

**SYNTHESIS AND EVALUATION OF PHOTOCHEMICALLY INDUCED
POLYMERIZATION IN NOVEL ACRYLIC MONOMERS**

A Thesis Submitted to the
UNIVERSITY OF PUNE

For the degree of
DOCTOR OF PHILOSOPHY

In
CHEMISTRY

By
HARIKRISHNA. R

Research guide
Dr. C. R. RAJAN

POLYMER SCIENCE AND ENGINEERING DIVISION
NATIONAL CHEMICAL LABORATORY
PUNE-411008, INDIA

DECEMBER 2010



राष्ट्रीय रासायनिक प्रयोगशाला
(वैज्ञानिक तथा औद्योगिक अनुसंधान परिषद)
डॉ. होमी भाभा मार्ग पुणे - 411 008. भारत
NATIONAL CHEMICAL LABORATORY



(Council of Scientific & Industrial Research)
Dr. Homi Bhabha Road, Pune - 411 008. India.

CERTIFICATE

Certified that the work incorporated in the thesis entitled **“Synthesis and Evaluation of Photochemically Induced Polymerization in Novel Acrylic Monomers”** submitted by **Mr. Harikrishna. R** was carried out by the candidate at National Chemical Laboratory, Pune – 411008, under my supervision. Such materials as obtained from other sources have been duly acknowledged in this thesis.

December 2010
Pune


Dr. C.R. Rajan
(Research guide)


Dr. S. Ponrathnam
(Co-Guide)

Communication
Channels


NCL Level DID : 2590
NCL Board No. : +91-20-25902000
EPABX : +91-20-25893300
+91-20-25893400

FAX

Director's Office : +91-20-25893355
COA's Office : +91-20-25893619
COS&P's Office : +91-20-25893008

WEBSITE

www.ncl-india.org

DECLARATION

I hereby declare that the thesis entitled "**Synthesis and Evaluation of Photochemically Induced Polymerization in Novel Acrylic Monomers**" submitted for PhD degree to the University of Pune has been carried out at National Chemical Laboratory, Pune, India, under the supervision of Dr. C.R. Rajan, Division of Polymer Science and Engineering, National Chemical Laboratory, Pune – 411008. The work is original and has not been submitted in part or full by me for any degree or diploma to this or any other university.

December 2010

Pune


(Harikrishna. R)

*Dedicated to all who have positively motivated
my life*

*A man in all his scientific glory is nothing compared to someone who has attained
supremacy over his own nature.*

*Dr.S.Radhakrishnan
(Philosopher and former president – Republic of India)*

CONTENTS

Contents	
List of figures	
List of tables	
Abstract	
List of abbreviations	

CHAPTER 1

Introduction to photopolymerization

<i>Section No.</i>		<i>Page No.</i>
1.1	Introduction	1
1.2	Reactions and properties of acrylate resins	3
1.2.1	General reactions of acrylate resins	3
1.2.2	Properties of acrylate resins	4
1.2.2.1	Influence of molecular weight	5
1.2.2.2	Growth rate of polymer chains	5
1.3	Theory of photoinitiated polymerization of acrylates	6
1.3.1	Initiation	6
1.3.2	Propagation	7
1.3.3	Termination	8
1.3.3.1	Chain transfer	10
1.3.3.1.1	Transfer to monomer	11
1.3.3.1.2	Transfer to modifier	11
1.3.4	Crosslinking in photo initiated polymerization	11
1.3.5	Photoinitiated polymerization in presence of reactive diluents	14
1.3.6	Factors influencing free radical photopolymerization	15
1.3.6.1	Reaction temperature	15
1.3.6.2	Monomer concentration	15
1.3.6.3	Solvents	15
1.3.6.4	Concentration of initiator	16
1.3.6.5	Chain transfer agents	16
1.3.6.6	Trommsdorff effect	16
1.3.6.7	Initiator half life	16

1.3.6.8	Influence of light intensity	17
1.3.6.9	Influence of added radical scavenger and UV absorber	17
1.3.7	Photoinitiated polymerization of high internal phase emulsions	18
1.4	Determination of rate constants by termination models	19
1.4.1	Bimolecular termination model	20
1.4.2	Monomolecular termination model	23
1.5	Determination of rate constants from classical and modified autocatalytic model	24
1.6	Measurement and interpretation of photopolymerization processes	26
1.6.1	Real time IR	26
1.6.2	Photo DSC	27
1.6.2.1	Determination of kinetic parameters by photo DSC	29
1.7	Applications of UV and visible photoinitiated polymerization	30
1.8	References	31

CHAPTER 2

Introduction to high internal phase emulsion

2.1	Introduction	43
2.2	Preparation and polymerization of HIPes	44
2.2.1	Preparation and polymerization of continuous phase HIPes	44
2.2.1.1	Preparation and polymerization of W/O HIPes	44
2.2.1.2	Preparation and polymerization of O/W HIPes	46
2.2.1.3	Non-aqueous polyHIPes	47
2.2.2	Dispersed phase polyHIPes	48
2.2.3	Polymerization of both phases of HIPes	49
2.3	Stability of HIPes	49
2.4	Morphology of polyHIPes	51
2.5	Properties of polyHIPes	53
2.6	Applications	54
2.7	References	55

CHAPTER 3

Aims and objectives

3	Aims and objectives	61
----------	---------------------	----

CHAPTER 4

Photopolymerization of mono and diacrylate based monomers

4.1	<i>PART-A: Photopolymerization of aliphatic and cycloaliphatic based di(meth)acrylate monomers</i>	66
4.1.1	Experimental	66
4.1.1.1	Materials	66
4.1.1.2	Measurements	67
4.1.1.2.1	Infrared spectroscopy	67
4.1.1.2.2	Nuclear magnetic resonance spectroscopy	67
4.1.1.2.3	Vapour pressure osmometry	67
4.1.1.2.4	Differential scanning calorimetry	68
4.1.1.2.5	Photo differential scanning calorimetry	68
4.1.1.2.6	Thermogravimetry	70
4.1.1.3	Photopolymerization of diurethane dimethacrylate based on 2-hydroxyethyl methacrylate and hexamethylene diisocyanate. [System 4A-1]	71
4.1.1.3.1	Procedure for synthesis	71
4.1.1.3.2	Formulation	72
4.1.1.3.3	Photocuring studies	72
4.1.1.3.4	Results and discussion	73
4.1.1.4	Photopolymerization of dimethacrylate macromonomer based on polypropylene glycol 3000, isophorone diisocyanate and 2-hydroxyethyl methacrylate. [System 4A-2]	78
4.1.1.4.1	Procedure for synthesis	79
4.1.1.4.2	Formulation	80
4.1.1.4.3	Photocuring studies	80
4.1.1.4.4	Result and discussion	81
4.1.1.5	Photopolymerization of diacrylate macromonomer based on polyethylene glycol 200, Polypropylene glycol 725, Polypropylene glycol 3000, isophorone diisocyanate and 2-hydroxyethyl acrylate. [System 4A-3]	84
4.1.1.5.1	Procedure for synthesis	85
4.1.1.5.2	Formulation	86
4.1.1.5.3	Photocuring studies	86
4.1.1.5.4	Results and discussion	87

4.1.1.6	Photopolymerization of diacrylate macromonomer based on polyethylene glycol 200, polyethylene glycol 400, polyethylene glycol 600, isophorone diisocyanate and 2-hydroxyethyl acrylate. [System 4A-4]	92
4.1.1.6.1	Procedure for synthesis	93
4.1.1.6.2	Formulation	94
4.1.1.6.3	Photocuring studies	94
4.1.1.6.4	Results and discussion	95
4.1.1.7	Photopolymerization of dimethacrylate macromonomer based on hydroxy terminated polybutadiene 2750, isophorone diisocyanate and 2-hydroxyethyl methacrylate. [System 4A-5]	101
4.1.1.7.1	Procedure for synthesis	101
4.1.1.7.2	Formulation	102
4.1.1.7.3	Photocuring studies	103
4.1.1.7.4	Results and discussion	103
4.1.1.8	Synthesis of dimethacrylate macromonomer based on hydroxy terminated polybutadiene 2750, polypropylene glycol 725, hexamethylene diisocyanate and 2-hydroxy ethyl methacrylate. [System 4A-6]	106
4.1.1.8.1	Procedure for synthesis	107
4.1.1.8.2	Formulation	108
4.1.1.8.3	Photocuring studies	108
4.1.1.8.4	Results and discussion	109
4.1.1.9	Photopolymerization of dimethacrylate macromonomer based on hydroxyl terminated polybutadiene 2750, isophorone diisocyanate and hydroxy propyl acrylate. [System 4A-7]	114
4.1.1.9.1	Procedure for synthesis	114
4.1.1.9.2	Formulation	116
4.1.1.9.3	Photocuring studies	116
4.1.1.9.4	Results and discussion	116
4.1.1.10	Photopolymerization of diacrylate macromonomer based on cyclohexane dimethanol, isophorone diisocyanate and 2-hydroxyethyl acrylate. [System 4A-8]	120
4.1.1.10.1	Procedure for synthesis	121
4.1.1.10.2	Formulation	122
4.1.1.10.3	Photocuring studies	123

4.1.1.10.4	Results and discussion	123
4.1.1.10.5	Post photopolymerization studies	159
4.1.1.11	Photopolymerization of diacrylate macromonomer based on polytetrahydrofuran 650, isophorone diisocyanate and polyethylene glycol methacrylate. [System 4A-9]	161
4.1.1.11.1	Procedure for synthesis	162
4.1.1.11.2	Formulation	163
4.1.1.11.3	Photocuring studies	163
4.1.1.11.4	Results and discussion	164
4.1.2	Conclusions	194
4.1.3	References	196
4.2	<i>PART – B: Photopolymerization of bisaromatic based di(meth)acrylate monomers</i>	198
4.2.1	Experimental	198
4.2.1.1	Materials and measurements	198
4.2.1.2	Photopolymerization of bisaromatic urethane diacrylate based on 2,2-bis[4-(β -hydroxyethoxy)-phenyl] propane, hexamethylene diisocyanate and 2-hydroxyethyl acrylate. [System 4B-1]	199
4.2.1.2.1	Procedure for synthesis	199
4.2.1.2.2	Formulation	200
4.2.1.2.3	Photocuring studies	201
4.2.1.2.4	Results and discussion	201
4.2.1.2.5	Post photopolymerization studies	207
4.2.1.3	Photopolymerization of bisaromatic diacrylate based on 2,2-bis[4-(β -hydroxypropoxy)-phenyl] propane, hexamethylene diisocyanate and 2-hydroxyethyl acrylate. [System 4B-2]	208
4.2.1.3.1	Procedure for synthesis	208
4.2.1.3.2	Formulation	209
4.2.1.3.3	Photocuring studies	210
4.2.1.3.4	Results and discussion	210
4.2.1.3.5	Post photopolymerization studies	223
4.2.1.4	Photopolymerization of bisaromatic urethane diacrylate based on bis [4-(β -hydroxypropoxy)-phenyl] sulphone, hexamethylene diisocyanate and 2-hydroxyethyl methacrylate. [System 4B-3]	224

4.2.1.4.1	Procedure for synthesis	225
4.2.1.4.2	Formulation	226
4.2.1.4.3	Photocuring studies	227
4.2.1.4.4	Results and discussion	227
4.2.1.4.5	Post photopolymerization studies	240
4.2.1.5	Photopolymerization of bisaromatic urethane diacrylate based on bis[4-(β -hydroxyethoxy)] biphenyl, isophorone diisocyanate and hydroxypropyl acrylate. [System 4B-4]	241
4.2.1.5.1	Procedure for synthesis	241
4.2.1.5.2	Formulation	242
4.2.1.5.3	Photocuring studies	243
4.2.1.5.4	Results and discussion	243
4.2.1.5.5	Post photopolymerization studies	251
4.2.2	Conclusions	251
4.2.3	References	255
4.3	<i>PART – C: Photopolymerization of high internal phase emulsions based (meth)acrylate monomers</i>	257
4.3.1	Experimental	257
4.3.1.1	Materials and measurements	257
4.3.1.2	Procedure for synthesis	257
4.3.1.3	Photocuring studies	258
4.3.1.4	Residual monomer analysis	259
4.3.2	Results and discussion	260
4.3.3	Conclusions	263
4.3.4	References	264

CHAPTER 5

Photopolymerization of multiacrylate based monomers

5.1	Introduction	265
5.2	Experimental	265
5.2.1	Materials and measurements	265
5.2.2	Photopolymerization of multiacrylate macromonomer based on polypropylene glycol 725, isophorone diisocyanate and pentaerythritol triacrylate. [System 5-1]	266
5.2.2.1	Procedure for synthesis	266

5.2.2.2	Formulation	267
5.2.2.3	Photocuring studies	267
5.2.2.4	Results and discussion	268
5.2.3	Photopolymerization of multiacrylate macromonomer based on hydroxy terminated polybutadiene 2750, isophorone diisocyanate and pentaerythritol triacrylate. [System 5-2]	272
5.2.3.1	Procedure for synthesis	273
5.2.3.2	Formulation	273
5.2.3.3	Photocuring studies	274
5.2.3.4	Results and discussion	274
5.2.4	Photopolymerization of multiacrylate macromonomer based on polyethylene glycol 200, polypropylene glycol 725, polypropylene glycol 3000, isophorone diisocyanate and glycerol diglycerolate diacrylate. [System 5-3]	276
5.2.4.1	Procedure for synthesis	277
5.2.4.2	Formulation	278
5.2.4.3	Photocuring studies	278
5.2.4.4	Results and discussion	279
5.2.5	Photopolymerization of multiacrylate macromonomer based on polytetrahydrofuran 650, isophorone diisocyanate and propylene glycol glycerolate diacrylate. [System 5-4]	287
5.2.5.1	Procedure for synthesis	287
5.2.5.2	Formulation	289
5.2.5.3	Photocuring studies	289
5.2.5.4	Results and discussion	289
5.3	Conclusions	296
5.4	References	298

CHAPTER 6

Synthesis of cation exchange resins and their catalytic evaluation for acid phase condensation reactions

6.1	Introduction	299
6.1.1	Functionalization of porous polymers for use as cation exchange resins	299
6.1.2	Preparation of bisphenol and trisphenol by acid phase catalysis	301
6.2	Experimental	303

6.2.1	Materials	303
6.2.2	Measurements	304
6.2.2.1	Elemental analysis	304
6.2.2.1.1	EDX	304
6.2.2.2	Infrared spectroscopy	304
6.2.2.3	BET surface area analysis	304
6.2.2.4	Surface morphology	304
6.2.2.4.1	Optical microscopy	304
6.2.2.4.2	Scanning electron microscopy	304
6.2.2.5	High resolution XPS	305
6.2.2.6	High performance liquid chromatography	305
6.2.3	Polymerization methods and surface modification reactions	305
6.2.3.1	Method of HIPE copolymerization	305
6.2.3.2	Surface modification for copolymerized HIPE beads	306
6.2.3.2.1	Method for sulphonation of oxirane ring in copolymerized HIPE beads	306
6.2.3.2.2	Method for mercapto sulphonation of oxirane ring in copolymerized HIPE beads	307
6.2.3.2.3	Method for mercapto sulphonation of thiirane ring in copolymerized HIPE beads	307
6.2.3.2.4	Method for aromatic sulphonation in copolymerized HIPE beads	308
6.2.3.3	Method for HIPE terpolymerization	308
6.2.3.4	Surface modifications for terpolymerized HIPE beads	310
6.2.3.4.1	Method for sulphonation of oxirane ring in terpolymerized HIPE beads	310
6.2.3.4.2	Method for mercapto sulphonation of oxirane ring in terpolymerized HIPE beads	310
6.2.3.4.3	Method for mercapto sulphonation of thiirane ring in terpolymerized HIPE beads	311
6.2.3.4.4	Method for aromatic sulphonation in terpolymerized HIPE beads	311
6.2.4	Calculation of acid exchange values	312
6.2.5	Acid phase catalysis	313
6.2.5.1	Condensation of phenol with acetone	313
6.2.5.2	Condensation of phenol with 4-hydroxy acetophenone	313
6.2.6	HPLC studies	313
6.2.6.1	HPLC study of condensation of phenol and acetone	313
6.2.6.2	HPLC study of condensation of phenol and 4-hydroxy acetophenone	314
6.3	Results and discussion	315

6.3.1	IR analysis	315
6.3.2	XPS analysis	316
6.3.3	EDX analysis	318
6.3.4	Calculation of acid exchange values	319
6.3.5	Surface area analysis	320
6.3.6	Surface morphology studies	321
6.3.6.1	Optical microscopy	321
6.3.6.2	Scanning electron microscopy	322
6.3.7	HPLC analysis for acid phase condensation reactions	323
6.3.7.1	Estimation of 4,4'-bisphenol A using HPLC	323
6.3.7.2	Estimation of 1,1,1-tris(4'-hydroxyphenyl) ethane using HPLC	326
6.4	Conclusions	329
6.5	References	330

CHAPTER 7

Summary and conclusions

7	Summary and conclusions	334
----------	-------------------------	-----

List of figures

<i>Fig No.</i>	<i>Caption</i>	<i>Page No.</i>
Chapter – 4		
4.1	Emission spectrum of high pressure mercury short arc lamp	69
4.2	Synthesis pathway of urethane diacrylate involving HEMA and HMDI [System 4A-1]	71
4.3(A-C)	Time dependent rate and conversion profiles of formulations containing 0.5, 1, 2 and 4 wt% of IRGACURE 651 [System 4A-1]	73
4.4(A-C)	Time dependent rate and conversion profiles of formulations containing 0.5, 1, 2 and 4 wt% of DAROCUR TPO [System 4A-1]	74
4.5(A-C)	Time dependent rate and conversion profiles of formulations containing 0.5, 1, 2 and 4 wt% of DAROCUR 1173 [System 4A-1]	75
4.6	Synthesis pathway of urethane dimethacrylate macromonomer based on PPG 3000, IPDI and HEMA [System 4A-2]	78
4.7(A-C)	Time dependent rate and conversion profiles of macromonomeric formulations containing 0.5, 1 and 1.5 wt% of IRGACURE 651 [System 4A-2]	81
4.8(A-C)	Time dependent rate and conversion profiles of macromonomeric formulations containing 0.5, 1 and 1.5 wt% of IRGACURE 184 [System 4A-2]	82
4.9	Synthesis pathway of urethane diacrylate macromonomer based on PEG 200, PPG 725, PPG 3000, IPDI and HEA [System 4A-3]	85
4.10(A-C)	Time dependent rate and conversion profiles of macromonomeric formulations containing 0.5 wt% of eight photoinitiators [System 4A-3]	87
4.11(A-C)	Time dependent rate and conversion profiles of macromonomeric formulations containing 1 wt% of eight photoinitiators [System 4A-3]	88
4.12(A-C)	Time dependent rate and conversion profiles of macromonomeric formulations containing 2 wt% of eight photoinitiators [System 4A-3]	89
4.13	Synthesis pathway of diacrylate macromonomer based on PEG 200, PEG 400, PEG 600, IPDI and HEA [System 4A-4]	93

4.14(A-C)	Time dependent rate and conversion profiles of macromonomeric formulations containing 0.5 wt% of five photoinitiators [System 4A-4]	96
4.15(A-C)	Time dependent rate and conversion profiles of macromonomeric formulations containing 1 wt% of five photoinitiators [System 4A-4]	97
4.16(A-C)	Time dependent rate and conversion profiles of macromonomeric formulations containing 2 wt% of five photoinitiators [System 4A-4]	98
4.17	Synthesis pathway of dimethacrylate macromonomer based on HTPB 2750, IPDI and HEMA [System 4A-5]	101
4.18(A-C)	Time dependent rate and conversion profiles of macromonomeric formulations containing 1 wt% of five photoinitiators [System 4A-5]	104
4.19	Synthesis pathway of dimethacrylate macromonomer based on HTPB 2750, PPG 725, HMDI and HEMA [System 4A-6]	107
4.20(A-C)	Time dependent rate and conversion profiles of macromonomeric formulations containing IRGACURE 651 at different concentrations [System 4A-6]	109
4.21(A-C)	Time dependent rate and conversion profiles of macromonomeric formulations containing DAROCUR TPO at different concentrations [System 4A-6]	110
4.22(A-C)	Time dependent rate and conversion profiles of macromonomeric formulations containing IRGACURE 819 at different concentrations [System 4A-6]	111
4.23	Synthesis pathway of dimethacrylate macromonomer based on HTPB 2750, IPDI and HPA [System 4A-7]	114
4.24(A-C)	Time dependent rate and conversion profiles of macromonomeric formulations containing 0.25 wt% of photoinitiator with respect to the weight of macromonomer at 30 °C [System 4A-7]	117
4.25(A-C)	Time dependent rate and conversion profiles of macromonomeric formulations containing 0.5 wt% of photoinitiator with respect to weight of macromonomer at 30 °C [System 4A-7]	118
4.26	The synthesis pathway of diacrylate macromonomer based on CHDM, IPDI and HEA [System 4A-8]	121

4.27(A-C)	Time dependent rate and conversion profiles of macromonomeric formulations containing 10 wt% HEA and 0.5 wt% of photoinitiator with respect to weight of macromonomer at 30°C [System 4A-8]	125
4.28(A-C)	Time dependent rate and conversion profiles of macromonomeric formulations containing 10 wt% HEA and 2 wt% of photoinitiator with respect to the weight of macromonomer at 30 °C [System 4A-8]	126
4.29(A-C)	Time dependent rate and conversion profiles of macromonomeric formulations containing 10 wt% HEA and 0.5 wt% of photoinitiator with respect to weight of macromonomer at 50 °C [System 4A-8]	127
4.30(A-C)	Time dependent rate and conversion profiles of macromonomeric formulations containing 10 wt% HEA and 2 wt% of photoinitiator with respect to weight of macromonomer at 50 °C [System 4A-8]	128
4.31(A-C)	Time dependent rate and conversion profiles of macromonomeric formulations containing 10 wt% HEA, 5 wt% NPGPDA and 0.5 wt% of photoinitiator with respect to weight of macromonomer at 30 °C [System 4A-8]	132
4.32(A-C)	Time dependent rate and conversion profiles of macromonomeric formulations containing 10 wt% HEA, 5 wt% NPGPDA and 2 wt% of photoinitiator with respect to weight of macromonomer at 30 °C [System 4A-8]	133
4.33(A-C)	Time dependent rate and conversion profiles of macromonomeric formulations containing 10 wt% HEA, 5 wt% NPGPDA and 0.5 wt% of photoinitiator with respect to weight of macromonomer at 50 °C [System 4A-8]	134
4.34(A-C)	Time dependent rate and conversion profiles of macromonomeric formulations containing 10 wt% HEA, 5 wt% NPGPDA and 2 wt% of photoinitiator with respect to weight of macromonomer at 50 °C [System 4A-8]	135
4.35(A-C)	Time dependent rate and conversion profiles of macromonomeric formulations containing 10 wt% HEA, 5 wt% TMPTA and 0.5 wt% of photoinitiator with respect to weight of macromonomer at 30 °C [System 4A-8]	139
4.36(A-C)	Time dependent rate and conversion profiles of macromonomeric formulations containing 10 wt% HEA, 5 wt% TMPTA and 2 wt% of photoinitiator with respect to weight of macromonomer at 30 °C [System 4A-8]	140

4.37(A-C)	Time dependent rate and conversion profiles of macromonomeric formulations containing 10 wt% HEA, 5 wt% TMPTA and 0.5 wt% of photoinitiator with respect to weight of macromonomer at 50 °C [System 4A-8]	141
4.38(A-C)	Time dependent rate and conversion profiles of macromonomeric formulations containing 10 wt% HEA, 5 wt% TMPTA and 2 wt% of photoinitiator with respect to weight of macromonomer at 50 °C [System 4A-8]	142
4.39(A-C)	Time dependent rate and conversion profiles of macromonomeric formulations containing 10 wt% HEA, 5 wt% NPGPDA, 0.006 wt% TEMPO and 0.5 wt% of photoinitiator with respect to weight of macromonomer at 30 °C [System 4A-8]	146
4.40 (A-C)	Time dependent rate and conversion profiles of macromonomeric formulations containing 10 wt% HEA, 5 wt% NPGPDA, 0.006 wt% TEMPO and 2 wt% of photoinitiator with respect to weight of macromonomer at 30 °C [System 4A-8]	147
4.41(A-C)	Time dependent rate and conversion profiles of macromonomeric formulations containing 10 wt% HEA, 5 wt% NPGPDA, 0.006 wt% TEMPO and 0.5 wt% of photoinitiator with respect to weight of macromonomer at 50 °C [System 4A-8]	148
4.42(A-C)	Time dependent rate and conversion profiles of macromonomeric formulations containing 10 wt% HEA, 5 wt% NPGPDA, 0.006 wt% TEMPO and 2 wt% of photoinitiator with respect to weight of macromonomer at 50 °C [System 4A-8]	149
4.43(A-C)	Time dependent rate and conversion profiles of macromonomeric formulations containing 10 wt% HEA, 5 wt% TMPTA, 0.012 wt% TEMPO and 0.5 wt% of photoinitiator with respect to weight of macromonomer at 30 °C [System 4A-8]	152
4.44(A-C)	Time dependent rate and conversion profiles of macromonomeric formulations containing 10 wt% HEA, 5 wt% TMPTA, 0.012 wt% TEMPO and 2 wt% of photoinitiator with respect to weight of macromonomer at 30 °C [System 4A-8]	153
4.45(A-C)	Time dependent rate and conversion profiles of macromonomeric formulations containing 10 wt% HEA, 5 wt% TMPTA, 0.012 wt% TEMPO and 0.5 wt% of photoinitiator with respect to weight of macromonomer at 50 °C [System 4A-8]	154

4.46(A-C)	Time dependent rate and conversion profiles of macromonomeric formulations containing 10 wt% HEA, 5 wt% TMPTA, 0.012 wt% TEMPO and 2 wt% of photoinitiator with respect to weight of macromonomer at 50 °C [System 4A-8]	155
4.47(A-C)	Scavenging effect of TEMPO [System 4A-8]	158
4.48	Thermogravimetric degradation profiles of (a) macromonomer with 10 wt% HEA (b) macromonomer containing 10 wt% HEA and 5 wt% of NPGPDA and (c) macromonomer containing 10 wt% HEA and 5 wt% of TMPTA with 0.5 wt% of IRGACURE 184 photocured at 50 °C. Analyses done after three days of storage [System 4A-8]	159
4.49	T _g of (a) macromonomer, (b) macromonomer containing 5 wt% of NPGPDA and (c) macromonomer containing 5 wt% of TMPTA with 0.5 wt% of IRGACURE 184 photocured at 50 °C [System 4A-8]	159
4.50	Synthesis pathway of diacrylate macromonomer based on PTHF 650, IPDI and PEGMA [System 4A-9]	161
4.51(A-C)	Time dependent rate and conversion profiles of macromonomeric formulations containing 0.5 and 2 wt% of IRGACURE 651 and DAROCUR TPO as photoinitiator with respect to weight of macromonomer at 30 °C [System 4A-9]	165
4.52(A-C)	Time dependent rate and conversion profiles of macromonomeric formulations containing 0.5 and 2 wt% of IRGACURE 651 and DAROCUR TPO as photoinitiator with respect to weight of macromonomer at 50 °C [System 4A-9]	166
4.53(A-C)	Deviation of experimental data from the autocatalytic and n th order models (A-B) and the corresponding heat flow profile (C) for macromonomer containing 0.5 wt% of DAROCUR TPO at 50 °C [System 4A-9]	169
4.54(A-C)	Time dependent rate and conversion profiles of macromonomeric formulations containing 10 wt% NPGPDA and 0.5 wt% of four photoinitiators with respect to weight of macromonomer at 30 °C [System 4A-9]	170
4.55(A-C)	Time dependent rate and conversion profiles of macromonomeric formulations containing 10 wt% NPGPDA and 2 wt% of four photoinitiators with respect to weight of macromonomer at 30 °C [System 4A-9]	171
4.56(A-C)	Time dependent rate and conversion profiles of macromonomeric formulations containing 10 wt% NPGPDA and 0.5 wt% of four photoinitiators with respect to weight of macromonomer at 50 °C [System 4A-9]	172

4.57(A-C)	Time dependent rate and conversion profiles of macromonomeric formulations containing 10 wt% NPGPDA and 2 wt% of four photoinitiators with respect to weight of macromonomer at 50 °C [System 4A-9]	173
4.58(A-C)	Better fit for the autocatalytic model and deviated nature of n^{th} order model (A-B) and the corresponding heat flow profile (C) for macromonomer containing 10 wt% NPGPDA and 0.5 wt% of DAROCUR TPO at 50 °C [System 4A-9]	176
4.59(A-C)	Time dependent rate and conversion profiles of macromonomeric formulations containing 10 wt% TMPTA and 0.5 wt% of four photoinitiators with respect to the weight of macromonomer at 30 °C [System 4A-9]	177
4.60(A-C)	Time dependent rate and conversion profiles of macromonomeric formulations containing 10 wt% TMPTA and 2 wt% of four photoinitiators with respect to weight of macromonomer at 30 °C [System 4A-9]	178
4.61(A-C)	The rate and conversion profiles of macromonomeric formulations containing 10 wt% TMPTA and 0.5 wt% of four photoinitiators with respect to weight of macromonomer at 50 °C [System 4A-9]	179
4.62(A-C)	Time dependent rate and conversion profiles of macromonomeric formulations containing 10 wt% TMPTA and 2 wt% of four photoinitiators with respect to weight of macromonomer at 50 °C [System 4A-9]	180
4.63(A-C)	Time dependent rate and conversion profiles of macromonomeric formulations containing 10 wt% NPGPDA, 0.006 wt% TEMPO and 0.5 wt% of four photoinitiators with respect to the weight of macromonomer at 30 °C [System 4A-9]	183
4.64(A-C)	Time dependent rate and conversion profiles of macromonomeric formulations containing 10 wt% NPGPDA, 0.006 wt% TEMPO and 2 wt% of four photoinitiators with respect to weight of macromonomer at 30 °C [System 4A-9]	184
4.65(A-C)	Time dependent rate and conversion profiles of macromonomeric formulations containing 10 wt% NPGPDA, 0.006 wt% TEMPO and 0.5 wt% of four photoinitiators with respect to weight of macromonomer at 50 °C [System 4A-9]	185
4.66(A-C)	Time dependent rate and conversion profiles of macromonomeric formulations containing 10 wt% NPGPDA, 0.006 wt% TEMPO and 2 wt% of four photoinitiators with respect to weight of macromonomer at 50 °C [System 4A-9]	186

4.67(A-C)	Time dependent rate and conversion profiles of macromonomeric formulations containing 10 wt% TMPTA, 0.012 wt% TEMPO and 0.5 wt% of four photoinitiators with respect to weight of macromonomer at 30 °C [System 4A-9]	189
4.68(A-C)	Time dependent rate and conversion profiles of macromonomeric formulations containing 10 wt% TMPTA, 0.012 wt% TEMPO and 2 wt% of four photoinitiators with respect to weight of macromonomer at 30 °C [System 4A-9]	190
4.69(A-C)	Time dependent rate and conversion profiles of macromonomeric formulations containing 10 wt% TMPTA, 0.012 wt% TEMPO and 0.5 wt% of four photoinitiators with respect to weight of macromonomer at 50 °C [System 4A-9]	191
4.70(A-C)	Time dependent rate and conversion profiles of macromonomeric formulations containing 10 wt% TMPTA, 0.012 wt% TEMPO and 2 wt% of four photoinitiators with respect to weight of macromonomer at 50 °C [System 4A-9]	192
4.71	Synthesis pathway of bisaromatic based urethane diacrylate based on HEPP, HMDI and HEA [System 4B-1]	199
4.72(A-C)	Time dependent rate as well as conversion profiles of macromonomeric formulations containing 50 wt% HEA and 0.5 wt% of three photoinitiators at 40 °C [System 4B-1]	202
4.73(A-C)	Time dependent rate as well as conversion profiles of macromonomeric formulations containing 50 wt% HEA and 1 wt% of three photoinitiators at 40 °C [System 4B-1]	203
4.74(A-C)	Time dependent rate as well as conversion profiles of macromonomeric formulations containing 50 wt% HEA and 2 wt% of three photoinitiators at 40 °C [System 4B-1]	204
4.75	Thermogravimetric degradation profiles of macromonomeric formulation containing 50 wt% of HEA and 0.5 wt% of DAROCUR TPO photocured at 40 °C and 0.03 min and 15 min of irradiation at 1.93 mW/cm ² . Analyses done after one week storage [System 4B-1]	207
4.76	The synthesis pathway of bisaromatic urethane diacrylate based on HPPP, HMDI and HEA [System 4B-2]	208
4.77(A-C)	Time dependent rate and conversion profiles of macromonomeric formulations containing 50 wt% HEA and 0.5 wt% of three photoinitiator at 40 °C and 1.93 mW/cm ² [System 4B-2]	211

4.78(A-C)	Time dependent rate and conversion profiles of macromonomeric formulations containing 50 wt% HEA and 1 wt% of three photoinitiator at 40 °C and 1.93 mW/cm ² [System 4B-2]	212
4.79(A-C)	Time dependent rate and conversion profiles of macromonomeric formulations containing 50 wt% HEA and 2 wt% of three photoinitiator at 40 °C and 1.93 mW/cm ² [System 4B-2]	213
4.80(A-C)	Time dependent rate and conversion profiles of macromonomeric formulations containing 50 wt% HEA and 0.5 wt% of three photoinitiator at 40 °C and 4.47 mW/cm ² [System 4B-2]	214
4.81(A-C)	Time dependent rate and conversion profiles of macromonomeric formulations containing 50 wt% HEA and 1 wt% of three photoinitiator at 40 °C and 4.47 mW/cm ² [System 4B-2]	215
4.82(A-C)	Time dependent rate and conversion profiles of macromonomeric formulations containing 50 wt% HEA and 2 wt% of three photoinitiator at 40 °C and 4.47 mW/cm ² [System 4B-2]	216
4.83(A-C)	Time dependent rate and conversion profiles of macromonomeric formulations containing 50 wt% HEA and 0.5 wt% of three photoinitiator at 70 °C and 4.47 mW/cm ² [System 4B-2]	219
4.84(A-B)	A plot of k_t^b/k_p at different percentage conversions for the formulation containing 50 wt% HEA and 0.5 wt% of (A) IRGACURE 651 and (B) DAROCUR TPO at 40 °C [System 4B-2]	222
4.85	Thermogravimetric degradation profiles at 20 °C/min of macromonomeric formulation containing 50 wt% of HEA and 0.5 wt% of DAROCUR TPO (A) photocured at 40 °C and 0.04 min and 5 min of irradiation at 1.93 mW/cm ² and (B) at 40 and 70 °C at 4.47 mW/cm ² . Analyses done after one week storage [System 4B-2]	223
4.86	Synthesis pathway of bisaromatic urethane diacrylate based on HPPS, HMDI and HEMA [System 4B-3]	225
4.87(A-C)	Time dependent rate and conversion profiles of macromonomeric formulations containing 75 wt% HEMA and 0.5 wt% of three photoinitiator at 40 °C and 1.78 mW/cm ² [System 4B-3]	228
4.88(A-C)	Time dependent rate and conversion profiles of macromonomeric formulations containing 75 wt% HEMA and 1 wt% of three photoinitiator at 40 °C and 1.78 mW/cm ² [System 4B-3]	229

4.89(A-C)	Time dependent rate and conversion profiles of macromonomeric formulations containing 75 wt% HEMA and 2 wt% of three photoinitiator at 40 °C and 1.78 mW/ cm ² [System 4B-3]	230
4.90(A-C)	Time dependent rate and conversion profiles of macromonomeric formulations containing 75 wt% HEMA and 0.5 wt% of three photoinitiator at 70 °C and 1.78 mW/ cm ² [System 4B-3]	231
4.91(A-C)	Time dependent rate and conversion profiles of macromonomeric formulations containing 75 wt% HEMA and 1 wt% of three photoinitiator at 70 °C and 1.78 mW/ cm ² [System 4B-3]	232
4.92(A-C)	Time dependent rate and conversion profiles of macromonomeric formulations containing 75 wt% HEMA and 2 wt% of three photoinitiator at 70 °C and 1.78 mW/ cm ² [System 4B-3]	233
4.93(A-C)	Time dependent rate and conversion profiles of macromonomeric formulations containing 75 wt% HEMA and 0.5 wt% of three photoinitiator at 40 °C and 3.26 mW/ cm ² [System 4B-3]	234
4.94(A-C)	Time dependent rate and conversion profiles of macromonomeric formulations containing 75 wt% HEMA and 1 wt% of three photoinitiator at 40 °C and 3.26 mW/ cm ² [System 4B-3]	235
4.95(A-C)	Time dependent rate and conversion profiles of macromonomeric formulations containing 75 wt% HEMA and 2 wt% of three photoinitiator at 40 °C and 3.26 mW/ cm ² [System 4B-3]	236
4.96	Thermogravimetric degradation profiles at 20 °C/min of macromonomeric formulation containing 75 wt% of HEMA and 0.5 wt% of IRGACURE 184 (A) photocured at 40 °C and 0.37 min and 5 min of irradiation at 1.78 mW/cm ² and (B) at 40 and 70 °C. Analyses done after one week storage [System 4B-3]	240
4.97	The synthesis pathway of bisaromatic urethane diacrylate based on HEBP, IPDI and HPA [System 4B-4]	241
4.98(A-C)	Time dependent rate and conversion profiles of macromonomeric formulations containing 300 wt% HPA, and three different concentration of IRGACURE 651 at 10, 40 and 70 °C at 2.27 mW/ cm ² [System 4B-4]	244
4.99(A-C)	Time dependent rate and conversion profiles of macromonomeric formulations containing 300 wt% HPA, and three different concentration of DAROCUR TPO at 10, 40 and 70 °C at 2.27 mW/ cm ² [System 4B-4]	245

4.100(A-C)	Time dependent rate and conversion profiles of macromonomeric formulations containing 300 wt% HPA, and three different concentration of IRGACURE 184 at 10, 40 and 70 °C at 2.27 mW/ cm ² [System 4B-4]	246
4.101	A plot of k_t^b/k_p at different percentage conversions for the formulation containing macromonomer, 300 wt% HPA and 0.5 wt% of IRGACURE 651 at 40 °C [System 4B-4]	250
4.102	Thermogravimetric degradation profiles at 20 °C/min of macromonomeric formulation containing 300 wt% of HPA and 0.5 wt% of DAROCUR TPO photocured at 10 and 70 °C and 2.27 mW/cm ² . Analyses done after one week storage [System 4B-4]	251
4.103(A-C)	Calibration plots obtained from GC data for the three monomers. (A) EHA, (B) EHMA and (C) EGDMA [System 4C]	260
4.104(A-E)	Time dependent percentage conversion profiles for formulations containing the three monomers and 0.5 wt% of photoinitiators photo cured using external lamp at ambient conditions with (A) IRGACURE 184, (B) IRGACURE 2959, (C) IRGACURE 1173, (D) IRGACURE 907 and (E) IRGACURE 819 [System 4C]	261

Chapter - 5

5.1	Synthesis pathway of urethane multiacrylate based on PPG 725, IPDI and PETA [System 5-1]	266
5.2(A-C)	Time dependent rate and conversion profiles of macromonomeric formulations containing 0.25 wt% of five photoinitiators [System 5-1]	269
5.3(A-C)	Time dependent rate and conversion profiles of macromonomeric formulations containing 1 wt% of five photoinitiators [System 5-1]	270
5.4	Synthesis pathway of urethane multiacrylate based on PPG 725, IPDI and PETA [System 5-2]	272
5.5(A-C)	Time dependent rate and conversion profiles of macromonomeric formulations containing 1 wt% of two photoinitiators [System 5-2]	275
5.6	Synthesis pathway of urethane multiacrylate based on PEG 200, PPG 725, PPG 3000, IPDI and GDGDA [System 5-3]	276
5.7(A-C)	Time dependent rate and conversion profiles of macromonomeric formulations containing 0.5 wt% of ten photoinitiators at 30 °C [System 5-3]	279

5.8(A-C)	Time dependent rate and conversion profiles of macromonomeric formulations containing 2 wt% of ten photoinitiators at 30 °C [System 5-3]	280
5.9(A-C)	Time dependent rate and conversion profiles of macromonomeric formulations containing 0.5 wt% of ten photoinitiators at 50 °C [System 5-3]	281
5.10(A-C)	Time dependent rate and conversion profiles of macromonomeric formulations containing 2 wt% of ten photoinitiators at 50 °C [System 5-3]	282
5.11	Synthesis pathway of urethane multiacrylate based on PTHF 650, IPDI and PGGDA [System 5-4]	287
5.12(A-C)	Time dependent rate and conversion profiles of macromonomeric formulations containing 0.5 wt% of four photoinitiators at 30 °C [System 5-4]	290
5.13(A-C)	Time dependent rate and conversion profiles of macromonomeric formulations containing 2 wt% of four photoinitiators at 30 °C [System 5-4]	291
5.14(A-C)	Time dependent rate and conversion profiles of macromonomeric formulations containing 0.5 wt% of four photoinitiators at 50 °C [System 5-4]	292
5.15(A-C)	Time dependent rate and conversion profiles of macromonomeric formulations containing 2 wt% of four photoinitiators at 50 °C [System 5-4]	293

Chapter - 6

6.1(A-C)	Formation of mercapto sulphonic acid catalyst from GMA-EGDM HIPE beads with 100% crosslink density in three steps using IR. (A) unmodified copolymer, (B) thiirated copolymer and (C) mercapto sulphonated copolymer	316
6.2(A-D)	Formation of mercapto sulphonic acid catalyst from ETMA-EGDM HIPE beads with 100% crosslink density in two steps using high resolution XPS. (A-B) unmodified copolymer and (C-D) mercapto sulphonated copolymer	317
6.3(A-C)	Formation of mercapto sulphonic acid catalyst from GMA-EGDM HIPE beads with 100% crosslink density in three steps using EDX. (A) unmodified copolymer, (B) thiirated copolymer and (C) mercapto sulphonated copolymer	319
6.4(A-B)	The surface morphology of the synthesized GMA-EGDM beads with 100% crosslink density measured at (A) 40 x and (B) 500 x	322
6.5(A-B)	The surface morphology of the synthesized GMA-ETMA-EGDM beads with 100% crosslink density measured at (A) 40 x and (B) 500 x	322
6.6(A-B)	The surface morphology of Amberlyst 15 copolymer beads with 100% crosslink density magnified to (A) 200 x and (B) 50k x	323
6.7(A-B)	The surface morphology of the synthesized GMA-ETMA - EGDM terpolymer beads with 100% crosslink density magnified to (A) 100 x and (B) 30k x	323

6.8(A-D)	Separation of (A) standard reactants and product obtained with 40% acetonitrile in water (B) product mixture after reaction with aliphatic mercapto sulphonated styrene-GMA-EGDM catalyst at 60 °C and (C) product mixture after reaction with two step sulphonated styrene-GMA-EGDM catalyst at 60 °C and (D) HPLC calibration plot for standard 4,4'-bisphenol A	324
6.9(A-E)	Separation of (A) standard solutions of reactants and product (B) example product mixture and (C) product mixture B after spiking with pure 1,1,1-THPE (D) product mixture after reaction with two step sulphonated styrene-GMA-DVB catalyst at 100 °C and (E) product mixture after reaction with Amberlyst 15 at 100 °C	327
6.10	HPLC calibration plot for standard 1,1,1-tris(4'-hydroxyphenyl) ethane	327

List of tables

<i>Table No.</i>	<i>Caption</i>	<i>Page No.</i>
Chapter - 4		
4.1	Photoinitiators used for curing studies	66
4.2	Physical properties of photoinitiators used in curing studies	67
4.3	Bandpass filters and their specific applications	69
4.4	Kinetic parameters of macromonomeric formulations calculated from the heat flow profiles at 30 °C [System 4A-1]	76
4.5	Kinetic parameters of macromonomeric formulations calculated from the heat flow profiles at 30 °C [System 4A-2]	83
4.6	Kinetic parameters of macromonomeric formulations calculated from the heat flow profiles at 30 °C [System 4A-3]	90
4.7	Kinetic parameters of macromonomeric formulations calculated from the heat flow profiles at 30 °C [System 4A-4]	99
4.8	Kinetic parameters of macromonomeric formulations calculated from the heat flow profiles at 1 wt% concentration of photoinitiator at 30 °C [System 4A-5]	105
4.9	Kinetic parameters of macromonomeric formulations calculated from the heat flow profiles at 30 °C [System 4A-6]	112
4.10	Kinetic parameters of macromonomeric formulations calculated from the heat flow profiles at 30 °C [System 4A-7]	119
4.11	Brookfield viscosity with spindle#4 at 80 rpm and 30 °C (Shear rate 266.4 s ⁻¹) [System 4A-8]	124
4.12	Kinetic parameters of macromonomeric formulations calculated from the heat flow profiles containing 10 wt% HEA [System 4A-8]	129
4.13	Evaluation of kinetic parameters of macromonomeric formulations as per autocatalytic model at 30 and 50 °C containing 10 wt% HEA [System 4A-8]	129

4.14	Kinetic parameters of macromonomeric formulations calculated from the heat flow profiles containing 10 wt% HEA and 5 wt% NPGPDA [System 4A-8]	136
4.15	Evaluation of kinetic parameters of macromonomeric formulations as per autocatalytic model at 30 and 50 °C containing 10 wt% HEA and 5 wt% NPGPDA [System 4A-8]	136
4.16	Kinetic parameters of macromonomeric formulations calculated from the heat flow profiles containing 10 wt% HEA and 5 wt% TMPTA [System 4A-8]	143
4.17	Evaluation of kinetic parameters of macromonomeric formulations as per autocatalytic model at 30 and 50 °C containing 10 wt% HEA and 5 wt% TMPTA [System 4A-8]	143
4.18	Kinetic parameters of macromonomeric formulations calculated from the heat flow profiles containing 10 wt% HEA, 5 wt% NPGPDA and 0.006 wt% TEMPO [System 4A-8]	150
4.19	Evaluation of kinetic parameters of macromonomeric formulations as per autocatalytic model at 30 and 50 °C containing 10 wt% HEA, 5 wt% NPGPDA and 0.006 wt% TEMPO [System 4A-8]	150
4.20	Kinetic parameters of macromonomeric formulations calculated from the heat flow profiles containing 10 wt% HEA, 5 wt% TMPTA and 0.012 wt% TEMPO [System 4A-8]	156
4.21	Evaluation of kinetic parameters of macromonomeric formulations as per autocatalytic model at 30 and 50 °C containing 10 wt% HEA, 5 wt% TMPTA and 0.012 wt% TEMPO [System 4A-8]	156
4.22	Post photopolymerization analyses [System 4A-8]	160
4.23	Kinetic parameters calculated from the heat flow profiles of macromonomeric formulations [System 4A-9]	167
4.24	Evaluation of kinetic parameters of macromonomeric formulations as per autocatalytic and n^{th} order models [System 4A-9]	167
4.25	Kinetic parameters of macromonomeric formulations calculated from the heat flow profiles containing 10 wt% of NPGPDA [System 4A-9]	174

4.26	Evaluation of kinetic parameters of macromonomeric formulations as per autocatalytic model at 30 and 50 °C containing 10 wt% of NPGPDA [System 4A-9]	174
4.27	Kinetic parameters of macromonomeric formulations calculated from the heat flow profiles containing 10 wt% of TMPTA [System 4A-9]	181
4.28	Evaluation of kinetic parameters of macromonomeric formulations as per autocatalytic model at 30 and 50 °C containing 10 wt% of TMPTA [System 4A-9]	181
4.29	Kinetic parameters of macromonomeric formulations calculated from the heat flow profiles containing 10 wt% of NPGPDA and 0.006wt% TEMPO [System 4A-9]	187
4.30	Evaluation of kinetic parameters of macromonomeric formulations as per autocatalytic model at 30 and 50 °C containing 10 wt% of NPGPDA and 0.006 wt% TEMPO [System 4A-9]	187
4.31	Kinetic parameters of macromonomeric formulations calculated from the heat flow profiles containing 10 wt% of TMPTA and 0.012 wt% TEMPO [System 4A-9]	193
4.32	Evaluation of kinetic parameters of macromonomeric formulations as per autocatalytic model at 30 and 50 °C containing 10 wt% of TMPTA and 0.012 wt% TEMPO [System 4A-9]	193
4.33	Kinetic parameters of macromonomeric formulations calculated from the heat flow profiles at 40 °C [System 4B-1]	205
4.34	Kinetic parameters of macromonomeric formulations calculated from the heat flow profiles at 40 °C [System 4B-2]	217
4.35	Kinetic parameters of macromonomeric formulations calculated from the heat flow profiles containing 0.5 wt% of photoinitiator at 70 °C and 4.47 mW/cm ² [System 4B-2]	219
4.36	Evaluation of kinetic parameters of macromonomeric formulations as per autocatalytic model at 40 °C [System 4B-2]	220
4.37	Evaluation of kinetic parameters of macromonomeric formulations as per autocatalytic model containing 0.5 wt% of photoinitiator at 4.47 mW/ cm ² [System 4B-2]	221

4.38	Kinetic parameters of macromonomeric formulations calculated from the heat flow profiles [System 4B-3]	237
4.39	Evaluation of kinetic parameters of macromonomeric formulations as per autocatalytic model at 40 and 70 °C at 1.78 mW/cm ² [System 4B-3]	238
4.40	Evaluation of kinetic parameters of macromonomeric formulations as per autocatalytic model at 40 °C and 3.26 mW/cm ² [System 4B-3]	239
4.41	Kinetic parameters of macromonomeric formulations calculated from the heat flow profiles at 2.27 mW/cm ² [System 4B-4]	247
4.42	Evaluation of kinetic parameters of macromonomeric formulations as per autocatalytic model at 2.27 mW/cm ² [System 4B-4]	249
4.43	Concentration of monomers in standard solutions for GC analysis	259
4.44	Induction time and maximum conversion calculated by residual monomer analysis using GC	262

Chapter - 5

5.1	Kinetic parameters of macromonomeric formulations calculated from the heat flow profiles at 30 °C and 22.6 mW/cm ² [System 5-1]	271
5.2	Kinetic parameters of macromonomeric formulations calculated from the heat flow profiles at 30 °C and 1.73 mW/cm ² [System 5-2]	275
5.3	Kinetic parameters of macromonomeric formulations calculated from the heat flow profiles at 4.6 mW/cm ² [System 5-3]	283
5.4	Evaluation of kinetic parameters of macromonomeric formulations as per autocatalytic model at 4.6 mW/cm ² [System 5-3]	286
5.5	Kinetic parameters of macromonomeric formulations calculated from the heat flow profiles at 4.6 mW/cm ² [System 5-4]	294
5.6	Evaluation of kinetic parameters of macromonomeric formulations as per autocatalytic model at 4.6 mW/cm ² [System 5-4]	294

Chapter - 6

6.1	Synthesis of copolymers of HIPE with 100% crosslink density	306
6.2	Surface modifications of copolymers of HIPE with 100% crosslink density	308
6.3	Synthesis of terpolymers of HIPE with 100% crosslink density	310

6.4	Surface modifications of copolymers of HIPE with 100% crosslink density	312
6.5	Acid exchange values for the catalysts	320
6.6	BET surface areas of unfunctionalized and functionalized beads	321
6.7	Percentage content and selectivity of 4,4'-bisphenol A calculated using aliphatic mercapto sulphonated catalysts	325
6.8	Percentage content and selectivity of 4,4'-bisphenol A calculated using aliphatic sulphonated catalysts	325
6.9	Percentage content and selectivity of 4,4'-bisphenol A calculated using two step sulphonated catalysts (aromatic sulphonated and aliphatic mercapto sulphonated catalysts) and commercial aromatic sulphonated catalysts	326
6.10	Percentage content and selectivity of 1,1,1-tris(4'-hydroxyphenyl) ethane calculated using two step sulphonated catalysts (aromatic sulphonated and aliphatic mercapto sulphonated catalysts) and commercial aromatic sulphonated catalysts	328

Acknowledgement

*It is my immense pleasure to express my gratitude towards many people who have helped me in various stages of research. First of all I like to thank my research guide **Dr. C.R. Rajan** for the support he has provided to me during my research career in National Chemical Laboratory. To me, he was a guardian as well as a research guide who has given valuable advices not only on research matters but also on divergent issues pertaining to general organized work in the laboratory. He has helped me in providing a decent accommodation during the hard time I have faced in N.C.L.*

*I am extremely indebted to my co-guide **Dr. S. Ponrathnam** for the valuable research discussions. His suggestions and criticisms had helped me to develop myself to carry out scientific research with minimum discussions and usage of available resources in the organization.*

*I express my sincerity to **Dr. S. Sivaram** (Director-N.C.L) for allowing me an opportunity to carry out my research at N.C.L. I like to thank **Dr. M.S. Qureshi** for the valuable discussions, support and suggestions provided to me in chromatographic analyses. I also like to thank **Dr. D.R. Saini** and **Dr. N.N. Chavan** for the support they have provided to me in the course of my research work.*

*I always have a high regard for my M.Phil research guide **Dr. S. Prathapan** as a person who has taught me the basics of scientific research in chemistry. I like to express my sincere thanks to all the teaching staff of polymer science and rubber technology department (CUSAT) who had taught me the basics and varied areas in Polymer Technology during my M.Tech career. I express my gratitude to **Mr. David. A. Lowe** (Former C.E.O-Yule Catto-Far East) for providing me an opportunity through campus interview to work in Revertex group technical centre. I am thankful to **Mr. M. Selvaraj** [Former M.D-Natural rubber division-Revertex (Malaysia)] for providing me moral support to go for Ph.D research, **Mr. Cheah Peck Kee** for introducing me to various organizations in Malaysian rubber industry, **Mr. Sivanyana Moorthy** and **Mr. Woon Sung Liang** [Technical managers-R&D/Tech Services-Revertex (Malaysia)] for providing me extensive training in the field of latex technology. I cannot forget the opportunity and exposure I got with **Dr. R.K. Mathan** (Director-Polymer Consultancy Services, Chennai) who has helped me to deal with hard technical problems in latex and dry rubber technology with limited man power by working as a junior technical*

consultant with him as well as his well wishes for doing Ph.D research. The moral support I got from the staff of A.V.T Rubber Processing and R&D wing to go for Ph.D research, including **Mr. Jayan Sekhar** (Former V.P-A.V.T group of companies), **Mr. Mathews** (Estate manager), **Mr. Joseph John** (General Manager-technical), **Mr. Renny Antony** (Deputy Manager-technical) as well as my friends and colleagues **Vinu Gopinath, Shaji, Vishwanath Pai** and support staffs-**Harikumar, Trijickumar, Anil, Renjith and Subash** are remembered at this time as well as the immense help they have provided to me in the development of my technical career.

I like to express my gratitude to my **father** (Mr. M. Reghunathan), **mother** (Dr. K. Santha Kumari), **wife** (Mrs. P.B. Pinky), **sisters** (Dr. Deepa Reghunathan and Dr. Deepthy Reghunathan), **brother in laws** (Dr. S. Ajaya kumar and Mr. P. Binu) **niece** (Miss Kavya Ajayan and Miss Sandra D. Binu) close cousins, friends from my native place and other dear ones for providing me moral support in taking a research career. The presence of my **daughter** Miss Lakshmi Krishna has immensely helped me by providing a enjoyable life in the final year of my research career at N.C.L.

I like to take this opportunity to express gratitude towards a group of friends and support staffs who had provided me a cordial environment in N.C.L. I am extremely thankful to **Mr. Wasif** who was always with me in lab during the course of my hectic research work. I am extremely thankful to **Dr. Smita Mule, Dr. Ganesh. C. Ingavle, Mr. Sunil Bhongale, Mr. Lijo Francis, Mr. Eldho Elias, Miss. Sonali. M. Bhosle, Mr. Mohasin Momin and Mr. Ravindra Ghorpade** for working with me in scientific research. I like to thank **Dr. Sarika Deokar** for the support she had provided in arranging this thesis. The help extended by **Mr. Gaikwad, Mr. Kashinath Patil, Mrs. Deepa Doble and Mr. Saroj** are remembered at this time. I also like to thank former colleagues **Dr. Rajkumar Patel, Dr. N.S. Pujari, Dr. Supriya Palimkar, Dr. Praveen Sher, Mr. Sunny Scaria, Mr. Timothy Ponrathnam** and present colleagues **Mr. K.B Mulani, Mrs. N. Archana, Mrs. S. Kalpana, Mr. Kishor and Mr. Punitarasu** for providing a helpful environment in the laboratory. I like to express my gratitude towards **Mr. Lalan Giri and Mr. S.N. Sathe** for extending me help in the laboratory. The moral support given by **Dr. Santhosh Paul, Mr. Shijo Cherian** and other close friends are remembered at this moment. Since it is difficult to name everyone, I like to thank all those people who have directly and indirectly helped me in the course of my research career at N.C.L.

Synthesis and Evaluation of Photochemically Induced Polymerization in Novel Acrylic Monomers

Abstract

The thesis has been divided into seven chapters comprising of introduction to photopolymerization, introduction to high internal phase emulsion, aims and objectives, photopolymerization of mono and diacrylate based monomers, photopolymerization of multiacrylate based monomers, synthesis of cation exchange resins and their catalytic evaluation for acid phase condensation reactions and summary and conclusions.

Various photopolymerizable oligomers (macromonomers) with acrylate or methacrylate end functionalities were synthesized and their photopolymerization kinetics were studied using photo DSC equipment. The acrylate end functionalized oligomers with polyurethane and polyether urethane linkages in backbone were synthesized and characterized by spectroscopic techniques. The photocurable formulations were prepared by mixing 0.25 to 4 wt% of photoinitiators with the macromonomer. Mono, di or trifunctional acrylates were added as reactive diluents to the formulation to obtain photopolymerizable compositions. The photopolymerization cure kinetic parameters such as rate of maximum photopolymerization, percentage conversion as well as other parameters such as time taken to reach peak maximum and induction time [time taken for 1% conversion] were studied from the exothermic heat flow profiles using universal analysis software. The conversion profiles based on theoretical heat flow values were noted. The post photopolymerization studies such as post photopolymerization IR, analyses of glass transition temperature of photocured sample using DSC as well as thermal degradation studies using TGA were carried out. Kinetic parameters based on variable autocatalytic kinetic model for the photopolymerized systems were calculated using TA advantage specialty library software. The effects of added radical scavenger on the photopolymerization kinetics were noted for certain compositions.

Certain soft segmented polyether urethane (meth)acrylates were synthesized by a two step process. The initial step involves the synthesis of a diisocyanate terminated prepolymer by treating poly glycols (such as polyethylene glycol, polypropylene glycol, polytetrahydrofuran as well as hydroxy terminated polybutadiene of molecular mass varying from 200 to 3000) with monomeric diisocyanates such as isophorone

diisocyanate and hexamethylene diisocyanate. The diisocyanate terminated prepolymers obtained were end capped with hydroxyl (meth)acrylates to obtain photopolymerizable oligomers. Linear oligomers were purified and formulated with requisite additives. Photocuring kinetics of the above systems were studied from the analyses of time dependent *in situ* photo DSC heat flow profiles and the kinetic parameters were estimated.

Certain bis aromatic based urethane (meth)acrylates were synthesized by a three step process. The initial step involves the synthesis of dihydroxy terminated bis aromatic precursor (involving 4,4'-bisphenol A, 4,4'-bisphenol S and 4,4'-biphenyl) which was subsequently treated with monomeric diisocyanate to obtain a diisocyanate terminated prepolymer. The final step involved the end capping of diisocyanate terminated prepolymers with hydroxyl (meth)acrylate to obtain photopolymerizable oligomers. Linear oligomers were purified and formulated with requisite additives. Photocuring kinetics of the above systems were studied from the analyses of time dependant *in situ* photo DSC heat flow profiles and kinetic parameters, including the applicability of variable autocatalytic kinetic model, were estimated. The non-steady state kinetics based on bimolecular termination model was evaluated for certain compositions.

Photopolymerization of high internal phase emulsions (HIPEs) involving acrylate monomers were carried out. Series of acrylates were used to prepare HIPEs with added photoinitiators. The monomers of choice were ethylhexyl acrylate, ethylhexyl methacrylate and ethylene dimethacrylate. The obtained emulsions were then subjected to photopolymerization studies under 400 W medium pressure mercury vapour lamp. The photopolymerized emulsions were then analyzed for residual monomer content. The analyses were done with GC from which the time dependent percentage conversions were estimated.

Linear and branched multiacrylate based polyether urethanes were synthesized by a two step process. The initial step involved the synthesis of diisocyanate terminated prepolymer. For linear multiacrylates the prepolymer was treated with pentaerythritol triacrylate to obtain hexaacrylated macromonomer. Treating the prepolymer with dihydroxy acrylate (propylene glycol glycerolate diacrylate) and trihydroxy acrylate (glycerol 1,3-diglycerolate diacrylate) resulted in the formation of branched urethane

acrylate oligomers. The oligomers were purified and formulated with requisite additives. Photocuring kinetics of the above systems were studied from the analyses of time dependant *in situ* photo DSC heat flow profiles and kinetic parameters.

Sulphonic/mercapto sulphonic acid functionalized porous polymers, that are potential catalysts for acid phase condensation reactions, were prepared by functionalization of polyHIPE beads. The monomers used for the polyHIPE syntheses were styrene, glycidyl methacrylate and 2,3-epithiopropyl methacrylate while the crosslinkers used were ethylene dimethacrylate and divinyl benzene. The obtained beads were characterized and functionalized to obtain cation exchange resins. Precursor of a monomer (4,4'-bisphenol A) used in photopolymerization studies was synthesized from excess of phenol and acetone using these functionalized beads. Similarly, acid phase catalysis for the condensation reactions involving a trisphenol [1,1,1-tris(4'-hydroxyphenyl) ethane] from excess of phenol and 4-hydroxy acetophenone were also estimated. The quantitative estimation of 4,4'-bisphenol A as well as 1,1,1-tris(4'-hydroxyphenyl) ethane were noted using a standard HPLC protocol.

Abbreviations

UV	Ultra violet
UVV	Ultra violet-visible
EPR	Electron paramagnetic resonance
DSC	Differential scanning calorimeter
DPC	Differential photo calorimetry
IR	Infra red
RTIR	Real time infrared spectroscopy
TEM	Transmission electron microscopy
SEM	Scanning electron microscopy
OM	Optical microscopy
HR-XPS	High resolution X-ray photoelectron spectroscopy
EDX	Energy dispersive spectroscopy
NMR	Nuclear magnetic resonance
VPO	Vapour pressure osmometry
RCS	Refrigerant cooling system
PCA	Photocalorimeter accessory
HPLC	High pressure/performance liquid chromatography
$d\alpha/dt$	Rate of reaction
α	Conversion
K	Specific rate constant
m	Autocatalytic exponent
n	Reaction order exponent
$R_{p \max}$	Maximum rate of polymerization
C_{\max}	Maximum conversion
T_g	Glass transition temperature
$t_{1/2}$	Half life
mW/cm^2	milliwatt per sq cm
Φ_a	Quantum yield for α -scission
E_T	Triplet energy

τ_T	Triplet lifetime
λ_{\max}	Maximum absorption wavelength
ϵ	Molar extinction coefficient
W/g	Watt/gram
ΔH_{theor}	Theoretical heat flow
IPN	Interpenetrating network
HALS	Hindered amine light stabilizer
TEMPO	2,2,6,6-Tetramethylpiperidinoxyl radical
HIPE	High internal phase emulsion
HLB	Hydrophile-lipophile balance
BET	Brunner Emmet Teller
ASTM	American system of testing and materials
O/W	Oil in water
W/O	Water in oil
O/O	Oil in oil
Span 80	Sorbitan monooleate
Arquad 2HT-75	Di(hydrogenated tallow) dimethyl ammonium chloride
Brij 72	Polyethylene glycol octadecyl ether
4,4'-BPA	4,4'-Bisphenol A
1,1,1-THPE	1,1,1-tris(4'-hydroxyphenyl) ethane
AIBN	2, 2'-azobisisobutyronitrile
DBTDL	Dibutyl tin dilaurate
DABCO	Diazabicyclo[2.2.2]octane
HQME	Hydroquinone monomethyl ether
PEG 200	Polyethylene glycol 200
PEG 400	Polyethylene glycol 400
PEG 600	Polyethylene glycol 600
PPG 725	Polypropylene glycol 725
PPG 3000	Polypropylene glycol 3000
PTHF 250	Polytetrahydro furan 250
PTHF 650	Polytetrahydro furan 650

HTPB 2750	Hydroxy terminated polybutadiene 2750
IPDI	Isophorone diisocyanate
HMDI	Hexamethylene diisocyanate
EHA	2-Ethylhexyl acrylate
EHMA	2-Ethylhexyl methacrylate
EGDMA	Ethylene dimethacrylate
HEA	2-Hydroxyethyl acrylate
HEMA	2-Hydroxyethyl methacrylate
HPA	Hydroxy propyl acrylate
NPGPDA	Neopentyl glycol propoxylate diacrylate
TMPTA	Trimethylol propane triacrylate
PGGDA	Propylene glycol glycerolate diacrylate
GDGDA	Glycerol 1,3-diglycerolate diacrylate
PETA	Pentaerythritol triacrylate
ETMA	2,3-Epithiopropyl methacrylate
GMA	Glycidyl methacrylate
DVB	Divinyl benzene
IRGACURE 651	2,2-dimethoxy-2-phenyl acetophenone
DAROCUR TPO	Diphenyl-(2,4,6-trimethylbenzoyl) phosphine oxide
IRGACURE 184	1-Hydroxy cyclohexyl phenyl ketone
IRGACURE 2959	2-Hydroxy-4'-(2-hydroxyethoxy)-2-methyl propiophenone
DAROCUR 1173	2-Hydroxy-2-methyl propiophenone
DAROCUR MBF	Methyl benzoyl formate
IRGACURE 907	2-Methyl-4'-(methylthio)-2-morpholino propiophenone
IRGACURE 819	Phenyl bis(2,4,6-trimethyl benzoyl) phosphine oxide
GENOCURE CQ	Camphoroquinone
GENOCURE BP	Benzophenone
HEPP	2,2-bis[4-(β -hydroxyethoxy)-phenyl] propane
HPPP	2,2-bis[4-(β -hydroxypropoxy)-phenyl] propane
HPPS	bis[4-(β -hydroxypropoxy)-phenyl] sulphone
HEBP	bis[4-(β -hydroxyethoxy)] biphenyl

Introduction to photopolymerization

1.1 Introduction

UV-radiation curing¹ is a well-accepted technology, which has found a large variety of industrial applications because of its distinct advantages. Light induced polymerization of multifunctional monomers is indeed a powerful method to achieve, selectively in the illuminated areas, a quasi-instantaneous transformation of a liquid resin into a solid polymer. UV radiation can cause changes in the mechanical and optical properties of polymer materials by breaking chemical bonds, thereby reducing their service life in outdoor applications. This problem can be overcome by the use of UV stabilizers.² However, UV radiation has many beneficial effects and can be used to initiate desired chemical reactions, like polymerization. By exposing a monomer for a brief time to intense UV radiation, in the presence of a photoinitiator, large amounts of free radicals are generated at once. Under such high initiation rate conditions, one would expect the polymerization to proceed with short kinetic chains, because of enhanced bimolecular termination,³ thus leading to low molecular weight waxy polymers. Actually, this prediction proved to be wrong for low molecular weight multifunctional monomers, such as di or triacrylates which were found to polymerize extensively within a fraction of a second upon UV or laser irradiation to form strongly crosslinked polymer networks.⁴ The steady development of the UV-curing technology in the past 20 years is a direct consequence of this unexpected behaviour, which has opened the way to an ever-increasing number of end-uses.

Ultraviolet (UV) radiation is electromagnetic radiation of a wavelength shorter than that of the visible region and longer than that of X-rays. As air is opaque to UV radiation of less than 200 nm wavelength, it is often subdivided into near UV (380-200 nm wavelength) and extreme or vacuum UV (200-10 nm). However, in connection with human health and the environment, it is subdivided into UV-A (380-315 nm), UV-B (315-280 nm) and UV-C (280-10 nm). Besides its great speed and spatial resolution, light-induced polymerization presents a number of other advantages, such as solvent-free formulation, low energy consumption, ambient temperature operations and tailor-made properties of the UV-cured polymers.⁵ During the last two decades, a considerable amount of work has been devoted to UV-radiation curing, most of the research efforts being focused both on the kinetics and mechanism of such ultra fast crosslinking

polymerization reactions,¹ and on the design of new photoinitiators⁶⁻²¹ including oligomeric²² and polymeric²³ photoinitiators, monomers,^{24,25} macromonomers, and telechelic oligomers²⁶⁻²⁹ best suited to producing high-performance polymer networks. The macromonomers include urethane,³⁰⁻³³ silicone,^{34,35} epoxy,³⁶ and aromatic ester³⁷ acrylates. In addition, macromonomers with ethylenically and acetylenically functionalized³⁸ as well as epoxy and acrylate³⁹ on the same molecule has been reported. The theory and methodologies involved in the photopolymerization process has been extensively covered in several textbooks and comprehensive review articles.^{39,40}

One of the basic laws in photochemistry states that a photochemical reaction can only occur if light has been absorbed by the medium. As most monomers are essentially transparent to radiation emitted by conventional UV sources such as mercury lamps, they do not produce initiating species with sufficiently high yields. Therefore, it is necessary to introduce a photoinitiator in the UV-curable formulation, which will effectively absorb the incident light and generate reactive free radicals or ions by cleavage of the electronically excited states.⁹

Acrylates are by far the most widely used resins in UV-curing applications because of their high reactivity, together with the large choice of acrylate functionalized oligomers (polyesters, polyethers, polyurethanes and polysiloxanes).⁵ Low-modulus elastomers are generally obtained with aliphatic compounds⁴¹ whereas hard and glassy materials are formed if the crosslinked segments contain aromatic structures.^{42,43} A typical UV-curable formulation is made of three basic components: a photoinitiator, a telechelic oligomer, and optionally monomer acting as a reactive diluent.¹ An increase of the monomer functionality was shown to speed up the reaction, but at the expense of the final conversion, because of premature mobility restrictions caused by gelation⁴⁴ and vitrification.⁴⁵ The increased crosslink density results in hard and brittle UV-cured polymer with high solvent resistance. Generally, the limiting conversion observed in photopolymerization is found to increase with an increase in temperature.⁴⁶

Monomers which are inactive towards free radicals, such as epoxides, or vinyl ethers, undergo rapid polymerization upon UV irradiation in the presence of aryl sulphonium or iodonium salts ($\phi_3 \text{S}^+ \text{PF}_6^-$, $\phi_2 \text{I}^+ \text{SbF}_6^-$) due to the formation of an intermediate photocation.⁴⁷⁻⁵⁰ These compounds were shown to generate protonic acids

up on their photolysis in the presence of a hydrogen donor molecule.⁵¹ The ring-opening polymerization of epoxides proceeds through the oxonium ion, with formation of a polyether chain. Vinyl ethers polymerize much faster than epoxides because of the electron rich C=C bond and the stabilization by resonance of the carbocation.¹ Three dimensional polymer networks with tailor-made properties have been obtained by UV irradiation of vinyl ether telechelic oligomers containing ether, ester, urethane or siloxane structures.^{52,53} One of the distinct advantages of cationic polymerization is its lack of sensitivity toward atmospheric oxygen, thus providing a rapid surface cure of protective coatings.

1.2 Reactions and properties of acrylate resins

1.2.1 General reactions of acrylate resins

The major types of functionalities, which are introduced in acrylic esters, include hydroxyl, carboxyl, amide and epoxy groups. There are two primary factors influencing monomer reactivity. The ease at which a monomer will form a monomer radical and the subsequent reactivity of the monomer radical so formed. Both these factors depend on the monomer structure. It has been observed that in the case of toluene as solvent, the chain transfer constant is found to decrease with increase in substitution in the carbon atom, showing reduced reactivity.

Acrylic polymers with hydroxyl side chain are found to react readily with butylated hydroxyl groups of amino formaldehyde or phenol formaldehyde resins under acidic conditions. The hydroxyl groups of polymeric acrylate can also react with diisocyanates to form diurethane linkages.⁵⁴ With polyanhydrides, they can form acrylic esters with free carboxylic acid groups in the side chain.⁵⁵ They also form ether linkage when treated with epoxy polymers under high temperature in presence of acidic catalyst with hydroxyl groups in side chain.⁵⁶ Hydroxyl containing acrylic polymers can also react with free carboxylic acid groups in the side chain of another polymer to form an ester.

Similarly, an acrylic polymer with a carboxylic acid group in side chain can react with a polymer containing epoxy group in side chain to form an ester with hydroxyl group in side chain.⁵⁷ This reaction is base catalyzed and in most cases occurs around 150 °C. An acrylic polymer with carboxylic acid side chain can also react with diisocyanates

to form diamide linkages.⁵⁸ It can also react with a hydroxyl alkyl ends or alkoxy methyl ester groups of an amino polymer chain to form an ester linkage.⁵⁹ The amino polymer chain can be either acrylamide, melamine or urea formaldehyde resins.

Self-condensation of side chain epoxy rings in acrylic polymer can result in the formation of ether linkage with methylol and hydroxyl groups in the side chain. With secondary amine containing polymers they form substituted amine with hydroxyl group in the side chain⁶⁰ and with alkoxy substituted amino formaldehyde resins they form ether linkage with alkoxy group in side chain, with phenol formaldehyde resins they react with aromatic hydroxyl groups in presence of acidic catalyst to form an ether linkage with hydroxyl group in side chain.⁶¹ Grafting reactions of epoxy acrylates on cellulose have been reported.⁶²

Acrylic polymers with amide group in side chain can react with formaldehyde to form methylolated acrylic polymers.⁶³ Unstabilized methylol group can undergo self-condensation. Further, the methylol group can be converted into alkoxy methylol group. Both these groups can readily react with epoxy, carboxy, hydroxyl and amino groups.⁶⁴ These reactions are the basis for a major proportion of the thermosetting acrylic surface coatings.

1.2.2 Properties of acrylate resins

The monomer units can combine together to provide head to head as well as head to tail linkages. The type of linkage depends on the relative stability of the monomer radical formed. For vinyl compounds with a structure $\text{CH}_2 = \text{CYX}$ in general, the $-\text{CYX}\cdot$ radical is more stable than the $-\text{CH}_2\cdot$ radical, since the electron excess can be stabilized over the substituent groups X and Y. In general, monomers which form free radicals easily tend to polymerize more slowly than monomers which do not form free radicals readily.⁴⁵ Electrostatic forces and steric hindrance play important role in polymerization processes. In the case of a free radical polymerization, the effects of electrostatic forces are not clearly defined. Due to their neutral nature, the attack can happen on either side of the C=C bond. In the case of ionic polymerization the electrostatic interaction has a major influence and occurs as a result of attraction between a polymeric ion and the permanent dipole on the monomer.

In free radical polymerization, the substitution will increase the stability of the formed radicals. Stability also increases with the polarization of the substituent in direct relationship to the ability to delocalize electrons. The stability of the free radicals is possibly the greatest influence on the orientation of the repeating unit in a polymer chain. Tacticity can play a key role in controlling the glass transition temperature, T_g .

1.2.2.1 Influence of molecular weight

In general, the properties of surface coatings are dependent on the molecular weight of the polymer and changes with an increase in the molecular weight and the complexity of molecular structures. Gloss retention, chemical resistance and film hardness increases with an increase in molecular weight while solubility, flexibility and adhesion increases with a decrease in molecular weight. Desired film properties may be obtained by producing a polymer of sufficiently high molecular weight. Such polymers have to be applied as solutions and form a coherent film by the evaporation of the solvent. These polymers are thermoplastic and the surface coating system is referred to as a lacquer.⁶⁵ The lacquers are air drying or force drying systems. Alternatively, a low molecular weight polymer can be produced with reactive sites capable of forming film by reaction with another polymer, chemical species or a catalyst. These high molecular weight complex films are termed thermosetting and the surface coating system is referred to as enamel.⁶⁶ Thermosetting acrylics require more specific conditions for film formation, although the final film tends to be more chemically resistant, particularly with respect to solvent, than the thermoplastic types.

1.2.2.2 Growth rate of polymer chains

A simple way to evaluate the actual rate at which the polymer chains are growing is by recording the polymerization profile after a very short and intense UV exposure, e.g. from a pulsed laser.⁶⁷ The rate of polymerization that proceeds in the dark depends primarily on the propagation rate constant, the number of initiating radicals generated by the laser flash (R_i) and the monomer concentration. By taking the ratio $R_p / [R_i]$ obtained from $R_p = k_p [R_i][M]$, evaluation of the initial growth rate of the polymer chains in a UV-curable urethane acrylate resin is around $5 \times 10^4 \text{ mol radical}^{-1} \text{ s}^{-1}$.¹ From this value, the average time for the addition of one monomer unit to the growing polymer chain was calculated to be 20 μs . As polymerization proceeds to above 20% conversion, R_p starts to

drop due to growing mobility restrictions and consumption of the monomer, thus leading to a concomitant increase of the addition time value.

It should be remembered that, in most UV-curing applications, the sample is exposed briefly to intense radiation by passing rapidly under a powerful UV lamp for a short time. This means that most of the polymerization reaction is actually proceeding in the dark, just after the UV exposure as initiation has already happened.

1.3 Theory of photoinitiated polymerization of acrylates

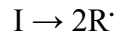
There are three distinct steps in this addition polymerization stage

- Initiation - Involves attack on the C=C bond by any initiating species
- Propagation - Involves growth of the polymer chain by successive addition of monomer units
- Termination - Involves deactivation of the polymer chain, terminating further addition of monomer units

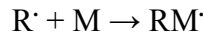
1.3.1 Initiation

It proceeds in two steps.

1. Decomposition of initiator into free radicals.



2. By the attack of free radical on the monomer molecule forming a monomer radical.



The rate of initiation is defined in terms of the rate of formation of polymer chains and is expressed as:

$$R_i = 2fk_d [I] \tag{1}$$

where, R_i is the rate of initiation, f is the frequency factor for free radicals reacting with monomer units, K_d is the decomposition rate of the initiator and $[I]$ is the molar concentration of the initiator. The number of chain ends present in any given time is determined by:

$$N_i = 2fk_d [I]_t \tag{2}$$

where, N_i is the number of initiated chains at time t .

The number of chain ends per monomer unit is given by:

$$M_i = N_i M_m / M_p \tag{3}$$

where, M_i is the number of chain ends per monomer unit, M_m is the molecular weight of the monomer and M_p is the mass of polymer formed during time t .

Resonance stabilized radicals will not initiate polymerization.⁹ Photoinitiator plays a key role by governing both the rate of initiation and the depth of cure through its absorbance. The rate of initiation (R_i) is directly related to the incident light intensity (I_0), absorbed light intensity (I_a), the sample thickness (l), the absorptivity (ϵ), concentration of the photoinitiator ($[PI]$) and the quantum yield of initiation (ϕ_i , the number of initiating species produced per photon absorbed).⁹

$$R_i = \phi_i I_0 [1 - e^{-\epsilon l [PI]}] \quad (4)$$

Then the rate constant for photochemical initiation is given by:

$$k = k_p / (k_t^b)^{0.5} \phi (I_a)^{0.5} \quad (5)$$

After initiation, the chain reaction proceeds very much as in the case of conventional thermal polymerization. The advantage of photopolymerization over thermal polymerization is that a much larger rate of initiation can be achieved by intense illumination at lower temperatures, which also reduces the curing time. With multifunctional monomers and telechelic oligomers, the polymerization will develop into three-dimensional structures to yield strongly crosslinked networks.

1.3.2 Propagation

The propagation rate is given by:

$$R_p = k_p [M^*] [M] \quad (6)$$

Thus an overall equation for acrylic polymerization can be written as:⁶⁸

$$R_p = k_p [M] (R_i / 2k_t)^{0.5} = k_p [M] (fk_d [I] / k_t)^{0.5} \quad (7)$$

where, $[I]$ is the concentration of initiator, $[M]$ is the concentration of monomer, f and k_d are the frequency and decomposition constants for the initiator and k_t is the rate coefficient of chain termination. A plot of R_p against $[M]$ for various monomers produces a straight line graph.

Once the monomer radical has been formed, propagation proceeds rapidly as the number of monomer units increases successively to produce a growing polymer chain. After each successive addition, the free radical is retained on the vinyl carbon atom of the end chain unit. The ease with which a monomer forms a free radical and the reactivity of the radical once formed determine the rate at which propagation proceeds. Each

propagation step is found to proceed at a speed determined by the propagation rate constant k_p , which is constant for a given monomer at a given temperature. The propagation rate constant is independent of the degree of polymerization of the growing chain.

$$R_p = k_p [M] [M\cdot] = k_p [M] (R_i / 2k_t)^{0.5} \quad (8)$$

Since the rate of initiation in photopolymerization is given by $R_i = \Phi I_a$, the equation becomes:

$$R_p = k_p / k_t^{0.5} [M] (\Phi I_a / 2)^{0.5} \quad (9)$$

where, Φ is the quantum yield for initiation, I_0 and I_a are the intensity of incident and absorbed radiation, $[M]$ is the concentration of the reactive functional group involved in photopolymerization and k_p and k_t are the rate constant of propagation and termination respectively. On applying Beer-Lamberts law, R_p becomes:¹

$$R_p = k_p / k_t^{0.5} [M] (\Phi I_0 (1 - e^{-\epsilon[A]D})^{0.5} \quad (10)$$

where, D is the thickness of the photopolymerized layer, ϵ is the molar extinction coefficient at the applied wavelength and $[A]$ is the concentration of the photoinitiator.

1.3.3 Termination

Termination involves the removal of free radical from the polymer chain. This involves either a combination reaction or disproportionation reaction or a transfer reaction. The exact mechanism will depend on the chemical structure of the monomer, the polymer chain and the nature of any other species present. In the combination as well as the disproportionation reaction the radical is quenched in the process, while in the case of transfer reaction, a chain stops growing and will result in the creation of a new propagation chain with a radical end. Transfer reactions are important in controlling the molecular weight of the polymer chain. The transfer reaction can occur in many ways. They include chain transfer to solvent, to monomer as well as to modifier. Generally solvents are weak chain transfer agents. Carbon tetrachloride has a relatively higher chain transfer constants among common solvents. The chain transfer constant is given by the relation⁶⁹

$$k_z = k_s / k_p \quad (11)$$

where, k_z is the chain transfer constant, k_s is the rate coefficient for transfer to solvent, and k_p is the rate coefficient for propagation of the polymer radicals. The value of k_z varies with temperature and the nature of the solvent.

In the case of photopolymerization, termination is diffusion controlled and the termination rate coefficient is dependent upon those parameters that can cause an effect on the diffusion of the polymeric radicals being terminated. It has been found that the termination rate coefficient varies with conversion. Hence, the rate determining process in termination is diffusion.⁴ It can be either both translational and segmental diffusion. Translational diffusion is chain dependent and decrease with increase in viscosity of the system under polymerization. The chain length dependence on the termination rate coefficient leads to their dependence on conversion. Segmental diffusion is chain independent and is found to increase with decreasing size of the polymer coils.³

The rate coefficient for the translational diffusion is given by k_{TD} and that of segmental diffusion is given by k_{SD} , respectively. If $k_{t,D}$ represents the termination rate coefficient for the diffusion controlled termination, then the overall termination is an effect of both translational and segmental diffusions. The overall termination rate coefficient for the diffusion-controlled termination is given below:

$$1 / k_{t,D} = 1 / k_{SD} + 1 / k_{TD} \quad (12)$$

An alternative mechanism for bimolecular termination is by reaction diffusion. It is important at intermediate conversions and is highly pronounced from 15% conversion after the onset of gel effect. At this stage all the free radicals are trapped to such an extent that their centre of mass is immobile on the time frame of propagation and the only possible diffusive motion the radical chain ends represents is the propagation reaction. Since the rate at which the monomer is consumed (R_p) is known, the value of rate coefficient for termination by reaction diffusion can be derived. The termination by reaction diffusion is given by:

$$k_{t, RD} = Rk_p [M] \quad (13)$$

where, R is the reaction diffusion parameter.³ Then the overall termination rate coefficient k_t is given by:

$$k_t = k_{t,D} + k_{t, RD} \quad (14)$$

The increase of segmental diffusion and the decrease in translational diffusion counterbalance each other so that k_t remains constant in most cases. Sometimes k_t is found to be decrease marginally due to a slight decrease in rate of translational diffusion with respect to the increase in segmental diffusion. Translational diffusion is found to decrease with increase in gel effect. Further, during the auto acceleration the termination becomes slower so that the termination rate coefficient decreases in several orders of magnitude. With further increase in conversion the gel effect appears to stop. Hence the termination becomes chain independent and it is the point at which reaction diffusion starts. This change in termination occurs near the maximum polymerization rate. The reaction diffusion process will keep the k_t to be a constant so that during the process a plateau is observed on the plot of k_t against conversion. The plateau for multifunctional systems in most cases is found from 30-50% to about 70-80%. As the reaction diffusion on k_t is found to depend up on the propagation rate coefficient and the monomer concentration, a rapid drop is observed toward the end of the reaction. This is known as autodeceleration.³ k_p is found to increase with increase in flexibility of the monomer. The reaction diffusion is found to be rate determining, if the value of k_p is higher.³ It is generally observed that k_p is generally smaller than k_t by a factor of 10^3 to 10^5 .

The analysis of polymer radicals trapped in a photopolymerized system can be found by electron paramagnetic resonance (EPR) studies.^{70,71} The polymer radicals can be classified into three types. Free radicals that are independent in the system, radicals which are attached to loosely crosslinked regions so that they have some mobility with restrictions, trapped radicals surrounded by dead polymer chains which cannot further react.

1.3.3.1 Chain transfer

The radical formed by abstraction is available to initiate propagation of another polymer chain. The effectiveness of the chain transfer agent is measured in terms of its ability to terminate a growing polymer chain and then to initiate the propagation of another chain. This is quantified as the chain transfer rate constant C_s , which is temperature dependent and is different for different monomers.

The number of chain ends arising from transfer reaction can be obtained from the equation:

$$N_s = 2C_s [S] / [M] \quad (15)$$

where, N_s is the number of chain ends containing modifier per monomer unit in the polymer, C_s is the rate coefficient of transfer for the modifier, $[S]$ is the molecular concentration of modifier and $[M]$ is the molecular concentration of monomer respectively.

This has been related empirically by Mayo⁷² in the equation:

$$1 / P = C_s [S] / [M] + 1 / P_0 \quad (16)$$

where, P is the degree of polymerization in presence of a modifier, P_0 is the degree of polymerization without the modifier.

1.3.3.1.1 *Transfer to monomer*

It can occur in two ways. Both involve an abstraction process through which a hydrogen atom is transferred to the propagating chain. The free radical is transferred to the monomer to form a monomer radical, which in turn continues the reaction. The monomer free radical formed is free to initiate the propagation of another polymer chain. The newly propagated chain will have an unsaturated end group. The end group is available for re-initiation.

1.3.3.1.2 *Transfer to a modifier*

Modifiers are species that contain a labile atom (most usually hydrogen or halogen) which can be abstracted by the propagating chain. Propagation of the chain is terminated and the radical is transferred to the modifier. The modifier radical can then act in one or two ways. It can act to initiate the propagation of a new polymer chain. The net result in this case is that the modifier has acted as an agent in the transfer of the radical from one propagating chain to another. Examples include carbon tetrabromide, ethane thiol and tertiary butyl mercaptan. It can be used for stabilizing free radicals, which will not take part in further initiation reactions. In effect, the free radical is removed from the system, and the modifier has acted as a polymerization inhibitor.

1.3.4 *Crosslinking in photoinitiated polymerization*

The bulk polymerization of multifunctional monomers is a complex process which exhibits a number of anomalous behaviour with respect to the reaction kinetics and mechanism.⁵ The process involves an initial auto-acceleration followed by auto-

deceleration due to gelation,^{73,74} radical trapping,⁷⁵⁻⁷⁷ formation of structural heterogeneities such as microgels,⁷⁸⁻⁷⁹ delayed volume shrinkage with respect to equilibrium^{80,81} and termination process controlled by reaction diffusion.⁴ While crosslinking polymerization proceeds, the physical state of the medium changes from a viscous liquid to a viscoelastic rubber and in some cases may develop a glassy appearance. This causes drastic variations of the reactive species mobility and will ultimately lead to a premature ending of the chain reaction.⁸² A most remarkable feature of ultra fast photopolymerization processes is that higher final degrees of conversion are usually attained than in thermal curing.⁴³ This is because volume shrinkage occurs over a much longer timescale than the chemical reaction, thus generating a temporary excess of free volume.⁸³ In addition, the heat instantly evolved by the exothermic reaction and the increase of the sample temperature also contributes to a more complete polymerization.

Crosslinking in polymerization can occur through 3 paths. It can occur by intermolecular, intramolecular (cyclization) and by the reaction of radical on a pendant double bond. Intermolecular crosslinking leads to network formation.⁸⁴ Extensive intramolecular reactions can lead to the formation of highly compact structures known as microgels.⁷⁹ Gel point is that stage at which microgels join together to form a huge molecule.³ It can occur at conversions as low as 1-2%. Cyclization can cause a delay in gel point conversion. Cyclization can be prevented by imparting more stiffness to system so that the chance of intermolecular reaction is minimized. Many of the pendant double bonds will get trapped in the microgel regime and the reactivity of these species will decrease due to steric hindrance. Further, reactive microgels can form macrogels by chemical reaction. Microgel formation causes inhomogeneity in the network and hence will drastically affect the mechanical properties of the cured system.⁸⁵ In photopolymerization the network is inhomogeneous from the initial stages itself. This has been proven for dimethacrylates by random walk percolation model.⁸⁶ The degree of termination will depend on the degree of double bond conversion and on reaction conditions such as temperature, monomer structure etc.

Three dimensional polymer networks can be readily obtained by photoinitiated polymerization of functional groups located on the polymer chains. A typical example is the photocrosslinking of epoxidized polybutadiene⁸⁷ or polyisoprene,⁸⁸ which was

performed at ambient temperature by UV exposure of the functionalized polymer in the presence of a sulphonium salt. The ring opening cationic polymerization of the oxirane functions leads to the formation of ether crosslinks between the rubber chains, and to complete insolubilization within a few seconds. The UV-cured polymer proved to be both hard and flexible, for it combines the elastomeric character of rubbers and the toughness of epoxy-based polymers. When used as coatings, these materials show excellent adhesion properties to various substrates, in particular aluminium, steel and glass. Similar results have been obtained by UV irradiation of rubbers bearing pendent acrylate double bonds.⁸⁹ In both types of functionalized polymers, intramolecular processes involving neighbouring reactive groups were shown to become increasingly important as the number of functional groups on the polymer chains increased. This accounts for the unexpectedly fast and extensive polymerization observed in these solid media exposed to UV light.

The glass transition temperature (T_g) of a polymer is a second order transition, involving a change in a solid polymer, from a flexible state to a rigid state. In other words, the glass transition point is the temperature below which all molecular movement including mobility about the bonds in the back bone of the polymer become frozen. Although T_g increases with molecular weight, it is largely a constant for all practical purposes over a range of molecular weights normally encountered with acrylic surface coatings. Crosslink density affects the T_g by several degrees per mole percentage of crosslinks. The chemical structure has the greatest effect on T_g as large changes are observed as the chemical structure is modified. In general, longer the side chain of the polymer, lower will be the T_g , where as the presence of methyl groups on the carbon atom (as with methacrylates) increases the T_g by increasing the propensity for steric hindrance.⁹⁰ Branching of the side chain also raise the T_g . Almost any intrinsic property of a polymer, which is temperature dependent, can be used to measure the T_g of the polymer. Properties, which may be used, include specific volume, specific heat and refractive index.

Fox-Johnston equation⁹¹ can be used to get a reasonable agreement between the theoretical and practical T_g of copolymers. The equation assumes that M_1M_1 , M_1M_2 or

M_2M_1 and M_2M_2 diads have their own glass transition temperature, with the overall T_g of a copolymer described by the following expression:

$$1 / T_g = W_1 P_{11} / T_{g11} + W_1 P_{22} / T_{g22} + W_1 P_{12} + W_2 P_{21} / T_{g12} \quad (17)$$

where, W_1 and W_2 are the weight fractions of the monomeric units in the main chain. P_{11} , P_{22} , P_{12} and P_{21} are the probabilities of having various linkages, which can be calculated considering the Mayo Lewis terminal model using the monomer feed composition and the monomer reactivity ratios.⁹² T_{g11} and T_{g22} are the glass transitions for the respective homopolymers and T_{g12} is the supposed glass transition for the alternating sequence M_1M_2 or M_2M_1 .

Generally, the polymers with T_g below 20-25 °C appear soft and flexible at ambient temperatures while that with T_g above 25 °C are rigid, hard and brittle at ambient temperatures. In photopolymerization, when the T_g of the sample reaches the isothermal cure temperature, the end of reaction is determined by vitrification.^{93,94} For a corresponding acrylate and methacrylate, the acrylate will show a higher elongation while the methacrylate will show a higher tensile strength and T_g .

1.3.5 Photoinitiated polymerization in presence of reactive diluents

The cure rate of solid functionalized polymers can be substantially enhanced by the addition of a monomer that will act as a reactive plasticizer.⁹⁵ Solution polymerization of acrylates can be done in the presence low molecular weight acrylates as reactive diluents. The difference between wide and narrow molecular weight distribution is generally evident in solution rheology and film performance characteristics. In general, polydispersed systems are more flexible and have lower solution viscosities. This is because the low molecular weight fractions generally exert a greater overall influence on the properties of a polydispersed polymer than the high molecular weight fractions.

Copolymerization will occur when the monomer and the polymer contain different functional groups. The addition of a diacrylate (20 wt%) to acrylated polyisoprene was found to cause a faster and more complete polymerization. Within 0.2 seconds, the low-modulus elastomer was transformed into a high-modulus and insoluble polymer.¹ The system can also act as mutual reactive diluents under certain cases. Interpenetrating as well as semi-interpenetrating polymer networks (IPN's and semi IPN's) can be produced by photopolymerization.⁹⁶ By mixing monomers that polymerize

by different mechanisms, e.g. vinyl ethers and acrylates⁵³ or epoxides and acrylates,^{47,48,97} two interpenetrating polymer networks can be produced within a few seconds by UV irradiation in the presence of both radical and cationic photoinitiators.⁵³ It has been reported that oxazolidone acrylate and other acrylates can form semi IPN's.⁹⁸ Different types of IPN have been generated by this UV technology^{99,100} such as acrylated polyisoprene plasticized by a vinyl ether or a cycloepoxide monomer and epoxidized polyisoprene associated with a di or triacrylate monomer. These UV cured polymers combine the properties of the elastomeric rubber network with those of the hard and glassy acrylate or epoxy polymer network. They have high impact, scratch and abrasion resistance, which makes these polymeric materials suitable for coating applications. The main advantage of such hybrid systems is to control precisely the final properties of the cured polymer by a proper selection of the two components, and by adjusting their proportions.

1.3.6 Factors influencing free radical photopolymerization

1.3.6.1 Reaction temperature

With increase in temperature at a low solution viscosity, molecular weight of the polymer will decrease, as the number of reactive species and its mobility are higher at higher temperatures.

1.3.6.2 Monomer concentration

Lower the concentration of the monomers, lower will be the molecular weight of the polymer formed, as the chance of collision between the active centers and free monomers get reduced during the propagation reaction facilitating chain terminations by any of the chain transfer processes.

1.3.6.3 Solvents

Solvents, in addition to reduction in viscosity as well as easy heat dissipation, can also influence the reactivity of monomer or initiator by chain transfer. Peroxides can easily undergo chain transfer with certain solvents reducing the number of effective free radicals, which can initiate the polymerization process. In the absence of chain transfer with solvent, the ratio of initiator to modifier plays an important role along with the temperature and the viscosity of the system in controlling the extent of polymerization.

1.3.6.4 Concentration of initiator

Commercial photopolymerizations usually employ between 0.2-4 wt% of initiator. When the concentration of initiator is reduced at low intensity, the molecular weight of the polymer is increased, but the conversion of monomer to polymer is reduced. Higher concentration of initiator form a greater number of polymer chains. These chains are shorter and hence molecular weight and viscosity are lower.

1.3.6.5 Chain transfer agents

The chain transfer agent terminates a propagating chain, while making the free radical available to initiate the propagation of another chain. The higher the concentration of chain transfer agent, lower is the molecular weight and hence lower will be the solution viscosity.

1.3.6.6 Trommsdorff effect

As polymerization proceeds, the system becomes progressively more viscous and the movement of all molecules is reduced with the larger molecules being most affected. Under these conditions, propagating radicals can no longer freely contact each other and the rate of termination is greatly reduced. The number of radicals increases and the rate of reaction increases correspondingly. At the same time, the half-life of the propagating radical is increased as a result of which the molecular weight of the polymer increases rapidly. Among (meth)acrylates, is most marked in systems containing methyl methacrylate.

1.3.6.7 Initiator half life

Polymerization can only proceed efficiently and economically if sufficient free radicals are present throughout the polymerization. However, the presence of too many free radicals can have a deleterious effect on the polymer, resulting in very low molecular weight or excessive chain grafting etc. Thus, it is desirable to know how the number of free radicals relates to the initiator concentration, initiator type and reaction conditions, including reaction temperature. This relationship is expressed as the initiator half-life and is defined as the time taken for half of a given mass of initiator to decompose. Initiators with high activation energies show large increase in decomposition rate for a small temperature rise and hence the half-life is shorter. In terms of reaction kinetics, the half-

life ($t_{1/2}$) is a first order reaction. Free radical formation does not follow the ideal first order kinetics, due to the influence of factors other than temperature on the decomposition rate. In practice, the rate of decomposition has been found to lie between that predicted for first order and second order reactions.¹⁰¹ Half-life of any given initiator does not only depend upon the reaction temperature, but also on the reaction environment and the concentration of the initiator.

1.3.6.8 Influence of the light intensity

One of the unique advantages of photoinduced reactions is the precise control of the initiation step with respect to both onset and magnitude, by acting on the light intensity. If desired, the initiation rate can even be varied in the course of the reaction through an intensity modulator. Numerous studies¹⁰²⁻¹⁰⁵ on the effect of the incident light intensity (I_0) on the polymerization kinetics of UV-curable resins have shown that an increase of I_0 leads not only to faster polymerization but also to a more extensive cure, so that the final product contains a lower amount of unreacted functional groups.¹⁰⁶ In the curing of polyurethane acrylate by real time IR, the final degree of conversion was found to rise from 80 to 95% when I_0 was increased from 10 to 80 mW/cm² reaching nearly 100% at 600 mW/cm². This trend was explained by two factors; (a) an increase in the sample temperature at high I_0 which provides more molecular mobility leading to higher ultimate conversion, and (b) a longer time lag between conversion and shrinkage, which generates a greater excess of free volume and thus increases the molecular mobility.¹⁰⁵ However, high extent of cure using photo DSC requires a much lower intensity due to higher energy of the source.

1.3.6.9 Influence of added radical scavenger and UV absorber

Addition of light stabilizers and UV absorbers^{107,108} can result in the reduction of effective number of free radicals involved in photo initiation process. Singlet oxygen induced inhibition¹⁰⁹ including on photo DSC with acrylates¹¹⁰ as well as on photolysis¹¹¹ of HALS (hindered amine light stabilizers) are reported. Many monomers¹¹²⁻¹¹⁷ and copolymers¹¹⁸ containing HALS are known. Other additives which can be added include inert solvent or reactive diluent, bifunctional¹¹⁹ and polymeric stabilizers¹²⁰ involving HALS, polymerizable antioxidants¹²¹ as well as aromatic monomeric UV absorbers.¹²² Addition of 2,2,6,6-tetramethylpiperidinoxyl radical (TEMPO) on photo DSC study with

acrylates was found to increase the heat flow in certain cases probably due to heat released on scavenging process involving radical radical combinations.¹²³

1.3.7 Photoinitiated polymerization of High Internal Phase Emulsions

High internal phase emulsions (HIPEs) are also known as double emulsions in which discontinuous phase is at least 74 volume percent of the emulsion. Photopolymerization of high internal phase emulsion foams can be done using actinic radiation between 200 and 400 nm. Recently, macroporous polyHIPEs with atom transfer radical polymerization initiators have been successfully photopolymerized.¹²⁴ The advantage of photopolymerization of HIPE over thermal is that the time taken for the photopolymerization is considerably low, varying from a few seconds to a few minutes, while thermal polymerization take several hours. As the stability of emulsions having high concentration of water deteriorated with time, the faster photopolymerization is found to be more efficient in getting high conversions. Emulsions which are stable for less than one minute can thus be successfully photopolymerized.¹²⁵ Concentration of surfactant can determine whether the emulsion formed has open or closed cells. Diverse physical properties can be achieved by altering types of monomer and comonomers, their ratios, cell size, percentage of open cells, density of foam and mixing methods.

Propagation of cationic photopolymerization in HIPE is found to be more effective even in the absence of light during the final stages of polymerization. It has been observed that the reactive species in the free radical photopolymerization of HIPE is found to be much short lived when the light source is removed.¹²⁵ The water to oil ratio can be varied from 3:1 to 11:1. Foams prepared by HIPE can take greater than 15 times their weight, while non-HIPE foams absorb up to 3 times the weight of the fluid. HIPE foams also have high storage capacity under load. Polymeric or non-polymeric emulsifiers which are cationic, anionic as well as non ionic can be used.¹²⁶ A surfactant with an optimum hydrophilic lipophilic balance (HLB) of 4 to 6 is usually preferred. Commonly used photoinitiators include a 1:1 blend of 2,4,6[trimethylbenzoyl diphosphine] oxide and 2-hydroxy-2-methyl 1-phenylpropan-1-one, 2-hydroxy-2-methyl propiophenone and 2-methyl-4'-(methylthio)-2-morpholino propiophenone. The concentration of photoinitiator can vary from 0.2 to 10 wt% of the composition.¹²⁷ Scattering of the radiation by the opaque nature of the emulsion has no effect on the cure

rate but it has been found that a lower optimum concentration of photoinitiator can result in a deeper cure in the foam layer. Small concentration of salts, preferably lower than 0.1 wt% of the immiscible phase, can be used.¹²⁸ Other additives, which are not soluble in reactive or immiscible phase, include pigments, carbon blacks, silica, reinforcing agents, solid fillers, toughening agents, antioxidants, flame retardants, UV stabilizers, grounded polymeric additives, expandable microspheres and glass beads.¹²⁹

1.4 Determination of rate constants by termination models

In the initial stage of the polymerization for a UV curable polyurethane acrylate resin, the propagation is reaction controlled and k_p remains relatively constant, of the order of $10^4 \text{ L mol}^{-1} \text{ s}^{-1}$. It starts to decrease above 20% conversion when propagation becomes controlled by diffusion, due to an increase in mobility restrictions. By contrast, the bimolecular termination process is controlled by radical diffusion at the very beginning of the polymerization, with the k_t value dropping rapidly as the polymer network is building up. At conversions beyond 10%, k_t was found to be proportional to the product $k_p [M]$, which indicates that diffusion dominates the termination step.

At this stage, polymer radicals are essentially moving by propagating through unreacted double bonds. The fact, that reaction diffusion controls the termination kinetics from low double bond conversion in photopolymerization of multifunctional monomers, was discovered by Anseth and Bowman.^{4,45,130} It must be emphasized that the resulting low value of k_t is one of the main reasons why polymerization of multifunctional monomers proceeds so effectively at high initiation rates, thus accounting for the present development of the UV-curing technology.

Generalized termination can be either by a bimolecular interaction of polymer radicals or by a first order process involving one polymer radical.

Consider the following reactions:



The reaction (a) represents the bimolecular termination while the reaction (b) represents the monomolecular termination where k_t^b represents the rate coefficient for the

termination by bimolecular pathway and k_t^m for the monomolecular pathway, respectively.

1.4.1 Bimolecular termination model

Increase in network mobility can reactivate the radicals eliminated by the monomolecular process while the radicals eliminated by bimolecular processes cannot be reactivated due to the irreversible nature of the polymer to provide radical on irradiation under the UV visible light energy used.¹³¹ Bimolecular termination can be strongly suppressed by chain transfer, which mostly is found to increase with the onset of vitrification. The limitation to the quasi steady state approximation is that at the early stages of photopolymerization, when the autoacceleration take place, the rate of termination is substantially reduced so that the rate of change of radical concentration becomes approximately equal to the rate of initiation, instead of being much less than the rate of initiation.⁸⁰

In UV assisted polymerization at high initiation rates, it has been observed that the volume shrinkage occurs at much slower rate than the chemical reaction. Hence, there will be a temporary excess of free volume which enhances the mobility of the system. Higher the mobility of the system, higher will be the diffusion and hence will lead to higher double bond conversion. In the case of higher intensities applied for photopolymerization, most of the reaction will occur in the unrelaxed state and hence it will have high segmental mobilities and conversions. In the case of lower intensities, the system is able to relax and hence will have reduced internal mobility and conversion.⁴

A plot of k_t against conversion shows a rapid initial decrease in the value of k_t due to the onset of gel effect. k_t value is reduced by several orders of magnitude during autoacceleration. As system approaches the maximum polymerization rate, the autoacceleration is reduced due to increase in viscosity and reduced diffusion and hence a plateau is observed in the reduced k_t value. When there is an onset of vitrification, the k_t value is reduced again due to the termination by predominance of reaction diffusion.¹³²

In the case of k_p vs conversion, it has been shown that the value remains constant until very high conversion is reached. At high conversion, the diffusion of monomer is significantly decreased and the propagation becomes diffusion controlled. At this stage, k_p also decreases mirroring the decrease in k_t towards the end of the reaction. On plotting

k_t / k_p against different conversions, it has been found that the ratio is quickly reduced and remains constant, forming a plateau. During vitrification, the rate of decrease of k_p is slightly more than the rate of decrease of k_t and hence the ratio shows a slight increase towards the end of the reaction. But this increase is not much pronounced as the value of both rate coefficients are very low. In the case of diacrylates and dimethacrylates, the value of k_p is of the order $10^4 \text{ M}^{-1} \text{ s}^{-1}$ and $10^2 \text{ M}^{-1} \text{ s}^{-1}$, respectively. The value of k_t in the plateau region is of the order $10^5 \text{ M}^{-1} \text{ s}^{-1}$ for diacrylates and $10^3 \text{ M}^{-1} \text{ s}^{-1}$ for dimethacrylates. The rate of decrease of k_t with conversion for the diacrylates is higher than the corresponding dimethacrylates.³

In the case of crosslinking, there is a network formation and reaction diffusion mechanism is found to predominate, leading to setting at lower conversions. The changes in the value of k_t and k_p occurring with increase in conversion depend not only on the type but also on the number of functional groups in the monomer molecule and on the nature of the polymerization conditions. Actual rate coefficient determination in the crosslinking system is very difficult due to a very early onset of autoacceleration. The experimental procedure involves initiation of the polymerization by irradiation followed by cutting the light after a particular time corresponding to the chosen degree of conversion and monitoring the reaction in the dark.^{133,134} Isothermal differential scanning calorimetry (photo DSC) as well as the real time infrared spectroscopy (RTIR) can be used for the purpose.

The dark polymerization is triggered in the absence of initiation by the radicals generated on irradiation prior to the dark period. The rate of propagation as well as termination of the dark polymerization is given below.

$$R_p = -d[M] / dt = k_p [M] [P^\cdot] \quad (18)$$

$$R_t^b = -d[P^\cdot] / dt = 2 k_t^b [P^\cdot]^2 \quad (19)$$

where, $[M]$ represents the concentration of double bonds and $[P^\cdot]$ is the radical concentration at the commencement of the dark period and k_t^b is the overall termination rate coefficient calculated under the assumption of exclusively bimolecular termination.

Rearranging and integrating equation (19) we get,

$$1 / [P^\cdot] = 2k_t^b t + 1 / [P^\cdot]_0 \quad (20)$$

where, $[P^*]_o$ is the concentration of the radical at the beginning of the dark period and t is time of the dark reaction.

$$[P^*] = R_p / k_p [M] \quad (21)$$

Substituting the value of $[P^*]$ from equation 21 in equation 20 and rearranging within the limits 0 to t , we obtain:^{133,135,136}

$$[M]_t / (R_p)_t = 2k_t^b / k_p \cdot t + [M]_o / (R_p)_o \quad (22)$$

where, the subscript ‘o’ denotes the polymerization parameter at the beginning of the dark period and the subscript ‘t’ denotes the parameter after the time ‘t’ for the dark reaction measured from the time frame of the dark period after the light has been cut off. The equation 22 is called the partly integrated bimolecular termination model. A plot of $[M]_t / (R_p)_t$ vs time must yield a straight line so that the linear equation on solving must give $2k_t^b / k_p$ as slope. In most cases at the beginning of the dark period a deviation from linearity is observed. The technique is applicable to those monomers which show an appreciable residual rate well beyond the time of reaching linearity in $[M]_t / (R_p)_t$ vs t . Deviations from linearity can occur if the kinetic model used is inadequate or the rate coefficients change with time of the dark reaction. The fully integrated model of equation 22 is given by:⁴

$$k_t^b / k_p = \{1/[2(t - t_o)]\} \{[M]_t / (R_p)_t - [M]_o / (R_p)_o\} \quad (23)$$

This model is based on the assumption that all processes that contribute to the termination process are represented by a single bimolecular termination rate coefficient; k_t^b . The classical rate of propagation in bimolecular photopolymerization is given as:

$$R_p^b = k_p / k_t^b \cdot 0.5 [M] (\Phi)^{0.5}; \text{ where, } \Phi = I_a \phi \quad (24)$$

From equation 24, the value of $k_p / k_t^b \cdot 0.5$ can be calculated.

The value of $2k_t^b / k_p$ can be obtained from equation 22 as the slope of the plot $[M]_t / (R_p)_t$ vs time.

In equation 24, the value of I_a can be calculated from the following equation:¹³⁷

$$I_a = I_o (1 - 10^{-\epsilon [A]d})/d \quad (25)$$

where, I_o is the intensity of incident radiation in mW/cm^2 , d is the thickness of the layer, ϵ is the molar extinction coefficient at a particular wavelength and $[A]$ is the concentration of the photoinitiator. Now if the ϕ and ϵ value for the photoinitiator used are known, then the value of Φ can be calculated and hence the ratio $k_p / k_t^b \cdot 0.5$ can be obtained from

equation 24. From equations 22 and 24, the individual values of k_p and k_t can be determined.

The expression of I_a in Einsteins/Ls is obtained by dividing I_a in mW/cm^3 by the quanta of energy of monochromatic light used in kJ mol^{-1} .³ In photopolymerization, the viscosity effect on the value of k_t^b / k_p against conversion for dimethacrylates^{138,139} as well as the value of $k_p / k_t^{b 0.5}$ against conversion for acrylate^{140,141} have been reported.

The fraction of radicals that are immobilized or deactivated is considered to be totally inactive on the time scale measured in photocalorimetry. But in reality, these radicals on a further time scale can react at very slow rate even though diffusion, and vitrification is associated with the system. In the case of crosslinking systems, the partly integrated bimolecular termination model has been extensively used for the determination of rate coefficients.^{4,45,84,131,142-144}

Tryson and Schultz¹⁴⁵ observed in the case of photopolymerization of two multifunctional acrylates, the value of k_t decreased more rapidly than k_p . Due to high reactivity of the acrylates, the termination and propagation rate coefficients were greater by two to three orders of magnitude relative to the methacrylates at the plateau region. The plateau value for k_p of acrylates and methacrylates were of the order 10^4 and $10^2 \text{ M}^{-1} \text{ s}^{-1}$ while the value of k_t were of the order 10^2 and $10^3 \text{ M}^{-1} \text{ s}^{-1}$, respectively.

As the number of acrylate and methacrylate groups in the monomer was increased, the rate coefficients correspondingly decreased due to the greater viscosity of the higher functionality monomers.⁴⁵ For the higher functionality monomers, the propagation become diffusion limited at much lower conversions. Increasing the number of functional groups decreased their average reactivities and the final conversion was found to decrease. Plateau region was most sensitive to polymerization temperature.

1.4.2 Monomolecular termination model

An assumption is made that the only mode of termination was by radical trapping. In vinyl ester photopolymerization, Batch and Macosko¹⁴⁶ derived the model based on the assumption that the only termination process for the system starting from the conversions near $R_{p \text{ max}}$ is the radical trapping process. At this stage the bimolecular termination was assumed to be negligible. Hence, the rate of termination was thus monomolecular.

$$R_t^m = -d[P^*] / dt = k_t^m[P^*] \quad (26)$$

where, k_t^m denotes the over all termination rate coefficient calculated under the assumption of exclusive monomolecular termination.

Rearrangement and integration of equation 26 gives:

$$[P^*] = \exp (-k_t^m t) [P^*]_o \quad (27)$$

Substituting $[P^*] = R_p / k_p [M]$ and rearranging, the partly integrated monomolecular termination model is obtained.

$$\ln [M]_t / (R_p)_t = k_t^m + \ln [M]_o / (R_p)_o \quad (28)$$

From the slope of the logarithm of the $[M]_t / (R_p)_t$ against time of the dark reaction, the value of k_t^m can be calculated. Here k_t^m represents the rate coefficient for all the processes which contributes to the termination reactions. Now, the propagation rate coefficient is obtained from the corresponding steady state equation for the polymerization rate under monochromatic initiation.

$$R_p^m = 2k_p / k_t^m [M] \Phi \quad (29)$$

Substituting the value of k_t^m in equation 29, the value of k_p can be obtained.

A mixed model or fully integrated model, based on the assumption that both bimolecular and monomolecular reactions occurred in parallel, was introduced by Timpe and Strehmel.¹⁰³

1.5 Determination of rate constants from classical and modified autocatalytic model

The autocatalytic model, which had two kinetic constants and two reaction orders, is highly applicable to those systems, where a polymerizing species is cured in presence of a catalyst. Hence, it is used widely in the case of thermal epoxy amine cure where the amine acts as a catalyst for the system. The different methods of analysis of kinetic constants for the autocatalytic model have been proposed. The classical autocatalytic equation for an isothermal process was proposed by Sestak and Berggren.¹⁴⁷⁻¹⁴⁹

$$d\alpha/dt = (k_1 + k_2 \alpha^m) (1-\alpha)^n \quad (30)$$

Since k_1 is negligible for many systems, Kamal¹⁵⁰⁻¹⁵² reduced the equation and applied it to calculate the kinetic parameters in epoxy reaction with amine.

$$d\alpha/dt = k \alpha^m (1-\alpha)^n \quad (31)$$

where, $d\alpha/dt$ is the rate of polymerization and α is the conversion. Here, k is the rate constant, n is the reaction order exponent and m is the autocatalytic exponent.

The isothermal acrylate photopolymerization reaction is dependent on the conversion and on maximum conversion as per another model. This model was derived from the autocatalytic Kamal model.¹⁵¹ This model was initially developed for the thermal cure of polyesters was later found to be applicable to the photopolymerization of acrylates. Further, the autoacceleration of acrylate, even though not autocatalytic in nature, was found to obey the equation, provided the system do not vitrify early. Since the volume relaxation of the polymer after vitrification was found to be less with respect to chemical conversion, no excess diffusion volume is available during the final stages of photocuring process. The model takes into account of the photopolymerization from zero conversion to the onset of vitrification.¹⁵³

As per the model,

$$d\alpha/dt = k (1-\alpha / \alpha_m)^n (\alpha / \alpha_m)^m \quad (32)$$

where, α_m represents the maximum conversion obtained in an isothermal cure and other parameters are as explained before.

After initiation, the reaction is accelerated due to sudden radical build up (Trommsdorff effect) and is later decelerated when the reaction becomes diffusion controlled. Here, the rate of radical radical termination is lowered due to rapid viscosity build up and the propagation reaction rate is reduced without any abrupt termination. As per equation 31, it has been found that the observed value of n is in excess of 1 and that of m is below 1, so that the overall sum is less than 3 in most acrylate photopolymerizations. The value of k is found to vary with temperature.¹⁵⁴ Hence, activation energy can be calculated for reactions studied at different isothermal conditions.

The usual expression for the total activation energy is given by the relation³

$$E_a = E_p + 0.5 E_i - 0.5 E_t \quad (33)$$

Where, E_p , E_i and E_t are the activation energy of the propagation, initiation and termination reactions, respectively. In the case of photochemical initiation, E_i is very small and hence:

$$E_a = E_p - 0.5 E_t \quad (34)$$

The above models, equations 31 and 32 can be subjected to non-linear regression analysis to obtain the kinetic constants for the isothermal photopolymerization reactions

under specified conditions. Marquardt's^{155,156} non-linear regression can be applied to calculate the three unknown parameters from experimental values.

Ryan and Dutta¹⁵⁷ on kinetic analysis of autocatalytic model proposed by Kamal found that the value of the orders can be determined if there is a peak maximum in the isothermal reaction rate against time. Hence, by considering the overall reaction order of epoxy amine cure to be of second order such that $m + n = 2$, the peak maximum was defined as follows.

At peak maximum:

$$m / (m + n) = \alpha_p \quad (35)$$

where, α_p is the value of conversion at the peak. From equations 31 and 35, equation 36 can be obtained.

$$\ln (d\alpha/dt) = \ln k + m [\ln \alpha + (1 - \alpha_p / \alpha_p) \ln (1 - \alpha)] \quad (36)$$

A plot of $\ln (d\alpha/dt)$ Vs $[\ln \alpha + (1 - \alpha_p / \alpha_p) \ln (1 - \alpha)]$ will give m as slope and $\ln k$ as intercept on plotting the straight portion of the graph.¹⁵⁸

The value of n is computed by substituting the value of m in equation 35. However, non-linear regression is more preferred than this method. The value of m , n , k and E_a of many di(meth)acrylates are reported. Andrzejewska et al.¹⁵⁹ reported that the value of n can be much higher during photopolymerization of di(meth)acrylates in air than in inert atmosphere. Grassino et al.⁴² calculated the value of m and k by fixing the value of n to 1.5 for aromatic multiacrylate photopolymerization. Khudyakov et al.¹⁶⁰ and L. Huang et al.¹⁵⁴ has observed that the value of m and n are reasonable for photopolymerization of acrylates, as they fall within the range for classical thermal cure.¹⁵⁶

1.6 Measurement and interpretation of photopolymerization processes

1.6.1 Real time IR

Real time infrared spectroscopy (RTIR) is useful for analysis of ultra fast photopolymerization reactions, which typically take place less than 1 sec. Real-time infrared spectroscopy, with its milliseconds time resolution, can be successfully used to monitor photopolymerizations occurring within a fraction of a second under intense UV¹⁶¹⁻¹⁶⁷ or laser^{168,169} (up to 500 mW/cm²) irradiation. Conversion (α) versus time curves is directly recorded by following the *in situ* disappearance of the IR peak upon UV

exposure, which is characteristic of the reactive group. The actual rate of polymerization (R_p) can be easily determined at any stage of the reaction from the slope of the RTIR curve (da/dt) and the initial concentration of reactive group ($[M_0]$).¹

$$R_p = [M_0] (da/dt) \quad (37)$$

The maximum value of R_p is usually reached between 10 and 30% conversion. It is one of the most reliable parameters for comparing the reactivity of different formulations. From the recorded profile one can also evaluate the final degree of conversion.¹⁶¹ RTIR curing study of self initiating monomers,¹⁶² epoxy vinyl ether mixtures,¹⁶³ epoxies for stereolithography,¹⁶⁴ diacrylates^{161,165} and urethane acrylates¹⁶⁶ by changing the concentration of mobile and trapped radicals¹⁶⁷ have been reported.

1.6.2 Photo DSC

Thermal DSC cure of various polymers¹⁷⁰ including acrylates,¹⁷¹ epoxy resins¹⁷² and urethanes^{173,174} as well the kinetics of thermogravimetry¹⁷⁵ and thermal decomposition of polymers,¹⁷⁶ which can give an idea of their stability and extent of crosslinking, were studied even before photo DSC came to existence. Photo DSC is used for the online monitoring of the photopolymerization process.^{145,177} Due to the transparent nature of the analysis composition, the irradiation intensity is kept low during analysis to prevent double reflection from the pans. Normally UV-visible (UVV) light source is used for photopolymerization studies. The polymerization initiated by free radical or by the formation of a photocation will result in the polymerization of one or more monomeric molecules in the formulation. Measurement of heat flow during polymerization can be done mostly by heat flux method. The molecular weight is heavily influenced by temperature and hence the *in situ* reaction must be done at isothermal conditions. As the polymerization increases, the viscosity of the system also increases and finally the system will vitrify. The increase in heat flow during the exothermic process is given by¹⁷⁸

$$\Delta T = \text{Total heat evolved} / \text{Total heat capacity} \quad (38)$$

The extent of cure as well as other parameters such as reaction rate, induction time and time to attain peak maximum can be calculated from the heat flow profile obtained during analyses there by facilitating photocuring kinetic studies. The major limitation of photo DSC is its relatively long response time (~2 sec), which makes it impossible to monitor accurately polymerization reactions occurring within 10 sec, thus requiring

operation with low intensity UV radiation. RTIR and thin film calorimeter¹⁷⁹ has a much faster response time than photo DSC. In photo DSC the light is transmitted to the DSC cell by using an external UV-visible source (mostly high pressure mercury short arc lamp) through a dual light guide system. The intensity of light through both the light guides is balanced to an accuracy of 0.1–0.4 mW/cm² so as to obtain a better baseline performance. As the thickness of the formulation in the pan can cause non-effective transmission of heat flow during photopolymerization, the thickness is kept to the lowest possible value. The analysis procedure involves transferring an accurately weighed amount (about 3 – 5 mg) of sample in aluminium pan and placing the sample containing pan on the sample platform. A blank reference pan is used in the reference platform. The pans were closed by a quartz window in order to prevent any monomer loss during irradiation. The isothermal analysis is conducted by using a cooling system, which instantly lowers the photopolymerization temperature during the analysis procedure under a continuous nitrogen or argon purge. The kinetic profiles are noted from the heat flow data.

Photo DSC studies of many acrylate and epoxy systems have been reported. Photopolymerization of monomers such as acrylic acid,¹⁸⁰ phosphate containing methacrylates,¹⁸¹ and acrylate containing cyclic carbonates¹⁸² have been reported. Similarly many di(meth)acrylate photopolymerization have been reported.¹⁸³ These include polyester diacrylates,¹⁸⁴ silicon based aromatic diacrylates¹⁸⁵ and dimethacrylates,¹⁸⁶ diacrylates with incorporated silica nanoparticles¹⁸⁷ and silicon based fillers,¹⁸⁸ sulphur containing aliphatic dimethacrylates,¹⁸⁹ other aromatic based di(meth)acrylates,¹⁹⁰⁻¹⁹² aromatic urethane diacrylates⁴² and dimethacrylates,¹⁹³ waterborne urethane diacrylates,^{28,29} polyurethane diacrylate dispersions,¹⁹⁴ hyperbranched urethane acrylates,^{195,196} methacrylates¹⁹⁷ and dispersions.¹⁹⁸ Other systems include inorganic organic hybrid materials involving silicone based sol–gel acrylates¹⁹⁹ and epoxies,²⁰⁰ dry film photoresist formulation,¹⁷⁷ multiacrylate monomers^{201,202} for stereolithography,⁹⁴ soft segmented aromatic urethane acrylate²⁰³ and copolymeric hydrogels²⁰⁴ for biomedical applications, soft segmented urethane acrylate involving hydroxy terminated polybutadiene,⁴¹ cholesteric blends with aromatic diacrylates,²⁰⁵ polymeric latex involving acrylates,²⁰⁶ ceramic suspensions,²⁰⁷

monodisperse microspheres^{208,209} including aerosols²¹⁰ and self initiating acrylic monomers.^{135,211} Dental materials involving acrylates which can cure under UV^{212,213} as well as visible²¹⁴ light radiation are also reported. Other studies involve photocopolymerization of acrylates,^{215,216} combination studies of acrylate photopolymerization with dilatometry,⁸³ real time IR¹⁶³ and fluorescence spectroscopy.²¹⁷ Post photopolymerization thermal DSC studies can result in further conversion for systems which vitrify early.²¹⁸ The post heating process results in the partial conversion of the system which has been terminated by the monomolecular process.²¹⁹ The resulting system will have less radicals trapped in the system.

Novel photoinitiator systems reported for radical photopolymerization using photo DSC include amine sensitized photopolymerization²²⁰ using 1,2-dichloro thioxanthone,^{221,222} camphoroquinone,²²³⁻²²⁵ benzophenone within macromonomer chain backbone²²⁶ and riboflavin²²⁷ as photoinitiator. Similarly, photosensitization using thioxanthone on anthracene is reported.²²⁸ Other novel systems involve PEG based macrophotoinitiator²²⁹ and photoinimer^{230,231} assisted photopolymerization and bimolecular photo initiating systems.^{232,233}

Photo cationic polymerization involving epoxies,²³⁴ epoxies based on negative photoresist,²³⁵ aromatic epoxy macromonomer,⁵⁰ aliphatic epoxies⁴⁹ including for stereolithography,⁹³ epoxy and acrylate on the same molecule^{47,48,97} and cyclic acetals²³⁶ are reported. Thiol-ene photopolymerization using photo DSC as well as RTIR spectroscopy of acrylates²³⁷ and methacrylates²³⁸ are reported.

1.6.2.1 Determination of kinetic parameters by Photo DSC

Different methods are proposed for obtaining kinetic data from DSC,^{239,240} including isothermal²⁴¹ and non-isothermal^{242,243} methods. Thermal autocatalytic kinetic^{244,245} investigation of epoxides²⁴⁶ and acrylates²⁴⁷ as well as thermal and photocurable systems⁴⁰ are reported. Autocatalytic kinetics of photocopolymerization²⁴⁸ as well as kinetics of bisphenol A based urethane formation²⁴⁹⁻²⁵¹ as well as that of corresponding acrylates²⁵² are also reported.

The *in situ* heat flow profile obtained from photo DSC can be used to calculate different parameters. If ΔH_t determines the heat flow during a particular interval and ΔH_0

determines the total theoretical heat flow,^{141,160,183,185} then the rate of photopolymerization (R_p) is given by:^{187,191,234,235}

$$R_p = (dH_t / dt) / \Delta H_o \quad (39)$$

Integrating the above rate equation within the time limits will provide the value of conversion (C).^{189,193,236,237}

$$C = \Delta H_t / \Delta H_o \quad (40)$$

Other parameters which can be calculated from the rate and conversion profile includes, induction time (time taken for 1% conversion), time to attain peak maximum, $R_{p \text{ max}}$ and C_{max} . Applying the values of rate and conversion in the kinetic models discussed above, the values of kinetic constants can be obtained.

1.7 Applications of UV and visible photoinitiated polymerization

UV visible photoinitiated polymerization has varied applications. In UV curing technology, UVV (450-395 nm) is also considered for systems which polymerize in presence of UV and visible light radiation and is used mainly for curing of thick layers. The most important applications are to be found in the coating industry for the surface protection of all kinds of materials (metals, plastics, glass, paper, wood, etc.) by fast-drying varnishes, paints, or printing inks.²⁵³ UV-A is generally used for curing heavier ink coats like silk screen, UV-B is used for through curing on flexo-printing as well as for curing general ink used in surface hardening and UV-C is used for general surface curing applications. Common applications include automotive paints,²⁵⁴ optic fiber coatings^{255,256} and household exterior paints. In photolithography,²⁵⁷ light-induced insolubilization of photoresists is being used to produce the high definition images needed for the manufacture of printing plates,²⁵⁸ optical disks²⁵⁹⁻²⁶⁰ and microcircuits.²⁶¹ Syntheses^{68,82,262} and application²⁶³ of PEG based soft segmented meth(acrylates) are reported. Designed photopolymerizable formulations are used in stereolithography,²⁶⁴⁻²⁶⁶ IPN's,²⁶⁷ high energy curing²⁶⁸ and other uses.²⁶⁹

The foams prepared by the photopolymerization of high internal phase emulsion can be used for fluid absorption, insulation, sound dampening and filtration.¹²⁵ It can also be used for the preparation of multilayer foam articles. Varying the starting material and processing conditions, the foam structure can be tailored to obtain required physical properties.

1.8 References

- [1] C. Decker., *Polym. Inter.* **45**, 133 (1998).
- [2] D.R. Bauer, M.J. Dean, J.L. Gerlock., *Ind. Eng. Chem. Res.* **27**, 65 (1988).
- [3] E. Andrzejewska., *Prog. Polym. Sci.* **26**, 605 (2001).
- [4] K.S. Anseth, C.M. Wang, C.N. Bowman., *Macromol.* **27**, 650 (1994).
- [5] C. Decker., *Macromol. Rapid Commun.* **23**, 1067 (2002).
- [6] X. Jiang, H. Xu, J. Yin., *Polymer* **45**, 133 (2004).
- [7] K.J. Schafer, J.M. Hales, M. Balu, K.D. Belfield, E.W.V. Stryland, D.J. Hagan., *J. Photochem. Photobiol. A Chem.* **162**, 497 (2004).
- [8] J. Alvarez, M.V. Encinas, E.A. Lissi., *Macromol. Chem. Phys.* **200**, 2411 (1999).
- [9] H.F. Gruber., *Prog. Polym. Sci.* **17**, 953 (1992).
- [10] T.B. Cavitt, C.E. Hoyle, K. Vishwanathan, Sonny Jonsson., *Polymer* **45**, 1119 (2004).
- [11] K. Studer, C. Decker, E. Beck, R. Schwalm, N. Gruber., *Prog. Org. Coat.* **53**, 126 (2005).
- [12] K. Studer, C. Decker, C. Babe, E. Beck, R. Schwalm, N. Gruber., *Prog. Org. Coat.* **53**, 134 (2005).
- [13] K. Studer, P.T. Nguyen, C. Decker, E. Beck, R. Schwalm., *Prog. Org. Coat.* **54**, 230 (2005).
- [14] A. Mishra, S. Daswal., *Colloid Polym. Sci.* **285**, 1109 (2007).
- [15] A. Mishra, S. Daswal., *Colloid Polym. Sci.* **285**, 397 (2007).
- [16] G.D. Ye, H. Zhou, J.W. Yang, Z.H. Zeng, Y.L. Chen., *J. Therm. Anal. Calorim.* **85**, 771 (2006).
- [17] L. Macarie, A. Petrean, G. Ilia, S. Iliescu, A. Popa, M.J.M. Abadie., *J. Polym. Res.* **12**, 331 (2005).
- [18] Y. Yan, X. Tao, Y. Sun, W. Yu, C. Wang, G. Xu, J. Yang, X. Zhao, M. Jiang., *J. Mater. Sci.* **40**, 597 (2005).
- [19] S.V. Zelentsov, S.V. Gusev, N.V. Zelentsova, M.V. Kuznetsov., *High Energy Chem.* **38**, 115 (2004).
- [20] J. Jakubiak, A. Sionkowska, L.A. Linden, J.F. Rabek., *J. Therm. Anal. Calorim.* **65**, 435 (2001).

- [21] J.D. Cho, E.O. Kim, H.K. Kim, J.W. Hong., *Polym. Test.* **21**, 781 (2002).
- [22] M.B. Purvis, I.V. Khudyakov, B.J. Overton, T.W. Gantt., *US Patent 6596786 B2* (2003).
- [23] D.E. Herr, Z. Hu, C.W. Paul, R.W.R. Humphreys., *PCT Patent Appln. WO 2004/000889 A2* (2004).
- [24] K.S. Jung, D.K. Kim, J.W. Kim, M.S. Kim, H.H. Byun, W.J. Oh, K.S. Han., *PCT patent WO03/076544 A1* (2003).
- [25] R. Wiesendanger, M. Reisinger., *US Patent 7087696 B2* (2006).
- [26] J.Y. Kim, K.D. Suh., *Macromol. Chem. Phys.* **197**, 2429 (1996).
- [27] C.Y. Lee, J.W. Kim, K.D. Suh., *J. Mater. Sci.* **34**, 5343 (1999).
- [28] J. Yang, Z. Wang, Z. Zeng, Y. Chen., *J. Appl. Polym. Sci.* **84**, 1818 (2002).
- [29] J.W. Kim, K.D. Suh., *J. Appl. Polym. Sci.* **69**, 1079 (1998).
- [30] B. Steinmann, J.P. Wolf, A. Schulthess, M. Hunziker., *US Patent 5658712* (1997).
- [31] Z. Komiya, A.G.M. Abel, D.P.W. Alkema, M. Mase, T. Ukachi., *US Patent 6858657 B2* (2005).
- [32] J.P. Wolf, A. Schulthess, B. Steinmann, M. Hunziker., *US Patent 5470689* (1995).
- [33] N. Miyata, H. Nakayama., *US Patent 3907865* (1975).
- [34] K.Aoki, K. Kanda, S. Urano, R. Mizuguchi., *US Patent 4902727* (1990).
- [35] H. Ohsugi, Y. Eguchi, S. Urano, R. Mizuguchi, M. Takarada., *US Patent 4888406* (1989).
- [36] M. Roth, R. Salvin, W. Rhein, K. Meier, B. Sailer, R. Wiesendanger., *US Patent 5576399* (1996).
- [37] R.L. Bowen., *US Patent 4514527* (1985).
- [38] M. Yamada, K. Aoki, S. Urano, R. Mizuguchi., *US Patent 5194655* (1993).
- [39] B. Steinmann, J.P. Wolf, A. Schulthess, M. Hunziker., *US Patent 5599651* (1997).
- [40] R. Chandra, R.K. Soni., *Prog. Polym. Sci.* **19**, 137 (1994).
- [41] F. Schapman, J.P. Couvercelle, C. Bunel., *Polymer* **42**, 7503 (2001).
- [42] S.B. Grassino, M.C. Strumia, J. Couve, M.J.M. Abadie., *Prog. Org. Coat.* **37**, 39 (1999).
- [43] M. Shirai, K. Mitsukura, H. Okamura., *Chem. Mater.* **20**, 1971 (2008).
- [44] P.J. Flory., *J. Am. Chem. Soc.* **63**, 3083 (1941).

- [45] K.S. Anseth, C.M. Wang, C.N. Bowman., *Polymer* **35**, 3243 (1994).
- [46] T.F. Scott, W.D. Cook, J.S. Forsythe., *Polymer* **43**, 5839 (2002).
- [47] G.V. Gatiyatullina, Y.A. Prochukhan, E.M. Battalov, N.G. Afzaletdinova, Y.I. Murinov., *Russ. J. Appl. Chem.* **76**, 623 (2003).
- [48] E.M. Battalov, G.V. Leplyanin, Y.I. Murinov., *Russ. J. Appl. Chem.* **76**, 1829 (2003).
- [49] M. Sangermano, G. Malucelli, R. Bongiovanni, G. Gozzelino, F. Peditto, A. Priola., *J. Mater. Sci.* **37**, 4753 (2002).
- [50] T. Wang, Z.H. Wang., *Polym. Bull.* **53**, 323 (2005).
- [51] M.Sangermano, G.Malucelli, F. Morel, C. Decker, A. Priola., *Eur. Polym. J.* **35**, 639 (1999).
- [52] Y.M. Kim, L.K. Kostanski, J.F. MacGregor, A.E. Hamielec., *J. Therm. Anal. Calorim.* **78**, 153 (2004).
- [53] N.K. Apohan, R. Demirci, M. Cakir, A. Gungor., *Rad. Phys. Chem.* **73**, 254 (2005).
- [54] D.M. Lamb, J.A. Simms., *US Patent 5286782* (1994).
- [55] S.S. Labana, A.N. Theodore., *US Patent 4069275* (1978).
- [56] S. Wu., *US Patent 3943187* (1976).
- [57] S. Sun, P. Sun, D. Liu., *Eur. Polym. J.* **41**, 913 (2005).
- [58] S.N. Lewis, R.A. Hoggard., *US Patent 4158736* (1979).
- [59] D.M. Geary, P.H. Pettit, M.L. Kaufman, S.K. Vicha., *US Patent 4801680* (1989).
- [60] V.D. McGinniss., *US Patent 4037018* (1977).
- [61] M.C. Gualpa, C.C. Riccardi, A. Vazuez., *Polymer* **39**, 2247 (1998).
- [62] M. Zeni, I.R. Bellobono, F. Muffato, A. Polissi, E. Selli., *J. Memb. Sci.* **36**, 277 (1988).
- [63] R.M. Christenson, D.P. Hart., *Ind. Eng. Chem.* **53**, 459 (1961).
- [64] B. Danner, H. Gerber, H. Pummer., *US Patent 4251410* (1981).
- [65] B. Neppel, J. Boysen., *US Patent 6939601 B2* (2005).
- [66] G. Kniajer, J.D. Cosby, I.H. Joyce, S. Sridharan, J.J. Maloney., *US Patent 6346493 B1* (2002).
- [67] F. Wang, B. He, X. Sun, H. Dai, J. Liu., *Appl. Phys. B.* **86**, 117 (2007).
- [68] J.H. Ward, K. Furman, N.A. Peppas., *J. Appl. Polym. Sci.* **89**, 3506 (2003).

- [69] P. Jones, *Chemistry of acrylic resins, chapter – 1. In waterborne and solvent based acrylics and their end user applications Vol. 1 (Ed. P. Oldring) Sita Technology, London, page 11 (1996).*
- [70] R.A. Sadykov, G.V. Gatiyatullina, E.M. Battalov, Y.A. Prochukhan., *Russ. J. Appl. Chem.* **76**, 629 (2003).
- [71] C. Decker, K. Moussa., *J. Polym. Sci. Polym. Chem.* **25**, 739 (1987).
- [72] R.A. Gregg, F.R. Mayo., *Discuss. Faraday. Soc.* **2**, 328 (1947).
- [73] J.G. Kloosterboer., *Adv. Polym. Sci.* **84**, 1 (1988).
- [74] P. Allen, G. Simon, D. Williams, E. Williams., *Macromol.* **22**, 809 (1989).
- [75] S. Zhu, Y. Tian, A.E. Hamielec, D.R. Eaton, *Macromol.* **23**, 1144 (1990).
- [76] M.E. Best, P.H. Kasai., *Macromol.* **22**, 2622 (1989).
- [77] D. Li, S. Zhu, A.E. Hamielec., *Polymer* **34**, 1383 (1993).
- [78] W. Funke., *Brit. Polym. J.* **21**, 107 (1989).
- [79] J. Bastide, L. Leibler., *Macromol.* **21**, 2649 (1988).
- [80] C.N. Bowman, N.A. Peppas., *Macromol.* **24**, 1914 (1991).
- [81] R. Greiner, F.R. Schwarzl., *Rheol. Acta.* **23**, 378 (1984).
- [82] J.H. Ward, A. Shahar, N.A. Peppas., *Polymer* **43**, 1745 (2002).
- [83] K.S. Anseth, C.N. Bowman, N.A. Peppas., *J. Polym. Sci. Polym. Chem.* **32**, 139 (1994).
- [84] K. Dusek., *Network formation involving polyfunctional polymer chains (Chapter-3), In (R.F.T. Stepto Ed.) Polymer networks: principles of their formation, structure and properties, Blackie Academic and Professional, London, Page 64 (1998).*
- [85] J.G. Kloosterboer, G.M.M.V. de Hei, H.M.J. Boots., *Polym. Commun.* **25**, 354 (1984).
- [86] K.S. Anseth, C.N. Bowman., *J. Polym. Sci. B Polym. Phys.* **33**, 1769 (1995).
- [87] J.V. Crivello, B. Yang., *J. Macromol. Chem. A* **31**, 517 (1994).
- [88] C. Decker, H.L. Xuan, T.V. Nguyen., *J. Polym. Sci Polym. Chem.* **34**, 1771 (1995).
- [89] C. Decker, T.V. Nguyen, H.L. Xuan., *Eur. Polym. J.* **32**, 549 (1996).
- [90] Ref 69, page 59 (1996).
- [91] N.W. Johnston., *J. Macromol. Sci. Rev. Macromol. Chem. C* **14**, 215 (1976).
- [92] H.J. Harwood, W.M. Ritchey., *J. Polym. Sci. B* **2**, 601 (1964).

- [93] C.E. Corcione, A. Greco, A. Maffezzoli., *J. Therm. Anal. Calorim.* **72**, 687 (2003).
- [94] A. Maffezzoli, R. Terzi., *Thermochim. Acta.* **321**, 111 (1998).
- [95] T.F. Scott, W.D. Cook, J.S. Forsythe., *Polymer* **44**, 671 (2003).
- [96] H. Kaczmarck, C.Decker., *J. Appl. Polym. Sci.* **54**, 2147 (1994).
- [97] G.V. Gatiyatullina, E.M. Battalov, Y.A. Prochukhan, R.R. Muslukhov., *Russ. J. Appl. Chem.* **76**, 448 (2003).
- [98] K. Moussa, C. Decker., *J. Polym. Sci. Polym. Chem. Ed.* **31**, 2633 (1993).
- [99] C. Decker, T.V.T. Nguyen, H.L. Xuan., *Eur. Polym. J.* **32**, 1319 (1996).
- [100] C. Decker, T.V.T. Nguyen, H.L. Xuan., *Eur. Polym. J.* **32**, 559 (1996).
- [101] Ref 69, page 79 (1996).
- [102] C.E. Hoyle., (S.P. Peppas Ed.) Radiation curing science and technology, Plenum Press, New York, page 57 (1992).
- [103] H.J. Timpe, B. Strehml., *Makromol. Chem.* **192**, 779 (1991).
- [104] H.J. Timpe, B. Strehml., *Angew. Makromol. Chem.* **178**, 131 (1990).
- [105] C. Decker, B. Elzaouk, D. Decker., *J. Macromol. Sci. Pure Appl. Chem.* **A 33**, 173 (1996).
- [106] D.L. Kurdikar, N.A. Peppas., *Polymer* **35**, 1004 (1994).
- [107]J.Q. Pan, W.W.Y. Lau, Z.F. Zhang, X.Z. Hu., *Polym. Degrad. Stab.* **53**, 153 (1996).
- [108]J.Q. Pan, N.C. Liu, W.W.Y. Lau., *Polym. Degrad. Stab.* **62**, 165 (1998).
- [109]P.J. Qing., *Polym. Degrad. Stab.* **32**, 219 (1991).
- [110]C.S.B. Ruiz, L.D.B. Machado, J.E. Volponi, E.S. Pino., *J. Therm. Anal. Calorim.* **75**, 507 (2004).
- [111]P.J. Qing, C. Song., *Polym. Degrad. Stab.* **40**, 375 (1993).
- [112]J.Q. Pan, W.W.Y. Lau, J. Lin, K.L. Tan., *Polym. Degrad. Stab.* **46**, 45 (1994).
- [113]J.Q. Pan, W.W.Y. Lau, J. Lin, K.L. Tan., *Polym. Degrad. Stab.* **46**, 51 (1994).
- [114]J.Q. Pan, W.W.Y. Lau, J. Lin., *Polym. Degrad. Stab.* **49**, 379 (1995).
- [115]T. Kurosaki, K.W. Lee, M. Okawara., *J. Polym. Sci. Polym. Chem.* **10**, 3295 (1972).
- [116]W.W.Y. Lau, J.Q. Pan., *Polym. Degrad. Stab.* **60**, 459 (1998).
- [117]N.C. Liu, J.Q. Pan, W.W.Y. Lau., *Polym. Degrad. Stab.* **63**, 71 (1999).
- [118]J.Q. Pan, W.W.Y. Lau, Z.F. Zhang, X.Z. Hu., *J. Appl. Polym. Sci.* **61**, 1405 (1996).
- [119]N.C. Liu, J.Q. Pan, W.W.Y. Lau., *Polym. Degrad. Stab.* **62**, 307 (1998).

- [120] J.Q. Pan, P.W. Quek, N.C. Liu, W.W.Y. Lau., *J. Appl. Polym. Sci.* **78**, 403 (2000).
- [121] J.Q. Pan, N.C. Liu, W.W.Y. Lau., *Polym. Degrad. Stab.* **62**, 315 (1998).
- [122] J.Q. Pan, W.W.Y. Lau, J. Lin, K.L. Tan, S.H. Goh., *Polym. Degrad. Stab.* **49**, 231 (1995).
- [123] M.J.M. Abadie, O.O. Novikova, V.Y. Voytekunas, V.G. Syromyatnikov, A.Y. Kolendo., *J. Appl. Polym. Sci.* **90**, 1096 (2003).
- [124] D. Cummins, P. Wyman, C.J. Duxbury, J. Thies, C.E. Koning, A. Heise., *Chem. Mater.* **19**, 5285 (2007).
- [125] K.L.V. Thunhorst, M.D. Gehlsen, R.E. Wright, E.W. Nelson, S.D. Koecher, D. Gold., *US Patent 6759080 B2* (2004).
- [126] T.M. Shiveley, T.A. Desmarais, J.C. Dyer, K.J. Stone., *US Patent 5856366* (1999).
- [127] M.C. Palazotto, F.A. Ubel, J.D. Oxman, M.Z. Ali., *US Patent 5545676* (1996).
- [128] T.A. Desmarais., *US Patent 5352711* (1994).
- [129] J.M. Williams, A.M. Nyitray, M.H. Wilkerson., *US Patent 5037859* (1991).
- [130] K.S. Anseth, L.M. Kline, T.A. Walker, K.J. Anderson, C.N. Bowman., *Macromol.* **28**, 2491 (1995).
- [131] E. Andrzejewska, M.B. Bogacki, M. Andrzejewski., *Macromol. Theory Simul.* **10**, 842 (2001).
- [132] E. Andrzejewska., *Macromol. Symp.* **171**, 243 (2001).
- [133] E.S. Jonsson, T.Y. Lee, K. Vishwanathan, C.E. Hoyle, T.M. Roper, C.A. Guymon, C. Nason, I.V. Khudyakov., *Prog. Org. Coat.* **52**, 63 (2005).
- [134] C. Decker, K. Moussa., *J. Appl. Polym. Sci.* **34**, 1603 (1987).
- [135] I.V. Khudyakov, W.S. Fox, M.B. Purvis., *Ind. Eng. Chem. Res.* **40**, 3092 (2001).
- [136] C. Decker, B. Elzaouk., *Eur. Polym. J.* **31**, 1155 (1995).
- [137] S.P. Peppas., Chapter – 1, Radiation curing science and technology, Plenum Press, New York, page 1 (1992).
- [138] E. Andrzejewska, M. Janaszczyk, M. Andrzejewski., *Conference proceedings, RadTech Europe 2005*, (2005) Barcelona, Spain.
- [139] K.S. Anseth, R.A. Scott, N.A. Peppas., *Macromol.* **29**, 8308 (1996).
- [140] E. Oral, N.A. Peppas., *Polymer* **45**, 6163 (2004).
- [141] J.E. Dietz, N.A. Peppas., *Polymer* **38**, 3767 (1997).

- [142] L. Lecamp, B. Youssef, C. Bunel, P. Lebaudy., *Nucl. Inst. Method Phy. Res. B.* **151**, 285 (1999).
- [143] J.L. Mateo, J. Serrano, P. Bosch., *Macromol.* **30**, 1285 (1997).
- [144] D. Nwabunma, K.J. Kim, Y. Lin, L.C. Chien, T. Kyu., *Macromol.* **31**, 6806 (1998).
- [145] G.R. Tryson, A.R. Shultz., *J. Polym. Sci. Polym. Phys.* **17**, 2059 (1979).
- [146] G.L. Batch, C.W. Macosko., *J. Appl. Polym. Sci.* **44**, 1711 (1992).
- [147] J. Sestak, G. Berggren., *Thermochim. Acta.* **3**, 1 (1971).
- [148] P.D. Garn., *Thermochim. Acta.* **5**, 485 (1973).
- [149] L. Abdellah, M.N. Dinia, B. Boutevin, M.J.M. Abadie., *Eur. Polym. J.* **33**, 869 (1997).
- [150] S. Sourour, M.R. Kamal., *Thermochim. Acta* **14**, 41 (1976).
- [151] M.R. Kamal, S. Sourour., *Polym. Engng. Sci.* **13**, 59 (1973).
- [152] M.R. Kamal., *Polym. Engng. Sci.* **14**, 230 (1974).
- [153] M.R. Keenan., *J. Appl. Polym. Sci.* **33**, 1725 (1987).
- [154] L. Huang, Y. Li, J. Yang, Z. Zeng, Y. Chen., *Polymer* **50**, 4325 (2009).
- [155] D.N. Marquardt., *J. Appl. Polym. Sci.* **7**, 1063 (1963).
- [156] U. Khanna, M. Chanda., *J. Appl. Polym. Sci.* **49**, 319 (1993).
- [157] M.E. Ryan, A. Dutta., *Polymer* **20**, 203 (1979).
- [158] L.H. Nguyen, H. Koerner, K. Lederer., *J. Appl. Polym. Sci.* **85**, 2034 (2002).
- [159] E. Andrzejewska, L.A. Linden, J.F. Rabek., *Polym. Inter.* **42**, 179 (1997).
- [160] I.V. Khudyakov, J.C. Legg, M.B. Purvis, B.J. Overton., *Ind. Eng. Chem. Res.* **38**, 3353 (1999).
- [161] T. Scherzer, U. Decker., *Vibrational Spectroscopy* **19**, 385 (1999).
- [162] T.Y. Lee, T.M. Roper, E.S. Jonsson, I. Kudyakov, K. Vishwanathan, C. Nason, C.A. Guymon, C.E. Hoyle., *Polymer* **44**, 2859 (2003).
- [163] Y.M. Kim, L.K. Kostanski, J.F. MacGregor, A.E. Hamielec., *J. Therm. Anal. Calorim.* **78**, 153 (2004).
- [164] K.C. Wu, J.W. Halloran., *J. Mater. Sci.* **40**, 71 (2005).
- [165] C. Peinado, E.F. Salvador, A. Alonso, T. Corrales, J. Baselga, F. Catalina., *J. Polym. Sci. Polym. Chem.* **40**, 4236 (2002).

- [166] S.M. Gasper, D.N. Schissel, L.S. Baker, D.L. Smith, R.E. Youngman, L.M. Wu, S.M. Sonner, R.R. Hancock, C.L. Hogue, S.R. Givens., *Macromol.* **39**, 2126 (2006).
- [167] Y. Zhang, D.E. Kranbuehl, H. Sautereau, G. Seytre, J. Dupuy., *Macromol.* **41**, 708 (2008).
- [168] C. Decker, K. Moussa., *Macromol.* **22**, 4455 (1989).
- [169] M. Fizet, C. Decker, J. Faure., *Eur. Polym. J.* **21**, 427 (1985).
- [170] R. Kay, A.R. Westwood., *Eur. Polym. J.* **11**, 25 (1975).
- [171] M.S. Hong, I.J. Chung., *Polym. J.* **23**, 747 (1991).
- [172] P. Peyser, W.D. Bascom., *J. Appl. Polym. Sci.* **21**, 2359 (1977).
- [173] E.B. Richter, C.W. Macosko., *Polym. Eng. Sci.* **18**, 1012 (1978).
- [174] D. Wang, G. Zhang, Y. Zhang, Y. Gao, Y. Zhao, C. Zhou, Q. Zhang, X. Wang., *J. Appl. Polym. Sci.* **103**, 417 (2007).
- [175] J.R. MacCallum, J. Tanner., *Eur. Polym. J.* **6**, 1033 (1970).
- [176] K.E.J. Barrett., *J. Appl. Polym. Sci.* **11**, 1617 (1967).
- [177] B.K. Applet, M.J.M Abadie., *Polym. Eng. Sci.* **28**, 367 (1988).
- [178] A. Boller, Y. Jin, B. Wunderlich., *J. Therm. Anal. Calorim.* **42**, 307 (1994).
- [179] T.M. Roper, C.A. Guymon, C.E. Hoyle, *Rev. Sci. Inst.* **76**, 54102 (2005).
- [180] K.S. Anseth, R.A. Scott, N.A. Peppas., *Macromol.* **29**, 8308 (1996).
- [181] D. Avci, L.J. Mathias., *Polym. Bull.* **54**, 11 (2005).
- [182] K. Moussa, C. Decker., *J. Polym. Sci. Polym. Chem.* **31**, 2197 (1993).
- [183] V. Pamedylyte, M.J.M Abadie, R. Makuska., *J. Appl. Polym. Sci.* **86**, 579 (2002).
- [184] H.K.Kim, H.T.Ju, J.W. Hong., *Eur. Polym. J.* **39**, 2235 (2003).
- [185] C. Iojoiu, M.J.M. Abadie, V. Harabagiu, M. Pinteala, B.C. Simionescu., *Eur. Polym. J.* **36**, 2115 (2000).
- [186] C.M. Chung, M.S. Kim, Y.S. Roh, J.G. Kim., *J. Mater. Sci. Lett.* **21**, 1093 (2002).
- [187] J.D. Cho, H.T. Ju, J.W. Hong., *J. Polym. Sci. Polym. Chem.* **43**, 658 (2005).
- [188] D.L. Starokadomskii, T.N. Soloveva., *Russ. J. Appl. Chem.* **75**, 138 (2002).
- [189] E. Andrzejewska., *Polymer* **37**, 1039 (1996).
- [190] Q. Yu, S. Nauman, J.P. Santerre, S. Zhu., *J. Mater. Sci.* **36**, 3599 (2001).
- [191] L. Lecamp, B. Youssef, C. Bunel, P. Lebaudy., *Polymer* **38**, 6089 (1997).

- [192] W.D. Cook, J.S. Forsythe, N. Irawati, T.F. Scott, W.Z. Xia., *J. Appl. Polym. Sci.* **90**, 3753 (2003).
- [193] T.Y. Inan, E. Ekinici, E. Yildiz, A. Kuyulu, A. Gungor., *Macromol. Chem. Phys.* **202**, 532 (2001).
- [194] Y.B. Kim, H.K. Kim, J.K. Yoo, J.W. Hong., *Surf. Coat. Tech.* **40**, 157 (2002).
- [195] E. Dzunuzovic, S. Tasic, B. Bozic, K. Jeremic, B. Dunjic., *React. Funct. Polym.* **66**, 1097 (2006).
- [196] L.E Schmidt, D. Schmah, Y. Leterrier, J.A.E. Manson., *Rheol. Acta.* **46**, 693 (2007).
- [197] K. Maruyama, H. Kudo, T. Ikehara, T. Nishikubo, I. Nishimura, A. Shishido, T. Ikeda., *Macromol.* **40**, 4895 (2007).
- [198] A. Asif, C.Y. Huang, W.F. Shi., *Colloid Polym. Sci.* **283**, 721 (2005).
- [199] C.C. Barghorn, O. Soppera, C. Carre., *J. Sol Gel Sci. Techn.* **41**, 93 (2007).
- [200] K. Zou, M.D. Soucek., *Macromol. Chem. Phys.* **205**, 2032 (2004).
- [201] J.E. Dietz, N.A. Peppas., *Polymer* **38**, 3767 (1997).
- [202] T.J. Smith, B.S. Shemper, J.S. Nobles, A.M. Casanova, C. Ott, L.J. Mathias., *Polymer* **44**, 6211 (2003).
- [203] K. Kobayashi, K. Obuchi, H. Hoshi, N. Morimoto, Y. Iwasaki, S. Takatani., *J. Artif. Organs* **8**, 237 (2005).
- [204] W.F. Lee, W.J. Lin., *J. Polym. Res.* **9**, 23 (2002).
- [205] N. Dadivanyan, A. Bobrovsky, V. Shibaev., *Colloid Polym. Sci.* **285**, 681 (2007).
- [206] J.Odeberg, J.Rassing, J.E.Jonsson, B.Wesslen., *J. Appl. Polym. Sci.* **62**, 435 (1996).
- [207] G.A. Brady, J.W. Halloran., *J. Mater. Sci.* **33**, 4551 (1998).
- [208] Z. Gao, E.A. Grulke, A.K. Ray., *Colloid Polym. Sci.* **285**, 847 (2007).
- [209] C. Esen, T. Kaiser, G. Schweiger., *J. Aerosol. Sci.* **27**, S-371 (1996).
- [210] M.T. Valdez, P. Jenouvrier, J. Fick, M. Langlet., *J. Mater. Sci.* **39**, 2801 (2004).
- [211] E.S. Jonsson, T.Y. Lee, K. Vishwanathan, C.E. Hoyle, T.M. Roper, C.A. Guymon, C. Nason, I.V. Khudyakov., *Prog. Org. Coat.* **52**, 63 (2005).
- [212] S.H. Dickens, J.W. Stansbury, K.M. Choi, C.J.E. Floyd., *Macromol.* **36**, 6043 (2003).

- [213] K.D. Ahn, D.K. Han, S.H. Lee, C.W. Lee., *Macromol. Chem. Phys.* **204**, 1628 (2003).
- [214] J. Augusto, C. Discacciati, R.L. Orefice., *J. Mater. Sci.* **42**, 3883 (2007).
- [215] N. Davidenko, C. Peniche, R. Sastre, J.S. Roman., *Polymer* **39**, 917 (1998).
- [216] E. Andrzejewska, E. Socha, M. Andrzejewski., *Polymer* **47**, 6513 (2006).
- [217] C. Peinado, A. Alonso, E.F. Salvador, J. Baselga, F. Catalina., *Polymer* **43**, 5355 (2002).
- [218] C.S.B. Ruiz, L.D.B. Machado, J.A. Vanin, J.E. Volponi., *J. Therm. Anal. Calorim.* **67**, 335 (2002).
- [219] L. Lecamp, B. Youssef, C. Bunel, P. Lebaudy., *Polymer* **40**, 6313 (1999).
- [220] J.P.Fouassier, D. Ruhlmann, B. Graff, F.M. Savary, F. Wieder., *Prog. Org. Coat.* **25**, 235 (1995).
- [221] C. Valderas, S. Bertolotti, C.M. Previtali, M.V. Encinas., *J. Polym. Sci. Polym. Chem.* **40**, 2888 (2002).
- [222] M.V. Encinas, A.M. Rufs, T. Corrales, F. Catalina, C. Peinado, K. Schmith, M.G. Neumann, N.S. Allen., *Polymer* **43**, 3909 (2002).
- [223] W.D. Cook., *Polymer* **33**, 600 (1992).
- [224] A. Sionkowska, A. Kaminska, L.A. Linden, J.F. Rabek., *Polym. Bull.* **43**, 349 (1999).
- [225] G. Ullrich, D. Herzog, R. Liska, P. Burtscher, N. Moszner., *J. Polym. Sci. Polym. Chem.* **42**, 4948 (2004).
- [226] X. Jiang, X. Luo, J. Yin., *J. Photochem. Photobiol. A Chem.* **174**, 165 (2005).
- [227] M.V. Encinas, A.M. Rufs, S. Bertolotti, C.M. Previtali., *Macromol.* **34**, 2845 (2001).
- [228] J.D. Cho, H.K. Kim, Y.S. Kim, J.W. Hong., *Polym. Test.* **22**, 633 (2003).
- [229] I. Cakmak, T. Ozturk., *J. Polym. Res.* **12**, 121 (2005).
- [230] B.R. Nayak, L.J. Mathias., *J. Polym. Sci. Polym. Chem.* **43**, 5661 (2005).
- [231] S.C. Clark, C.E. Hoyle, S. Jonsson, F. Morel, C. Decker., *Polymer* **40**, 5063 (1999).
- [232] J.L. Mateo, P. Bosch., *Polym. Adv. Tech.* **5**, 561 (1994).
- [233] A. Costela, I.G. Moreno, F. Diaz, J. Dabrio, R. Sastre., *Acta Polymer.* **48**, 423 (1997).

- [234] J.D. Cho, J.W. Hong., *Eur. Polym. J.* **41**, 367 (2005).
- [235] J.D. Cho, H.T. Ju, Y.S. Park, J.W. Hong., *Macromol. Mater. Eng.* **291**, 1155 (2006).
- [236] M. Pantiru, D.M. Vuluga, D.S. Vasilescu, M.J.M. Abadie., *Polym. Bull.* **47**, 485 (2002).
- [237] T.M. Roper, T. Kwee, T.Y. Lee, C.A. Guymon, C.E. Hoyle., *Polymer* **45**, 2921 (2004).
- [238] L. Lecamp, F. Houllier, B. Youssef, C. Brunel., *Polymer* **42**, 2727 (2001).
- [239] A.A. Duswalt., *Thermochim. Acta* **8**, 57 (1974).
- [240] N. Sbirrazzuoli, D. Brunel, L. Elegant., *J. Therm. Anal.* **38**, 1509 (1992).
- [241] D.N. Waters, J.L. Paddy., *Anal. Chem.* **60**, 53 (1988).
- [242] F.Y.C. Boey, W. Qiang., *Polymer* **41**, 2081 (2000).
- [243] V.M. Gorbachev., *J. Therm. Anal.* **18**, 13 (1980).
- [244] J.D. Nam, J.C. Seferis., *J. Appl. Polym. Sci.* **50**, 1555 (1993).
- [245] S.N. Lee, M.T. Chiu, H.S. Lin., *Polym. Eng. Sci.* **32**, 1037 (1992).
- [246] R. Chandra, B.P. Thapliyal, B. Sehgal, R.K. Soni., *Polym. Inter.* **29**, 185 (1992).
- [247] R. Chandra, R.K. Soni., *Polym. Inter.* **31**, 239 (1993).
- [248] R. Chandra, R.K. Soni, S.S. Murthy., *Polym. Inter.* **31**, 305 (1993).
- [249] I. Yilgor, E.H. Orhan, B.M. Baysal., *Makromol. Chem.* **179**, 109 (1978).
- [250] Y. Iwakura, H. Okada, S. Yamashiro., *Makromol. Chem.* **58**, 237 (1962).
- [251] H. Okada, Y. Iwakura., *Makromol. Chem.* **66**, 91 (1963).
- [252] E. Andrzejewska, M. Andrzejewski., *J. Polym. Sci. Polym. Chem.* **36**, 665 (1998).
- [253] A.V. Rao, D.S. Kanitkar, A.K. Parab., *Prog. Org. Coat.* **25**, 221 (1995).
- [254] K. Magg, W. Lenhard, H. Loffles., *Prog. Org. Coat.* **40**, 93 (2000).
- [255] I.V. Khudyakov, B.J. Overton, M. Purvis., *US Patent 6171698 B1* (2001).
- [256] P.J. Shustack., *US Patent 5146531* (1992).
- [257] L.F. Thompson. R.E. Kerwin., *Annual Rev. Mater. Sci.* **6**, 267 (1976).
- [258] J.V. Crivello., *US Patent 4193799* (1980).
- [259] M. Kuwahara, T. Nakano, J. Taminaga, M.B. Lee, N. Atoda., *Jpn. J. Appl. Phys.* **38**, 1079 (1999).

- [260] A. Kouchiyama, K. Aratani, Y. Takemoto, T. Nakao, S. Kai, K. Osato, K. Nakagawa., *Jpn. J. Appl. Phys.* **42**, 769 (2003).
- [261] R.E. Sheets., *US Patent 3941475* (1976).
- [262] V.A. Liu, S.N. Bhatia., *Biomed. Microdevices* **4**, 257 (2002).
- [263] B. Kim, N.A. Peppas., *Biomed. Microdevices* **5**, 333 (2003).
- [264] Y. Tamura, T. Hagiwara., *US Patent 6203966 B1* (2001).
- [265] J.P. Wolf, A. Schulthess, B. Steinmann, M. Hunziker., *US Patent 5629133* (1997).
- [266] T. Suzuki, T. Osaki, H. Matsueda., *US Patent 5731388* (1998).
- [267] R. Breeveld, J. Schutyser., *PCT Patent Appln. WO93/11465* (1993).
- [268] Y. Wang., *US Patent 6569602 B1* (2003).
- [269] L. Schon, W. Rogler, V. Muhrer, M. Fedtke, A. Palinsky., *US Patent 6127092* (2000).

Introduction to high internal phase
emulsion

2.1 Introduction

High internal phase emulsions (HIPE's) are concentrated systems possessing a large volume of internal or dispersed phase. PolyHIPE polymers are highly porous materials obtained by polymerizing the continuous phase of a high internal phase emulsion (HIPE).^{1,2} Lissant³ classified high internal phase emulsions or HIPEs, as emulsions containing greater than 70% internal phase volume. This value represents the maximum volume occupiable by a number of uniform spheres packed into a given volume in the most efficient manner.⁴ The volume fraction above 0.74, results in deformation of the dispersed phase droplets into polyhedra, which are separated by thin films of continuous phase and can exceed 0.99. Its formation depends critically on the nature of the surfactant, which must be soluble in the continuous phase. If it does not happen, then emulsion inversion will occur. The foams obtained by this method have well defined cellular morphology, which is different from the foams formed by other methods such as gas blowing. The morphological features such as cell size⁵, interconnecting hole size⁶ and porosity can be efficiently controlled⁷, which make polyHIPEs a superior product than the gas blown foams. Their structure, which is analogous to conventional gas-liquid foam of low liquid content, gives rise to a number of peculiar and fascinating properties such as high viscosity. Like dilute emulsions, HIPEs are both kinetically and thermodynamically unstable. It is possible to prepare metastable systems, which show no change in properties or appearance over long periods of time. Polymer materials can easily be prepared from HIPEs if one or the other (or both) phases of the emulsion contain monomeric species. This process yields a range of products with widely differing properties. Additionally, as the concentrated emulsion acts as a scaffold or template, the microstructure of the resultant material is determined by the emulsion structure immediately prior to polymerization. These concentrated emulsions have been referred to by a number of different names in the literature, including high internal phase ratio emulsions (HIPREs)⁸⁻¹¹, HIPEs, gel-emulsions¹²⁻¹⁵ and hydrocarbon gels¹⁶. Styrene divinyl benzene copolymeric HIPE was extensively studied in the initial stages of the discovery of the system. However, this has opened a vast area of research that can be applied to a series of monomers of various types including acrylates.

The first criterion for the formation of a HIPE is the presence of two immiscible liquids, one of which is water (or aqueous solution), almost without exception. The nature of the organic or oil phase can vary to a considerable extent, although the most stable HIPEs are generally produced with more hydrophobic liquids. However, it is the nature of the surfactant employed to stabilize the HIPE which will ultimately facilitate its formation. Above a certain critical limit of internal phase volume, an emulsion will tend to invert to the opposite type, i.e. an oil-in-water (O/W) emulsion will become the water in oil (W/O) variety, and vice versa. This can be prevented from occurring by careful choice of surfactant, such that it is completely insoluble in the dispersed phase of the emulsion.

HIPE is formed generally by careful addition of the internal phase to a solution of surfactant in the external phase, under constant agitation. HIPEs may also form under certain other circumstances.¹⁷ When a centrifugal field is applied to an emulsion, the droplets can be forced into contact with each other and deformation into polyhedra occurs. The excess continuous phase is forced out of the emulsion, forming a separate phase. This process is known as "creaming". Additionally, emulsions may cream over a period of time under the influence of gravity, forming a layer of HIPE either on top of the dilute emulsion, in the case of oil-in-water emulsions, or below the bulk emulsion for W/O system.

Other researchers have also observed an increase in HIPE viscosity with increasing phase volume ratio.¹⁸ Further studies¹⁹ revealed that the viscosity increased for smaller mean droplet radii, which was found to be greater at higher internal phase ratios. The total interfacial area increases as droplet size decreases, so viscosity also increases, as more energy is required to deform the larger network of thin films.²⁰

2.2 Preparation and polymerization of HIPEs

2.2.1 Preparation and polymerization of continuous phase HIPEs

2.2.1.1 Preparation and polymerization of W/O polyHIPEs

The suspension polymerization technique is generally used for the preparation of macroporous copolymer networks in the form of beads of diameter ranging between 0.1 and 1.5 mm. First, a water insoluble monovinyl–divinyl monomer mixture containing a

free-radical initiator is mixed with an inert diluent. The inert diluent must usually be soluble in the monomer mixture but insoluble in the continuous phase of the suspension polymerization. The reaction mixture is then added into the continuous phase under agitation, so that it distributes in the form of droplets inside the continuous phase. The copolymerization and crosslinking reactions taking place in the monomer–diluent droplets result in the formation of beads having a glassy, opaque, or milky appearance. The beads are then extracted with a good solvent to remove the soluble polymers and the diluent from the network. Although the inert diluent must be soluble in the monomer mixture (organic phase) and insoluble in the continuous water phase, organized surfactant assemblies such as inverse micelles can be used to capture monomer-insoluble diluents such as water inside the organic phase. Thus, the crosslinking copolymerization in the continuous phase of a water-in-oil micro emulsion also yields macroporous networks.²¹⁻²³ The nature of the porous structure is largely dependent on the microstructure of the microemulsion.^{24,25} Short chain alcohols have been used as cosurfactants together with conventional surfactants for the formation of microemulsions.²⁶⁻²⁸

If water is added slowly to a stirred solution of a surfactant of low hydrophilic–lipophilic balance (HLB) dissolved in the oil phase, an internal phase volume of water up to 99% is achievable, and in this state, the water droplets in the oil phase strongly interact.²⁹ When the continuous oil phase is composed of a monovinyl–divinyl monomer mixture, the crosslinking polymerization in the continuous phase results in a solid crosslinked polymer which contains the water droplets.³⁰ Removal of the water droplets by washing with ethanol, and vacuum drying, yields a highly porous monolith of extremely low density (about 0.2 g/mL compared to 1.1 g/mL polymer).^{30,31} This porous material has an open pore structure indicating that there are holes in the walls separating the water droplets. Such porous materials are called polyHIPE (polymeric water-in-oil high internal phase emulsion) using the nomenclature devised by Unilever scientists.³⁰ They also discovered that the surfactant used to form the HIPEs must be of low HLB value (between 2 and 6), as would be expected for W/O emulsions.³² The optimum surfactant was sorbitan monooleate (Span 80), which has an HLB value of 4.3. However, the HLB number of the surfactant is not the only criterion for the preparation of stable HIPEs as the chemical nature was also found to be of importance.³³ The concentration of

the surfactant in the monomer phase was found to be critical to the formation of stable polymeric foam.³⁴ At least 4% surfactant, relative to the total oil phase, was required for polyHIPE formation, whereas formulations containing above 80% resulted in the formation of an unconnected or closed-cell material. Surfactant levels between 20 and 50% were deemed to be optimum at all internal phase volumes. Litt and coworkers³⁴ demonstrated that block copolymer surfactants can be used to prepare water-in-styrene HIPEs. From these, highly porous uncrosslinked polystyrene polyHIPE materials were synthesized.

A general procedure³⁰ for the synthesis of the extensively studied W/O styrene-DVB HIPE system involves the preparation of an aqueous HIPE phase by mixing styrene, DVB and a non-ionic surfactant at high rpm. Both water soluble (e.g. potassium persulphate) and oil-soluble (2,2'-azobisisobutyronitrile or AIBN) initiators were employed and polymerizations were carried out by heating the emulsion in a sealed plastic container for 24 hours at 50 °C. This yielded a solid crosslinked monolithic polymer material with the aqueous dispersed phase retained inside the porous microstructure. On exhaustive extraction of the material in a Soxhlet extractor with a lower alcohol followed by drying in vacuum, low-density polystyrene foam was produced with a permanent macroporous open-cellular structure of very high porosity.

The range of monomers, which can be employed, is largely dictated by the physical chemistry of the emulsion system. For instance, monomers must be sufficiently hydrophobic to allow the formation of stable W/O HIPEs. In addition, most systems studied have used polymerization methods requiring either an initiation step, or addition of a catalyst. The first step in the preparation of polymer is the preparation of HIPE without any significant degree of polymerization. Thus it can be seen that radical addition polymerization is suitable for the synthesis of polyHIPE polymers, whereas condensation polymerization can be more problematical. Also, the latter reactions often generate water as the by-product, making the aqueous component of HIPE to inhibit polycondensation.

2.2.1.2 Preparation and polymerization of O/W polyHIPEs

PolyHIPE materials have also been prepared by polycondensation in high internal phase emulsions.³⁵ Thus a resorcinol-formaldehyde porous copolymer was synthesised from an O/W HIPE of cyclohexane in an aqueous solution of resorcinol, formaldehyde

and surfactant. Addition of an acid catalyst to the emulsion followed by heating resulted in copolymerization. Other systems prepared included urea-formaldehyde, phenol-formaldehyde, melamine-formaldehyde and polysiloxane-based elastomeric species.³⁵

The resorcinol-formaldehyde polymers have been used to prepare highly porous carbon materials by controlled pyrolysis in an inert atmosphere.^{36,37} The microstructure of the carbon is an exact copy of the porous polymer precursor. Poly(methacrylonitrile) polyHIPE polymers have also been used for this purpose. These monolithic highly porous carbons are potentially useful in electrochemical applications particularly re-chargeable batteries and super-capacitors.

Open-cell polyHIPE materials have also been prepared from hydrophilic methacrylates which, on hydrolysis, yield hydrophilic polymethacrylic acid based species. Stable HIPEs containing high levels of glycidyl methacrylate can also be formed from which porous polymers can be made. These have considerable potential for further exploitation due to the reactive epoxide group.

2.2.1.3 Non-aqueous polyHIPEs

Non-aqueous or oil in oil (O/O) emulsions, where the phases are two immiscible organic liquids. Riess and coworkers^{38,39} have studied the stabilization of waterless systems with block and graft copolymers, where one of the liquids is a good solvent for one of the blocks and a non-solvent for the other, and vice versa. Sharma has published a considerable volume of work on non-aqueous emulsions involving ethylene glycol as the polar organic phase and either benzene⁴⁰ or chlorobenzene⁴¹ as the non-polar organic phase. The surfactants used were anionic or nonionic, low molecular weight materials. More recently, attention is focused on the formation of non-aqueous microemulsions,⁴² usually with formamide as the polar organic phase, and the first example of liposome formation in a non-aqueous solvent was reported.⁴³ The above emulsions were not highly concentrated.

Highly concentrated non-aqueous HIPE emulsions are used as safety fuels in military applications.⁴⁴ Here the emulsifier system used was a blend of two nonionics, with an optimal HLB value of 12. One of the most important factors was the solubility of the emulsifier in the continuous (formamide) phase. Thus, higher the surfactant solubility, the more stable will be the emulsion. The emulsifier concentration was also important.

The stability increased to a maximum and then decreased with an increase in surfactant concentration. Surprisingly, the HLB number did not appear to have much effect on the stability of the emulsions over the range studied (11 to 14). This was attributed to the high concentration of emulsifier in the continuous phase, although the narrow HLB value range is probably also a factor. The non-aqueous HIPEs showed similar properties to their water-containing counterparts. Examination by optical microscopy revealed a polyhedral, polydisperse microstructure.

2.2.2 Dispersed phase polyHIPEs

The dispersed phase of HIPEs may also be used to prepare polymeric materials. In this case, conversion of monomer dispersed droplets to polymer results in latexes or particulates. Lissant⁴⁵ prepared polymer particles by polymerization of HIPEs of vinyl chloride monomer in water. Concentrated emulsions with high phase volume ratios (above 0.9) gave agglomerates of particles with a relatively monodisperse size distribution. The particles themselves appeared to be hollow. The explanation given for this was that poly(vinyl chloride) is considerably more dense than vinyl chloride monomer. Since polymerization is probably initiated on the surface of the droplets, by a water-soluble initiator, polymer will grow until the surface is covered. This resulted in a rigid sphere encapsulating unreacted monomer. Polymerization will continue inside the shell with concomitant shrinkage until all the monomer is consumed resulting in hollow spheres. The presence of the rigid shell prevents additional initiator from reaching unreacted monomer resulting in the formation of a high molecular weight polymer. Using this method, synthesis of monodispersed polystyrene latexes are reported.^{46,47}

Copolymer particles can also be prepared from HIPEs.⁴⁸ Other latexes which have been produced by this method include poly(butyl methacrylate), poly(butyl acrylate) and poly(styrene/DVB).⁴⁹ Dispersed phase polymerization of HIPEs has also been used to prepare polymer-supported quaternary onium phase transfer catalysts.⁵⁰ Polyurethane/polypyrrole composites,⁵¹ poly(methyl methacrylate)/polypyrrole composite,⁵² polypyrrole /poly(ethylene-co-vinyl acetate), polyaniline/polystyrene⁵³ and polyaniline/poly(alkyl methacrylate)⁵⁴ composites were synthesized. A rubber-like copolymer/carbon fibre composite material has also been prepared.⁵⁵ Rubber-toughened polystyrene composites were obtained by polymerizing the dispersed phase of a

styrene/styrene-butadiene-styrene solution of O/W HIPE.⁵⁶ Kim and Ruckenstein⁵⁷ reported the preparation of polyacrylamide particles from a HIPE of aqueous acrylamide solution in a non-polar organic solvent. Crosslinked polyacrylamide latexes encapsulating microparticles of silica and alumina have also been prepared by this method.⁵⁸

2.2.3 Polymerization of both phase of polyHIPEs

If both continuous and dispersed phases of highly concentrated emulsions contain monomeric species, it is possible to obtain hydrophilic/hydrophobic polymer composite materials. Polyacrylamide/polystyrene composites have been prepared in this manner⁵⁹ from both W/O and O/W HIPEs containing aqueous acrylamide and a solution of styrene in an organic solvent. The composite materials have been used to form selective membranes for the separation of liquid mixtures.⁶⁰ Other hydrophilic/hydrophobic membranes have been generated from HIPEs of aqueous sodium acrylate solution in divinylbenzene.⁶¹ The emulsions were more stable than corresponding styrene-containing systems leading to more favourable membrane preparation. The mechanical properties of these membranes were improved by including a crosslinker, methylene bisacrylamide, in the aqueous phase, and by using a styrene/butyl acrylate mixture as the continuous phase.⁶² The styrene/butyl acrylate mixture had to be prepolymerized to low conversion to allow HIPE formation. The permeation rate of the membrane was improved by including a porogen (hexane) in the organic phase, generating a permanent porous structure.⁶³ Gelatin-poly(methyl methacrylate) composite materials can also be prepared through HIPE pathway.⁶⁴ Concentrated emulsions of methyl methacrylate in aqueous gelatin/surfactant solutions on polymerization at 50 °C yielded composite membrane materials. A comb-like polymer, possessing hydrophilic and hydrophobic side chains anchored to an amphiphilic backbone⁶⁵ was prepared. A quaternary ammonium and quaternary phosphonium monomers were copolymerized and used for this purpose.

2.3 Stability of HIPEs

A number of factors greatly influence the stability of HIPEs such as nature of the surfactant, concentration, nature of the continuous phase, temperature and the presence of salts in the aqueous phase. Ford and coworker⁶⁶ have studied HIPEs of water-in-xylenes, stabilized by a variety of surfactants, and postulated three properties which an emulsifier should possess in order to form stable W/O HIPEs of high volume fraction: a) a lowering

of the interfacial tension between water and oil phases, b) the formation of a rigid interfacial film and c) rapid adsorption at the interface. The most important factor was suggested to be the formation of a rigid film at the interface.

Gel emulsions of water/nonionic surfactant/oil systems⁶⁷ are either in the water-rich or oil-rich regions of the ternary phase diagrams, depending on the surfactant and system temperature. The latter parameter is important as a result of the property of nonionic surfactants known as the HLB temperature or phase inversion temperature. Below the phase inversion temperature, nonionic surfactants are water-soluble (hydrophilic and form O/W emulsions) whereas above the phase inversion temperature they are oil-soluble (hydrophobic and form W/O emulsions).

The HLB temperature was found to be the most important factor in the formation of stable emulsions. In each case, W/O polyHIPEs⁶⁷ would only form at temperatures above the HLB temperature of the systems, while O/W polyHIPEs⁶⁸ formed below the phase inversion temperature. The nature of the oil phase was also found to be of importance for the formation of stable W/O polyHIPEs⁶⁹.

Ruckenstein and coworkers⁷⁰ showed that the maximum volume of hydrocarbon, which could be incorporated in an O/W HIPE, increased with increasing surfactant concentration, presumably due to a concomitant decrease in the interfacial tension. Generally more hydrophobic is one phase and more hydrophilic is the other phase the more stable are the emulsions.⁷¹ Thus the greater the interfacial tension between oil and water phases in absence of surfactant, the greater will be the stability of HIPE.

The viscosity of the continuous phase was also found to affect the stability of highly concentrated emulsions.⁷² It was demonstrated that increasing the viscosity of the continuous phase, either by using a more viscous organic liquid (for W/O systems) or increasing the nonionic surfactant concentration (for O/W systems), gave low maximum volume fractions. Increasing temperature has the effect of decreasing emulsion stability.^{69,70} This is due to the increase of the rate of coalescence of the dispersed phase droplets with increasing thermal energy. Pons and coworkers⁷³ also noted that a temperature increase caused an increase in average droplet size due to increased interfacial tension.

Another process, which leads to HIPE instability, is gravitational syneresis or creaming, where the continuous phase drains from the thin films as a result of density differences between the phases. This produces a separated layer of bulk continuous phase and a more concentrated emulsion phase. The separated liquid can be located either above or below the emulsion, depending on whether the continuous phase is more or less dense respectively, than the dispersed phase. This process has been studied by Princen⁷⁴ who suggests that it can be reduced by a number of parameters including a high internal phase volume, small droplet sizes, a high interfacial tension and a small density difference between phases.

The addition of salts to the aqueous phase of concentrated emulsions can have profound effects on their stabilities. W/O HIPEs are generally stabilized by salt addition.^{14,67} However, the nature of the salt used was found to be important.⁷⁵ The interactions of the surfactant molecules at the oil/water interface increased due to dehydration of the hydrophilic ethylene oxide groups on addition of salt. This was verified experimentally⁷⁶ by an ESR method, which demonstrated that the surfactant molecules at the oil/water interface become more ordered if the salt concentration is increased. Salts in the aqueous phase are stabilized W/O HIPEs by two means. First the Ostwald ripening process is inhibited due to the decreased solubility of the aqueous solution in the continuous oil phase. Secondly, the attractive forces between adjacent aqueous droplets are lowered, as a result of the increase in refractive index of the aqueous phase towards that of the oil phase. When the refractive indices of the two phases are matched, the attractive forces are minimum and highly stable transparent emulsions are formed.

2.4 Morphology of polyHIPEs

It is now well understood that a phase separation during the formation of the network is mainly responsible for the formation of porous structures in a dried state. Major factors effecting formation of pores include effect of diluent, crosslinker, temperature and initiator.⁷⁷ In order to obtain macroporous structures, a phase separation must occur during the course of the crosslinking process so that the two-phase structure is fixed by the formation of additional crosslinks.⁷⁸ Depending on the synthesis parameters, phase separation takes place on a macro scale (macrosyneresis) or on a micro scale

(microsyneresis).⁷⁸ Macroporous networks usually have a broad pore size distribution ranging from 10-10⁴ Å. In general, macroporous copolymers refer to materials prepared in the presence of a pore forming agent and having a dry porosity, characterized by a lower density of the network due to the voids than that of the matrix polymer.⁷⁹

Another problem with the definition of macroporosity arises from the variation of the pore structure of the networks depending on their post treatment process.⁸⁰ A macroporous copolymer may become nonporous if it is first swollen in a good solvent and then dried at an elevated temperature. Subsequently the loss of porosity can be recovered by a solvent exchange procedure and the original swollen state porosity called maximum porosity can be preserved in the dried state. Because only the maximum porosity is a characteristic property for a given material, it is appropriate to define the macroporosity with respect to the maximum porosity.⁷⁷

IUPAC classification of pores based on the pore width as follows⁸¹

- a. Micropores have widths of up to 20 Å
- b. Mesopores have widths in the range 20–500 Å
- c. Macropores have widths greater than 500 Å

A typical pore size distribution of a styrene–divinylbenzene copolymer network prepared in the presence of a non-solvating diluent shows pores from a few tens of angstroms up to several thousands of angstroms in radius exist inside the macroporous material. Agglomerates of particles of various sizes inside the porous copolymer are responsible for this broad size distribution of pores. The pores are, in fact, irregular voids between agglomerates, which are typically interconnected.⁸² The formation process of the porous structure can be divided into three stages.⁸³

- a. The smaller particles called nuclei are about 10² Å in diameter. The nuclei are nonporous and constitute the highly crosslinked regions of the network. Micropores defined with widths of up to 20 Å appear between the nuclei.
- b. The agglomerations of nuclei are called microspheres and they are about 10³ Å in diameter. Mesopores constitute the interstices between the microspheres.
- c. Microspheres are agglomerated again into larger irregular moieties of 2500-10,000 Å inside the polymer material. Meso and macropores appear between the agglomerates of the microspheres.⁸⁴

Williams^{7,85} discovered that the surfactant level had a profound effect on the cellular structure of polyHIPE materials. Below a surfactant concentration of 5%, the polymers produced had a closed-cell structure. The aqueous phase in this material remained trapped inside the structure, resulting in a high density polymer. Above a surfactant concentration of 7%, open-cell foam was produced with an entirely interconnected microstructure. The aqueous phase could easily be removed yielding a dry, low density polymer matrix. Surprisingly, the surfactant concentration was found to be more important than the phase volume in determining the final cellular structure. A material prepared from a HIPE of as much as 97% internal phase volume and 5% surfactant still gave a closed-cell polymer.

Williams and coworkers⁸⁶ investigated the effect of variation of the DVB content of the monomer phase on the cellular structure of the resulting foam. The phase volume and surfactant and initiator concentrations were kept constant while the DVB content was increased from 0 to 100% which caused a drop in average cell size from 15 μm to 6 μm . Sherrington and coworkers⁸⁷ produced polyHIPE materials with an additional porous structure within the walls of the macro cells. It was observed that an increase in high internal phase volume with chlorobenzene as porogen resulted in a decrease in surface area.⁸⁸ The internal phase volume ratio can have a profound influence on the surface area.^{89,90}

2.5 Properties of polyHIPEs

PolyHIPE materials possess novel properties as a result of their unique cellular structure. Referring specifically to open-cell polymers, they are characterized by a very low dry bulk density, typically less than 0.1 g/cm^3 , due to their highly porous and interconnected structure. The cell sizes can range from 5 to 100 μm , surface areas of less than $10 \text{ m}^2 \text{ g}^{-1}$. The addition of porogen can lead to high surface area and will possess low bulk density ($< 0.1 \text{ g/cm}^3$) and very high pore volumes which can go even above 90%.⁸⁸ Another important property of open-cell PolyHIPE materials is their ability to absorb large quantities of solvent by capillary action.⁹² Simply immersing a piece of the material in the liquid causes absorption with displacement of the air from inside the matrix. This occurs until all voids are filled.

2.6 Applications

PolyHIPEs has been found to be successful in various applications. The applications include uniform functionalized monoliths as precursors to supported species,⁹³ in solid phase peptide synthesis,⁹⁴ as sulphonated materials for superadsorbents,⁹⁵ as monolithic support for heterogenous catalysis,⁹⁶⁻⁹⁸ as amine and free radical scavenger in chromatographic processes,⁹⁹⁻¹⁰¹ monolithic solid phase acid catalyst,¹⁰² ion exchange resins,¹⁰³ as detergents,¹⁰⁴ for immobilization of cells¹⁰⁵ and enzymes,^{106,107} in agricultural sprays,¹⁰⁸ in cosmetic compositions,¹⁰⁹⁻¹¹¹ for transport of flammable liquids,³⁰ in electrochemical applications,^{112,113} as support for conducting polymers,¹¹⁴ as monoliths for heavy metal separation,¹¹⁵⁻¹¹⁷ as (interpenetrating networks)IPN's,¹¹⁸ as porous carbon precursors,³⁶ as elastomeric materials,^{119,120} as polycondensation materials of high thermo oxidative stability,^{121,122} in biotechnological and biomedical applications,¹²³ in invitro application including tissue engineering,¹²⁴⁻¹²⁸ for recovery of oil from tar and oil sands,¹²⁹ as safety fuel for military applications^{44,130} and as membrane filters for removing particulates from aerosols.¹³¹

O/W HIPEs can be used as detergents.¹⁰⁴ Grease can be removed from a surface by dissolution in the internal oil phase; the aqueous surfactant solution then wets the surface, preventing the oil from returning to the surface and allowing it to be rinsed with water. The same principle can be applied to remove soil from fabrics by using O/W HIPEs.

Applications in physics include formation of a silver film on the interior of PolyHIPE polymers, with a view to producing materials with good thermal insulation. PolyHIPE foams have also found uses in high energy physics experiments, such as inertially confined fusion.¹³² High density polymers are prepared by impregnating open-cell poly(styrene/DVB) polyHIPE with a heptane solution of styrene, DVB and AIBN, followed by polymerisation.¹³³ Upon drying, a composite material of higher density is obtained. Another use for polystyrene PolyHIPE materials was suggested by Williams and coworkers and involves the intact capture of microparticles of cosmic dust.¹³⁴ Poly(styrene/DVB) PolyHIPE materials have also been employed as supports for conducting polymers.¹³⁵⁻¹³⁷

2.7 References

- [1] D. Barby, Z. Haq., *U.S. Patent 4522953* (1985).
- [2] E. Ruckenstein, *Adv. Polym. Sci.*, **127**, 1 (1997).
- [3] K.J. Lissant., *Emulsions and Emulsion Technology, Part 1, Marcel Dekker, New York, Chap. 1* (1974).
- [4] W. Ostwald., *Kolloidz* **6**, 103 (1910).
- [5] A. Barbetta, N. R. Cameron, S. J. Cooper., *Chem. Commun.* **3**, 221 (2000).
- [6] D. Gregory, M. Sharples, I. M. Tucker, *European Patent 299762* (1989).
- [7] N.R.Cameron., *Polymer* **46**, 1439 (2005).
- [8] K.J. Lissant., *J. Coll. Interf. Sci.* **22**, 462 (1966).
- [9] K.J. Lissant., *J. Soc. Cosmetic. Chem.* **21**, 141 (1970).
- [10] K.J. Lissant, K.G. Mayhan., *J. coll. Interf. Sci.* **42**, 201 (1973).
- [11] H.M. Princen., *Langmuir* **4**, 486 (1988).
- [12] J.C. Ravey, M.J. Stebe., *Progr. Coll. Polym. Sci.* **82**, 218 (1990).
- [13] C. Solans, J.G. Dominguez, J.L. Parra, J. Heuser, S.E. Friberg., *Coll. Polym. Sci.* **266**, 570 (1992).
- [14] R. Pons, C. Solans, M.J. Stebe , P. Erra, J.C. Ravey., *Prog. Coll. Polym. Sci.* **89**, 110 (1992).
- [15] C. Solans, R. Pons, S. Zhu, H.T. Davis, D.F. Evans, K. Nakamura, H. Kunieda., *Langmuir* **9**, 1479 (1993).
- [16] H. Hoffmann., *Adv. Coll. Interf. Sci.* **32**, 123 (1990).
- [17] H.M. Princen., *J. Coll. Interf. Sci.* **71**, 55 (1979).
- [18] R. Pal, E. Rhodes., *J. Coll. Interf. Sci.* **107**, 301 (1985).
- [19] A.K. Das, D. Mukesh, V. Swayambunathan, D.D. Kotkar, P.K. Ghosh., *Langmuir* **8**, 2427 (1992).
- [20] Y. Otsubo, R.K. Prudhomme., *Rheol. Acta* **33**, 101 (1994).
- [21] F.M. Menger, T. Tsuno, G.S. Hammond., *J. Am. Chem. Soc.* **112**, 1263 (1990).
- [22] J.O. Stoffer, T. Bone., *J. Dispersion Sci. Technol.***1**, 393 (1980).
- [23] M. Sasthav, W.R.P. Raj, H.M. Cheung., *J. Coll. Inter. Sci.***152**, 376 (1992).
- [24] E. Haque, S. Qutubuddin., *J. Polym. Sci. Polym. Lett.* **26**, 429 (1988).
- [25] M. Sasthar, H.M. Cheung., *Langmuir* **7**, 1378 (1991).

- [26] J.S. Guo, M.S. El-Aasser, J.W. Vanderhoff., *J. Polym. Sci. Polym. Chem.* **27**, 691 (1989).
- [27] A. Jayakrishna, D.O.Shah., *J. Polym. Sc. Polym. Lett.* **22**, 31 (1984).
- [28] F. Candau., In: H.F. Mark, N.M. Bikales, C.G. Overberger, G. Menges, Editors., *Encyclopedia of polymer science and engineering*, Wiley, New York **9**, 718 (1987).
- [29] D.H. Smith., *J. Coll. Interf. Sci.* **108**, 471 (1985).
- [30] D. Barby, Z. Haq., *European Patent* 0,060,138 (1982).
- [31] D.C. Sherrington., *Makromol. Chem. Macromol. Symp.* **70/71**, 303 (1993).
- [32] D. Barby, Z. Haq., *European Patent* 68830 B1 (1982).
- [33] J.M. Williams., *Langmuir* **7**, 1370 (1991).
- [34] M.H. Litt, B.R. Hsieh, I.M. Krieger, T.T Chen, H.L. Lu., *J. Coll. Interf. Sci.* **115**, 312 (1987).
- [35] A.R. Elmes, K.Hammond, D.C.Sherrington., *European Patent Appl.* 0289238 (1988).
- [36] W. R. Even Jr., D. P. Gregory., *MRS Bull.* **19**, 29 (1994).
- [37] C.J.C. Edwards, D.A. Hitchen, M. Sharpies., *U.S. Patent* 4755655 (1988).
- [38] J.Periard, A. Branderet, G.Riess., *J. Polym. Sci. Polym. Lett.* **8**, 109 (1970).
- [39] G. Riess., *Makromol. Chem. Suppl.* **13**, 157 (1985).
- [40] M.K. Sharma., *Prog. Coll. Polym. Sci.* **63**, 75 (1978).
- [41] M.K. Sharma., *Prog. Coll. Polym. Sci.* **63**, 87 (1978).
- [42] H.D. Dorfler, C. Swaboda., *Coll. Polym. Sci.* **271**, 586 (1993).
- [43] A. Meliani, E. Perez, I. Rico, A. Lattes, A. Moisand., *New J. Chem.* **15**, 871 (1991).
- [44] A. Beerbower, J. Nixon, T.J. Wallace., *J. Aircraft* **5**, 367 (1968).
- [45] K.J. Lissant, B.W. Pearce, S.H. Wu, K.G. Mayhan., *J. Coll. Interf. Sci.* **47**, 416 (1974).
- [46] E. Ruckenstein, K.J. Kim., *J. Appl. Polym. Sci.* **36**, 907 (1988).
- [47] F. Sun, E. Ruckenstein., *J. Appl. Polym. Sci.* **48**, 1279 (1993).
- [48] E. Ruckenstein, K.J. Kim., *J. Polym. Sci. Pt. A. Polym. Chem.* **27**, 4375 (1989).
- [49] E. Ruckenstein, J.S.Park., *Polymer* **31**, 2397 (1990).
- [50] L.Hong, E. Ruckenstein., *Polymer* **33**, 1968 (1992).
- [51] E. Ruckenstein, J.H. Chen., *Polymer* **32**, 1230 (1991).

- [52] E. Ruckenstein, S. Yang., *Polymer* **34**, 4655 (1993).
- [53] E. Ruckenstein, S. Yang., *Synth. Metals* **53**, 283 (1993).
- [54] S. Yang, E. Ruckenstein., *Synth. Metals* **59**, 1 (1993).
- [55] E. Ruckenstein, L.Hong., *J. Appl. Polym. Sci.* **53**, 923 (1994).
- [56] H.Li, E. Ruckenstein., *J. Appl. Polym. Sci.* **52**, 1949 (1994).
- [57] K.J.Kim, E. Ruckenstein., *Macromol. Chem. Rapid Commun.* **9**, 285 (1988).
- [58] J.S.Park, E. Ruckenstein., *Polymer* **31**, 175 (1990).
- [59] E. Ruckenstein, J.S.Park., *J. Polym. Sci. Polym. Lett.* **26**, 529 (1988).
- [60] E. Ruckenstein., *Coll. Polym. Sci.* **267**, 792 (1989).
- [61] H.H.Chen, E. Ruckenstein., *J. Appl. Polym. Sci.* **42**, 2429 (1991).
- [62] F.Sun, E. Ruckenstein., *J. Memb. Sci.* **81**, 191 (1993).
- [63] F.Sun, E. Ruckenstein., *J. Memb. Sci.* **85**, 59 (1993).
- [64] G.Xu, E. Ruckenstein., *J. Appl. Polym. Sci.* **46**, 683 (1992).
- [65] E. Ruckenstein, L. Hong., *Macromol.* **26**, 1363 (1993).
- [66] R.E. Ford, C.G.L. Furnidge., *J. Coll. Interf. Sci.* **22**, 331 (1966).
- [67] C. Solans, N. Azemar, J.L. Parra., *Prog. Coll. Polym. Sci.* **76**, 224 (1988).
- [68] H. Kunieda, D.F. Evans, C. Solans, M. Yoshida., *Coll. Surf.* **47**, 35 (1990).
- [69] H. Kunieda, C. Solans, N. Shida, J.L. Parra., *Coll. Surf.* **24**, 225 (1987).
- [70] E. Ruckenstein, G. Ebert, G.Platz., *J. Coll. Interf. Sci.* **133**, 432 (1989).
- [71] H.H. Chen, E. Ruckenstein., *J. Coll. Interf. Sci.* **138**, 473 (1990).
- [72] H.H. Chen, E. Ruckenstein., *J. Coll. Interf. Sci.* **145**, 260 (1991).
- [73] R. Pons, J.C. Ravey, S. Sauvage, M.J. Stebe, P. Erra , C. Solans., *Coll. Surf.* **76**, 171 (1993).
- [74] H.M. Princen., *J Coll. Interf. Sci.* **134**, 188 (1990).
- [75] H. Kunieda, N. Yano, C. Solans., *Coll. Surf.* **36**, 313 (1989).
- [76] V. Rajagopalan, C. Solans, H. Kunieda., *Coll. Polym. Sci.* **272**, 1166 (1994).
- [77] O.Okay., *Prog. Polym. Sci.* **25**, 711 (2000).
- [78] J. Seidl, J. Malinsky, K. Dusek, W. Heitz., *Adv. Polym. Sci.* **5**, 113 (1967).
- [79] K. Dusek., In: E.N. Haward, Editor. *Developments in polymerization, Applied Science, London* **3**,143 (1982).
- [80] K. Haupke, G. Schwachula., *Plaste und Kautschuck* **2**, 48 (1985).

- [81] K.S.W. Sing, D.H. Everett, R.A.W. Haul, L. Moscou, R.A. Pierotti, J. Rouquerol, T.Siemieniewska., *Pure Appl. Chem.* **57**, 603 (1985).
- [82] D.C. Sherrington, P. Hodge., *Syntheses and separations using functional polymers.* Wiley, New York (1989).
- [83] H. Jacobelli, M. Bartholin, A. Guyot., *J. Appl. Polym. Sci.* **23**, 927 (1979).
- [84] C.M. Cheng, F.J. Micale, J.W. Vanderhoff, M.S. El-Aasser., *J. Coll. Interf. Sci.* **150**, 549 (1992).
- [85] J.M. Williams, D.A. Wroblewski., *Langmuir* **4**, 656 (1988).
- [86] J.M. Williams, A.J. Gray, M.H. Wilkerson., *Langmuir* **6**, 437 (1990).
- [87] P. Hainey, I.M. Huxham, B. Rowatt, D.C. Sherrington, L. Tetley., *Macromol.* **24**, 117 (1991).
- [88] A. Barbetta, N.R. Cameron., *Macromol.* **37**, 3188 (2004).
- [89] H. Zhang, A. I. Cooper., *Chem. Mater.* **14**, 4017 (2002).
- [90] Y.Sergienko, H. Tai, M. Narkis, M. S. Silverstein., *J. Appl. Polym. Sci.* **94**, 2233 (2004).
- [91] N.R. Cameron, A. Barbetta., *J. Mater. Chem.* **10**, 2466 (2000).
- [92] T.A. DesMarias, K.J. Stone, J.C. Dyer, B. Hird, S.A. Goldman, M.R. Peace, Seiden *PCT Patent 9621680 A1* (1996).
- [93] N. R. Cameron, D. C. Sherrington, I. Ando and H. Kurosu., *J. Mater. Chem.* **6**, 719 (1996).
- [94] P.W. Small, D.C. Sherrington., *J. Chem. Soc. Chem. Commun.* 1589 (1989).
- [95] Z. Haq., *U.S. Patent. 4536521* (1985).
- [96] S. Sotiropoulos, I. J. Brown, G. Akay, E. Lester., *Mater. Lett.* **35**, 383 (1998).
- [97] H. F. M. Schoo, G. Challa, B. Rowatt, D. C. Sherrington., *React. Polym.* **16**, 125 (1992).
- [98] E. Ruckenstein, L. Hong., *Chem. Mater.* **4**, 122 (1992).
- [99] P. Krajnc, N. Leber, D. Stefanec, S. Kontrec, A. Podgornik., *J. Chrom. A* **1065**, 69 (2005).
- [100] L. Moine, H. Deleuze, B. Maillard., *Tetrahedon Lett.* **44**, 7813 (2003).
- [101] A. Desforges, M. Arpontet, H. Deleuze, O. M. Monval., *React. Funct. Polym.* **53**, 183 (2002).

- [102] M. Ottens, G. Leene, A. Beenackers, N. Cameron, D. C. Sherrington., *Ind. Eng. Chem. Res.* **39**, 259 (2000).
- [103] R. J. Wakeman, Z. G. Bhumgara, G. Akay, *Chem. Eng. J. (Lausanne)*. **70**, 133 (1998).
- [104] N.R. Cameron, R.C. Sherrington., *Adv. Polym. Sci.* **126**, 199 (1996).
- [105] E. Ruckenstein, X. B. Wang, *Biotechnol. Bioeng.* **44**, 79 (1994).
- [106] E. Ruckenstein, X. Wang, *Biotechnol. Bioeng.* **42**, 821 (1993).
- [107] S.J. Peirre, J.C. Thies, A. Dureault, N.R. Cameron, J.C.M. Van Hest, N. Carette, T. Michon, R. Weberskirch., *Adv. Mater.* **18**, 1822 (2006).
- [108] K.J. Kim, E. Ruckenstein., *J. Appl. Polym. Sci.* **38**, 441 (1989).
- [109] Z. Ma, P.H. Neill, L.M. Brandt, A.A. Scafidi, B. Nogaj, G.P. Newell., *US Patent 6685952 B1* (2004).
- [110] I.R. Cox, Z. Haq., *European Patent 154465 B1* (1991).
- [111] C.I.Park, W.G. Cho, S. J. Lee., *Korea Australia Rheol. J.* **15**, 125 (2003).
- [112] I.J. Brown, S. Sotiropoulos., *Electrochim. Acta* **46**, 2711 (2001).
- [113] P.J. Blood, I.J. Brown, S. Sotiropoulos., *J. Appl. Electrochem.* **34**, 1 (2004).
- [114] E. Ruckenstein, J.S. Park., *J. Appl. Polym. Sci.* **42**, 925 (1991).
- [115] B. C. Benicewicz, G. D. Jarvinen, D. J. Kathios, B. S. Jorgensen, *J. Radioanal. Nucl. Chem.* **235**, 31 (1998).
- [116] S. D. Alexandratos, R. Beauvais, J. R. Duke and B. S. Jorgensen, *J. Appl. Polym. Sci.* **68**, 1911 (1998).
- [117] Z.A. Katsoyiannis, A.I. Zounboulis., *Water Res.* **36**, 5141 (2002).
- [118] H.Tai, A.Sergienko, M.S.Silverstein., *Polym. Eng. Sci.* **41**, 1540 (2001).
- [119] C. J. C. Edwards, D. P. Gregory, M. Sharples., *U.S. Patent 4788225* (1988).
- [120] N. R. Cameron, D. C. Sherrington., *J. Mater. Chem.* **7**, 2209 (1997).
- [121] N. R. Cameron, D. C. Sherrington., *Macromol.* **30**, 5860 (1997).
- [122] M. A. Hoisington, J. R. Duke, P. G. Apen, *Polymer* **38**, 3347 (1997).
- [123] H.P. Hentze, M. Antonietti., *Rev. Molecular Biotechnology* **90**, 27 (2002).
- [124] W. Busby, N.R. Cameron, C.A.B. Jahoda., *Polym. Int.* **51**, 871 (2002).
- [125] V. Karageorgiou, D. Kaplan., *Biomaterials* **26**, 5474 (2005).
- [126] G. Akay, M.A. Birch, M.A. Bokhari., *Biomaterials* **25**, 3991 (2004).

- [127] M.A. Bokhari, G. Akay, S. Zhang, M.A. Birch., *Biometaterials* **26**, 5198 (2005).
- [128] M.W. Hayman, K.H. Smith, N.R. Cameron, S.A. Przyborski., *J. Biochem. Biophys. Methods* **62**, 231 (2005).
- [129] F. Sebba, *Chem. Ind. (London)* **10**, 367 (1984).
- [130] J. Nixon, A. Beerbower., *Am. Chem. Soc. Div. Petrol. Chem. Prepr.* **14**, 49 (1969).
- [131] G. Akay, Z. Bhumgara, R. J. Wakeman., *Chem. Eng. Res. Des.* **73**, 782 (1995).
- [132] J.M. Williams, *Langmuir* **4**, 44 (1988).
- [133] J.M. Williams, M.H. Wilkerson., *Polymer* **31**, 2162 (1990).
- [134] J.M Williams, D.A. Wroblewski., *J. Mat. Sci. Lett.* **24**, 4062 (1989).
- [135] E. Ruckenstein, J.S. Park., *Polym. Comp.* **12**, 289 (1991).
- [136] E. Ruckenstein, J.H. Chen., *J. Appl. Polym. Sci.* **43**, 1209 (1991).
- [137] E. Ruckenstein, J.S. Park., *Synth. Metals* **44**, 293 (1991).

Aims and objectives

3 Aims and objectives

Acrylates form a major workhorse in surface coating industry. Photopolymerization is the preferred choice of process to cure photopolymerizable compositions. This process also offers advantages of short cure time, faster throughput and curing of intricate shapes of articles where photocurable compositions are applied. A typical photocurable composition is a formulation comprising of acrylate based oligomers with a polyether, polyester or a polyurethane backbone, one or more photoinitiators as well as optionally monoacrylate based reactive diluent and/or multifunctional crosslinkers. Other additives such as radical scavengers as well as UV stabilizers and dyes can be added to the composition as per the application requirement.

Various photopolymerizable oligourethane based macromonomers are to be synthesized and subjected to photopolymerization in presence of different photo initiators. The photopolymerizable macromonomers would consist of certain soft segmented as well as hard segmented acrylate based macromonomers. The soft segment can be imparted in the macromonomer by using polyols / low molecular weight elastomers as one of the components in the synthesis process. The poly glycols that can be used include polyethylene glycols, polypropylene glycols and polytetrahydrofurans of varying molecular weights ranging from 200 to 3000. Low molecular weight elastomer of choice is hydroxy terminated polybutadiene. The hard segmented macromonomers during formulation has to be mixed with excess of di or trifunctional acrylate as a crosslinker (which can also act as a reactive diluent) so as to provide an optimum viscosity to the composition. The hard segments can be imparted easily by using low molecular weight bifunctional molecules as components in the synthesis process. They include isocyanates like isophorone diisocyanate, and toluene-2,5-diisocyanate and diols such as cyclohexane-1,4-dimethanol. The kinetics of photopolymerization needs to be evaluated by noting induction time, peak maximum time, rate of photopolymerization as well as the percentage conversions using photo DSC equipment. The analyses would be done using a polychromatic radiation emerging from a dual light guide system. Studies at different isothermal conditions have to be carried out. Compositions have to be made with varying concentration of photo initiator. In addition to reactive diluents, effects of added free radical scavenger on the composition have to be studied for certain systems. Soft

segmented polyols have to be used as components in the synthesis of certain systems as it can impart viscous liquid nature to the synthesized macromonomer. These oligourethane acrylates are expected to be stable and free flowing.

Other types of oligourethane acrylate macromonomers to be studied include hard segmented systems involving alicyclic as well as bis aromatic based linear oligourethane acrylates. Bis aromatic systems are highly rigid and hence have to be made moderately flexible to obtain photopolymerizable oligomers. The hard segmented bis aromatic molecules which can be used include 4,4'-bisphenol A, 4,4'-bisphenol S, 4,4'-dihydroxy biphenyl and similar molecules. For this purpose, these molecules need to be subjected to chain extension with ethylene carbonate or propylene carbonate to obtain the diethylenated or dipropylenated bis aromatic diols. These diols thus obtained can be used for reacting with excess of diisocyanates and subsequently with hydroxyl acrylates to obtain oligourethanes acrylates with bis aromatic moieties in the backbone. These hard segmented oligomers have to be formulated with reactive diluents in addition to photo initiators so as to enable them to photopolymerize efficiently. Studies at different isothermal conditions/intensity will be carried out. The photocuring kinetics as well as the applicability of variable autocatalytic kinetic model needs to be evaluated for all the formulations.

Photopolymerization of high internal phase emulsions (HIPEs) using acrylates with non-polar moieties and with high concentration of aqueous phase would be carried out using an external irradiation source. A 400W medium pressure mercury vapor lamp can be used at a constant irradiation distance. The photopolymerizations have to be carried out at a predetermined interval of time up to a period for each system. Polymerization reactions have to be quenched in liquid nitrogen and the residual monomers have to be subsequently extracted in a suitable solvent. A GC protocol has to be developed for the quantitative estimation of residual monomers remaining after photopolymerization process from which the percentage monomer conversion can be estimated.

Photopolymerization of certain multiacrylate based monomers would be evaluated. One approach involves reaction of hydroxyl multiacrylates such as pentaerythritol triacrylate as an end capping agent to a diisocyanate terminated

prepolymer to obtain a linear multiacrylate. Second approach involves reaction of di or trihydroxy acrylates to a diisocyanate terminated prepolymer to obtain branched multiacrylates. The dihydroxy acrylates such as glycerol-1,3-diglycerolate diacrylate and trihydroxy acrylates such as propylene glycol glycerolate diacrylate can be used for the purpose. The synthesized multiacrylates are to be photopolymerized with varying concentration of photoinitiators under different isothermal conditions. The photocuring kinetics of multiacrylates has to be calculated. The applicability of variable autocatalytic kinetic model needs to be evaluated for all the formulations.

Certain monomers will be considered for the synthesis of co- as well as terpolymers based on HIPEs. The monomers of choice include 2,3-epithiopropyl methacrylate, glycidyl methacrylate and styrene along with suitable crosslinkers. The use of suitable surfactants needs to be tested followed by HIPE polymerization to obtain polyHIPE beads. The polymeric beads would be subjected to functionalization to obtain a sulphonic acid or/and thiol groups for evaluation as heterogeneous catalyst. The beaded catalysts need to be evaluated for morphological and physico-chemical characterization studies. The acid exchange values of the prepared catalysts are to be established. The catalytic efficiency of the catalysts needs to be evaluated for acid phase condensation reactions. The analyses of acid phase condensation reactions will be carried out using a HPLC protocol with pure products as standards. The efficacies of the prepared catalysts need to be compared with a commercial one such as Amberlyst 15.

Photopolymerization of mono and
diacrylate based monomers

This chapter is divided into three parts. Part A deals with the synthesis, photopolymerization and estimation of kinetic parameters of aliphatic and cycloaliphatic based urethane (meth)acrylates while part B deals with aromatic urethane (meth)acrylates. Part C deals with the UV assisted photopolymerization of high internal phase emulsions.

PART – A

Dihydroxy terminated linear soft segmented compounds such as polyethylene glycol, polypropylene glycol and polytetrahydrofuran of varying molecular mass were treated with excess aliphatic and alicyclic diisocyanates such as hexamethylene diisocyanate and isophorone diisocyanate and subsequently with hydroxyl acrylates to obtain photopolymerizable macromonomers. These transparent and viscous soft segmented urethane acrylates were formulated with excess amount of end capping agent as reactive diluent and photoinitiators with different weight proportions prior to photopolymerization studies. The photocuring kinetics including rate and conversion profiles and other kinetic parameters were computed using photo DSC. The photocuring kinetics and kinetic parameters based on autocatalytic kinetic model was computed from the photo DSC cure curves.

PART – B

Dihydroxy bis aromatic compounds such as 4,4'-bisphenol A, 4,4'-bisphenol S and 4,4'-dihydroxy biphenyl being rigid were subjected to chain extension using ethylene or propylene carbonate to obtain chain extended bis aromatic monomers. These chain extended monomers were then treated with excess diisocyanates and subsequently with hydroxyl acrylates to obtain photopolymerizable macromonomers. Unlike aliphatic soft segmented urethane acrylates based on polyols, bis aromatic based urethane acrylate macromonomers were found to be highly viscous. Hence excess amount of end capping agent was added to the system as reactive diluent prior to photopolymerization studies resulting in optimum viscosity formulations. The photocuring kinetics and kinetic parameters based on autocatalytic kinetic model were computed.

PART – C

Water in oil HIPes in which the oil phase is composed of mono acrylate monomers and crosslinker were prepared and subjected to photopolymerization studies. The photoinitiators of choice were acetophenone and phosphine oxide types. Photopolymerization was attempted for maximization of monomer conversion at short reaction times. The process involves usage of an external UV lamp source at a definite distance from the source under constant flux and ambient conditions. HIPE polymerization of 2-ethylhexyl acrylate (EHA) and 2-ethylhexyl methacrylate (EHMA) with ethylene dimethacrylate (EGDMA) as crosslinker were carried out using different photoinitiators. The extents of conversion were computed by residual monomer analyses using gas chromatography.

Photopolymerization of aliphatic and
cycloaliphatic based di(meth)acrylate
monomers

4.1 PART – A: Photopolymerization of aliphatic and cycloaliphatic based di(meth)acrylate monomers

4.1.1 Experimental

4.1.1.1 Materials

Polyethylene glycol 200, 400 and 600 (SD fine), Polypropylene glycol 725 and 3000 (Aldrich), polytetrahydrofuran 650 (Aldrich), hydroxy terminated polybutadiene 2750 (VSSC-Thiruvananthapuram), isophorone diisocyanate (Fluka), hexamethylene diisocyanate (Fluka), cyclohexane-1,4-dimethanol (Fluka), 2-hydroxyethyl acrylate (Aldrich), 2-hydroxyethyl methacrylate (Fluka), hydroxy propyl acrylate (Aldrich), poly(ethylene glycol) methacrylate (Aldrich), neopentyl glycol propoxylate diacrylate (Aldrich), trimethylolpropane triacrylate (Aldrich), dibutyl tin dilaurate (Aldrich), 1,4-diazabicyclo[2.2.2]octane (Aldrich), 2,2,6,6-tetramethylpiperidinoxyl radical or TEMPO (Aldrich), hydroquinone monomethyl ether (Fluka) and chloroform (Merck) were used as received.

Commercial photoinitiators belonging to different class were procured from Aldrich and used as received. Detailed description of the photoinitiators used and their physical properties are given in Tables 4.1 and 4.2.^{1,2}

Table 4.1 Photoinitiators used for curing studies

No.	Commercial name	Code used	Chemical class	Chemical name	Main use
1	IRGACURE 651	IRG 651	Benzil-dialkyl ketal	2,2-Dimethoxy-2-phenyl acetophenone	Wood, PCB, printing plates
2	DAROCUR TPO / LUCIRIN TPO	IRG TPO	Acyl phosphine oxide	Diphenyl-(2,4,6-trimethyl benzoyl) phosphine oxide	General through cure - pigmented inks.
3	IRGACURE 184	IRG 184	α -hydroxy ketone	1-Hydroxy cyclohexyl phenyl ketone	General surface - non yellowing cure
4	IRGACURE 2959	IRG 2959	α -hydroxy ketone	2-Hydroxy-4'-(2-hydroxy ethoxy)-2-methyl propiophenone	Clear coats
5	DAROCUR 1173	DAR 1173	α -hydroxy ketone	2-Hydroxy-2-methyl propiophenone	-
6	DAROCUR MBF / GENOCURE MBF	MBF	Phenyl glyoxylate	Methyl benzoyl formate	Labelling free
7	IRGACURE 907	IRG 907		2-Methyl-4'-(methyl thio)-2-morpholino propiophenone	-
8	IRGACURE 819	IRG 819	Acyl phosphine oxide	Phenyl bis (2,4,6-trimethyl benzoyl) phosphine oxide	UV absorber containing exterior coatings

Table 4.2 Physical properties of photoinitiators used in curing studies

No.	Commercial name	Physical state	Φ_{α}	E_T (kJ/mol)	τ_T (nano sec)	In acetonitrile ¹ (most prominent)		In methanol ² (all absorptions)*
						λ_{\max} (nm)	ϵ (L mol ⁻¹ sec ⁻¹)	λ (nm)
1	IRGACURE 651	Solid	0.57	278	< 0.1	252	12800	250, 340
2	DAROCUR TPO / LUCIRIN TPO	Solid	0.5-0.56	263	0.08-0.1	380	525	295, 368, 380, 393
3	IRGACURE 184	Solid	-	-	-	243	10000	246, 280, 333
4	IRGACURE 2959	Solid	0.29	295	13	272	16200	276
5	DAROCUR 1173	Liquid	0.3-0.38	298	30	243	10900	245, 280, 331
6	DAROCUR MBF / GENOCURE MBF	Liquid	-	-	-	254	11200	255, 325
7	IRGACURE 907	Solid	0.88	256	10	303	18600	230, 304
8	IRGACURE 819	Solid	-	233	0.47	369	933	295, 370

* Higher energies denote allowed transitions while lower energies denote forbidden transitions.

Φ_{α} – Quantum yield for α -scission

E_T - Triplet energy

τ_T – Triplet lifetime

4.1.1.2 Measurements

4.1.1.2.1 Infrared spectroscopy

The infrared (IR) spectroscopic analyses were carried out using a Perkin Elmer (Spectrum 1) infrared spectrophotometer. The analyses of prepolymers and macromonomers were carried out from 400 to 4000 cm⁻¹. The analyses were done using a thin layer of material placed in between a pair of sodium chloride cell.

4.1.1.2.2 Nuclear magnetic resonance spectroscopy

The structural elucidation of the synthesized prepolymers and macromonomers were carried out using a Bruker 500 MHz nuclear magnetic resonance (NMR) spectrophotometer. Both ¹H and ¹³C NMR spectra were recorded. Distortionless enhancement by polarization transfer (DEPT) technique was used in assigning the nature of carbon-hydrogen absorptions.

4.1.1.2.3 Vapour pressure osmometry

The molecular mass of the synthesized macromonomers were evaluated using a vapour pressure osmometer. A K-7000 vapour pressure osmometer (Knauer, Germany) was used to calculate the M_n of the synthesized macromonomers. The vapour pressure osmometer (VPO) was initially calibrated using benzil. Accurately weighed (about 0.5g)

of the oligomer was solvated in a 10 mL standard flask using HPLC grade tetrahydrofuran or chloroform. Exactly 5 mL of the made up solution was pipetted out using a 5 mL calibrated pipette in to another 10 mL standard flask and made up to the mark using the solvent. Further two more series of dilutions were made. The solvent as well as the polymer at different concentrations was carefully added to the thermister and the readings were noted. The ratio of the slope obtained from the calibration curve to the y intercept of the plot $\Delta T/c$ against concentration in g/L for the sample gave the number average molecular mass of the polymer. The variations in two analyses were found to be less than 2%. The average of two values was taken as the molecular mass (M_n).

4.1.1.2.4 Differential scanning calorimetry

The glass transition temperature (T_g) of the photocured matrix were noted using a differential scanning calorimeter (DSC) Q 10 from TA instruments, U.S.A. The samples were analyzed in nitrogen atmosphere from 30 to 150 °C at a heating rate of 10 °C/min. The machine data was processed using universal analysis software provided by TA instruments, U.S.A.

4.1.1.2.5 Photo differential scanning calorimetry

Photo differential scanning calorimetry (photo DSC) is a combination of two instruments. DSC Q 100 differential scanning calorimeter (TA instruments, USA) was connected to Q Series PCA (TA instruments, USA) for online monitoring of photopolymerization process. The photo DSC measures isothermal heat flow during polymerization as a function of time. Refrigerant cooling system (RCS) was used in maintaining isothermal condition in DSC unit under nitrogen purge. Polychromatic radiation from a 100 W high pressure mercury short arc lamp (EXFO) was passed through the dual light guide system of PCA during analyses. The emission spectrum of the lamp is given below in Figure 4.1.

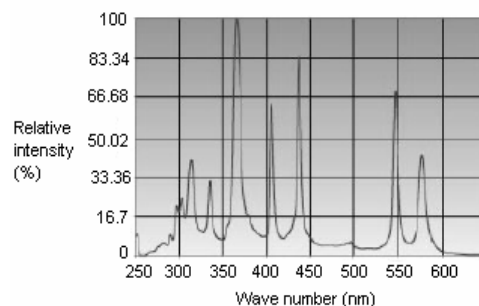


Figure 4.1 Emission spectrum of high pressure mercury short arc lamp

Bandpass filters can be used to select the range of radiation for the requisite application. The bandpass filters provided by the manufacturer as well as their uses are given in Table 4.3.³ Specific analysis parameters set for different analyses are explained under photocuring studies in subsequent sections. Two bandpass filters used in the studies range from 250-450 nm and 320-500 nm.

Table 4.3 Bandpass filters and their specific applications

No.	Filter range (nm)	Name of typical applications	Maximum irradiance (mW/cm ²)
1	320-500	General purpose-Suitable for most UV and visible light curing epoxy and acrylic adhesives on a broad variety of substrates.	23400
2	400-500	Variable light output-Used with visible curing acrylic adhesives, particularly when UV sensitive substrates are involved.	8700
3	320-390	Narrow band filter-Some epoxy adhesives have superior response to this filter. May also be used when unwanted substrate heating results from visible light irradiation.	11100
4	365	Peak filter – May be used when unwanted substrate heating results from UV and / or visible light irradiation.	6000
5	250-450	Provides some UVC input that can be helpful for certain epoxy adhesives, as well as surface curing of acrylic adhesives. Must be used in conjunction with an extended range liquid light guide or a quartz fiber light guide.	24600

The output heat flows in W/g against time in minutes were recorded from the machine. From the obtained data, the kinetic parameters were calculated from the corresponding theoretical heat flow values.⁴ The machine data was processed using universal analysis software provided by TA instruments, U.S.A. An extrapolated baseline was used to calculate the total area under the peak. The partial areas on each analysis over the entire heat flow profiles were also noted at a fixed interval. From the values

obtained, the rates of polymerization in sec^{-1} as well as the percentage conversions were calculated and the plots were generated. From the plots obtained, kinetic parameters such as induction time (time taken for 1% conversion), peak maximum time, maximum polymerization rate ($R_{p \text{ max}}$) as well as maximum percentage conversion attained (C_{max}) were also noted for all the formulations.

The theoretical heat flow in joules per gram was calculated using the following expression:⁴

$\Delta H_{\text{theor}} = (\text{monomer functionality} \times \text{heat flow in joules per mole}) / \text{molecular weight in grams per mole.}$

For formulations containing two or more monomers / crosslinkers the equation can be modified as the sum of fractional heat flows.^{5,6}

$$\Delta H_{\text{theor}} = f_1 \times N_1 \times \Delta H_1 / M_1 + f_2 \times N_2 \times \Delta H_2 / M_2 + f_3 \times N_3 \times \Delta H_3 / M_3 \text{ etc.} \quad (1)$$

where, f_1, f_2 etc. represents mass fractions, N_1, N_2 etc. represents average functionalities, $\Delta H_1, \Delta H_2$ etc. represents the theoretical heat flows and M_1, M_2 etc. represents average molecular weights of each (meth)acrylates in the composition.

The theoretical heat flow for acrylates and methacrylates used in calculations are 86190.4 J/mol and 54810.4 J/mol, respectively. This is based on the general heat flow of acrylate (20.6 kcal/mol) and methacrylate (13.1 kcal/mol) monomers used in literature.⁷⁻⁹

The evaluation of variable autocatalytic kinetic model¹⁰⁻¹³ for the photopolymerization reactions were carried out using TA advantage specialty library software provided by TA instruments, U.S.A. The isothermal kinetics analyses were carried out using a linear baseline with variable values option for the two exponents, m and n. The analyses of the formulations were carried out by providing respective theoretical heat flow values (in J/g) to the software.^{4,6,7} A plot of $\log(dC/dt)$ against $\log(1-C)C^{m/n}$ was plotted using the software. From the plot the values of autocatalytic exponent (m), reaction order exponent (n) as well as specific rate constant (k) were computed for all the formulations using the software by non linear regression analysis.

4.1.1.2.6 Thermogravimetry

Thermogravimetric analyses were carried out using TGA Q-5000 (TA instruments, U.S.A). The samples were heated under nitrogen atmosphere from 30 to 650

°C at a heating rate of 20 °C/min. The degradation profiles of the photopolymerized matrixes with and without crosslinkers were noted.

4.1.1.3 Photopolymerization of diurethane dimethacrylate based on hydroxyethyl methacrylate and hexamethylene diisocyanate (System 4A-1)

A diurethane diacrylate based on hydroxyethyl methacrylate (HEMA) and hexamethylene diisocyanate (HMDI) was synthesized and their photocuring studies were carried out. Estimation of kinetic parameters were done based on the heat flow profile obtained during the photopolymerization process.

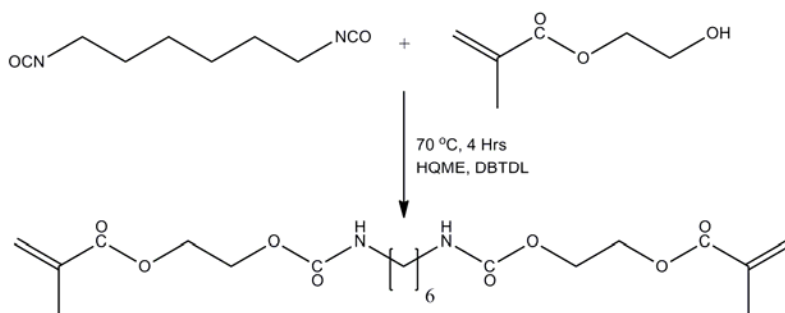


Figure 4.2 Synthesis pathway of urethane diacrylate involving HEMA and HMDI

4.1.1.3.1 Procedure for synthesis

Polymerization was carried out in a 100 mL three necked round bottomed flask provided with half moon stirrer rod through the central neck provided with a teflon stuffing box. The stirrer rod was connected to an overhead stirrer. Nitrogen gas was flushed to the flask through one side neck for a period of 2 min. To it was added 13.2 mL (81.62 mmol) of hexamethylene diisocyanate and 4.7 mg (0.03786 mmol) or 125 ppm of hydroquinone monomethyl ether. 166 mg (0.2629 mmol) or 0.05% of dibutyl tin dilaurate was added to the system after solvating in 30 mL of chloroform. The system was homogenized well at 80 rpm in nitrogen atmosphere. 22 mL (181.4 mmol) of 2-hydroxyethyl methacrylate was added drop-wise through one side neck under stirring at a rate of 1 mL/min. After the addition, it was stirred further for 5 min and the temperature was increased to 70 °C. The reaction was continued for 4 h until the isocyanate peak disappeared from the IR spectrum. 20 mL of chloroform was added to the reaction mixture and the product mixture was poured into water followed by 3 times washing with

100 mL distilled water. The chloroform layer was separated and dried over activated molecular sieves for 1 h. Chloroform was removed using a rotavapour under vacuum at 50 °C. Final drying was done by applying vacuum for 12 h at 60 °C. IR spectrum was noted. The molecular mass was found by VPO.

IR: 1714 (C=O, urethane), 1723 (C=O, methacrylate), 3390 and 1532 (-CO-NH-, urethane), 1638 and 816 (C=C-, methacrylate), 1170 (C-O), 2934, 2862 (-CH₂-) cm⁻¹.

4.1.1.3.2 Formulation

The formulations were made in 5 mL sample vials. 1 g (2.347 mmol) of monomer was weighed accurately in all the vials. 5 mg (0.5 wt%), 10 mg (1 wt%), 20 mg (2 wt%) and 40 mg (4 wt%) of three photoinitiators were added to obtain twelve compositions. Each composition was homogenized in a vibrating mill for 2 min. The photoinitiators used were IRGACURE 651, DAROCUR TPO and DAROCUR 1173.

4.1.1.3.3 Photocuring studies

DSC Q 100 differential scanning calorimeter connected to Q Series PCA was used for the online monitoring of the photopolymerization process. The intensity of irradiation on either side of the dual light guide system was balanced and adjusted to the required value with blank pans on the DSC platform prior to the irradiation of sample. The formulation was homogenized in the glass sample tube using a vibrating mill. About 10 mg of the composition was accurately weighed on a DSC pan and subjected to photo DSC studies under a nitrogen purge of 50 mL/min. The pans were closed by a quartz window in order to prevent any monomer loss during irradiation. The sample was preconditioned at the isothermal condition under nitrogen purge for a period of 1 min prior to irradiation. It was followed by irradiation for a period of 5 min under a constant photo flux from the machine. The heat flow profiles obtained during the *in situ* photocuring process were recorded as a function of time under an isothermal condition of 30 °C. The intensity of irradiation was kept at 17.4 mW/cm² using a polychromatic radiation of 320-500 nm using a 100 W high pressure mercury short arc lamp. The normalized output signals in W/g against time were recorded. The rates of photopolymerizations as well as the conversions were calculated for all the compositions.

4.1.1.3.4 Results and discussion

The complete conversion of isocyanate group during the formation of macromonomer was confirmed by IR spectroscopy. The molecular mass was found 426 g/mol by VPO. The total theoretical heat flow⁷ (ΔH_{theor}) for the system was calculated to be 257.33 J/g.

The rate and conversion profiles obtained from photocuring studies of formulations with three photoinitiators at 0.5, 1, 2 and 4 wt% compositions at 30 °C and 17.4 mW/cm² are given below in Figures 4.3 to 4.5 (A-C).

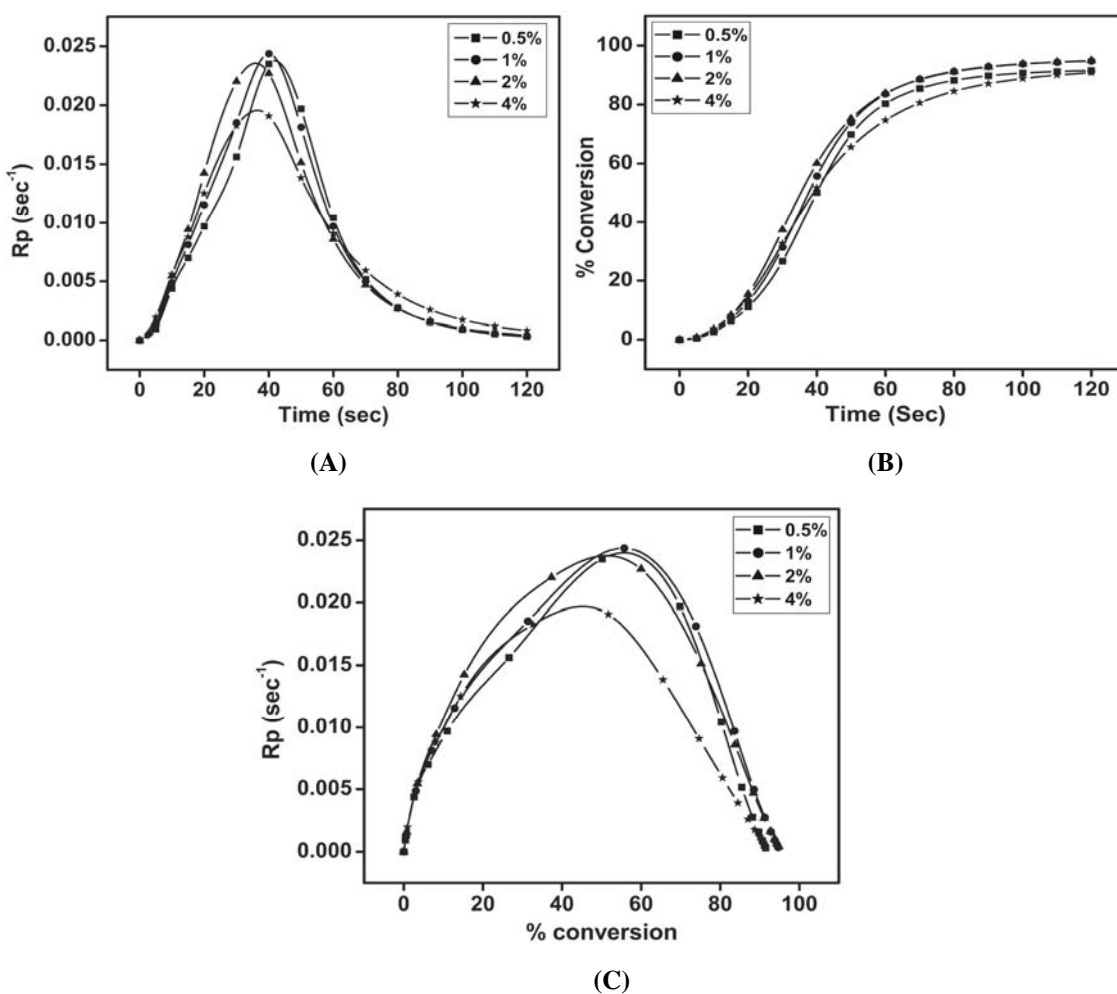
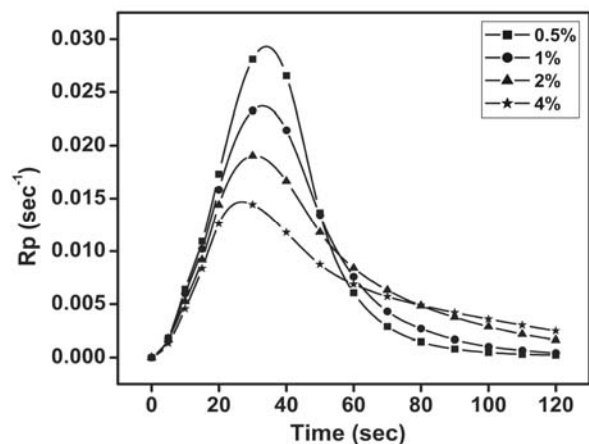
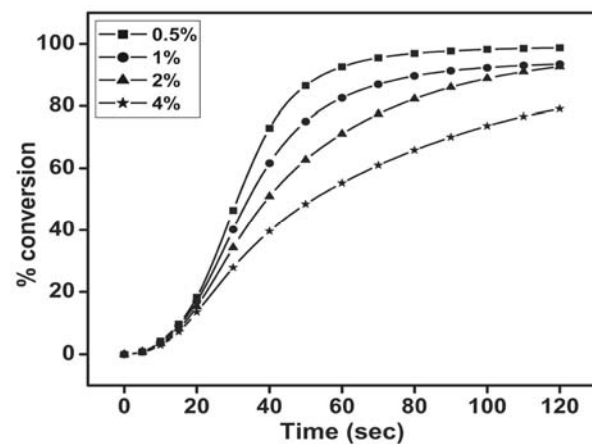


Figure 4.3(A-C) Time dependent rate and conversion profiles of formulations containing 0.5, 1, 2 and 4 wt% of IRGACURE 651

(A)



(B)



(C)

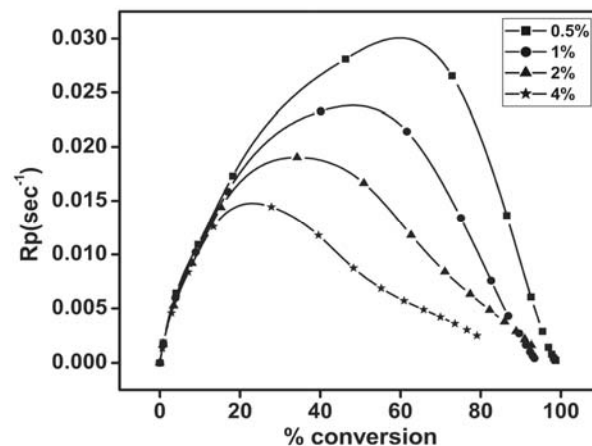
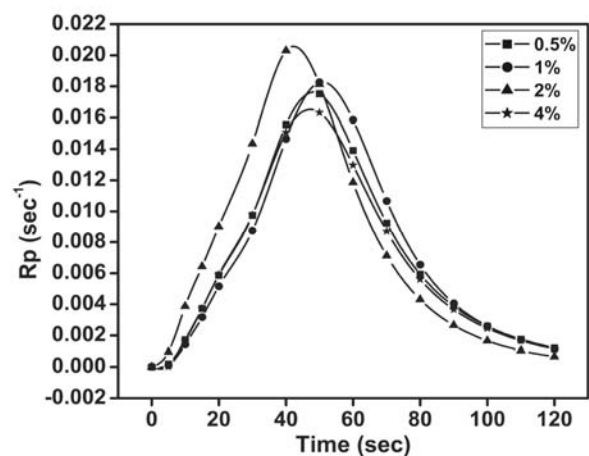
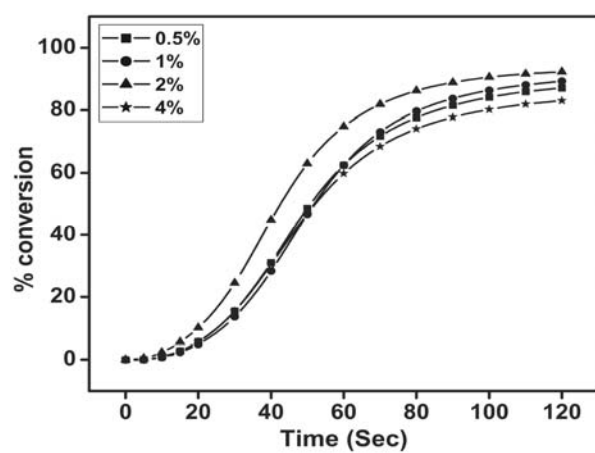


Figure 4.4(A-C) Time dependent rate and conversion profiles of formulations containing 0.5, 1, 2 and 4 wt% of DAROCUR TPO

(A)



(B)



(C)

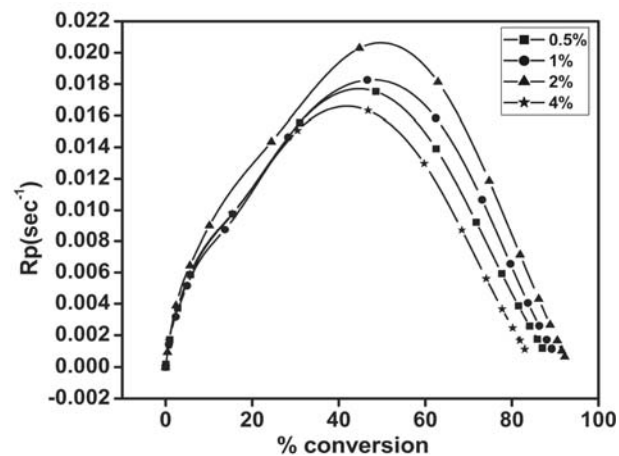


Figure 4.5(A-C) Time dependent rate and conversion profiles of formulations containing 0.5, 1, 2 and 4 wt% of DAROCUR 1173

The kinetic parameters calculated are given in Table 4.4.

Table 4.4 Kinetic parameters of macromonomeric formulations calculated from the heat flow profiles at 30 °C

Photo Initiator	% conc. of photo-initiator (w/w)	Induction Time (sec)	Peak Maximum Time (sec)	$R_{p \max}$ ($\times 10^{-2}$) (sec^{-1})	C_{\max} (%)	Heat of reaction (J/g)	Autocatalytic		
							n	m	k
IRGACURE 651	0.5	6.64	41.96	2.38	92.61	238.3	1.28	0.91	6.21
	1	6.14	39.94	2.43	95.91	246.8	1.23	0.85	5.94
	2	5.64	36.10	2.35	96.18	247.5	1.42	0.83	6.44
	4	5.10	36.53	1.95	93.07	239.5	1.71	0.83	5.98
DAROCUR TPO	0.5	5.23	34	2.93	99.8	256.8	1.18	0.88	7.55
	1	5.27	32.89	2.38	94.43	243	1.57	0.85	7.14
	2	5.39	30.55	1.91	97.23	250.2	1.93	0.76	5.67
	4	6.09	26.99	1.47	87.01	223.9	2.29	0.56	3.38
DAROCUR 1173	0.5	10.14	48.15	1.76	89.77	231	1.67	0.88	5.46
	1	10.99	50.60	1.83	91.75	236.1	1.48	0.87	5.14
	2	6.80	42.33	2.06	93.77	241.3	1.44	0.87	5.66
	4	10.56	47.23	1.65	85.69	220.5	1.81	0.85	5.26

Table 4.4 represents the kinetic parameters calculated from the heat flow profiles. This system has a monomer with low molecular mass and hence the acrylate terminations are higher which is reflected in the heat of reaction. As a result an increase in concentration of photoinitiator results in initiation of more chains. This resulted in an initial high rate of photopolymerization and the induction time was found to decrease with increase in concentration of photoinitiator due to negligible effect of viscosity build up before autoacceleration. Corresponding time to attain peak maximum was found to show a similar trend with variations at high concentration in certain cases. This explains that the peak maximum is influenced by reaction diffusion.^{12,14} Due to high viscosity build up after autoacceleration, the effect of reaction diffusion was much pronounced soon after autoacceleration. This resulted in variations for the value of $R_{p \max}$ and C_{\max} for the formulations. On close observation, we can find from Table 4.4 that for each photoinitiator containing compositions, the value of $R_{p \max}$ has increased to a certain level followed by a decrease with increase in concentration of photoinitiator. Photoinitiation happens throughout the entire photoirradiation process. The $R_{p \max}$ is influenced by reaction diffusion (propagation of mobility restricted macroradical) as well as radical

diffusion (propagation of initiating radical), since for a particular system value of $R_{p \text{ max}}$ is not continuously increasing with increase in concentration of photoinitiator.^{12,15}

Here, increase in concentration of photoinitiator will result in an initial increase in the rate of photopolymerization after autoacceleration. So after autoacceleration, the terminations get drastically reduced when reaction diffusion sets in.¹⁶ The effective number of radicals which can initiate more chains increase with an increase in concentration of photoinitiator up to a limit. Beyond this limit, the effective number of radicals is found to decrease with an increase in concentration of photoinitiator due to enhanced terminations which decreases the quantum yield.¹⁷ Even though the $R_{p \text{ max}}$ is controlled by reaction diffusion, this effect will be observable at $R_{p \text{ max}}$ if the viscosity is not highly pronounced at $R_{p \text{ max}}$. A similar observation in the value of C_{max} as $R_{p \text{ max}}$ was not observed as the autodeceleration step is highly limiting to radical diffusion. However, considering the system as a whole, a high conversion was observed due to a longer time scale for reaction diffusion and delayed vitrification.

The photopolymerization kinetics were studied using polychromatic radiation (320-500 nm). All the photoinitiators have multiple absorptions within the range of radiation.² In acetonitrile solution, the most prominent λ_{max} and the corresponding extinction coefficients for the photoinitiators are as follows - IRGACURE 651 (252 nm, $\epsilon = 12800 \text{ L mol}^{-1} \text{ cm}^{-1}$), DAROCUR TPO (380.4 nm, $\epsilon = 525 \text{ L mol}^{-1} \text{ cm}^{-1}$) and DAROCUR 1173 (243 nm, $\epsilon = 10900 \text{ L mol}^{-1} \text{ cm}^{-1}$).¹ The Table 4.2 shows that the DAROCUR TPO has $n - \pi^*$ transition while the other two photoinitiators shows $\pi - \pi^*$ transition in the principal absorption region. Since the analysis range was from 320-500 nm, DAROCUR TPO showed a higher initiating efficiency and lower induction time than other photoinitiators. The absorption at various wavelengths within the analysis range was also found to be higher for DAROCUR TPO, which resulted in highest value of $R_{p \text{ max}}$ among the studied photoinitiators.

From Table 4.4 we can infer that the photopolymerization rate fits to the variable autocatalytic kinetic model over a wide range in the cure profile as the values of m and n are constant.¹⁸ With increase in concentration of photoinitiator, the specific rate constant (k) as per autocatalytic model was found to show an initial decrease followed by an increase for IRGACURE 651 and DAROCUR 1173 while a consistent decrease was

observed for DAROCUR TPO. The system during photocuring can be assumed to undergo both bimolecular as well as monomolecular terminations.¹⁹ The bimolecular termination is expected to occur over a wide range of cure while monomolecular termination predominates when the *in situ* viscosity build up totally prevents the propagating chains from continuing the reaction.¹² This happens towards vitrification.

4.1.1.4 Photopolymerization of dimethacrylate macromonomer based on polypropylene glycol 3000, isophorone diisocyanate and 2-hydroxyethyl methacrylate (System 4A-2)

A dimethacrylate macromonomer based on polypropylene glycol 3000 (PPG 3000), isophorone diisocyanate (IPDI) and HEMA was synthesized and formulated. The photocuring studies of the formulations were carried out. Estimation of kinetic parameters were done based on the heat flow profile obtained during the photopolymerization process.

The telechelic synthesis of macromonomer was done in two steps. An initial condensation of the diol and diisocyanate to form a diisocyanate terminated urethane prepolymer followed by end capping of the formed prepolymer with excess of 2-hydroxyethyl methacrylate to form soft segmented urethane dimethacrylate macromonomer.

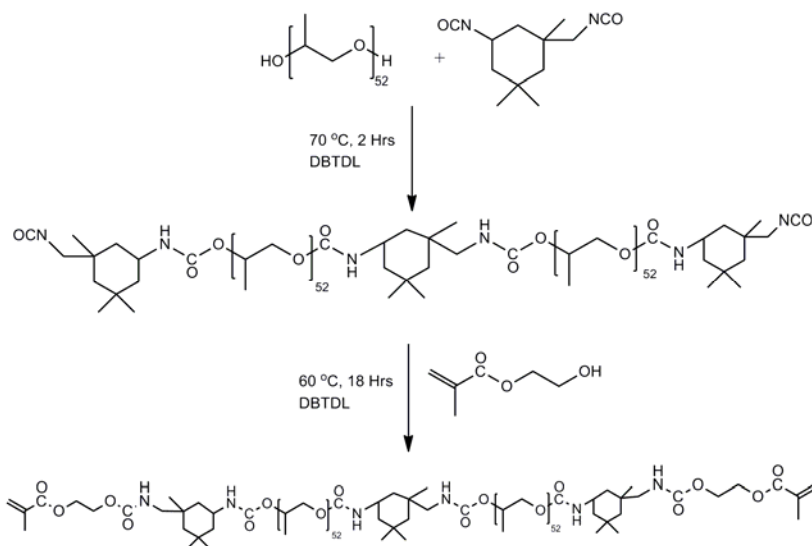


Figure 4.6 Synthesis pathway of urethane dimethacrylate macromonomer based on PPG 3000, IPDI and HEMA

4.1.1.4.1 Procedure for synthesis

Polymerization was carried out in a 100 mL three necked round bottomed flask provided with half moon stirrer rod through the central neck provided with a teflon stuffing box. The stirrer rod was connected to an overhead stirrer. Nitrogen gas was flushed to the flask through one side neck for a period of 2 min. 6 mg dibutyl tin dilaurate was added to it followed by the addition of 11.25 g (3.75 mmol) of polypropylene glycol (Mn =3000) and homogenized at 40 °C at 80 rpm. Using a dropping funnel 0.8025 mL (3.787 mmol) of isophorone diisocyanate was added at a rate of 0.2 mL/min. The system was homogenized well at 100 rpm and the temperature was increased to 70 °C. After 2 h, 0.09 mL (0.749 mmol) of 2-hydroxyethyl methacrylate in 20 mL of chloroform was added drop-wise through one side neck under stirring at a rate of 4 mL/min and stirred at 100 rpm for 5 min. The stirring speed was reduced thereafter to 80 rpm. The temperature was reduced to 60 °C and the reaction was continued in nitrogen atmosphere for 18 h until the isocyanate peak disappeared from the IR spectrum. 50 mL of chloroform was added to the contents of the flask and transferred to a 250 mL separating funnel. It was washed thrice with 100 mL of deionised water until the washings are devoid of excess HEMA. About 1 g of activated molecular sieves were added to it and kept over night. The material was transferred to a 100 mL RB flask and vacuum was applied for 2 h. The viscous macromonomer was transferred to a petri dish and further dried in a vacuum oven at 50 °C for 10 h. IR and NMR spectra were noted. The molecular mass was found by VPO.

Prepolymer

IR: 1721 (C=O, urethane), 3344 and 1529 (-CO-NH-, urethane), 2265 (NCO), 1111 (C-O), 2968, 2871 (-CH₂-) cm⁻¹

¹H NMR (CDCl₃): 0.96 and 1.04 (CH₃, alicyclic), 1.11 (-CH(CH₃)-CH₂-O-), 2.77 (-CH₂-NH-CO-), 3.03 (-CH₂-NCO), 3.49 (-CH(CH₃)-CH₂-O-), 3.53 (-CH(CH₃)-CH₂-O-), 4.53 (-NH-CO-O-) ppm.

¹³C NMR (CDCl₃): 17.34 and 18.35 (-CH(CH₃)-CH₂-O-, propyloxy), 27.43 and 34.59 (=C(CH₃)₂, alicyclic), 23.24 (-CH₃, alicyclic), 31.78 (=C(CH₃)₂, alicyclic), 36.40 (=C(CH₃)-CH₂-NH-CO-, alicyclic), 43.25, 46.16 and 47.93 (-CH₂-, alicyclic), 56.71 (-CH₂-NCO), 73.25 (-CH(CH₃)-CH₂-O-, propyloxy), 75.26 (-CH(CH₃)-CH₂-O-, propyloxy), 121.89 (-CH₂-NCO), 122.77 (-NCO), 155.74 (-NH-CO-O-), 157.15 (-CH₂-NH-CO-O-) ppm.

Macromonomer

IR: 1722 (C=O, urethane), 3346 and 1531 (-CO-NH-, urethane), 1640 (C=C-, methacrylate), 1114 (C-O), 2971, 2872 (-CH₂-) cm⁻¹.

¹H NMR (CDCl₃): 0.94 and 1.05 (CH₃, alicyclic), 1.12 (-CH(CH₃)-CH₂-O-), 2.92 (-CH₂-NH-CO-), 3.40 (-CH(CH₃)-CH₂-O-), 3.54 (-CH(CH₃)-CH₂-O-), 3.91 and 4.29 (-O-CH₂-CH₂-O-CO-C(CH₃)=CH₂), 4.88 (-CH₂-NH-CO-O-), 4.53 (-NH-CO-O-), 5.60 and 6.13 (-CO-C(CH₃)=CH₂) ppm.

¹³C NMR (CDCl₃): 17.37 and 18.35 (-CH(CH₃)-CH₂-O-, propyloxy), 27.45 and 34.96 (=C(CH₃)₂, alicyclic), 23.29 (-CH₃, alicyclic), 31.76 (=C(CH₃)₂, alicyclic), 36.43 (=C(CH₃)-CH₂-NH-CO-, alicyclic), 44.38, 45.90 and 46.47 (-CH₂-, alicyclic), 61.06 (-CH₂-NH-CO-), 73.26 (-CH(CH₃)-CH₂-O-, propyloxy), 75.21 (-CH(CH₃)-CH₂-O-, propyloxy), 125.96 (-O-CO-C(CH₃)=CH₂), 134.75 (-O-CO-C(CH₃)=CH₂), 155.29 (-NH-CO-O-), 156.55 (-CH₂-NH-CO-O-), 167.62 (-O-CO-C(CH₃)=CH₂) ppm.

4.1.1.4.2 Formulation

The macromonomer was found to be viscous. 15 wt% of HEMA was added to the macromonomer for better homogenization during formulation. The formulations were made in 5 mL sample vials. 1 g of monomer containing 15 wt% HEMA was weighed accurately in all the vials. 5 mg (0.5 wt%), 10 mg (1 wt%) and 15 mg (1.5 wt%) of two photoinitiators were added to obtain six compositions. Each composition was homogenized in a vibrating mill for 2 min. The photoinitiators used were IRGACURE 651 and IRGACURE 184.

4.1.1.4.3 Photocuring studies

About 10 mg of the composition was accurately weighed on a DSC pan and subjected to photo DSC studies under a nitrogen purge of 50 mL/min. The heat flow profile obtained during the *in situ* photocuring process was recorded as a function of time under an isothermal condition of 30 °C. The intensity of irradiation was kept at 21.1 mW/cm² using a polychromatic radiation of 250-450 nm and 100 W high pressure mercury short arc lamp. The normalized output signal in W/g against time were recorded. The rates of photopolymerizations as well as corresponding conversions were noted for all the compositions.

4.1.1.4.4 Results and discussion

The existence of terminal isocyanate group in the prepolymer as well as complete conversion of isocyanate group during the formation of macromonomer was confirmed by IR, ^1H and ^{13}C NMR spectroscopy. The molecular mass was found to be 7805 g/mol by VPO. The total theoretical heat flow^{6,7,20} (ΔH_{theor}) for the system containing 15 wt% HEMA was calculated to be 67.17 J/g.

The rate and conversion profiles obtained from photocuring studies of macromonomeric formulations containing 15 wt% of HEMA as reactive diluent with two photoinitiators at 0.5, 1 and 1.5 wt% compositions at 30 °C and 21.1 mW/cm² are given below in Figures 4.7 to 4.8 (A-C).

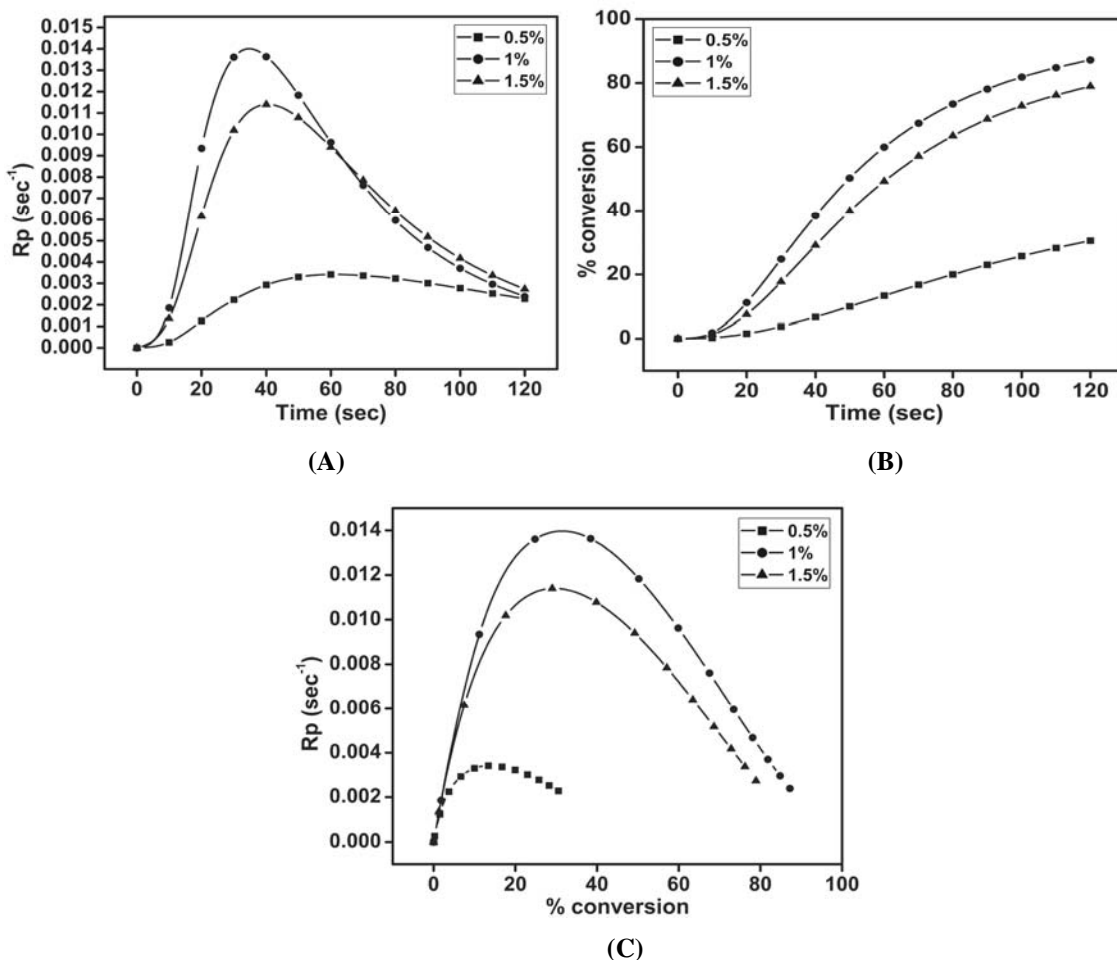
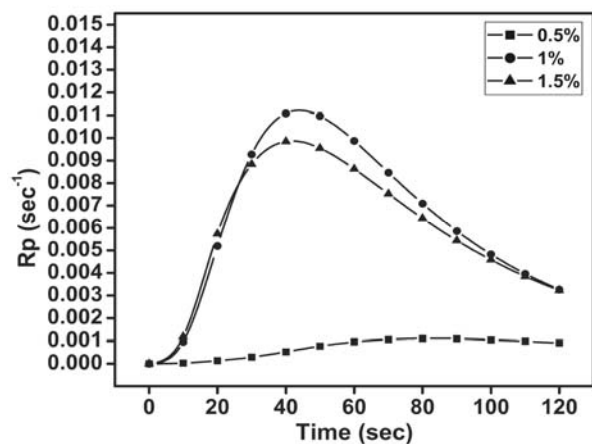
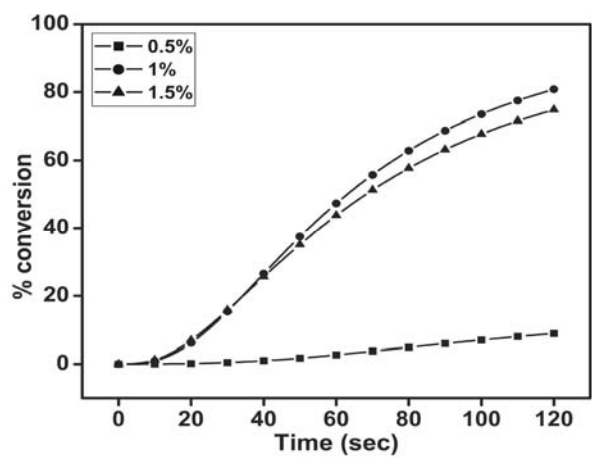


Figure 4.7(A-C) Time dependent rate and conversion profiles of macromonomeric formulations containing 0.5, 1 and 1.5 wt% of IRGACURE 651

(A)



(B)



(C)

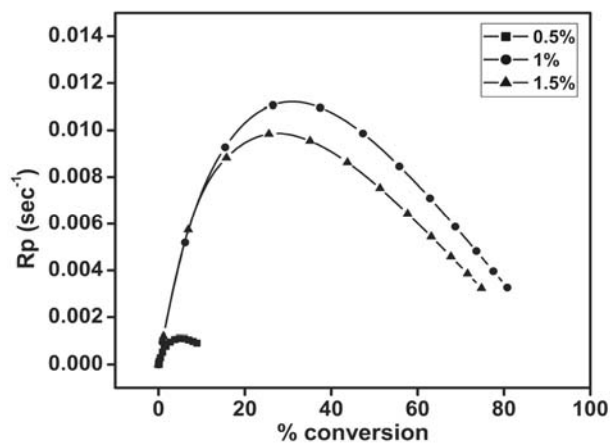


Figure 4.8(A-C) Time dependent rate and conversion profiles of formulations containing 0.5, 1 and 1.5 wt% of IRGACURE 184

The kinetic parameters calculated are given in Table 4.5.

Table 4.5 Kinetic parameters of macromonomeric formulations calculated from the heat flow profiles at 30 °C

Photo Initiator	% conc of photo-initiator (w/w)	Induction Time (sec)	Peak Maximum Time (sec)	$R_{p \max}$ ($\times 10^{-2}$) (sec^{-1})	C_{\max} (%)	Heat of reaction (J/g)	Autocatalytic		
							n	m	k
IRGACURE 651	0.5	16.83	60.37	0.34	44.30	29.76	4.19	0.56	1.16
	1	8	34.78	1.40	97.69	65.62	1.44	0.47	2.46
	1.5	8.83	40.92	1.14	90.74	60.95	1.64	0.53	2.29
IRGACURE 184	0.5	40.35	82.74	0.11	14.72	9.89	16.4	0.75	1.44
	1	10.06	43.97	1.12	95.23	63.97	1.44	0.50	2.05
	1.5	9.38	41.98	0.99	90.13	60.54	1.56	0.46	1.74

From Table 4.5, the induction time and the peak maximum time for IRGACURE 651 was found to decrease followed by an increase with increase in concentration of photoinitiator. As the concentration of photoinitiator was increased, the system attains an optimum value of radical concentration at 1 wt% concentration of photoinitiator. A further increase thus resulted in the reduced quantum yield of initiation, which accounts for this effect.¹⁷ In the case of IRGACURE 184, continuous reductions in the value of induction times and peak maxima times with an increase in the concentration of photoinitiator were observed. This shows the radical concentration has not reached the optimum value, even at 1.5 wt% concentration of photoinitiator.

The $R_{p \max}$ as well as the C_{\max} for both the photo initiating systems show an initial increase followed by a decrease. Since a continuous increase in the value was not observed, the value of $R_{p \max}$ is controlled by reaction diffusion.^{12,14} In both the cases, the value of $R_{p \max}$ and C_{\max} was found to increase followed by a decrease. The viscosity build up at 1.5 wt% concentration of both the photoinitiators were high enough to cause reduction in radical diffusion. This resulted in reduction of formation of new chains and hence a low value was observed for $R_{p \max}$. This effect was also found to remain in the decelerating step resulting in a similar behaviour for the value of C_{\max} . As the oligomer has flexible propyleneoxy linkages, the system was found to show a longer time scale for reaction diffusion and hence higher conversions are readily observed at higher concentration of photoinitiator.²¹ The polymerization rate diminished and stopped when

the volume shrinkage towards the end of photopolymerization process exceeds the chemical reaction.²²

The photopolymerizations were studied using polychromatic radiation (250-450 nm). All the photoinitiators have multiple absorptions within the range of radiation.² In acetonitrile solution, the most prominent λ_{\max} and the corresponding extinction coefficients for the photoinitiators are as follows - IRGACURE 651 (252 nm, $\epsilon = 12800 \text{ L mol}^{-1} \text{ cm}^{-1}$) and IRGACURE 184 (243 nm, $\epsilon = 10000 \text{ L mol}^{-1} \text{ cm}^{-1}$).¹ The Table 4.5 shows that the IRGACURE 651 has a higher rate of initiation as the $\pi - \pi^*$ absorption maximum lies within the analysis range. This result in a high initiating efficiency for IRGACURE 651, which can be understood from the induction time data in Table 4.5.

From Table 4.5, we can infer that the photopolymerization rate fits to the variable autocatalytic kinetic model over a wide range in the cure profile as the values of m and n are constant.¹⁸ With increase in concentration of photoinitiator, the specific rate constant (k) as per autocatalytic model was found to show an initial increase followed by decrease for both the photoinitiators. The system during photocuring can be assumed to undergo both bimolecular as well as monomolecular terminations.¹⁹

4.1.1.5 Photopolymerization of diacrylate macromonomer based on polyethylene glycol 200, Polypropylene glycol 725, Polypropylene glycol 3000, isophorone diisocyanate and 2-hydroxyethyl acrylate ((System 4A-3)

A diacrylate macromonomer based on polyethylene glycol 200 (PEG 200), polypropylene glycol 725 (PPG 725), PPG 3000, IPDI and 2-hydroxyethyl acrylate (HEA) was synthesized and formulated. The photocuring studies of the formulations were carried out. Estimation of kinetic parameters were done based on the heat flow profile obtained during the photopolymerization process.

The telechelic synthesis of macromonomer was done in two steps. An initial condensation of the diol and diisocyanate to form a diisocyanate terminated urethane macromonomer followed by end capping of the formed macromonomer with excess of 2-hydroxyethyl acrylate to form soft segmented urethane diacrylate macromonomer.

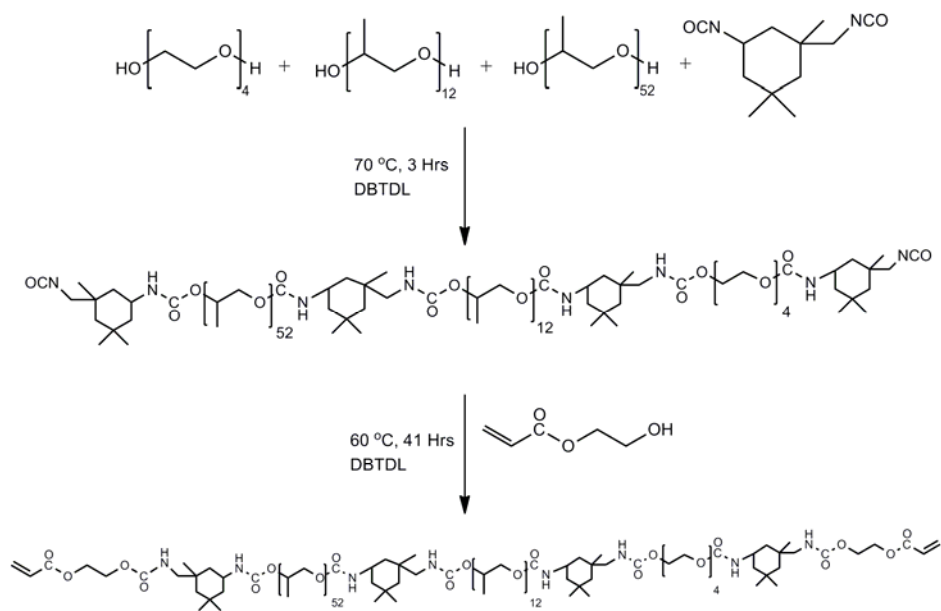


Figure 4.9 Synthesis pathway of urethane diacrylate macromonomer based on PEG 200, PPG 725, PPG 3000, IPDI and HEA

4.1.1.5.1 Procedure for synthesis

Polymerization was carried out in a 100 mL three necked round bottomed flask provided with half moon stirrer rod through the central neck provided with a teflon stuffing box. The stirrer rod was connected to an overhead stirrer. Nitrogen gas was flushed to the flask through one side neck for a period of 2 min. 50 mg (0.07917 mmol) dibutyl tin dilaurate was added to it followed by the addition of 3.85 g (19.25 mmol) of polyethylene glycol 200, 23.08 g (7.69 mmol) of polypropylene glycol 725, 8.365 g (11.54 mmol) of polypropylene glycol 3000 and homogenized at 40 °C at 80 rpm. Using a dropping funnel, 8.55 mL (40.4 mmol) of isophorone diisocyanate was added at a rate of 0.5 mL/min. The system was homogenized well at 100 rpm and the temperature was increased to 70 °C. After 3 hours, 0.89 g (7.66 mmol) of 2-hydroxyethyl acrylate in 20 mL of chloroform was added drop-wise through one side neck under stirring at a rate of 1 mL/min and stirred at 100 rpm for 10 min. The temperature was reduced to 60 °C and further stirred at 80 rpm. The reaction was continued in nitrogen atmosphere for 41 h until the isocyanate peak disappeared from the IR spectrum. 80 mL of chloroform was added to the contents of the flask and transferred to a 500 mL separating funnel. It was washed thrice with 150 mL of deionised water until the washings were devoid of excess HEA. About 2 g of activated molecular sieves were added to it and kept over night. The

material was transferred to a 250 mL RB flask and vacuum was applied to it for 2 h. The viscous macromonomer was transferred to a petri dish and further dried in a vacuum oven at 50 °C for 10 h. IR and NMR spectra were noted. The molecular mass was found by VPO.

IR: 1722 (C=O, urethane), 3343 and 1536 (-CO-NH-, urethane), 1640, 836 (C=C-, acrylate), 1107 (C-O), 2971, 2930, 2871 (-CH₂-) cm⁻¹.

¹H NMR (CDCl₃): 1.13 and 1.23 (CH₃, alicyclic), 1.88 (-CH(CH₃)-CH₂-O-), 2.88 (-CH₂-NH-CO-), 3.29 to 3.56 (-CH(CH₃)-CH₂-O-), 3.64 and 3.59 (-O-CH₂-CH₂-O-), 4.56 (-CH₂-NH-CO-O-), 4.87 (-NH-CO-O-), 6.47 and 5.88 (-O-CO-CH=CH₂), 6.15 (-O-CO-CH=CH₂) ppm.

¹³C NMR (CDCl₃): 17.37 and 18.36 (-CH(CH₃)-CH₂-O-, propyloxy), 27.53 and 34.97 (=C(CH₃)₂, alicyclic), 23.26 (-CH₃, alicyclic), 31.75 (=C(CH₃)₂, alicyclic), 36.28 (=C(CH₃)-CH₂-NH-CO-, alicyclic), 44.02, 46.10 and 46.97 (-CH₂-, alicyclic), 65.47 and 67.18 (-O-CH₂-CH₂-O-), 73.27 (-CH(CH₃)-CH₂-O-, propyloxy), 75.27 (-CH(CH₃)-CH₂-O-, propyloxy), 126.96 (-O-CO-CH=CH₂), 132.66 (-O-CO-CH=CH₂), 155.52 (-NH-CO-O-), 157.82 (-CH₂-NH-CO-O-), 165.58 (-O-CO-CH=CH₂) ppm.

4.1.1.5.2 Formulation

The macromonomer was found to be viscous. 15 wt% of HEA was added to the macromonomer for better homogenization and during formulation. The formulations were made in 5 mL sample vials. 1 g each of macromonomer containing 15 wt% HEA was weighed accurately in all the vials. 5 mg (0.5 wt%), 10 mg (1 wt%) and 20 mg (2 wt%) of eight photoinitiators were added to obtain twenty four compositions. Each composition was homogenized in a vibrating mill for 2 min. The photoinitiators used were IRGACURE 651, DAROCUR TPO, IRGACURE 184, IRGACURE 2959, DAROCUR 1173, DAROCUR MBF, IRGACURE 907 and IRGACURE 819.

4.1.1.5.3 Photocuring studies

About 10 mg each of the composition were accurately weighed on a DSC pan and subjected to photo DSC studies under a nitrogen purge of 50 mL/min. The heat flow profiles obtained during the *in situ* photocuring process were recorded as a function of time under an isothermal condition of 30 °C. The intensity of irradiation was kept constant at 22.1 mW/cm² using a polychromatic radiation of 250-450 nm using a 100 W high pressure mercury short arc lamp. The normalized output signals in W/g against time were recorded. The rates of photopolymerizations as well as corresponding conversions were calculated for all the compositions.

4.1.1.5.4 Results and discussions

The complete conversion of isocyanate group during the formation of macromonomer was confirmed by IR, ^1H and ^{13}C NMR spectroscopy. The molecular mass was found 4342 g/mol by VPO. The total theoretical heat flow^{4,6,7} (ΔH_{theor}) for the system containing 15 wt% HEA was calculated to be 131.38 J/g.

The rate and conversion profiles obtained from photocuring studies of macromonomeric formulations containing 15 wt% of HEA as reactive diluent with eight photoinitiators at 0.5,1 and 2 wt% compositions at 30 °C and 22.1 mW/cm² are given below in Figures 4.10 to 4.12 (A-C).

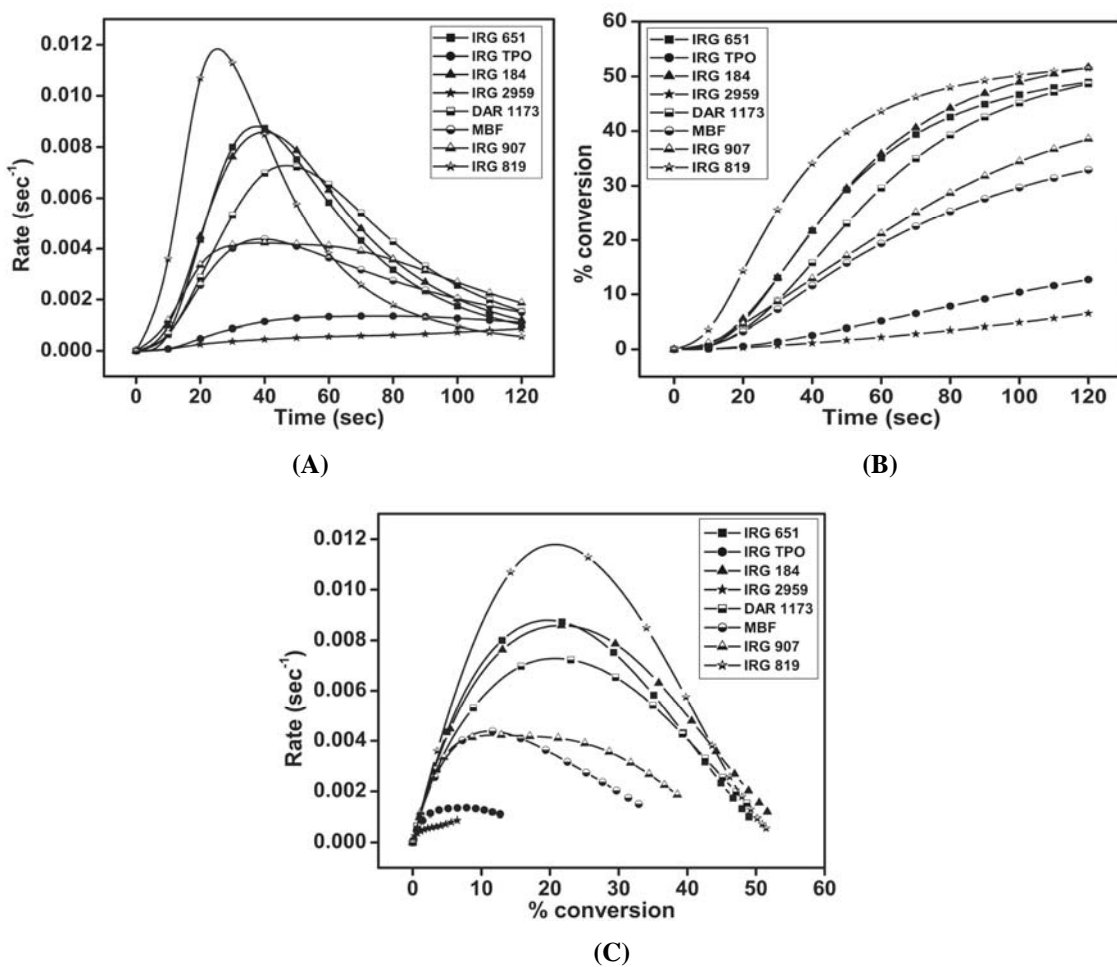
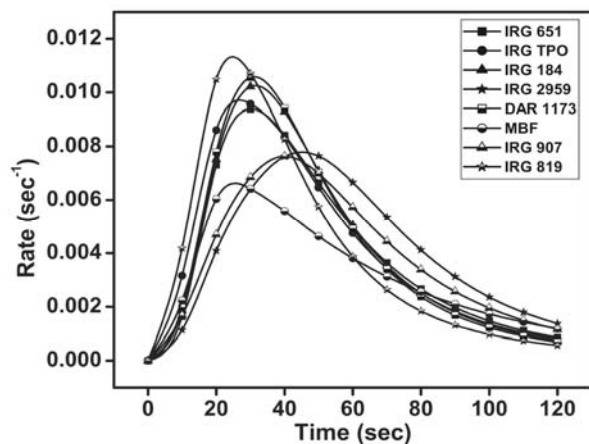
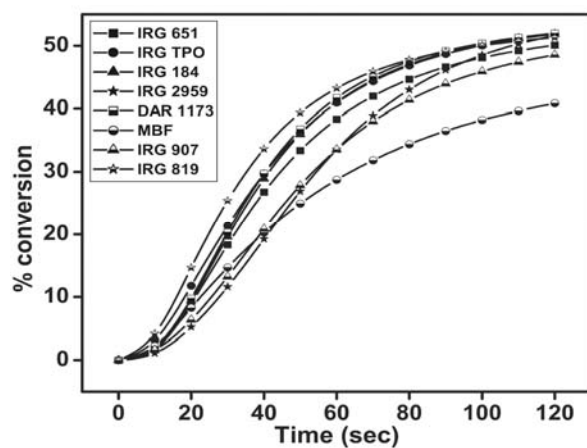


Figure 4.10(A-C) Time dependent rate and conversion profiles of macromonomeric formulations containing 0.5 wt% of eight photoinitiators

(A)



(B)



(C)

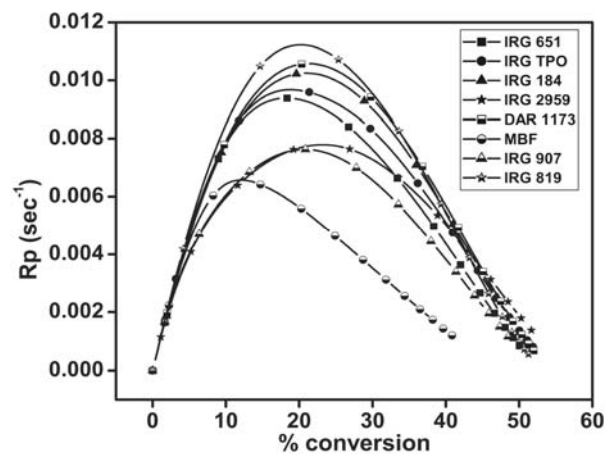
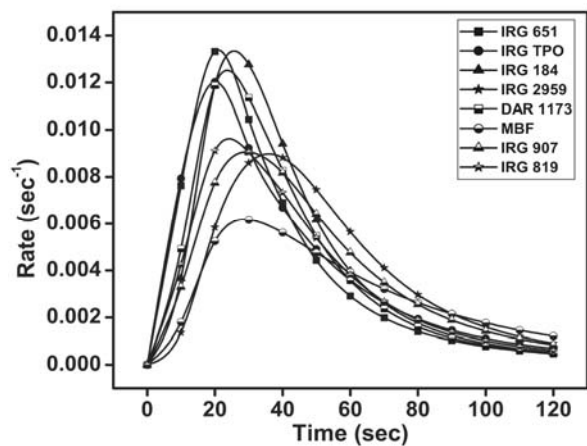
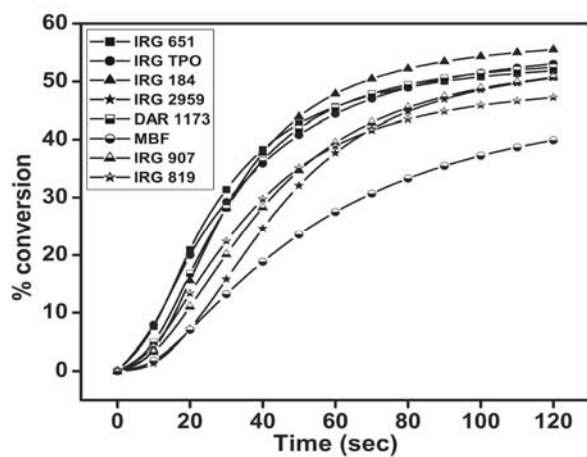


Figure 4.11(A-C) Time dependent rate and conversion profiles of macromonomeric formulations containing 1 wt% of eight photoinitiators

(A)



(B)



(C)

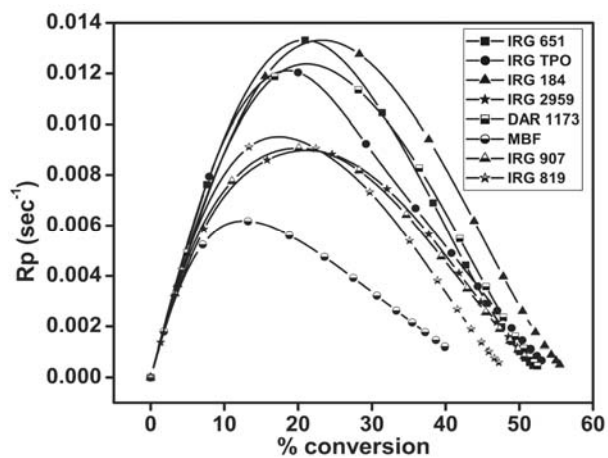


Figure 4.12(A-C) Time dependent rate and conversion profiles of macromonomeric formulations containing 2 wt% of eight photoinitiators

The kinetic parameters calculated are given in Table 4.6.

Table 4.6 Kinetic parameters of macromonomeric formulations calculated from the heat flow profiles at 30 °C

Photo Initiator	% conc. of photo-initiator (w/w)	Induction Time (sec)	Peak Maximum Time (sec)	$R_{p \max}$ ($\times 10^{-3}$) (sec^{-1})	C_{\max} (%)	Heat of reaction (J/g)	Autocatalytic		
							n	m	k
IRGACURE 651	0.5	11.34	37.43	8.81	52.77	69.33	4.70	0.74	4.62
	1	8.26	30.24	9.39	53.38	70.13	4.44	0.69	3.92
	2	1.66	21.04	13.38	53.92	70.84	4.78	0.64	6.06
DAROCUR TPO	0.5	25.57	76.36	1.35	19.63	25.79	10.4	0.44	0.42
	1	4.78	26.80	9.71	55.01	72.27	4.03	0.61	3.58
	2	1.47	20.26	12.05	55.87	73.40	4.32	0.49	3.64
IRGACURE 184	0.5	10.05	40.24	8.57	56.12	73.73	4.21	0.73	4.15
	1	7.59	31.69	10.26	54.70	71.87	4.40	0.73	5.17
	2	4.87	25.66	13.34	57.53	75.58	4.27	0.75	6.90
IRGACURE 2959	0.5	36.77	-	-	17.48	22.97	3.73	0.47	0.24
	1	9.42	45.05	7.79	56.54	74.28	3.79	0.73	3.47
	2	8.87	36.06	8.99	54.06	71.02	4.48	0.72	4.36
DAROCUR 1173	0.5	12.01	46.66	7.28	54.32	71.37	4.34	0.76	3.73
	1	7.39	31.26	10.58	54.60	71.73	4.49	0.74	5.48
	2	3.10	23.70	12.52	54.19	71.20	4.37	0.67	5.50
DAROCUR MBF	0.5	11.98	38.75	4.38	40.52	53.24	6.76	0.55	1.67
	1	6.14	25.44	6.62	46.43	61	5.76	0.51	2.19
	2	7.24	28.62	6.18	45.44	59.70	5.97	0.56	2.43
IRGACURE 907	0.5	9.19	38.97	4.23	46.57	61.19	3.36	0.39	0.87
	1	7.35	40.21	7.64	52.82	69.39	4.49	0.76	3.96
	2	4.22	29.65	9.07	53.92	70.84	4.34	0.66	3.91
IRGACURE 819	0.5	4.59	25.41	11.84	53.81	70.70	4.82	0.73	6.36
	1	3.62	24.79	11.32	53.65	70.48	4.57	0.68	5.20
	2	3.24	24.17	9.62	49.60	65.17	4.72	0.59	3.72

From Table 4.6, the induction time of all the systems were found to decrease with an increase in concentration of photoinitiator. The results show all the systems have a high initiation rate which increase with increase in concentration of photoinitiator. The peak maximum time also follow a similar trend showing that the influence of reaction diffusion is not much pronounced at peak maximum. The difference in *in situ* viscosity during the onset of gelation up to peak maximum time resulted in marginal variations in certain cases. This is observed in the case of DAROCUR MBF and IRGACURE 907 as photoinitiators.

Considering the value of $R_{p \max}$, for all the formulations except IRGACURE 819, an increase in concentration of photoinitiator resulted in an increase in the value of $R_{p \max}$. This shows that the viscosity build up after autoacceleration is not high enough to slow

down the rate of radical diffusion.¹⁵ As a result the $R_{p \text{ max}}$ was found to increase with an increase in concentration of photoinitiator. In the case of formulations containing IRGACURE 819, the variation in peak maximum time was negligible with an increase in concentration of photoinitiator. This shows a comparative higher viscosity build up for IRGACURE 819 formulations as compared to other formulations which resulted in a reduction in the value of $R_{p \text{ max}}$. The final conversions for all formulations were almost of the same range at higher concentration of photoinitiator. Due to the reduced effect of reaction as well as radical diffusion during the deceleration step resulted in comparatively less variations in final conversions.^{12,15} In other words, the rate of increase in volume shrinkage with respect to reduction in chemical conversion towards the end of polymerization did not vary much for all the formulations.²² The flexibility imparted by the propyleneoxy linkages and a much lesser flexibility imparted by ethyleneoxy linkages resulted in a final conversion of below 60% for all the formulations.

The photopolymerizations were studied using a polychromatic radiation (250-450 nm). All the photoinitiators with the exception of IRGACURE 2959 have multiple absorptions within the range of radiation.² In acetonitrile solution, the most prominent λ_{max} and the corresponding extinction coefficients for the photoinitiators are as follows - IRGACURE 651 (252 nm, $\epsilon = 12800 \text{ L mol}^{-1} \text{ cm}^{-1}$), DAROCUR TPO (380 nm, $\epsilon = 525 \text{ L mol}^{-1} \text{ cm}^{-1}$), IRGACURE 184 (243 nm, $\epsilon = 10000 \text{ L mol}^{-1} \text{ cm}^{-1}$), IRGACURE 2959 (272 nm, $\epsilon = 16200 \text{ L mol}^{-1} \text{ cm}^{-1}$), DAROCUR 1173 (243 nm, $\epsilon = 10900 \text{ L mol}^{-1} \text{ cm}^{-1}$), DAROCUR MBF (255 nm, $\epsilon = 11200 \text{ L mol}^{-1} \text{ cm}^{-1}$), IRGACURE 907 (303 nm, $\epsilon = 18600 \text{ L mol}^{-1} \text{ cm}^{-1}$) and IRGACURE 819 (369 nm, $\epsilon = 933 \text{ L mol}^{-1} \text{ cm}^{-1}$).¹ The Table 4.6 shows that the formulations containing IRGACURE 651 and DAROCUR TPO have a higher rate of initiation with an increase in concentration of photoinitiator. At the lowest concentration, formulations containing IRGACURE 819 showed highest initiation rate. Since the excitation energy of DAROCUR TPO and IRGACURE 819, lies near to the most prominent emission line of the high pressure mercury arc at 365 nm, faster initiation at 0.5 wt% concentration of IRGACURE 819 can be attributed to attainment of initial radical concentration much closer to the optimum value.¹⁷ For all other formulations, optimum radical concentration was not attained even at 2 wt% concentration. At 2 wt%

concentration, the effective radical concentration was higher for IRGACURE 651 and DAROCUR TPO.

From Table 4.6, we can infer that the photopolymerization rate fits to the variable autocatalytic kinetic model over a wide range in the cure profile as the values of m and n are constant.¹⁸ With increase in concentration of photoinitiator, the specific rate constant (k) as per autocatalytic model was found to show an increase with increase in concentration of photoinitiator with the exception of IRGACURE 819, where a gradual decrease was observed. This observation is in accordance with the value of $R_{p \text{ max}}$. This system as a whole during photocuring can be assumed to undergo bimolecular termination as well as monomolecular terminations.¹⁹

4.1.1.6 Photopolymerization of diacrylate macromonomer based on polyethylene glycol 200, polyethylene glycol 400, polyethylene glycol 600, isophorone diisocyanate and 2-hydroxyethyl acrylate (System 4A-4)

A diacrylate macromonomer based on PEG 200, polyethylene glycol 400 (PEG 400), polyethylene glycol 600 (PEG 600), IPDI and HEA was synthesized and formulated. The photocuring studies of the formulations were carried out. Estimation of kinetic parameters were done based on the heat flow profile obtained during the photopolymerization process.

The telechelic synthesis was done in two steps. An initial condensation of the mixture of diols and excess of diisocyanate to form a diisocyanate terminated urethane prepolymer followed by end capping of the formed prepolymer with excess of 2-hydroxyethyl acrylate to form soft segmented urethane diacrylate macromonomer.

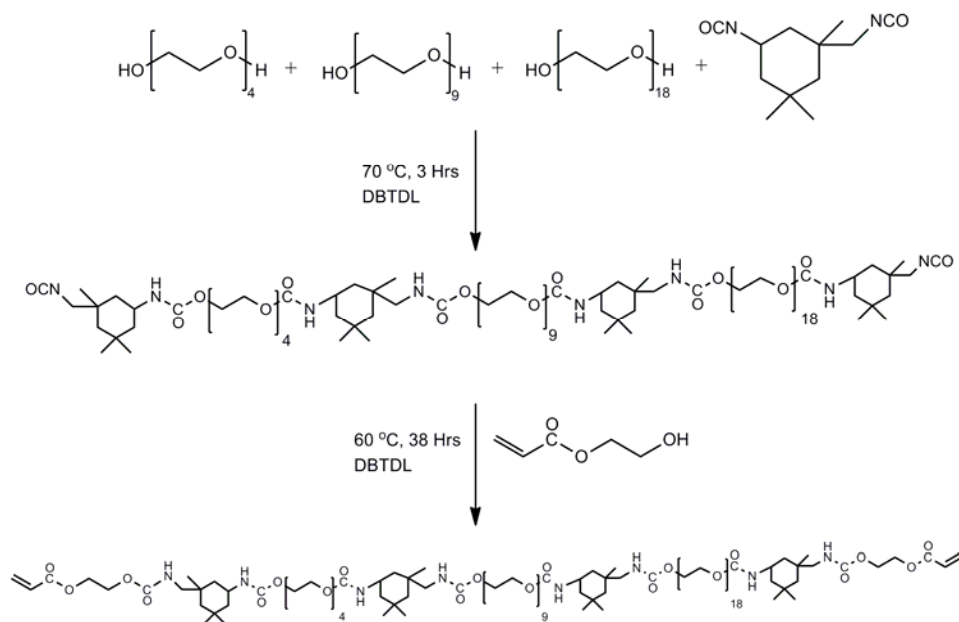


Figure 4.13 Synthesis pathway of diacrylate macromonomer based on PEG 200, PEG 400, PEG 600, IPDI and HEA

4.1.1.6.1 Procedure for synthesis

Polymerization was carried out in a 100 mL three necked round bottomed flask provided with half moon stirrer rod through the central neck provided with a teflon stuffing box. The stirrer rod was connected to an overhead stirrer. Nitrogen gas was flushed to the flask through one side neck for a period of 2 min. 7 mg (0.01128 mmol) dibutyl tin dilaurate was added to it followed by the addition of 1 g (5 mmol) of polyethylene glycol 200, 4 g (10 mmol) of polyethylene glycol 400 and 24 g (40 mmol) of polyethylene glycol 600. The system was homogenized at 40 °C at 80 rpm. Using a dropping funnel 12.24 mL (57.7 mmol) of isophorone diisocyanate was added at a rate of 1 mL/min. The system was homogenized well at 100 rpm and the temperature was increased to 70 °C. After 3 h, 5 mg of hydroquinone and 2.25 g (19.38 mmol) of 2-hydroxyethyl acrylate in 20 mL chloroform was added drop-wise through one side neck under stirring at a rate of 2 mL/min and stirred at 100 rpm for 5 min. The temperature was reduced to 60 °C and the system was stirred further at 80 rpm. The reaction was continued in nitrogen atmosphere for 38 h until the isocyanate peak disappeared from the IR spectrum. IR and NMR spectra were noted. The molecular mass was found by VPO.

Prepolymer

IR: 2260 (-NCO), 1715 (C=O, urethane), 3349 and 1557 (-CO-NH-, urethane), 1114 (C-O), 2918, 2856 (-CH₂-) cm⁻¹.

¹H NMR (CDCl₃): 0.95 and 1.04 (CH₃, alicyclic), 1.08 to 1.83 (CH₂, alicyclic), 3.03 (-CH₂-NCO), 3.57 to 3.70 (-CH₂-CH₂-O-CH₂-CH₂-O-), 4.51 (=NH-CO-O-), 4.71 (-CH₂-NH-CO-O-) ppm.

¹³C NMR (CDCl₃): 27.29 and 34.45 (=C(CH₃)₂, alicyclic), 23.09 (-CH₃, alicyclic), 43.07, 45.99 and 47.75 (-CH₂-, alicyclic), 31.64 (=C=(CH₃)₂, alicyclic), 36.24 (=C-(CH₃)-CH₂-NCO, alicyclic), 48.32 (=CH-NH-, alicyclic), 56.53 (-CH₂-NCO), 69.36 to 72.43 (-O-CH₂-CH₂-O-CH₂-CH₂-O-), 121.39 (-CH₂-NCO), 122.55 (-NCO), 155.43 (-NH-CO-O-), 156.67 (-CH₂-NH-CO-O-) ppm.

Macromonomer

IR: 1716 (C=O, urethane), 3333 and 1557 (-CO-NH-, urethane), 1647, 812 (C=C-, acrylate), 1118 (C-O), 3003, 2949, 2872 (-CH₂-) cm⁻¹.

¹H NMR (CDCl₃): 0.91 and 1.04 (CH₃, alicyclic), 1.12 to 1.84 (CH₂, alicyclic), 2.90 (-CH₂-NH-CO-), 3.48 to 3.87 (-O-CH₂-CH₂-O-CH₂-CH₂-O-), 4.18 and 4.30 (-CH₂-CH₂-O-CO-CH=CH₂), 4.71 (-CH₂-NH-CO-O-), 6.42 and 5.85 (-O-CO-CH=CH₂), 6.16 (-O-CO-CH=CH₂) ppm.

¹³C NMR (CDCl₃): 27.55 and 34.09 (=C(CH₃)₂, alicyclic), 23.11 (-CH₃, alicyclic), 44.43, 46.05 and 47 (-CH₂-, alicyclic), 31.67 (=C=(CH₃)₂, alicyclic), 36.19 (=C-(CH₃)-CH₂-NH-CO-, alicyclic), 60.60 (-CH₂-NH-CO-), 69.45 to 72.51 (-O-CH₂-CH₂-O-CH₂-CH₂-O-), 155.57 (-NH-CO-O-), 156.73 (-CH₂-NH-CO-O-), 127.98 (-O-CO-CH=CH₂), 131.17 (-O-CO-CH=CH₂), 166.30 (-O-CO-CH=CH₂) ppm.

4.1.1.6.2 Formulation

The macromonomer was found to be viscous. 10 wt% of HEA was added to the macromonomer for better homogenization and during formulation. The formulations were made in 5 mL sample vials. 1 g of macromonomer containing 15 wt% of HEA was weighed accurately in all the vials. 5 mg (0.5 wt%), 10 mg (1 wt%) and 20 mg (2 wt%) of five photoinitiators were added to obtain fifteen compositions. Each composition was homogenized in a vibrating mill for 2 min. The photoinitiators used were DAROCUR TPO, IRGACURE 184, IRGACURE 2959, DAROCUR 1173 and DAROCUR MBF.

4.1.1.6.3 Photocuring studies

About 10 mg each of the compositions were accurately weighed on a DSC pan and subjected to photo DSC studies under a nitrogen purge of 50 mL/min. The heat flow

profiles obtained during the *in situ* photocuring process were recorded as a function of time under an isothermal condition of 30 °C. The intensity of irradiation was kept constant at 20.2 mW/cm² using a polychromatic radiation of 250-450 nm using a 100 W high pressure mercury short arc lamp. The normalized output signals in W/g against time were recorded. The rates of photopolymerizations as well as corresponding conversions were calculated for all the compositions.

4.1.1.6.4 Results and discussion

The existence of isocyanate group in the prepolymer as well as the complete conversion of isocyanate group during the formation of macromonomer was confirmed by IR, ¹H and ¹³C NMR spectroscopy. The molecular mass was found to be 1961 g/mol by VPO. The total theoretical heat flow^{4,6,7} (ΔH_{theor}) for the system containing 10 wt% HEA was calculated to be 147.39 J/g.

The rate and conversion profiles obtained from photocuring studies of macromonomeric formulations containing 10 wt% of HEA as reactive diluent with five photoinitiators at 0.5, 1 and 2 wt% compositions at 30 °C and 20.2 mW/cm² are given below in Figures 4.14 to 4.16 (A-C).

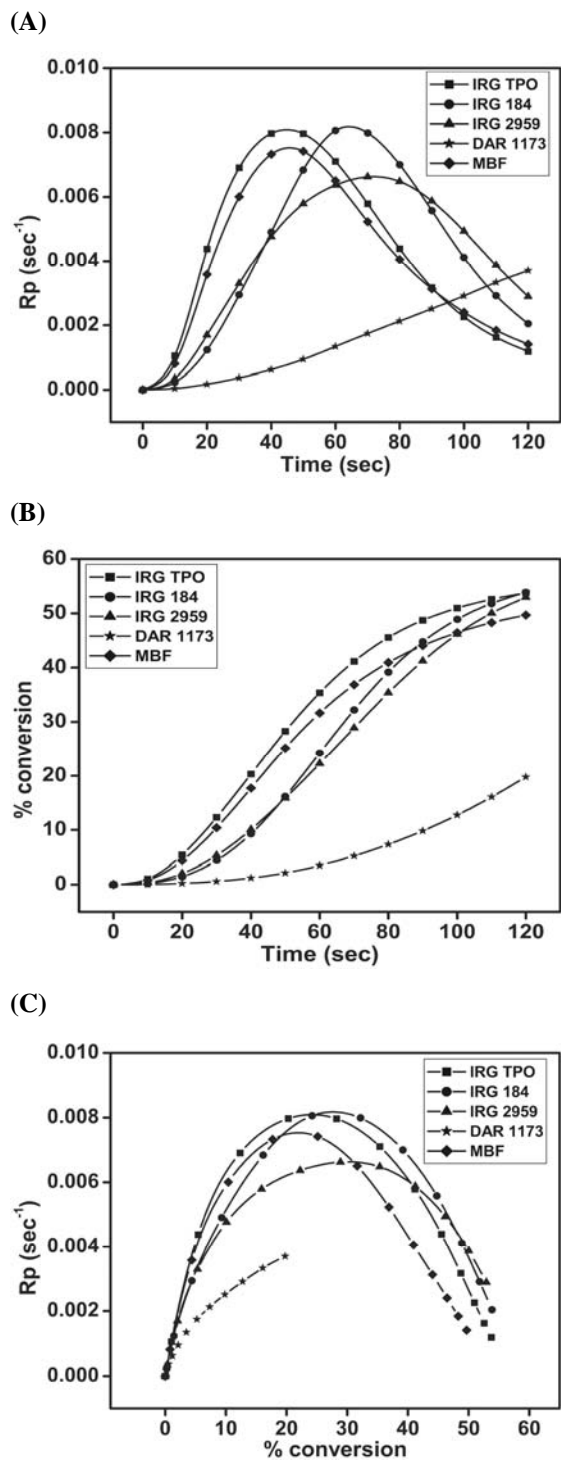
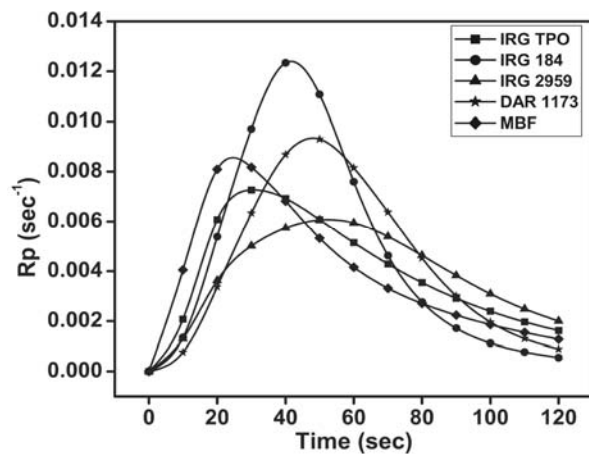
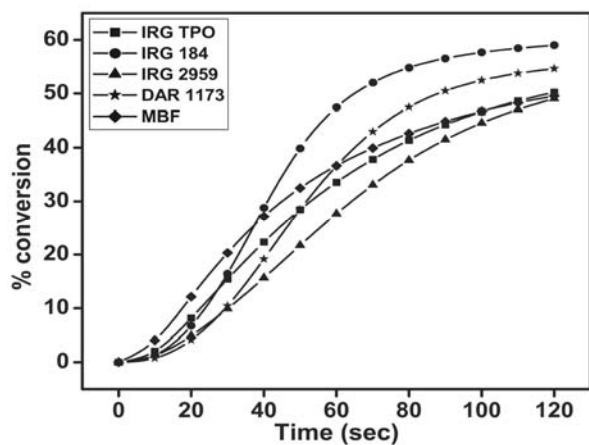


Figure 4.14(A-C) Time dependent rate and conversion profiles of macromonomeric formulations containing 0.5 wt% of five photoinitiators

(A)



(B)



(C)

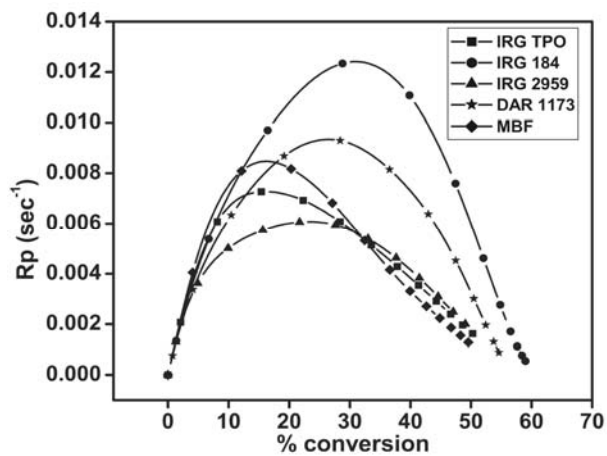
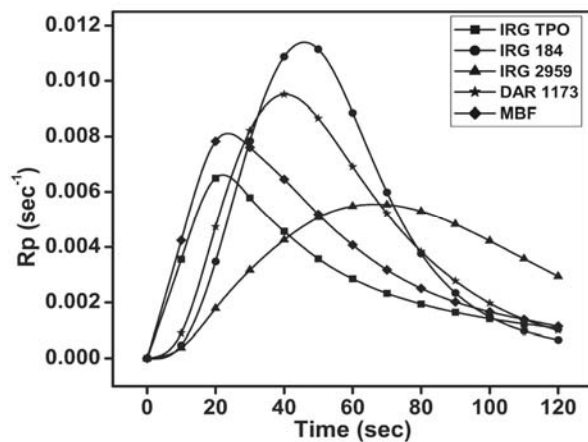
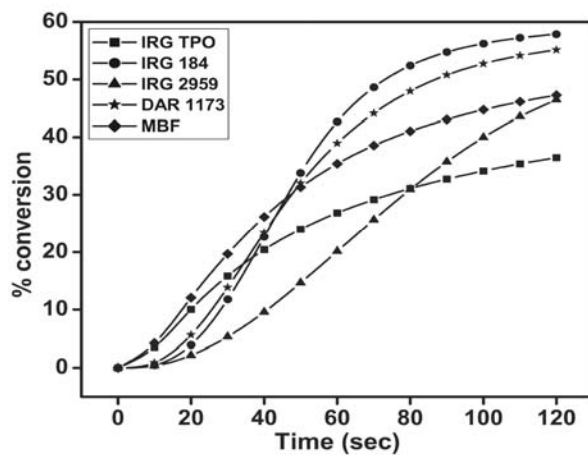


Figure 4.15(A-C) Time dependent rate and conversion profiles of macromonomeric formulations containing 1 wt% of five photoinitiators

(A)



(B)



(C)

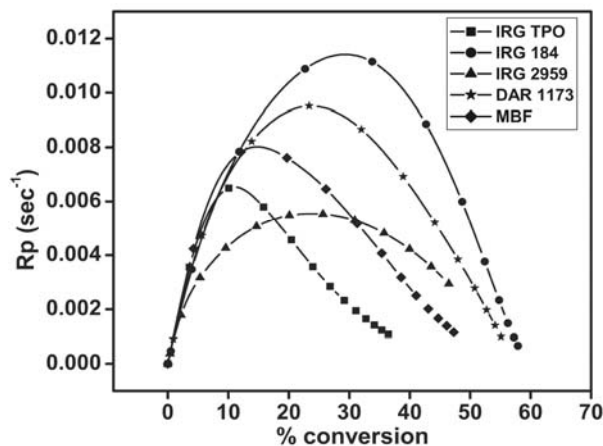


Figure 4.16(A-C) Time dependent rate and conversion profiles of macromonomeric formulations containing 2 wt% of five photoinitiators

The kinetic parameters calculated are given in Table 4.7.

Table 4.7 Kinetic parameters of macromonomeric formulations calculated from the heat flow profiles at 30 °C

Photo Initiator	% conc. of photo-initiator	Induction Time (sec)	Peak Maximum Time (sec)	$R_{p \max}$ ($\times 10^{-3}$) (sec^{-1})	C_{\max} (%)	Heat of reaction (J/g)	Autocatalytic		
							n	m	k
DAROCUR TPO	0.5	9.78	44.96	8.09	57.71	85.06	3.06	0.62	2.55
	1	6.58	30.70	7.26	57.01	84.02	3.79	0.50	2.02
	2	3.49	22.23	6.61	43.05	63.45	8.27	0.54	2.77
IRGACURE 184	0.5	17.46	64.26	8.18	59.52	87.73	3.15	0.81	3.55
	1	8.72	41.62	12.41	60.79	89.60	3.14	0.83	5.58
	2	12.61	45.92	11.40	59.81	88.15	3.08	0.78	4.74
IRGACURE 2959	0.5	15	72.48	6.64	60.86	89.70	2.19	0.62	1.70
	1	8.67	52.74	6.07	57.28	84.43	2.63	0.54	1.57
	2	14.52	66.93	5.56	57.41	84.61	2.88	0.64	1.71
DAROCUR 1173	0.5	37.14	-	-	49.13	72.42	3.48	0.69	1.59
	1	11.20	48.16	9.35	57.17	84.26	3.24	0.77	3.92
	2	10.34	40.32	9.51	58	85.49	3.58	0.72	3.99
DAROCUR MBF	0.5	10.80	45.75	7.52	54.73	80.66	4.13	0.73	3.50
	1	3.22	24.30	8.56	54.86	80.86	4.84	0.57	3.14
	2	2.96	23.57	8.12	51.75	76.27	4.75	0.52	2.64

From Table 4.7, the induction times for most systems were found to decrease with an increase in concentration of photoinitiator, showing faster initiation. The peak maximum time also follows a similar trend. However, in the case of formulations containing IRGACURE 184 and IRGACURE 2959, the optimum concentration of photoinitiator was reached below a concentration of 2 wt%, which resulted in an increase in induction time at a concentration of 2 wt%.¹⁷ This effect was pronounced at peak maximum time, showing a similar reduced rate of radical diffusion. DAROCUR TPO and DAROCUR MBF showed highest initiation rate, which was also reflected in the peak maximum time.

The value of $R_{p \max}$ showed much variation for all formulations. A reduction in the value of $R_{p \max}$ with an increase in concentration of photoinitiator was observed for DAROCUR TPO and IRGACUR 2959. These shows increase in viscosity build up near at $R_{p \max}$ with increase in concentration of photoinitiator. This effect also reduces the radical diffusion. Hence the influences of reaction diffusion at $R_{p \max}$ for the formulations

are higher.^{12,14} Variations such as increase or decrease in the value of $R_{p \max}$ in many formulations were observed due to competing factors such as competition between initiating / propagating radicals and between radicals and monomers.²³ If the viscosity build up is higher with reduced radical diffusion, then terminations as well as propagation will get reduced, resulting in a lower value of $R_{p \max}$. If the viscosity build up is less and radical diffusion is higher, then termination as well as propagation rate will be higher.^{12,14,15} Under these conditions, in most cases, the rate of propagation occurs faster than terminations as a certain viscosity has already attained, resulting in an increase in the value of $R_{p \max}$. Since the formulations are highly influenced by reaction diffusion even at $R_{p \max}$, the variations in radical as well as reaction diffusion occurring during the deceleration step resulted in variation in C_{\max} values from 43 to 61%.

The photopolymerizations were studied using polychromatic radiation (250-450 nm). All the photoinitiators except IRGACURE 2959 have multiple absorptions within the range of radiation.² In acetonitrile solution, the most prominent λ_{\max} and the corresponding extinction coefficients for the photoinitiators are as follows - DAROCUR TPO (380 nm, $\epsilon = 525 \text{ L mol}^{-1} \text{ cm}^{-1}$), IRGACURE 184 (243 nm, $\epsilon = 10000 \text{ L mol}^{-1} \text{ cm}^{-1}$), IRGACURE 2959 (272 nm, $\epsilon = 16200 \text{ L mol}^{-1} \text{ cm}^{-1}$), DAROCUR 1173 (243 nm, $\epsilon = 10900 \text{ L mol}^{-1} \text{ cm}^{-1}$) and DAROCUR MBF (255 nm, $\epsilon = 11200 \text{ L mol}^{-1} \text{ cm}^{-1}$).¹ The Table 4.7 shows that the DAROCUR TPO and DAROCUR MBF have a higher rate of initiation with an increase in concentration of photoinitiator. Due to multiple absorptions occurring within analysis range, DAROCUR TPO showed higher initiation rate. Considering the $\pi - \pi^*$ transition of DAROCUR MBF, we can find that this photoinitiator has highest initiation rate as it falls in the high energy region of analysis with a moderately high value of ϵ .¹ This effect is less pronounced for IRGACURE 184 and DAROCUR 1173 as their λ_{\max} for $\pi - \pi^*$ transition is outside the analysis range.¹

From Table 4.7, we can infer that the photopolymerization rate fits to the variable autocatalytic kinetic model over a wide range in the cure profile as the values of m and n are constant.¹⁸ With increase in concentration of photoinitiator, the specific rate constant (k) as per autocatalytic model was found to show variations for different systems. The cure process involves both bimolecular as well as monomolecular terminations.¹⁹ A gradual increase in the value of k was observed for DAROCUR 1173, while a gradual

decrease was observed for DAROCUR MBF. For DAROCUR TPO and IRGACURE 2959 an initial decrease followed by an increase was observed, while in the case of IRGACURE 184, an increase followed by a decrease was observed. This shows high combination effect of viscosity dependent reaction diffusion and radical diffusion (overall diffusion processes) occurring during the deceleration step.^{12,14,15}

4.1.1.7 Photopolymerization of dimethacrylate macromonomer based on hydroxy terminated polybutadiene 2750, isophorone diisocyanate and 2-hydroxyethyl methacrylate (System 4A-5)

A dimethacrylate macromonomer based on hydroxy terminated polybutadiene (HTPB 2750), IPDI and HEMA was synthesized and formulated. The photocuring studies of the formulations were carried out. Estimation of kinetic parameters were done based on the heat flow profile obtained during the photopolymerization process.

The telechelic synthesis was done in two steps. An initial condensation of the elastomeric diol and excess of diisocyanate to form a diisocyanate terminated urethane prepolymer followed by end capping of the formed prepolymer with excess of 2-hydroxyethyl methacrylate to form a soft segmented urethane dimethacrylate macromonomer.

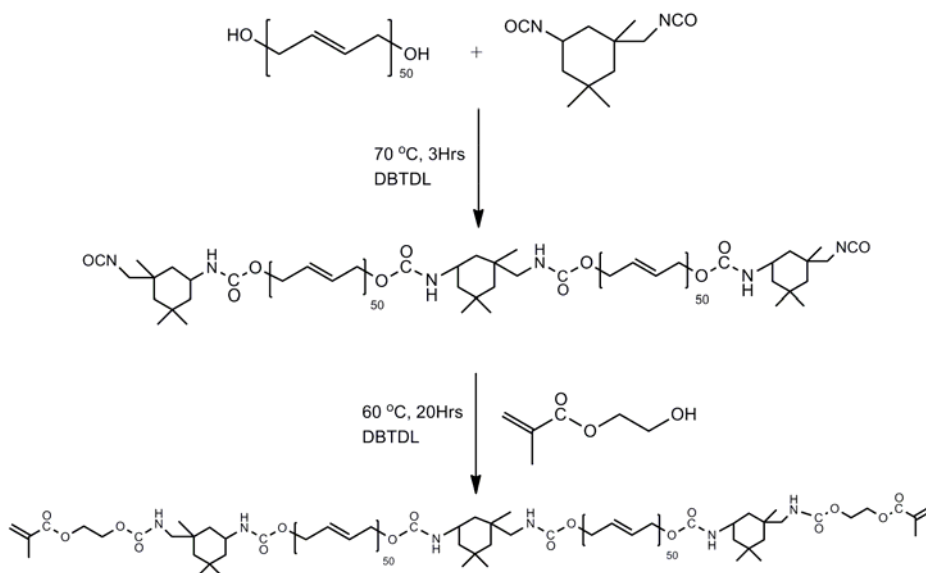


Figure 4.17 Synthesis pathway of dimethacrylate macromonomer based on HTPB 2750, IPDI and HEMA

4.1.1.7.1 Procedure for synthesis

Polymerization was carried out in a 100 mL three necked round bottomed flask provided with half moon stirrer rod through the central neck provided with a teflon stuffing box. The stirrer rod was connected to an overhead stirrer. Nitrogen gas was flushed to the flask through one side neck for a period of 2 min. 5 mg (0.007917 mmol) dibutyl tin dilaurate was added to it followed by the addition of 10.45 g (3.8 mmol) of dihydroxy terminated polybutadiene 2750 and homogenized at 40 °C at 80 rpm. 0.9135 g (4.11 mmol) of isophorone diisocyanate was weighed in a 25 mL beaker and was solvated in 5 mL chloroform and the contents of the beaker was transferred to the dropping funnel. The beaker was further washed with 5 mL of chloroform. Under stirring, the solvated diisocyanate was added at a rate of 2 mL/min. The system was homogenized well at 100 rpm and the temperature was increased to 70 °C. After 3 h, 1.018 g (0.007822 mmol) of 2-hydroxyethyl methacrylate in 20 mL of chloroform was added drop-wise through one side neck under stirring at a rate of 1 mL/min at 100 rpm for 5 min. The stirring speed was reduced thereafter to 80 rpm. The temperature was reduced to 60 °C and the reaction was continued in nitrogen atmosphere for 20 h until the isocyanate peak disappeared from the IR spectrum. IR and NMR spectra were noted. The molecular mass was found by VPO.

IR: 1727 (C=O, urethane), 3341 and 1521 (-CO-NH-, urethane), 1130 (C-O), 1640 and 826 (C=C-, methacrylate), 3003 (-C=C-), 2989, 2849 (-CH₂-) cm⁻¹.

¹³C NMR (CDCl₃): 18.29 (-O-CO-C(CH₃)=CH₂), 27.36, 32.69, 30.10, 24.83, 33.92 and 38.14 (CH₂, aliphatic, polybutadiene), 23.25, 27.64 and 35.07 (-CH₃, alicyclic), 41.78, 44.56 and 46.98 (-CH₂-, alicyclic), 62.83 (-CH₂-NH-CO-O-CH₂-CH₂-O), 62.72 (-CH₂-NH-CO-O-CH₂-CH₂-O), 114.22 and 142.68 (1,2- unsaturation, polybutadiene), 129.41 (1,4-cis unsaturation, polybutadiene), 129.97 (1,4 - trans unsaturation, polybutadiene), 131.22 (-CH=CH-CH₂-O-CO-NH-, terminal), 128.32 (-CH=CH-CH₂-O-CO-NH-, terminal), 156.46 (-NH-CO-O-CH₂-CH=CH-), 157.43 (-CH₂-NH-CO-O-CH₂-CH₂-O), 126.02(-O-CO-C(CH₃)=CH₂), 135.95 (-O-CO-C(CH₃)=CH₂), 168.57 (-O-CO-C(CH₃)=CH₂) ppm.

4.1.1.7.2 Formulation

The macromonomer was found to be viscous. 30 wt% of HEMA was added to the macromonomer for better homogenization and during formulation. The formulations were made in 5 mL sample vials. 1 g of macromonomer containing 30 wt% of HEMA as diluent was weighed accurately in all the vials. 10 mg (1 wt%) of five photoinitiators

were added to obtain five compositions. Each composition was homogenized in a vibrating mill for 2 min. The photoinitiators used were IRGACURE 651, DAROCUR 1173, DAROCUR MBF, IRGACURE 915 and IRGACURE 819.

4.1.1.7.3 Photocuring studies

About 10mg of each composition was accurately weighed on a DSC pan and subjected to photo DSC studies under a nitrogen purge of 50 mL/min. The heat flow profiles obtained during the *in situ* photocuring process were recorded as a function of time under an isothermal condition of 30 °C. The intensity of irradiation was kept at 23.7 mW/cm² using a polychromatic radiation of 250-450 nm using a 100 W high pressure mercury short arc lamp. The normalized output signals in W/g against time were recorded. The rates of photopolymerizations as well as corresponding conversions were calculated for all the compositions.

4.1.1.7.4 Results and discussion

The complete conversion of isocyanate group during the formation of macromonomer was confirmed by IR and ¹³C NMR spectroscopy. The molecular mass was found to be 3246 g/mol by VPO. The total theoretical heat flow^{6,7,20} (ΔH_{theor}) for the system containing 30 wt% HEMA was calculated to be 123.17 J/g.

The rate and conversion profiles obtained from photocuring studies of macromonomeric formulations containing 30 wt% of HEMA as reactive diluent with five photoinitiators at 1 wt% compositions at 30 °C and 20.2 mW/cm² are given below in Figure 4.18 (A-C).

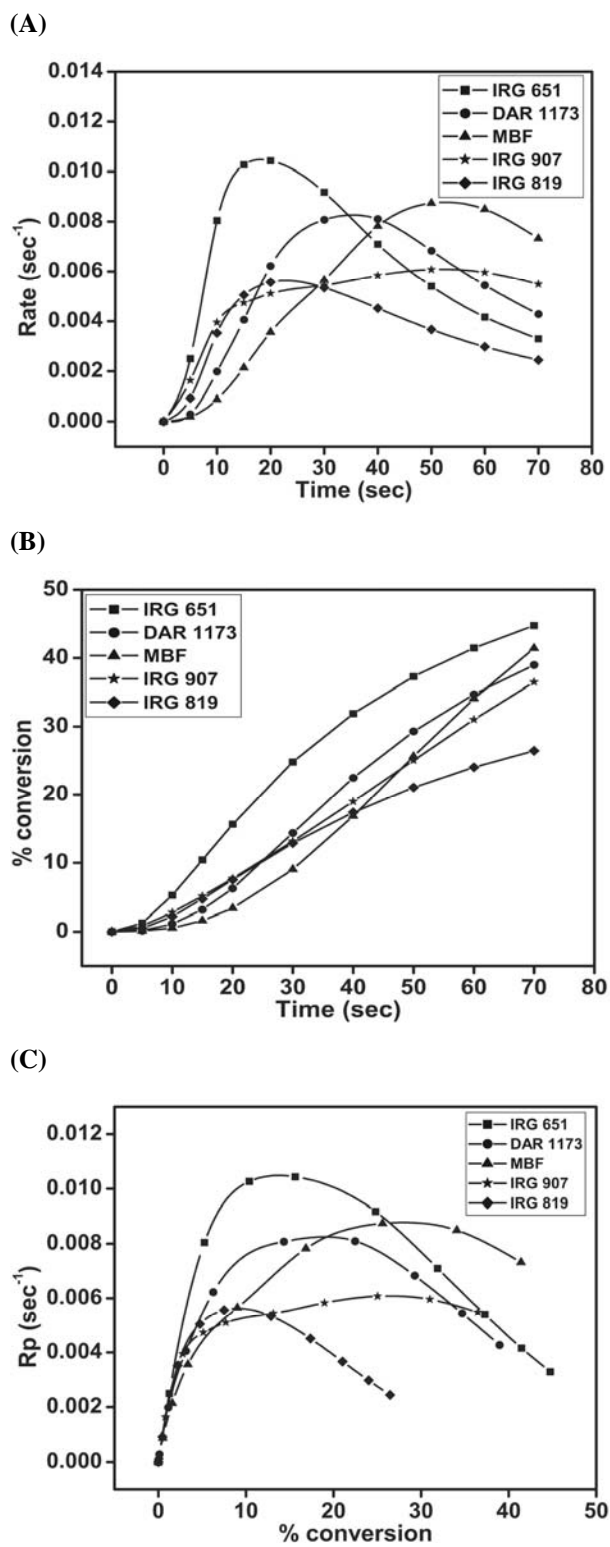


Figure 4.18(A-C) Time dependent rate and conversion profiles of macromonomeric formulations containing 1 wt% of five photoinitiators

The kinetic parameters calculated are given in Table 4.8.

Table 4.8 Kinetic parameters of macromonomeric formulations calculated from the heat flow profiles at 1wt% concentration of photoinitiator at 30 °C

Photoinitiator	Induction Time (sec)	Peak Maximum Time (sec)	$R_{p \max}$ ($\times 10^{-3}$) (sec^{-1})	C_{\max} (%)	Heat of reaction (J/g)	Autocatalytic		
						n	m	k
IRGACURE 651	3.99	18.20	10.48	60.44	74.45	5.39	0.56	3.78
DAROCUR 1173	9.34	35.36	8.27	57.73	71.10	5.73	0.68	4.10
DAROCUR MBF	12.18	52.74	8.78	68.70	84.62	3.41	0.69	3.15
IRGACURE 907	5.44	52.25	6.08	65.20	80.31	2.78	0.47	1.20
IRGACURE 819	6.50	23.02	5.62	38.14	46.98	9.01	0.56	2.60

From Table 4.8, the induction time for formulation containing IRGACURE 651 was found to be lowest while that for formulation with DAROCUR MBF, if found to be highest. Thus before the effect of viscosity build up, the rate of initiation is fastest for formulation containing IRGACURE 651. The peak maximum time also is found to be least for formulation containing IRGACURE 651. The peak maximum time of formulation containing IRGACURE 907 is nearly equal to that of DAROCUR MBF, even though IRGACURE 907 had a faster initial rate of reaction. This can be due to earlier onset of reaction diffusion or reduction in radical diffusion for the active species in IRGACURE 907, before attaining peak maximum.

The $R_{p \max}$ was highest for the formulations containing IRGACURE 651 and lowest for IRGACURE 819 due to better radical diffusion initiated by high excitation energy.² Here the effect of retardation by overall diffusion process is much pronounced for formulation containing IRGACURE 819 than for formulation containing IRGACURE 651. The final conversion was found to be highest for formulation containing DAROCUR MBF and lowest for IRGACURE 819. Due to a probable high *in situ* viscosity at $R_{p \max}$, the value of C_{\max} for formulation containing IRGACURE 819 was found to be least. Contrary to the expectation, the formulation containing DAROCUR MBF showed higher conversion than formulation containing IRGACURE 651 due to a probable better radical diffusion or reduced viscosity build up in the deceleration step.^{12,14,15}

The photopolymerizations were studied using polychromatic radiation (250-450 nm). All the photoinitiators have multiple absorptions within the range of radiation.² In acetonitrile solution, the most prominent λ_{\max} and the corresponding extinction

coefficients for the photoinitiators are as follows - IRGACURE 651 (252 nm, $\epsilon = 12800 \text{ L mol}^{-1} \text{ cm}^{-1}$), DAROCUR 1173 (243 nm, $\epsilon = 10900 \text{ L mol}^{-1} \text{ cm}^{-1}$), DAROCUR MBF (255 nm, $\epsilon = 11200 \text{ L mol}^{-1} \text{ cm}^{-1}$), IRGACURE 907 (303 nm, $\epsilon = 18600 \text{ L mol}^{-1} \text{ cm}^{-1}$) and IRGACURE 819 (369 nm, $\epsilon = 933 \text{ L mol}^{-1} \text{ cm}^{-1}$).¹ The Table 4.8 shows that IRGACURE 651 has the highest initiation rate. Even though, DAROCUR MBF has the second highest absorption energy; an unexpected low initiation rate was observed probably due to very low initial radical diffusion. But this delay in radical diffusion has helped the system to undergo longer time scale of segmental diffusion, which in turn resulted in a delay in onset of reaction diffusion. The system thus achieved the highest final conversion than other systems.^{12,14}

From Table 4.8, we can infer that the photopolymerization rate fits to the variable autocatalytic kinetic model over a wide range in the cure profile as the values of m and n are constant.¹⁸ The value of specific rate constant as per the model was found to be highest for DAROCUR 1173 and lowest for IRGACURE 907. As the final conversion was below 69%, the formulations during photocuring can be assumed to undergo both bimolecular and monomolecular terminations.¹⁹

4.1.1.8 Synthesis of dimethacrylate macromonomer based on hydroxy terminated polybutadiene 2750, polypropylene glycol 725, hexamethylene diisocyanate and 2-hydroxy ethyl methacrylate (System 4A-6)

A dimethacrylate macromonomer based on HTPB 2750, PPG 725, HMDI and HEMA was synthesized and formulated. The photocuring studies of the formulations were carried out. Estimation of kinetic parameters were done based on the heat flow profile obtained during the photopolymerization process.

The telechelic synthesis was done in two steps. An initial condensation of the mixture of diols and excess of diisocyanate to form a diisocyanate terminated urethane prepolymer followed by end capping of the formed prepolymer with excess of 2-hydroxy ethyl methacrylate to form soft segmented urethane dimethacrylate macromonomer.

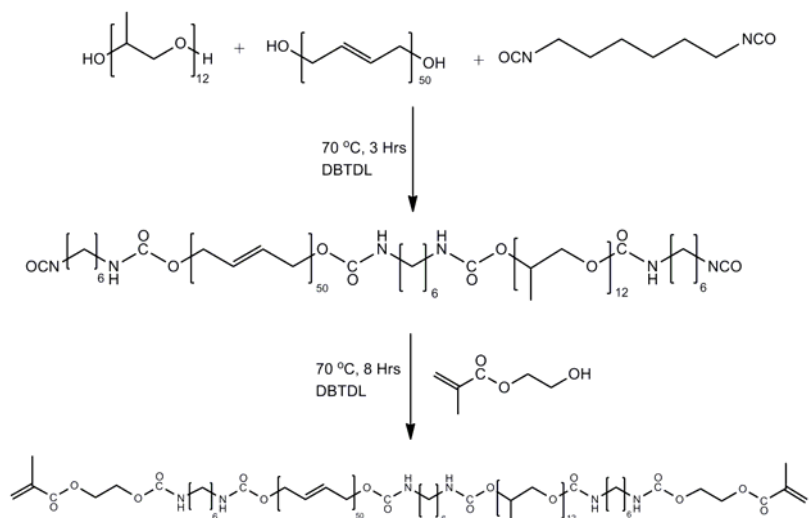


Figure 4.19 Synthesis pathway of dimethacrylate macromonomer based on HTPB 2750, PPG 725, HMDI and HEMA

4.1.1.8.1 Procedure for synthesis

Polymerization was carried out in a 100 mL three necked round bottomed flask provided with half moon stirrer rod through the central neck provided with a teflon stuffing box. The stirrer rod was connected to an overhead stirrer. Nitrogen gas was flushed to the flask through one side neck for a period of 2 min. 42 mg (0.0665 mmol) of dibutyl tin dilaurate was added to it followed by the addition of 14.785 g (20.39 mmol) of PPG 725 and 13 g (4.73 mmol) of dihydroxy terminated polybutadiene 2750. The system was homogenized at 40 °C at 80 rpm. Using a dropping funnel 4.27 mL (26.38 mmol) of hexamethylene diisocyanate was added at a rate of 0.5 mL/min. After complete addition, the dropping funnel was washed with 5 mL of chloroform and the washings were also allowed to pour into the flask. The system was homogenized well at 100 rpm and the temperature was increased to 70 °C. After 3 h, 1.99 g (15.29 mmol) of 2-hydroxyl ethyl methacrylate in 5 mL chloroform was transferred to the flask using a dropping funnel. The addition was done under stirring at a rate of 1 mL/min. It was then stirred for five minutes at 100 rpm. The stirring speed was reduced thereafter to 80 rpm. The reaction was continued at 70 °C in nitrogen atmosphere for 8 h until the isocyanate peak disappeared from the IR spectrum. IR and NMR spectra were noted. The molecular mass was found by VPO.

IR: 1710 (C=O, urethane), 3340 and 1511 (-CO-NH-, urethane), 1131 (C-O), 1639 and 825 (C=C-, methacrylate), 3003 (-C=C-), 2989, 2921, 2849 (-CH₂-) cm⁻¹.

¹H NMR (CDCl₃): 2.02 (-CH₂-CH=CH-CH₂-), 3.14 (-CH₂-NH-CO-O-), 3.31 to 3.63 (-CH(CH₃)-CH₂-O-), 4.46 and 4.49 (-CH₂-NH-CO-O-, internal), 4.30 (-CH₂-NH-CO-O-, terminal), 5.39 (-CH₂-CH=CH-CH₂-), 5.58 and 6.12 (-CO-C(CH₃)=CH₂) ppm.

¹³C NMR (CDCl₃): 17.28 and 18.17 (-CH(CH₃)-CH₂-O-), 27.33, 32.65, 30.06, 24.81, 33.88 and 38.10 (CH₂, aliphatic, polybutadiene), 73.26 (-CH(CH₃)-CH₂-O-), 75.29 (-CH(CH₃)-CH₂-O-), 114.18 and 142.64 (1,2- unsaturation, polybutadiene), 129.37 (1,4-cis unsaturation, polybutadiene), 129.96 (1,4 – trans unsaturation, polybutadiene), 131.18 (-CH=CH-CH₂-O-CO-NH-, terminal), 128.28 (-CH=CH-CH₂-O-CO-NH-, terminal), 125.95 (-O-CO-C(CH₃)=CH₂), 136.66 (-O-CO-C(CH₃)=CH₂), 156.17 (-NH-CO-O-CH₂-CH=CH-), 166.62 (-O-CO-C(CH₃)=CH₂) ppm.

4.1.1.8.2 Formulation

The macromonomer was found to be viscous. 30 wt% of HEMA was added to the macromonomer for better homogenization during formulation. The formulations were made in 5 mL sample vials. 1 g of macromonomer containing 30 wt% diluent was weighed accurately in all the vials. 2.5 mg (0.25 wt%), 5 mg (0.5 wt%), 10 mg (1 wt%) and 20 mg (2 wt%) of three photoinitiators were added to obtain twelve compositions. Each composition was homogenized in a vibrating mill for 2 min. The photoinitiators used were IRGACURE 651, DAROCUR TPO and IRGACURE 819.

4.1.1.8.3 Photocuring studies

About 10 mg each of the composition was accurately weighed on a DSC pan and subjected to photo DSC studies under a nitrogen purge of 50 mL/min. The heat flow profiles obtained during the *in situ* photocuring process were recorded as a function of time under an isothermal condition of 30 °C. The intensity of irradiation was kept at 25.2 mW/cm² using a polychromatic radiation of 250-450 nm using a 100 W high pressure mercury short arc lamp. The normalized output signals in W/g against time were recorded. The rates of photopolymerizations as well as corresponding conversions were calculated for all the compositions.

4.1.1.8.4 Results and discussion

The complete conversion of isocyanate group during the formation of macromonomer was confirmed by IR, ^1H and ^{13}C NMR spectroscopy. The molecular mass was found to be 4124 g/mol by VPO. The total theoretical heat flow^{6,7,20} (ΔH_{theor}) for the system containing 30 wt% HEMA was calculated to be 117.64 J/g.

The rate and conversion profiles obtained from photocuring studies of macromonomeric formulations containing 30 wt% of HEMA as reactive diluent with three photoinitiators at 0.25, 0.5, 1 and 2 wt% compositions at 30 °C and 25.2 mW/cm² are given below in Figures 4.20 to 4.22 (A-C).

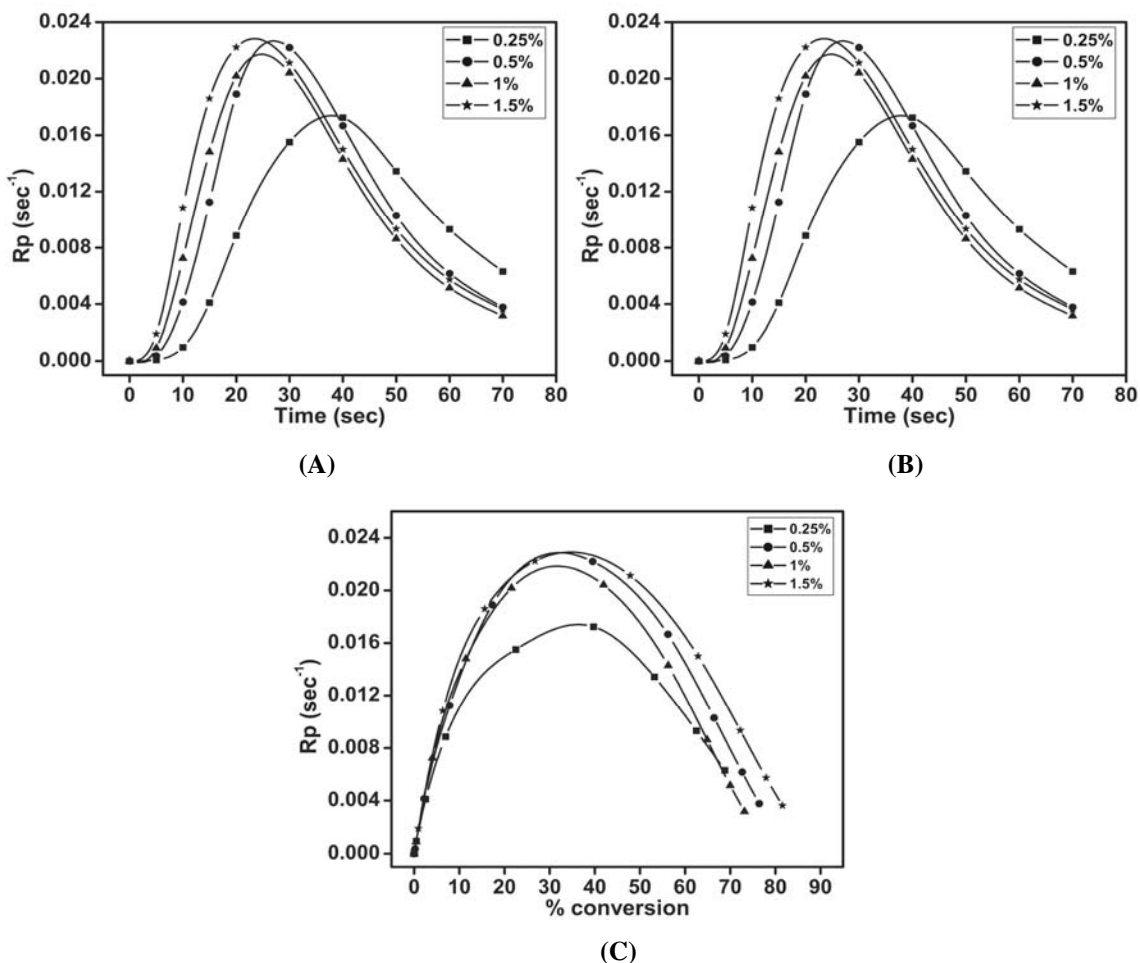
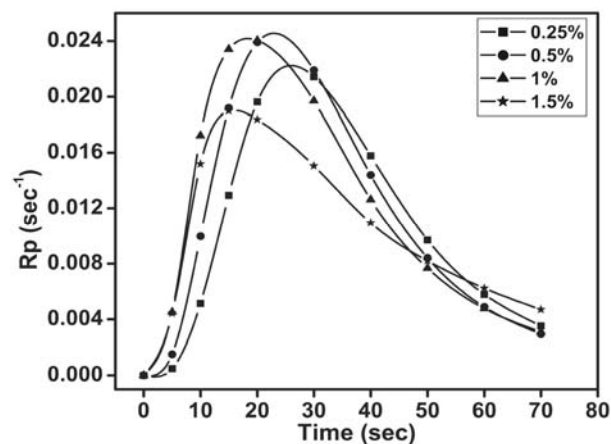
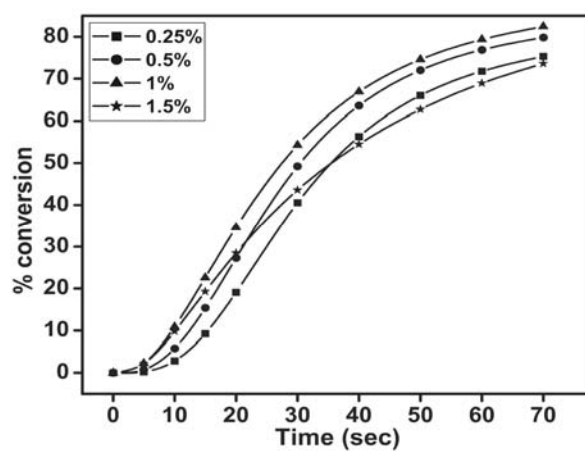


Figure 4.20(A-C) Time dependent rate and conversion profiles of macromonomeric formulations containing IRGACURE 651 at different concentrations

(A)



(B)



(C)

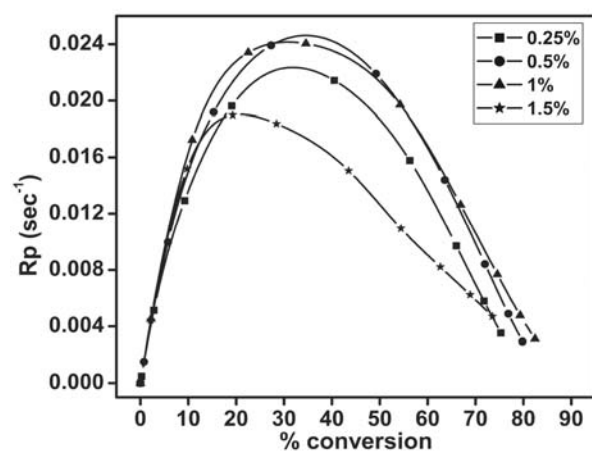
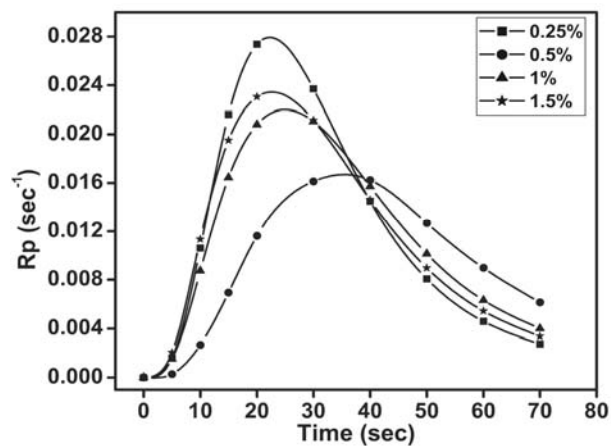
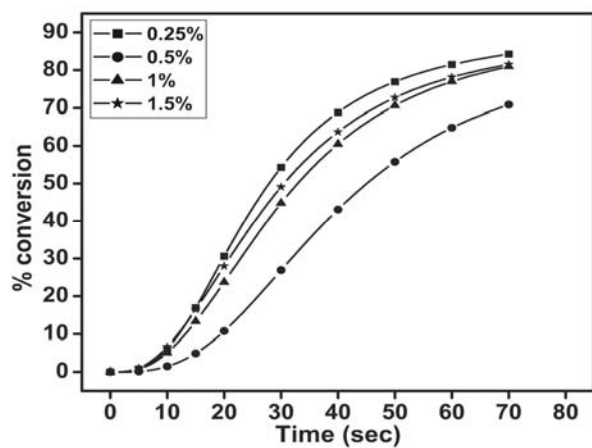


Figure 4.21(A-C) Time dependent rate and conversion profiles of macromonomeric formulations containing DAROCUR TPO at different concentrations

(A)



(B)



(C)

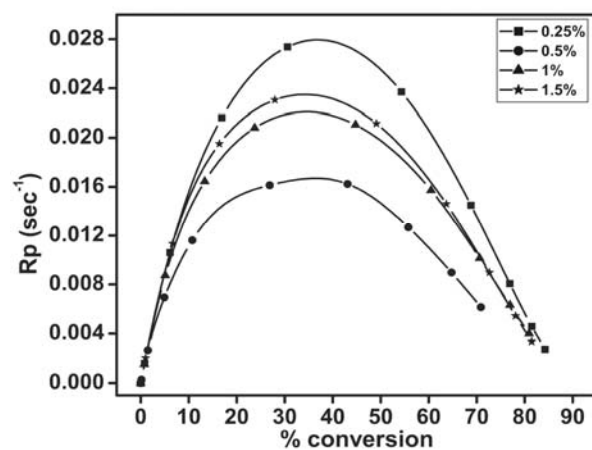


Figure 4.22(A-C) Time dependent rate and conversion profiles of macromonomeric formulations containing IRGACURE 819 at different concentrations

The kinetic parameters calculated are given in Table 4.9.

Table 4.9 Kinetic parameters of macromonomeric formulations calculated from the heat flow profiles at 30 °C.

Photoinitiator	% conc of photo-initiator	Induction Time (sec)	Peak Maximum Time (sec)	$R_{p \max}$ ($\times 10^{-2}$) (sec^{-1})	C_{\max} (%)	Heat of reaction (J/g)	Autocatalytic		
							n	m	k
IRGACURE 651	0.25	11.72	37.97	1.74	85	99.99	2.24	0.71	5.43
	0.5	7.83	26.93	2.27	85.18	100.2	2.23	0.73	7.15
	1	6.22	24.82	2.17	80.8	95.05	2.38	0.70	6.70
	1.5	5.04	23.46	2.28	90.53	106.5	1.77	0.58	5.08
DAROCUR TPO	0.25	7.28	25.93	2.22	85.07	98.9	2.21	0.69	6.61
	0.5	5.44	22.91	2.46	87.47	102.9	2	0.64	6.33
	1	3.43	18.33	2.42	89.94	105.8	1.77	0.52	5.03
	1.5	3.34	15.70	1.90	89.09	104.8	1.92	0.36	3.01
IRGACURE 819	0.25	6.59	22.25	2.80	91.55	107.7	1.88	0.67	7.22
	0.5	8.83	35.38	1.67	85.86	101	1.97	0.66	4.53
	1	6.24	24.95	2.20	90.62	106.6	1.77	0.60	4.99
	1.5	4.95	22.65	2.35	89.94	105.8	1.80	0.58	5.27

From Table 4.9, the rate of initiation was found to be fastest with formulation containing DAROCUR TPO and least with formulation containing IRGACURE 651 due to multiple absorption of DAROCUR TPO.¹⁴ In most cases, induction time was found to decrease with increase in concentration of photoinitiator.²⁴ The peak maximum time was also found to follow the same trend.²⁴ For all systems, the value of $R_{p \max}$ was found to show varying patterns with increase in concentration of photoinitiator. This trend is observed when the reaction diffusion sets in soon after auto acceleration.¹² The segmental diffusion time period is very much reduced and the variations in $R_{p \max}$ are observed rather than a particular trend (increase or decrease). In general, the earlier is the onset of reaction diffusion after autoacceleration the lower will be observed $R_{p \max}$.¹² Variations can occur depending on the other parameters such as analyses temperature and intensity, initial viscosity of the formulation as well as on the rate of initiation, propagation, termination and diffusion of radicals.^{15,16} In this case, the radical diffusion during the onset of reaction diffusion soon after gelation may have a contributing effect to an increase or decrease in $R_{p \max}$ value. At an optimum viscosity, increase in radical diffusion before peak maximum can increase the value of $R_{p \max}$.¹² The interplay of the above two factors which are totally dependent on the *in situ* viscosity from the onset of gelation to the peak maximum is responsible for the observed variations. The final

conversion was found to vary from 80 to 92%. High conversion was possible in this system as the backbone is not having any hard segments.^{14,21,25} IRGACURE 819 is efficient for through cure applications.²⁶ The highest conversions were observed with formulations containing IRGACURE 819 due to a high radical diffusion on the flexible system. The lowest conversion was observed with IRGACURE 651 at 1 wt% concentration most probably due to a combination of earlier onset of reaction diffusion and comparatively low rate of radical diffusion, forcing the system to terminate the process soon after auto deceleration.

The photopolymerizations were carried out using polychromatic radiation (250-450 nm). All the photoinitiators have multiple absorptions within the range of radiation.² In acetonitrile solution, the most prominent λ_{max} and the corresponding extinction coefficients for the photoinitiators are as follow - IRGACURE 651 (252 nm, $\epsilon = 12800 \text{ L mol}^{-1} \text{ cm}^{-1}$), DAROCUR TPO (380 nm, $\epsilon = 525 \text{ L mol}^{-1} \text{ cm}^{-1}$) and IRGACURE 819 (369 nm, $\epsilon = 933 \text{ L mol}^{-1} \text{ cm}^{-1}$).¹ The Table 4.9 shows that DAROCUR TPO has the fastest rate of initiation probably due to higher initial rate of radical diffusion in the matrix than IRGACURE 819 due to multiple excitations. IRGACURE 819 shows only two instead of four excitation regions for DAROCUR TPO within the analysis range.² The allowed $\pi - \pi^*$ transition of IRGACURE 651 is responsible for the initiation in formulations containing IRGACURE 651 while the forbidden $n - \pi^*$ transition occurring in the formulations containing DAROCUR TPO and IRGACURE 819 is responsible for their initiation.²⁶

From Table 4.9, we can infer that the photopolymerization rate fits to the variable autocatalytic kinetic model over a wide range in the cure profile as the values of m and n are constant.¹⁸ The value of specific rate constant (k) did not show any trend with increase in concentration of photoinitiator.²⁴ Due to the presence of soft segments, the system showed a maximum conversion around 92%.^{14,21} The system during photocuring can be assumed to undergo both bimolecular and monomolecular terminations.¹⁹

4.1.1.9 Photopolymerization of dimethacrylate macromonomer based on hydroxyl terminated polybutadiene 2750, isophorone diisocyanate and hydroxy propyl acrylate (System 4A-7)

A diacrylate macromonomer based on HTPB 2750, IPDI and hydroxypropyl acrylate (HPA) was synthesized and formulated. The photocuring studies of the formulations were carried out. Estimation of kinetic parameters were carried out based on the heat flow profile obtained during the photopolymerization process.

The synthesis was done in two steps. The initial step involves condensation of the hydroxyl acrylate with monomeric diisocyanate to obtain a urethane with isocyanate and acrylate end groups followed by end capping of the hydroxyl terminated polybutadiene with the above synthesized isocyanate adduct to obtain soft segmented diacrylated diurethane macromonomer.

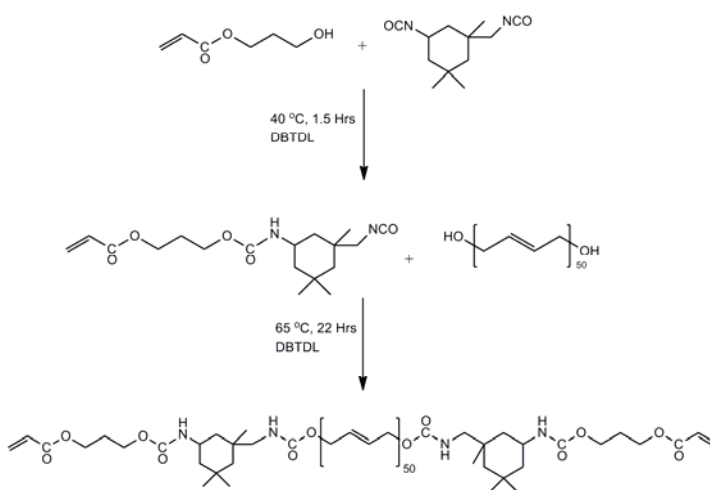


Figure 4.23 Synthesis pathway of dimethacrylate macromonomer based on HTPB 2750, IPDI and HPA

4.1.1.9.1 Procedure for synthesis

Synthesis of end capping agent

The end capping agent was synthesized from isophorone diisocyanate and hydroxy propyl acrylate. A 100 mL three necked round bottomed flask provided with half moon stirrer rod and teflon stuffing box through the central neck was flushed for 2 min with nitrogen. The stirrer rod was connected to an overhead stirrer. 29.57 g (133 mmol) of isophorone diisocyanate and 0.0595 g (0.09421 mmol) dibutyl tin dilaurate was added to it and stirred at 40 °C and stirred at 80 rpm for 2 minutes under nitrogen purge.

17.3086 g (133 mmol) of hydroxyl propyl acrylate was added drop-wise within a period of 30 min under the same conditions. After 1 h, the system became viscous and was transferred to a container and stored under refrigeration. IR and NMR spectra were noted.

IR: 2269 (NCO), 1728 (C=O, urethane), 3346 and 1530 (-CO-NH-, urethane), 1637, 809 (C=C-, acrylate), 2956, 2893 (-CH₂-) cm⁻¹.

¹H NMR (CDCl₃): 0.94 and 1.06 (-CH₃, alicyclic), 1.18-1.25 (-CH₂-, alicyclic), 3.01 (-CH₂-NCO), 4.31 and 4.39 (-CH₂-CH₂-CH₂-, propyl), 4.55 (=NH-CO-O-) ppm.

¹³C NMR (CDCl₃): 23.30, 27.45 and 34.85 (-CH₃, alicyclic), 31.77 (=CH₃)₂, alicyclic), 36.44 (=CH₃-CH₂-, alicyclic), 41.40, 45.99 and 46.46 (-CH₂-, alicyclic), 56.72 (-NH-CO-O-CH₂-), 62.70 (-CH₂-NCO), 121.71 (-NCO), 131.31 (CH₂=CH-CO-O-), 127.96 (CH₂=CH-CO-O-), 155.23 (-NH-CO-O-CH=CH₂), 165.36 (-O-CO-CH=CH₂) ppm.

Synthesis of macromonomer

Polymerization was carried out in a 100 mL three necked round bottomed flask provided with half moon stirrer rod through the central neck provided with a teflon stuffing box. The stirrer rod was connected to an overhead stirrer. Nitrogen gas was flushed to the flask through one side neck for a period of 2 min. 25.5 g (9.273 mmol) of dihydroxy terminated polybutadiene 2750 and 0.08 g (0.1267 mmol) dibutyl tin dilaurate was added to it at stirred at room temperature at 80 rpm for 15 min. 6.4107 g (18.19 mmol) of IDI-HPA adduct was accurately weighed in a 25 mL beaker and solvated in 10 mL of chloroform. It was then added drop-wise under stirring at a rate of 1 mL/min. After the addition, the temperature of the system was raised to 65 °C and stirred at 80 rpm for 22 h under nitrogen purge, until the isocyanate peak disappeared from the IR spectrum. IR and NMR spectra were noted. The molecular mass was found by VPO.

IR: 1729 (C=O, urethane), 1534 (-CO-NH-, urethane), 1639, 809 (C=C-, acrylate), 3001 (-C=C-), 2956, 2916, 2840 (-CH₂-) cm⁻¹.

¹H NMR (CDCl₃): 0.91 and 1.04 (-CH₃, alicyclic), 2.02 (-CH₂-CH=CH-CH₂-), 4.19 (-CH₂-NH-CO-O-), 4.49 (=NH-CO-O-), 4.74 (-CH₂-NH-CO-O-), 5.39 (-CH₂-CH=CH-CH₂-), 5.87, 6.47 (-CO-CH=CH₂), 6.14 (-CO-CH=CH₂) ppm.

^{13}C NMR (CDCl_3): 27.34, 32.66, 30.08, 24.83, 33.90 and 38.12 (CH_2 , aliphatic, polybutadiene), 56.68 ($-\text{NH}-\text{CO}-\text{O}-\underline{\text{C}}\text{H}_2-$), 66.39 ($-\underline{\text{C}}\text{H}_2-\text{NH}-\text{CO}-\text{O}-\text{CH}_2-$), 114.20 and 142.62 (1,2- unsaturation, polybutadiene), 129.38 (1,4-cis unsaturation, polybutadiene), 129.96 (1,4 – trans unsaturation, polybutadiene), 131.21 ($-\text{CH}=\underline{\text{C}}\text{H}-\text{CH}_2-\text{O}-\text{CO}-\text{NH}-$, terminal), 128.30 ($-\underline{\text{C}}\text{H}=\text{CH}-\text{CH}_2-\text{O}-\text{CO}-\text{NH}-$, terminal), 156.78 ($-\text{NH}-\underline{\text{C}}\text{O}-\text{O}-\text{CH}_2-\text{CH}=\text{CH}-$), 156.96 ($-\text{CH}_2-\text{NH}-\underline{\text{C}}\text{O}-\text{O}-\text{CH}_2-\text{CH}_2-\text{O}$), 165.45 ($-\text{O}-\underline{\text{C}}\text{O}-\text{CH}=\text{CH}_2$) ppm.

4.1.1.9.2 Formulations

The formulations were made in 1 mL disposable centrifuge tubes. 500 mg of macromonomer (0.1643 mmol) was accurately weighed in all the vials. 1.25 mg (0.25 wt%) and 2.5 mg (0.5 wt%) of four photoinitiators were added to obtain eight compositions. Each composition was homogenized in a vibrating mill for 3 min. The photoinitiators used were IRGACURE 651, IRGACURE 184, IRGACURE 2959 and IRGACURE 819.

4.1.1.9.3 Photocuring studies

About 3 mg of the composition was accurately weighed on a DSC pan and subjected to photo DSC studies under a nitrogen purge of 50 mL/min. The heat flow profile obtained during the *in situ* photocuring process was recorded as a function of time under an isothermal condition of 30 °C. The intensity of irradiation was kept at 2.14 mW/cm² using a polychromatic radiation of 320-500 nm using a 100 W high pressure mercury short arc lamp. The normalized output signals in W/g against time were recorded. The rates of photopolymerizations as well as corresponding conversions were calculated for all the compositions.

4.1.1.9.4 Results and discussion

The existence of isocyanate group in the end capping agent as well as the complete conversion of isocyanate group during the formation of macromonomer was confirmed by IR, ^1H and ^{13}C NMR spectroscopy. The molecular mass was found to be 3044 g/mol by VPO. The total theoretical heat flow^{4,7} (ΔH_{theor}) for the system was calculated to be 56.63 J/g.

The rate and conversion profiles obtained from photocuring studies of macromonomeric formulations with four photoinitiators at 0.25 and 0.5 wt% compositions at 30 °C and 2.14 mW/cm² are given below in Figures 4.24 to 4.25 (A-C).

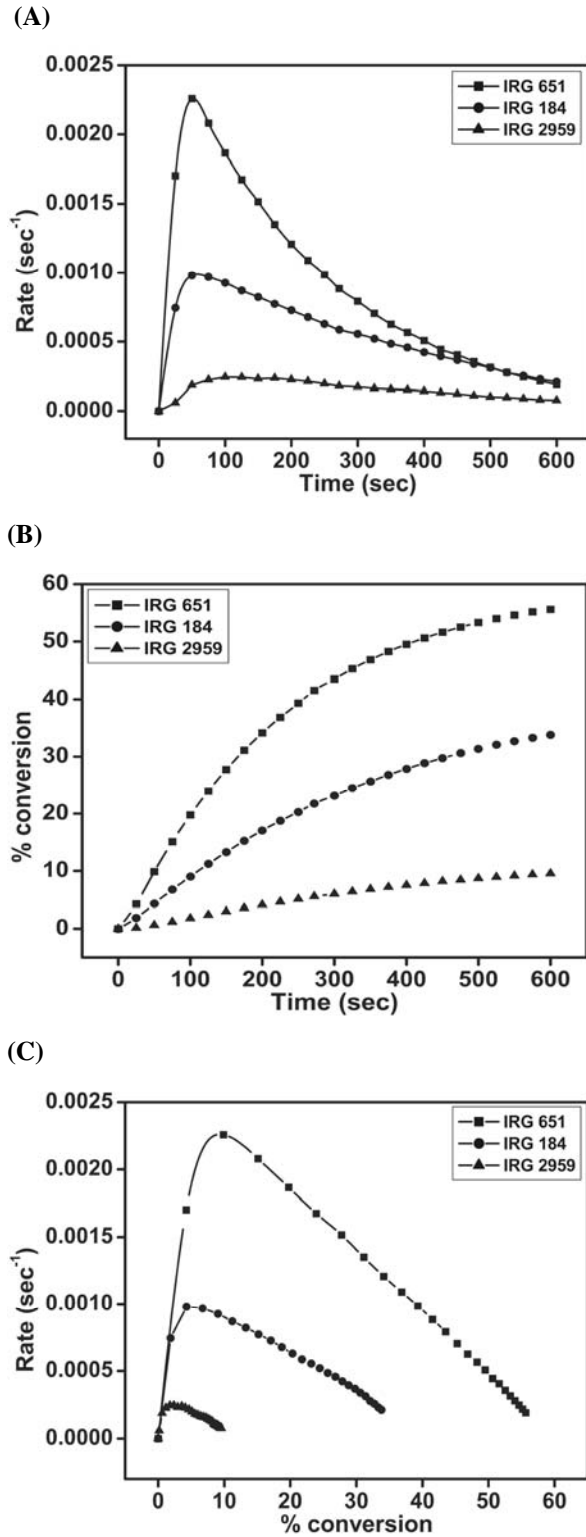


Figure 4.24(A-C) Time dependent rate and conversion profiles of macromonomeric formulations containing 0.25 wt% of photoinitiator with respect to weight of macromonomer at 30 °C

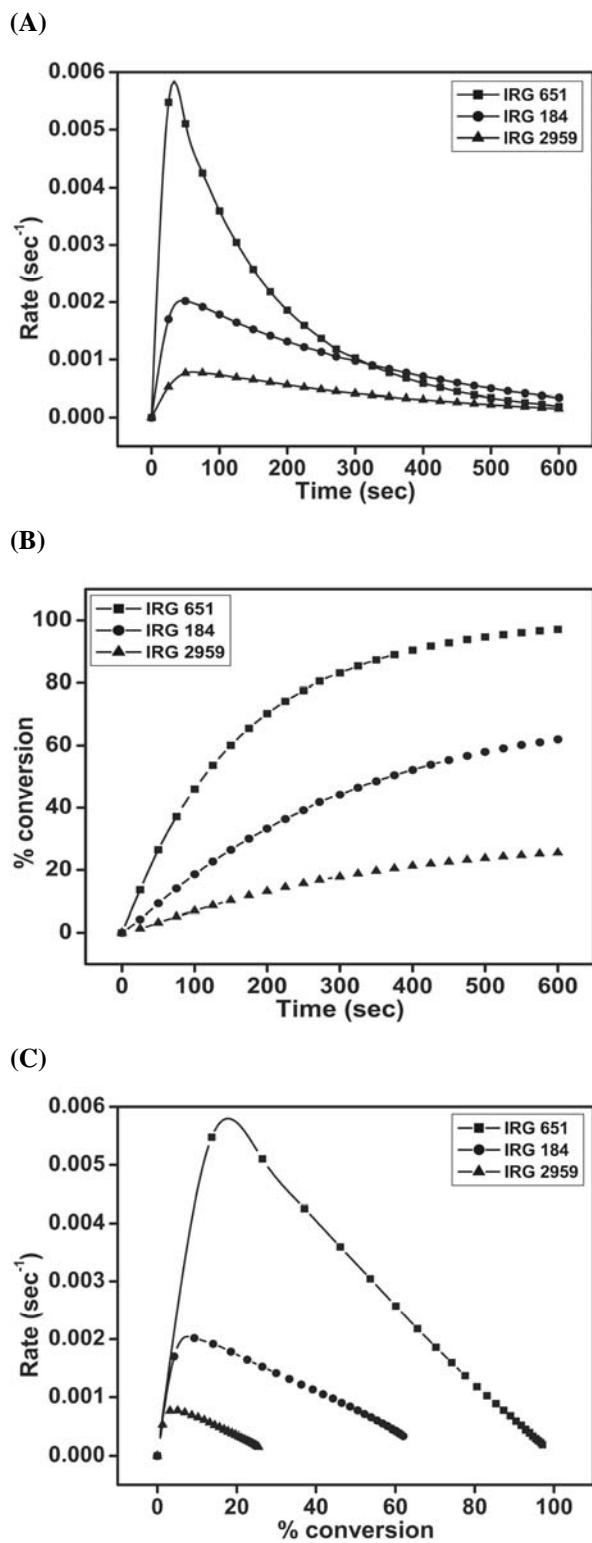


Figure 4.25(A-C) Time dependent rate and conversion profiles of macromonomeric formulations containing 0.5 wt% of photoinitiator with respect to weight of macromonomer at 30 °C

The kinetic parameters calculated are given in Table 4.10.

Table 4.10 Kinetic parameters of macromonomeric formulations calculated from the heat flow profiles at 30 °C.

Photo Initiator	% conc. of photo-initiator	Induction Time (sec)	Peak Maximum Time (sec)	$R_{p \text{ max}}$ ($\times 10^{-4}$) (sec^{-1})	C_{max} (%)	Heat of reaction (J/g)	Autocatalytic		
							n	m	k
IRGACURE 651	0.25	6.38	51.78	22.6	57.67	32.66	2.67	0.15	0.25
	0.5	1.74	33.27	58.4	99.13	56.14	1.45	0.09	0.38
IRGACURE 184	0.25	14.18	57.52	9.89	36.43	20.63	4.05	0.16	0.12
	0.5	6.09	44.94	20.32	66.06	37.41	1.79	0.08	0.17
IRGACURE 2959	0.25	67.20	112.24	2.42	10.47	5.93	16.2	0.30	0.07
	0.5	20.13	61.39	7.86	27.35	15.49	6.78	0.24	0.13

In Table 4.10, for all the studied formulations, the induction time as well as the peak maximum time was found to decrease with increase in concentration of photoinitiator showing higher rate of initiation which is unaffected even at peak maximum.²⁴ The $R_{p \text{ max}}$ as well as the C_{max} was found to increase with an increase in concentration of photoinitiator. In this system, since the irradiation intensity is very low (2.14 mW/cm^2), the influence of reaction diffusion soon after gelation is much reduced. Due to this reduced barrier of reaction diffusion, an enhancement in radical diffusion is possible in all systems during segmental diffusion.^{12,14,15} Further, an optimum level of radical concentration was used in analyses. This system can be assumed to have a reduced time scale for reaction diffusion as its onset may be delayed even after peak maximum time in certain cases.

The photopolymerization was carried out using a polychromatic radiation (320-500 nm). Since $\pi - \pi^*$ transitions for all studied photoinitiators fall below 320 nm, the photo initiation will occur only by low energetic and forbidden $n - \pi^*$ transition.²⁶ As a result, the value of $R_{p \text{ max}}$ was found to be much lower. IRGACURE 2959 has no major absorptions above 300 nm and hence the formulations containing it were found to be least cured.^{1,2,26} The induction time and peak maximum time in this case was also found to be higher showing very slow rate of polymerization. IRGACURE 651 and IRGACURE 184 has prominent absorptions corresponding to $n - \pi^*$ transitions around 330-340 nm and hence showed a better polymerization profile.² Due to low initiation rate, the time scale for reaction diffusion was higher and the system showed very high conversions with 0.5

wt% of IRGACURE 651. The induction time for this system was also found to be least. At low irradiation intensity, the chances of radical radical combinations are reduced as the initiation can be assumed to occur in a controlled manner. Other parameters such as quantum yield for α scission can have a higher influence on the initiation rate at low irradiation intensities.¹ Even though, in the case of formulation containing 0.5 wt% of IRGACURE 184 did not give very high conversion, this system can be expected to give higher conversion with increase in concentration of photoinitiator, as the system has not still attained the optimum concentration of effective number of radicals for photopolymerization.¹⁷

This system on analyses using variable autocatalytic kinetic model gave low values of m . However the value of specific rate constant (k) was found to increase with increase in concentration of photoinitiator. The lowest value of k was observed for 0.25 wt% of IRGACURE 2959 and highest value of k was observed for 0.5 wt% of IRGACURE 651. The steady behaviour of the system can be due to a relatively slow and steady viscosity build up during the entire time scale of reaction diffusion. This was possible probably due to lower excitation energies involved, flexible nature in the backbone of matrix, steady radical diffusion with reduced radical radical combinations and low rate of *in situ* viscosity build up.^{12,14} The formulations during photocuring can be assumed to undergo both bimolecular and monomolecular terminations.¹⁹

4.1.1.10 Photopolymerization of diacrylate macromonomer based on cyclohexane dimethanol, isophorone diisocyanate and 2-hydroxyethyl acrylate (System 4A-8)

A diacrylate macromonomer based on cyclohexane-1,4-dimethanol (CHDM), IPDI and HEA was synthesized and formulated. The photocuring studies of the formulations were carried out. Estimation of kinetic parameters were done based on the heat flow profile obtained during the photopolymerization process.

The telechelic synthesis of macromonomer was done in two steps. An initial condensation of the diol and diisocyanate to form a diisocyanate terminated urethane prepolymer followed by end capping of the formed prepolymer with excess of 2-hydroxyethyl acrylate was carried out to obtain urethane diacrylate macromonomer.

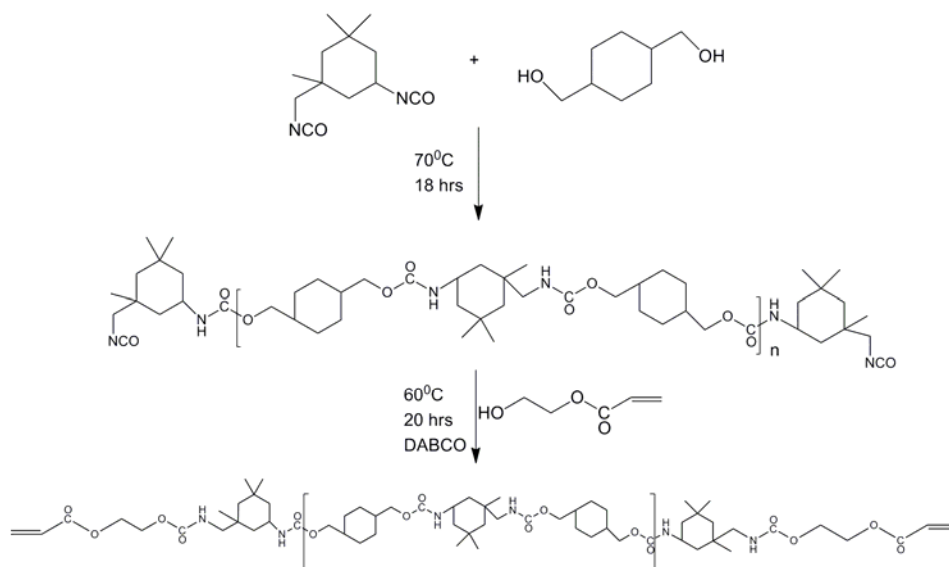


Figure 4.26 The synthesis pathway of diacrylate macromonomer based on CHDM, IPDI and HEA

4.1.1.10.1 Procedure for synthesis

Synthesis of prepolymer

Polymerization was carried out in a 100 mL three necked round bottomed flask provided with half moon stirrer rod through the central neck provided with a teflon stuffing box. The stirrer rod was connected to an overhead stirrer. Nitrogen gas was flushed to the flask through one side neck for a period of 2 min. 14.67 g (65.6 mmol) IPDI and was added to it and stirred at 40 °C at 80 rpm. 8.6526 g (60 mmol) of CHDM was solvated in 30 mL of chloroform and added to the reactor using a dropping funnel at a flow rate of 1 mL/min so that the ratio of NCO:OH was 1.1:1. During addition, the system was homogenized by increasing the stirring speed to 150 rpm. The temperature was further increased to 70 °C and stirred for 18 h to obtain the prepolymer. The residual isocyanate content was found to be 2.49% (ASTM D 2572). IR and NMR spectra were noted.

IR: 1699 (C=O, urethane), 2268 (NCO), 1520 (N-H, urethane), 1134 (C-O), 3008, 2925, 2857 (C-H) cm^{-1} .

¹H NMR (CDCl_3): 0.91 and 1.04 (=C(CH₃)₂, alicyclic - isophorone), 2.89 and 2.91 (-CH₂-NH-CO-O-), 3.01 (-CH₂-NCO), 4.49 (-NH-CO-O-), 4.76 (-CH₂-NH-CO-O-) ppm.

$^{13}\text{C NMR (CDCl}_3\text{)}$: 27.57 and 34.99 ($=\text{C}(\underline{\text{C}}\text{H}_3)_2$, alicyclic - isophorone), 23.13 ($=\text{C}(\underline{\text{C}}\text{H}_3)\text{-CH}_2\text{-}$, alicyclic - isophorone), 25.23 and 28.75 ($-\underline{\text{C}}\text{H}_2\text{-}$, alicyclic - cyclohexane), 31.79 ($=\underline{\text{C}}(\text{CH}_3)_2$, alicyclic - isophorone) and 36.47 ($=\underline{\text{C}}(\text{CH}_3)\text{-CH}_2\text{-}$, alicyclic - isophorone), 37.38 ($=\underline{\text{C}}\text{H-}$, alicyclic - cyclohexane), 41.84, 46.51 and 47 ($-\text{CH}_2\text{-}$, alicyclic - isophorone), 56.92 ($-\underline{\text{C}}\text{H}_2\text{-NCO}$), 67.52 and 69.59 ($-\text{NH-CO-O-}\underline{\text{C}}\text{H}_2\text{=}$, (exo) cyclohexane ring), 121.67 ($-\text{N}\underline{\text{C}}\text{O}$), 155.97 ($-\text{NH-}\underline{\text{C}}\text{O-O-}$), 157.17 ($-\text{CH}_2\text{-NH-}\underline{\text{C}}\text{O-O-CH}_2\text{-}$) ppm.

Synthesis of macromonomer

To 22 g of synthesized prepolymer was added 1.3949 g (12 mmol) of HEA followed by addition of 0.1092 g (0.9735 mmol) of DABCO as catalyst. 200 ppm of HQME was added as stabilizer and the reaction was continued at 60 °C for 20 h until all the isocyanate groups were completely consumed as observed from IR spectrum. 40 mL of chloroform was added to the contents of the flask and transferred to 250 mL water taken in a 500 mL beaker. The precipitated macromonomer was washed three times with water and initially dried in vacuum at room temperature for 12 h and further dried in vacuum oven for a period of 10 h at 60 °C. IR and NMR spectra were noted. The molecular mass was found by VPO.

IR: 1698 (C=O, urethane), 3332 and 1524 (N-H, urethane), 1637 and 809 (C=C, acrylate), 1134 and 1196 (C-O), 3000, 2924, 2853 (C-H) cm^{-1} .

$^1\text{H NMR (CDCl}_3\text{)}$: 0.91 and 1.04 ($=\text{C}(\underline{\text{C}}\text{H}_3)_2$, alicyclic - isophorone), 2.88 and 2.90 ($-\underline{\text{C}}\text{H}_2\text{-NH-CO-O-}$), 4.53 ($-\text{NH-}\underline{\text{C}}\text{O-O-}$), 4.80 ($-\text{CH}_2\text{-NH-}\underline{\text{C}}\text{O-O-}$), 5.83 and 6.40 ($-\text{O-CO-CH=}\underline{\text{C}}\text{H}_2$), 6.16 ($-\text{O-CO-}\underline{\text{C}}\text{H=CH}_2$) ppm.

$^{13}\text{C NMR (CDCl}_3\text{)}$: 27.60 and 35.02 ($=\text{C}(\underline{\text{C}}\text{H}_3)_2$, alicyclic - isophorone), 23.17 ($=\text{C}(\underline{\text{C}}\text{H}_3)\text{-CH}_2\text{-}$, alicyclic - isophorone), 25.27 and 28.80 ($-\underline{\text{C}}\text{H}_2\text{-}$, alicyclic - cyclohexane), 31.83 ($=\underline{\text{C}}(\text{CH}_3)_2$, alicyclic - isophorone) and 36.36 ($=\underline{\text{C}}(\text{CH}_3)\text{-CH}_2\text{-}$, alicyclic - isophorone), 37.43 ($=\underline{\text{C}}\text{H-}$, alicyclic - cyclohexane), 41.90, 46.37 and 47.02 ($-\text{CH}_2\text{-}$, alicyclic - isophorone), 60.99 ($-\underline{\text{C}}\text{H}_2\text{-NH-CO-O-}$), 67.44 and 69.65 ($-\text{NH-CO-O-}\underline{\text{C}}\text{H}_2\text{=}$, (exo) cyclohexane ring), 128 ($-\text{O-CO-}\underline{\text{C}}\text{H=CH}_2$), 131.41 ($-\text{O-CO-CH=}\underline{\text{C}}\text{H}_2$), 155.97 ($-\text{NH-}\underline{\text{C}}\text{O-O-}$), 157.17 ($-\text{CH}_2\text{-NH-}\underline{\text{C}}\text{O-O-CH}_2\text{-}$), 165.98 ($-\text{O-}\underline{\text{C}}\text{O-CH=CH}_2$) ppm.

4.1.1.10.2 Formulation

The macromonomer was a solid. Hence 10 wt% excess HEA was added as reactive diluent to obtain an optimum viscosity material. Macromonomer and 10 wt% (0.8612 mmol) of HEA were homogenized in sample vials using a vibrating mill. The formulations were made in 5 mL sample vials. 1 g (0.1687 mmol) of formulation was added in each of the sample vials. The photoinitiators of choice were IRGACURE 651,

DAROCUR TPO, IRGACURE 184 and IRGACURE 819. 0.5 and 2 wt% of photoinitiator were homogenized with the macromonomer containing 10 wt% HEA to obtain eight photopolymerizable formulations.

The isothermal photocalorimetry was studied at 30 and 50 °C. Under the same isothermal conditions and concentrations of photoinitiators, the effect of crosslinker (reactive diluent) on the photopolymerization was studied by the addition of 5 wt% (0.1524 mmol) of neopentyl glycol propoxylate diacrylate (NPGPDA) as the difunctional crosslinker. Studies using 5 wt% (0.1687 mmol) of trimethylolpropane triacrylate (TMPTA) as trifunctional crosslinker was also carried out. The radical scavenging effect was also studied by addition of TEMPO to 0.006 wt% on the difunctional crosslinking system and 0.012 wt% to the trifunctional crosslinking system, respectively. The radical scavenging effect was studied at 30 and 50 °C to understand the effect of temperature on the rate of polymerization of the formulation with and without the presence of radical scavenger.

4.1.1.10.3 Photocuring studies

About 10 mg of the composition was accurately weighed on a DSC pan and subjected to photo DSC studies under a nitrogen purge of 50 mL/min. The heat flow profile obtained during the *in situ* photocuring process was recorded as a function of time under an isothermal condition of 30 and 50 °C. The intensity of irradiation was kept constant at 4.6 mW/cm² using a polychromatic radiation of 250-450 nm and 100 W high pressure mercury short arc lamp. The normalized output signals in W/g against time were recorded. The rates of photopolymerizations as well as corresponding conversions were calculated for all the compositions.

4.1.1.10.4 Results and discussion

The existence of isocyanate group in the prepolymer as well as the complete conversion of isocyanate group during the formation of macromonomer was confirmed by IR, ¹H and ¹³C NMR spectroscopy. The molecular mass of the macromonomer was found by VPO to be 5929 g/mol. The total theoretical heat flow^{4,6,7} (ΔH_{theor}) for the macromonomeric system containing 10 wt% of HEA was calculated to be 93.91 J/g, that for the macromonomeric system containing 10 wt% of HEA and 5 wt% NPGPDA was calculated to be 112.68 J/g and that for the macromonomeric system containing 10 wt%

of HEA and 5 wt% TMPTA was calculated to be 127.77 J/g. The Brookfield viscosity of the crosslinkers and macromonomeric formulations noted are given in Table 4.11.

Table 4.11 Brookfield viscosity with spindle#4 at 80 rpm and 30°C (Shear rate 266.4 s⁻¹)

Type of crosslinker/formulation	Brookfield viscosity ^a (cP)
NPGPDA	450 ± 9
TMPTA	375 ± 2
Diacrylate terminated macromonomer + 10wt% HEA	4387 ± 36
Diacrylate terminated macromonomer + 10wt% HEA + 5wt% NPGPDA	11630 ± 55
Diacrylate terminated macromonomer + 10wt% HEA + 5wt% TMPTA	5481 ± 17

a) Average of three readings.

The diacrylate showed a higher viscosity than the triacrylate due to the presence of glycol moiety. This same trend was also observed on formulating with the macromonomer. From the results we can infer that the formulation containing diacrylate has the highest initial viscosity followed by triacrylate containing formulation.

The rate and conversion profiles obtained from photocuring studies of macromonomeric formulations containing 10 wt% HEA with four photoinitiators at 0.5 and 2 wt% compositions at 30 and 50 °C are given below in Figures 4.27 to 4.30 (A-C).

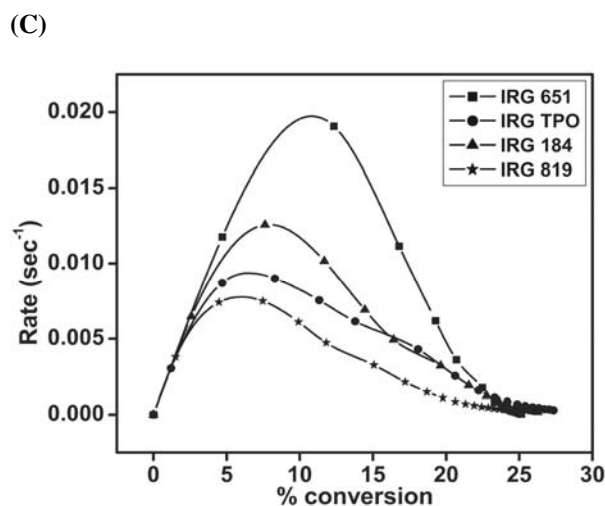
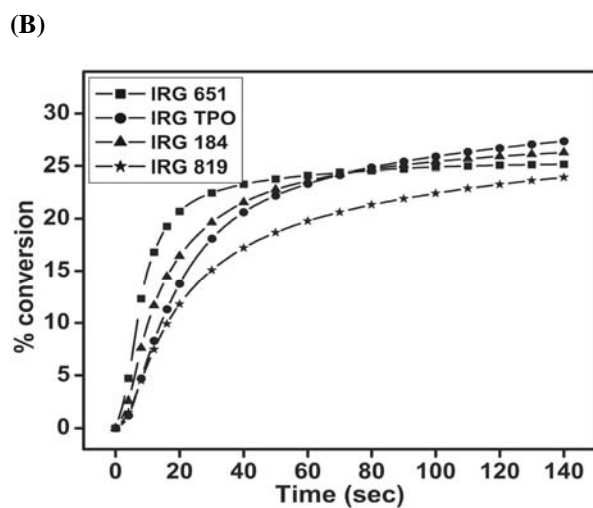
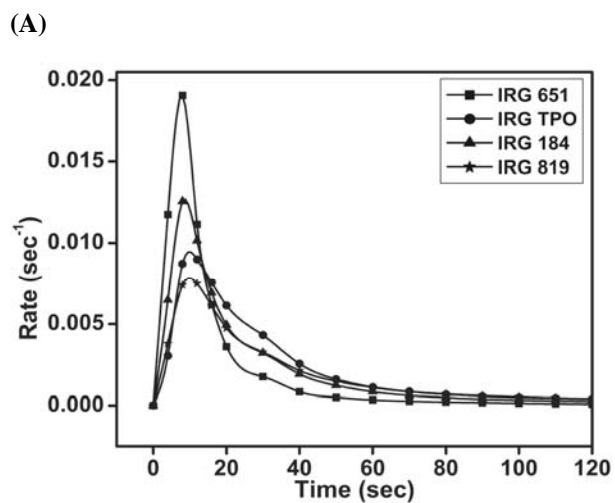
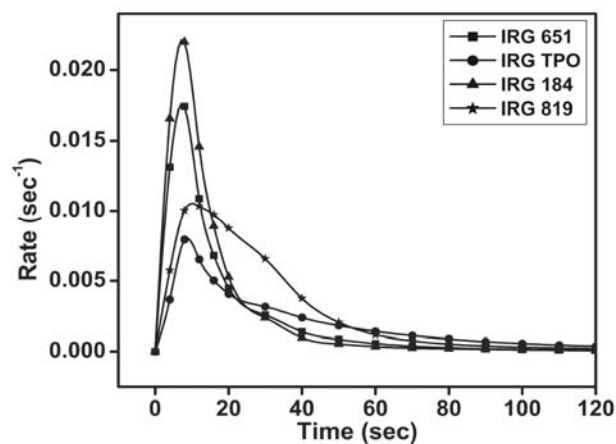
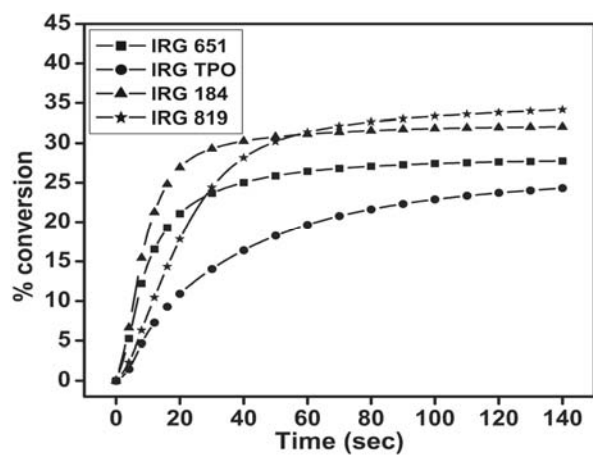


Figure 4.27(A-C) Time dependent rate and conversion profiles of macromonomeric formulations containing 10 wt% HEA and 0.5 wt% of photoinitiator with respect to weight of macromonomer at 30 °C

(A)



(B)



(C)

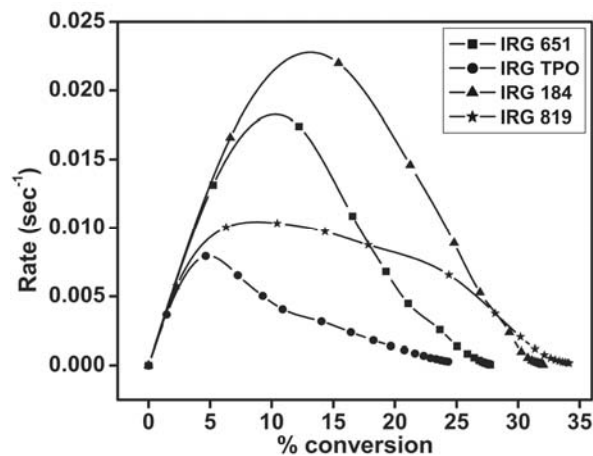


Figure 4.28(A-C) Time dependent rate and conversion profiles of macromonomeric formulations containing 10 wt% HEA and 2 wt% of photoinitiator with respect to weight of macromonomer at 30 °C

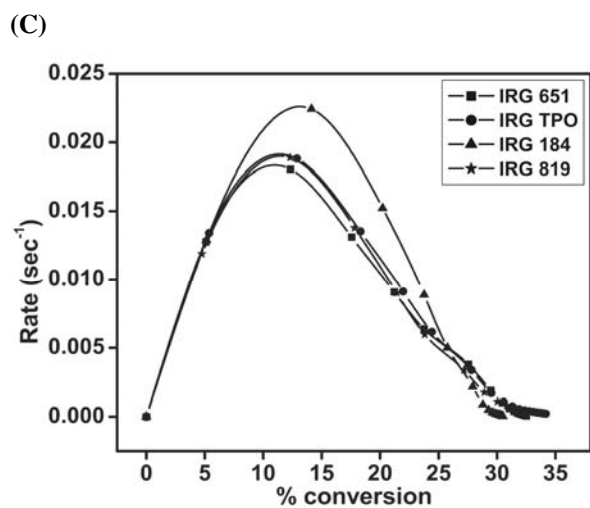
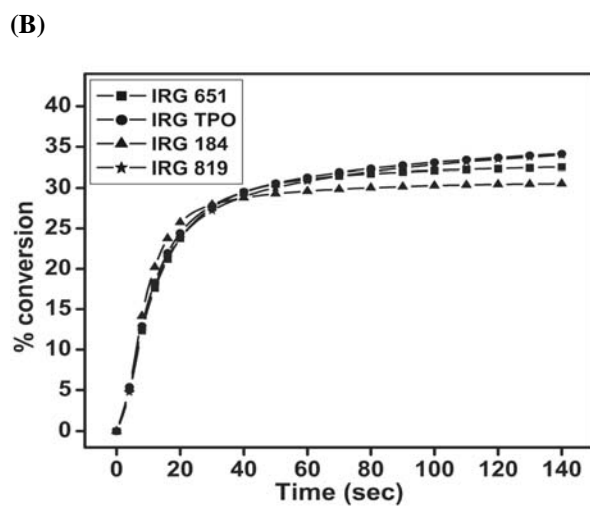
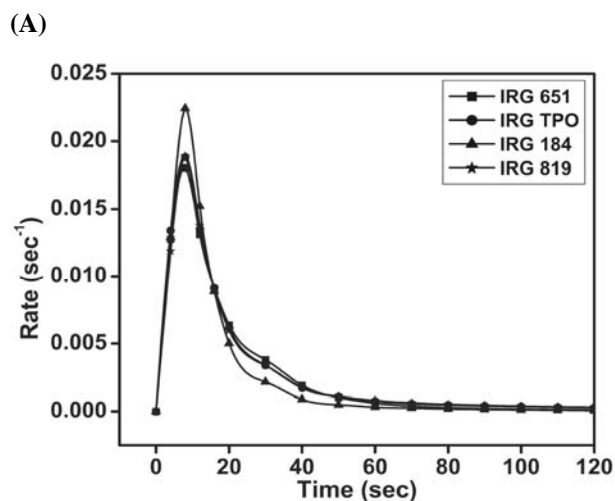
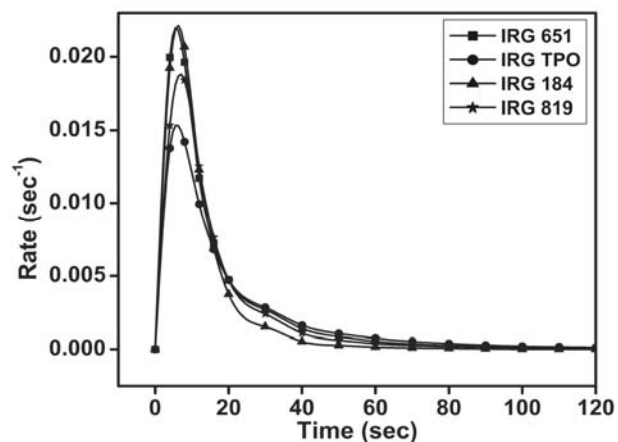
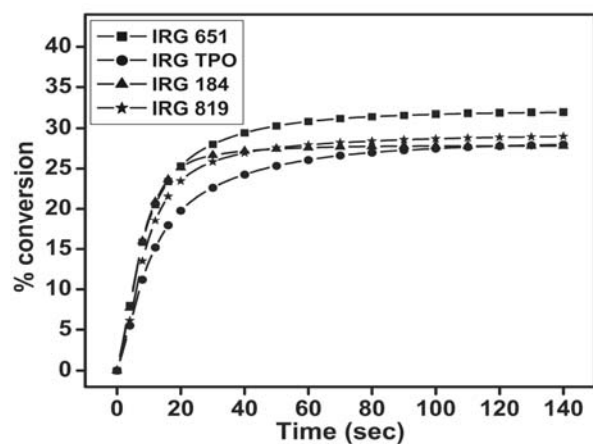


Figure 4.29(A-C) Time dependent rate and conversion profiles of macromonomeric formulations containing 10 wt% HEA and 0.5 wt% of photoinitiator with respect to weight of macromonomer at 50 °C

(A)



(B)



(C)

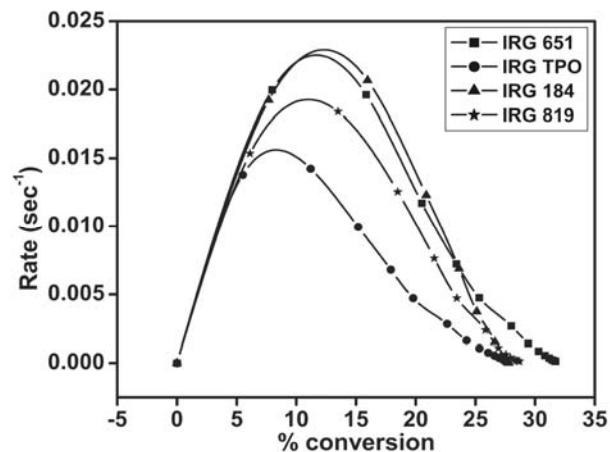


Figure 4.30(A-C) Time dependent rate and conversion profiles of macromonomeric formulations containing 10 wt% HEA and 2 wt% of photoinitiator with respect to weight of macromonomer at 50 °C

The kinetic parameters calculated are given in Tables 4.12 and 4.13.

Table 4.12 Kinetic parameters of macromonomeric formulations calculated from the heat flow profiles containing 10 wt% HEA

Photo Initiator	% conc. of photo-initiator	Temp (°C)	Induction Time (sec)	Peak Maximum Time (sec)	$R_p \text{ max}$ ($\times 10^{-2}$) (sec^{-1})	C_{max} (%)	Heat of reaction (J/g)
IRGACURE 651	0.5	30	1.07	7.83	1.91	25.11	23.58
	2	30	0.84	7.32	1.76	27.78	26.09
	0.5	50	0.90	7.78	1.81	32.69	30.7
	2	50	0.51	5.68	2.20	31.86	29.92
DAROCUR TPO	0.5	30	3.60	9.91	0.95	29.09	27.32
	2	30	3.12	8.66	0.81	25.57	24.01
	0.5	50	0.85	7.80	1.89	35.53	33.37
	2	50	0.75	5.90	1.54	28.26	26.54
IRGACURE 184	0.5	30	1.94	8.57	1.27	26.95	25.31
	2	30	0.67	7.42	2.22	32.05	30.10
	0.5	50	0.98	8.11	2.25	30.52	28.66
	2	50	0.55	6.19	2.21	27.37	25.7
IRGACURE 819	0.5	30	2.96	9.83	0.79	25.78	24.21
	2	30	2.03	10.07	1.05	34.81	32.69
	0.5	50	1.02	8.09	1.89	35.44	33.28
	2	50	0.70	6.92	1.88	29.04	27.27

Table 4.13 Evaluation of kinetic parameters of macromonomeric formulations as per autocatalytic model at 30 and 50 °C containing 10 wt% HEA

Photo Initiator	% conc. of photo-initiator	Temperature (°C)	Autocatalytic		
			n	m	k (min^{-1})
IRGACURE 651	0.5	30	15.9	0.86	41.7
	0.5	50	9.99	0.60	12.1
	2	30	14.7	0.75	26.2
	2	50	11.6	0.65	21.3
DAROCUR TPO	0.5	30	14.6	0.77	12.5
	0.5	50	11.6	0.78	23.8
	2	30	11.7	0.22	1.46
	2	50	13.5	0.59	12.6
IRGACURE 184	0.5	30	17.3	0.89	28.8
	0.5	50	10.9	0.84	30.5
	2	30	9.18	0.60	15.2
	2	50	10.2	0.60	16.4
IRGACURE 819	0.5	30	18.5	0.81	14.2
	0.5	50	12.9	0.89	35.8
	2	30	6.61	0.49	3.96
	2	50	11.3	0.66	17.1

From Table 4.12, the induction time and peak maximum time were found to decrease with increase in temperature at similar concentration of photoinitiator as well as

with increase in concentration of photoinitiator at same temperature.²⁴ Due to multiple absorptions,² DAROCUR TPO was found to show a reduced induction time with increase in temperature. The peak maximum time also showed a similar trend. This system can be assumed to have an onset of reaction diffusion before attaining peak maximum.^{12,14} But the influence of *in situ* viscosity at $R_{p \text{ max}}$ is not much sufficient to cause a reduction in the radical diffusion which resulted in similar trend of peak maximum time as that of induction time. The fact that the macromonomer is rigid also has a high influence on the rate of radical and reaction diffusion processes. From the values of $R_{p \text{ max}}$, we can infer that in many cases an increase in concentration of photoinitiator from 0.5 to 2 wt%, has resulted in a reduction in the value of $R_{p \text{ max}}$. In the case of lower isothermal condition, it can be either due to radical trapping or by attaining an optimum limit in the effective number of initiating species.¹⁷ In the case of higher isothermal condition, the initial viscosity is lower and the radical diffusion can be expected to be higher. But the *in situ* viscosity build up can prevent the system from attaining higher conversions.²⁷ For all the formulations, the final conversion varied from 25 to 36%. As the photo cured system has a T_g of around 113 °C which is higher than the analyses temperature, it readily vitrifies on cure.²⁷ This early vitrification cannot predict that that all the systems must have a higher final conversion at higher isothermal condition. The rate of photopolymerization during the onset of reaction diffusion has a higher influence on the overall *in situ* viscosity build up which also depends on radical diffusion.^{12,15}

The photopolymerization was carried out using polychromatic radiation (250-450 nm). All the photoinitiators have multiple absorptions within the range of radiation.² In acetonitrile solution, the most prominent λ_{max} and the corresponding extinction coefficients for the considered photoinitiators are as follows - IRGACURE 651 (252 nm, $\epsilon = 12800 \text{ L mol}^{-1} \text{ cm}^{-1}$), DAROCUR TPO (380 nm, $\epsilon = 525 \text{ L mol}^{-1} \text{ cm}^{-1}$), IRGACURE 184 (243 nm, $\epsilon = 10000 \text{ L mol}^{-1} \text{ cm}^{-1}$) and IRGACURE 819 (369 nm, $\epsilon = 933 \text{ L mol}^{-1} \text{ cm}^{-1}$).¹ Since the λ_{max} of $\pi - \pi^*$ transition for IRGACURE 651 falls within the range of analysis than that of IRGACURE 184, a lower induction time is expected for IRGACURE 651.^{1,26} Considering increase in temperature at similar concentration of photoinitiator, formulations containing DAROCUR TPO showed highest reduction in

induction time. Considering photoinitiators, DAROCUR TPO has four absorption bands within the analysis range, which accounts for this effect.²

From Table 4.13, we can infer that the photopolymerization rate fits to the variable autocatalytic kinetic model over a wide range in the cure profile as the values of m being nearly constant¹⁸ with a higher variation in the value of n .²⁸ The autocatalytic model can predict the kinetic behavior from the onset of initiation to the onset of vitrification.¹² The photopolymerization of the macromonomer with added HEA is autoaccelerating during photo initiation reaction and hence can be assumed to follow the autocatalytic model to a great extent.¹² A reduction in specific rate constant was observed with increase in temperature for IRGACURE 651, while a decrease was observed for other photoinitiators.^{18,24,29} This shows that the system is not following the autocatalytic model to high conversions.¹⁸ At high conversions, the reaction is diffusion limited and hence may follow n^{th} order mechanism during the final diffusion controlled crosslinking process.¹⁸ Chandra et al.^{16,26} have observed an increase as well as a decrease in specific rate constant at higher isothermal conditions using autocatalytic model on photopolymerization reactions. These reactions were done using photo DSC at polychromatic conditions. The diffusion of radical (created by multiple excitations of polychromatic radiation) within the *in situ* viscosity build up creates variations, which effects the extent of applicability of autocatalytic behaviour. As a result, the model may give an increase or decrease in the value of specific rate constant with increase in temperature.²⁴

The rate and conversion profiles obtained from photocuring studies of macromonomeric formulations containing 10 wt% HEA and 5 wt% of NPGPDA as crosslinker with four photoinitiators at 0.5 and 2 wt% compositions at 30 and 50 °C are given below in Figures 4.31 to 4.34 (A-C).

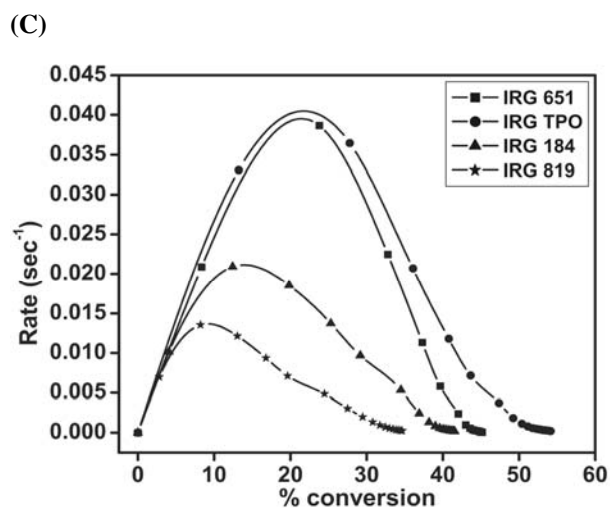
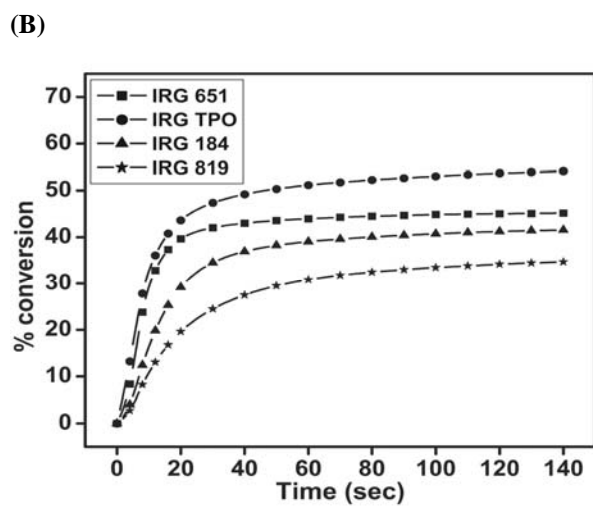
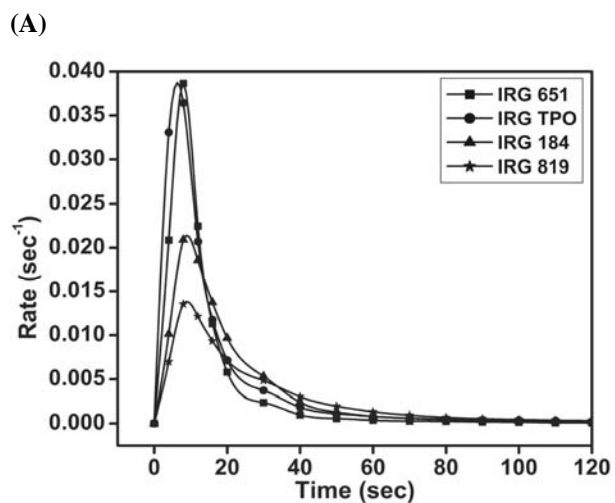


Figure 4.31(A-C) Time dependent rate and conversion profiles of macromonomeric formulations containing 10 wt% HEA, 5 wt% NPGPDA and 0.5 wt% of photoinitiator with respect to weight of macromonomer at 30 °C

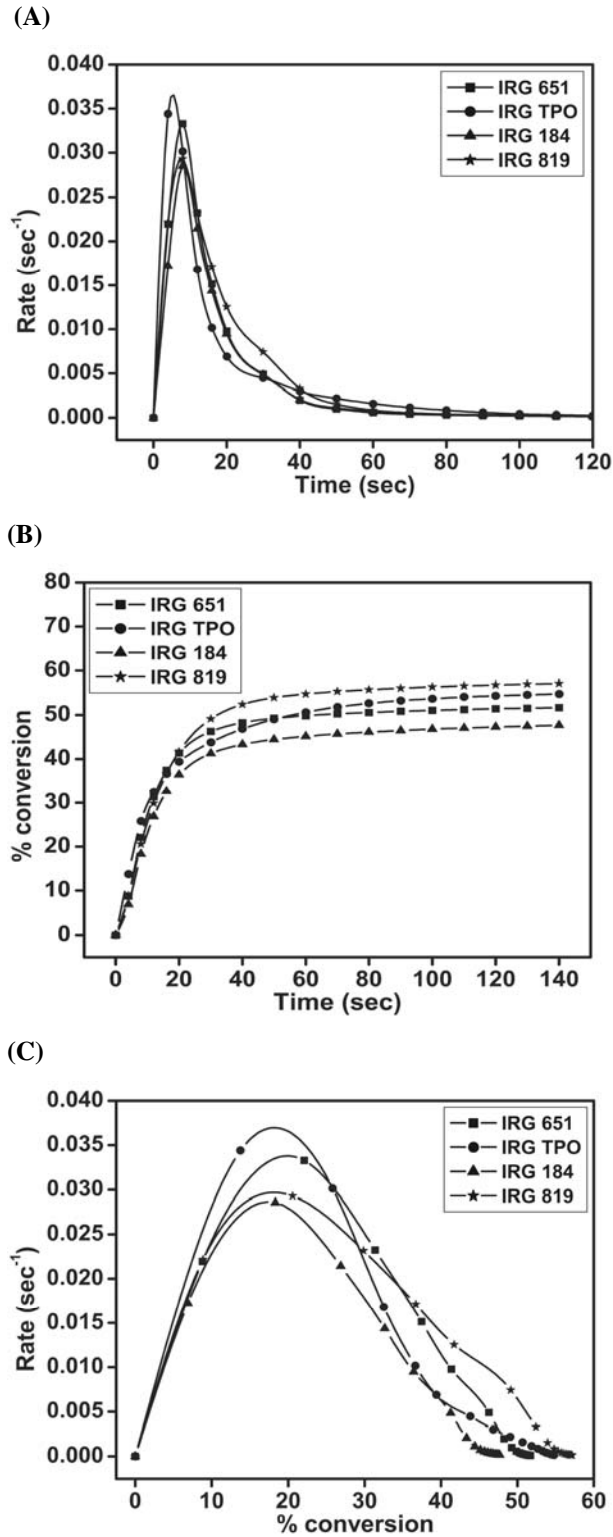


Figure 4.32(A-C) Time dependent rate and conversion profiles of macromonomeric formulations containing 10 wt% HEA, 5 wt% NPGPDA and 2 wt% of photoinitiator with respect to weight of macromonomer at 30 °C

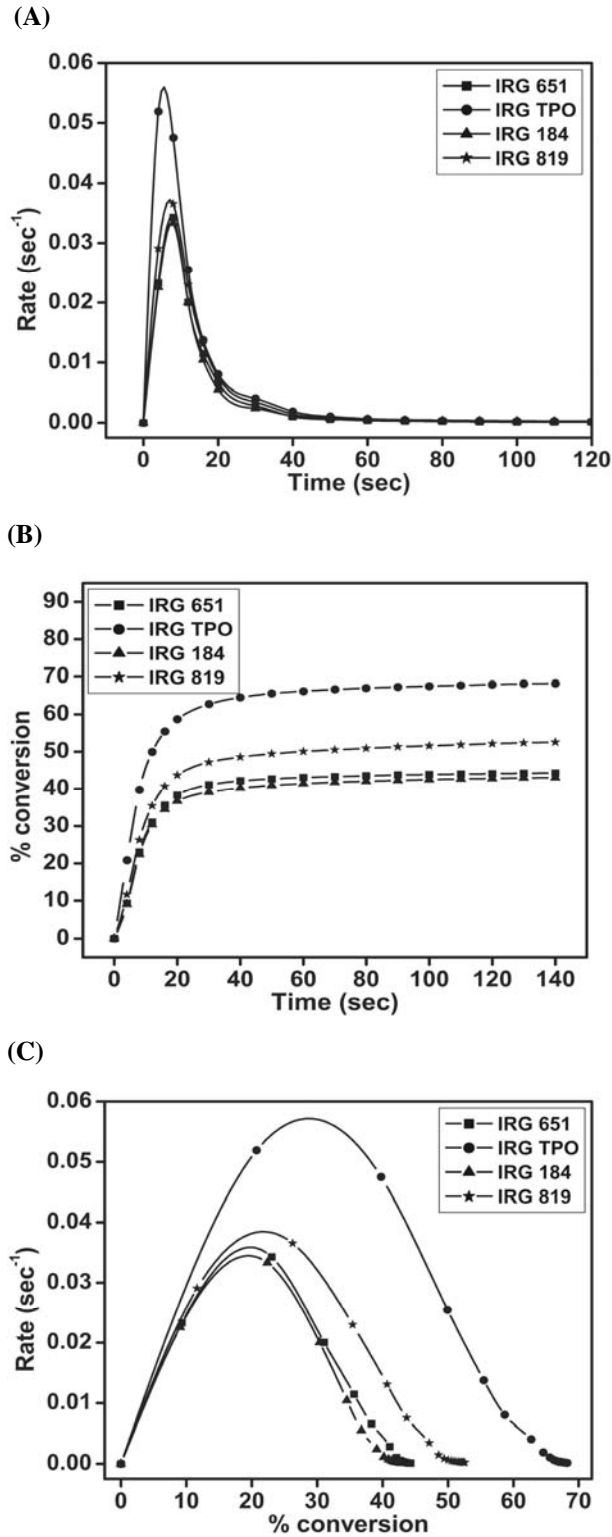


Figure 4.33(A-C) Time dependent rate and conversion profiles of macromonomeric formulations containing 10 wt% HEA, 5 wt% NPGPDA and 0.5 wt% of photoinitiator with respect to weight of macromonomer at 50 °C

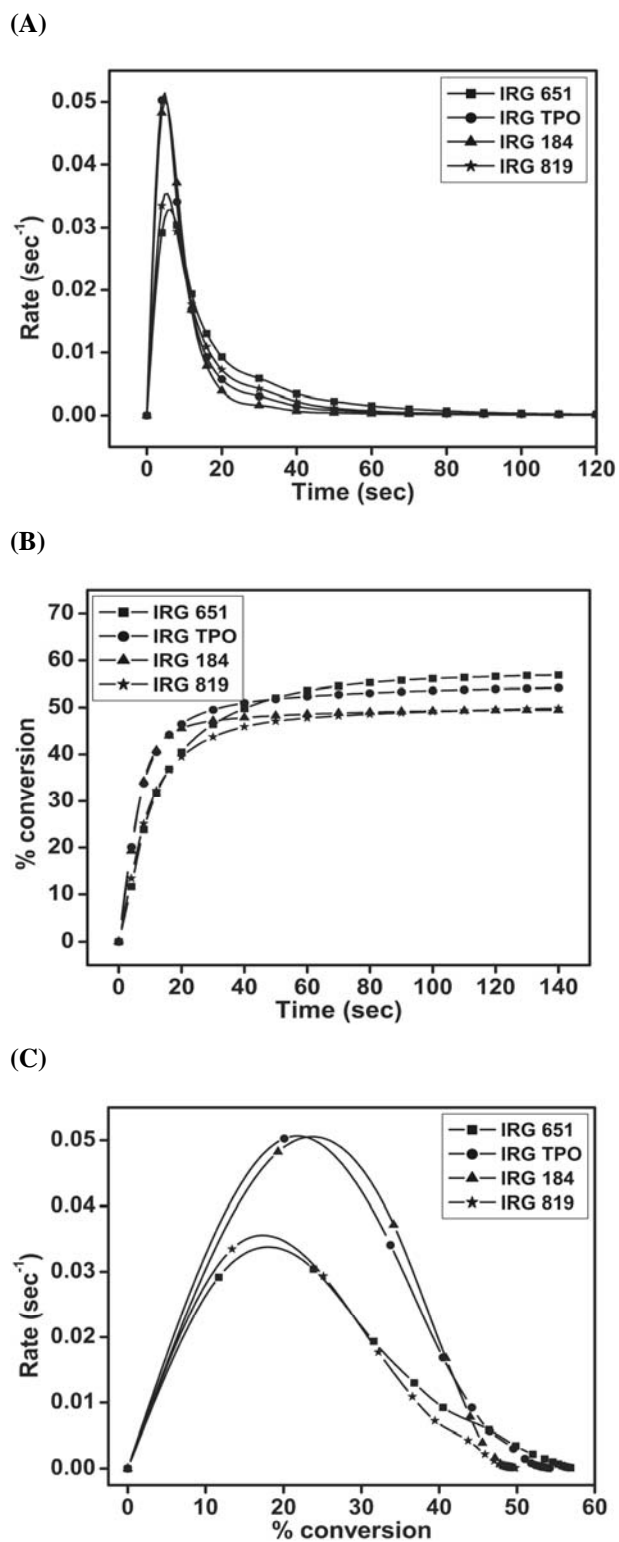


Figure 4.34(A-C) Time dependent rate and conversion profiles of macromonomeric formulations containing 10 wt% HEA, 5 wt% NPGPDA and 2 wt% of photoinitiator with respect to weight of macromonomer at 50 °C

The kinetic parameters calculated are given in Tables 4.14 and 4.15.

Table 4.14 Kinetic parameters of macromonomeric formulations calculated from the heat flow profiles containing 10 wt% HEA and 5 wt% NPGPDA

Photo Initiator	% conc. of photo-initiator	Temp (°C)	Induction Time (sec)	Peak Maximum Time (sec)	$R_{p \text{ max}}$ ($\times 10^{-2}$) (sec^{-1})	C_{max} (%)	Heat of reaction (J/g)
IRGACURE 651	0.5	30	0.64	7.98	3.87	45.29	51.03
	2	30	0.54	7.91	3.33	52.18	58.80
	0.5	50	0.49	7.59	3.45	44.61	50.27
	2	50	0.35	6.01	3.30	57.44	64.72
DAROCUR TPO	0.5	30	0.32	6.34	3.87	55.49	62.53
	2	30	0.29	5.29	3.67	55.63	62.68
	0.5	50	0.19	5.42	5.60	69.16	77.93
	2	50	0.18	4.63	5.15	54.77	61.71
IRGACURE 184	0.5	30	1.30	8.98	2.14	42.30	47.66
	2	30	0.72	8.22	2.86	48.51	54.66
	0.5	50	0.52	7.68	3.35	43.49	49.01
	2	50	0.20	4.90	5.03	49.51	55.79
IRGACURE 819	0.5	30	1.76	8.94	1.39	36	40.56
	2	30	0.50	7.67	2.94	57.93	65.27
	0.5	50	0.38	7.08	3.73	53.74	60.55
	2	50	0.29	5.22	3.56	50.45	56.85

Table 4.15 Evaluation of kinetic parameters of macromonomeric formulations as per autocatalytic model at 30 and 50 °C containing 10 wt% HEA and 5 wt% NPGPDA

Photo Initiator	% conc. of photo-initiator	Temperature (°C)	Auto catalytic		
			n	m	k (min^{-1})
IRGACURE 651	0.5	30	6.76	0.83	36.6
	0.5	50	7.09	0.79	31.4
	2	30	5.05	0.56	13.8
	2	50	5.36	0.47	12.2
DAROCUR TPO	0.5	30	6.19	0.70	28.7
	0.5	50	3.68	0.56	21.5
	2	30	7.38	0.66	28
	2	50	5.92	0.58	28.5
IRGACURE 184	0.5	30	7.46	0.72	15.6
	0.5	50	7.49	0.84	35.7
	2	30	6.09	0.64	15.7
	2	50	6.07	0.72	39.7
IRGACURE 819	0.5	30	10	0.62	9.06
	0.5	50	5.52	0.68	22.6
	2	30	3.82	0.42	7.52
	2	50	6.19	0.52	15.9

From Table 4.14, it is observed that the induction time and peak maximum time was found to decrease with increase in temperature at similar concentration of

photoinitiator as well as with increase in concentration of photoinitiator at same temperature.²⁴ A higher reduction was observed at higher isothermal condition due to reduction in initial viscosity and increase in mobility of radicals during initiation. Due to multiple absorptions,² DAROCUR TPO was found to show least induction time which was more pronounced at higher isothermal condition. Due to the presence of difunctional reactive diluent, the system showed similar trend for induction time and peak maximum time. The reactive diluent in this case can be assumed to cause an initial delay in onset of reaction diffusion mainly due to the presence of soft segments in neopentyl glycol propoxylate diacrylate which is also associated in the crosslinking reaction of rigid macromonomer.¹⁶ Hence, we can infer that the segmental diffusion is enhanced in this case rather than the previous case where the difunctional soft segmented crosslinker was not present. Due to the presence of NPGPDA, with the exception of IRGACURE 651, all other photoinitiators showed an increase in $R_{p \text{ max}}$ with increase in temperature at a particular concentration. This behaviour readily shows an efficient radical and segmental diffusion occur due to low initial system viscosity at higher temperature which in turn is observed up to peak maximum. In the case of IRGACURE 651 the reduction in $R_{p \text{ max}}$ at higher temperature may be arising due to a comparatively reduced radical diffusion or radical radical combinations which can reduce the quantum yield for photo initiation.¹⁷

The final conversion varied from 36 to 70% for all the systems which is higher than the macromonomeric formulations containing 10 wt% HEA. The increase is expected due to the plasticization effect of the reactive diluent coupled with reduced terminations and gradual viscosity build up. As the photo cured system with difunctional crosslinker has a glass transition of around 117 °C, it readily vitrifies on cure. This early vitrification cannot predict that that all the systems must have a higher final conversion at higher isothermal condition. The rate of photopolymerization during the onset of reaction diffusion has a high influence on the overall *in situ* viscosity build up which also depends on radical diffusion.^{12,15} As a result in certain cases, a decrease in final conversion was observed at higher temperature. During the course of reaction diffusion, an increase in *in situ* viscosity occurs leading to an increase in the final conversion as compared to the formulation without difunctional crosslinker. As this formulation has highest initial viscosity (Table 4.11), after autoacceleration the terminations are reduced and the

propagation is mostly dependent on reaction diffusion.¹² The formulations containing NPGPDA showed a faster initiation rate and high $R_{p \text{ max}}$ values than the initial macromonomeric formulation.

The photopolymerization were carried out using polychromatic radiation (250-450 nm). Hence, all the photoinitiators have multiple absorptions within the range of radiation.² In acetonitrile solution, the most prominent λ_{max} and the corresponding extinction coefficients for the photoinitiators are as follows - IRGACURE 651 (252 nm, $\epsilon = 12800 \text{ L mol}^{-1} \text{ cm}^{-1}$), DAROCUR TPO (380 nm, $\epsilon = 525 \text{ L mol}^{-1} \text{ cm}^{-1}$), IRGACURE 184 (243 nm, $\epsilon = 10000 \text{ L mol}^{-1} \text{ cm}^{-1}$) and IRGACURE 819 (369 nm, $\epsilon = 933 \text{ L mol}^{-1} \text{ cm}^{-1}$).¹ The Table 4.14 shows that DAROCUR TPO has the faster rate of initiation than IRGACURE 819 with increase in temperature as well as increase in concentration. Unlike previous system, this system shows better radical diffusion on plasticization which account for the effect.^{15,30} In addition, the presence of more absorption bands for DAROCUR TPO resulted in a better performance than IRGACURE 819. Since the λ_{max} of $\pi - \pi^*$ transition for IRGACURE 651 falls within the range of analysis than that of IRGACURE 184, a lower induction time as expected for IRGACURE 651 was observed. This effect was better pronounced than initial system due to plasticization effect of NPGPDA.

From Table 4.15, we can infer that the photopolymerization rate fits the variable autocatalytic kinetic model over a wide range in the cure profile as the values of m is constant¹⁸ with higher variations for n .²⁸ The photopolymerization of the macromonomer with added HEA and NPGPDA was found to follow the autocatalytic model to a great extent.¹² IRGACURE 651 at 0.5 and 2 wt% and DAROCUR TPO at 0.5 wt% showed a reduction in specific rate constant with increase in temperature. The system during photocuring can be assumed to follow both monomolecular and bimolecular terminations.¹⁹

The rate and conversion profiles obtained from photocuring studies of macromonomeric formulations containing 10 wt% HEA and 5 wt% of TMPTA as crosslinker with four photoinitiators at 0.5 and 2 wt% compositions at 30 and 50 °C are given below in Figures 4.35 to 4.38 (A-C).

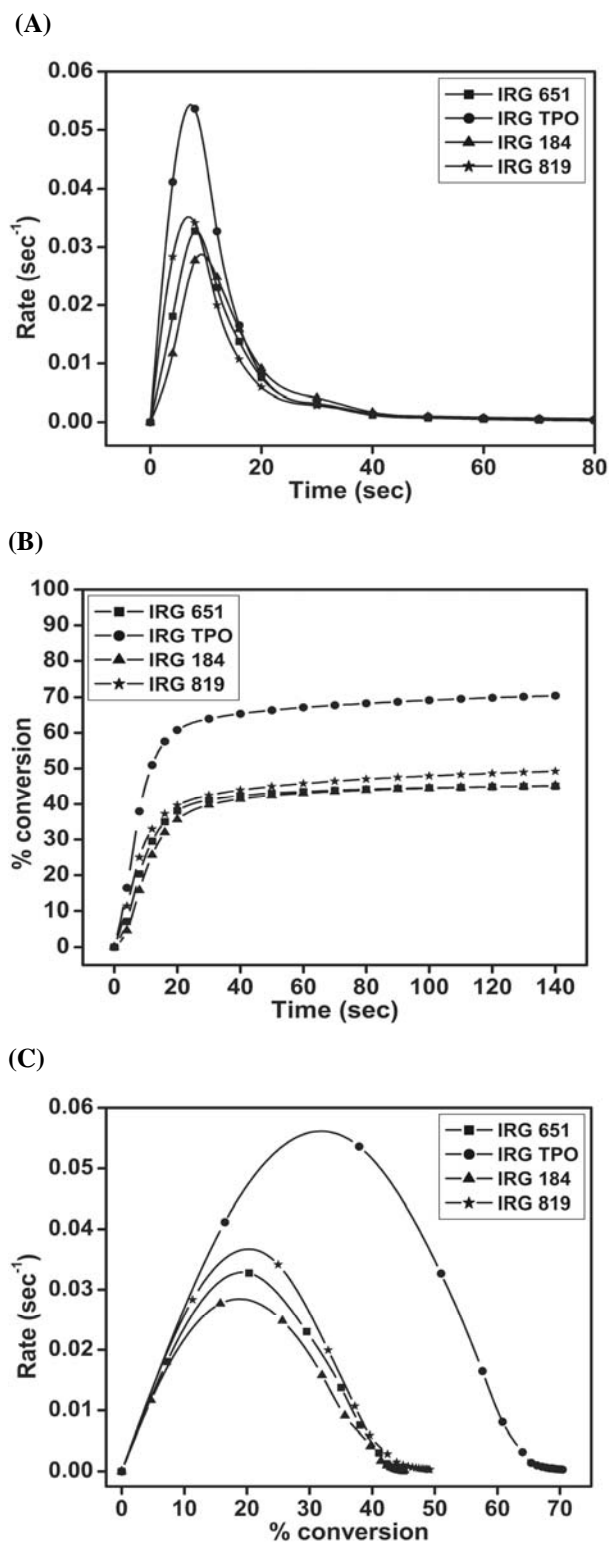


Figure 4.35(A-C) Time dependent rate and conversion profiles of macromonomeric formulations containing 10 wt% HEA, 5 wt% TMPTA and 0.5 wt% of photoinitiator with respect to weight of macromonomer at 30 °C

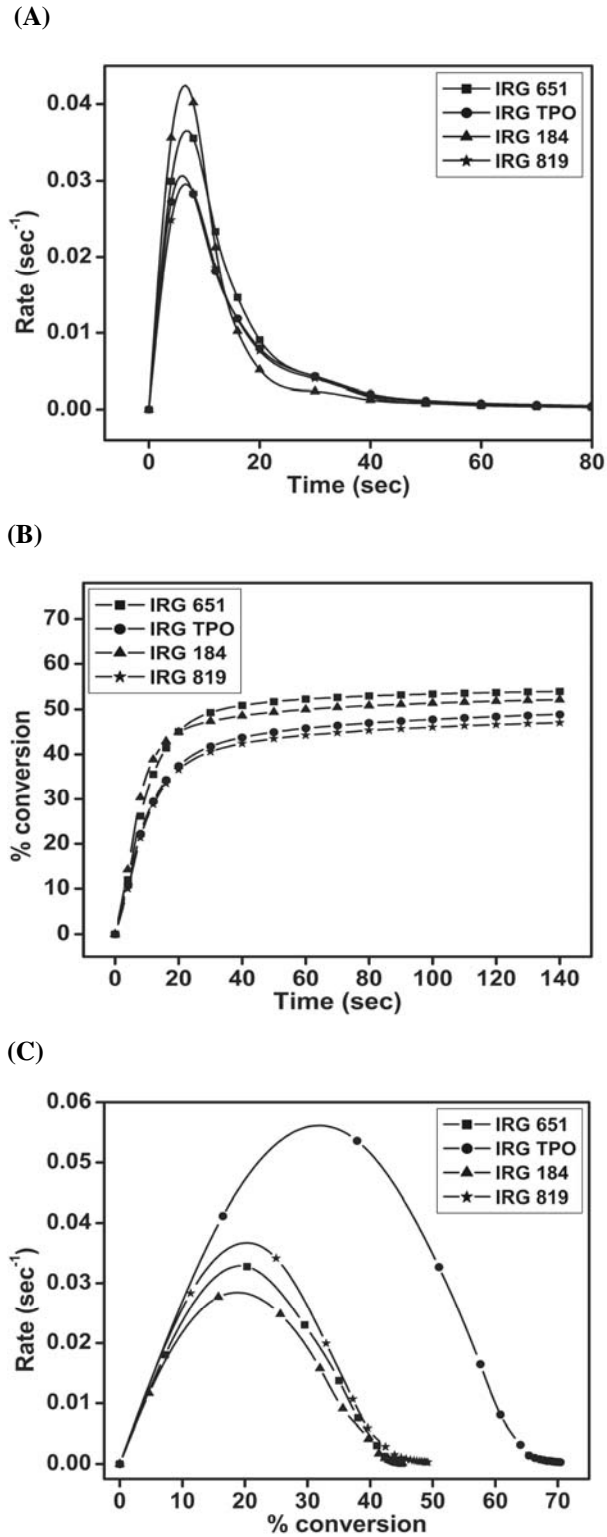


Figure 4.36(A-C) Time dependent rate and conversion profiles of macromonomeric formulations containing 10 wt% HEA, 5 wt% TMPTA and 2 wt% of photoinitiator with respect to weight of macromonomer at 30 °C

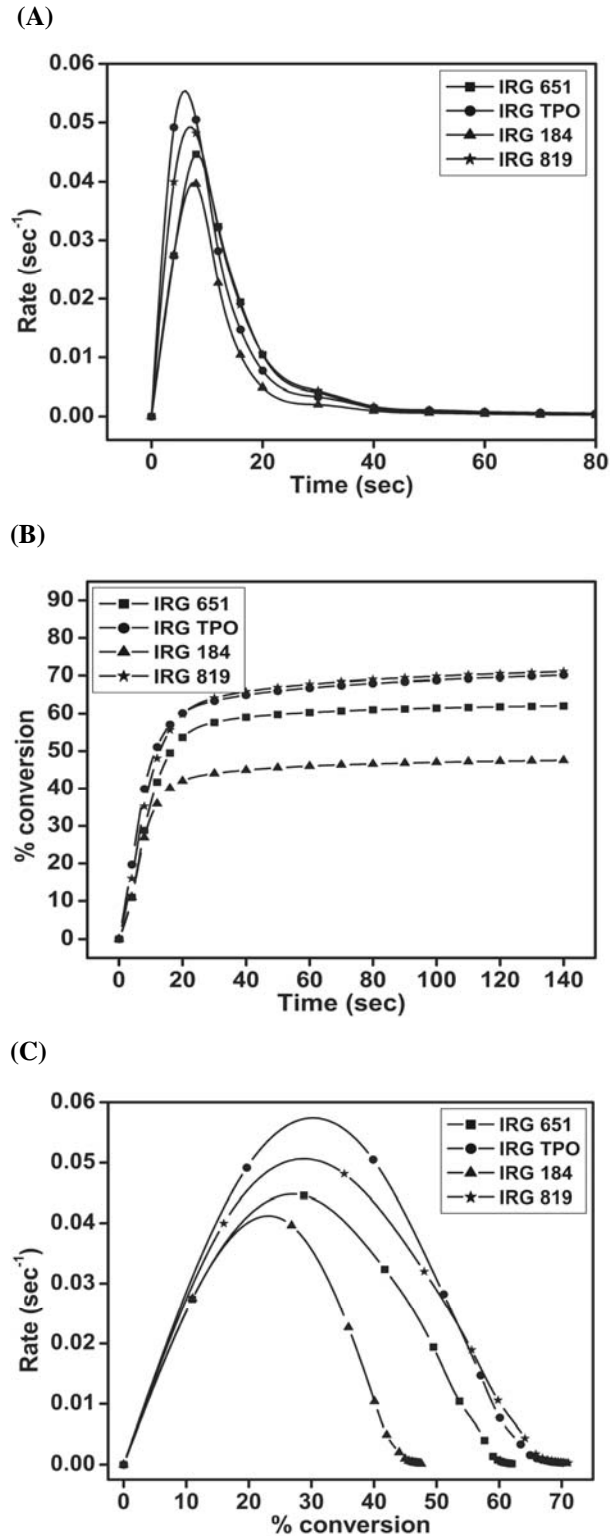
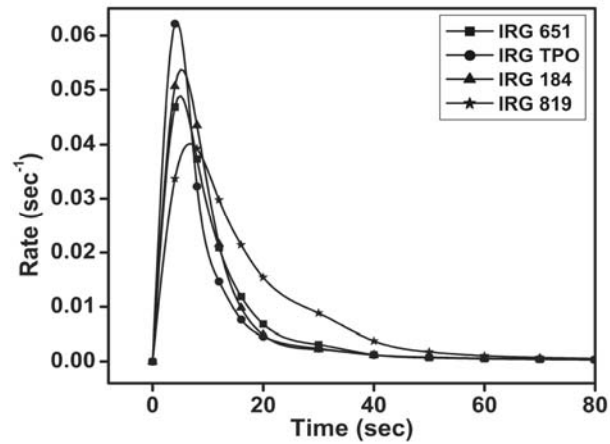
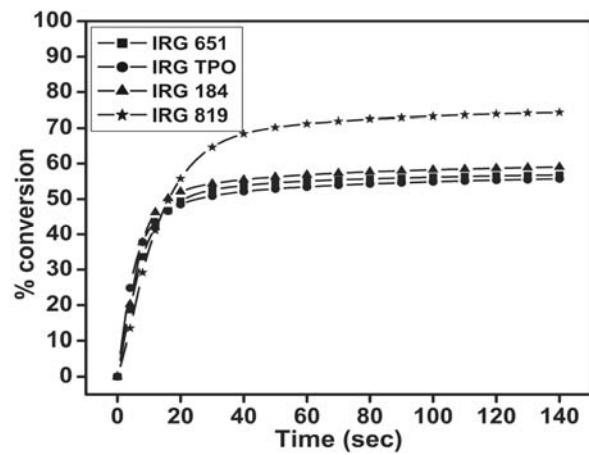


Figure 4.37(A-C) Time dependent rate and conversion profiles of macromonomeric formulations containing 10 wt% HEA, 5 wt% TMPTA and 0.5 wt% of photoinitiator with respect to weight of macromonomer at 50 °C

(A)



(B)



(C)

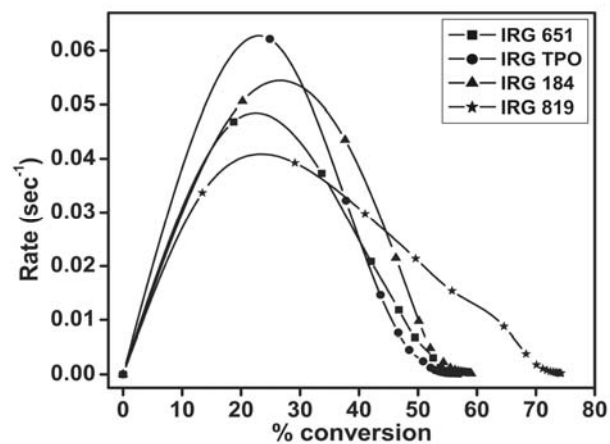


Figure 4.38(A-C) Time dependent rate and conversion profiles of macromonomeric formulations containing 10 wt% HEA, 5 wt% TMPTA and 2 wt% of photoinitiator with respect to weight of macromonomer at 50 °C

The kinetic parameters calculated are given in Tables 4.16 and 4.17.

Table 4.16 Kinetic parameters of macromonomeric formulations calculated from the heat flow profiles containing 10 wt% HEA and 5 wt% TMPTA

Photo Initiator	% conc. of photo-initiator	Temp (°C)	Induction Time (sec)	Peak Maximum Time (sec)	$R_p \text{ max}$ ($\times 10^{-2}$) (sec^{-1})	C_{max} (%)	Heat of reaction (J/g)
IRGACURE 651	0.5	30	0.73	8.23	3.29	45.51	58.15
	2	30	0.35	6.83	3.65	54.51	69.65
	0.5	50	0.45	8.15	4.46	62.56	79.93
	2	50	0.21	4.96	4.88	57.43	73.38
DAROCUR TPO	0.5	30	0.27	7.32	5.44	72.07	92.08
	2	30	0.38	5.96	3.07	50.18	64.11
	0.5	50	0.20	5.96	5.54	71.74	91.66
	2	50	0.14	4.35	6.26	56.73	72.48
IRGACURE 184	0.5	30	1.29	9.13	2.89	45.82	58.54
	2	30	0.30	6.51	4.25	52.95	67.65
	0.5	50	0.42	7.57	4	48.07	61.42
	2	50	0.19	5.20	5.38	59.90	76.54
IRGACURE 819	0.5	30	0.38	6.81	3.52	50.78	64.88
	2	30	0.43	6.58	2.96	48.06	61.41
	0.5	50	0.27	6.91	4.93	72.51	92.64
	2	50	0.32	6.72	4.02	75.32	96.24

Table 4.17 Evaluation of kinetic parameters of macromonomeric formulations as per autocatalytic model at 30 and 50 °C containing 10 wt% HEA and 5 wt% TMPTA

Photo Initiator	% conc of photo-initiator	Temperature (°C)	Autocatalytic		
			n	m	k (min^{-1})
IRGACURE 651	0.5	30	6.08	0.70	20.5
	0.5	50	3.28	0.56	14.3
	2	30	4.58	0.52	13.8
	2	50	4.69	0.48	18.6
DAROCUR TPO	0.5	30	3.18	0.63	20.8
	0.5	50	3.34	0.54	19.4
	2	30	6.19	0.48	12.9
	2	50	6.04	0.59	37.6
IRGACURE 184	0.5	30	7.02	0.89	30.3
	0.5	50	6.04	0.84	35.3
	2	30	5.77	0.73	31.9
	2	50	4.39	0.59	24.7
IRGACURE 819	0.5	30	7.38	0.82	38
	0.5	50	2.95	0.51	14.4
	2	30	6.76	0.62	17.7
	2	50	2.47	0.35	7.48

From Table 4.16, the induction time and peak maximum time of most systems were found to decrease with increase in temperature at similar concentration of

photoinitiator as well as with increase in concentration of photoinitiator at same temperature. Exception was seen in the case of DAROCUR TPO at 30 °C and IRGACURE 819 at 30 and 50 °C. Both these photoinitiators belong to phosphine oxide type. With increase in concentration of photoinitiator, the radicals generated are more and radical radical combinations can cause a reduction in the quantum yield for photo initiation beyond an optimum concentration of photoinitiator which account for this effect.¹⁷ At a particular concentration, an increase in peak maximum time with an increase in temperature was observed for IRGACURE 819 due to a comparatively earlier onset of reaction diffusion. Many variations were observed for the value of $R_{p \text{ max}}$ with increase in concentration of photoinitiator at same temperature. This is due to the competition between initiating/propagating radicals as well as between the radicals and the double bond.²³ But it has to be noted that an increase in temperature at a particular concentration was found to increase the $R_{p \text{ max}}$ in all cases. This shows that the combined plasticization provided by the trifunctional crosslinker and HEA to the macromonomer helped the formulations to undergo sufficient volume relaxation during auto acceleration. In other words the rate on onset of reaction diffusion was delayed by a better segmental diffusion towards peak maximum.¹²

The final conversion varied from 45 to 76% for all the systems which is higher than the macromonomeric formulations containing 10 wt% HEA and also with diacrylate. The may be due to the plasticization effect of the reactive diluent and due to a lower initial viscosity of TMPTA containing formulations (Table 4.11) than NPGPDA containing formulations.³⁰ Anseth et al.⁷ have observed that an increase in functionality of crosslinker can reduce the final conversion in many cases for similar class of monomers as an increase in functionality will increase its initial viscosity. Based on such observations we can infer that the major factor for our observation is due the selection of different class of di and trifunctional crosslinkers. We used a trifunctional crosslinker with a lower initial viscosity than that of difunctional crosslinker, which resulted in higher conversion with increase in functionality. An almost consistent behaviour of increase in conversion with increase in temperature was observed. Further, the photo cured system with trifunctional crosslinker has a glass transition of around 126 °C, it shows that this system has crosslinked higher than the diacrylate system. Since the

triacrylate system has a higher ultimate T_g than that of diacrylate system, the former can be assumed to vitrify early for photopolymerization carried out at 30 and 50 °C. This is due to a higher extent of volume shrinkage occurring as compared to chemical reaction for the triacrylate system during the deceleration step, forcing the system to vitrify early.²²

The photopolymerizations were carried out using polychromatic radiation (250-450 nm) showed comparable extent of initiation for the triacrylate and diacrylate systems. Variations in induction or peak maximum time were not observed for these systems.

From Table 4.17, we can infer that the photopolymerization rate fits to the variable autocatalytic kinetic model over a wide range in the cure profile as the values of m and n are constant.¹⁸ Many systems showed reduction in the value of specific rate constant (k) with increase in temperature showing the non fitting nature of the autocatalytic equation from onset to vitrification. The system can also be assumed to follow the n^{th} order model to certain extent.¹⁸ The system during photocuring can be assumed to undergo both monomolecular and bimolecular terminations.¹⁹

The rate and conversion profiles obtained from photocuring studies of macromonomeric formulations containing 10 wt% HEA, 5 wt% of NPGPDA as crosslinker and 0.006 wt% TEMPO with four photoinitiators at 0.5 and 2 wt% compositions at 30 and 50 °C are given below in Figures 4.39 to 4.42 (A-C).

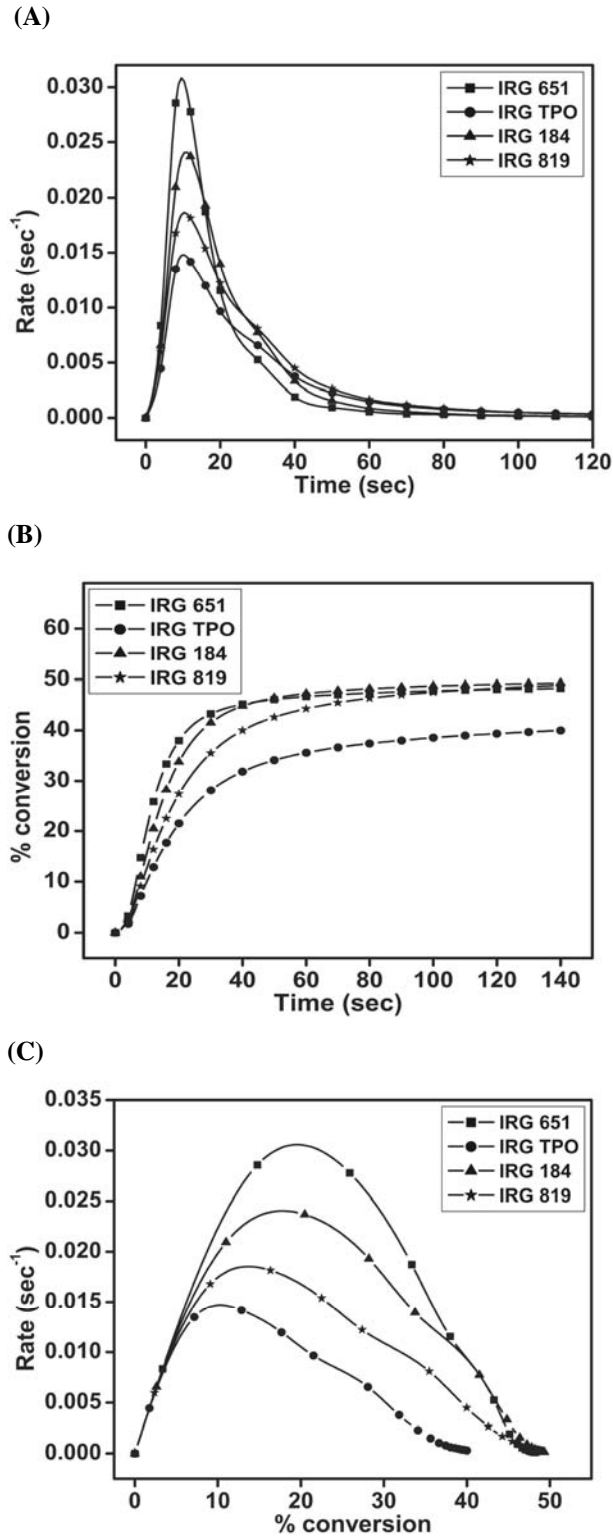


Figure 4.39(A-C) Time dependent rate and conversion profiles of macromonomeric formulations containing 10 wt% HEA, 5 wt% NPGPDA, 0.006 wt% TEMPO and 0.5 wt% of photoinitiator with respect to weight of macromonomer at 30 °C

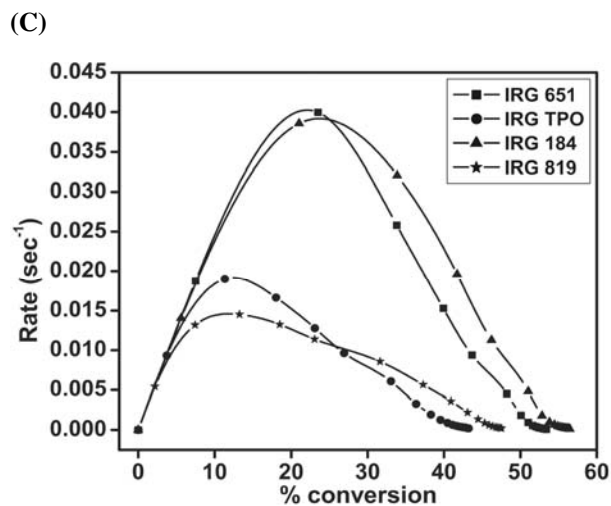
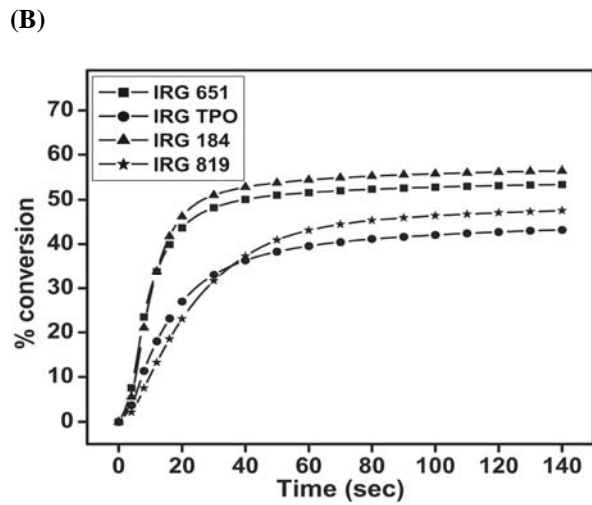
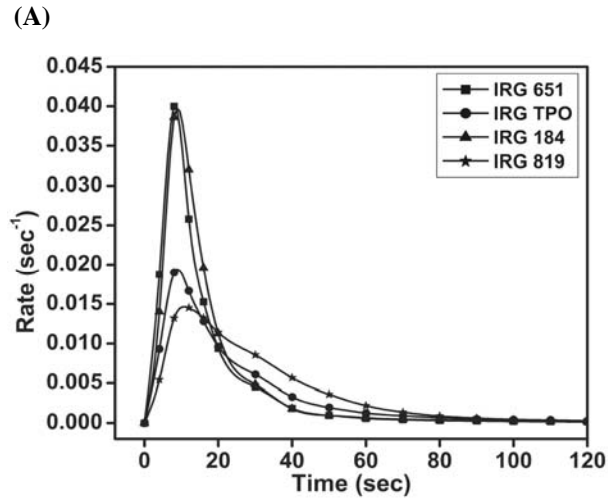


Figure 4.40 (A-C) Time dependent rate and conversion profiles of macromonomeric formulations containing 10 wt% HEA, 5 wt% NPGPDA, 0.006 wt% TEMPO and 2 wt% of photoinitiator with respect to weight of macromonomer at 30 °C

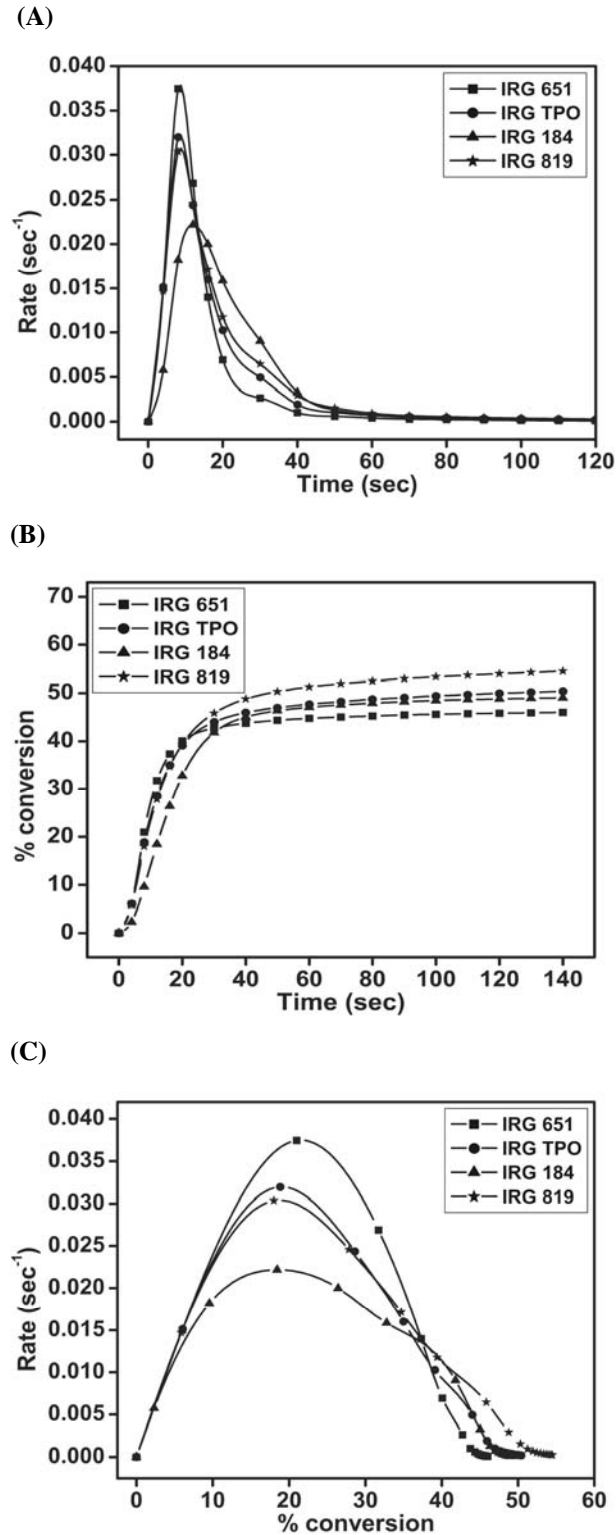


Figure 4.41(A-C) Time dependent rate and conversion profiles of macromonomeric formulations containing 10 wt% HEA, 5 wt% NPGPDA, 0.006 wt% TEMPO and 0.5 wt% of photoinitiator with respect to weight of macromonomer at 50 °C

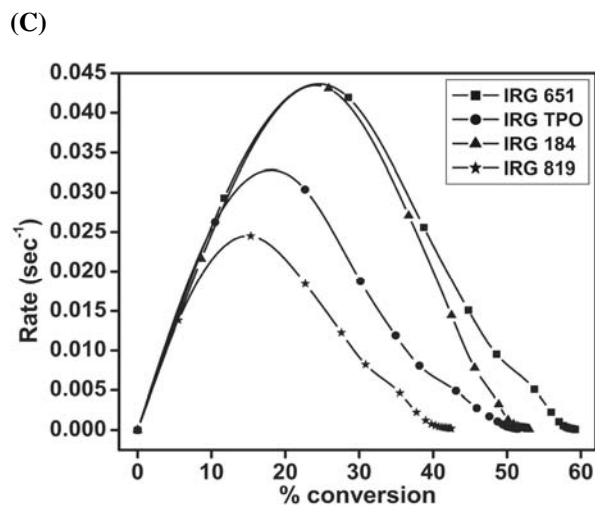
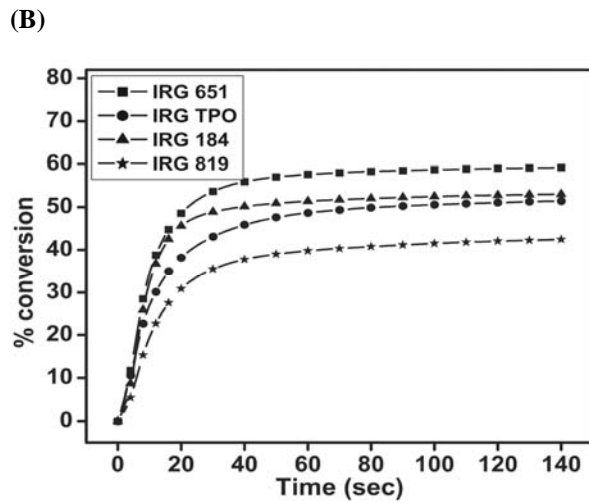
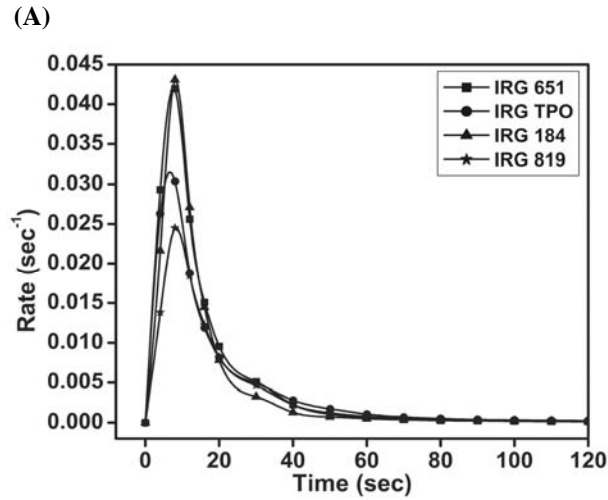


Figure 4.42(A-C) Time dependent rate and conversion profiles of macromonomeric formulations containing 10 wt% HEA, 5 wt% NPGPDA, 0.006 wt% TEMPO and 2 wt% of photoinitiator with respect to weight of macromonomer at 50 °C

The kinetic parameters calculated are given in Tables 4.18 and 4.19.

Table 4.18 Kinetic parameters of macromonomeric formulations calculated from the heat flow profiles containing 10 wt% HEA, 5 wt% NPGPDA and 0.006 wt% TEMPO

Photo Initiator	% conc. of photo-initiator	Temp (°C)	Induction Time (sec)	Peak Maximum Time (sec)	$R_p \text{ max}$ ($\times 10^{-2}$) (sec^{-1})	C_{max} (%)	Heat of reaction (J/g)
IRGACURE 651	0.5	30	2.18	9.59	3.08	48.68	54.85
	2	30	0.79	8.25	4.01	53.91	60.75
	0.5	50	1.11	8.51	3.79	46.32	52.19
	2	50	0.39	7.49	4.22	59.64	67.20
DAROCUR TPO	0.5	30	2.96	10.03	1.48	41.63	46.91
	2	30	1.44	8.91	1.95	44.43	50.06
	0.5	50	0.95	8.51	3.22	51.55	58.09
	2	50	0.41	6.64	3.17	52.43	59.08
IRGACURE 184	0.5	30	2.36	10.74	2.41	49.76	56.07
	2	30	1.26	8.91	3.98	57	64.23
	0.5	50	2.54	11.84	2.22	49.49	55.77
	2	50	0.66	8.20	4.31	53.34	60.10
IRGACURE 819	0.5	30	2.40	10.35	1.86	50.29	56.67
	2	30	2.40	10.69	1.47	48.64	54.81
	0.5	50	0.95	8.66	3.08	55.87	62.95
	2	50	0.92	8.33	2.46	43.50	49.02

Table 4.19 Evaluation of kinetic parameters of macromonomeric formulations as per autocatalytic model at 30 and 50 °C containing 10 wt% HEA, 5 wt% NPGPDA and 0.006 wt% TEMPO

Photo Initiator	% conc of photo-initiator	Temperature (°C)	Autocatalytic		
			n	m	k (min^{-1})
IRGACURE 651	0.5	30	5.96	0.83	24.7
	0.5	50	6.19	0.84	32
	2	30	5.63	0.73	25.9
	2	50	4.76	0.64	21.6
DAROCUR TPO	0.5	30	8.02	0.65	9.34
	0.5	50	5.70	0.67	17.9
	2	30	7.29	0.62	10.7
	2	50	6.61	0.58	18.2
IRGACURE 184	0.5	30	5.44	0.75	14.8
	0.5	50	4.59	0.68	10.5
	2	30	4.69	0.78	23.3
	2	50	5.47	0.80	31.8
IRGACURE 819	0.5	30	5.99	0.66	9.93
	0.5	50	5.34	0.68	16.3
	2	30	4.84	0.49	4.60
	2	50	8.16	0.74	20.8

The addition of free radicals will result in the scavenging of the *in situ* photo radical formed.¹⁷ A photoinitiator undergoing fragmentation under UV irradiation in most

cases will create unsymmetrical radical pairs, of which one type of radical will initiate the reaction.¹⁷ The added free radical may have equal or unequal scavenging affinity to the two types of radical produced on photoinitiation. This difference in affinity can affect the kinetic parameters such as rate constants, time to attain peak maximum, maximum rate and conversions. The important effect of addition of radical scavenger was observed at the induction time, when the system had not undergone autoacceleration as the *in situ* viscosity effects can be ignored. The radical scavengers are found to increase the induction time by scavenging the photo initiating species there by reducing the quantum yield for photo initiation.¹⁷ Other kinetic factors are also influenced by the scavenger. The various disparities in peak maximum time, maximum rate and conversion occur due to several competing factors such as autoacceleration, segmental and radical diffusions, radical radical combination, radical trapping, earlier onset of reaction diffusion, vitrification etc.^{12,14,15} The above factors control the termination and propagation kinetics during the entire process.

From Table 4.18, it can be seen that the induction time of the systems with TEMPO varied from 0.39 to 2.96 sec, while the variation without added scavenger for NPGPDA system varied from 0.18 to 1.76 sec. The final conversion for the diacrylate system containing TEMPO varied from 41 to 60% unlike 36 to 70% for the diacrylate system without added scavenger. This shows a reduction in the range of final conversion on addition of TEMPO. With all other kinetic parameters being constant, we can infer that the primary effect is due to the reduction in induction time for the TEMPO systems. The time scale for reaction diffusion can be increased in many cases due to a slower initiation rate on addition of radical scavenger. Higher conversion of around 70% was shown by the diacrylate system without scavenger as against 60% by diacrylate system with scavenger due to the influence of initiation rate and diffusion processes. In short, the accelerating and decelerating factors, which control the *in situ* viscosity, resulted in the variations.

From Table 4.19, it was observed that the system was found to obey the variable autocatalytic kinetic model to a better level than the NPGPDA added system without TEMPO. In general, for n^{th} order model, the R_p is highest at the starting of the reaction while for the autocatalytic model the R_p is maximum after a certain time.³¹ This accounts

for the better autocatalytic behavior in presence of TEMPO. The system showed an increase in the value of specific rate constant with increase in temperature for most of the formulations. The reduction in the rate of initiation as observed from the induction time as well as the time delay in attaining $R_{p\text{ max}}$ can be considered as the major contributing factor to this effect.

The rate and conversion profiles obtained from photocuring studies of macromonomeric formulations containing 10 wt% HEA, 5 wt% of TMPTA as crosslinker and 0.012 wt% TEMPO with four photoinitiators at 0.5 and 2 wt% compositions at 30 and 50 °C are given below in Figures 4.43 to 4.46 (A-C).

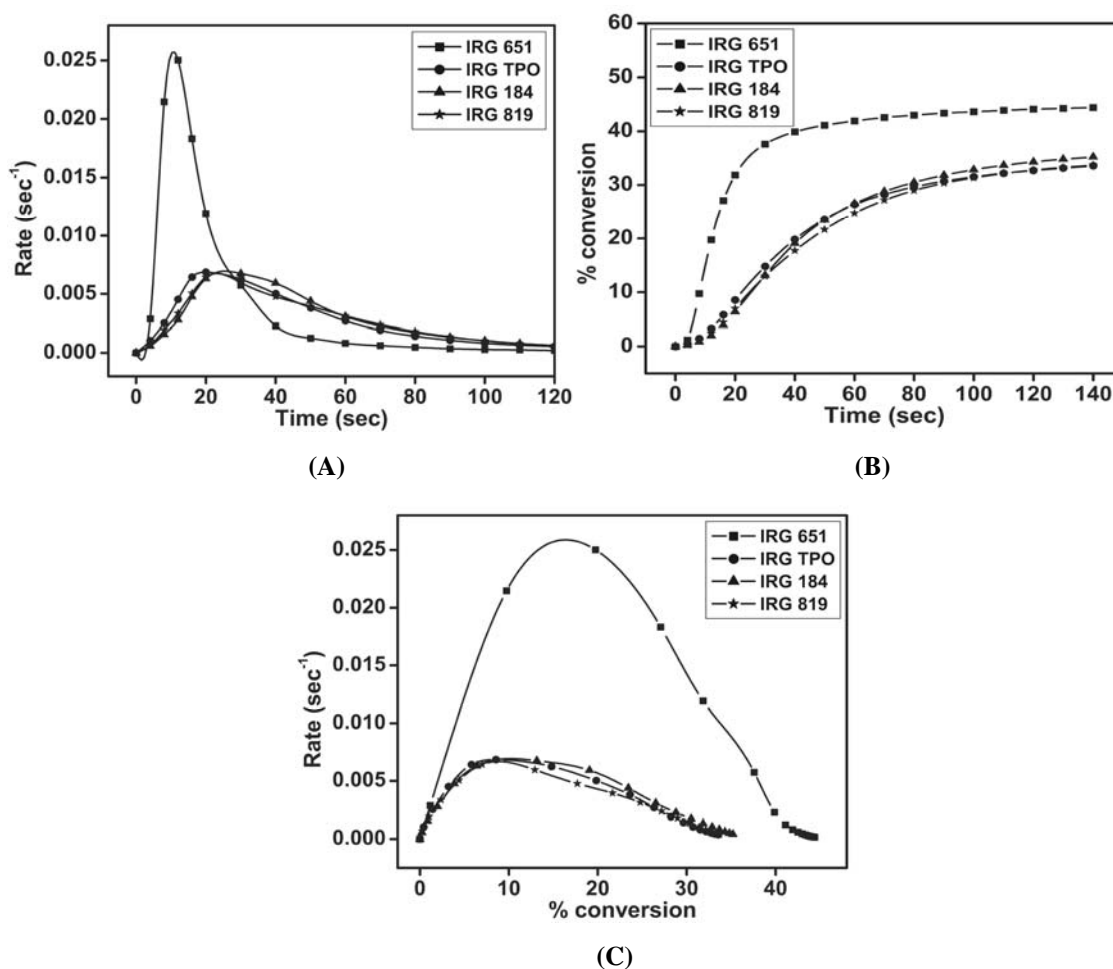


Figure 4.43(A-C) Time dependent rate and conversion profiles of macromonomeric formulations containing 10 wt% HEA, 5 wt% TMPTA, 0.012 wt% TEMPO and 0.5 wt% of photoinitiator with respect to weight of macromonomer at 30 °C

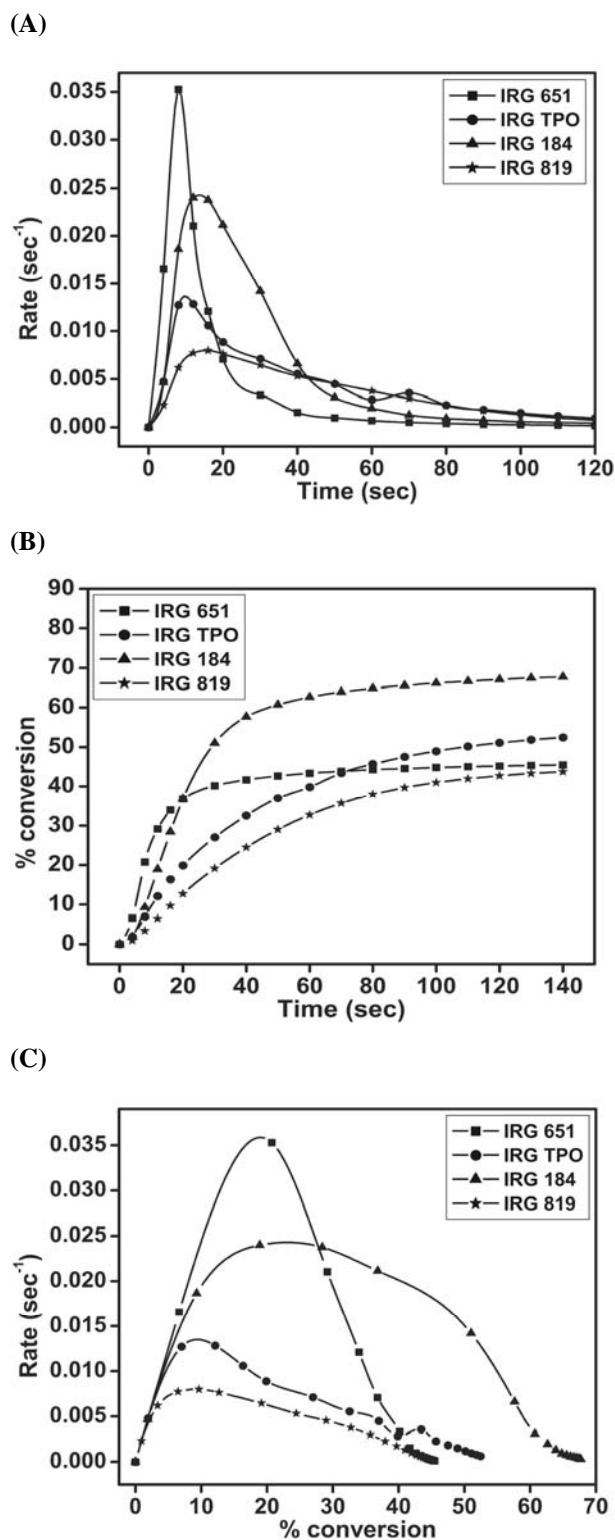


Figure 4.44(A-C) Time dependent rate and conversion profiles of macromonomeric formulations containing 10 wt% HEA, 5 wt% TMPTA, 0.012 wt% TEMPO and 2 wt% of photoinitiator with respect to weight of macromonomer at 30 °C

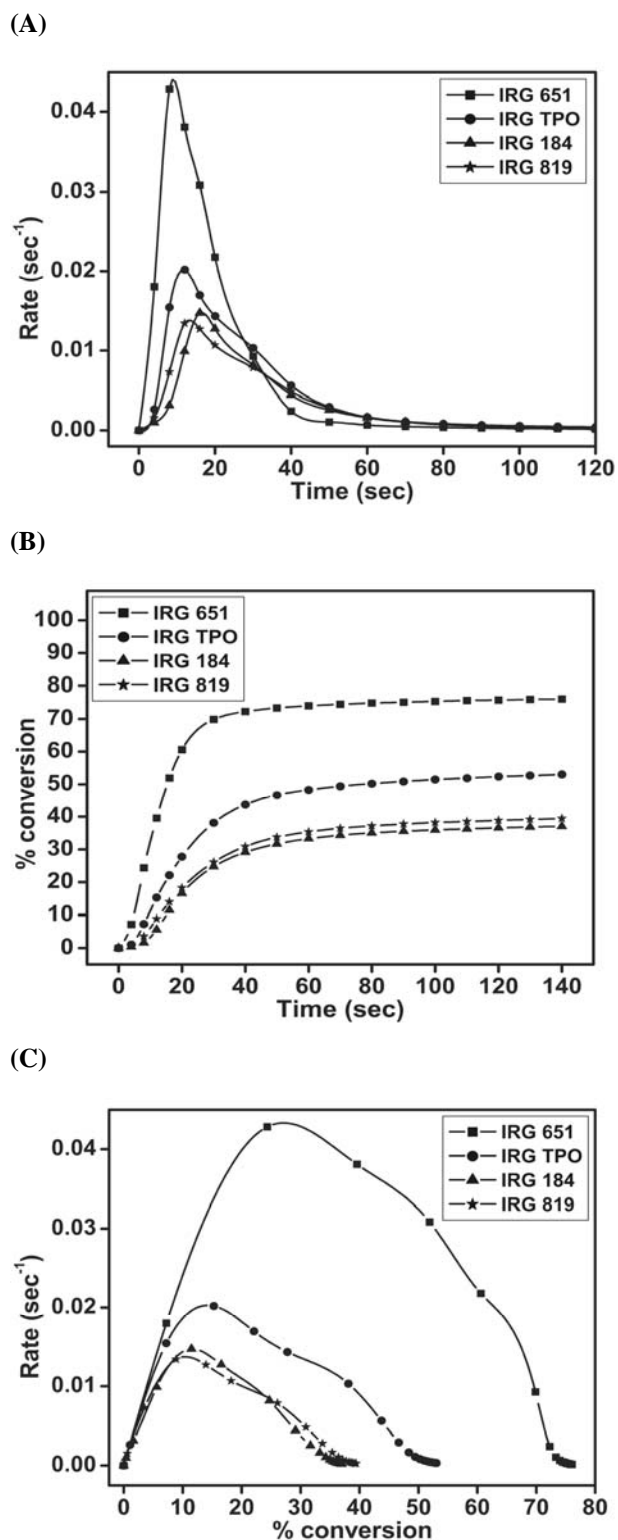


Figure 4.45(A-C) Time dependent rate and conversion profiles of macromonomeric formulations containing 10 wt% HEA, 5 wt% TMPTA, 0.012 wt% TEMPO and 0.5 wt% of photoinitiator with respect to weight of macromonomer at 50 °C

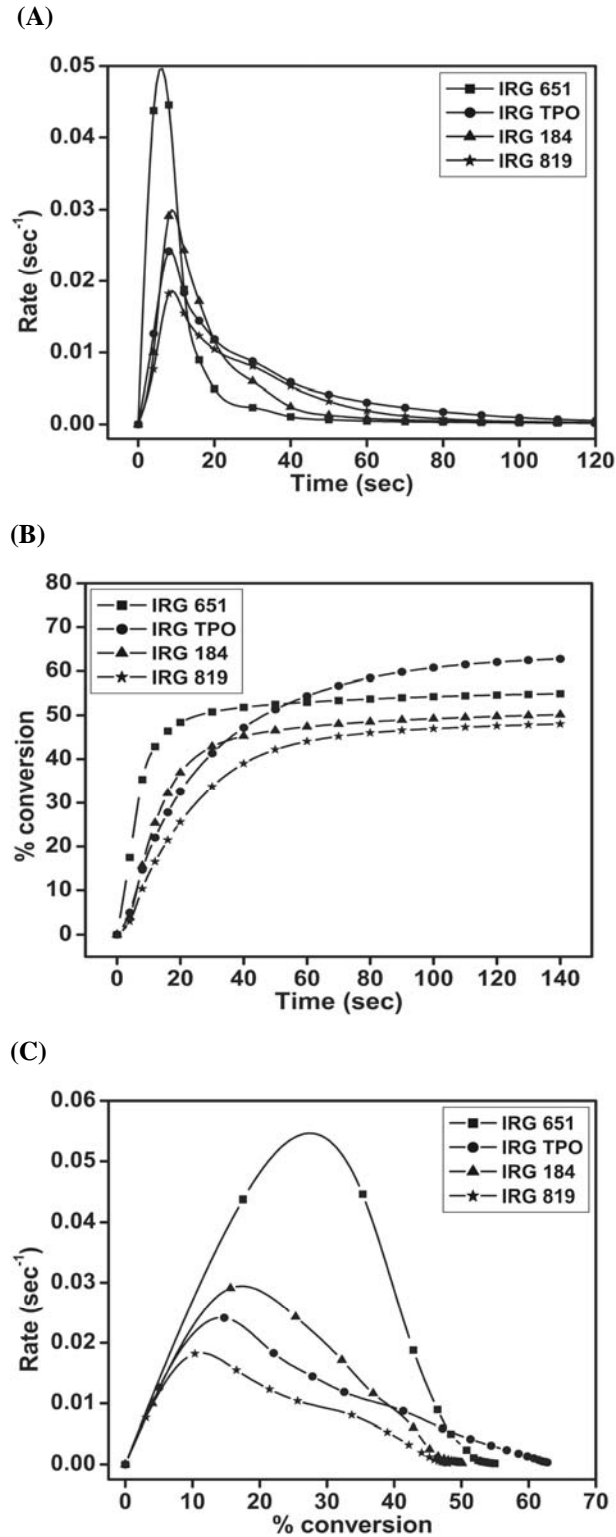


Figure 4.46(A-C) Time dependent rate and conversion profiles of macromonomeric formulations containing 10 wt% HEA, 5 wt% TMPTA, 0.012 wt% TEMPO and 2 wt% of photoinitiator with respect to weight of macromonomer at 50 °C

The kinetic parameters calculated are given in Tables 4.20 and 4.21.

Table 4.20 Kinetic parameters of macromonomeric formulations calculated from the heat flow profiles containing 10 wt% HEA, 5 wt% TMPTA and 0.012 wt% TEMPO

Photo Initiator	% conc. of photo-initiator	Temp (°C)	Induction Time (sec)	Peak Maximum Time (sec)	$R_p \text{ max}$ ($\times 10^{-2}$) (sec^{-1})	C_{max} (%)	Heat of reaction (J/g)
IRGACURE 651	0.5	30	2.88	10.64	2.58	45.07	57.59
	2	30	0.88	8.15	3.53	46.07	58.87
	0.5	50	0.87	8.98	4.41	76.79	98.12
	2	50	0.22	5.99	4.98	55.73	71.21
DAROCUR TPO	0.5	30	6.61	19.52	0.69	35.42	45.25
	2	30	2.71	9.76	1.37	54.69	69.88
	0.5	50	3.92	11.69	2.02	54.90	70.15
	2	50	1.05	8.31	2.43	64.39	82.27
IRGACURE 184	0.5	30	8.67	25.60	0.70	37.06	47.35
	2	30	3.07	13.66	2.43	69.51	88.81
	0.5	50	6.66	16.55	1.48	37.98	48.53
	2	50	1.75	8.90	3.01	51.04	65.22
IRGACURE 819	0.5	30	7.78	23.08	0.68	35.65	45.55
	2	30	4.18	15.30	0.80	45.60	58.26
	0.5	50	4.86	13.22	1.38	40.86	52.21
	2	50	1.87	8.84	1.86	49.17	62.83

Table 4.21 Evaluation of kinetic parameters of macromonomeric formulations as per autocatalytic model at 30 and 50 °C containing 10 wt% HEA, 5 wt% TMPTA and 0.012 wt% TEMPO

Photo Initiator	% conc. of photo-initiator	Temperature (°C)	Autocatalytic		
			n	m	k (min^{-1})
IRGACURE 651	0.5	30	7.10	0.79	22.2
	0.5	50	1.66	0.35	6.58
	2	30	7.63	0.76	32
	2	50	6.02	0.76	48.3
DAROCUR TPO	0.5	30	8.69	0.75	5.72
	0.5	50	4.41	0.48	5.94
	2	30	3.73	0.16	1.52
	2	50	3.37	0.15	2.89
IRGACURE 184	0.5	30	9.01	0.89	8.68
	0.5	50	10.8	1.07	33.5
	2	30	2.92	0.59	7.56
	2	50	5.52	0.63	14.2
IRGACURE 819	0.5	30	8.06	0.69	4.19
	0.5	50	7.39	0.66	8.07
	2	30	4.01	0.30	1.38
	2	50	4.26	0.27	2.97

The induction time of the triacrylate systems with TEMPO varied from 0.22 to 8.67 sec, while the variations without added scavenger for triacrylate systems varied from 0.14 to 1.29 sec. The final conversion for the triacrylate system containing TEMPO

varied from 35 to 77% unlike 45 to 76% for the triacrylate system without added scavenger. This shows the scavenging effect of TEMPO does not have much effect on maximum conversion, while an increase in induction time can be considered as a major factor for variations in conversions for the formulations containing TEMPO. We can infer that the time scale for reaction diffusion increased by the effect of TEMPO did not make significant contribution to final conversion due to reduction in the value of $R_{p \max}$. In other words the onset of vitrification is delayed when the viscosity build up is gradual, which can result in higher conversions. Here also the accelerating and decelerating factors which control the *in situ* viscosity resulted in the variations.^{12,15}

This system was found to obey variable autocatalytic kinetic model to a better level than the TMPTA systems without TEMPO. The system showed an increase in the value of specific rate constant (k) with increase in temperature for most of the formulations. The reduction in the rate of initiation as observed from the induction time as well as a delay in attaining $R_{p \max}$ can be considered as the major contributing factor to this effect.^{12,31}

Scavenging effect of TEMPO

It has to be noted that in photopolymerization reactions, during initiation and before onset of autoacceleration the value of k_t was found to be much higher than k_p .^{12,14} The heat flow profile of the macromonomeric formulation containing diacrylate, radical scavenger and 0.5 wt% of photoinitiator at 30 °C was found to show a trend in delay of induction time in photocuring as compared to the photopolymerization of the same system at 50 °C. The results are given in Figure 4.47 (a). This is due to the combined effect of radical trapping at low temperature and radical radical combination which delays the rate of propagation of photopolymerization.^{12,17} A portion of the photo radical formed will be scavenged *in situ* in the photocalorimeter during analyses which reduces the quantum yield of initiation and hence the induction time will increase.¹⁷ The amount of photo radical scavenged depends on the quantum yield of α scission as well as the mobility of the photoinitiator and the radical scavenger in the formulation.¹⁷ On increasing the concentration of the initiator to 2 wt% for the same system, the effect is less pronounced as evident from Figure 4.47 (b). On analyses of the system with triacrylate and twice the concentration of radical scavenger than the diacrylate system

with 2 wt% of initiator concentration showed a higher induction time than the diacrylate system. This shows that the concentration of radical scavenger rather than the nature of crosslinker in the matrix is more responsible for the lesser extent of polymerization rate. Further, the heat flow profile is also found to increase with increase in temperature, which clarifies that the effective number of radicals causing the initiation reaction increases with temperature even though radical radical combination exist at considered temperatures. The comparative plots for the triacrylate system is given in Figure 4.47 (c).

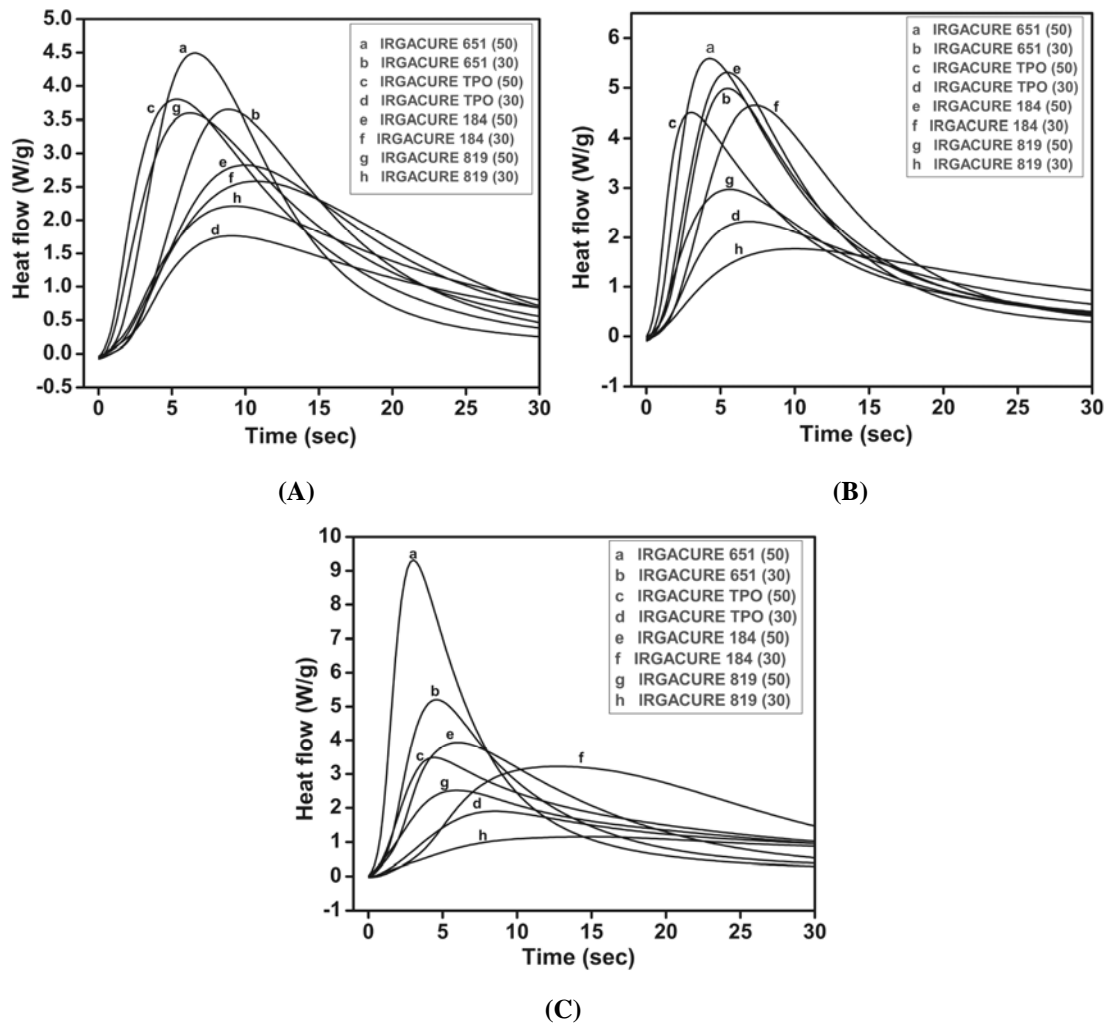


Figure 4.47(A-C) Scavenging effect of TEMPO

4.1.1.10.5 Post photopolymerization studies

Thermogravimetric analysis

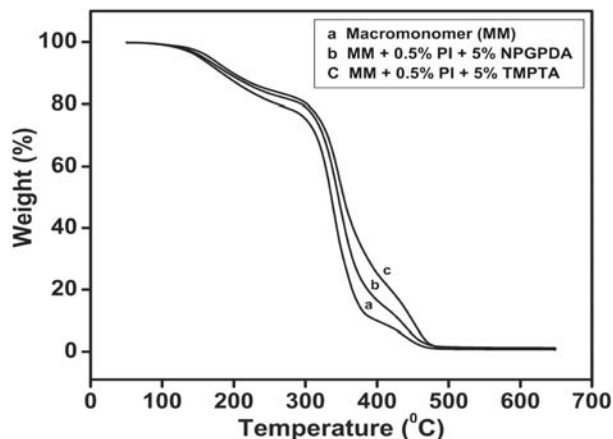


Figure 4.48 Thermogravimetric degradation profiles of (a) macromonomer with 10 wt% HEA (b) macromonomer containing 10 wt% HEA and 5 wt% of NPGPDA and (c) macromonomer containing 10 wt% HEA and 5 wt% of TMPTA with 0.5 wt% of IRGACURE 184 photocured at 50 °C. Analyses done after three days of storage

From the thermogravimetric degradation profile given in Figure 4.48, we can infer that the macromonomeric formulation containing triacrylate as crosslinker showed least degradation profile followed by diacrylate as crosslinker. The macromonomeric formulation containing 10 wt% HEA as reactive diluent showed fastest degradation profile.

DSC analysis

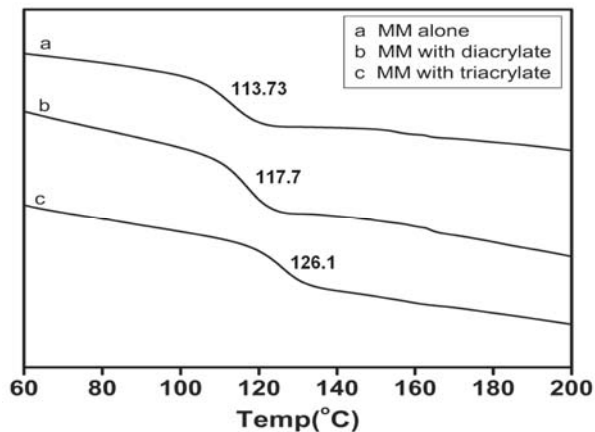


Figure 4.49 T_g of (a) macromonomer, (b) macromonomer containing 5 wt% of NPGPDA and (c) macromonomer containing 5 wt% of TMPTA with 0.5 wt% of IRGACURE 184 photocured at 50 °C

From Figure 4.49, we can infer that an increase in the functionality of the crosslinker has increased the extent of crosslinking by showing a corresponding increase in T_g .

Determination of gel content

The gel content of the photopolymerized systems were calculated by swelling studies.³² Accurately weighed (~10 mg) of the material after 16 h of photopolymerization was extracted with chloroform in a Soxhlet extractor for a period of 24 h and repeatedly weighed to a constant weight.

$$\text{Percentage gel content} = W/W_0 \times 100$$

where, W is the weight of the resin after extraction and W_0 is the weight of the original resin.

Once initiated, the photopolymerization occur even in dark at a low rate.³³ As a result the gel contents in all the three cases were found to show less variation (Table 4.22). The results of post polymerization studies are condensed in Table 4.22.

Table 4.22 Post polymerization analyses

Composition ^a	90% weight loss ^b (°C)	T_g ^b (°C)	Gel content ^b (%)
Macromonomer with 10% HEA	399 ± 2.1	113 ± 1.2	90 ± 2.6
Macromonomer with 10% HEA and 5% of NPGPDA	432 ± 3.2	117 ± 0.7	93 ± 1.9
Macromonomer with 10% HEA and 5% of TMPTA	449 ± 2.4	125 ± 1.1	93 ± 2.5

a) With 0.5% IRGACURE 184 as photoinitiator cured at 50°C.

b) Errors based on duplicate analysis.

4.1.1.11 Photopolymerization of diacrylate macromonomer based on polytetrahydrofuran 650, isophorone diisocyanate and poly(ethylene glycol) methacrylate (System 4A-9)

A diacrylate macromonomer based on polytetrahydrofuran 650 (PTHF 650), isophorone diisocyanate and poly(ethylene glycol) methacrylate (PEGMA) was synthesized and formulated. The photocuring studies of the formulations were carried out. Estimation of kinetic parameters were done based on the heat flow profiles obtained during the photopolymerization process.

The telechelic synthesis of macromonomer was done in two steps. An initial condensation of the diol and diisocyanate to form a diisocyanate terminated urethane prepolymer followed by end capping of the formed prepolymer with excess of PEGMA to form soft segmented urethane diacrylate macromonomer.

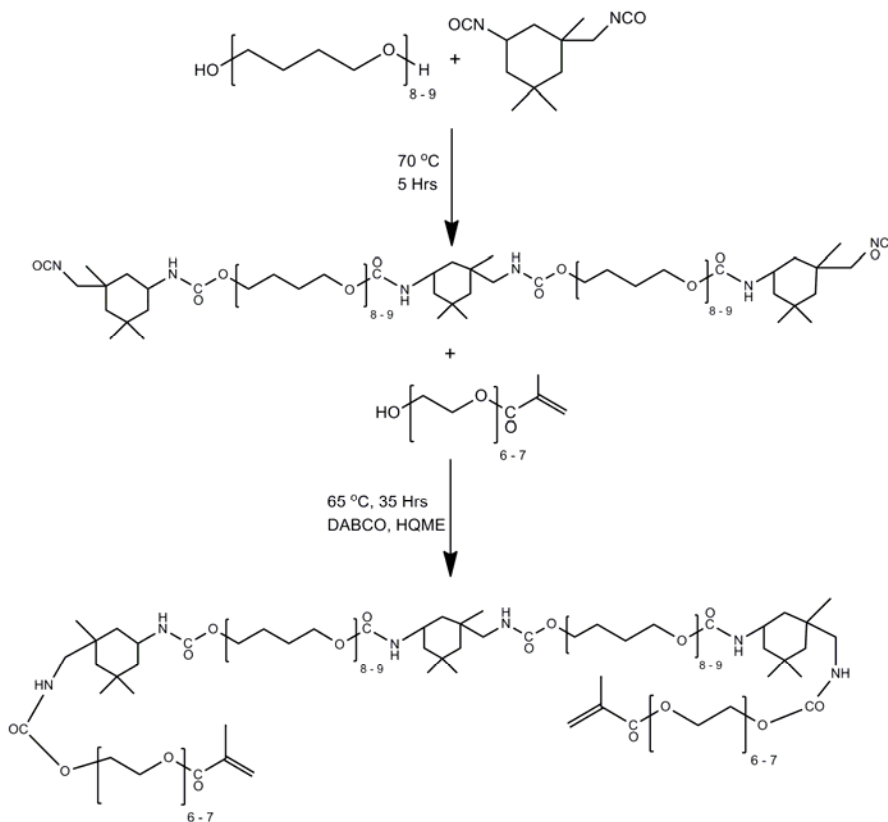


Figure 4.50 Synthesis pathway of diacrylate macromonomer based on PTHF 650, IPDI and PEGMA

4.1.1.11.1 Procedure for synthesis

Synthesis of prepolymer

The prepolymer was synthesized by the addition of 15.52 g (23.88 m mol) PTHF 650 in to a 100 mL three necked glass reaction vessel, which was initially purged with nitrogen. The reaction mixture was stirred at 100 rpm. To it 5.33 g (23.99 m mol) of IPDI was added followed by addition of 10 mL of chloroform as solvent. The ratio of NCO:OH was 1.005:1. The system was stirred at 70 °C under nitrogen atmosphere for a period of five hours to obtain diisocyanate terminated prepolymer. The residual isocyanate content was noted (ASTM D 2572). The residual isocyanate was found to be 5.477%. IR and NMR spectra were noted.

IR: 2260 (NCO), 1713 (C=O, urethane), 3341 and 1534 (-CO-NH-, urethane), 1109 (C-O), 2928 and 2856 (-CH₂-) cm⁻¹.

¹HNMR (CDCl₃): 0.84, 0.94 and 1.05 (CH₃, alicyclic), 1.16 to 1.24 (-CH₂-, alicyclic), 1.60, 1.66 (-O-CH₂-CH₂-CH₂-CH₂-O-), 2.91 (-CH₂-NH-CO-), 3.01 (-CH₂-NCO), 3.40 and 3.44 (-O-CH₂-CH₂-CH₂-CH₂-O-), 3.61 (-CH-NH-, alicyclic), 4.05 (-NH-CO-O-CH₂-), 4.75 (-CH₂-NH-CO-O-CH₂-).

¹³C NMR (CDCl₃): 26.39 and 25.80 (-O-CH₂-CH₂-CH₂-CH₂-O-), 27.44 and 34.95 (CH₃, gem, alicyclic), 23.14 (CH₃, alicyclic), 41.84, 45.94 and 46.50 (-CH₂-, alicyclic), 31.75 (=C-(CH₃)₂, alicyclic), 36.29 (=C-(CH₃)-CH₂-NH-CO-, alicyclic), 56.92 (-CH₂-NCO), 64.46 (-NH-CO-O-CH₂-CH₂-), 62.51 (-CH₂-NH-CO-O-CH₂-CH₂-), 70.11 and 70.70 (-O-CH₂-CH₂-CH₂-CH₂-O-), 155.88 (-NH-CO-O-), 157.05 (-CH₂-NH-CO-O-) ppm.

Synthesis of macromonomer

To the synthesized prepolymer was added 0.676 g (1.88 mmol) of PEGMA so that the ratio of NCO:OH was 1:4. 0.108 g (0.9628 mmol) of DABCO was added followed by the addition of 4.3 mg of HQME (200 ppm) as stabilizer. The reaction was continued at 65 °C for 35 h until all the isocyanate groups were completely consumed from the IR spectrum. The reaction mixture was then poured into 100 mL chloroform in a 500 mL separating funnel. It was then washed thrice with 100 mL deionised water until devoid of excess PEGMA. The chloroform layer was dried over activated molecular sieves for 6 h and filtered and dried for 12 h. It was further dried in vacuum oven at 60 °C for 12 h to obtain viscous macromonomer. IR and NMR spectra were noted. The molecular mass was found by VPO.

IR: 1703 (C=O, urethane), 3331 and 1538 (-CO-NH-, urethane), 1111 (C-O), 815 (-CO-C(CH₃)=CH₂, methacrylate), 2945 and 2856 (-CH₂-) cm⁻¹.

¹*H*NMR (CDCl₃): 0.86, 0.91 and 1.04 (CH₃, alicyclic), 1.11 to 1.29 (-CH₂-, alicyclic), 1.60, 1.64 (-O-CH₂-CH₂-CH₂-CH₂-O-), 2.90 (-CH₂-NH-CO-), 3.39 and 3.43 (-O-CH₂-CH₂-CH₂-CH₂-O-), 3.77 (-CH-NH-, alicyclic), 4.51 (-NH-CO-O-CH₂-), 4.78 (-CH₂-NH-CO-O-CH₂-), 5.62 and 6.15 (-CO-C(CH₃)=CH₂) ppm.

¹³*C* NMR (CDCl₃): 26.46, 26.17 and 25.86 (-O-CH₂-CH₂-CH₂-CH₂-O-), 27.59 and 35.02 (CH₃, gem, alicyclic), 23.20 (CH₃, alicyclic), 41.91, 46.35 and 47 (-CH₂-, alicyclic), 31.83 (=C-(CH₃)₂, alicyclic), 36.35 (=C-(CH₃)-CH₂-NH-CO-, alicyclic), 55.03 (-CH₂-NH-CO-), 64.69 (-NH-CO-O-CH₂-CH₂-) 62.67 (-CH₂-NH-CO-O-CH₂-CH₂-) 70.21 and 70.81 (-O-CH₂-CH₂-CH₂-CH₂-O-), 126.2 (-O-CO-C(CH₃)=CH₂), 134.5 (-O-CO-C(CH₃)=CH₂), 155.96 (-NH-CO-O-), 157.12 (-CH₂-NH-CO-O-), 167.4 (-O-CO-C(CH₃)=CH₂) ppm

4.1.1.11.2 Formulation

The macromonomer was viscous and transparent. The formulations were made in 5 mL sample vials. 1 g each of the formulation was added in each of the sample vials. The photoinitiators of choice were IRGACURE 651, DAROCUR TPO, IRGACURE 184 and IRGACURE 819. 0.5 wt% and 2 wt% of photoinitiator were homogenized with the macromonomer to obtain eight photopolymerizable formulations.

The isothermal photocalorimetry was studied at 30 and 50 °C. Under the same isothermal conditions and concentrations of photoinitiators, the effect of crosslinker on the photopolymerization was studied by adding 10 wt% of neopentyl glycol propoxylate diacrylate (NPGPDA) as the difunctional crosslinker. Studies using 10 wt% of trimethylolpropane triacrylate (TMPTA) as trifunctional crosslinker was also carried out. The radical scavenging effect was also studied by addition of TEMPO at 0.006 wt% on the difunctional crosslinking system and 0.012 wt% on the trifunctional crosslinking system respectively. The radical scavenging effect was studied at 30 and 50 °C to understand the effect of temperature on the rate of polymerization of the formulation with and without the presence of radical scavenger.

4.1.1.11.3 Photocuring studies

About 10 mg of the composition was accurately weighed on a DSC pan and subjected to photo DSC studies under a nitrogen purge of 50 mL/min. The heat flow profiles obtained during the *in situ* photocuring process were recorded as a function of time under an isothermal condition of 30 and 50 °C. The intensity of irradiation was kept

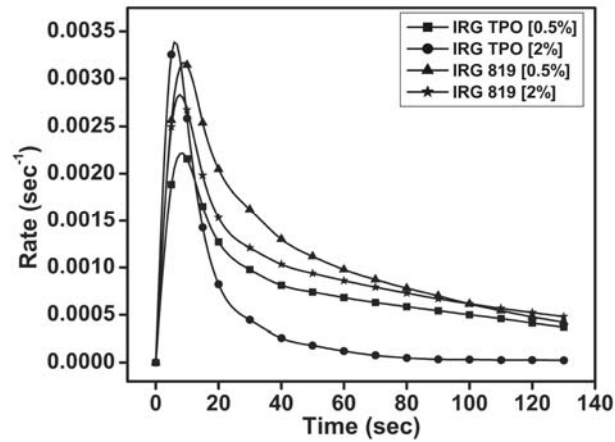
constant at 4.6 mW/cm^2 using a polychromatic radiation of 250-450 nm and 100 W high pressure mercury short arc lamp. The normalized output signals in W/g against time were recorded. The rates of photopolymerizations as well as corresponding conversions were calculated for all the compositions.

4.1.1.11.4 Results and discussion

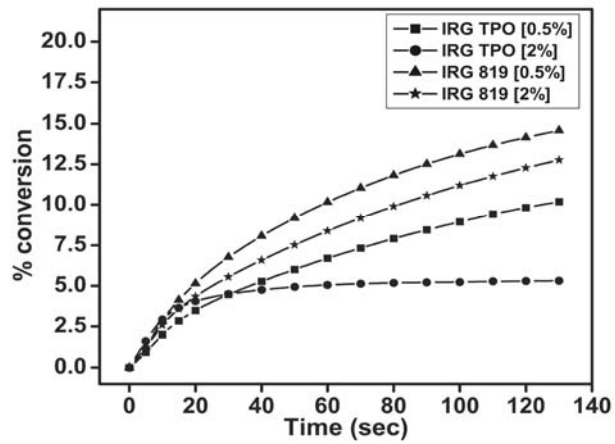
The existence of isocyanate group in the prepolymer as well as the complete conversion of isocyanate group during the formation of macromonomer was confirmed by IR, ^1H and ^{13}C NMR spectroscopy. The molecular mass was found by VPO to be 2937 g/mol. The total theoretical heat flow^{7,20} (ΔH_{theor}) for the system was calculated to be 37.32 J/g. The total theoretical heat flow^{4,6,7} on addition of 10 wt% of NPGPDA was calculated to be 81.7 J/g and on addition of 10 wt% of TMPTA was calculated as 113.26 J/g.

The rate and conversion profiles obtained from photocuring studies of macromonomeric formulations containing 0.5 and 2 wt% of IRGACURE 651 and DAROCUR TPO at 30 and 50 °C are given below in Figures 4.51 and 4.52 (A-C).

(A)



(B)



(C)

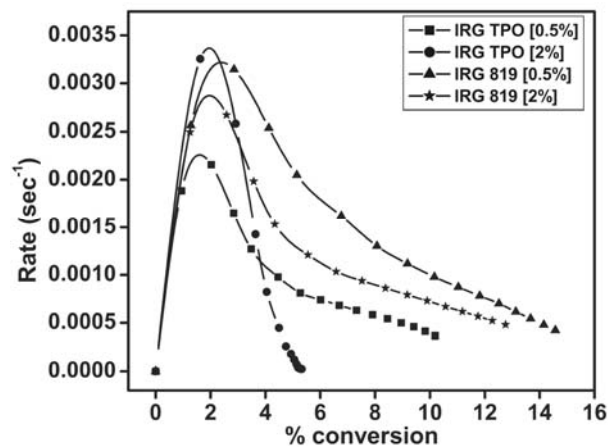
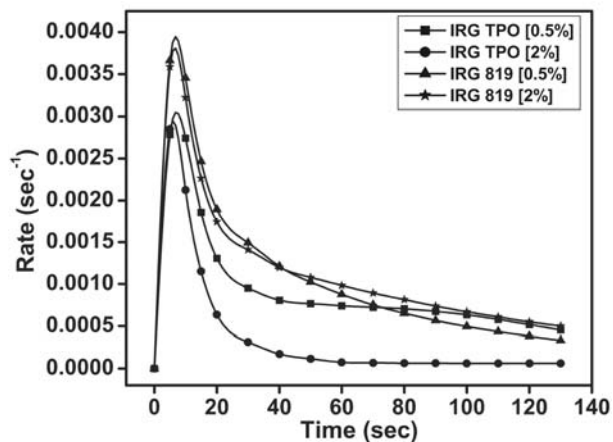
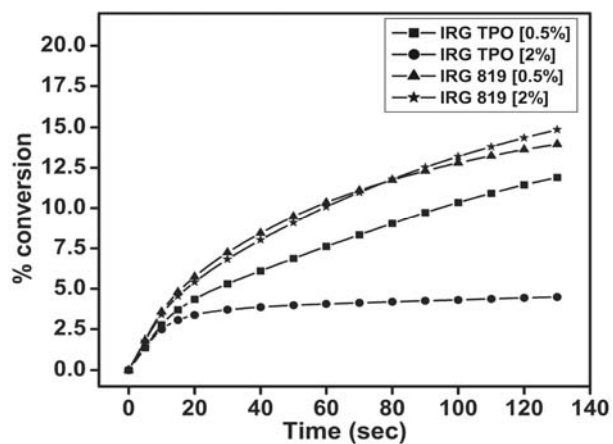


Figure 4.51(A-C) Time dependent rate and conversion profiles of macromonomeric formulations containing 0.5 and 2 wt% of IRGACURE 651 and DAROCUR TPO as photoinitiator with respect to weight of macromonomer at 30 °C

(A)



(B)



(C)

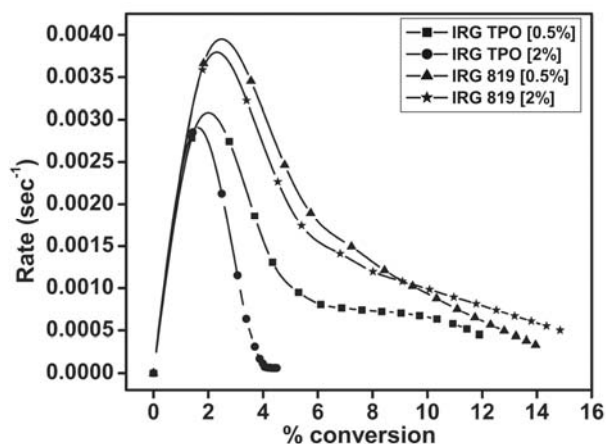


Figure 4.52(A-C) Time dependent rate and conversion profiles of macromonomeric formulations containing 0.5 and 2 wt% of IRGACURE 651 and DAROCUR TPO as photoinitiator with respect to weight of macromonomer at 50 °C

The kinetic parameters calculated are given in Tables 4.23 and 4.24.

Table 4.23 Kinetic parameters of macromonomeric formulations calculated from the heat flow profiles

Photo Initiator	% conc. of photo-initiator	Temp (°C)	Induction Time (sec)	Peak Maximum Time (sec)	$R_p \text{ max}$ ($\times 10^{-3}$) (sec ⁻¹)	C_{max} (%)	Heat of reaction (J/g)
DAROCUR TPO	0.5	30	5.29	8.36	2.22	11.75	4.38
	2	30	3	6.13	3.40	5.59	2.09
	0.5	50	3.63	7.07	3.06	13.71	5.12
	2	50	3.41	5.92	2.95	5.03	1.88
IRGACURE 819	0.5	30	3.99	9.02	3.18	16.89	6.31
	2	30	4.06	7.74	2.83	16.03	5.98
	0.5	50	2.71	6.77	3.94	15.87	5.92
	2	50	2.78	6.50	3.82	18.12	6.76

Table 4.24 Evaluation of kinetic parameters of macromonomeric formulations as per autocatalytic and nth order models

Photo Initiator	% conc. of photo-initiator	Temp (°C)	Autocatalytic			n th order	
			n	m	k (min ⁻¹)	n	k (min ⁻¹)
DAROCUR TPO	0.5	30	10.3	-0.34	0.03	18.1	0.15
	2	30	96.7	0.88	38.1	49.5	0.39
	0.5	50	3.77	-0.65	0.01	17.8	0.19
	2	50	152	1.28	389	75.4	0.43
IRGACURE 819	0.5	30	12.6	-0.08	0.16	13.8	0.24
	2	30	7.36	-0.11	0.19	15.2	0.18
	0.5	50	15.5	-0.43	0.03	17.3	0.31
	2	50	6.48	-0.45	0.04	14	0.25

These formulations do not have any reactive diluent. From Table 4.23, we can infer that the formulation containing IRGACURE 819 had a faster rate of initiation than formulation containing DAROCUR TPO. This is against expectation and is probably due to a better radical diffusion/reduced terminations for the active species in IRGACURE 819 during the initial stages of the polymerization. In general, a reduction in induction time and peak maximum time was observed for most of the formulations with increase in concentration of photoinitiator at isothermal conditions or with increase in temperature at similar concentrations. It has to be noted that the trend was seen at peak maximum time and not at induction time. This behaviour is unusual and can be due to a delayed initiation caused by high initial viscosity or due to low density of functionality in the formulation. The $R_p \text{ max}$ was not found to be consistently increasing with increase in temperature. This

shows an earlier onset of reaction diffusion and the competence of radical and reaction diffusion before $R_{p \text{ max}}$ which accounts for this effect.^{15,23} The final conversions were relatively lower due to high initial system viscosity and low density of functionality.

The photopolymerization were carried out using polychromatic radiation (250-450 nm). From the induction time values, it was observed that the formulation containing IRGACURE 819 showed a faster rate of initiation than that of DAROCUR TPO. Both the photoinitiators being of phosphine oxide type, has primary excitation lying within $n-\pi^*$ forbidden transition.^{1,26} Even though DAROCUR TPO has multiple excitations within the irradiation range than IRGACURE 819, it was found to show a reduced initiation rate probably due to reduced radical diffusion/enhanced terminations. The viscous formulation did not contain any reactive diluent and hence had a high initial viscosity. As a result in addition to reaction diffusion, the rate of radical diffusion from the starting of the reaction had much influence on the kinetics.^{14,15} So the induction time can be assumed to be controlled by radical diffusion/effective number of radical species generated.^{14,15,17}

From Table 4.24, we can infer that the photopolymerization rate did not fit to variable autocatalytic kinetic model as the values of m and n were not constant. The value of autocatalytic exponent (m) was negative in certain cases. So the values of specific rate constants (k) calculated by the autocatalytic model for the formulations are not correct. For an n^{th} order model, the conversion is maximum at the initial stages of the reaction.³¹ The system was also found to deviate from the n^{th} order model.

The heat flow profile for the formulations containing DAROCUR TPO at 0.5 wt% concentration of photoinitiator at 50 °C as well as the deviations of both the models from the experimental values (represented by dots) are given in the Figure 4.53(A-C)

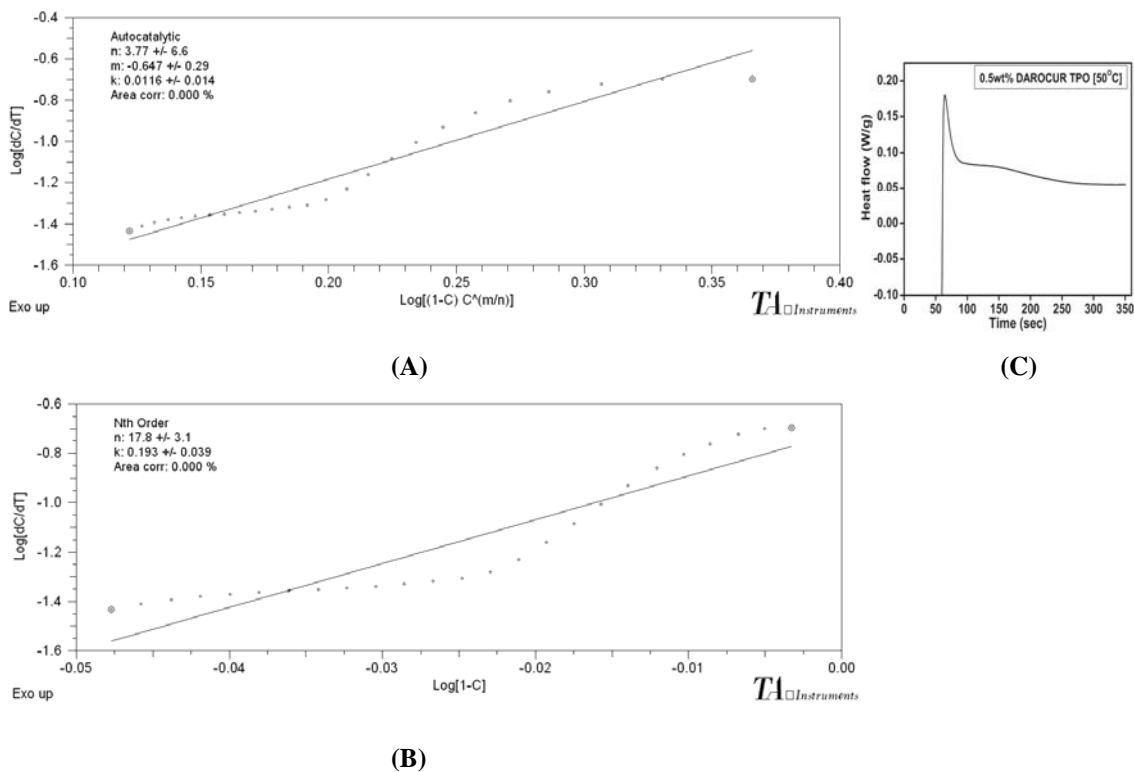
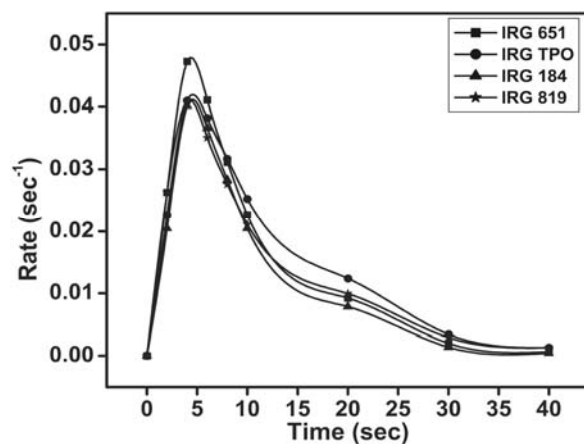


Figure 4.53(A-C) Deviation of experimental data from the autocatalytic and n^{th} order models (A-B) and the corresponding heat flow profile (C) for macromonomer containing 0.5 wt% of DAROCUR TPO at 50 °C

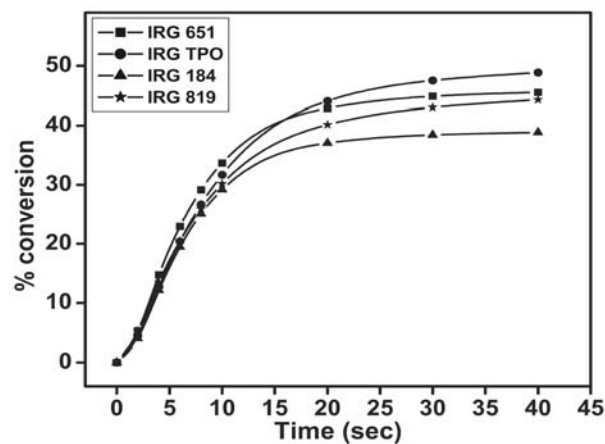
From the above Figures, we can infer that the system may be following either model for a short time during the course of polymerization. But the value of constants obtained cannot be considered. The system showed very low rate of polymerization and final conversions. The cure curve showed a short peak and did not reach the baseline during deceleration step [Figure 4.53(C)]. The rate and conversion profiles were calculated by taking the baseline at the inflection region and are represented in Figure 4.51 and 4.52 (A-C). Here, the deceleration step was found to be very low which resulted in very low conversions.

The rate and conversion profiles obtained from photocuring studies of the macromonomeric formulation containing 10 wt% of NPGPDA as crosslinker with four photoinitiators at 0.5 and 2 wt% compositions at 30 and 50 °C are given below in Figures 4.54 to 4.57 (A-C).

(A)



(B)



(C)

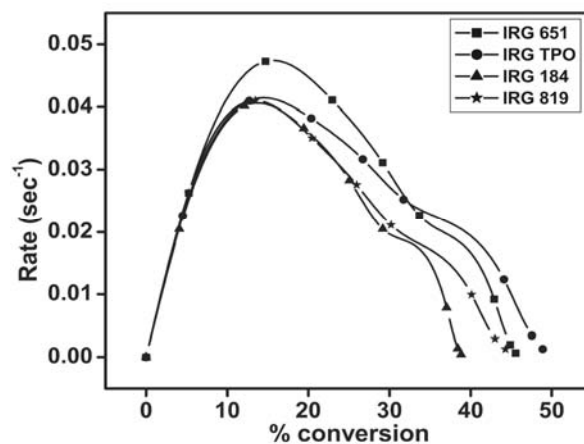
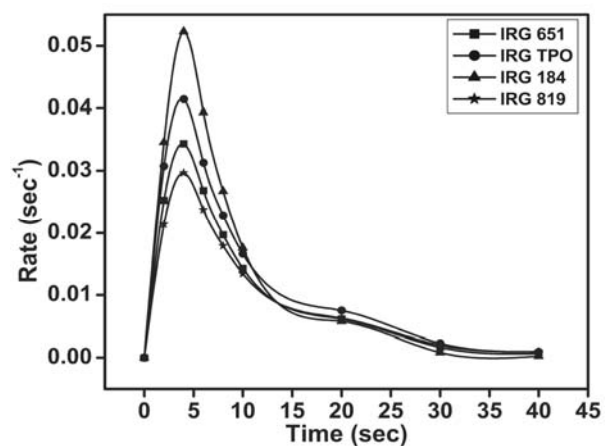
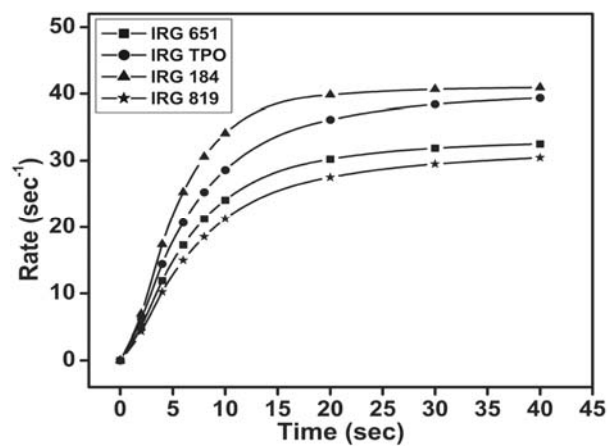


Figure 4.54(A-C) Time dependent rate and conversion profiles of macromonomeric formulations containing 10 wt% NPGPDA and 0.5 wt% of four photoinitiators with respect to weight of macromonomer at 30 °C

(A)



(B)



(C)

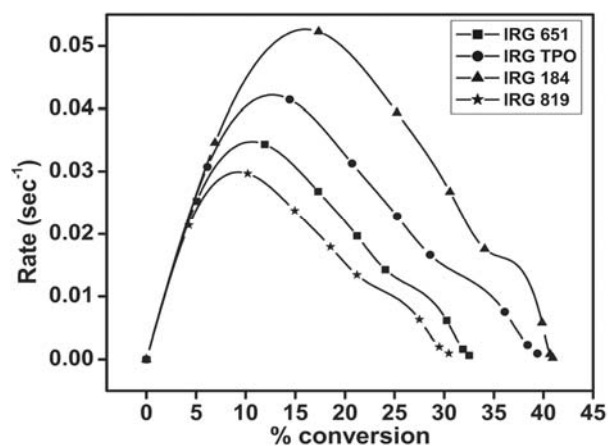
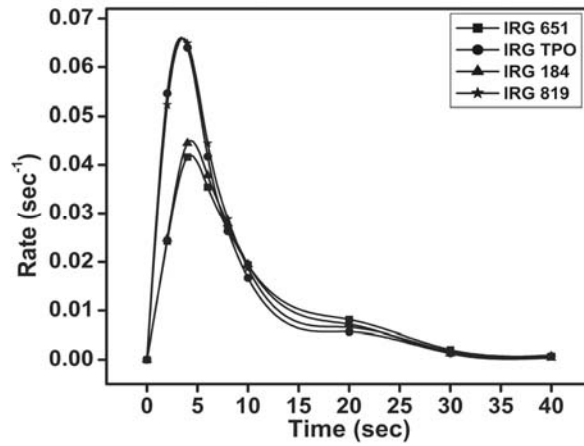
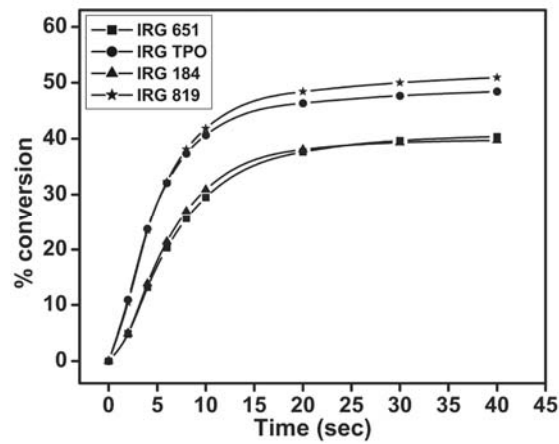


Figure 4.55(A-C) Time dependent rate and conversion profiles of macromonomeric formulations containing 10 wt% NPGPDA and 2 wt% of four photoinitiators with respect to weight of macromonomer at 30 °C

(A)



(B)



(C)

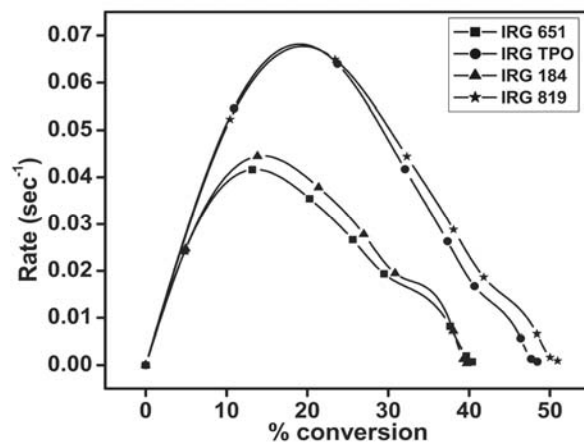
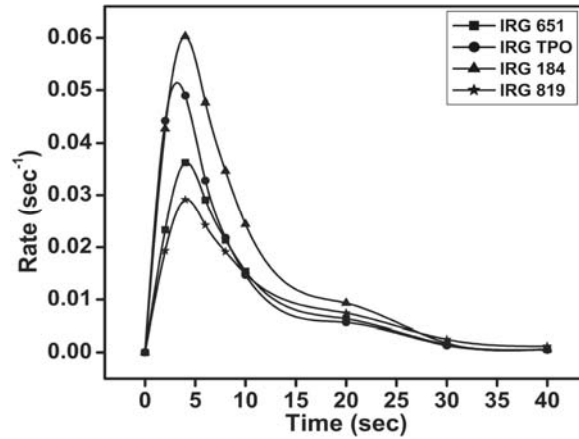
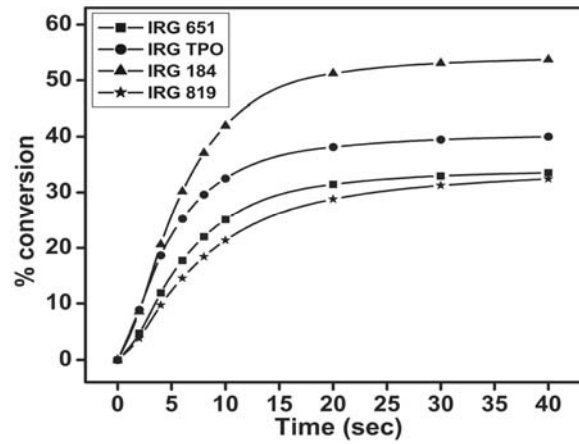


Figure 4.56(A-C) Time dependent rate and conversion profiles of macromonomeric formulations containing 10 wt% NPGPDA and 0.5 wt% of four photoinitiators with respect to weight of macromonomer at 50 °C

(A)



(B)



(C)

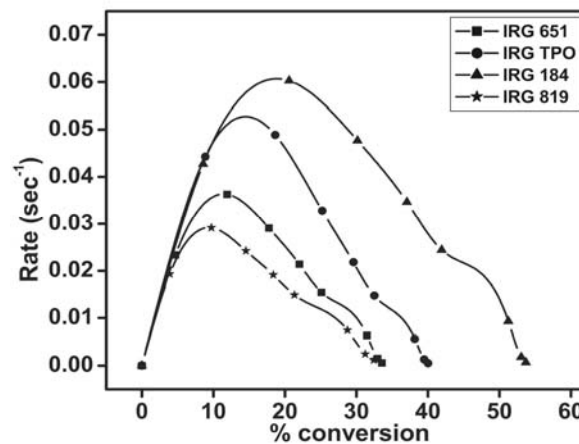


Figure 4.57(A-C) Time dependent rate and conversion profiles of macromonomeric formulations containing 10 wt% NPGPDA and 2 wt% of four photoinitiators with respect to weight of macromonomer at 50 °C

The kinetic parameters calculated are given in Tables 4.25 and 4.26.

Table 4.25 Kinetic parameters of macromonomeric formulations calculated from the heat flow profiles containing 10 wt% of NPGPDA

Photo Initiator	% conc. of photo-initiator	Temp (°C)	Induction Time (sec)	Peak Maximum Time (sec)	$R_p \text{ max}$ ($\times 10^{-2}$) (sec^{-1})	C_{max} (%)	Heat of reaction (J/g)
IRGACURE 651	0.5	30	0.48	4.36	4.79	45.97	37.56
	2	30	0.44	3.81	3.44	33.62	27.47
	0.5	50	0.51	4.31	4.20	41.70	34.07
	2	50	0.51	4.09	3.63	34.86	28.48
DAROCUR TPO	0.5	30	0.56	4.54	4.20	54.39	44.44
	2	30	0.36	3.84	4.16	42.18	34.46
	0.5	50	0.28	3.37	6.61	54.13	44.23
	2	50	0.36	3.17	5.15	41.64	34.02
IRGACURE 184	0.5	30	0.64	4.54	4.12	39.96	32.65
	2	30	0.34	4.04	5.23	41.44	33.86
	0.5	50	0.51	4.32	4.51	40.63	33.20
	2	50	0.41	3.99	6.02	55.76	45.56
IRGACURE 819	0.5	30	0.45	4.23	4.12	49.18	40.18
	2	30	0.52	3.97	2.98	34.92	28.53
	0.5	50	0.30	3.57	6.60	55.41	45.27
	2	50	0.60	4.07	2.92	37.07	30.29

Table 4.26 Evaluation of kinetic parameters of macromonomeric formulations as per autocatalytic model at 30 and 50 °C containing 10 wt% of NPGPDA

Photo Initiator	% conc. of photo-initiator	Temperature (°C)	Autocatalytic		
			n	m	k (min^{-1})
IRGACURE 651	0.5	30	5.42	0.58	20
	0.5	50	6.52	0.59	20.2
	2	30	9.14	0.60	21.7
	2	50	8.30	0.57	19.6
DAROCUR TPO	0.5	30	5.03	0.57	16.5
	0.5	50	6.20	0.69	44.5
	2	30	7.42	0.55	20.4
	2	50	7.21	0.57	27.2
IRGACURE 184	0.5	30	6.11	0.58	18.3
	0.5	50	7.10	0.70	30.4
	2	30	6.48	0.65	30
	2	50	4.16	0.51	19.5
IRGACURE 819	0.5	30	6.20	0.59	19.6
	0.5	50	5.67	0.68	39.7
	2	30	11.6	0.71	30.2
	2	50	9.99	0.63	21.1

From Table 4.25, for most of the formulations, the induction time and peak maximum time was found to decrease with increase in temperature at similar concentration of photoinitiator as well as with increase in concentration of photoinitiator at the same temperature. An increase in temperature from 30 to 50 °C results in a reduction of induction time showing that the system has either enhanced radical diffusion or a reduction in initial viscosity with increase in temperature.^{12,15} DAROCUR TPO showed the fastest initiation with NPGPDA as reactive diluent in the formulation. At higher temperature, an increase in induction time was observed by formulations containing 0.5 and 2 wt% of IRGACURE 651 and 2 wt% of IRGACURE 184 and IRGACURE 819. The concentration of active species in the above formulations are above the optimum value, which accounts for the increase in induction time due to reduced quantum yield for photo initiation.¹⁷ A more consistent increase in the value of $R_{p \text{ max}}$ with increase in temperature was observed against the non consistent behaviour shown by macromonomeric formulation without NPGPDA. This behaviour is shown due to plasticization effect caused by the reactive diluent.³⁰ The variations such as decrease in the value of $R_{p \text{ max}}$ with increase in concentration of photoinitiator at a particular temperature can be due to the influence of opposing factors such as reaction diffusion and diffusion of radical/ propagating chains.^{12,14,15} The final conversion with diacrylate varied from 33 to 56% against 5 to 18% for the macromonomeric system without diacrylate. The variations in final conversion with temperature and concentration may be due to the effect of competing factors which slows down and terminates the system in the deceleration step as explained before.^{22,23}

The photopolymerizations were carried out using polychromatic radiation (250-450 nm). As expected the lowest induction time and peak maximum was observed for DAROCUR TPO at 50°C due to enhanced mobility.³⁴ Since the λ_{max} of $\pi - \pi^*$ transition for IRGACURE 651 falls within the range of analysis than that of IRGACURE 184, a lower induction time is expected for IRGACURE 651.^{1,26}

From Table 4.26, we can infer that the photopolymerization rate fits to variable autocatalytic kinetic model over a wide range in the cure profile as the values of m being constant with much larger variations for n .^{18,28} The photopolymerization of the macromonomer with added NPGPDA is autoaccelerating during photo initiation reaction

and hence was found to follow the autocatalytic model. The heat evolved during the end of polymerization is due to crosslinking reactions. For similar compositions, the value of specific rate constant (k) can be expected to increase with an increase in temperature, if the system follows autocatalytic kinetics to high levels of achieved conversions. An increase in temperature did not show a consistent behaviour in increased value of k , showing partial autocatalytic behaviour.^{18,29} The increase in photoinitiator concentration at 30 °C resulted in reduction in value of k while a decrease was observed at 50 °C.

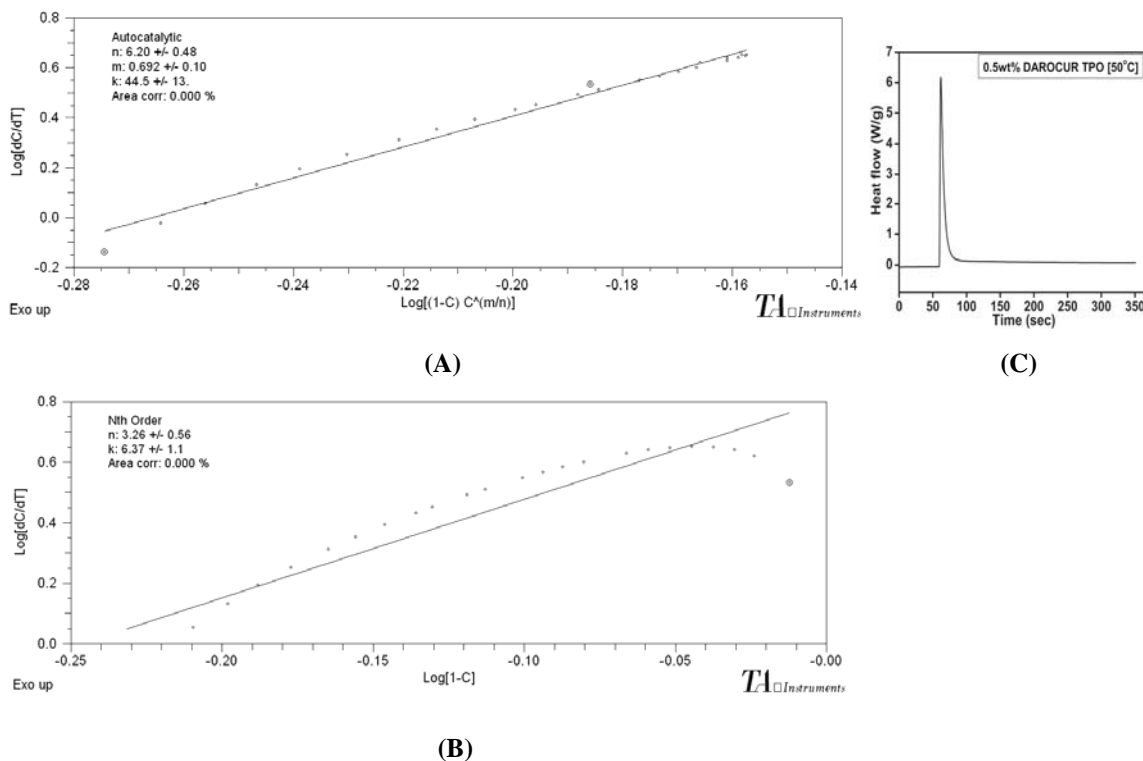


Figure 4.58(A-C) Better fit for the autocatalytic model and deviated nature of n^{th} order model (A-B) and the corresponding heat flow profile (C) for macromonomer containing 10 wt% NPGPDA and 0.5 wt% of DAROCUR TPO at 50 °C

The evaluation of kinetic models for the composition containing the reactive diluent is given in Figure 4.58(A-B). The system obeys autocatalytic model to a great extent, even though the n^{th} order model fails to fit beyond a particular level. The system can be thus assumed to undergo both (n^{th} and autocatalytic) behaviour at various stages of photopolymerization.¹⁸ Unlike the previous case, where photopolymerization was carried out without reactive diluent, this system showed more pronounced autocatalytic

behaviour as observed from consistency in the value of autocatalytic exponent (m). The system can be assumed to undergo both monomolecular and bimolecular terminations.¹⁹

The rate and conversion profiles obtained from photocuring studies of the macromonomeric formulation containing 10wt% of TMPTA as crosslinker with four photoinitiators at 0.5 and 2 wt% compositions at 30 and 50 °C are given below in Figures 4.59 to 4.62 (A-C).

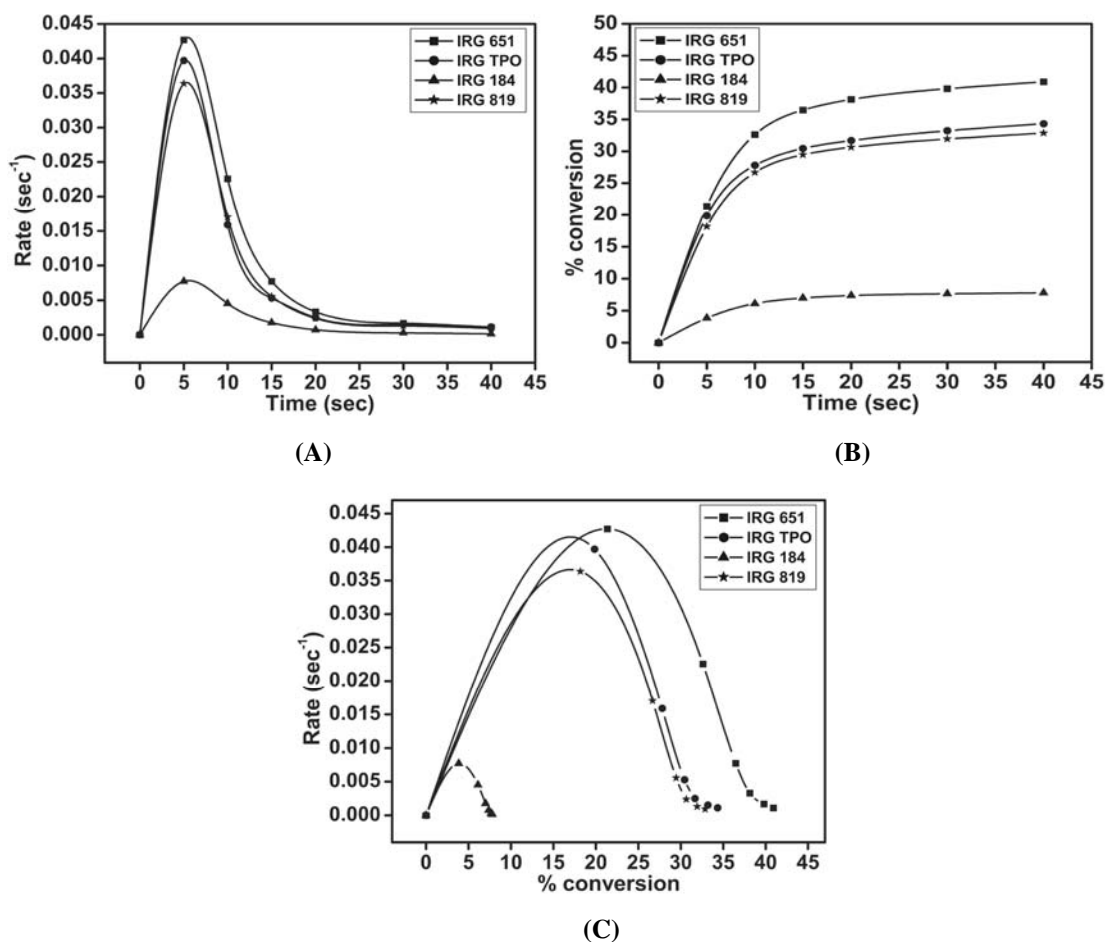
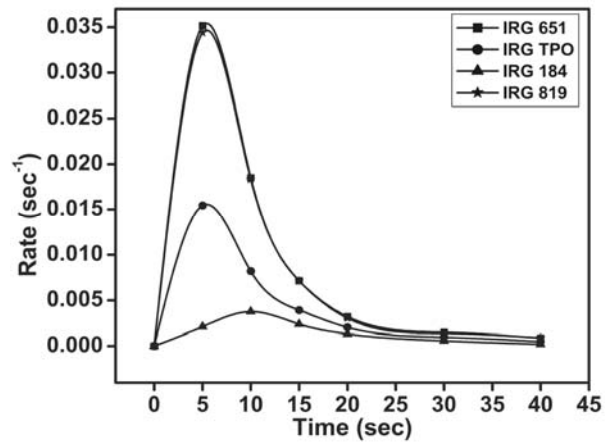
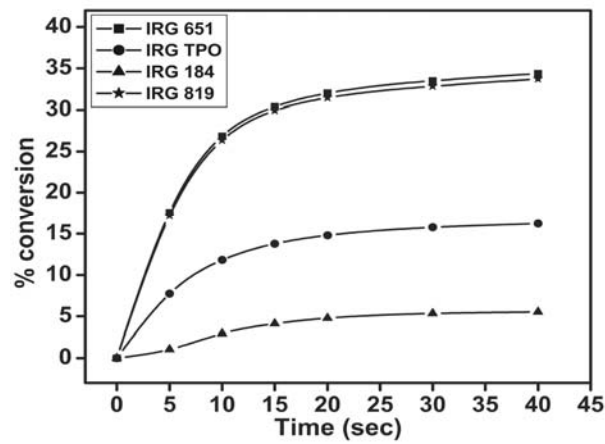


Figure 4.59(A-C) Time dependent rate and conversion profiles of macromonomeric formulations containing 10 wt% TMPTA and 0.5 wt% of four photoinitiators with respect to weight of macromonomer at 30 °C

(A)



(B)



(C)

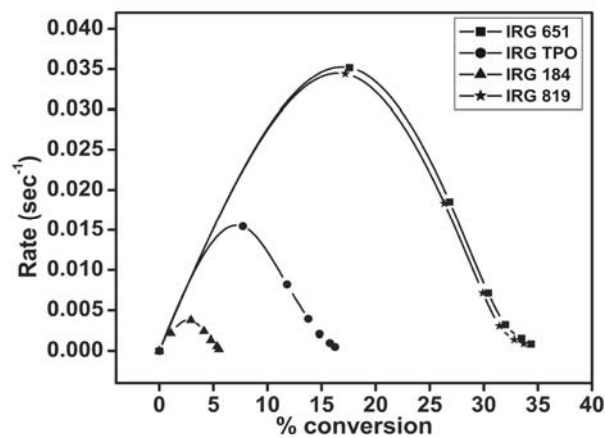
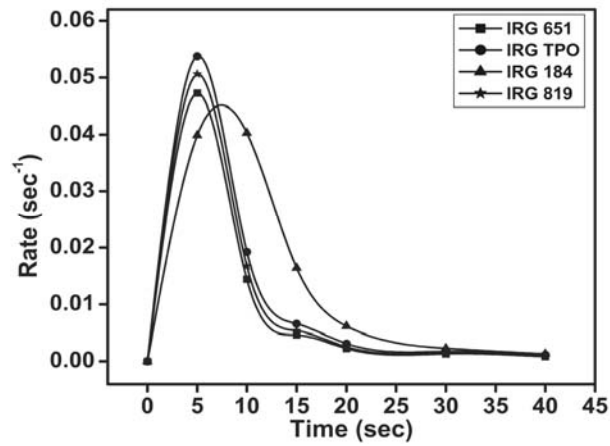
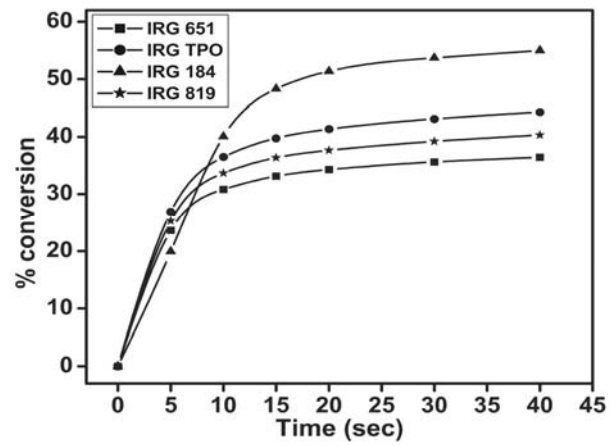


Figure 4.60(A-C) Time dependent rate and conversion profiles of macromonomeric formulations containing 10 wt% TMPTA and 2 wt% of four photoinitiators with respect to weight of macromonomer at 30 °C

(A)



(B)



(C)

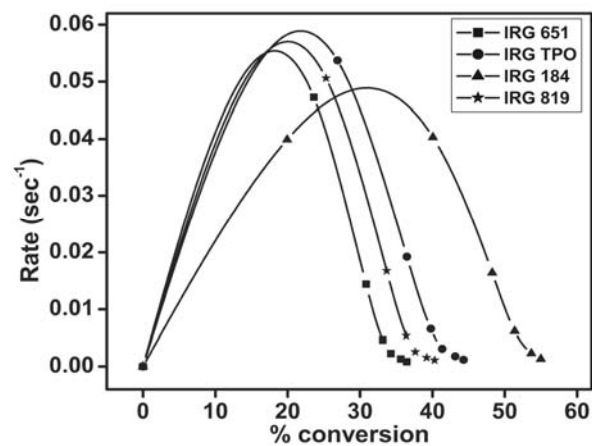


Figure 4.61(A-C) Time dependent rate and conversion profiles of macromonomeric formulations containing 10 wt% TMPTA and 0.5 wt% of four photoinitiators with respect to weight of macromonomer at 50 °C

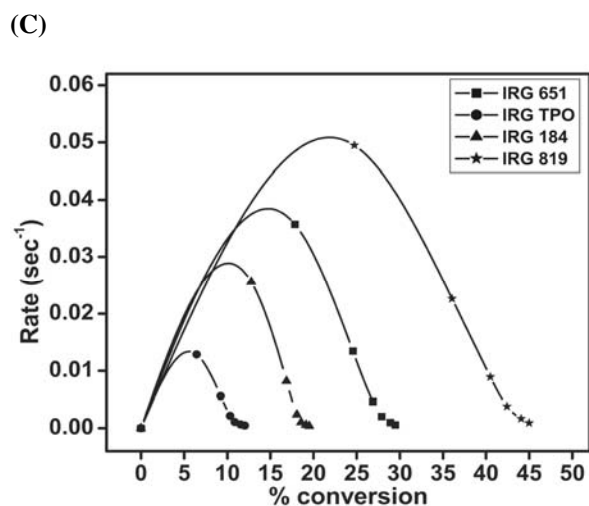
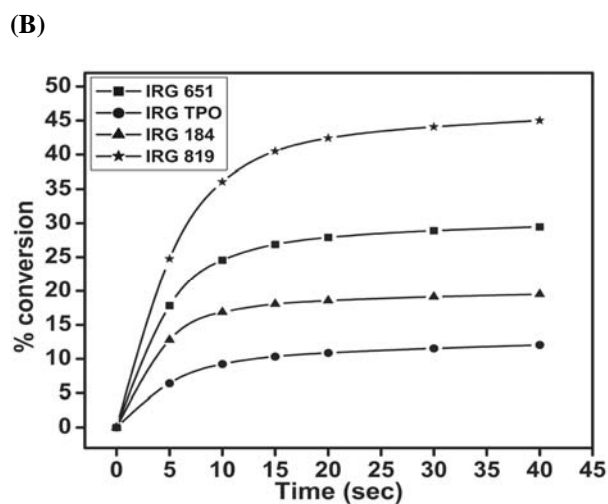
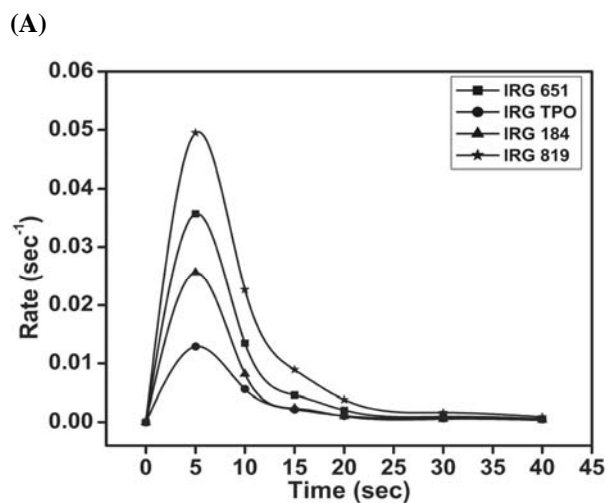


Figure 4.62(A-C) Time dependent rate and conversion profiles of macromonomeric formulations containing 10 wt% TMPTA and 2 wt% of four photoinitiators with respect to weight of macromonomer at 50 °C

The kinetic parameters calculated are given in Tables 4.27 and 4.28.

Table 4.27 Kinetic parameters of macromonomeric formulations calculated from the heat flow profiles containing 10 wt% of TMPTA

Photo Initiator	% conc. of photo-initiator	Temp (°C)	Induction Time (sec)	Peak Maximum Time (sec)	$R_p \text{ max}$ ($\times 10^{-2}$) (sec^{-1})	C_{max} (%)	Heat of reaction (J/g)
IRGACURE 651	0.5	30	0.23	5.45	4.31	45.55	51.59
	2	30	0.30	5.43	3.55	37.28	42.22
	0.5	50	0.18	5.01	4.73	38.69	43.82
	2	50	0.26	5.11	3.58	31.17	35.30
DAROCUR TPO	0.5	30	0.22	5.20	3.98	40.31	45.65
	2	30	0.59	5.39	1.56	17.62	19.96
	0.5	50	0.16	5.10	5.38	49.36	55.90
	2	50	0.68	5.26	1.30	14.41	16.32
IRGACURE 184	0.5	30	1.19	5.58	0.78	8.14	9.22
	2	30	4.83	10.06	0.37	5.64	6.38
	0.5	50	0.26	7.42	4.52	61.22	69.34
	2	50	0.34	5.07	2.55	20.38	23.08
IRGACURE 819	0.5	30	0.25	5.32	3.65	37.47	42.44
	2	30	0.32	5.45	3.47	39.48	44.72
	0.5	50	0.17	5.02	5.06	44.91	50.87
	2	50	0.26	5.27	4.97	49.47	56.03

Table 4.28 Evaluation of kinetic parameters of macromonomeric formulations as per autocatalytic model at 30 and 50 °C containing 10 wt% of TMPTA

Photo Initiator	% conc. of photo-initiator	Temperature (°C)	Autocatalytic		
			n	m	k (min^{-1})
IRGACURE 651	0.5	30	9.11	0.93	80.5
	0.5	50	12.4	1.12	220
	2	30	9.99	0.74	41.7
	2	50	12.5	0.74	54.5
DAROCUR TPO	0.5	30	14.7	1.21	269
	0.5	50	8.83	0.88	93.5
	2	30	22.8	0.59	20.1
	2	50	50.2	1.22	396
IRGACURE 184	0.5	30	48.9	0.74	30.7
	0.5	50	4.79	0.79	34.9
	2	30	55.4	0.66	9.34
	2	50	24.6	1.11	244
IRGACURE 819	0.5	30	12.5	0.98	108
	0.5	50	9.74	0.84	89.2
	2	30	12.4	0.98	98.5
	2	50	6.41	0.51	25.7

It can be seen from Table 4.27 that the system with triacrylate as reactive diluent showed better plasticization than the diacrylate containing formulations due to low initial

viscosity of triacrylate. Both the induction time and peak maximum time in many cases were found to increase with increase in concentration of photoinitiator in many cases. This showed the attainment of an optimum concentration of photoinitiator even at 0.5 wt% concentration. A decrease in induction as well as peak maximum time with increase in temperature at similar concentration of photoinitiator was observed due to reduced viscosity at higher temperature and better radical mobility and diffusion.^{12,14,15} The $R_{p\ max}$ was found to increase with increase in temperature at similar concentration of photoinitiator showing better volume relaxation occurring at higher isothermal condition during autoacceleration in addition to plasticization effect imparted by the added triacrylate.³⁰ The value of $R_{p\ max}$ at a particular temperature was also found to decrease with increase in concentration of photoinitiator predominantly due to a probable reduction in effective radical concentration at higher concentration of photoinitiator due to radical radical combinations.¹⁷ The final conversions varied from 5 to 62% showing the influence of reaction diffusion soon after $R_{p\ max}$. The autodeceleration step can be assumed to undergo all the competent reactions to different extent.¹⁴ The variations in viscosity build up during the autodeceleration process resulted in the variations in final conversion.¹² It has to be noted that the maximum conversion in the case of TMPTA containing formulation was around 61%, which was slightly higher than that of NPGPDA containing formulation. At the same time the minimum conversion of TMPTA containing formulation was around 5% against 33% for NPGPDA containing formulation.

The analyses were done using polychromatic radiation (250-450 nm). As expected the lowest induction time and peak maximum was observed for DAROCUR TPO. Since the most prominent λ_{max} of $\pi - \pi^*$ transition for IRGACURE 651 falls within the range of analysis than that of IRGACURE 184, a lower induction time is expected for IRGACURE 651.^{1,26}

From Table 4.28, we can infer that the photopolymerization rate fits the autocatalytic kinetic model over a certain range only in the cure profile as the values of m and n showed large variations. A constant value of m was not observed. Still this system can be assumed to obey the autocatalytic equation for a short duration in the entire photopolymerization process better than the macromonomer without any reactive diluents as explained before.

The rate and conversion profiles obtained from photocuring studies of the macromonomeric formulation containing 10 wt% of NPGPDA as crosslinker with 0.006 wt% TEMPO and four photoinitiators at 0.5 and 2 wt% compositions at 30 and 50 °C are given below in Figures 4.63 to 4.66 (A-C).

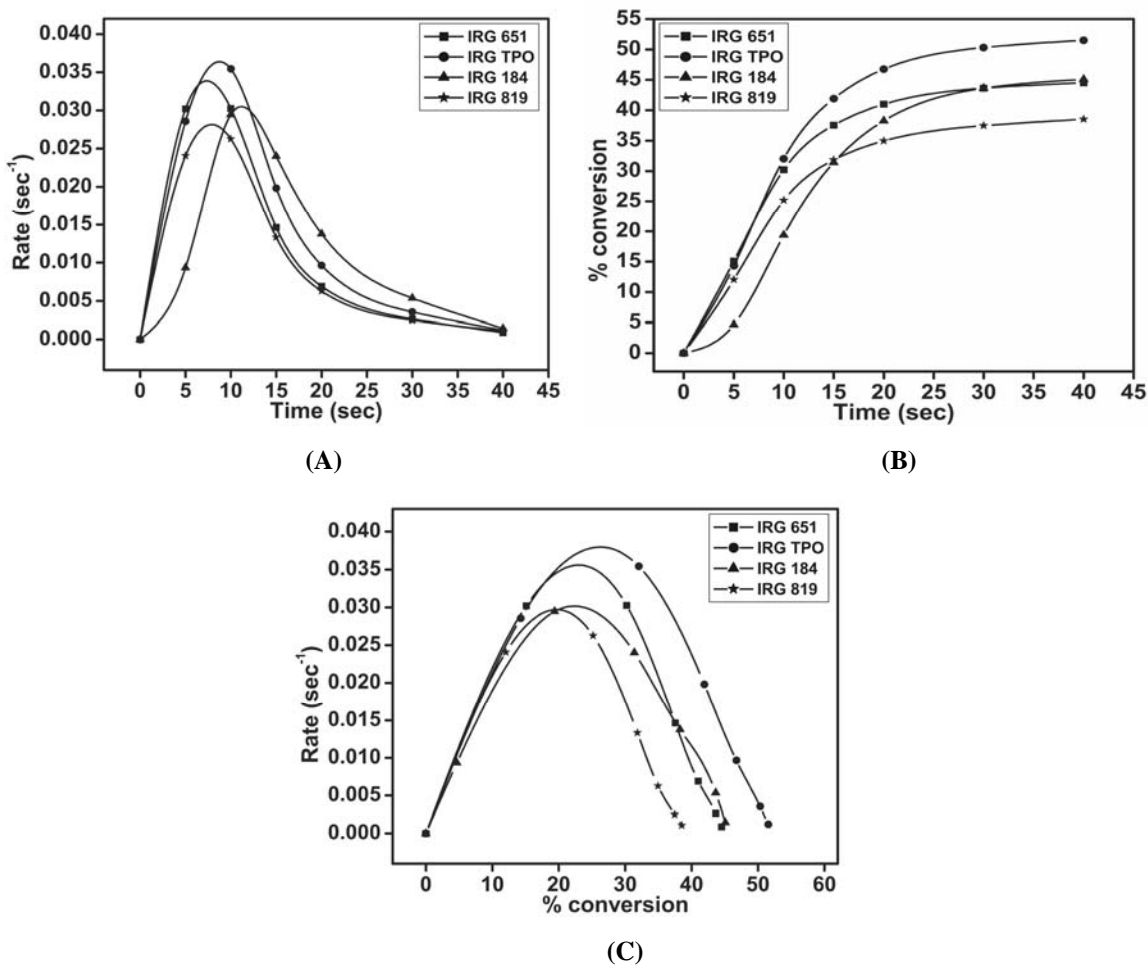
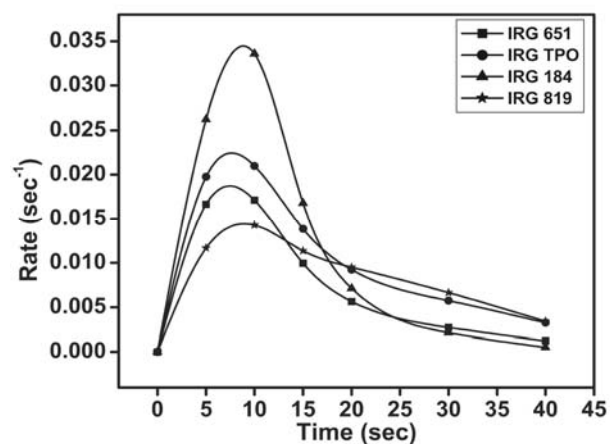
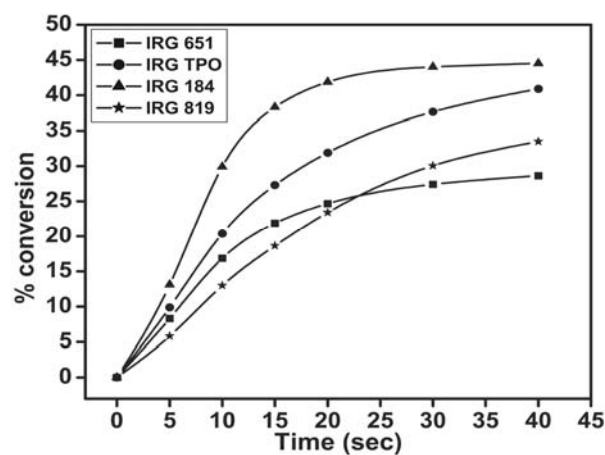


Figure 4.63(A-C) Time dependent rate and conversion profiles of macromonomeric formulations containing 10 wt% NPGPDA, 0.006 wt% TEMPO and 0.5 wt% of four photoinitiators with respect to weight of macromonomer at 30 °C

(A)



(B)



(C)

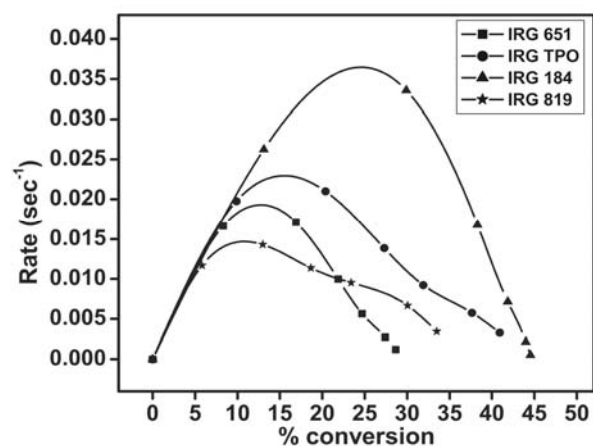
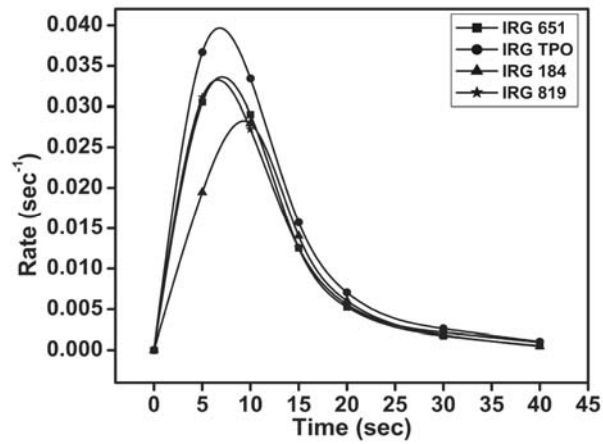
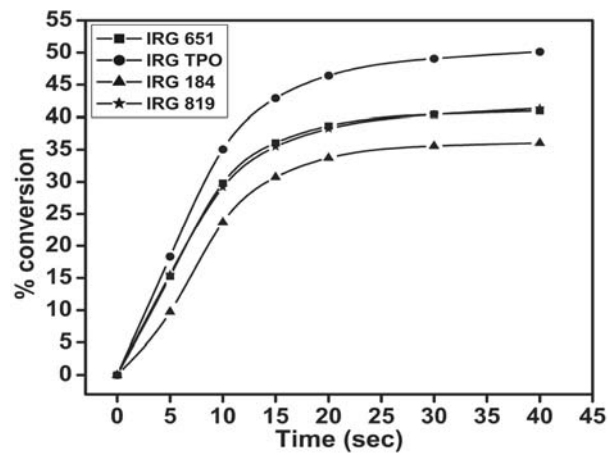


Figure 4.64(A-C) Time dependent rate and conversion profiles of macromonomeric formulations containing 10 wt% NPGPDA, 0.006 wt% TEMPO and 2 wt% of four photoinitiators with respect to weight of macromonomer at 30 °C

(A)



(B)



(C)

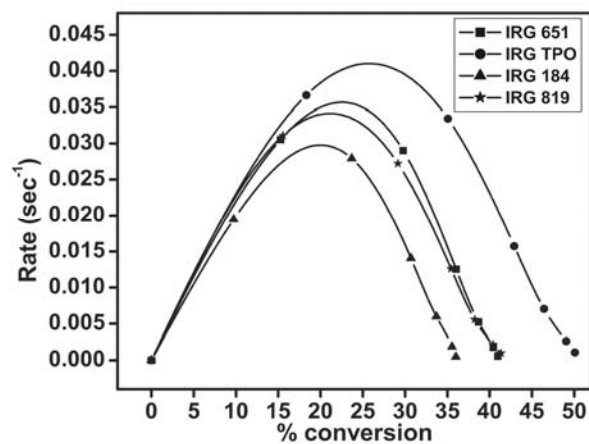


Figure 4.65(A-C) Time dependent rate and conversion profiles of macromonomeric formulations containing 10 wt% NPGPDA, 0.006 wt% TEMPO and 0.5 wt% of four photoinitiators with respect to weight of macromonomer at 50 °C

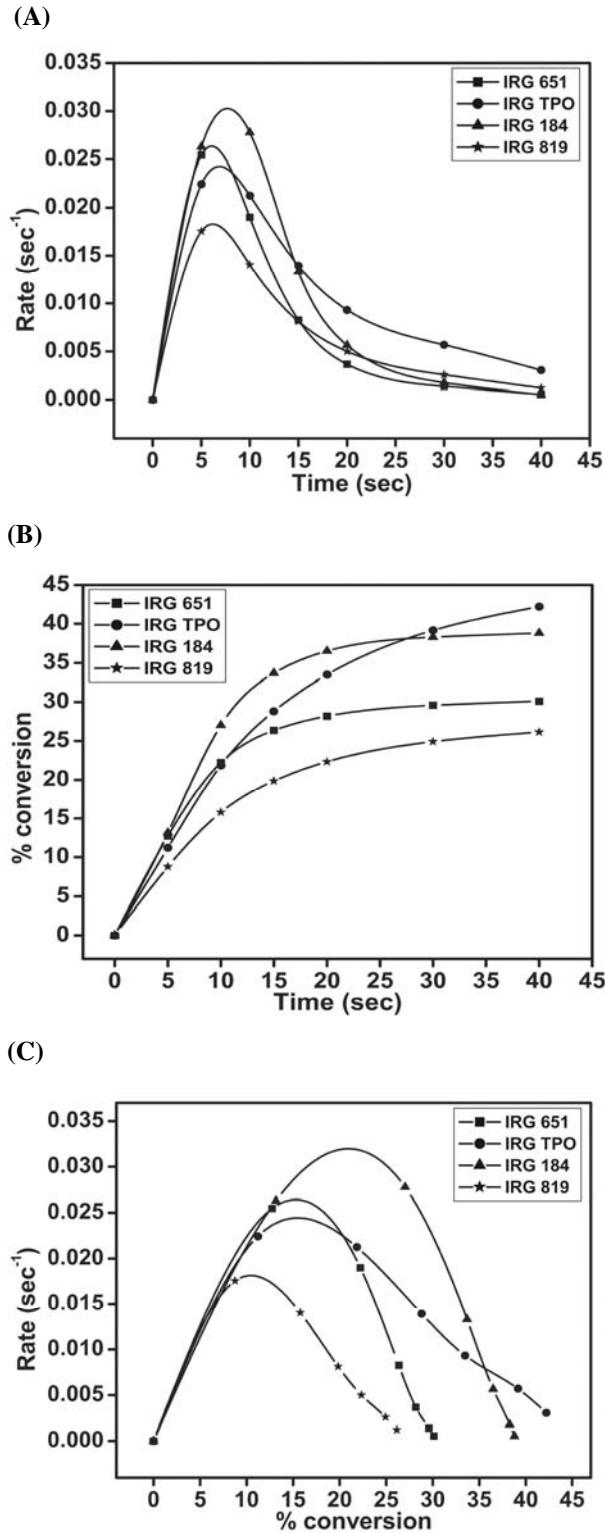


Figure 4.66(A-C) Time dependent rate and conversion profiles of macromonomeric formulations containing 10 wt% NPGPDA, 0.006 wt% TEMPO and 2 wt% of four photoinitiators with respect to weight of macromonomer at 50 °C

The kinetic parameters calculated are given in Tables 4.29 and 4.30.

Table 4.29 Kinetic parameters of macromonomeric formulations calculated from the heat flow profiles containing 10 wt% of NPGPDA and 0.006 wt% TEMPO

Photo Initiator	% conc. of photo-initiator	Temp (°C)	Induction Time (sec)	Peak Maximum Time (sec)	$R_p \text{ max}$ ($\times 10^{-2}$) (sec^{-1})	C_{max} (%)	Heat of reaction (J/g)
IRGACURE 651	0.5	30	0.34	7.35	3.39	45.37	37.07
	2	30	0.62	7.50	1.89	30.66	25.05
	0.5	50	0.33	7.10	3.37	41.81	34.16
	2	50	0.37	6.05	2.64	31.5	25.74
DAROCUR TPO	0.5	30	0.38	8.75	3.64	56.40	46.08
	2	30	0.52	7.64	2.25	45.31	37.02
	0.5	50	0.26	6.84	3.97	55.68	45.49
	2	50	0.45	6.83	2.43	47.46	38.78
IRGACURE 184	0.5	30	2.10	11.18	3.05	46.96	38.37
	2	30	0.42	8.88	3.45	45.44	37.13
	0.5	50	0.60	9.37	2.82	36.55	29.86
	2	50	0.41	7.70	3.03	39.75	32.48
IRGACURE 819	0.5	30	0.44	7.88	2.83	43.03	35.16
	2	30	0.91	8.94	1.44	40.32	32.94
	0.5	50	0.31	6.58	3.33	45.03	36.79
	2	50	0.55	6.22	1.83	30.57	24.98

Table 4.30 Evaluation of kinetic parameters of macromonomeric formulations as per autocatalytic model at 30 and 50 °C containing 10 wt% of NPGPDA and 0.006 wt% TEMPO

Photo Initiator	% conc. of photo-initiator	Temperature (°C)	Autocatalytic		
			n	m	k (min^{-1})
IRGACURE 651	0.5	30	5.89	0.63	21.4
	0.5	50	6.25	0.63	22.3
	2	30	10.3	0.6	14.5
	2	50	9.48	0.60	20
DAROCUR TPO	0.5	30	4.41	0.61	16.8
	0.5	50	5.09	0.64	22.7
	2	30	6.13	0.46	8.52
	2	50	5.72	0.42	7.74
IRGACURE 184	0.5	30	5.07	0.73	17.2
	0.5	50	7.02	0.71	22.1
	2	30	4.97	0.62	17.8
	2	50	6.27	0.64	19.4
IRGACURE 819	0.5	30	7.48	0.71	24.3
	0.5	50	6.64	0.69	24.4
	2	30	5.08	0.27	2.74
	2	50	13.3	0.64	18.7

As observed from Table 4.29, it can be inferred that the system was found to undergo better radical diffusion and radical radical combination due to low initial

viscosity and plasticization effect.³⁰ Comparing with diacrylate composition without TEMPO (Table 4.25), the quantum yield for initiation is not affected by the addition of radical scavenger. This can be understood by noting the induction times in Table 4.25 and 4.29. But the system showed reduction in $R_{p \text{ max}}$ on addition of radical scavenger. This shows that the system has an enhancement in scavenging action only after autoacceleration. The terminations are higher momentarily after autoacceleration and the scavenging effect is much pronounced during the subsequent volume relaxation, which accounts for the reduction in $R_{p \text{ max}}$. The influence of this effect at $R_{p \text{ max}}$ is further enhanced by the fact that the initiations are much controlled and hence the viscosity build up is not as high to prevent the scavenging radical from undergoing high level of terminations. The evaluation of autocatalytic model is given in Table 4.30. The enhanced terminations occurring near $R_{p \text{ max}}$ resulted in a gradual reaction diffusion, which helped the system to fit the autocatalytic model to better.

The rate and conversion profiles obtained from photocuring studies of the macromonomeric formulation containing 10 wt% of TMPTA as crosslinker with 0.012 wt% TEMPO and four photoinitiators at 0.5 and 2 wt% compositions at 30 and 50 °C are given below in Figures 4.67 to 4.70 (A-C).

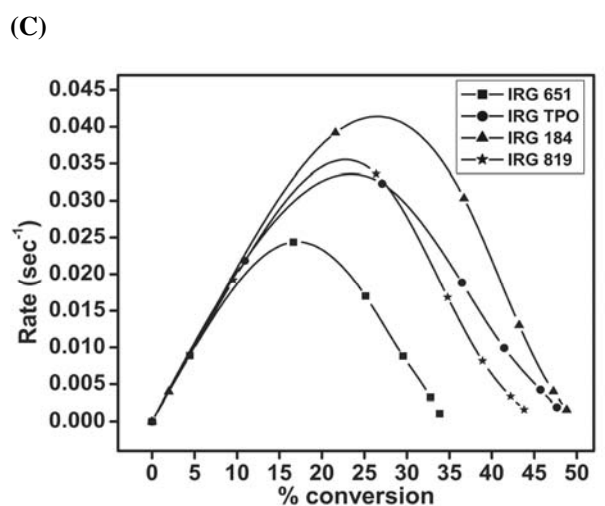
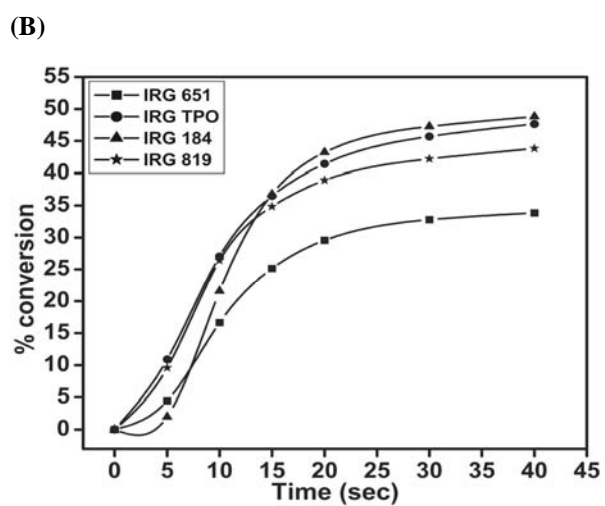
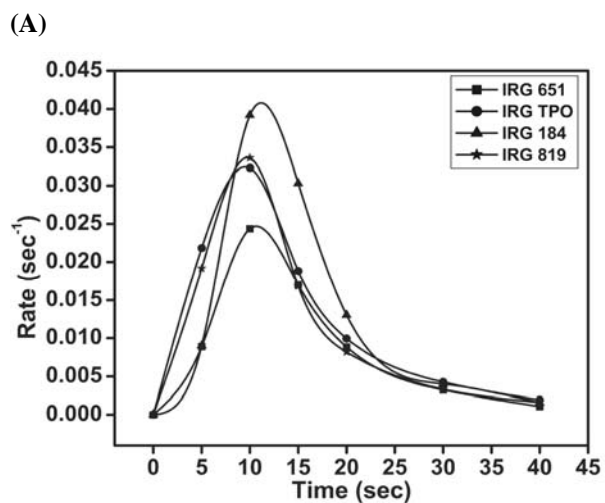


Figure 4.67(A-C) Time dependent rate and conversion profiles of macromonomeric formulations containing 10 wt% TMPTA, 0.012 wt% TEMPO and 0.5 wt% of four photoinitiators with respect to weight of macromonomer at 30 °C

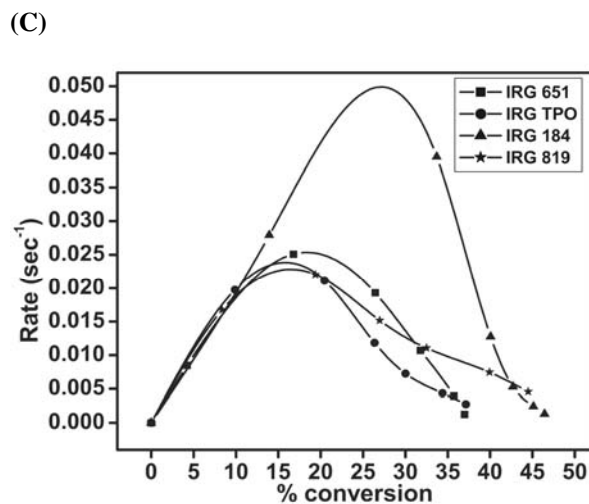
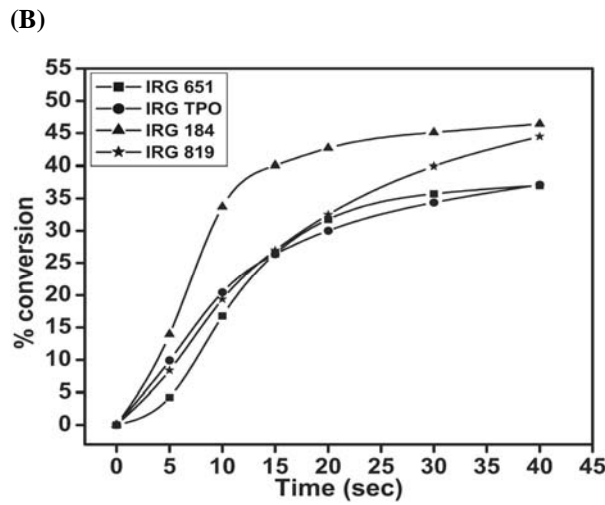
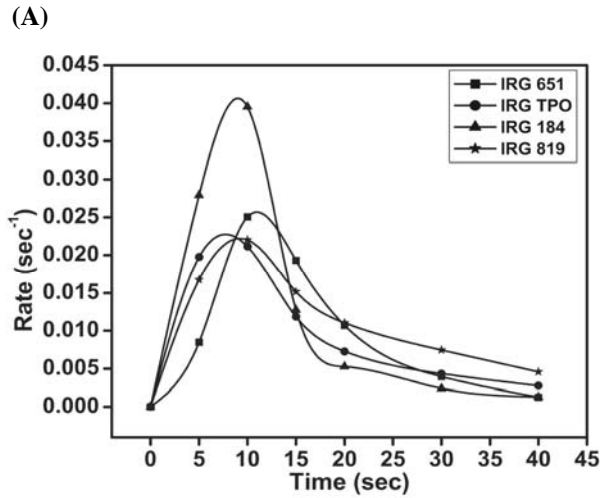


Figure 4.68(A-C) Time dependent rate and conversion profiles of macromonomeric formulations containing 10 wt% TMPTA, 0.012 wt% TEMPO and 2 wt% of four photoinitiators with respect to weight of macromonomer at 30 °C

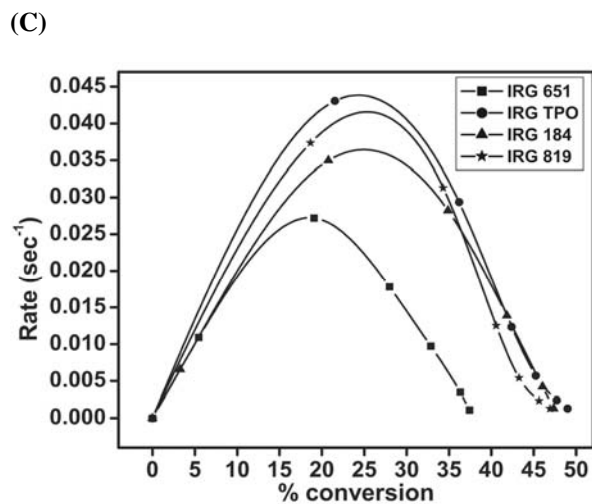
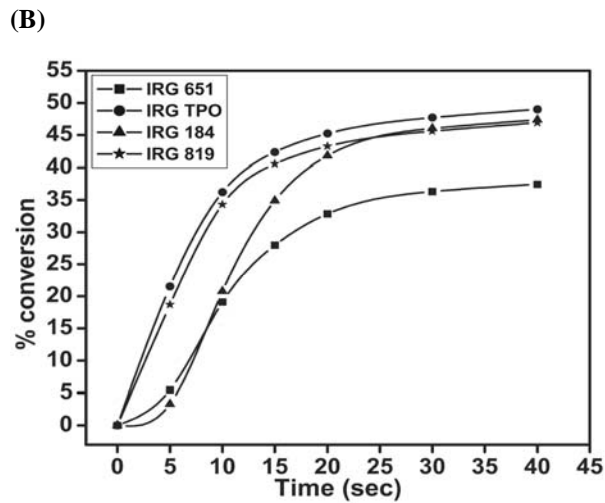
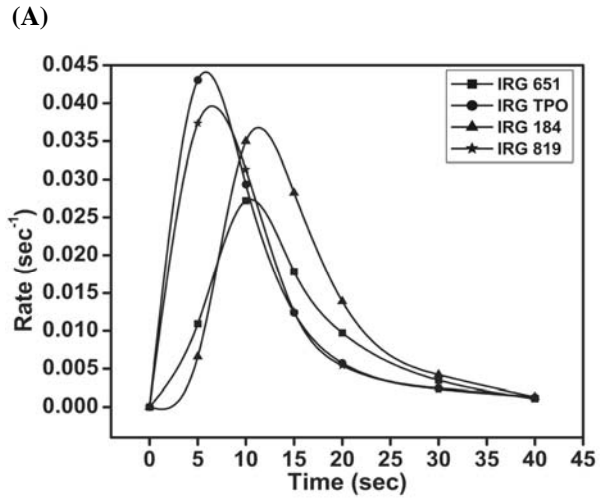
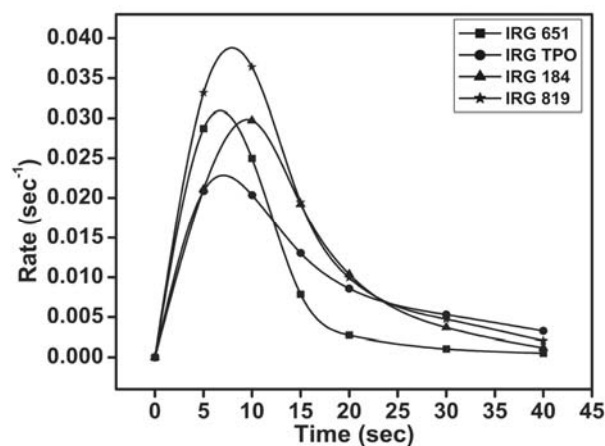
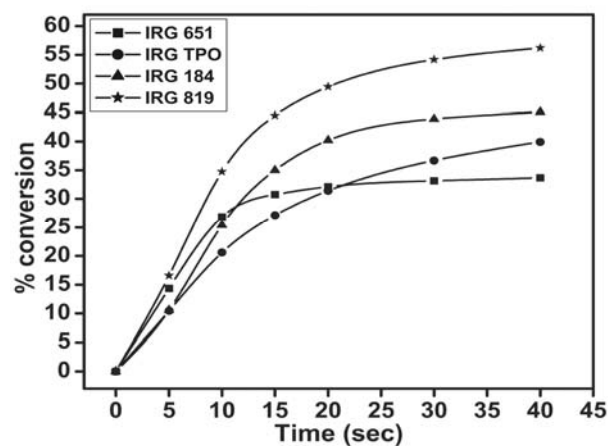


Figure 4.69(A-C) Time dependent rate and conversion profiles of macromonomeric formulations containing 10 wt% TMPTA, 0.012 wt% TEMPO and 0.5 wt% of four photoinitiators with respect to weight of macromonomer at 50 °C

(A)



(B)



(C)

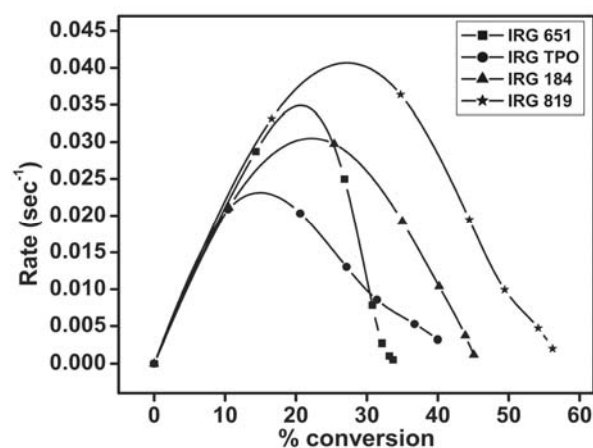


Figure 4.70(A-C) Time dependent rate and conversion profiles of macromonomeric formulations containing 10 wt% TMPTA, 0.012 wt% TEMPO and 2 wt% of four photoinitiators with respect to weight of macromonomer at 50 °C

The kinetic parameters calculated are given in Tables 4.31 and 4.32.

Table 4.31 Kinetic parameters of macromonomeric formulations calculated from the heat flow profiles containing 10 wt% of TMPTA and 0.012 wt% TEMPO

Photo Initiator	% conc. of photo-initiator	Temp (°C)	Induction Time (sec)	Peak Maximum Time (sec)	$R_{p \text{ max}}$ ($\times 10^{-2}$) (sec^{-1})	C_{max} (%)	Heat of reaction (J/g)
IRGACURE 651	0.5	30	1.99	10.68	2.46	36.77	41.65
	2	30	2.15	10.97	2.57	40.84	46.26
	0.5	50	1.53	10.49	2.74	39.93	45.23
	2	50	0.34	6.72	3.09	33.39	37.82
DAROCUR TPO	0.5	30	0.55	9.52	3.24	56.60	64.11
	2	30	0.54	7.69	2.28	49.42	55.97
	0.5	50	0.20	5.83	4.42	53.96	61.11
	2	50	0.47	7.08	2.30	48.39	54.81
IRGACURE 184	0.5	30	3.87	11.15	4.08	55.22	62.54
	2	30	0.43	9.03	4.07	50.1	56.74
	0.5	50	3.61	11.33	3.68	50.96	57.72
	2	50	0.54	9.52	2.98	47.71	54.04
IRGACURE 819	0.5	30	0.70	9.70	3.37	51.47	58.29
	2	30	0.66	9.25	2.24	55.79	63.19
	0.5	50	0.30	6.50	3.96	51.99	58.88
	2	50	0.31	7.93	3.88	62.06	70.29

Table 4.32 Evaluation of kinetic parameters of macromonomeric formulations as per autocatalytic model at 30 and 50 °C containing 10 wt% of TMPTA and 0.012 wt% TEMPO

Photo Initiator	% conc. of photo-initiator	Temperature (°C)	Autocatalytic		
			n	m	k (min^{-1})
IRGACURE 651	0.5	30	7.26	0.62	14.3
	0.5	50	6.31	0.58	13.3
	2	30	6.43	0.65	14.3
	2	50	8.95	0.79	43.5
DAROCUR TPO	0.5	30	6.99	0.90	41.9
	0.5	50	6.70	0.73	44.5
	2	30	9.57	0.75	26.5
	2	50	6.80	0.46	9.34
IRGACURE 184	0.5	30	6.10	0.96	48
	0.5	50	4.69	0.70	19
	2	30	8.33	1.12	124
	2	50	4.12	0.39	8.12
IRGACURE 819	0.5	30	8.22	1.02	64.3
	0.5	50	7.67	0.97	75.9
	2	30	4.69	0.31	5
	2	50	4.46	0.64	19.9

As can be seen from Table 4.31, we can find that the system was found to undergo simultaneous radical diffusion and radical radical combination in the initial

stages due to low initial viscosity and plasticization effect.³⁰ The radical scavenging action of TEMPO during initiation was observed.³⁵ These formulations also had negligible effect on induction time while reduction in peak maximum time was observed on addition of TEMPO which confirms that the scavenging effect is much pronounced soon after autoacceleration.

The evaluation of autocatalytic model is given in Table 4.32. The system showed better extent of autocatalytic behaviour as the value of m and n was more consistent as compared to the macromonomeric formulation containing TMPTA without TEMPO (Table 4.28). The shift in peak maximum time created by the scavenging action of TEMPO (as evident from Table 4.27 and 4.31) has resulted in a better autocatalytic behaviour by delaying the time to attain $R_{p \text{ max}}$.

4.1.2 Conclusions

Photopolymerization of oligomers synthesized in the presence of reactive diluents and photoinitiators of various classes were carried out. The synthesized oligomers were based on urethane di(meth)acrylates possessing aliphatic and cycloaliphatic backbone. Photopolymerization was carried out with polychromatic radiation at isothermal conditions and varying photoinitiator concentrations under a constant nitrogen purge. The addition of reactive diluents decreased the viscosity as well as increased the density of reactive sites in the formulations. As a result, the photopolymerization took place in an efficient manner with high conversions in certain cases. High conversions were observed with flexible oligomers having long chain ethyleneoxy and propyleneoxy linkages with selected irradiation intensities.^{14,21,25} The low molecular mass urethane dimethacrylate was found to show high conversions due to a steady segmental diffusion, autoacceleration and volume relaxation followed radical and reaction diffusions occurring during the deceleration step.

In the presence of 15 wt% of HEMA as reactive diluent with high molecular weight propyleneoxy linkages in the backbone of methacrylate macromonomer, it was observed that the final conversions at 21.1 mW/cm^2 with 250-450 nm polychromatic radiation were higher than that of diacrylates with HEA as reactive diluent. With an irradiation range of 250-450 nm, the formulations with 15 wt% and 10 wt% of HEA

evaluated with a respective intensity of 20.2 and 22.1 mW/cm² showed comparable final conversions.

In the presence of reactive diluent (30 wt% of HEMA) and 250-450 nm radiation, oligomers containing polybutadiene moieties under analyses intensities of 23.7 and 25.2 mW/cm² showed consistency in the value of final cure. This shows better radical and reaction diffusion occurring for these formulations after autoacceleration. The volume relaxation occurring soon after autoacceleration helped these systems to undergo enhancement in diffusion processes such as segmental and reaction diffusions. However, in the absence of reactive diluents and high energy radiation below 320 nm, oligomers containing polybutadiene moiety in the backbone showed large variations in conversions at low intensity of 2.14 mW/cm².

It was found that photopolymerization occurred efficiently in presence of reactive diluents, even from a low intensity of 4.6 mW/cm². It was found that the addition of crosslinker increased the final conversion while the addition of radical scavenger increased the induction time or in other words slows down the photo initiation process by undergoing rapid terminations.

The efficacies of variable autocatalytic kinetic model on photopolymerization processes were studied using TA advantage specialty library software. The model takes into account of the heat flow profiles signal from onset of initiation to the onset of vitrification. It was observed that in many cases the value of autocatalytic exponent (m) is closer to the ideal value of 0.5 observed in the case of amine assisted epoxy/anhydride cure reactions.³⁶ The value of specific rate constant (k) was inconsistent with an increase in temperature.

4.1.3 References

- [1] I. Reetz, Y. Yagci, M.K. Mishra., *Photoinitiated radical vinyl polymerization (Chap. 7). In - Handbook of radical vinyl polymerization (M.K. Mishra and Y. Yagci Ed.)*, Marcel Decker Inc. NY (1998).
- [2] *Photoinitiators for UV curing – Key products selection guide*, Ciba Speciality Chemicals Inc., Switzerland.
- [3] *Novacure®2100 - Ultraviolet/visible spot curing system – manual*, EXFO Photonic Solutions, Mississauga, Canada.
- [4] I.V. Khudyakov, J.C. Legg, M.B. Purvis, B.J. Overton., *Ind. Eng. Chem. Res.* **38**, 3353 (1999).
- [5] S.R. Sauerbrunn., *RadTech'88-North American conference proceedings, New Orleans*, 24-28 April, 219 (1988).
- [6] S.R. Sauerbrunn, D.C. Armbruster, P.D. Shickel., *Differential photocalorimetry: Advancements for the analysis and characterization of free radical, cationic and hybrid photopolymers. Thermal analysis and rheology application library*, TA instruments, U.S.A.
- [7] K.S. Anseth, C.M. Wang, C.N. Bowman., *Polymer* **35**, 3243 (1994).
- [8] J.E. Mark., *Calorimetric analysis of UV curable systems. UV curing science and technology*, Tech Market Corporation, New York 133 (1980).
- [9] J.E. Moore., *Photopolymerization of multifunctional acrylate and methacrylates. In - chemistry and properties of crosslinked polymers, (S.S Labana Ed.) Academic press, New York* 535 (1977).
- [10] J. Sestak, G. Berggren., *Thermochim. Acta* **3**, 1 (1971).
- [11] M.R. Keenan., *J. Appl. Polym. Sci.* **33**, 1725 (1987).
- [12] E. Andrzejewska., *Prog. Polym. Sci.* **26**, 605 (2001).
- [13] J.D Cho, J.W. Hong., *Eur. Polym. J.* **41**, 367 (2005).
- [14] K.S. Anseth, L.M. Kline, T.A. Walker, K.J. Anderson, C.N. Bowman., *Macromolecules* **28**, 2491 (1995).
- [15] C. Decker., *Polym. Inter.* **45**, 133 (1988).
- [16] C. Decker., *Macromol. Rapid Commun.* **23**, 1067 (2002).
- [17] H.F. Gruber., *Prog. Polym. Sci.* **17**, 953 (1992).

- [18] R. Chandra, R.K. Soni, S.S. Murthy., *Polym. Inter.* **31**, 305 (1993).
- [19] E. Andrzejewska, M.B. Bogacki., *Macromol. Chem. Phys.* **198**, 1649 (1997).
- [20] A.R. Kannurpatti, S. Lu, G.M. Bunker, C.N. Bowman., *Macromolecules* **29**, 7310 (1996).
- [21] J.H Ward, A. Shahar, N.A. Peppas., *Polymer* **43**, 1745 (2002).
- [22] J.G. Kloosterboer, G.M.M. van de Hei, R.G. Gossink, G.C.M. Dortant., *Polym. Commun.* **25**, 322 (1984).
- [23] L. Lecamp, B. Youssef, C. Bunel, P. Lebaudy., *Polymer* **38**, 6089 (1997).
- [24] N.S. Allen, S.J. Hardy, A.F. Jacobine, D.M. Glaser, B. Yang, D. Wolf., *Eur. Polym. J.* **26**, 1041 (1990).
- [25] J.H. Ward, K. Furman, N.A. Peppas., *J. Appl. Polym. Sci.* **89**, 3506 (2003).
- [26] N.S. Allen, J. Segurolo, M. Edge, E. Santamari, A. Mc Mahon., *Surf. Coat. Inter.* **2**, 67 (1999).
- [27] J.G. Kloosterboer, G.F.C.M Lijten., *Polymer* **31**, 95 (1990).
- [28] E. Andrzejewska, L.A. Linden, J.F. Rabek., *Polym. Inter.* **42**, 179 (1997).
- [29] R. Chandra, R.K. Soni., *Polym. Inter.* **31**, 239 (1993).
- [30] T.F. Scott, W.D. Cook, J.S. Forsythe., *Polymer* **44**, 671 (2003).
- [31] R. Chandra, R.K. Soni., *Prog. Polym. Sci.* **19**, 137 (1994).
- [32] W.Y. Chiang, W.J. Shu, *Die Angew. Macromol. Chem.* **160**, 41 (1988).
- [33] C. Decker, K. Moussa., *Makromol. Chem.* **189**, 2381 (1988).
- [34] T.F. Scott, W.D. Cook, J.S. Forsythe., *Polymer* **44**, 5839 (2002).
- [35] M.J.M Abadie, O.O. Novikova, V.Y. Voytekunas, V.G. Syromatnikov, A.Y. Kolendo., *J. Appl. Polym. Sci.* **90**, 1096 (2003).
- [36] U. Khanna, M. Chanda., *J. Appl. Polym. Sci.* **49**, 319 (1993).

Photopolymerization of bisaromatic
based di(meth)acrylate monomers

4.2 PART – B: Photopolymerization of bisaromatic based di(meth)acrylate monomers

4.2.1 Experimental

4.2.1.1 Materials and measurements

4,4'-Bisphenol A (SD Fine), 4,4'-bisphenol S (Aldrich), 4,4'-dihydroxy biphenyl (Fluka), ethylene carbonate (Aldrich), propylene carbonate (Aldrich), hexamethylene diisocyanate (Fluka), isophorone diisocyanate (Fluka), 2-hydroxyethyl acrylate (Aldrich), 2-hydroxyethyl methacrylate (Aldrich), hydroxylpropyl acrylate (Aldrich), 1,4-diazabicyclo[2.2.2]octane or DABCO (Aldrich), dibutyl tin dilaurate (Aldrich), tetrahydrofuran (Merck) and chloroform (Merck) were used as received.

The measurements used are same as given in Section 4.1.1.2

4.2.1.2 Photopolymerization of bisaromatic urethane diacrylate based on 2,2-bis[4-(β -hydroxyethoxy)-phenyl] propane, hexamethylene diisocyanate and 2-hydroxyethyl acrylate (System 4B-1)

A bisaromatic urethane diacrylate based on 2,2-bis[4-(β -hydroxyethoxy)-phenyl] propane (HEPP), HMDI and HEA was synthesized and the photocuring studies were carried out. Estimation of kinetic parameters were done based on the heat flow profile obtained during the photopolymerization process.

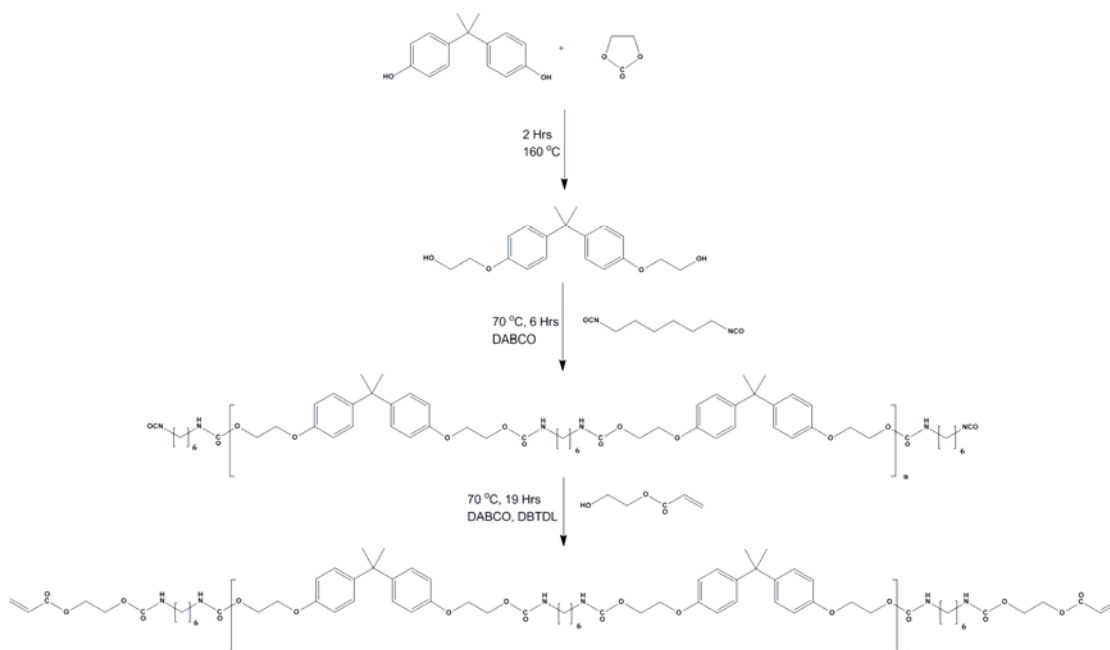


Figure 4.71 Synthesis pathway of bisaromatic based urethane diacrylate based on HEPP, HMDI and HEA

4.2.1.2.1 Procedure for synthesis

Synthesis of 2,2-bis[4-(β -hydroxyethoxy)-phenyl] propane (HEPP)

The monomer was synthesized from 4,4'-bisphenol A and ethylene carbonate using a reported procedure.¹

Synthesis of prepolymer

To a 100 mL three necked round bottom flask provided with a half moon stirrer and stuffing box was flushed with nitrogen for 2 min. To it was added 10 g (31.61 mmol) of HEPP followed by addition of 10 mg (0.08915 mmol) of DABCO and 40 mL dry

chloroform. The system was homogenized by stirring at 80 rpm at 50 °C under nitrogen purge. 5.62 mL (34.77 mmol) of hexamethylene diisocyanate was added to it drop-wise at 100 rpm. After addition, the temperature was increased to 70 °C and continued for a period of 6 h to obtain the diisocyanate terminated prepolymer. The residual isocyanate was noted (ASTM D2572). The residual isocyanate content was found to be 3.528%. IR and NMR spectra were noted.

IR: 1705 (C=O, urethane), 2270 (NCO), 3338 and 1511 (N-H, urethane), 1246 (C-O), 3008, 2934, 2867 (C-H) cm^{-1} .

¹H NMR (CDCl₃): 1.62 (-CH₃, gem), 1.46 and 1.6 (-CH₂-, hexamethylene), 3.14 (CH₂-NCO, terminal), 2.16 (CH₂-NH), 4.84 (-NH-), 4.37 (-CH₂-O-), 4.07 (-CH₂-CH₂-O-), 6.59 and 7.1 (CH, aromatic ring)

¹³C NMR (CDCl₃): 25.91, (-CH₂- hexamethylene), 29.47 (-CH₂-CH₂-NCO), 30.69 (-CH₃, gem), 40.52 (-CH₂-NH), 41.38 (=C=, bis), 42.55 (CH₂-NCO), 62.88 (-O-CH₂-CH₂-), 66.11 (-O-CH₂-CH₂-), 122.59 (-NCO, terminal), 113.6 and 127.45 (CH, aromatic), 143 and 156.9 (C, aromatic), 156.01 (-CO-)

Synthesis of macromonomer

In the second step, 1.45 mL (12.62 mmol) of HEA and 380 mg (0.6017 mmol) of dibutyl tin dilaurate were added to the system at 50 °C under stirring. The temperature was raised to 70 °C and held under stirring for 19 h until the isocyanate peak disappeared from the IR spectrum. The product thus obtained was purified by washing three times with 200 mL methanol until the washings are devoid of HEA. IR and NMR spectra were noted. The molecular mass was found by VPO.

IR: 1699 (C=O, urethane), 3340 and 1511 (N-H, urethane), 810, 1457, 1637 (C=O, acrylate), 1244 (C-O), 2932, 2861 (C-H) cm^{-1} .

¹H NMR (CDCl₃): 1.76 (-CH₃, gem), 1.3 and 1.46 (-CH₂-, hexamethylene), 3.15 (CH₂-NH-), 4.87 (-NH-), 4.37 (-CH₂-O-), 4.09 (-CH₂-CH₂-O-), 6.80 and 7.08 (CH, aromatic ring)

¹³C NMR (CDCl₃): 25.86 and 29.50, (-CH₂- hexamethylene), 30.65 (-CH₃, gem), 40.47 (-CH₂-NH), 41.33 (=C=, bis), 60.34 (-NH-CO-O-CH₂-CH₂-O-CO-, acrylate) and 61.04 (-NH-CO-O-CH₂-CH₂-O-CO-, acrylate) 66.06 (-O-CH₂-CH₂-O-CO-), 62.85 (-O-CH₂-CH₂-O-CO-), 113.57 and 127.42 (CH, aromatic), 143.18 and 156.06 (C, aromatic), 155.96 (-CO-NH), 166.71 (C=O, acrylate)

4.2.1.2.2 Formulation

The macromonomer being highly viscous was formulated by addition of 50 wt% excess HEA and photoinitiators to obtain photopolymerizable compositions. The photoinitiators of choice were IRGACURE 651, DAROCUR TPO and IRGACURE 814.

To 500 mg of macromonomer containing excess HEA was added 0.5, 1 and 2 wt% of above photoinitiator to obtain nine photopolymerizable compositions. The compositions were stirred using a vibrating mill prior to weighing. The Brookfield viscosity of the macromonomer with 50 wt% HEA with a shear rate of 133.3 sec^{-1} at $50 \text{ }^\circ\text{C}$ was noted with spindle number 1 at 10 rpm.

4.2.1.2.3 Photocuring studies

5 mg of the material was taken in a DSC pan and subjected to photo curing studies. The heat flow profiles obtained during the *in situ* photocuring process was recorded as a function of time under an isothermal condition of $40 \text{ }^\circ\text{C}$. The intensity of irradiation was kept at 1.93 mW/cm^2 using a polychromatic radiation of 250-450 nm using a 100 W high pressure mercury short arc lamp. The normalized outputs in W/g against time were recorded. The rates of polymerization as well as corresponding conversions were calculated for all the compositions. The results are provided in Figures 4.72 to 4.74 (A-C). The evaluation of variable autocatalytic kinetic model were carried out using TA advantage specialty library software. Post polymerization degradation profile and glass transition temperature of photocured matrix were noted using TGA (ramp rate of $20 \text{ }^\circ\text{C/min}$ from 30 to $650 \text{ }^\circ\text{C}$) and DSC (ramp rate of $10 \text{ }^\circ\text{C/min}$ from 30 to $150 \text{ }^\circ\text{C}$) methods, respectively.

4.2.1.2.4 Results and discussion

The existence of terminal isocyanate group in the prepolymer as well as complete conversion of isocyanate group during the formation of macromonomer were confirmed by IR, ^1H and ^{13}C NMR spectroscopic methods. The molecular mass was found to be 1508 g/mol by VPO. The total theoretical heat flow² (ΔH_{theor}) for the system was calculated to be 323.59 J/g . The viscosity of the macromonomeric formulation was found to be 1781 cP .

The rate and conversion profiles obtained from photocuring studies of macromonomeric formulations containing 50 wt% of HEA as reactive diluent with three photoinitiators at 0.5, 1 and 2 wt% compositions at $40 \text{ }^\circ\text{C}$ and 1.93 mW/cm^2 are given in Figures 4.72 to 4.74 (A-C).

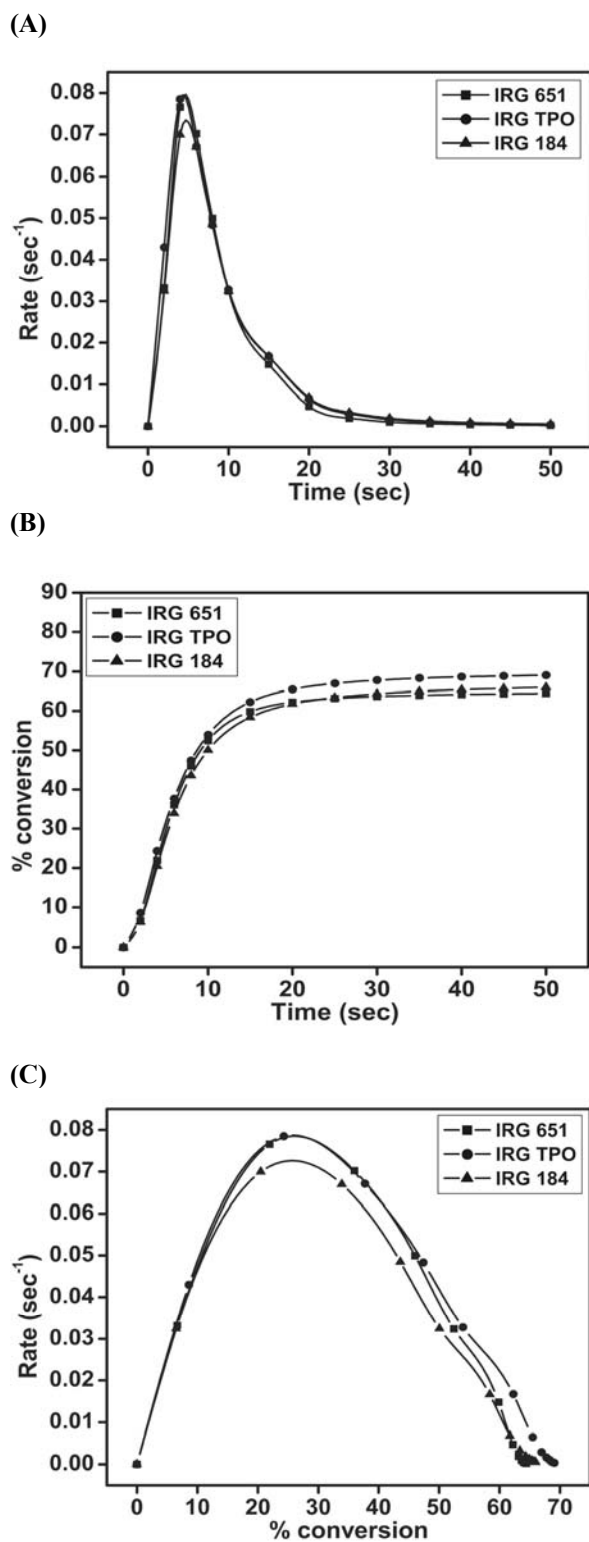


Figure 4.72(A-C) Time dependent rate and conversion profiles of macromonomeric formulations containing 50 wt% HEA and 0.5 wt% of three photoinitiators at 40 °C

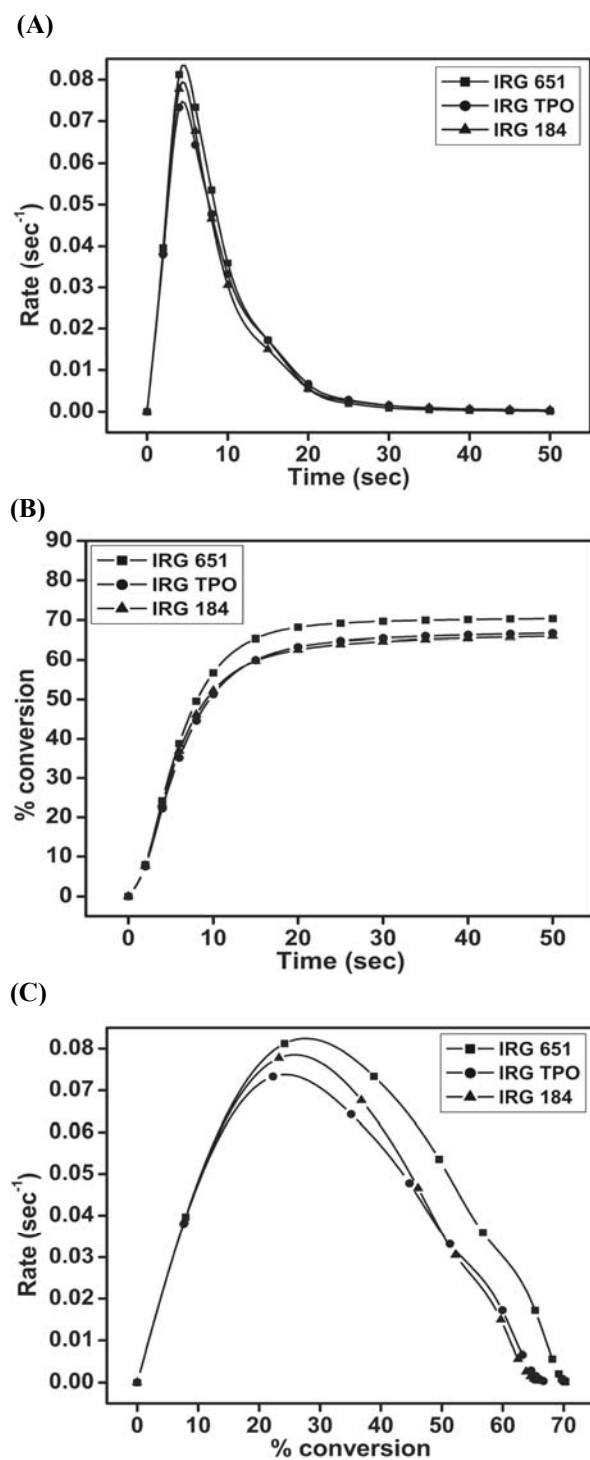


Figure 4.73(A-C) Time dependent rate and conversion profiles of macromonomeric formulations containing 50 wt% HEA and 1 wt% of three photoinitiators at 40 °C

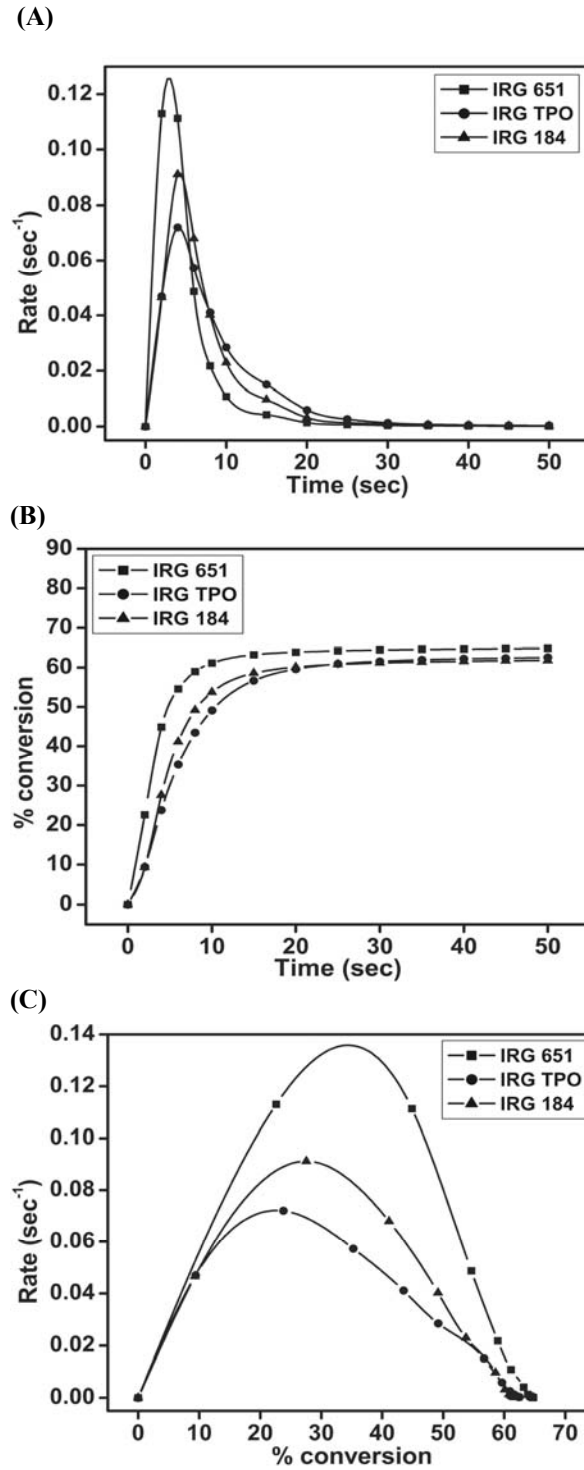


Figure 4.74(A-C) Time dependent rate and conversion profiles of macromonomeric formulations containing 50 wt% HEA and 2 wt% of three photoinitiators at 40 °C

Table 4.33 Kinetic parameters of macromonomeric formulations calculated from the heat flow profiles at 40 °C

Photo Initiator	% conc. of photo-initiator	Induction Time (sec)	Peak Maximum Time (sec)	$R_p \text{ max}$ ($\times 10^{-2}$) (sec^{-1})	C_{max} (%)	Heat of reaction (J/g)	Autocatalytic		
							n	m	k (min^{-1})
IRGACURE 651	0.5	0.46	4.62	7.97	64.77	209.6	3.08	0.62	26.1
	1	0.35	4.55	8.36	70.80	229.1	2.58	0.57	22.7
	2	0.12	2.90	12.63	64.90	210	4.26	0.85	101
DAROCUR TPO	0.5	0.30	4.35	7.95	69.56	225.1	2.98	0.60	24.9
	1	0.35	4.44	7.47	67.83	219.5	3.04	0.56	22.1
	2	0.25	4.09	7.22	62.86	203.4	3.43	0.54	22.3
IRGACURE 184	0.5	0.44	4.75	7.34	67.12	217.2	3.55	0.72	31.9
	1	0.36	4.48	7.95	66.66	215.7	3.44	0.69	31.9
	2	0.30	4.20	9.19	61.96	200.5	3.96	0.75	47.5

Initial viscosity of bisaromatic macromonomers gets reduced on addition of reactive diluents.³ Radical recombination can occur at lower initial viscosity due to enhanced collisions and lower half life of initiating species.⁴ But the deciding factor in a faster initiation is the radical diffusion through the matrix which depends on the interactions between the matrix and initiating species such as their mobility and diffusion rates.⁴ A viscous macromonomer is always found to have a higher induction time than the same system containing a reactive diluent under similar conditions do to the above effect.

The formulations as given in Table 4.33 showed a consistent decrease in induction time as well as peak maximum time with an increase in concentration of photoinitiator effected by the addition of 50 wt% excess HEA added to the system leading to reduced viscosity. An anomaly in induction and peak maximum times were observed in the case of 1 wt% concentration of DAROCUR TPO as this photoinitiator has the highest rate of initiation due to multiple excitations occurring within the irradiation range.⁵ For the formulation under study, an optimum value of effective radical concentration was attained at a concentration around 0.5 wt%. As a result, an increase in concentration of photoinitiator to 1 wt%, quantum yield of initiation was reduced by radical radical combination which resulted in an increase in induction time and peak maximum time.⁶ A further increase to 2 wt% resulted in much faster rate of initiation showing that the concentration of radicals produced are much higher and the radical diffusion exceeds the combinations resulting in an enhancement.

The value of $R_{p \text{ max}}$ was found to increase for IRGACURE 651 and IRGACURE 184 with increase in concentration of photoinitiator while a decrease was observed for DAROCUR TPO. DAROCUR TPO can be assumed to have a faster autoacceleration along with a better radical diffusion, which resulted in a faster onset of reaction diffusion as compared to other photoinitiators before attaining $R_{p \text{ max}}$, which resulted in a decrease in the value of $R_{p \text{ max}}$ was observed with increase in concentration of photoinitiator.⁵ The rate of initiation of reaction diffusion with IRGACURE 651 and IRGACURE 184 can be assumed to occur gradually and hence the nature of propagation follows initiation, as is evident from induction time and $R_{p \text{ max}}$ values. The final conversions are found to vary from 61 to 71%. A trend of increase/decrease in final conversion with increase in concentration of photoinitiator was observed. This is due to the influence of competing factors in the deceleration step such as competition between primary/propagating radical with double bond and between radicals themselves.⁷ For these formulations in general, it can be said that an increase in concentration of photoinitiator resulted in earlier vitrification, there by reducing final conversions due to an earlier influence of volume shrinkage which exceeds the chemical reaction in the deceleration step.⁸

The evaluation of variable autocatalytic kinetic model as given in Table 4.33 shows that the values of m and n are constant. The value of specific rate constant (k) was also within a range. An unexpected high value of k was observed in a few cases for those systems which had a higher $R_{p \text{ max}}$ value. This variation may be due to a higher extent of shift from the autocatalytic behaviour for these formulations.⁹

4.2.1.2.5 Post photopolymerization studies

Thermogravimetric analysis

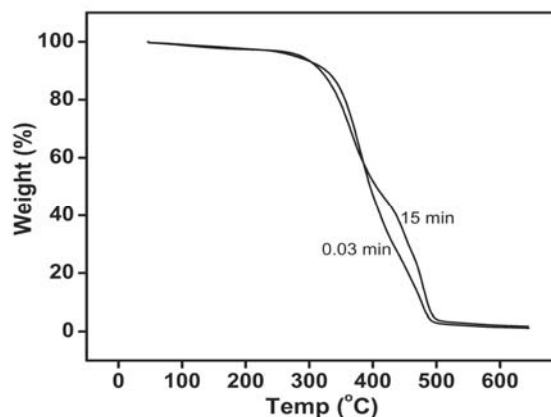


Figure 4.75 Thermogravimetric degradation profiles of macromonomeric formulation containing 50 wt% of HEA and 0.5 wt% of DAROCUR TPO photocured at 40 °C and 0.03 min and 15 min of irradiation at 1.93 mW/cm². Analyses done after one week storage.

The thermogravimetric degradation profile given in Figure 4.75 shows that the extent of crosslinking occurring on a photocured matrix (15 min irradiated) and that of a photo initiated matrix (0.03 min irradiated) which were kept in dark for a week showed more or less similar extent of cure. They follow an almost similar trend up to 50% weight loss. A faster degradation of photoinitiated matrix was observed after 50% weight loss. This shows that the photoinitiated matrix has undergone polymerization in dark in an efficient manner. This supports the observation that photoinitiated matrix undergo further conversion in dark.¹⁰ This efficient conversion can be due to slow and large time scale of radical/reaction diffusions occurring due to the plasticization effect of HEA.

DSC analysis

Macromonomeric formulation containing 50 wt% excess HEA and 1 wt% of IRGACURE 651 photocured at 40 °C and 1.93 mW/cm² was subjected to thermal analysis using DSC. The T_g of the photocured sample was found to be 60.3 °C. The extent of vitrification was found to depend on many parameters of which the initial viscosity as well as the ultimate T_g of the photocured sample have greater influence. Vitrification is enhanced, with increase in initial viscosity and increase in T_g of the cured network.¹¹ For this system, the initial viscosity was found to be 1781 cP and the photocured material had a T_g of 60.3 °C.

4.2.1.3 Photopolymerization of bisaromatic diacrylate based on 2,2-bis[4-(β -hydroxypropoxy)-phenyl] propane, hexamethylene diisocyanate and 2-hydroxyethyl acrylate (System 4B-2)

A bisaromatic diacrylate based on 2,2-bis[4-(β -hydroxypropoxy)-phenyl] propane (HPPP), HMDI and HEA was synthesized and their photocuring studies were carried out. Estimation of kinetic parameters were done based on the heat flow profile obtained during the photopolymerization process.

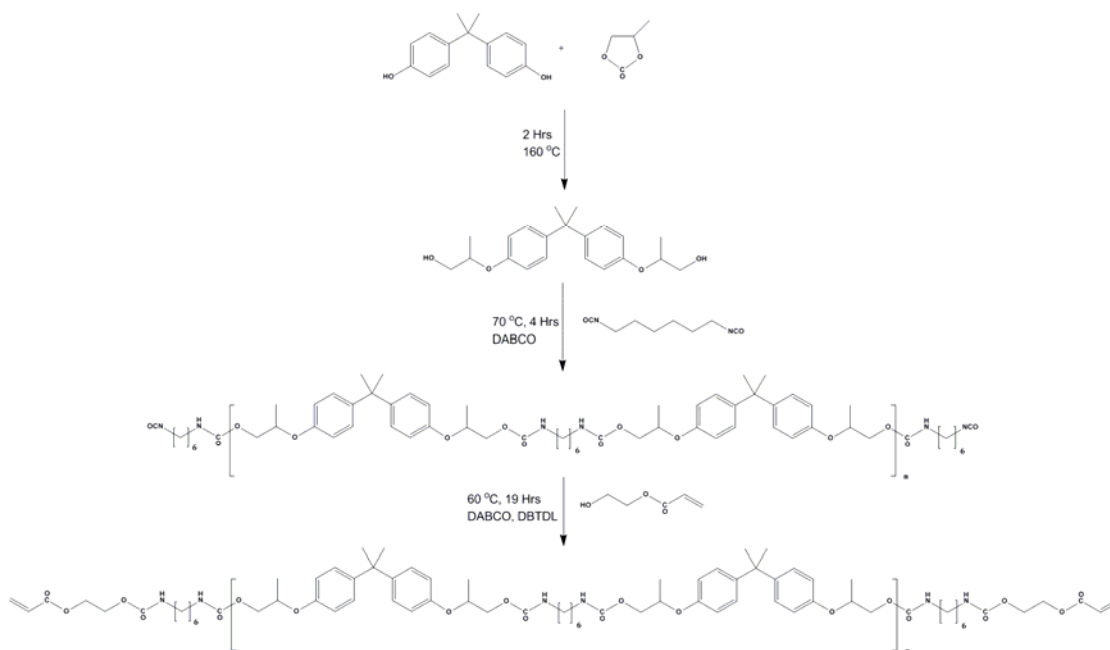


Figure 4.76 Synthesis pathway of bisaromatic urethane diacrylate based on HPPP, HMDI and HEA

4.2.1.3.1 Procedure for synthesis

Synthesis of 2,2-bis[4-(β -hydroxypropoxy)-phenyl] propane.(HPPP)

The monomer was synthesized from 4,4'- bisphenol A and propylene carbonate using a reported procedure.¹

Synthesis of prepolymer

To a 100 mL three necked round bottom flask provided with a half moon stirrer and stuffing box was flushed with nitrogen for 2 minutes. To it was added 10 g (29 mmol) of HPPP followed by addition of 10 mg of DABCO and 30 mL dry chloroform. The system was homogenized by stirring at 80 rpm at 50 °C under nitrogen purge. 5.17

mL (31.97 mmol) of HMDI was added to it drop-wise under stirring at 100 rpm. After addition, the temperature was increased to 70 °C and continued for a period of four hours to obtain the diisocyanate terminated prepolymer. The residual isocyanate was noted (ASTM D 2572). The residual isocyanate content was found to be 2.352%. IR spectrum was noted.

IR: 2275 (NCO), 3420 and 1510 (N-H, urethane), 1706 (C=O, urethane), 1248 (N-CO-O, sym str) and 1040 (N-CO-O, asym str), 2969, 2935, 2870 (C-H) cm⁻¹

Synthesis of macromonomer

1.34 mL (11.58 mmol) of HEA and 380 mg (0.6017 mmol) of dibutyl tin dilaurate were added to the prepolymer at 100 rpm and stirred at 60 °C and 80 rpm for 19 h until the isocyanate peak disappeared from the IR spectrum. 30 mL of chloroform was then added and the product was transferred to a 500 mL separation funnel. It was then purified by washing three times with 200 mL distilled water until the washings are devoid of excess HEA. The chloroform layer was transferred to a 100 mL R B flask and vacuum was applied to the viscous product at 40 °C for 2 h. The viscous polymer was solvated in minimum amount of dichloromethane and dried in vacuum oven for 10 h at 60 °C. IR and NMR spectra were noted. The molecular mass was found by VPO.

IR: 1707 (C=O, urethane), 3355 and 1510 (N-H, urethane), 810, 1462, 1636 (C=O, acrylate), 1248 (N-CO-O, sym str) and 1042 (N-CO-O, asym str), 2968, 2833 and 2869 (C-H) cm⁻¹.

¹H NMR (CDCl₃): 1.61 (-CH₃, gem), 1.31 (-O-CH₂-CH(CH₃)-O-), 1.26 and 1.46 (-CH₂, hexamethylene), 3.13 (CH₂-NH-), 4.81 (terminal -NH-) and 5.1 (internal -NH-), 4.17 (-O-CH₂-CH(CH₃)-O-), 3.88 (-O-CH₂-CH(CH₃)-O-), 4.31 (-O-CH₂-CH₂-O-CO-NH-), 3.94 (-O-CH₂-CH₂-O-CO-NH-), 6.09, 6.14 and 6.4 (CH₂=CH-, acrylate) 6.80 and 7.10 (CH, aromatic ring)

¹³C NMR (CDCl₃): 26.09 and 29.65 (-CH₂- hexamethylene), 30.88 (-CH₃, gem), 40.63 (-CH₂-NH-), 41.54 (=C=, bis), 62.70 (-CO-O-CH₂-CH₂-O-CO-NH-, acrylate) and 62.34 (-CO-O-CH₂-CH₂-O-CO-NH-, acrylate) 66.06 (-CO-O-CH₂-CH(CH₃)-O-), 73.1 (-CO-O-CH₂-CH(CH₃)-O-), 113.78 and 127.62 (CH, aromatic), 131.44 (CH₂=CH-, acrylate), 128.04 (CH₂=CH-, acrylate) 143.36 and 156.27 (C, aromatic), 155.98 (-CO-NH), 165.86 (C=O, acrylate)

4.2.1.3.2 Formulation

The macromonomer being highly viscous was then formulated by addition of 50 wt% HEA and photoinitiator to obtain photopolymerizable compositions. The photoinitiators of choice were IRGACURE 651, DAROCUR TPO and IRGACURE 814.

To 500 mg of macromonomer containing excess HEA was added 0.5, 1 and 2 wt% of above photoinitiators to obtain nine photopolymerizable compositions. The compositions were mixed in a vibrating mill prior to weighing. The Brookfield viscosity of the macromonomer with 50 wt% HEA with a shear rate of 133.3 sec^{-1} at $50 \text{ }^\circ\text{C}$ was noted with spindle number 1 at 10 rpm.

4.2.1.3.3 Photocuring Studies

5 mg of the material was taken in a DSC pan and subjected to photo curing studies. The heat flow profiles obtained during the *in situ* photocuring process was recorded as a function of time under an isothermal condition of $40 \text{ }^\circ\text{C}$. The intensity of irradiation was kept at 1.93 mW/cm^2 using a polychromatic radiation of 250-450 nm using a 100 W high pressure mercury short arc lamp. The normalized outputs in W/g against time were recorded. The rates of polymerization as well as corresponding conversions were calculated for all the compositions. The reaction was also carried out at a higher intensity of 4.47 mW/cm^2 at 40 and $70 \text{ }^\circ\text{C}$ to understand the effect of intensity and temperature on cure. The evaluation of variable autocatalytic kinetic model was carried out using TA advantage specialty library software. Post polymerization degradation profile and glass transition temperature of photocured matrix were noted using TGA (ramp rate of $20 \text{ }^\circ\text{C/min}$ from 30 to $650 \text{ }^\circ\text{C}$) and DSC (ramp rate of $10 \text{ }^\circ\text{C/min}$ from 30 to $150 \text{ }^\circ\text{C}$) methods, respectively.

4.2.1.3.4 Results and discussion

The existence of terminal isocyanate group in the prepolymer was confirmed by IR spectroscopy. Confirmation for complete conversion of isocyanate group during the formation of macromonomer was noted by IR, ^1H and ^{13}C NMR spectroscopy. The molecular mass was found to be 1872 g/mol by VPO. The total theoretical heat flow² (ΔH_{theor}) for the system was calculated to be 308.8 J/g . The viscosity of the macromonomer was found to be 993 cP .

The rate and conversion profiles obtained from photocuring studies of macromonomeric formulations containing 50 wt% of HEA as reactive diluent with three photoinitiators at 0.5, 1 and 2 wt% compositions at $40 \text{ }^\circ\text{C}$ and 1.93 mW/cm^2 are given below in Figures 4.77 to 4.79 (A-C).

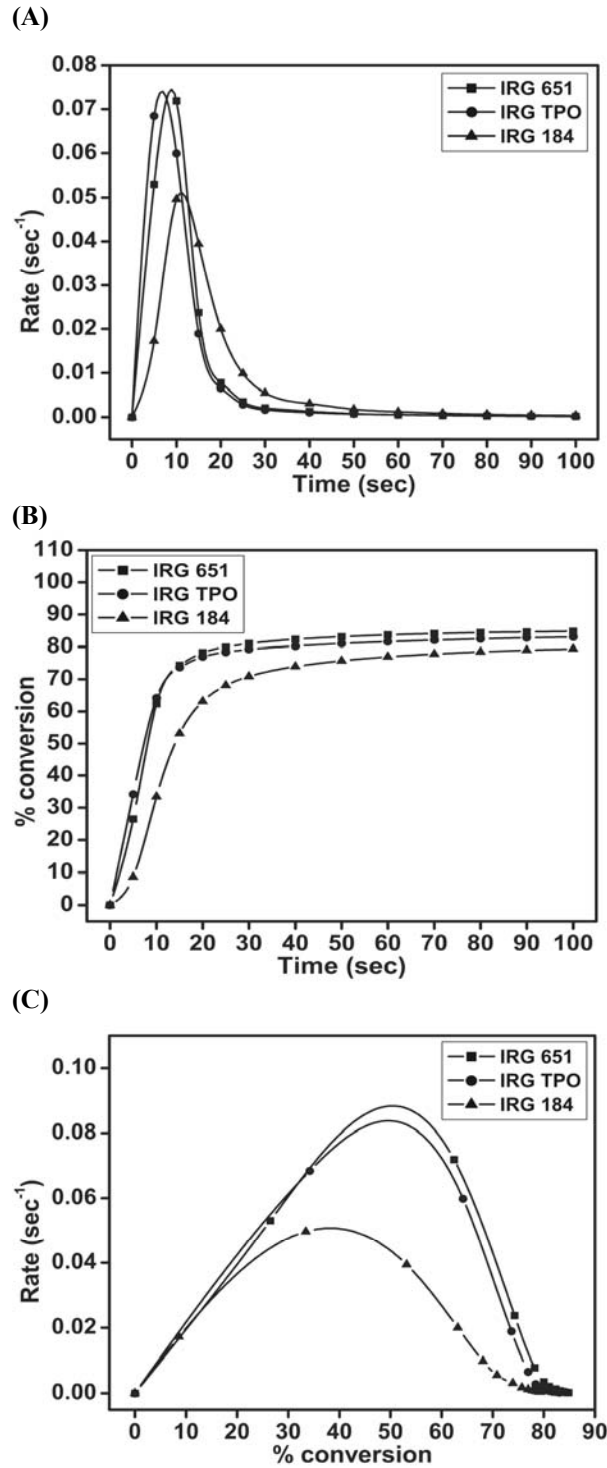


Figure 4.77(A-C) Time dependent rate and conversion profiles of macromonomeric formulations containing 50 wt% HEA and 0.5 wt% of three photoinitiator at 40 °C and 1.93 mW/cm²

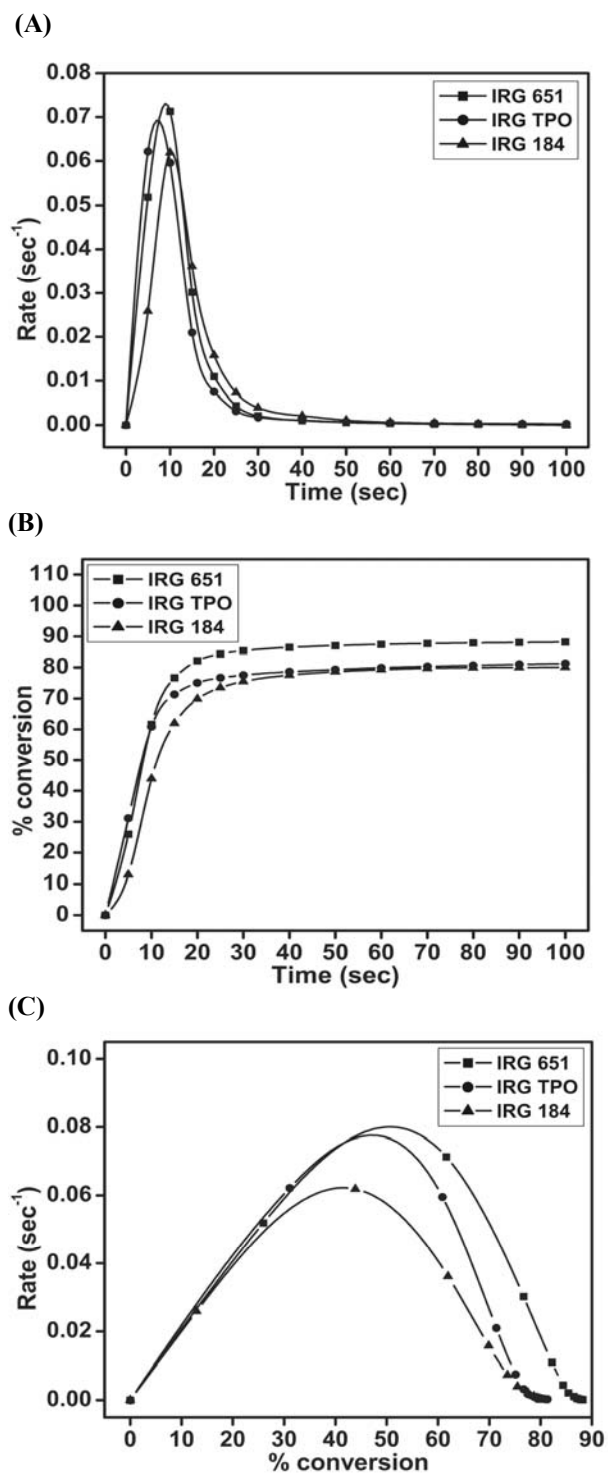


Figure 4.78(A-C) Time dependent rate and conversion profiles of macromonomeric formulations containing 50 wt% HEA and 1 wt% of three photoinitiator at 40 °C and 1.93 mW/cm²

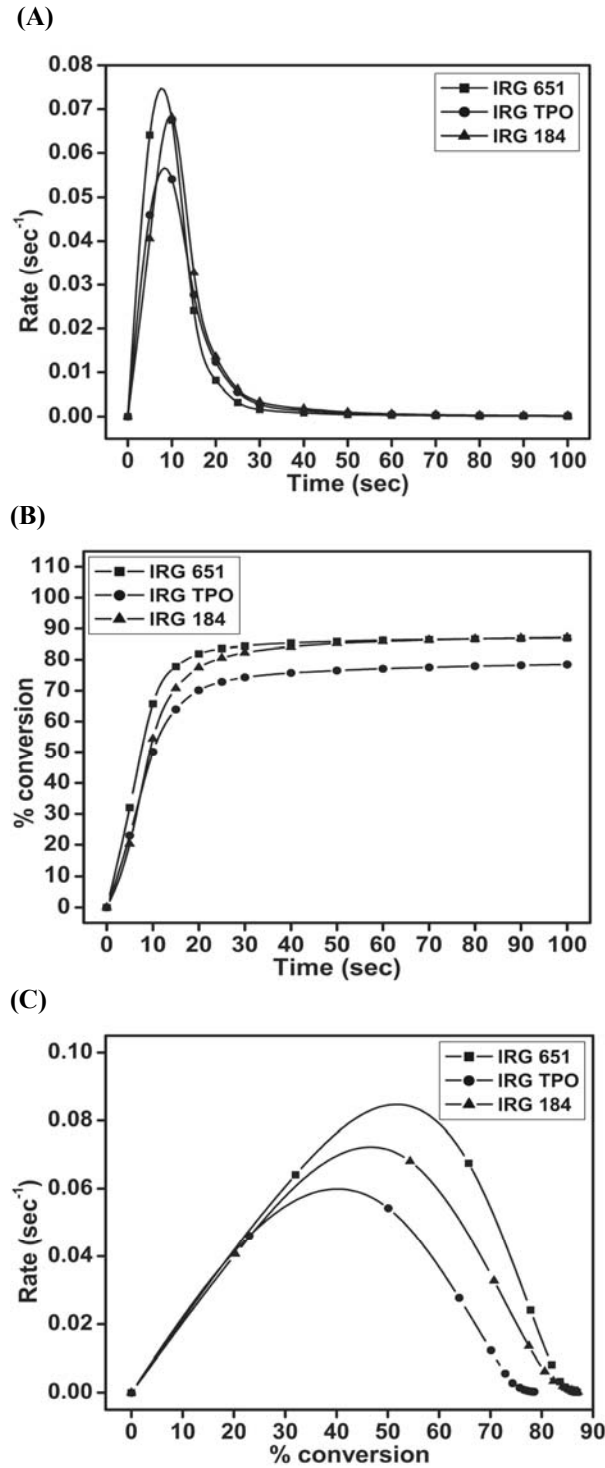


Figure 4.79(A-C) Time dependent rate and conversion profiles of macromonomeric formulations containing 50 wt% HEA and 2 wt% of three photoinitiator at 40 °C and 1.93 mW/cm²

The rate and conversion profiles obtained from photocuring studies of the macromonomeric formulation containing 50 wt% of HEA as reactive diluent with three photoinitiators at 0.5, 1 and 2 wt% compositions at 40 °C and 4.47 mW/cm² are given below in Figures 4.80 to 4.82 (A-C).

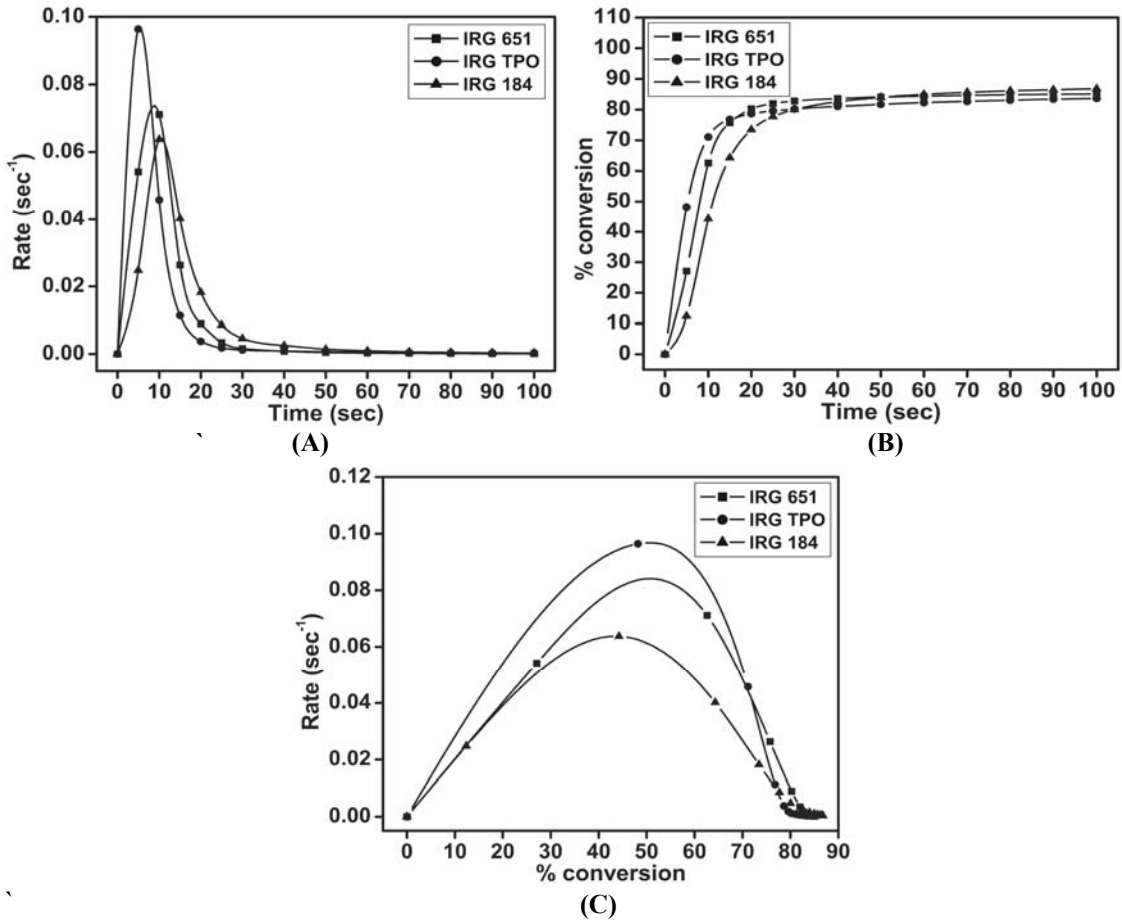


Figure 4.80(A-C) Time dependent rate and conversion profiles of macromonomeric formulations containing 50 wt% HEA and 0.5 wt% of three photoinitiator at 40 °C and 4.47 mW/cm²

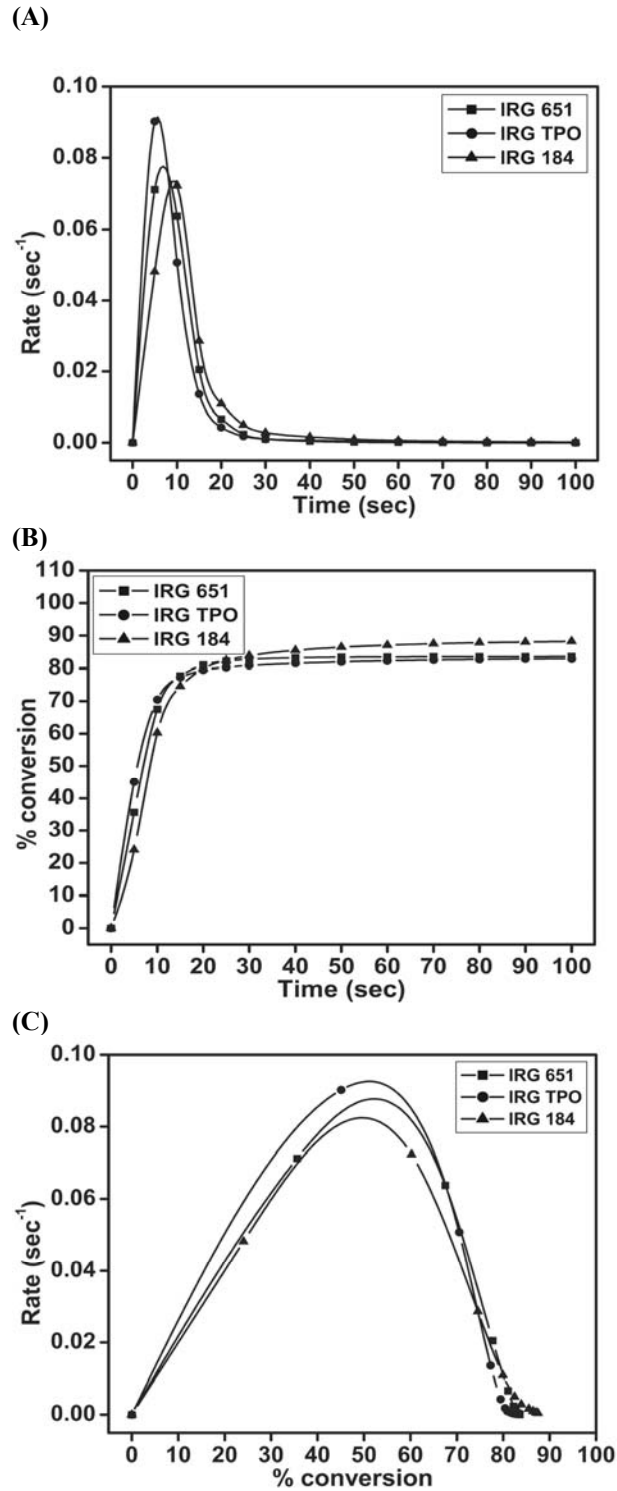


Figure 4.81(A-C) Time dependent rate and conversion profiles of macromonomeric formulations containing 50 wt% HEA and 1 wt% of three photoinitiator at 40 °C and 4.47 mW/cm²

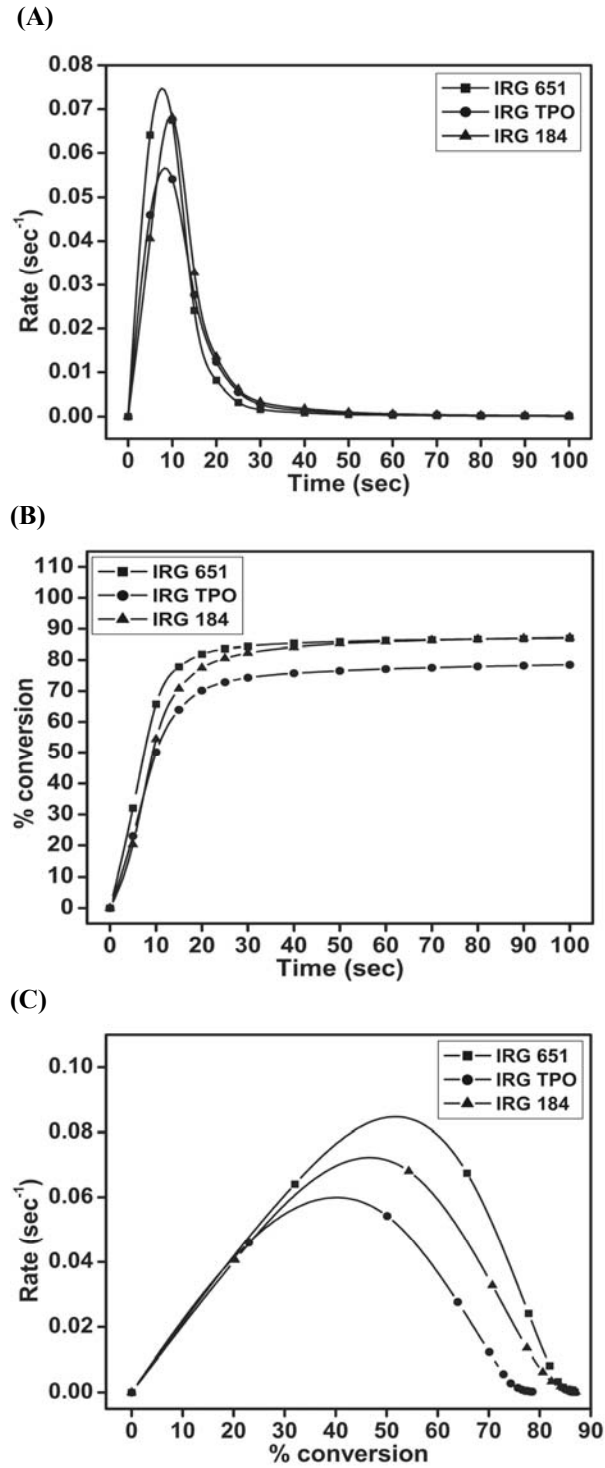


Figure 4.82(A-C) Time dependent rate and conversion profiles of macromonomeric formulations containing 50 wt% HEA and 2 wt% of three photoinitiator at 40 °C and 4.47 mW/cm²

Table 4.34 Kinetic parameters of macromonomeric formulations calculated from the heat flow profiles at 40 °C

Photo Initiator	% conc. of photo-initiator	Intensity (mW/cm ²)	Induction Time (sec)	Peak Maximum Time (sec)	R _p max (x 10 ⁻²) (sec ⁻¹)	C _{max} (%)	Heat of reaction (J/g)
IRGACURE 651	0.5	1.93	0.23	8.90	7.43	85.78	264.9
	1	1.93	0.24	9.04	7.30	88.86	274.4
	2	1.93	0.22	7.71	7.46	87.5	270.2
	0.5	4.47	0.22	8.82	7.35	85.62	264.4
	1	4.47	0.21	6.83	7.75	83.52	257.9
	2	4.47	0.16	7.71	7.46	83.81	258.8
DAROCUR TPO	0.5	1.93	0.17	6.77	7.40	84.84	262
	1	1.93	0.21	7.18	6.92	82.93	256.1
	2	1.93	0.24	8.40	5.67	80.12	247.4
	0.5	4.47	0.12	5.35	9.69	85.49	264
	1	4.47	0.18	5.53	9.13	82.90	256
	2	4.47	0.23	8.39	5.66	81.12	250.5
IRGACURE 184	0.5	1.93	1.15	11.06	5.11	81.28	251
	1	1.93	0.67	10.26	6.21	80.08	247.3
	2	1.93	0.32	9.66	6.83	87.99	271.7
	0.5	4.47	0.75	10.47	6.43	88.15	272.2
	1	4.47	0.26	9.26	7.35	89.18	275.4
	2	4.47	0.32	9.65	6.83	86.82	268.1

From Table 4.34, it was observed that the addition of 50 wt% HEA as diluent to the compositions were found to give optimum cure characteristics. The formulations containing IRGACURE 651 and IRGACURE 184 in most cases were found to show a decrease in induction time as well as peak maximum time with an increase in concentration of photoinitiator. This behaviour happens below an optimum value, where the quantum yield of initiation increases with increase in concentration of photoinitiator.⁶ An increase in the rate of initiation was also observed with an increase in intensity of irradiation at 40 °C. The competing effect such as initial radical diffusion and radical radical combinations resulted in variations of induction time and peak maximum time in some cases.⁵ In the case of DAROCUR TPO an increase in induction time as well as peak maximum time was observed with increase in concentration of photoinitiator as well as an increase in irradiation intensity. This shows that these formulations have a very high rate of initiation and the radical radical combinations exceed the radical diffusion with increase in concentration of photoinitiator thereby reducing the quantum yield of initiation.⁴

With increase in irradiation intensity, the same effect is observed at a faster rate of initiation. The value of $R_{p \text{ max}}$ in the case of formulations containing IRGACURE 651 and IRGACURE 184 showed variations due to the variations in radical diffusion after autoacceleration. These systems during the initial stages of reaction diffusion before attaining $R_{p \text{ max}}$ showed variations in radical diffusion due to rapid build up of *in situ* viscosity. In the case of DAROCUR TPO, a reduction in $R_{p \text{ max}}$ was observed with increase in the concentration of photoinitiator. This shows that the radical combination effects as well as its diffusion rates were unaffected from initiation to $R_{p \text{ max}}$. The final conversion levels varied from 80 to 90% for all formulations and an increase in intensity did not have any pronounced effect on the final conversion due to enhanced effect of viscosity assisted overall diffusion processes. For formulations containing IRGACURE 651 and IRGACURE 184, the final conversions did not show any trend with increase in concentration of photoinitiator due to competing factors occurring within the deceleration step up to vitrification.⁷ In the case of DAROCUR TPO, a consistent reduction in final conversion with increase in concentration of photoinitiator was observed due to consistent reduction in radical diffusion occurring during gradual reaction diffusion in the deceleration step. As a result the formulation having the highest concentration of photoinitiator got vitrified faster resulting in lowest conversions. Irrespective of the nature of initiation, these formulations can be thus assumed to have a gradual reaction diffusion process up to vitrification arising from a lower initial viscosity as compared to that of corresponding ethoxylated system as described in Section 4.2.1.2 resulting in higher ultimate conversions.¹²

The rate and conversion profiles obtained from photocuring studies of macromonomeric formulations containing 50 wt% of HEA as reactive diluent with three photoinitiators at 0.5 wt% compositions at 70 °C and 4.47 mW/cm² are given below in Figure 4.83 (A-C).

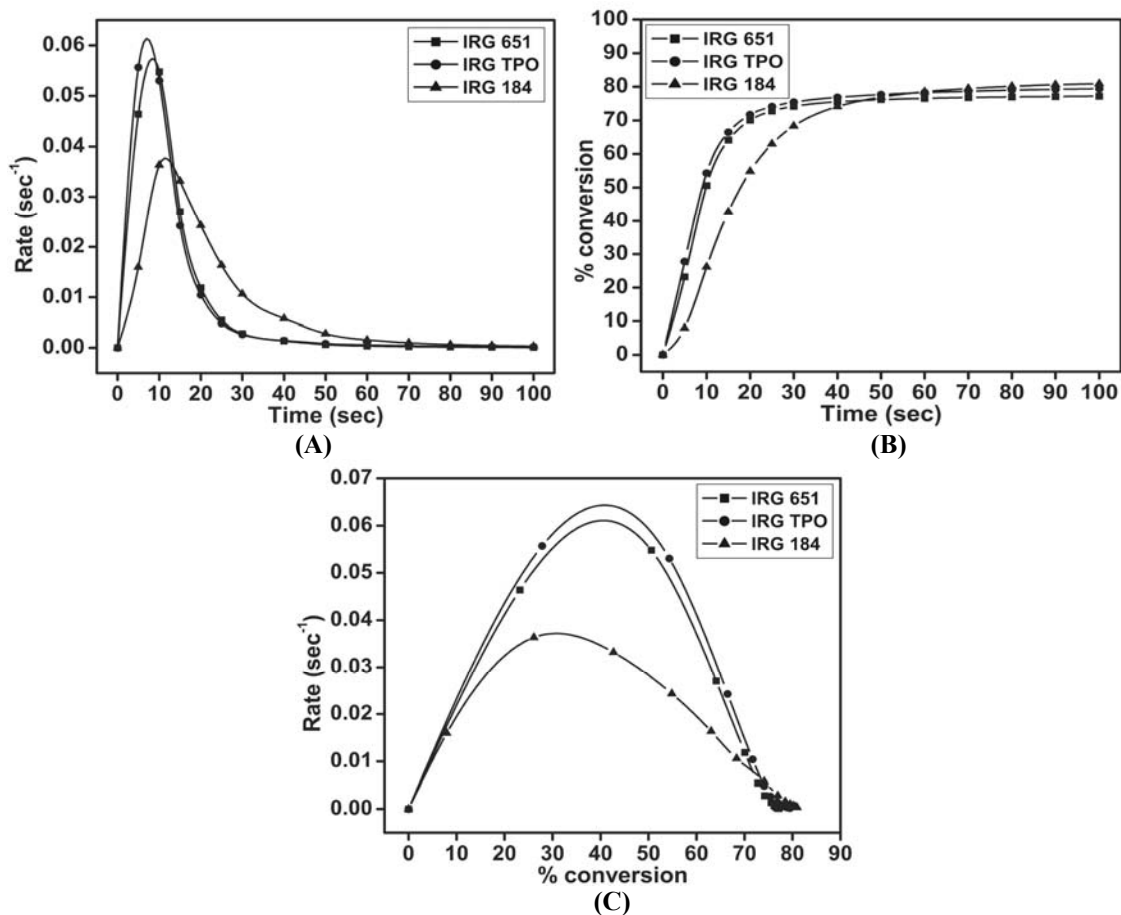


Figure 4.83(A-C) Time dependent rate and conversion profiles of macromonomeric formulations containing 50 wt% HEA and 0.5 wt% of three photoinitiator at 70 °C and 4.47 mW/cm²

Table 4.35 Kinetic parameters of macromonomeric formulations calculated from the heat flow profiles containing 0.5 wt% of photoinitiator at 70 °C and 4.47 mW/cm²

Photo Initiator	Induction Time (sec)	Peak Maximum Time (sec)	R _p max (x 10 ⁻²) (sec ⁻¹)	C _{max} (%)	Heat of reaction (J/g)
IRGACURE 651	0.24	8.38	5.73	77.62	239.7
DAROCUR TPO	0.18	7.07	6.12	80.51	248.6
IRGACURE 184	0.95	11.47	3.77	81.54	251.8

The effect of increased temperature (70 °C) on the photopolymerization kinetics of formulations containing 0.5 wt% of three photoinitiators at 4.47 mW/cm² are presented in Table 4.35. Comparing with corresponding data at 40 °C given in Table 4.34, we can infer that an increase in temperature has increased the induction as well as peak maximum time. It has also resulted in a decrease in R_p max as well as final conversion. This typically shows that rate of reactions decreased at higher temperature resulting in

reduced final conversions. Here the radical radical combinations or terminations occurring at reduced initial system viscosity due to higher isothermal condition and enhanced mobility has reduced the quantum yield for initiation.⁶ Since the system is formulated with reactive diluent and the reaction diffusion was gradual due to plasticization effect, the rate of termination had greater influence over the entire time scale of reaction, which resulted in lower cure profiles.⁴

Table 4.36 Evaluation of kinetic parameters of macromonomeric formulations as per autocatalytic model at 40 °C

Photo Initiator	% conc. of photo-initiator	Intensity (mW/cm ²)	Autocatalytic		
			n	m	k (min ⁻¹)
IRGACURE 651	0.5	1.93	2.30	0.82	35.5
	1	1.93	1.81	0.62	21.7
	2	1.93	1.93	0.62	25.1
	0.5	4.47	2.06	0.68	27.4
	1	4.47	2.09	0.65	29.9
	2	4.47	2.06	0.61	28.3
DAROCUR TPO	0.5	1.93	2.47	0.73	35.2
	1	1.93	2.39	0.65	27.6
	2	1.93	2.26	0.52	15.9
	0.5	4.47	2.67	0.77	54.5
	1	4.47	2.33	0.65	37.3
	2	4.47	2.24	0.56	27.4
IRGACURE 184	0.5	1.93	2.80	0.84	23.4
	1	1.93	2.51	0.79	25.1
	2	1.93	2.09	0.69	22.7
	0.5	4.47	2.21	0.76	22.5
	1	4.47	2.16	0.74	28.9
	2	4.47	2.02	0.52	23.4

The evaluation of variable autocatalytic kinetic model as given in Table 4.36 showed that the values of m and n are constant. The value of specific rate constant (k) was also within a range and the system can be assumed to follow the model to high levels of achieved conversions. The variations in reaction diffusion have pronounced effect on the value of specific rate constant. The system during photocuring can be assumed to undergo both monomolecular and bimolecular terminations.¹³

Table 4.37 Evaluation of kinetic parameters of macromonomeric formulations as per autocatalytic model containing 0.5 wt% of photoinitiator at 4.47 mW/ cm²

Photo Initiator	Temp. (°C)	Autocatalytic		
		n	m	k (min ⁻¹)
IRGACURE 651	40	2.06	0.68	27.4
	70	2.40	0.60	19
DAROCUR TPO	40	2.67	0.77	54.5
	70	2.33	0.53	18.2
IRGACURE 184	40	2.21	0.76	22.5
	70	2.11	0.55	8.99

From Table 4.37, we can infer that the value of specific rate constant as per variable autocatalytic kinetic model was found to decrease with increase in temperature. Due to high final conversions, the formulations obey autocatalytic kinetic model up to higher levels of achieved conversions. The value of m and n were also found to be constant.

Evaluation of bimolecular termination model

With the polychromatic light source, the initiation was done at 4.24 mW/cm² followed by dark polymerization to study the ratio of rate constants using bimolecular termination model. This model is based on the assumption that all the processes which results in termination are bimolecular and hence cannot be applied to any system which vitrifies early.⁴ The dark polymerization was done after irradiating the sample up to 5, 10, 15, 20, 30, 40, 50, 60 and 70% conversion. As per the bimolecular termination model, a plot of $[M]_t/(R_p)_t$ against time gives the ratio $2k_t^b/k_p$ as slope. At initiation, the termination is high than the propagation due to the high concentration of radicals and low viscosity of the system favouring termination process, the ratio (k_t^b/ k_p) at the beginning will be very high. As the polymerization proceeds, the viscosity of the polymer increases and as a result the ratio will decrease due to a drastic drop in k_t values, which may approach k_p at higher conversions due to rapid propagation after autoacceleration. However, it was observed that when the viscosity of the system becomes high, the propagation is controlled by reaction diffusion and finally the system will vitrify. During vitrification process towards the end of photopolymerization the growing chain as well as active radicals will get trapped in the matrix resulting in a slight increase in ratio due to a relatively higher rate of decrease in propagation than termination.^{4,14,15}

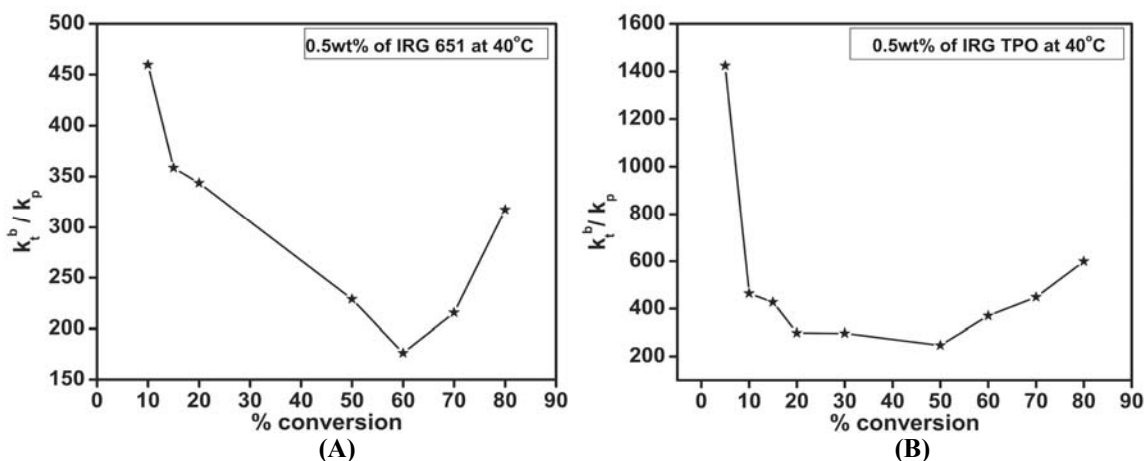


Figure 4.84(A-B) Plot of k_t^b/k_p at different percentage conversions for the formulation containing 50 wt% HEA and 0.5 wt% of (A) IRGACURE 651 and (B) DAROCUR TPO at 40 °C

Since the formulations did not vitrify very early, it can be thought to undergo bimolecular termination to a great extent. Hence, the bimolecular termination model was applied to two formulations at 0.5 wt% of two photoinitiators. Figures 4.84A and 4.84B shows the value of the ratio of rate constants calculated as per bimolecular termination model at various conversions for formulations containing 0.5 wt% of IRGACURE 651 and DAROCUR TPO respectively. It was observed that the value of the ratio (k_t^b/k_p) at low conversions was found to be much higher than at higher conversions. The terminations occurring in the case of formulation containing 0.5 wt% of DAROCUR TPO at lower conversions are much higher than that for IRGACURE 651. This confirms that for formulation containing 0.5 wt% DAROCUR TPO, the radical radical terminations were much pronounced in the initial stages of reaction as compared to formulation containing 0.5 wt% of IRGACURE 651.

At higher conversions due to influence of diffusion controlled reactions, the ratio represents a more or less plateau for formulation containing 0.5 wt% of DAROCUR TPO showing a steady and gradual reaction diffusion which was not noted in formulation containing 0.5 wt% of IRGACURE 651. Or in other words, the plateau represents a similar rate of propagation and termination reactions occurring at the same time.¹⁴ It has to be noted that the value of the ratio at high conversions are found to show an increase towards the onset of vitrification for both systems. This is because the decrease in the rate of propagation towards vitrification is slightly lower than termination due to very high

mobility restrictions, which is much pronounced in long radical chains. In other words the system at high conversions can be assumed to follow the monomolecular termination model to a greater extent as radical trapping predominates over any other termination phenomena.⁴ Since majority of the termination phenomena is bimolecular before the upper limit of attained conversions, the evaluation of the kinetics using this model is appropriate. The occurrence of the monomolecular termination is higher, if the system vitrifies very early.¹³ Similar observation of increase in the value of ratio (k_t^b/k_p) at high conversion as per bimolecular termination model is reported by Andrzejewska et al.^{14, 15}

4.2.1.3.5 Post photopolymerization studies

Thermogravimetric analysis

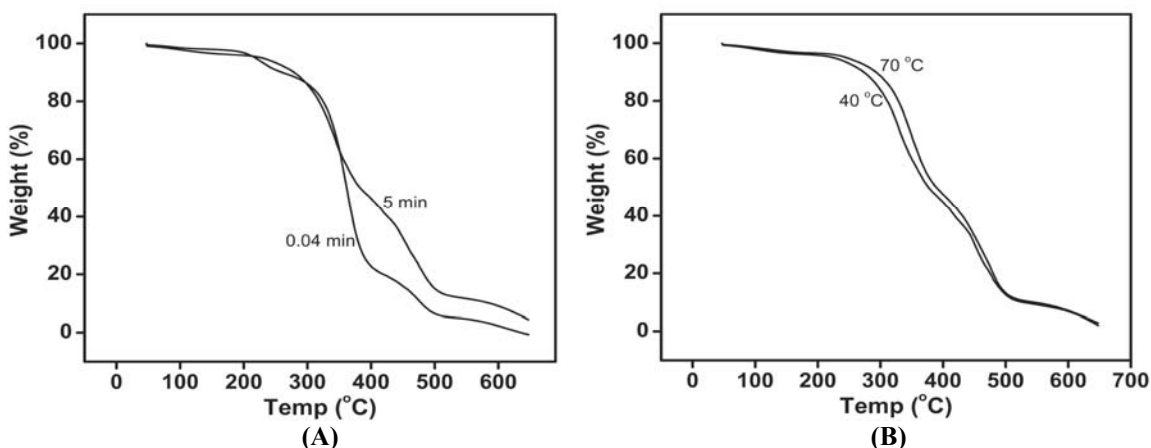


Figure 4.85 Thermogravimetric degradation profiles at 20 °C/min of macromonomeric formulation containing 50 wt% of HEA and 0.5 wt% of DAROCUR TPO (A) photocured at 40 °C and 0.04 min and 5 min of irradiation at 1.93 mW/cm² and (B) at 40 and 70 °C at 4.47 mW/cm². Analyses done after one week storage.

The thermogravimetric degradation profile given in Figure 4.83 (A) shows that the extent of crosslinking occurring in a photocured matrix (5 min irradiated) and that of a photo initiated matrix (0.04 min irradiated) which were left alone in dark for a week showed certain variations in the extent of cure. They follow a similar trend up to 45% loss. A faster degradation of photoinitiated matrix was observed after 45% weight loss. The photoinitiated matrix had undergone polymerization in dark in an efficient manner. This can be due to slow and large time scale of radical diffusion or reaction diffusion occurring due to the plasticization effect of HEA. The degradation profile given in Figure 4.83 (B) shows that the system is more crosslinked at higher temperature.

DSC analysis

Macromonomeric formulation containing 50 wt% excess HEA and 1 wt% of IRGACURE 651 photocured at 40 °C and 1.93 mW/cm² were subjected to thermal analysis using DSC. The T_g of the photocured sample was found to be 62.6 °C. The extent of vitrification is found to depend on many parameters of which the initial viscosity as well as the ultimate T_g of the photocured sample have higher influence. Vitrification is enhanced, with increase in initial viscosity of the formulation and increase in T_g of the cured network.¹¹ For this system, the initial viscosity was found to be 993 cP while the photocured material had a T_g of 62.6 °C. As compared to the ethoxylated system studied in Section 4.2.1.2, the T_g values are similar, and hence the delay in vitrification in this system is most probably due to a reduction in initial viscosity as well as a much gradual onset of reaction diffusion leading to higher conversions.

4.2.1.4 Photopolymerization of bisaromatic urethane diacrylate based on bis[4-(β-hydroxypropoxy)-phenyl] sulphone, hexamethylene diisocyanate and 2-hydroxyethyl methacrylate ((System 4B-3)

A bisaromatic diacrylate based on bis[4-(β-hydroxypropoxy)-phenyl] sulphone (HPPS), HMDI and HEMA was synthesized and their photocuring studies were carried out. Estimation of kinetic parameters were done based on the heat flow profile obtained during the photopolymerization process.

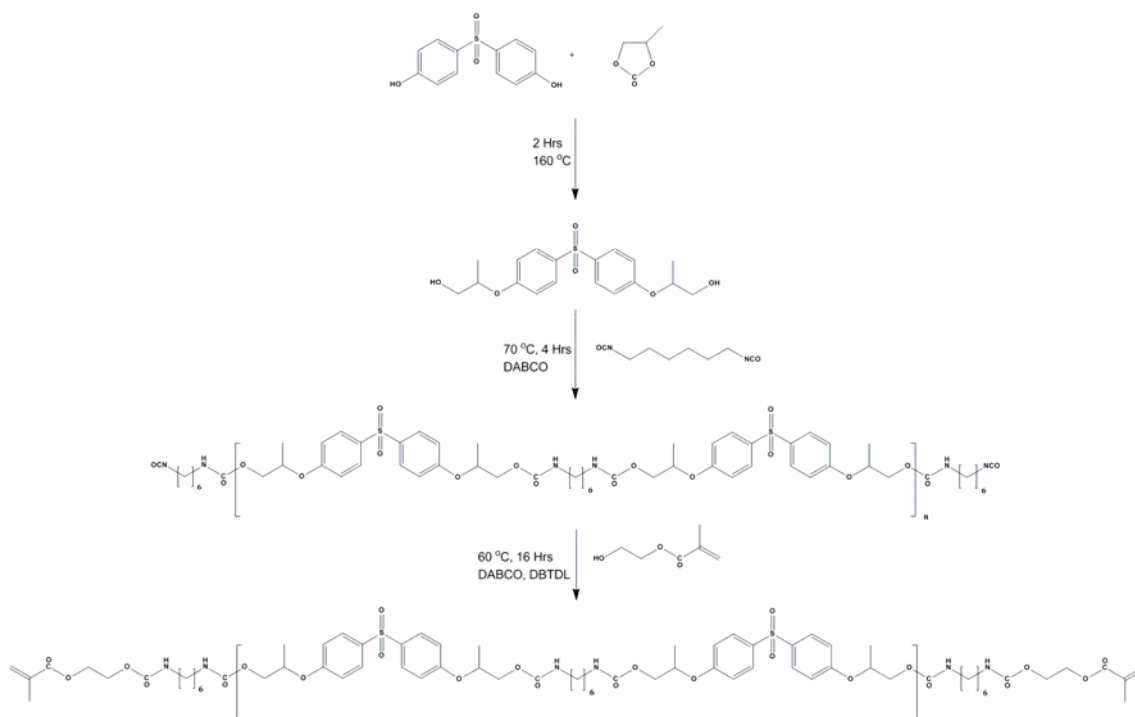


Figure 4.86 Synthesis pathway of bisaromatic urethane diacrylate based on HPPS, HMDI and HEMA

4.2.1.4.1 Procedure for synthesis

Synthesis of bis[4-(β-hydroxypropoxy)-phenyl] sulphone (HPPS)

The monomer was synthesized from 4,4'- bisphenol S and propylene carbonate using a reported procedure.¹

Synthesis of prepolymer

To a 100 mL three necked round bottom flask provided with a half moon stirrer and stuffing box was flushed with nitrogen for 2 min. To it was added 12 g (32.76 mmol) of HPPS followed by addition of 12 mg (0.107 mmol) of DABCO and 36 mL dry tetrahydrofuran. The system was homogenized by stirring at 80 rpm at 50 °C under nitrogen purge. 5.83 mL (36.05 mmol) of HMDI was added to it drop-wise under 100 rpm. After addition, the temperature was increased to 70 °C and continued for a period of 4 h to obtain the diisocyanate terminated prepolymer. The residual isocyanate was noted (ASTM D 2572). The residual isocyanate content was found to be 3.253%. IR spectrum was noted.

IR: 3351 and 1534 (NH, urethane), 2273 (NCO), 1743 (CO, urethane), 1210 (N-CO-O, sym str) and 959 (N-CO-O, asym str), 2973, 2935 and 2862 (C-H) cm^{-1} .

Synthesis of macromonomer

1.59 mL (13.11 mmol) of HEMA and 200 mg (0.3167 mmol) of dibutyl tin dilaurate were added to the prepolymer and stirred under 60 °C at 80 rpm for 16 h until the isocyanate peak disappeared from the IR spectrum.

To the flask, 20 mL of tetrahydrofuran was added and the product was transferred to 200 mL distilled water in a 500 mL beaker under stirring during addition. The crude product settled down and the top water layer was decanted. The washing was repeated for three more times with stirring for five minutes followed by settling time of 15 minutes until the washings are devoid of excess HEMA. The macromonomer was solvated with minimum amount of tetrahydrofuran and transferred to a 100 mL R B flask after solvation and vacuum was applied to the viscous product at 40 °C for 2 h. The viscous polymer was then dried in vacuum oven for 10 h at 60 °C. IR and NMR spectra were noted. The molecular mass was found by VPO.

IR: 3365 and 1537 (NH, urethane), 1714 (CO, urethane), 1638, 1455 (C=C, acrylate), 1215 (N-CO-O, sym str) and 954 (N-CO-O, asym str), 2973, 2935 and 2861 (C-H) cm^{-1} .

$^1\text{H NMR}$ (DMSO- D_6): 1.23 and 1.75 (-CH₂-, hexamethylene), 1.86 (-CH₃, methacrylate), 2.06 (-CH₂-CH(CH₃-), 2.93 (CH₂-NH-), (-NH-CO-O-CH₂-CH(CH₃-), (methylene and chain extension overlaps with water peak in DMSO), 4.98 (-NH-, internal), 4.20 (-NH-, terminal), 5.68 and 6.02 (CO-O-C(CH₃)=CH₂), 6.91 and 7.71 (CH, aromatic ring)

$^{13}\text{C NMR}$ (CDCl₃): 16.9 (-CH₂-CH(CH₃-), 18.19 (CH₃, methacrylate), 26.16 and 29.57, (-CH₂-hexamethylene), 39.42 (-CH₂-NH), 63.38 (-CO-O-CH₂-CH₂-O-CO-NH-) and 61.78 (-CO-O-CH₂-CH₂-O-CO-NH-) 70.76 (-CO-O-CH₂-CH(CH₃)-O-), 68.04 (-CO-O-CH₂-CH(CH₃)-O-) 62.85 (-O-CH₂-CH₂-O-CO-), 116.21 and 129.61 (CH, aromatic), 126.27 (CH₂=C(CH₃-), 129.32 (CH₂=C(CH₃-), 132.35 and 161.86 (C, aromatic), 155.92 (-CO-NH, terminal) and 158.43 (-CO-NH, internal), 166.71 (C=O, acrylate)

4.2.1.4.2 Formulation

The macromonomer being highly viscous was then formulated using addition of 75 wt% HEMA and photoinitiator to obtain photopolymerizable compositions. The photoinitiators of choice were IRGACURE 651, DAROCUR TPO and IRGACURE 184. To 500 mg of macromonomer containing excess HEMA were added 0.5, 1 and 2 wt% of above photoinitiators to obtain nine photopolymerizable compositions. The compositions

were mixed in a vibrating mill prior to weighing. The Brookfield viscosity of the macromonomer with 75 wt% HEMA with a shear rate of 133.3 sec^{-1} at $50 \text{ }^{\circ}\text{C}$ was noted with spindle number 1 at 10 rpm.

4.2.1.4.3 Photocuring studies

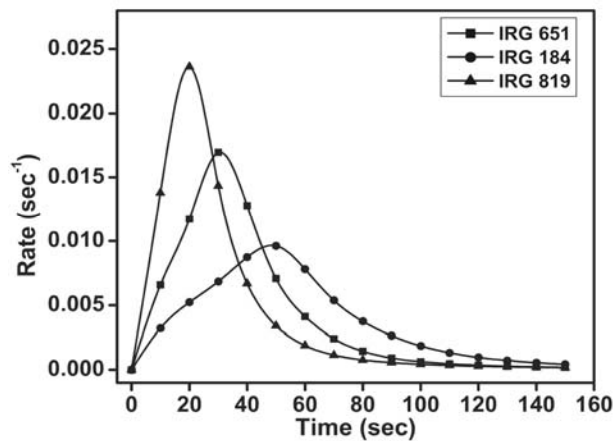
5 mg of the material was taken in a DSC pan and subjected to photo curing studies. The heat flow profiles obtained during the *in situ* photocuring process was recorded as a function of time under an isothermal condition of 40 and $70 \text{ }^{\circ}\text{C}$. The intensity of irradiation was kept at 1.78 mW/cm^2 using a polychromatic radiation of $250\text{-}450 \text{ nm}$ using a 100 W high pressure mercury short arc lamp. The normalized outputs in W/g against time were recorded. The rates of polymerization as well as corresponding conversions were calculated for all the compositions. The reaction was also carried out at a higher intensity of 3.26 mW/cm^2 at $40 \text{ }^{\circ}\text{C}$ to understand the effect of intensity and temperature on cure. The evaluation of variable autocatalytic kinetic model was carried out using TA advantage specialty library software. Post polymerization degradation profile and glass transition temperature of photocured matrix were noted using TGA (ramp rate of $20 \text{ }^{\circ}\text{C/min}$ from 30 to $650 \text{ }^{\circ}\text{C}$) and DSC (ramp rate of $10 \text{ }^{\circ}\text{C/min}$ from 30 to $150 \text{ }^{\circ}\text{C}$) methods, respectively.

4.2.1.4.4 Results and discussion

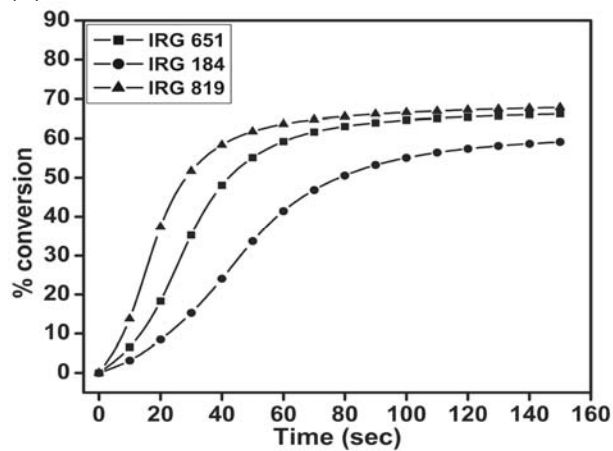
The existence of terminal isocyanate group in the prepolymer was confirmed by IR spectroscopy. Confirmation for complete conversion of isocyanate group during the formation of macromonomer was noted by IR, ^1H and ^{13}C NMR spectroscopy. The molecular mass was found to be 1102 g/mol by VPO. The total theoretical heat flow¹⁶ (ΔH_{theor}) for the system was calculated to be 237.34 J/g . The viscosity of the macromonomer with 75 wt% HEMA with a shear rate of 133.3 sec^{-1} at $50 \text{ }^{\circ}\text{C}$ was found to be 1856 cP .

The rate and conversion profiles obtained from photocuring studies of macromonomeric formulations containing 75 wt% of HEMA as reactive diluent with three photoinitiators at 0.5, 1 and 2 wt% compositions at $40 \text{ }^{\circ}\text{C}$ and 1.78 mW/cm^2 are given below in Figures 4.87 to 4.89 (A-C).

(A)



(B)



(C)

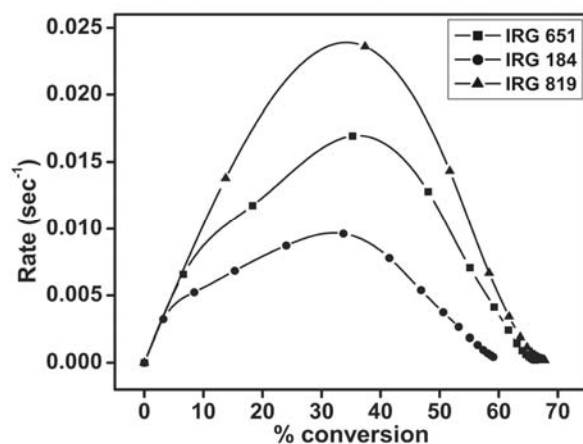
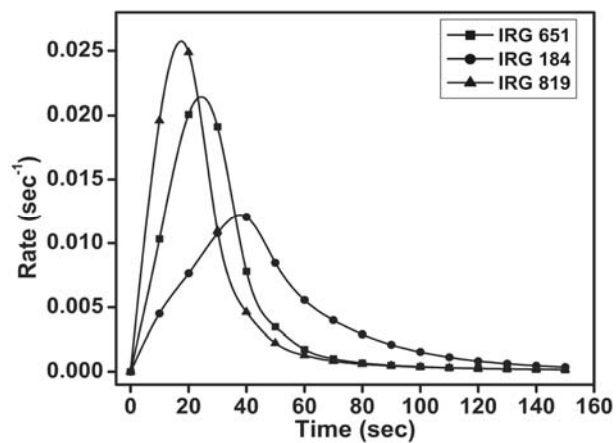
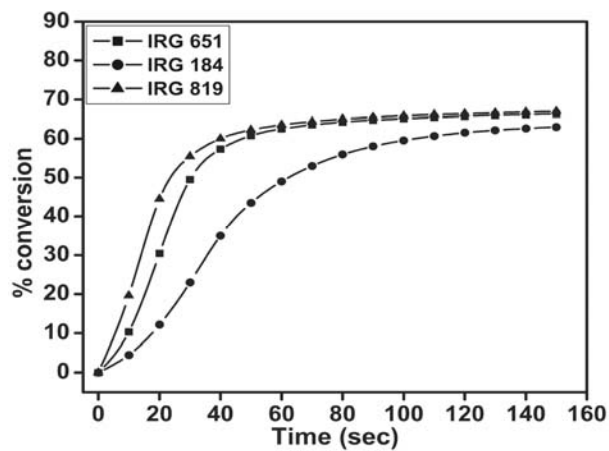


Figure 4.87(A-C) Time dependent rate and conversion profiles of macromonomeric formulations containing 75 wt% HEMA and 0.5 wt% of three photoinitiator at 40 °C and 1.78 mW/ cm²

(A)



(B)



(C)

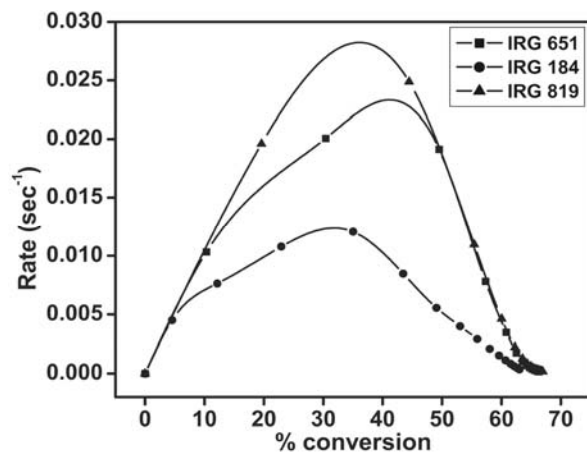


Figure 4.88(A-C) Time dependent rate and conversion profiles of macromonomeric formulations containing 75 wt% HEMA and 1 wt% of three photoinitiator at 40 °C and 1.78 mW/ cm²

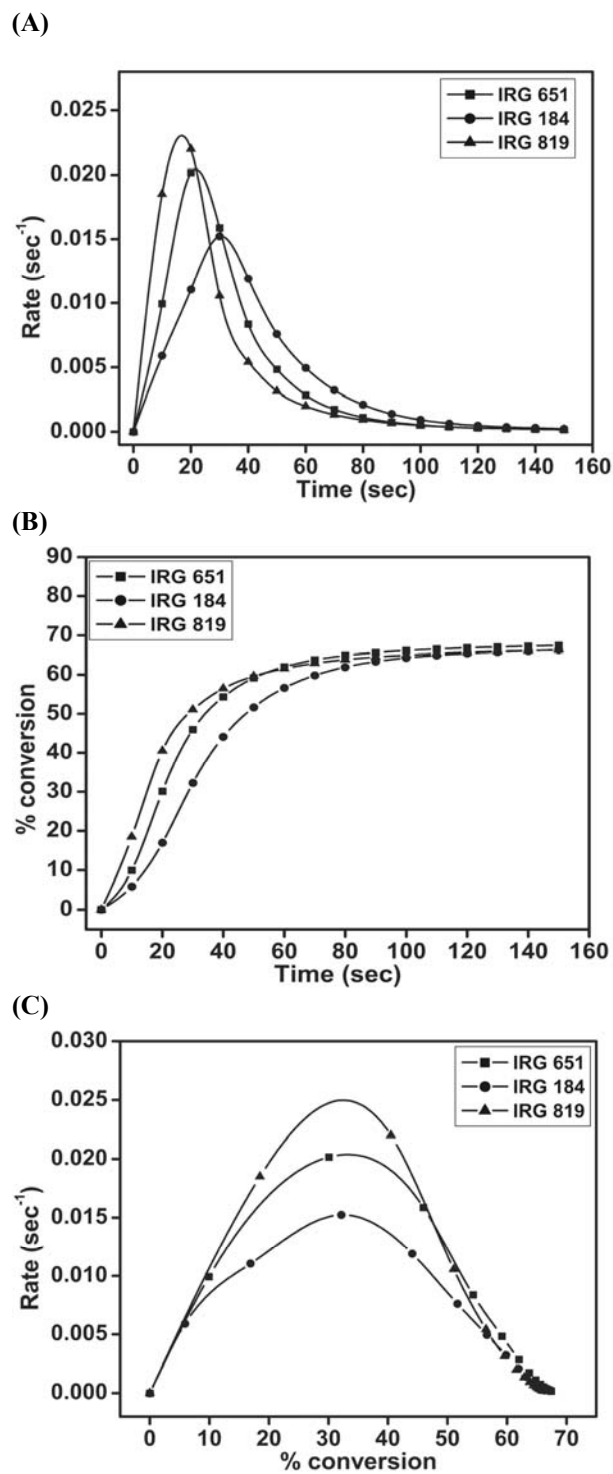


Figure 4.89(A-C) Time dependent rate and conversion profiles of macromonomeric formulations containing 75 wt% HEMA and 2 wt% of three photoinitiator at 40 °C and 1.78 mW/ cm²

The rate and conversion profiles obtained from photocuring studies of macromonomeric formulations containing 75 wt% of HEMA as reactive diluent with three photoinitiators at 0.5, 1 and 2 wt% compositions at 70 °C and 1.78 mW/cm² are given below in Figures 4.90 to 4.92 (A-C).

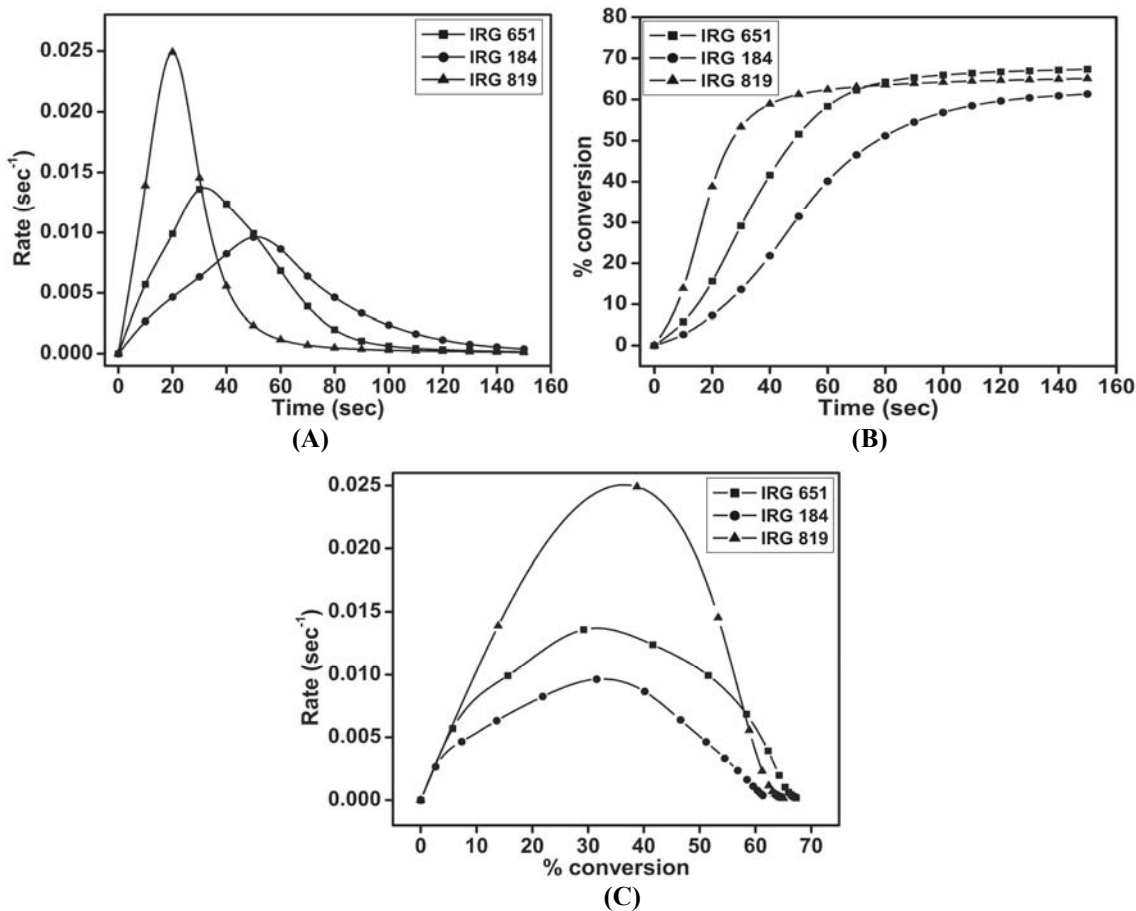


Figure 4.90(A-C) Time dependent rate and conversion profiles of macromonomeric formulations containing 75 wt% HEMA and 0.5 wt% of three photoinitiator at 70 °C and 1.78 mW/ cm²

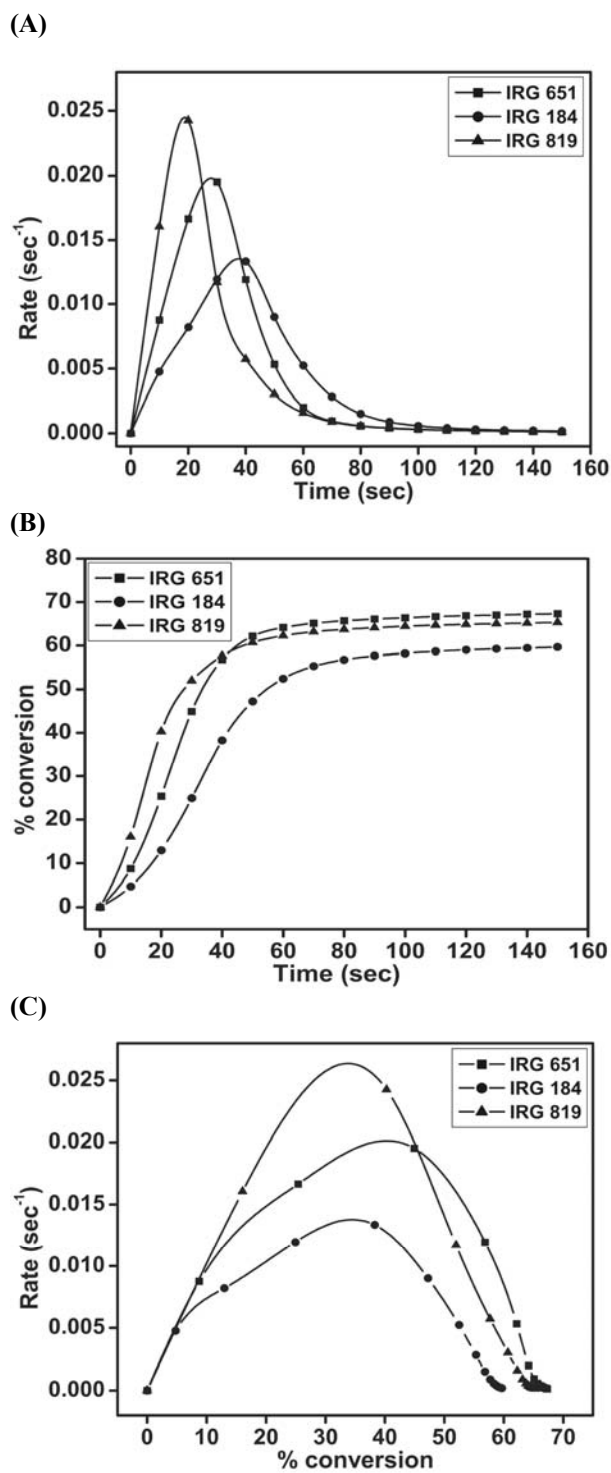


Figure 4.91(A-C) Time dependent rate and conversion profiles of macromonomeric formulations containing 75 wt% HEMA and 1 wt% of three photoinitiator at 70 °C and 1.78 mW/ cm²

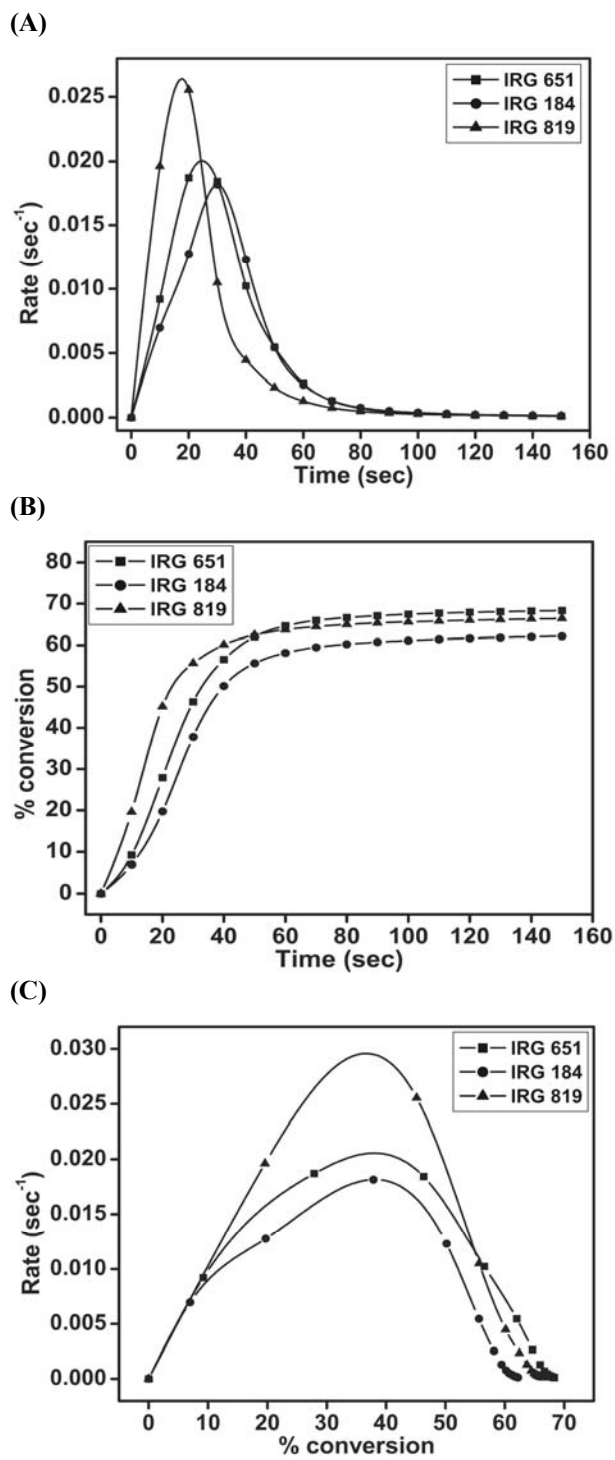


Figure 4.92(A-C) Time dependent rate and conversion profiles of macromonomeric formulations containing 75 wt% HEMA and 2 wt% of three photoinitiator at 70 °C and 1.78 mW/ cm²

The rate and conversion profiles obtained from photocuring studies of macromonomeric formulations containing 75 wt% of HEMA as reactive diluent with three photoinitiators at 0.5, 1 and 2 wt% compositions at 40 °C and 3.26 mW/cm² are given below in Figures 4.93 to 4.95 (A-C).

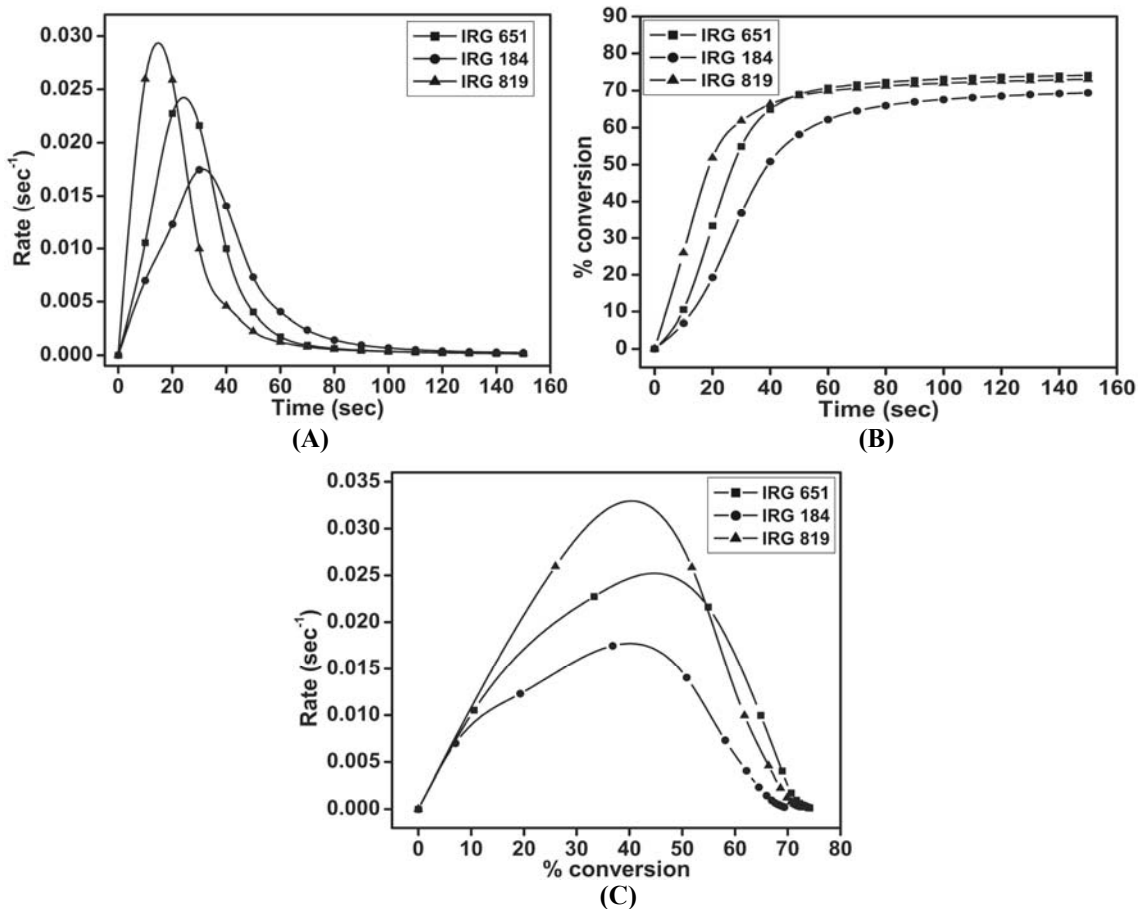


Figure 4.93(A-C) Time dependent rate and conversion profiles of the macromonomeric formulations containing 75 wt% HEMA and 0.5 wt% of three photoinitiator at 40 °C and 3.26 mW/cm²

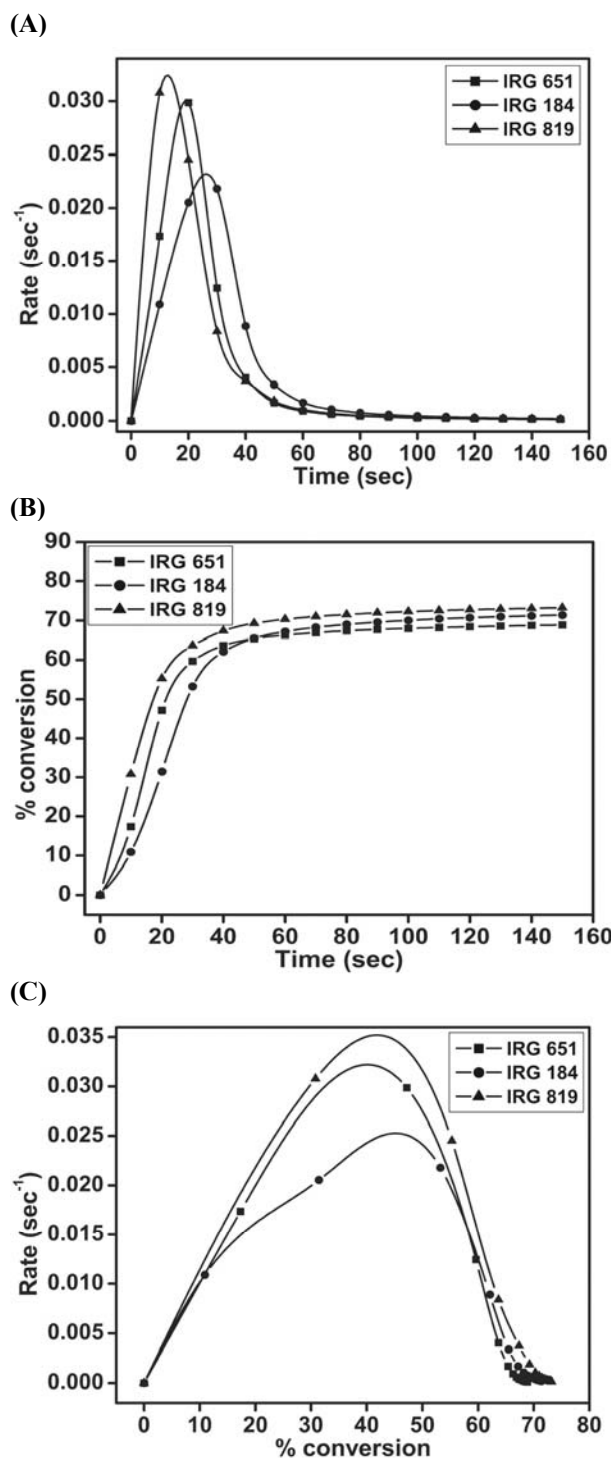


Figure 4.94(A-C) Time dependent rate and conversion profiles of the macromonomeric formulations containing 75 wt% HEMA and 1 wt% of three photoinitiator at 40 °C and 3.26 mW/cm²

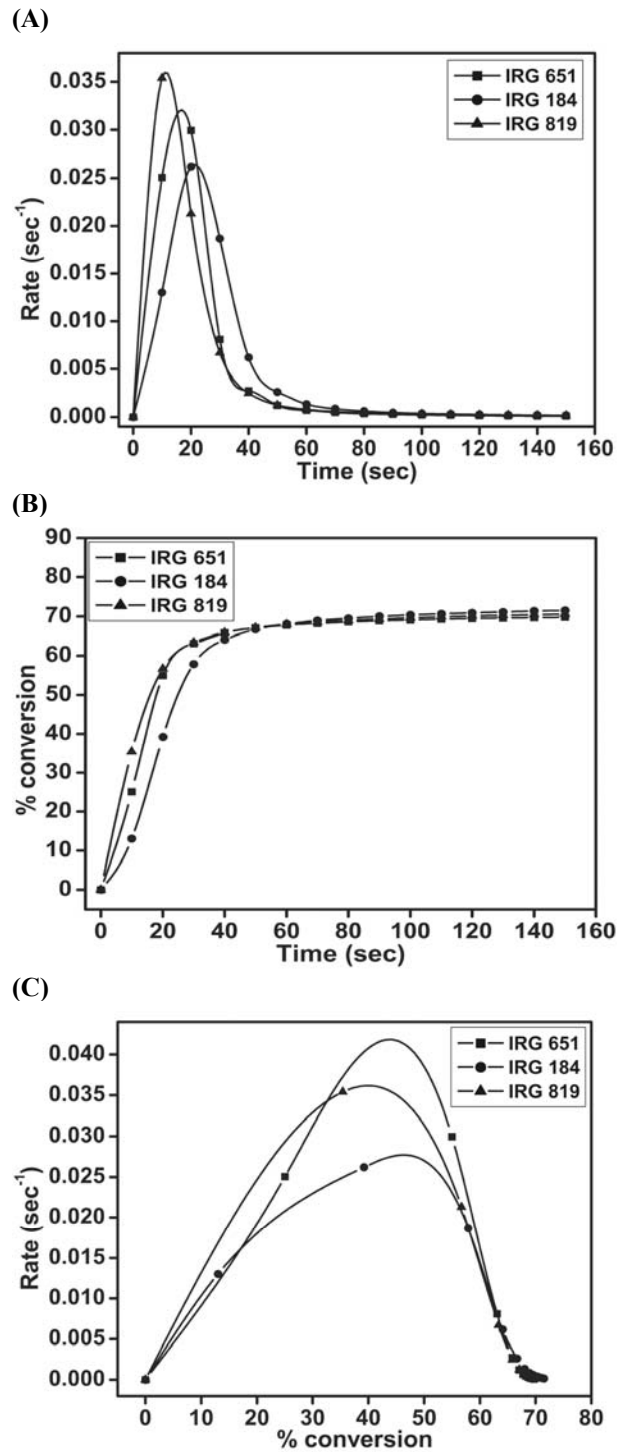


Figure 4.95(A-C) Time dependent rate and conversion profiles of the macromonomeric formulations containing 75 wt% HEMA and 2 wt% of three photoinitiator at 40 °C and 3.26 mW/cm²

Table 4.38 Kinetic parameters of macromonomeric formulations calculated from the heat flow profiles

Photo-initiator	% conc. of photo-initiator	Temp. (°C)	Intensity (mW/cm ²)	Induction Time (sec)	Peak Maximum Time (sec)	R _{p max} (x 10 ⁻²) (sec ⁻¹)	C _{max} (%)	Heat of reaction (J/g)
IRGACURE 651	0.5	40	1.78	1.78	30.47	1.70	67.16	159.4
	1	40	1.78	1.27	24.45	2.14	67.12	159.3
	2	40	1.78	1.41	21.64	2.05	68.26	162
	0.5	40	3.26	1.35	24.19	2.43	74.87	177.7
	1	40	3.26	0.78	19.16	3	69.39	164.7
	2	40	3.26	0.44	16.77	3.20	70.19	166.6
	0.5	70	1.78	2.01	31.87	1.37	68.13	161.7
	1	70	1.78	1.42	27.89	1.98	67.88	161.1
	2	70	1.78	1.44	24.45	2	68.89	163.5
IRGACURE 184	0.5	40	1.78	3.55	48.64	0.97	60.84	144.4
	1	40	1.78	2.53	37.91	1.22	64.51	153.1
	2	40	1.78	2.02	30.54	1.52	67.41	160
	0.5	40	3.26	1.66	31.15	1.76	70.49	167.3
	1	40	3.26	1.16	26.26	2.32	72.34	171.7
	2	40	3.26	1.09	21.28	2.64	72.26	171.5
	0.5	70	1.78	4.32	51.02	0.97	62.69	148.8
	1	70	1.78	2.41	37.62	1.36	60.50	143.6
	2	70	1.78	1.68	30.21	1.82	62.86	149.2
IRGACURE 819	0.5	40	1.78	0.93	19.93	2.36	68.68	163
	1	40	1.78	0.57	17.53	2.58	67.79	160.9
	2	40	1.78	0.58	16.89	2.30	67.12	159.3
	0.5	40	3.26	0.40	14.70	2.93	73.82	175.2
	1	40	3.26	0.31	12.67	3.24	73.99	175.6
	2	40	3.26	0.25	11.31	3.60	71.29	169.2
	0.5	70	1.78	0.95	19.94	2.49	65.64	155.8
	1	70	1.78	0.75	18.87	2.45	65.90	156.4
	2	70	1.78	0.59	17.67	2.64	66.99	159

In Table 4.38 the kinetic parameters obtained from the photo DSC heat flow profiles are presented. The formulations have 75 wt% excess HEMA and hence is expected to show the effect of added reactive diluent. From the Table, a decrease in induction time and peak maximum time was observed with increase in concentration of photoinitiator. At 40 °C, both the induction as well as peak maximum time were found to show a decrease with increase in irradiation intensity from 1.78 to 3.26 mW/cm². All the above observations show that the systems have enhanced mobility and better radical diffusion. At 70 °C the value of induction time and peak maximum time were increased than that observed at 40 °C under similar intensity. This shows a greater extent of radical combinations taking place at higher temperature thereby reducing the quantum yield for

intitiation.⁶ The value of $R_{p \text{ max}}$ was found to show an increase with increase in concentration of photoinitiator showing a gradual onset of reaction diffusion. The increase in irradiation intensity at 40 °C for a particular concentration of photoinitiator was found to show an enhancement in value of $R_{p \text{ max}}$ showing better radical diffusion.¹⁷ A reduction in the value of $R_{p \text{ max}}$ was observed for irradiation done at 1.78 mW/cm² from 40 to 70 °C due to enhanced propagation and lesser number of effective radicals involved in propagation.¹⁸ The final conversion ranged from 60 to 74%. Higher conversions were observed for irradiation done at higher intensity. During the entire course of the heat flow profile, the system at higher intensity can initiate more radicals which resulted in higher conversions.¹⁷

Table 4.39 Evaluation of kinetic parameters of macromonomeric formulations as per autocatalytic model at 40 and 70 °C at 1.78 mW/ cm²

Photoinitiator	% conc. of photo-initiator	Temperature (°C)	Autocatalytic		
			n	m	k (min ⁻¹)
IRGACURE 651	0.5	40	2.74	0.84	6.94
	0.5	70	2.06	0.67	3.67
	1	40	2.51	0.83	8.71
	1	70	2.07	0.74	6
	2	40	3.61	0.93	12.9
	2	70	2.80	0.85	9.22
IRGACURE 184	0.5	40	2.66	0.76	3.31
	0.5	70	2.59	0.80	3.44
	1	40	3.51	0.89	6.53
	1	70	2.44	0.77	4.50
	2	40	3.15	0.85	7.19
	2	70	2.08	0.74	5.24
IRGACURE 819	0.5	40	3.13	0.80	10.8
	0.5	70	2.87	0.82	11.1
	1	40	3.45	0.83	15
	1	70	3.70	0.88	15.3
	2	40	4.07	0.84	15.9
	2	70	3.15	0.78	12.7

Table 4.39 shows the value of kinetic parameters as per variable autocatalytic kinetic model at 40 and 70 °C using 0.5, 1 and 2 wt% photoinitiator at 1.78 mW/cm². The system was found to follow the model over a considerable range during the course of reaction. Andrzejewska et al.¹⁹ have reported that in the case of photopolymerization of di(meth)acrylates, the value of n is found to decrease with increase in temperature at a

low irradiation intensity of 1.8 mW/cm². This effect was pronounced in the reaction by a decrease in final conversion. Similar observation was obtained in the above systems.

Table 4.40 Evaluation of kinetic parameters of macromonomeric formulations as per autocatalytic model at 40 °C and 3.26 mW/cm²

Photoinitiator	% conc. of photoinitiator	Autocatalytic		
		n	m	k (min ⁻¹)
IRGACURE 651	0.5	2.11	0.82	8.69
	1	2.63	0.84	13.1
	2	3	0.93	21.2
IRGACURE 184	0.5	2.27	0.79	5.85
	1	1.83	0.74	6.62
	2	2.07	0.78	8.76
IRGACURE 819	0.5	3.36	0.85	19.1
	1	3.50	0.9	24.6
	2	3.43	0.81	22.1

Table 4.40 shows the value of kinetic parameters as per variable autocatalytic kinetic model at 40 °C using 0.5, 1 and 2 wt% photoinitiator at 3.26 mW/cm². The system was found to follow the model to certain extent as the value of n and m are constant. The value of specific rate constant (k) was found to show an increase in most cases with increase in concentration of photoinitiator at 40 °C and 3.26 mW/cm². From the autocatalytic analyses, we can infer that the formulations showed deviations from autocatalytic behaviour to certain extent.⁹ Both bimolecular as well as monomolecular terminations have influence on the reaction kinetics.¹³

4.2.1.4.5 Post photopolymerization studies

Thermogravimetric analysis

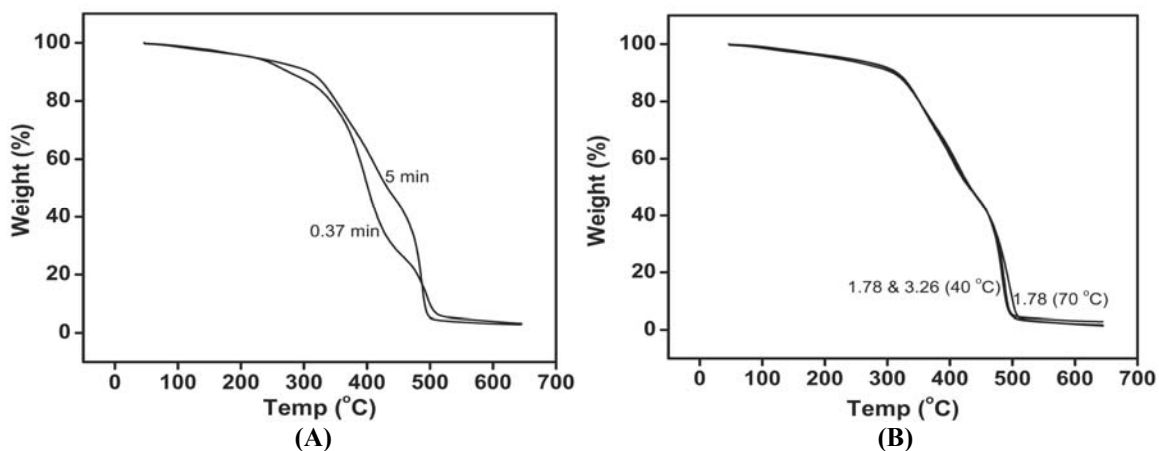


Figure 4.96 Thermogravimetric degradation profiles at 20 °C/min of macromonomeric formulation containing 75 wt% of HEMA and 0.5 wt% of IRGACURE 184 (A) photocured at 40 °C and 0.37 min and 5 min of irradiation at 1.78 mW/cm² and (B) at 40 and 70 °C. Analyses done after one week storage

The thermogravimetric degradation profile given in Figure 4.96 (A) show that the extent of crosslinking occurring on a photocured matrix (5 min irradiated) and that of a photo initiated matrix (0.37 min irradiated) which was left in dark for a week showed variations in the extent of cure. They follow a similar trend up to 10% weight loss. A faster degradation of photoinitiated matrix was observed after 10 to 15% weight loss. This shows that the photo initiated matrix has undergone the polymerization in dark.²⁰ This can be due to slow and large time scale of radical/reaction diffusion occurring due to the plasticization effect of HEMA. The degradation profile given in Figure 4.96 (B) shows that the system is more crosslinked at higher temperature. The effect of intensity of the degradation profile at 40 °C for 1.78 and 3.26 mW/cm² was found to be negligible on storage.

DSC analysis

Macromonomeric formulation containing 75 wt% excess HEMA and 1 wt% of IRGACURE 651 photocured at 40 °C and 1.78 mW/cm² was subjected to thermal analysis using DSC. The T_g of the photocured sample was found to be 55.5 °C. The extent of vitrification is found to depend on many parameters of which the initial viscosity of the formulation as well as the ultimate T_g of the photocured sample have

higher influence.¹¹ For this system, the initial viscosity was found to be 1856 cP while the photocured material had a T_g of 55.5 °C.

4.2.1.5 Photopolymerization of bisaromatic urethane diacrylate based on bis[4-(β -hydroxyethoxy)] biphenyl, isophorone diisocyanate and hydroxypropyl acrylate. (System 4B-4)

A bisaromatic diacrylate based on bis[4-(β -hydroxyethoxy)] biphenyl (HEBP), IPDI and HPA was synthesized and their photocuring studies were carried out. Estimation of kinetic parameters were done based on the heat flow profile obtained during the photopolymerization process.

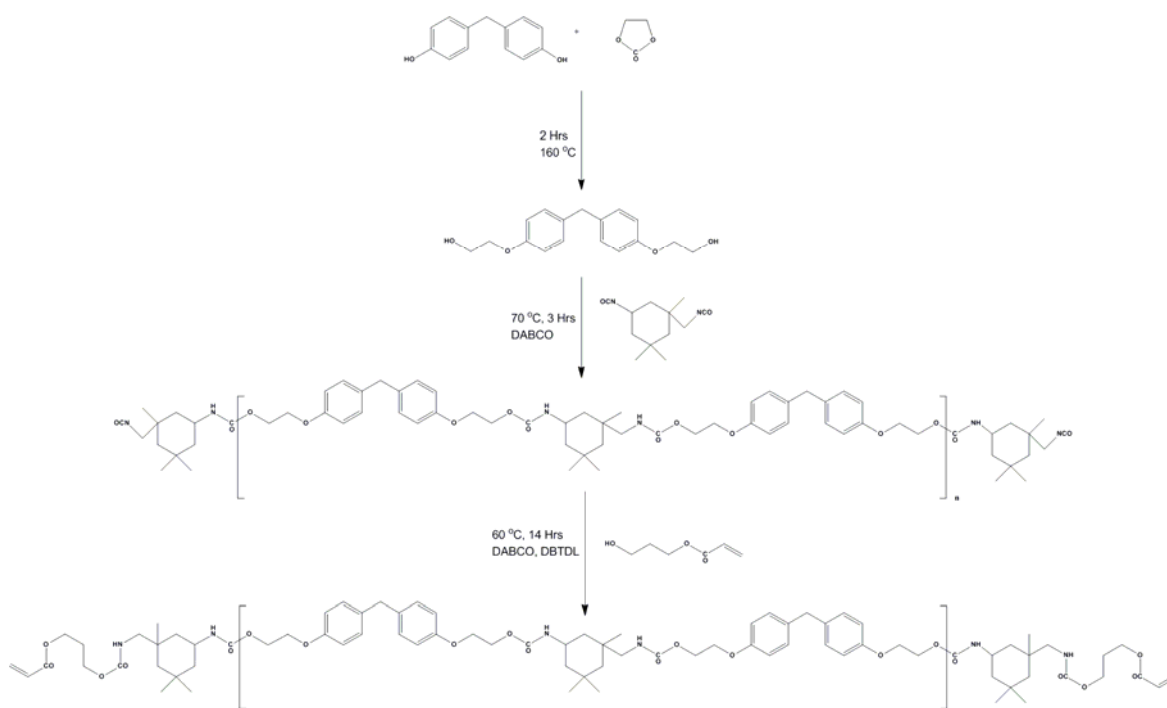


Figure 4.97 Synthesis pathway of bisaromatic urethane diacrylate based on HEBP, IPDI and HPA

4.2.1.5.1 Procedure for synthesis

Synthesis of bis[4-(β -hydroxyethoxy)] biphenyl (HEBP)

The monomer was synthesized from 4,4'-dihydroxy biphenyl and ethylene carbonate using a reported procedure.¹

Synthesis of prepolymer

To a 100 mL three necked round bottom flask provided with a half moon stirrer and stuffing box was flushed with nitrogen for 2 min. To it was added 10 g (36.46 mmol) of HEBP followed by addition of 10 mg (0.08915 mmol) of DABCO and 30 mL dry N,N'-dimethylacetamide. The system was homogenized by stirring at 80 rpm at 50 °C under nitrogen purge. 8.11 mL (38.27 mmol) of IPDI was added to it drop-wise under 100 rpm. After addition, the temperature was increased to 70 °C and continued for a period of three hours to obtain the diisocyanate terminated prepolymer. The residual isocyanate was noted (ASTM D 2572). The residual isocyanate content was found to be 3.921%. IR spectrum was noted.

IR: 3444 and 1551 (NH, urethane), 2257 (NCO), 1718 (CO, urethane), 1242 (N-CO-O, sym str) and 1057 (N-CO-O, asym str), 2934 (C-H) cm^{-1} .

Synthesis of macromonomer

0.9 mL (7.22 mmol) of HPA and 200 mg (0.3167 mmol) of dibutyl tin dilaurate were added to HEBP under 100 rpm and stirred at 60 °C and 80 rpm for 14 h until the isocyanate peak disappeared from the IR spectrum. The product was transferred to 200 mL distilled water in a 500 mL beaker with stirring during addition. The crude solid product settled down and the top water layer was decanted. 200 mL water was again added and the product was filtered under suction until devoid of solvent and excess HPA. It was then dried in vacuum oven for 10 h at 60 °C. The solid macromonomer obtained was subjected to molecular mass analysis by VPO.

IR: 3444 and 1551 (NH, urethane), 1716 (CO, urethane), 1633, 814 (C=C, acrylate), 1239 (N-CO-O, sym str) and 961 (N-CO-O, asym str), 2936 (C-H) cm^{-1} .

*¹H NMR (DMSO-*D*₆):* 0.85 and 0.96 (-CH₃, alicyclic), 1.08 and 1.16 (-CH₂-, alicyclic), 1.43 (-CO-O-CH₂-CH₂-CH₂-, acrylate), 2.72 (-CH₂-NH-), 3.83 (=CH-NH-, alicyclic ring), 3.93 (-NH-CO-O-CH₂-CH₂-O-), 4.16 (-NH-CO-O-CH₂-CH₂-O-), 4.26 (-CO-O-CH₂-CH₂-CH₂-, acrylate), 4.93 (CH₂=CH-CO-O-CH₂-CH₂-, acrylate), 4.45 (-NH-, internal), 5.54 (-NH-, terminal), 5.96 and 6.32 (CH₂=CH-CO-O-, acrylate), 6.19 (CH₂=CH-CO-O-, acrylate), 7 and 7.5 (CH, aromatic ring)

4.2.1.5.2 Formulation

The macromonomer being solid was then formulated using addition of 300 wt% HPA and photoinitiator to obtain photopolymerizable compositions. The photoinitiators of choice were IRGACURE 651, DAROCUR TPO and IRGACURE 184. To 500 mg of

macromonomer containing excess HPA were added 0.5, 1 and 2 wt% of photoinitiators to obtain nine photopolymerizable compositions. The compositions were mixed in a vibrating mill prior to weighing. The Brookfield viscosity of the macromonomer with 300 wt% HPA with a shear rate of 133.3 sec^{-1} at $50 \text{ }^\circ\text{C}$ was noted with spindle number 1 at 10 rpm.

4.2.1.5.3 Photocuring studies

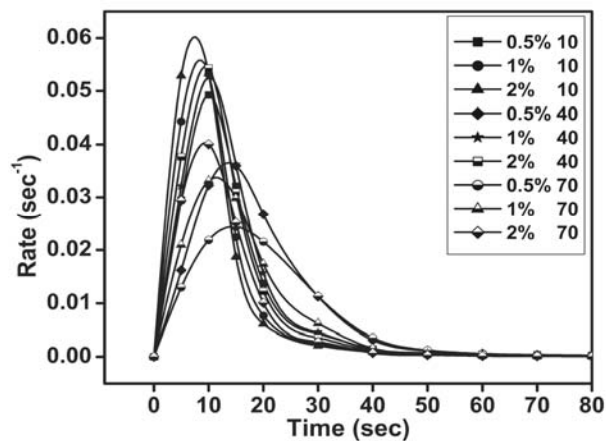
5 mg of the material was taken in a DSC pan and subjected to photo curing studies. The heat flow profiles obtained during the *in situ* photocuring process was recorded as a function of time under an isothermal condition of 10, 40 and $70 \text{ }^\circ\text{C}$. The intensity of irradiation was kept at 2.27 mW/cm^2 using a polychromatic radiation of 250-450 nm using a 100W high pressure mercury short arc lamp. The normalized outputs in W/g against time were recorded. The rates of polymerization as well as corresponding conversions were calculated for all the compositions. The evaluation of variable autocatalytic kinetic model was carried out using TA advantage specialty library software. Post polymerization degradation profile and glass transition temperature of photocured matrix were noted using TGA (ramp rate of $20 \text{ }^\circ\text{C/min}$ from 30 to $650 \text{ }^\circ\text{C}$) and DSC (ramp rate of $10 \text{ }^\circ\text{C/min}$ from 30 to $150 \text{ }^\circ\text{C}$) methods, respectively.

4.2.1.5.4 Results and discussion

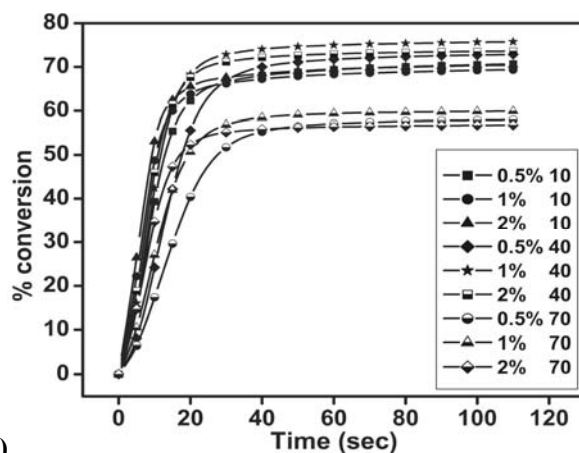
The existence of terminal isocyanate group in the prepolymer was confirmed by IR spectroscopy. Confirmation for complete conversion of isocyanate group during the formation of macromonomer was noted by IR and ^1H NMR spectroscopy. The molecular mass was found to be 1518 g/mol by VPO. The total theoretical heat flow² (ΔH_{theor}) for the system was calculated to be 525.1 J/g . The viscosity of the macromonomer with 300 wt% HPA with a shear rate of 133.3 sec^{-1} at $50 \text{ }^\circ\text{C}$ was found to be 1406 cP .

The rate and conversion profiles obtained from photocuring studies of macromonomeric formulations containing 300 wt% of HPA as reactive diluent with IRGACURE 651, DAROCUR TPO and IRGACURE 184 at 0.5,1 and 2 wt% compositions analyzed at 10,40 and $70 \text{ }^\circ\text{C}$ and 2.27 mW/cm^2 are given below in Figure 4.98 to 4.100 (A-C).

(A)



(B)



(C)

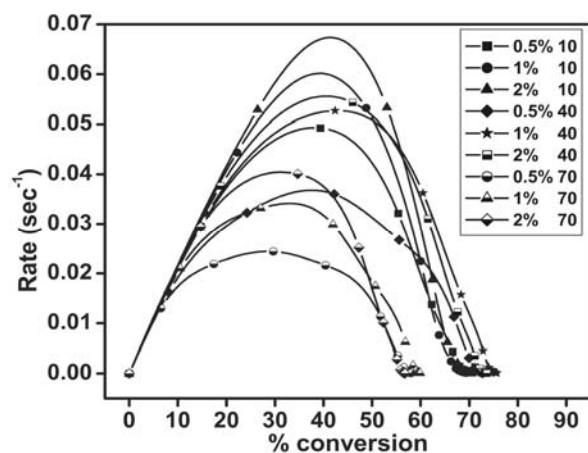
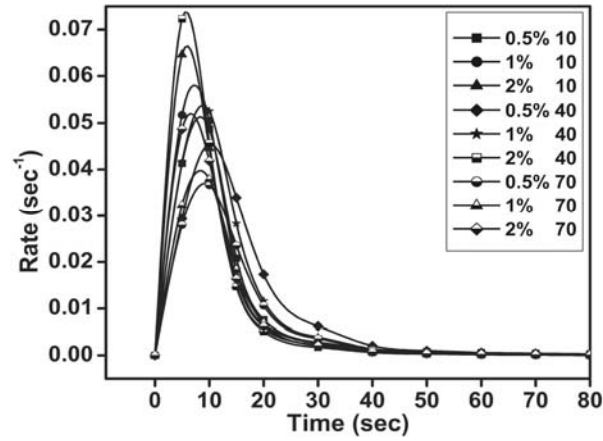
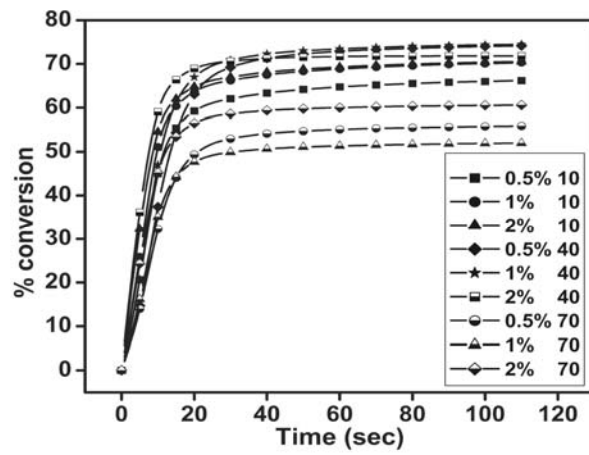


Figure 4.98(A-C) Time dependent rate and conversion profiles of the macromonomeric formulation containing 300 wt% HPA, and three different concentration of IRGACURE 651 at 10, 40 and 70 °C at $2.27 \text{ mW}/\text{cm}^2$

(A)



(B)



(C)

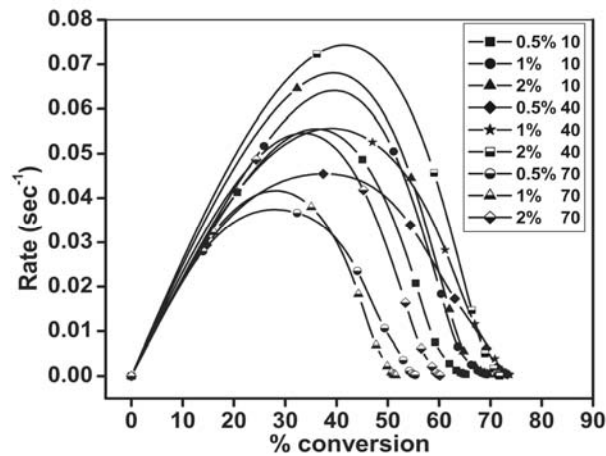
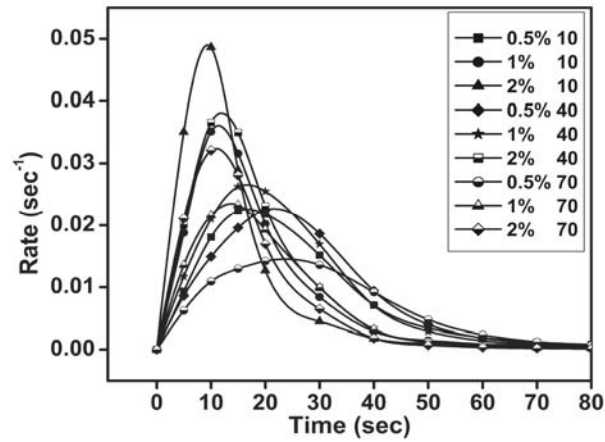
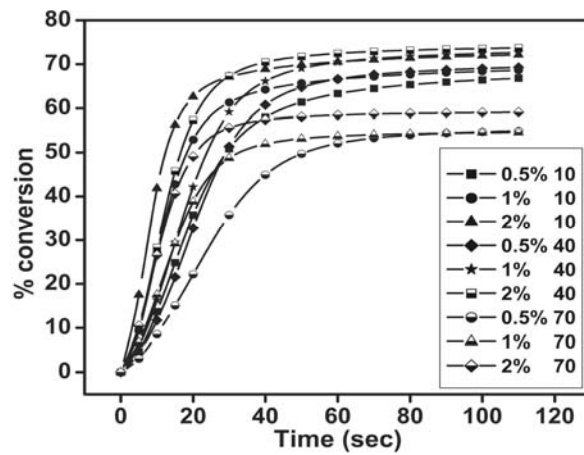


Figure 4.99(A-C) Time dependent rate and conversion profiles of the macromonomeric formulations containing 300 wt% HPA, and three different concentration of DAROCUR TPO at 10, 40 and 70 °C at 2.27 mW/cm^2

(A)



(B)



(C)

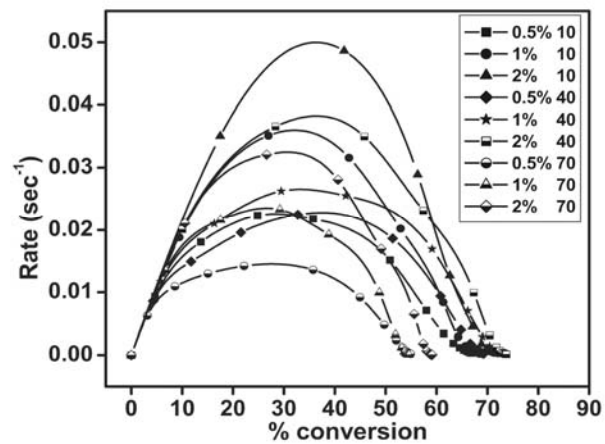


Figure 4.100(A-C) Time dependent rate and conversion profiles of the macromonomeric formulations containing 300 wt% HPA, and three different concentration of IRGACURE 184 at 10, 40 and 70 °C at 2.27 mW/ cm^2

Table 4.41 Kinetic parameters of macromonomeric formulations calculated from the heat flow profiles at 2.27 mW/cm²

Photo-initiator	% conc. of photo-initiator	Temperature (°C)	Induction Time (sec)	Peak Maximum Time (sec)	R _{p max} (x 10 ⁻²) (sec ⁻¹)	C _{max} (%)	Heat of reaction (J/g)
IRGACURE 651	0.5	10	0.43	10.09	4.92	71.61	376
	1	10	0.25	8.5	5.58	70.12	368.2
	2	10	0.19	7.47	6.02	71.87	373.8
	0.5	40	0.80	13.69	3.66	73.43	385.6
	1	40	0.38	10.20	5.26	76.16	399.9
	2	40	0.31	9.57	5.46	73.99	388.5
	0.5	70	0.92	14.75	2.44	58.31	306.2
	1	70	0.56	11.37	3.38	60.14	315.8
	2	70	0.39	9.42	4.02	56.92	298.9
DAROCUR TPO	0.5	10	0.25	8.33	5.13	67.21	352.9
	1	10	0.19	7.28	5.8	71.30	374.4
	2	10	0.16	5.94	6.65	71.47	375.3
	0.5	40	0.41	10.17	4.55	74.90	393.3
	1	40	0.28	8.86	5.38	75.17	394.7
	2	40	0.13	5.73	7.38	71.81	377.1
	0.5	70	0.40	9.27	3.70	56.37	296
	1	70	0.32	8.38	3.97	52.41	275.2
	2	70	0.20	6.59	5.20	61	320.3
IRGACURE 184	0.5	10	1.35	16.50	2.25	68.50	359.7
	1	10	0.69	11.39	3.61	69.83	366.7
	2	10	0.40	9.37	4.90	73.21	384.4
	0.5	40	1.37	21.66	2.26	70.37	369.5
	1	40	1.04	16.52	2.66	73.59	386.4
	2	40	0.63	11.93	3.82	74.39	390.6
	0.5	70	1.9	23.8	1.45	55.68	292.4
	1	70	0.87	13.78	2.35	55.04	289
	2	70	0.55	10.93	3.24	59.44	312.1

Table 4.41 gives the kinetic parameters obtained from the photo DSC heat flow profiles. The formulations have 300 wt% excess HPA and hence is expected to show the effect of added reactive diluent. A comparatively high heat flow values were obtained in this case due to an increase in density of reactive species. From the Table, at a particular temperature, an increase in induction time was observed with increase in isothermal condition showing a better radical combination occurring at a low system viscosity as the system has high excess of reactive diluent.⁴ As expected, a comparatively higher initiation rate was shown by DAROCUR TPO due to multiple absorbtions.⁵ The peak maximum time was also found to follow the same trend. As expected, an increase in the value of R_{p max} was observed with increase in concentration of photoinitiator at a particular temperature showing similar trend of induction time due to relatively lower

effect of reaction diffusion at $R_{p \text{ max}}$. The value of $R_{p \text{ max}}$ was comparatively lesser at 70 °C than at 10 or 40 °C mainly due to the effect of radical combinations at higher temperature. The same trend can also be found in the case of final conversion due to the same reason. To conclude, this system has a steady radical diffusion even in the reaction diffusion process, which makes the parameters to show reduced effect of reaction diffusion at initial stages of polymerization. The most probable reason for this behaviour is due to effect of very high volume of reactive diluent in the composition. The high volume of reactive diluent in addition to reduction in initial viscosity of the macromonomeric formulation has facilitated various diffusion processes, which resulted in a gradual rather than an abrupt increase in *in situ* viscosity. The diffusion process includes initial translational and segmental diffusions,⁴ radical diffusion,²¹ initial volume relaxation and enhanced chemical reaction or autoacceleration, final volume shrinkage and reduced chemical reaction leading to vitrification.⁸

Table 4.42 Evaluation of kinetic parameters of macromonomeric formulations as per autocatalytic model at 2.27 mW/cm²

Photo-initiator	% conc. of photo-initiator	Temperature (°C)	Autocatalytic		
			n	m	k (min ⁻¹)
IRGACURE 651	0.5	10	2.38	0.64	14.9
	0.5	40	1.93	0.64	9.42
	0.5	70	2.16	0.50	5.33
	1	10	2.52	0.63	18.9
	1	40	1.81	0.59	12.6
	1	70	2.33	0.53	8.21
	2	10	2.69	0.68	24.3
	2	40	2	0.59	14.1
	2	70	2.36	0.49	9.19
DAROCUR TPO	0.5	10	3.03	0.66	20.5
	0.5	40	2.14	0.60	12.1
	0.5	70	3.07	0.55	11.1
	1	10	3.01	0.70	26.2
	1	40	2.17	0.59	14.8
	1	70	3.62	0.60	14.9
	2	10	3.01	0.61	26
	2	40	2.46	0.54	21.9
	2	70	3.11	0.54	17
IRGACURE 184	0.5	10	2.65	0.65	7.07
	0.5	40	1.94	0.64	5.55
	0.5	70	2.43	0.53	3.47
	1	10	2.31	0.56	8.82
	1	40	1.97	0.62	6.71
	1	70	2.53	0.51	5.61
	2	10	2.53	0.63	15.6
	2	40	2.03	0.59	9.43
	2	70	2.61	0.54	8.62

Since the formulations have excess reactive diluent, it can be said to have high plasticization effect. From Table 4.42, the system showed similar values for the constants n and m due to better radical diffusion occurring along with reaction diffusion as explained above. The value of specific rate constant was found to show a similar reduction with increase in temperature at a particular concentration. The decrease in the value of k with an increase in temperature may be due to the shift for the formulations in behaving the autocatalytic kinetic model to high levels of achieved conversions.⁹ The system during photocuring can be assumed to undergo both bimolecular as well as monomolecular terminations.¹³

Evaluation of bimolecular termination model

With the polychromatic light source, photoinitiation was done at 4.51 mW/cm^2 followed by dark polymerization to study the ratio of rate constants using bimolecular termination model. The dark polymerization was done by initial irradiation of the sample for 5, 10, 15, 20, 30, 40, 50, 60 and 70% conversions.

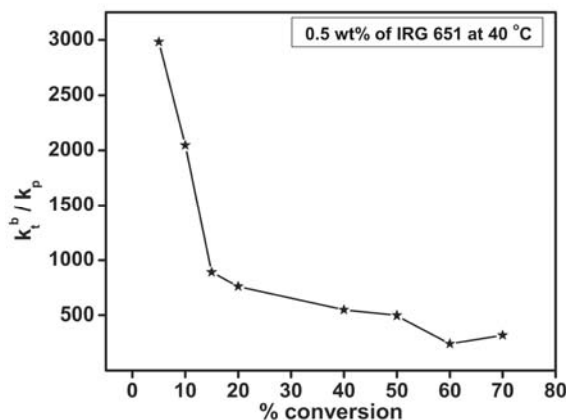


Figure 4.101 Plot of k_t^b/k_p at different percentage conversions for the formulation containing macromonomer, 300 wt% HPA and 0.5 wt% of IRGACURE 651 at 40 °C

A plot k_t^b/k_p against percentage conversion is given in Figure 4.101. From the Figure, we can infer that this reaction has a better radical diffusion as well as enhanced terminations at the beginning of photopolymerization process. At very low conversions, the value of the ratio (k_t^b/k_p) was found to be around 3000, which was more than six times the value observed in System 4B-2 [Figure 4.84(A)]. Even though the initial viscosity of this system is higher than previous case, the terminations at very low conversions can be to be higher for this system due to a higher density of reactive species imparted by 300% excess HPA as compared to 50wt% HEA in system 4B-2. Hence, the high concentration of reactive diluent at the initial stages, allow fast radical diffusion with high termination rates which accounts for this observation.⁴ The Figure 4.101 also provides an idea of the propagation rates, as a better consistency (plateau behaviour) is observed in the ratio with increase in conversion.¹⁴ As expected, the value of ratio towards vitrification showed a slight increase showing the influence of monomolecular termination towards vitrification.^{4,15}

4.2.1.5.5 Post photopolymerization studies

Thermogravimetric analysis

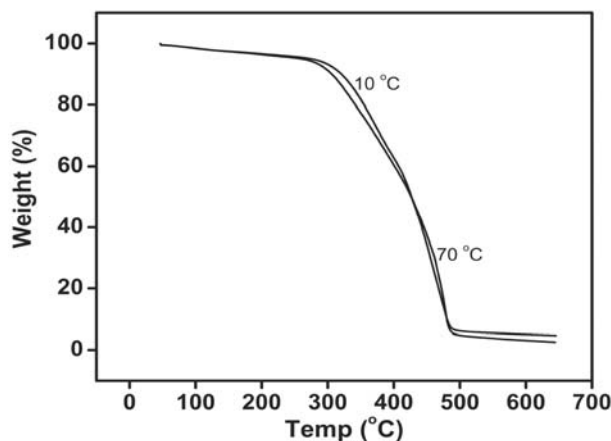


Figure 4.102 Thermogravimetric degradation profiles at 20 °C/min of macromonomeric formulation containing 300 wt% of HPA and 0.5 wt% of DAROCUR TPO photocured at 10 and 70 °C and 2.27 mW/cm². Analyses done after one week storage

The degradation profiles show that the extent of crosslinking at higher temperature is comparatively low. After 10% weight loss, the decomposition profile of the film photocured at 70 °C showed faster degradation due to early vitrification. This is a reflection of the conversion data observed in Table 4.41.

DSC analysis

Macromonomeric formulation containing 300 wt% excess HPA and 1 wt% of IRGACURE 651 photocured at 40 °C and 2.27 mW/cm² was subjected to thermal analysis using DSC. The T_g of the photocured sample was found to be 57.6 °C. The extent of vitrification is found to depend on many parameters of which the initial viscosity of the formulation as well as the ultimate T_g of the photocured sample have higher influence.¹¹ For this system, the initial viscosity was found to be 1406 cP while the photocured material had a T_g of 57.6 °C.

4.2.2 Conclusions

Photopolymerization of synthesized oligomers in presence of reactive diluents and photoinitiators of various classes were carried out at low irradiation intensities. The synthesized oligomers were based on bis aromatic based urethane di(meth)acrylates possessing aliphatic/cycloaliphatic and aromatic backbone. Photopolymerization was

carried out with polychromatic radiation at different isothermal conditions and intensities under a constant nitrogen purge of 50 mL/min. The addition of reactive diluents decreases the viscosity as well as increases the density of reactive sites in the formulations. As a result, the photopolymerization took place in an efficient manner with moderate to high conversions in certain cases. High conversions were observed with formulations having low initial viscosity.

The bis aromatic based urethane diacrylate with ethyleneoxy linkages containing 50 wt% of monoacrylate as reactive diluent (system 4B-1) showed a initial viscosity of 1781 cP and a maximum conversion around 71%, when irradiated at a very low intensity of 1.93 mW/cm² at 40 °C. High conversion was not occurring in this case due to the effect of radical/reaction diffusions occurring during the deceleration step and enhanced vitrification.²² Bis aromatic based urethane diacrylate with propyleneoxy linkages containing 50wt% of monoacrylate as reactive diluent (system 4B-2) showed a initial viscosity of 993cP and a maximum conversion around 89%, when irradiated at a low intensity of 1.93 mW/cm² at 40 °C. An increase in irradiation intensity to 4.47 mW/cm² did not cause much effect on final conversion due to influence of limitations imparted by overall diffusion processes under polychromatic conditions. An increase in isothermal condition to 70 °C at 4.47 mW/cm² resulted in an overall decrease in final conversion due to reduction in initial system viscosity and enhanced terminations occurring during the initial stages of photopolymerization. A high conversion was achieved for formulations in system 4B-2 as compared to formulations in system 4B-1 mainly due to low initial system viscosity. In addition, the radical and reaction diffusions occurring in system 4B-2 during the deceleration step happened efficiently over a longer time scale before the onset of vitrification as compared to system 4B-1. The compositions cured at higher temperature vitrified faster due to comparatively faster volume shrinkage with respect to the chemical reaction in the deceleration step.⁸

Bis aromatic based urethane dimethacrylate with propyleneoxy linkages and sulphone moieties in the backbone and containing 75 wt% of monomethacrylate as reactive diluent (system 4B-3) showed a initial viscosity of 1856 cP. For this system, the maximum conversion of above 68% was found to occur at an irradiation intensity of 1.78 mW/cm² at 40 and 70 °C. On increasing the irradiation intensity to 3.26 mW/cm² at 40

°C, a maximum conversion of around 75% was obtained. This shows that the final conversion during the photopolymerization process for this system is influenced by intensity rather than increase in temperature from 40 to 70 °C.¹⁷ In system 4B-3 with methacrylate end functionalities, an increase in timescale of reaction diffusion with a decrease in rate as compared to acrylate systems (system 4B-1 and system 4B-2) were obtained and is evident from the heat flow profiles. A very high conversion as expected for methacrylates was not obtained in system 4B-3, probably due to a positive glass transition temperature of 55.5 °C for the photocured matrix, which has forced the system to vitrify early.²³

Bis aromatic based urethane diacrylate with ethyleneoxy linkages and biphenyl moieties in the backbone and containing 300 wt% of monoacrylate as reactive diluent (system 4B-4) showed a initial viscosity of 1406 cP. The solid macromonomer was solvated with high excess of monoacrylate as reactive diluent to obtain an optimum viscosity and the maximum conversion of above 76% was obtained when irradiated at a low intensity of 2.27 mW/cm². An increase in temperature from 10 to 40 °C showed a trend of increase in final conversion which got reduced when analyzed at 70 °C. This shows the effect of reaction diffusion at higher temperature as well as effect of enhanced bimolecular terminations occurring during the initial stages of photopolymerization at 70 °C. Due to reduced initial viscosity and enhanced terminations, the quantum yield of initiation was reduced, which were reflected in the final conversions.⁶

A trend in decrease of induction time and peak maximum time as well as overall diffusion processes occurs readily during a gradual rise in reaction diffusion. An increase in $R_{p \text{ max}}$ and final conversion occurred and was observed in some formulations with an increase in temperature as well as with increase in concentration of photoinitiator. Disparities in the trend were found in many formulations due to variations in the onset and course of viscosity dependent reaction diffusion which restricts all diffusion processes such as radical and propagating chain diffusions throughout the photopolymerization process.^{21,24}

The efficacies of variable autocatalytic kinetic model on photopolymerization processes were studied by considering theoretical heat flow values using TA advantage specialty library software. The model takes into account of the heat flow signals from

onset of initiation to the onset of vitrification. It was observed that in many cases, the value of autocatalytic exponent (m) is closer to the ideal value of 0.5 observed in the case of epoxy/anhydride cure using amines.²⁵ However, it cannot be said that the model is a fit to the reaction kinetics as in many cases all the experimental points did not lie within the calculated value on plotting $\log(dC/dt)$ against $\log(1-C)C^{m/n}$, due to probable partial n^{th} order behaviour.⁹ The value of specific rate constant (k) did not show consistent increase with increase in temperature in most cases. At the same time an increase in the value of k with increase in irradiation intensity was found in many cases.

The formulation did not vitrify so early and hence the applicability of bimolecular termination model was studied for three formulations. It was observed that the ratio of rate constants as per the model (k_t^b/k_p) was found to show a higher value for low conversions. As conversion proceeds, the ratio got decreased as expected from theory.^{4,14,15} Considering the studies for formulations using 0.5wt% of IRGACURE 651 at 40 °C in systems 4B-2 and 4B-4, we can infer that due to higher density of reactive sites imparted by excess reactive diluent, the later showed a initial ratio of about six times than the former at 5% conversion. This shows that value of rate constant for bimolecular termination increases with an increase in density of reactive sites.

From thermogravimetric analyses, we can infer that samples photocured at higher temperature showed a decrease in degradation profiles due to better crosslinking. It was also observed that photoinitiated samples on storage had undergone dark polymerization to a considerable extent as compared to completely photocured samples. Extent of dark polymerization varied depending on the nature of photoinitiated matrix. This supports the theory that photoinitiated matrix can undergo polymerization in dark over a much longer time scale of days or even months.²⁶

4.2.3 References

- [1] L. Soos, G.Y. Deak, S. Keki, M. Zsuga., *J. Polym. Sci. A Polym. Chem.* **37**, 545 (1999).
- [2] I.V. Khudyakov, J.C. Legg, M.B. Purvis, B.J. Overton., *Ind. Eng. Chem. Res.* **38**, 3353 (1999).
- [3] E. Andrzejewska, A. Marcinkowska., *J. Appl. Polym. Sci.* **110**, 2780 (2008).
- [4] E. Andrzejewska., *Prog. Polym. Sci.* **26**, 605 (2001).
- [5] Photoinitiators for UV curing – Key products selection guide, Ciba Speciality Chemicals Inc., Switzerland.
- [6] H.F. Gruber., *Prog. Polym. Sci.* **17**, 953 (1992).
- [7] L. Lecamp, B. Youssef, C. Bunel, P. Lebaudy., *Polymer* **38**, 6089 (1997).
- [8] J.G. Kloosterboer, G.M.M. van de Hei, R.G. Gossink, G.C.M. Dortant., *Polym. Commun.* **25**, 322 (1984).
- [9] R. Chandra, R.K. Soni, S.S. Murthy., *Polym. Inter.* **31**, 305 (1993).
- [10] A. Asif, C.Y. Huang, W.F. Shi., *Colloid Polym Sci.* **283**, 721 (2005).
- [11] Q. Yu, S. Nauman, J.P. Santerre, S. Zhu., *J. Mater. Sci.* **36**, 3599 (2001).
- [12] K.S. Anseth, C.M. Wang, C.N. Bowman., *Macromolecules* **27**, 650 (1994).
- [13] E. Andrzejewska, M.B. Bogacki., *Macromol. Chem. Phys.* **198**, 1649 (1997).
- [14] E. Andrzejewska, M. Janaszczyk, M. Andrzejewski., *Conferenece proceedings - RadTech Europe* (2005).
- [15] E. Andrzejewska, D.Z. Tomkowiak, M.B. Bogacki, M. Andrzejewski., *Macromolecules* **37**, 6346 (2004).
- [16] A.R. Kannurpatti, S. Lu, G.M. Bunker, C.N. Bowman., *Macromolecules* **29**, 7310 (1996).
- [17] A. Maffezzoli, R. Terzi., *Thermochim. Acta* **321**, 111 (1998).
- [18] T.F. Scott, W.D. Cook, J.S. Forsythe., *Polymer* **43**, 5839 (2002).
- [19] E. Andrzejewska, L.A. Linden, J.F. Rabek., *Polym. Inter.* **42**, 179 (1997).
- [20] C. Decker, K. Moussa., *J. Polym. Sci. Polym. Chem.* **25**, 739 (1987).
- [21] C. Decker., *Polym. Inter.* **45**, 133 (1988).
- [22] C. Decker., *Macromol. Rapid Commun.* **23**, 1067 (2002).
- [23] J.G. Kloosterboer., *Adv. Polym. Sci.* **84**, 1 (1988).

- [24] C. Decker, B . Elzaouk, D. Decker., *J. Macromol. Sci. Pure Appl. Chem.* **A33**, 173 (1996).
- [25] U. Khanna, M. Chanda., *J. Appl. Polym. Sci.* **49**, 319 (1993).
- [26] K.S. Anseth, K.J. Anderson, C.N. Bowman., *Macromol. Chem. Phys.* **197**, 833 (1996).

Photopolymerization of high internal
phase emulsions based on (meth)acrylate
monomers

4.3 PART – C: Photopolymerization of high internal phase emulsions based on (meth)acrylate monomers

4.3.1 Experimental

4.3.1.1 Materials and measurements

Potassium persulphate (SD fine), cyclohexane 99% (Rankem), sorbitan monooleate or Span 80 (Loba chemie), (Di(hydrogenated tallow) dimethyl ammonium chloride or Arquad 2HT-75 (Fluka), 2-ethylhexyl acrylate (EHA) 98%, ethylene glycol dimethacrylate (EGDM) 98%, 2-ethylhexyl methacrylate (EHMA) 98%, IRGACURE 184 or 1-hydroxycyclohexyl phenyl ketone, IRGACURE 2959 or 2-hydroxyl-4'-(2-hydroxyethoxy)-2-methyl propiophenone, DAROCUR 1173 or 2-hydroxy-2-methyl propiophenone, IRGACURE 907 or 2-methyl-4'-(methylthio)-2-morpholino propiophenone, IRGACURE 819 or phenyl bis(2,4,6-trimethyl benzoyl) phosphine oxide and butyl acrylate 99% (all from Aldrich) were used as received.

Gas Chromatograph

A gas chromatograph (Model GC-14B) from Shimadzu Corporation, Japan equipped with an auto sampler (AOC 20i) was used for the experiments. Ultra high pure nitrogen gas was used as carrier gas. Pure hydrogen and zero air were used for flame ionization detector flame. The data processing was carried out using Shimadzu C-R7A plus Chromatopac software.

4.3.1.2 Procedure for synthesis

Preparation of photopolymerizable high internal phase emulsion

HIPE was prepared from EHA, EHMA and EGDMA and polymerized using photoinitiators and other additives in a glass vessel. The photoinitiators of choice were IRGACURE 184, IRGACURE 2959, DAROCUR 1173, IRGACURE 907 and IRGACURE 819. Glass vessels with 4 cm diameter and 17 cm length were used for the photopolymerization of HIPEs. The vessels were provided with B 50 joint and stopper. Initially, the organic phase was prepared by the addition of 0.185 g (0.001 mol) of EHA, 0.19 g (0.00095 mol) of EHMA and 0.0875 g (0.00044 mol) of EGDMA in to the glass vessel. This was followed by the addition of 0.0325 g (6.513 wt % of monomer phase) of Span 80 and 0.004 g (0.8016 wt % of monomer phase) of (Di(hydrogenated tallow)

dimethyl ammonium chloride or Arquad 2HT-75 and 0.0023 g (0.5 wt% of monomer phase) of photoinitiator. The contents in the glass vessel were mixed well.

13.5 mL of distilled water (27 times the volume of monomer phase) was purged with ultra high pure nitrogen gas. The aqueous phase was added to the organic phase under stirring in a controlled manner so that the addition was completed in 5 min. The system was then stirred further for 5 minutes to obtain a stable W/O HIPE.

4.3.1.3 Photocuring studies

Photopolymerization of high internal phase emulsion involving 2-ethyl hexyl acrylate, 2-ethyl hexyl methacrylate and ethylene dimethacrylate.

The HIPE prepared was purged with nitrogen for two minutes and kept on the irradiation chamber on a marked platform at a distance of 19 cm below the radiation source. Irradiation was done under a constant photo flux with a 400 W medium pressure mercury vapour lamp (HPL-N series, Philips). The polychromatic radiation from the lamp has wavelength ranging from 340 to 800 nm with a luminous flux of 22000 lumens. The luminous efficacy of the lamp used (luminous flux in lumens / power in watts) was 55 lm/W. A stopwatch was used to monitor the irradiation time. After specified and differing irradiation times, the HIPE was quenched rapidly in liquid nitrogen. 100 mL of cyclohexane containing 2500 ppm of butyl acrylate as internal standard was added to it. The lumps formed, if any were dispersed well. The system was then kept in liquid nitrogen for 5 min and left overnight in water bath at ambient conditions. The cyclohexane layer was analyzed for residual monomer content using gas chromatography. Identical samples were irradiated for differing periods ranging from 2 to 12 minutes, with 2 minute interval, to effect polymerization to differing conversions.

Highest achieved polymerization of HIPE within least time was obtained using a variety of photoinitiators at ambient conditions. About 4 to 6 samples were prepared for the kinetic study of the photopolymerization of each composition. A two min interval was kept for each analysis and the percentage conversion was noted. The induction times (time taken for 1% conversion) as well as the percent conversions in the photopolymerization processes were studied by analyses of the residual monomer per unit volume of the cured material, using gas chromatography. The polyHIPE prepared had a thickness of 5 mm.

4.3.1.4 Residual monomer analysis

Analysis of residual monomers using gas chromatography (GC)

The unreacted monomers extracted after the photopolymerization were estimated by G C. A J & W Scientific, DB-1 (polydimethyl siloxane) column having a dimension of 100 m x 0.25 mm with a film thickness of 0.5 μm was used for the analyses. The carrier gas pressure was kept constant at 220 kPa, while the hydrogen and zero air pressure at the FID were kept at 60 and 50 kPa respectively. The column oven temperature was kept constant at 225 $^{\circ}\text{C}$, whereas the temperatures of injector and detector were kept at 275 and 300 $^{\circ}\text{C}$, respectively. 1 μL of sample solution was injected (with a split ratio of 23:1) to the injector provided with deactivated glass wool filter.

Preparation of standards

Preparation of internal standard solution

The internal standard solution at a concentration of 2500 ppm (w/v) was prepared by dissolving 625 mg of butyl acrylate in 250 mL of cyclohexane in standard (class A) volumetric flask.

Preparation of monomer standard solutions

Five compositions of EHA, EHMA and EGDM with varying concentrations were prepared by dissolving appropriate quantities of individual monomer standards in 25 mL of cyclohexane containing internal standard in a standard (class A) volumetric flask. The concentrations of monomers in each composition (ppm based on w/v) are given in Table 4.43.

Table 4.43 Concentration of monomers in standard solutions for GC analysis

Compositions	Monomer concentration (mg / 25 mL)			Monomer concentration (ppm, w/v)		
	EHA	EHMA	EGDM	EHA	EHMA	EGDM
1	12.2	11.2	6	488	448	240
2	24.4	25.8	12.1	976	1032	484
3	52.4	51.3	24.3	2096	2052	972
4	76.1	74.7	44.1	3044	2988	1764
5	101.8	113.3	50.6	4072	4532	2024

1 μL each of monomer standards were injected into GC and the calibration curves for three monomers were generated by plotting concentration in ppm against peak area of corresponding monomers. 1 μL of cyclohexane solution containing internal standard and

extracted monomers from the photopolymerized HIPE samples were then injected into GC and the individual amount of residual or unreacted monomers were calculated using the corresponding response factors. From the experimental and calibration values, the final conversions of individual monomers in the photopolymerized matrix were calculated.

4.3.2 Results and discussion

The residual monomers were analyzed based on the calibration curves obtained from three monomer standards. The calibration plots are given in Figure 4.103 (A-C)

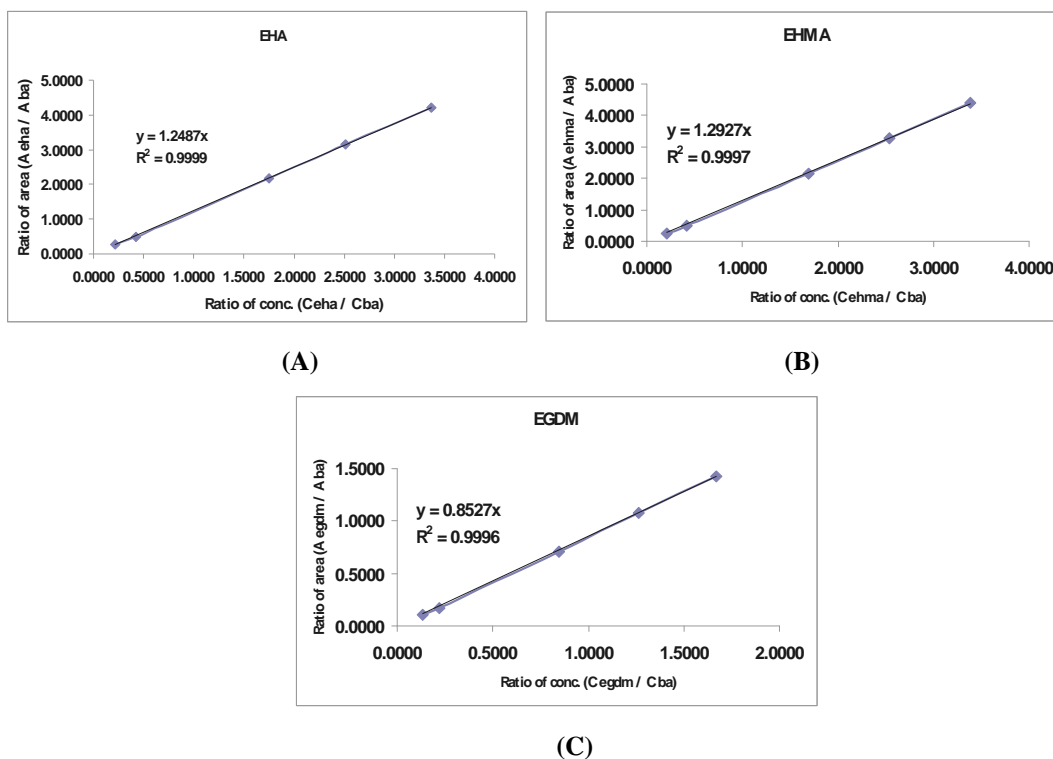


Figure 4.103(A-C) Calibration plots obtained from GC data for the three monomers. (A) EHA, (B) EHMA and (C) EGDMA

The time dependant percentage conversion profiles of three monomers during the photopolymerization of formulated HIPE emulsions containing 0.5 wt% of five photoinitiators calculated based on residual monomer analyses using GC are given in Figure 4.104 (A-E).

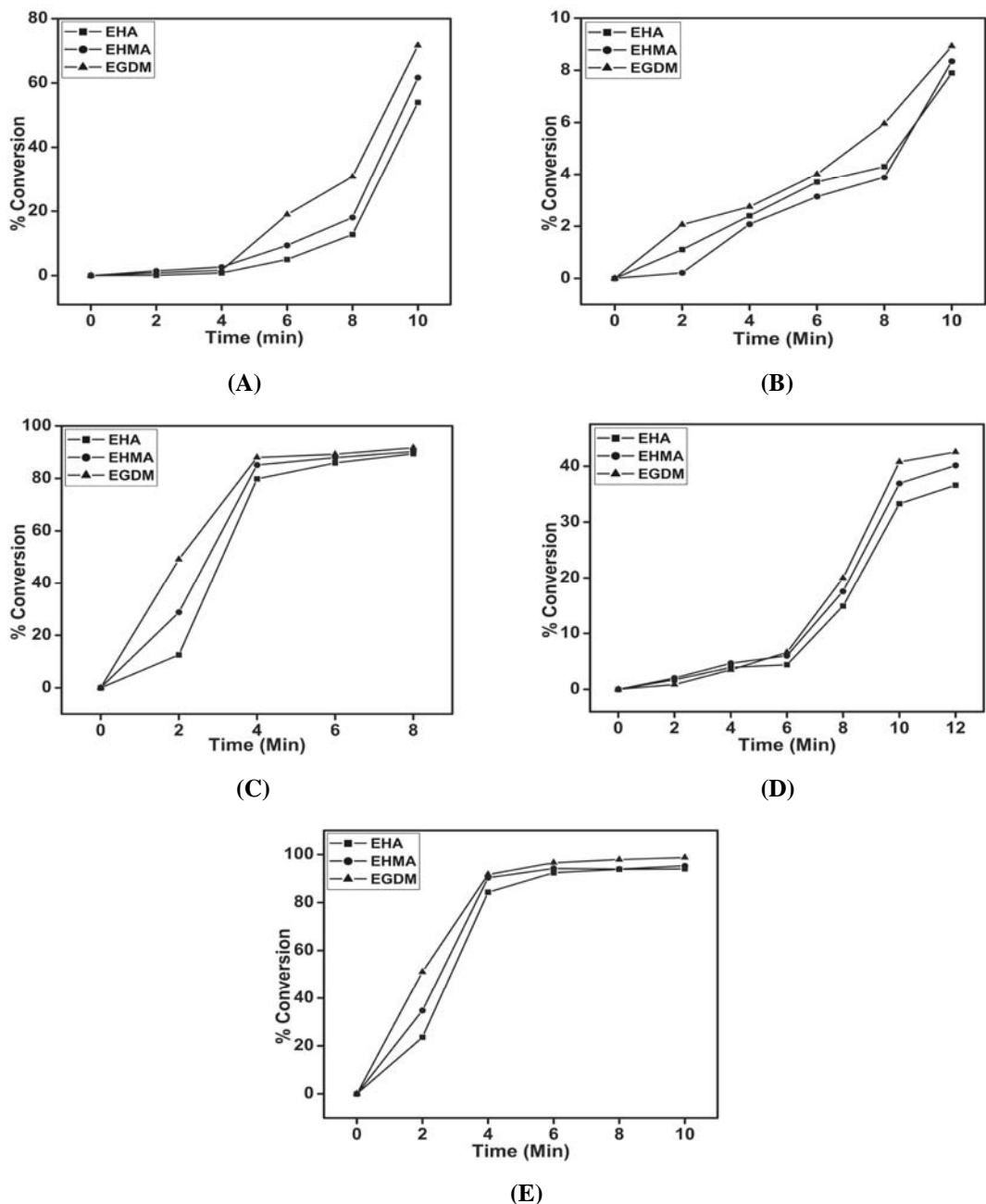


Figure 4.104(A-E) The time dependant percentage conversion profiles for the formulation containing the three monomers and 0.5 wt% of photoinitiators photo cured using external lamp at ambient conditions with (A) IRGACURE 184, (B) IRGACURE 2959, (C) IRGACURE 1173, (D) IRGACURE 907 and (E) IRGACURE 819

The plots show that the ethylene glycol dimethacrylates have higher conversion rate as well as final conversion than the other mono(meth)acrylates used for the photopolymerization studies. This is due to efficient cross linking associated with the

dimethacrylate than mono(meth)acrylates.¹ From the plots it can be inferred that IRGACURE 819 was most efficient and resulted in maximum monomer conversion as compared to others. DAROCUR 1173 also showed reasonably good monomer conversion. Less than 50% conversion of the monomers were observed using IRGACURE 907. Very low conversion of less than 10% was observed in the case of IRGACURE 2959.

The above observations can be due to various factors. Being an opaque emulsion, the system can reduce penetration of radiation.² Secondly, the migration of photoinitiator in the micelle, even though not much hindered by the diffusion processes like free radical polymerization, can result in variations in final conversion. The photoinitiators will not undergo π - π^* transition, since the irradiation source has a lower energy (340 to 800 nm).³ The major factor contributing to the variations in final conversion can thus be considered as the excitation energy from the light source as well as the radical diffusibility. IRGACURE 819 belongs to phosphine oxide type photoinitiator and is normally used for through cure and hence can cure thicker sections. The irradiated foams had a thickness of 5 mm. In addition, n- π^* transition of IRGACURE 819, which corresponds to the λ_{\max} value of the photoinitiator around 370 nm is much closer to a major emission line in mercury spectrum at 365 nm.³ This helps in a faster initiation rate for HIPE containing IRGACURE 819 as photoinitiator. This is also reflected from the induction time results given in Table 4.44.

Table 4.44 Induction time and maximum conversion calculated by residual monomer analyses using GC

Photoinitiator	Induction time (sec)			Time taken for 5% conversion (sec)			Maximum conversion (%)		
	EHA	EHMA	EGDM	EHA	EHMA	EGDM	EHA	EHMA	EGDM
IRGACURE 184	4.09	1.38	2.41	6	4.7	4.4	54	61.6	71.6
IRGACURE 2959	1.81	2.85	0.97	8.4	8.5	7	7.9	8.3	8.9
DAROCUR 1173	0.16	0.07	0.04	0.8	0.4	0.2	89.4	90.2	91.7
IRGACURE 907	1.17	0.98	2.09	6.1	4.5	5	36.6	40.1	42.5
IRGACURE 819	0.08	0.06	0.04	0.4	0.3	0.2	94	95.3	98.7

The second highest conversion was observed for DAROCUR 1173. The n- π^* transitions for DAROCUR 1173 and IRGACURE 184 are 331 and 333 nm; respectively.⁴ DAROCUR 1173, being a liquid, can mix readily with the monomers under study. This can impart a better diffusion of reactive radical species and hence a higher conversion

was obtained for the formulation with DAROCUR 1173 as compared to that of IRGACURE 184. IRGACURE 907 has n- π^* transition at 304 nm.⁴ Since the proximity of the nearest major emission band in the radiation at 365 nm is much more widened, the HIPEs containing this photoinitiator showed low level of conversion. The least conversion was observed in HIPEs containing IRGACURE 2959. IRGACURE 2959 has no major absorptions above 300 nm and hence the system showed very low conversions.³

4.3.3 Conclusions

Photopolymerization of HIPEs containing acrylate monomers were evaluated. The final conversions in photopolymerized HIPEs vary with the choice, type and concentration of photoinitiators. For emulsions containing IRGACURE 819, high conversion was obtained possibly due to the through cure (thick layer curing) property of the monomer arising from the proximity of the major absorption maximum of the photoinitiator to the major emission line of the mercury spectrum. The other factors such as diffusion of radical species can also affect the final conversion. This has been observed in the case of emulsions containing DAROCUR 1173 as compared to IRGACURE 184. The foams prepared by this method can be used in various applications such as fluid absorption, insulation, sound dampening and multilayer foam articles.² By varying the starting material and processing conditions, the foam structure can be tailored to obtain required physical properties. The feasibility of photopolymerization of HIPE systems involving acrylates has been established.

4.3.4 References

- [1] S.J. Pierre, J.C. Thies, A. Dureault, N.R. Cameron, J.C.M. Vanhest, N. Carette, T. Michon, R. Weberskirch., *Adv. Mater.* **18**, 1822 (2006).
- [2] K.L.V. Thunhorst, M.D. Gehlsen, R.E. Wright, E.W. Nelson, S.D. Koecher, D. Gold., *US Patent 6759080* (2004).
- [3] N.S. Allen, J. Segurola, M. Edge, E. Santamari, A. Mc Mahon., *Surf. Coat. Inter.* **2**, 67 (1999).
- [4] Photoinitiators for UV curing - Key products selection guide, Ciba Speciality Chemicals Inc., Basel, Switzerland.

Photopolymerization of multiacrylate
based monomers

5.1 Introduction

Dihydroxy terminated linear soft segmented compounds such as polyethylene glycol, polypropylene glycol and polytetrahydrofuran of varying molecular mass were treated with excess alicyclic diisocyanate such as IPDI and subsequently treated with triacrylate such as pentaerythritol triacrylate to obtain hexaacrylated macromonomers or with di or trihydroxy diacrylates to obtain branched photopolymerizable macromonomers. Propylene glycol glycerolate diacrylate (PGGDA) was used as the dihydroxy diacrylate while glycerol 1,3-diglycerolate diacrylate (GDGDA) was used as trihydroxy diacrylate respectively. These transparent and viscous urethane multiacrylates were formulated with photoinitiators with different weight proportions prior to photopolymerization studies. The photocuring kinetics including rate and conversion profiles and certain other kinetic parameters were computed using photo DSC.

5.2 Experimental

5.2.1 Materials and measurements

Polyethylene glycol 200 (SD fine), polypropylene glycol 725 and 3000 (Aldrich), polytetrahydrofuran 650 (Aldrich), hydroxy terminated polybutadiene 2750 (VSSC-Thiruvananthapuram), isophorone diisocyanate (Fluka), glycerol 1,3-diglycerolate diacrylate (Aldrich), propylene glycol glycerolate diacrylate (Aldrich), pentaerythritol triacrylate (Aldrich), dibutyl tin dilaurate (Aldrich), 1,4-diazabicyclo[2.2.2]octane or DABCO (Aldrich), hydroquinone (Aldrich), hydroquinone monomethyl ether (Fluka) and chloroform (Merck) were used as received.

The measurements used are same as given in Section 4.1.1.2.

5.2.2 Photopolymerization of multiacrylate macromonomer based on polypropylene glycol 725, isophorone diisocyanate and pentaerythritol triacrylate (System 5-1)

A hexaacrylated macromonomer based on PPG 725, IPDI and pentaerythritol triacrylate (PETA) was synthesized and formulated. The photocuring studies of the formulations were carried out. Estimation of kinetic parameters were done based on the heat flow profile obtained during the photopolymerization process.

The telechelic synthesis of macromonomer was done in two steps. An initial condensation of the diol and diisocyanate to form a diisocyanate terminated urethane prepolymer followed by end capping of the formed prepolymer with excess of pentaerythritol triacrylate to form soft segmented urethane hexaacrylate macromonomer.

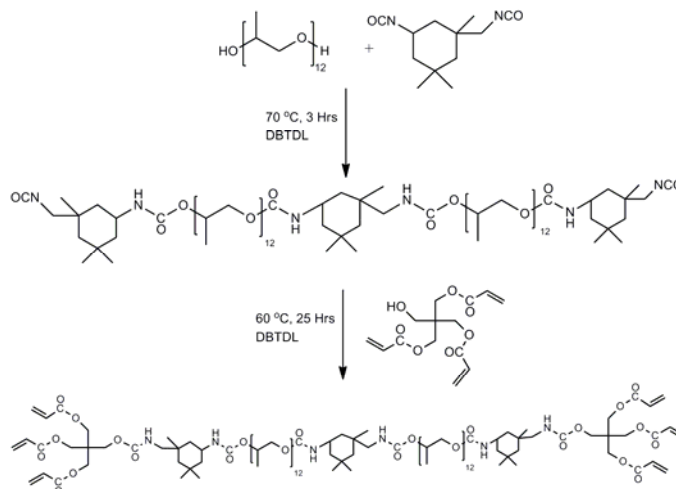


Figure 5.1 Synthesis pathway of urethane multiacrylate based on PPG 725, IPDI and PETA

5.2.2.1 Procedure for synthesis

Synthesis of macromonomer

A 100 mL three necked round bottomed flask was dried and flushed with nitrogen gas through one side neck. 18 mg (0.02847 mmol) of dibutyl tin dilaurate was added to it followed by the addition of 10.07 g (13.89 mmol) of polypropylene glycol 725 and homogenized at 40 °C at 80 rpm. 3.09 mL (14.58 mmol) of isophorone diisocyanate was added at a rate of 0.5 mL/min. The system was homogenized well at 100 rpm and the temperature was increased to 70 °C. After 3 h, 2.073 g (6.95 mmol) of pentaerythritol

triacrylate in 20 mL of chloroform was added drop-wise over a period of 5 min. The stirring speed was reduced thereafter to 80 rpm. The temperature was reduced to 60 °C and the reaction was continued in nitrogen atmosphere for 25 h until the isocyanate peak disappeared from the IR spectrum.

The product mixture was solvated in 30 mL of chloroform and was transferred into a 250 mL separating funnel. It was then washed thrice with 100 mL of distilled water until devoid of excess acrylate. The chloroform layer was separated and dried over activated molecular sieves for one hour. The chloroform layer was decanted and transferred into a 100 mL RB flask and vacuum was applied for a period of 6 h followed by solvating in minimum amount of dichloromethane and dried in vacuum oven for a period of 10 h at 60 °C to obtain a viscous macromonomer. IR and NMR spectra were noted. The molecular mass was found by VPO.

IR: 1728 (C=O, urethane), 1723 (C=O, acrylate), 3375 and 1530 (-CO-NH-, urethane), 1635 and 809 (C=C-, acrylate), 1093 (C-O), 2972, 2912 and 2868 (-CH₂-) cm⁻¹.

¹H NMR(CDCl₃): 0.90 and 1.09 (-CH₃, alicyclic), 1.11 to 1.70 (-CH₂-, alicyclic), 3.33 to 3.62 (-CH₂- and -CH-, propyloxy (internal)), 3.88 to 3.95 (-CH₂- and -CH-, propyloxy (terminal)), 2.89 (-CH₂-NH-), 4.86 (-CH₂-NH-CO-O-CH₂-), 4.59 (-NH-CO-O-CH₂-), 4.08 (-NH-CO-O-CH=CH₂), 5.84 and 6.36 (-CO-O-CH=CH₂), 6.11 (-CO-O-CH=CH₂).

¹³C NMR(CDCl₃): 23.12, 27.54 and 34.99 (-CH₂-, alicyclic), 31.77 (=C(CH₃)₂, alicyclic), 36.28 (=C(CH₃)CH₂-, alicyclic), 42.02, 46.28 and 47.16 (-CH₂-, alicyclic), 62.53 (-CH₂-NH-CO), 127.49 (CH₂=CH-CO-O-), 131.82 (CH₂=CH-CO-O-), 156.52 (-CH₂-NH-CO-O-), 155.32 (-NH-CO-O-), 165.49 (CH₂=CH-CO-O-)

5.2.2.2 Formulation

The formulations were made in 5 mL sample vials. 1 g (0.5828 mmol) of macromonomer was weighed accurately in all the vials. 2.5 mg (0.25 wt%) and 10 mg (1 wt%) of five photoinitiators were added to obtain ten compositions. Each composition was homogenized in a vibrating mill for 2 min. The photoinitiators used were IRGACURE 651, DAROCUR TPO, IRGACURE 184, DAROCUR 1173 and IRGACURE 819.

5.2.2.3 Photocuring studies

10 mg of the composition was accurately weighed on a DSC pan and subjected to photo DSC studies under a nitrogen purge of 50 mL/min. The pans were closed by a

quartz window in order to prevent any monomer loss during irradiation. The sample was preconditioned at the isothermal condition under nitrogen purge for a period of 1 min prior to irradiation. It was followed by irradiation for a period of 5 min under a constant photo flux from the machine. The heat flow profile obtained during the *in situ* photocuring process was recorded as a function of time under an isothermal condition of 30 °C. The intensity of irradiation was kept at 22.6 mW/cm² using a 100 W high pressure mercury short arc lamp. A polychromatic radiation having a range of 250-450 nm was used for analyses. The normalized output signals in W/g against time were recorded. The rates of photopolymerizations as well as corresponding conversions were calculated for all the compositions.

5.2.2.4 Results and discussion

The macromonomer was characterized using IR, ¹H and ¹³C NMR spectroscopy. The molecular mass was found to be 1716 by VPO. The total theoretical heat flow¹ (ΔH_{theor}) for the system was calculated to be 301.37 J/g.

The rate and conversion profiles obtained from photocuring studies of macromonomeric formulations containing five photoinitiators at 0.25 and 1 wt% compositions at 30 °C and 22.6 mW/cm² are given below in Figures 5.2 (A-C) and 5.3 (A-C).

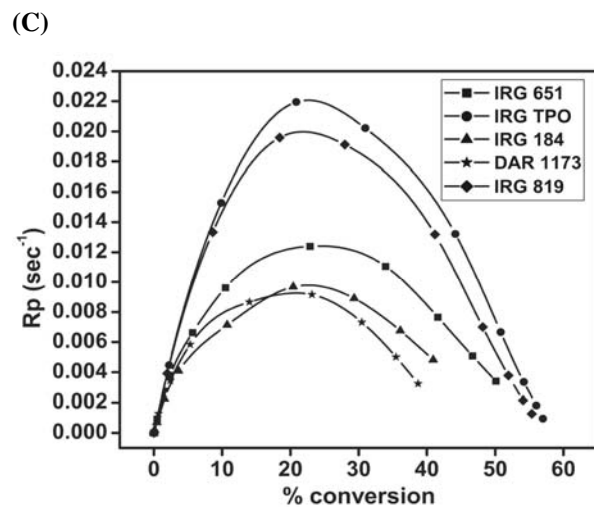
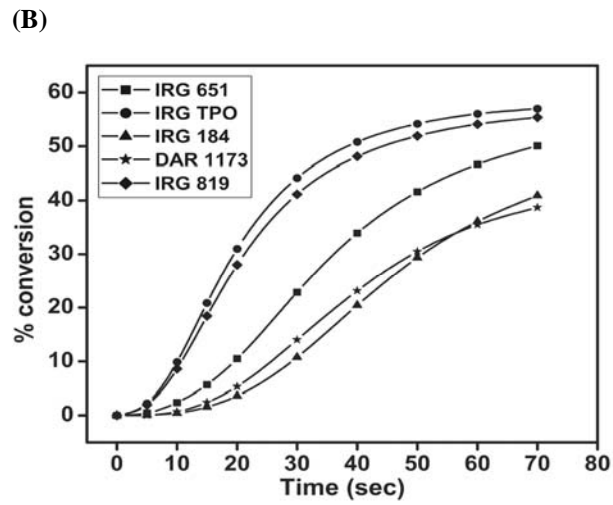
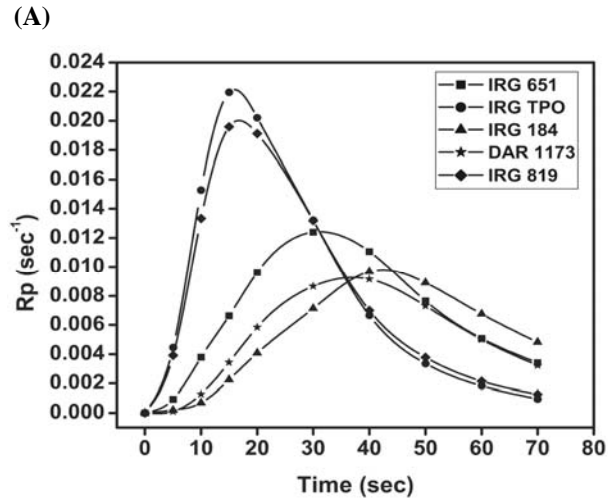
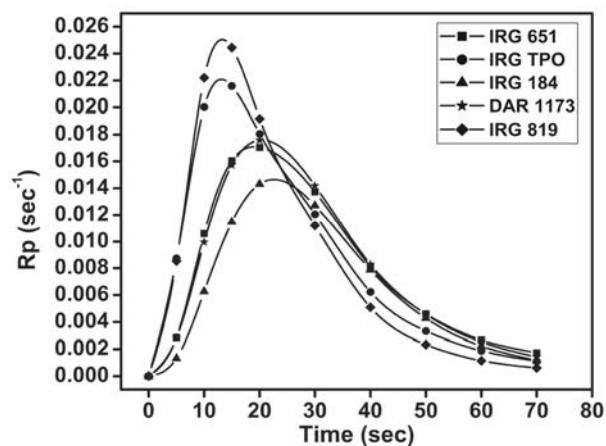
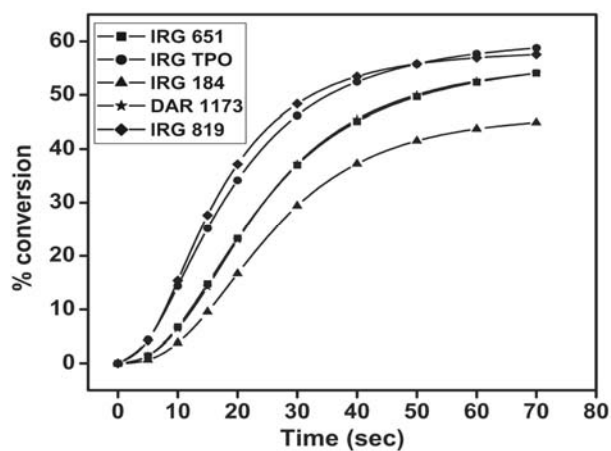


Figure 5.2(A-C) Time dependent rate and conversion profiles of macromonomeric formulations containing 0.25 wt% of five photoinitiators

(A)



(B)



(C)

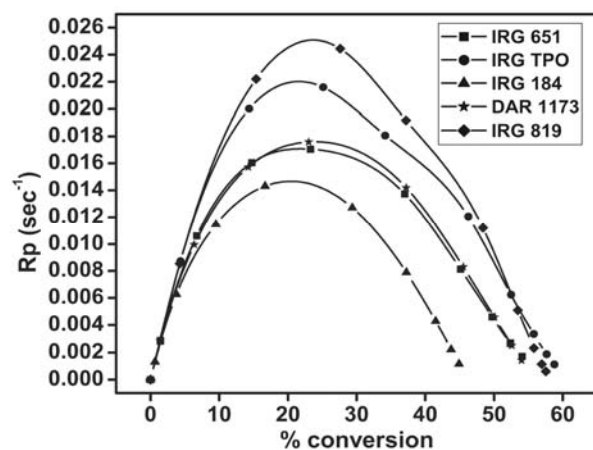


Figure 5.3(A-C) Time dependent rate and conversion profiles of macromonomeric formulations containing 1 wt% of five photoinitiators

The kinetic parameters calculated are given in Table 5.1.

Table 5.1 Kinetic parameters of macromonomeric formulations calculated from the heat flow profiles at 30 °C and 22.6 mW/cm²

Photoinitiator	% conc. of photo-initiator (w/w)	Induction Time (sec)	Peak Maximum Time (sec)	R _p max (x 10 ⁻²) (sec ⁻¹)	C _{max} (%)	Heat of reaction (J/g)	Autocatalytic		
							n	m	k (min ⁻¹)
IRGACURE 651	0.25	6.91	31.03	1.24	57.50	173.3	4.18	0.88	7.90
	1	4.21	19.02	1.71	58.47	176.2	4.02	0.74	8.31
DAROCUR TPO	0.25	3.22	16	2.21	59.49	179.3	4.05	0.79	11.9
	1	1.61	13.10	2.21	61.59	185.6	3.43	0.60	7.43
IRGACURE 184	0.25	12.93	42.55	0.98	51.07	153.9	4.52	0.86	6.32
	1	5.91	22.62	1.47	47.25	142.4	5	0.81	9.21
DAROCUR 1173	0.25	11.22	37.09	0.93	44.93	135.4	5.09	0.80	5.97
	1	4.25	20.50	1.76	57.07	172	3.96	0.78	8.95
IRGACURE 819	0.25	3.54	16.71	2	57.87	174.4	4.23	0.79	11.2
	1	1.80	13.21	2.51	59.36	178.9	3.78	0.71	11.1

As can be seen from Table 5.1, the induction time and the peak maximum time were found to decrease with an increase in concentration of photoinitiator showing a faster rate of photo initiation with increase in concentration of photoinitiator. The rate of polymerization maximum as well as the conversion maximum were found to increase with an increase in concentration of photoinitiator. When the viscosity build up after the volume relaxation occurring during the auto acceleration is low, it will result in a higher R_p max with increase in concentration of photoinitiator. This can be either due to enhancement in segmental diffusion and/or radical diffusion occurring just after autoacceleration.² Percentage conversion in this case is also showing a similar trend as R_p max. This is due to an optimum radical diffusion occurring along with gradual reaction diffusion in the deceleration step.³ In the case of IRGACURE 184, at higher concentration of photoinitiator, the conversion was found to decrease. The final conversion in this case was found to decrease probably due to predominance of reaction diffusion with reduced radical diffusion during the deceleration step.

From the values for induction time, we can infer that phosphine oxide type photoinitiators (DAROCUR TPO and IRGACURE 819) had a much faster rate of initiation. The trend was also observed during the entire photopolymerization process due the effect of a gradual reaction diffusion, which slowed down instantaneous viscosity build up. Better photopolymerization profiles for formulations containing DAROCUR TPO over formulations containing IRGACURE 819 can be due to multiple absorptions

occurring for the former as compared to later within the range of polychromatic radiation.⁴

The value of m and n showed consistency, explaining that the system fits variable autocatalytic kinetic model in the range of achieved conversions.⁵ System during photocuring can be assumed to undergo both bimolecular and monomolecular terminations.²

5.2.3 Photopolymerization of multiacrylate macromonomer based on hydroxy terminated polybutadiene 2750, isophorone diisocyanate and pentaerythritol triacrylate (System 5-2)

A hexamethacrylate macromonomer based on HTPB 2750, IPDI and PETA was synthesized and formulated. The photocuring studies of the formulations were carried out. Estimation of kinetic parameters was done based on the heat flow profile obtained during the photopolymerization process. The telechelic synthesis was done in two steps. An initial condensation of the HTPB and excess of diisocyanate to form a diisocyanate terminated urethane prepolymer followed by end capping of the formed prepolymer with excess of PETA to form a soft segmented urethane hexaacrylate macromonomer.

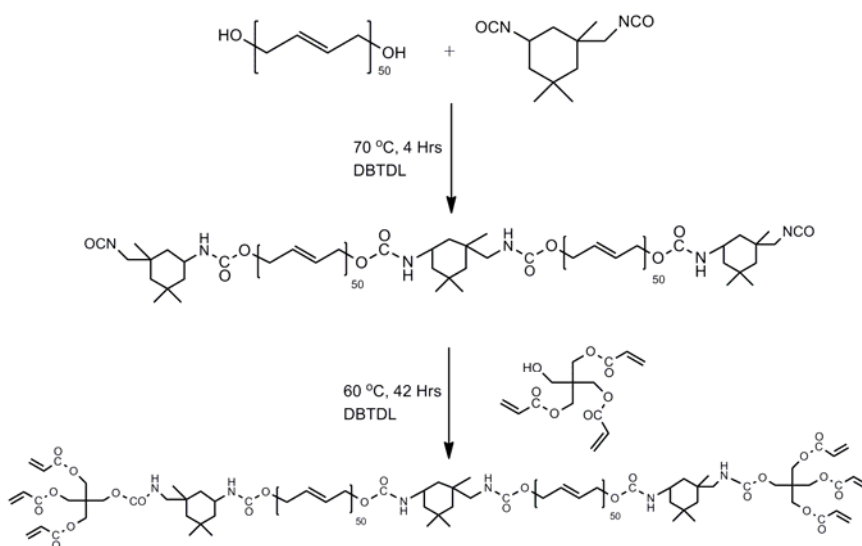


Figure 5.4 Synthesis pathway of urethane multiacrylate based on PPG 725, IPDI and PETA

5.2.3.1 Procedure for synthesis

Synthesis of macromonomer

A 100 mL three necked round bottomed flask was dried and flushed with nitrogen gas through one side neck. 10 mg (0.001584 mmol) dibutyl tin dilaurate was added to it followed by the addition of 10 g (3.636 mmol) of HTPB 2750 and homogenized at 40 °C at 80 rpm. 0.8746 g (3.935 mmol) of IPDI was weighed in a 25 mL beaker and was solvated in 5 mL chloroform and the contents of the beaker were transferred to the dropping funnel. The beaker was further washed with 5 mL of chloroform. The solvated diisocyanate was added at a rate of 1 mL/min and the system was homogenized by stirring at 100 rpm and the temperature was increased to 70 °C. After 4 h, 5 mg hydroquinone and 0.6712 g (2.25 mmol) of PETA in 10 mL of chloroform was added drop-wise under stirring at a rate of 1 mL/min and stirred for 5 min. The stirring speed was reduced thereafter to 80 rpm. The temperature was reduced to 60 °C and the reaction was continued in nitrogen atmosphere for 42 h until the isocyanate peak disappeared from IR spectrum. IR and NMR spectra were noted. The molecular mass was found by VPO.

IR: 1727 (C=O, urethane), 3350 and 1514 (-CO-NH-, urethane), 1193 (C-O), 1639 and 808 (C=C-, acrylate), 3006 (-C=C-), 2917, 2845 (-CH₂-) cm⁻¹.

¹H NMR(CDCl₃): 0.92 and 1.05 (CH₃, alicyclic), 1.24, 1.42 and 1.57 (CH₂, alicyclic), 2.16 (-CH₂-NH-), 2.90 (-CH-NH-, alicyclic), 4.16 (CH₂-O-CO-NH-), 4.29 (-CH₂-O-CO-CH=CH₂), 4.92 (-NH-CO-O-CH₂-CH=CH-CH₂-O-), 4.95 (-NH-CO-O-CH₂-CH=CH-CH₂-O-), 4.47 (-CH₂-NH-), 4.71 (=CH-NH-CO-, alicyclic), 5.40 and 5.36 (-CO-O-CH=CH-CH₂-O-), 6.11 (-O-CO-CH=CH₂), 5.86 and 6.39 (-O-CO-CH=CH₂).

¹³C NMR(CDCl₃): 30.10 (CH₃, gem, alicyclic), 23.19 (CH₃, alicyclic), 41.08, 44.55 and 47 (-CH₂-, alicyclic), 31.83 (=C-(CH₃)₂, alicyclic), 36.34 (=C-(CH₃)-CH₂-NH-CO-, alicyclic), 43.47 (=CH-NH-, alicyclic), 54.91 (-CH₂-NH-CO-), 62.61 and 64.10 (-CO-O-CH₂-CH=CH-CH₂-O-CH₂-), 129.98 and 130.42 (-O-CH₂-CH=CH-CH₂-O-), 128.32 (CH₂=CH-CO-O-), 131.23 (CH₂=CH-CO-O-), 153.96 (-CH₂-NH-CO-O-), 156.75 (-NH-CO-O-), 165.52 (CH₂=CH-CO-O-)

5.2.3.2 Formulation

The formulations were made in 5 mL sample vials. 1 g (0.296 mmol) of macromonomer was weighed accurately in all the vials. 10 mg (1 wt%) of two photoinitiators were added to obtain two compositions. Each composition was

homogenized in a vibrating mill for 2 min. The monomer was mixed with 1 wt% of two photoinitiators to obtain two photopolymerizable formulations. The photoinitiators used were IRGACURE 651 and DAROCUR 1173.

5.2.3.3 Photocuring studies

About 10 mg of the composition was accurately weighed on a DSC pan and subjected to photo DSC studies under a nitrogen purge of 50 mL/min. The heat flow profile obtained during the *in situ* photocuring process was recorded as a function of time under an isothermal condition of 30 °C. A 100 W high pressure mercury short arc lamp was used as source. The intensity of irradiation was kept constant at 1.73 mW/cm², under a polychromatic radiation of 320-500 nm. The normalized output signals in W/g against time were recorded. The rates of photopolymerizations as well as corresponding conversions were calculated for all the compositions.

5.2.3.4 Results and discussion

The macromonomer was characterized using IR, ¹H and ¹³C NMR spectroscopic techniques. The molecular mass was found to be 3378 by VPO. The total theoretical heat flow¹ (ΔH_{theor}) for the system was calculated to be 153.09 J/g.

The rate and conversion profiles obtained from photocuring studies of macromonomeric formulations containing two photoinitiators at 1 wt% compositions at 30 °C and 1.73 mW/cm² are given below in Figure 5.5 (A-C).

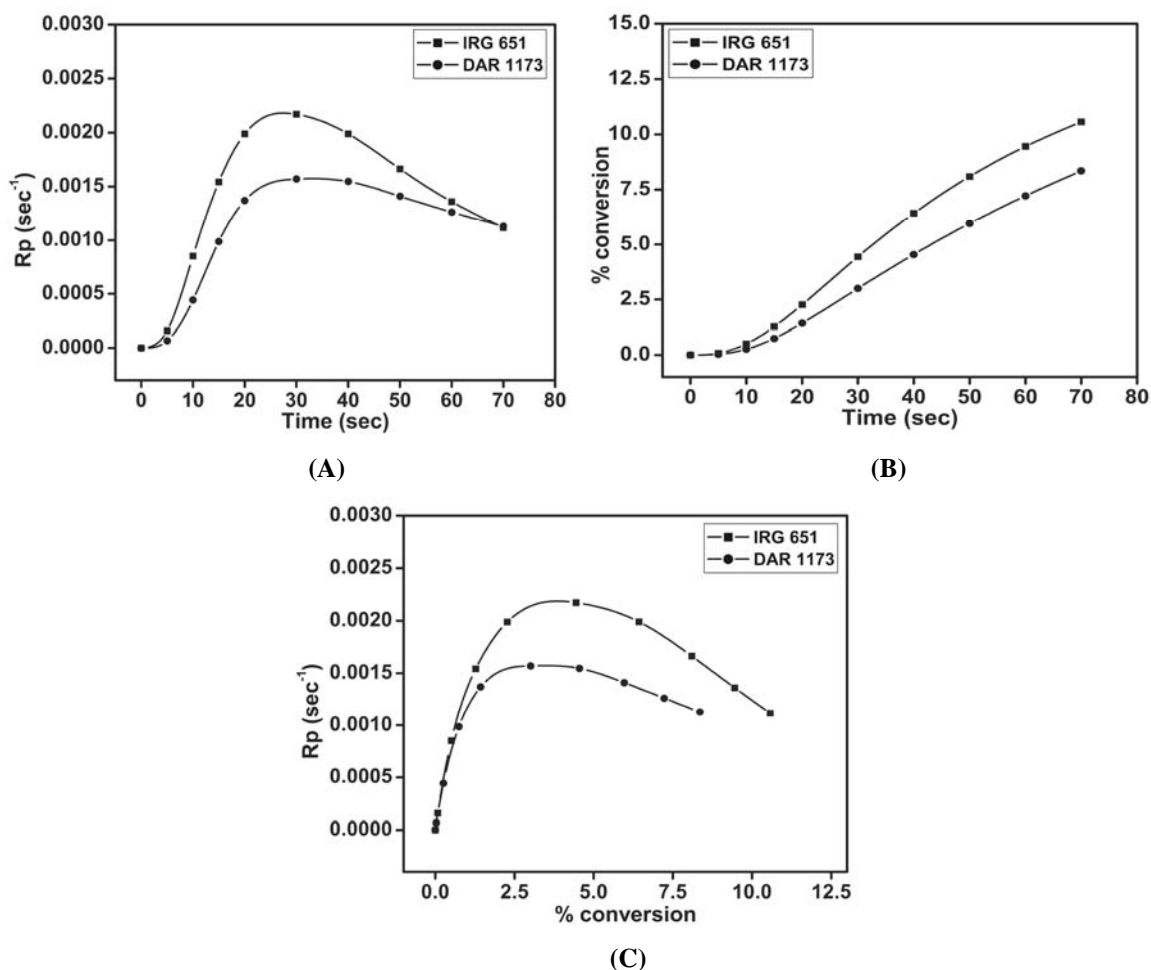


Figure 5.5(A-C) Time dependent rate and conversion profiles of macromonomeric formulations containing 1 wt% of two photoinitiators

The kinetic parameters calculated are given in Table 5.2.

Table 5.2 Kinetic parameters of macromonomeric formulations calculated from the heat flow profiles at 30 °C and 1.73 mW/cm²

Photoinitiator	Induction Time (sec)	Peak Maximum Time (sec)	$R_{p \max}$ ($\times 10^{-3}$) (sec^{-1})	C_{\max} (%)	Heat of reaction (J/g)	Autocatalytic		
						n	m	k (min^{-1})
IRGACURE 651	13.41	27.72	2.18	16.16	24.74	27.1	0.66	2.63
DAROCUR 1173	16.96	32.84	1.58	22.01	33.70	21.8	0.51	0.967

From Table 5.2, it can be inferred that the induction time was considerably higher than the system studied earlier. This shows that these formulations polymerized very slowly even from initiation at low irradiation intensity. The systems attained

comparatively faster peak maximum time as compared to initiation. The system also showed low values for $R_{p \text{ max}}$ and conversions. The major reason for a low conversion may be due to low irradiation intensity and usage of 320-500 nm filter, which prevents major absorption at wavelength below 300 nm ($\pi-\pi^*$ transitions) from causing spontaneous initiation. A weak absorption band around 330 – 340 nm for both the photoinitiators resulted in feeble initiations and final conversions.⁴ It has to be noted that variable autocatalytic kinetic model showed certain level of applicability as the value of m was within the expected range.⁶ The system is viscous and it did not show high levels of curing. The terminations occurring in this system during photocuring process can be assumed to be both bimolecular and monomolecular as radical combination and trapping can be assumed to occur together.²

5.2.4 Photopolymerization of multiacrylate macromonomer based on polyethylene glycol 200, polypropylene glycol 725, polypropylene glycol 3000, isophorone diisocyanate and glycerol diglycerolate diacrylate (System 5-3)

A multiacrylate based on PEG 200, PPG 725, PPG 3000, IPDI and glycerol diglycerolate diacrylate (GDGDA) was synthesized and its photocuring studies were carried out. Estimation of kinetic parameters were done based on the heat flow profile obtained during the photopolymerization process.

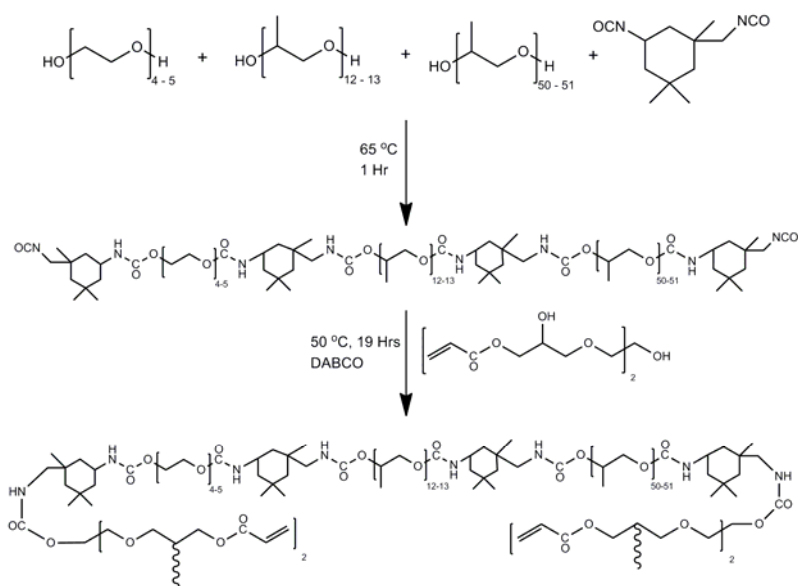


Figure 5.6 Synthesis pathway of urethane multiacrylate based on PEG 200, PPG 725, PPG 3000, IPDI and GDGDA

5.2.4.1 Procedure for synthesis

Preparation of prepolymer

To a 100 mL three neck round bottomed flask provided with a half moon stirrer and stuffing box was flushed with dry nitrogen gas for 3 min. It was then charged with 4 g (20 mmol) of PEG 200, 8.4 g (11.59 mmol) of PPG 725, 23 g (7.67 mmol) of PPG 3000 and 13 g (58.48 mmol) of IPDI at room temperature. The system was stirred at 150 rpm. The reaction temperature was increased to 65 °C and the reaction was carried out for a period of 1 h, until the oligomer is formed. The reaction was monitored by estimation of residual isocyanate (ASTM D 2572). IR and NMR spectra were noted.

IR: 2261 (NCO), 1718 (C=O, urethane), 3340 and 1539 (-CO-NH-, urethane), 1108 (C-O), 2967, 2928, 2901 and 2871 (-CH₂-) cm⁻¹.

¹³C NMR (CDCl₃): 17.14, 17.25, 18.11 and 18.37 (-O-[CH(CH₃)-CH₂-O]-), 27.58 and 35.03 (CH₃, gem, alicyclic), 23.23 (CH₃, alicyclic), 44.57, 46.20 and 46.86 (-CH₂-, alicyclic), 31.79 (=C=(CH₃)₂, alicyclic), 36.32 (=C-(CH₃)-CH₂-NH-CO-, alicyclic), 54.83 (-CH₂-NCO), 63.66 and 69.59 (-NH-CO-O-CH₂-CH₂-O-) and 70.47 (-O-CH₂-CH₂-O-), 72.82 and 73.27 (-O-[CH(CH₃)-CH₂-O]-), 75.04, 75.24 and 75.44(-O-[CH(CH₃)-CH₂-O]-), 155.73 (-NH-CO-O-), 156.89 (-CH₂-NH-CO-O-)

Synthesis of macromonomer

A reaction vessel equipped with a stirrer and nitrogen inlet was charged with 22 g of diisocyanate terminated urethane prepolymer and 22 mg (0.177 mmol) of hydroquinone monomethyl ether. The system was stirred at 100 rpm for 15 min at room temperature at 5 °C. 10 mL of chloroform was added to 6 g (17.22 mmol) of glycerol 1, 3-diglycerolate diacrylate in a dropping funnel. The stirring speed was increased to 150 rpm and the contents of the dropping funnel were added over a period of 10 minutes. After stirring for 30 min, the temperature was raised to 50 °C and the reaction was allowed to continue for 6 h followed by addition of 280 mg (2.496 mmol) of DABCO. The reaction was further continued for 13 h, until the isocyanate was completely consumed.

20 mL of chloroform was added to the R B flask and the contents were poured in to 100 mL deionised water taken in a 500 mL separating funnel. It was further washed three times with 100 mL water until the washings are devoid of excess acrylate. The chloroform layer was separated and kept over night over activated molecular sieves. The

chloroform layer was decanted and vacuum was applied at room temperature for a period of 6 h followed by drying in vacuum oven at 60 °C for 10 h to obtain the viscous macromonomer. IR and NMR spectra were noted. The molecular mass was found by VPO.

IR: 1723 (C=O, urethane), 3465 and 1547 (-CO-NH-, urethane), 1105 (C-O), 1635 and 812 (CH=CH-CO-, acrylate), 2972, 2928, 2901 and 2868 (-CH₂-) cm⁻¹.

¹³C NMR (CDCl₃): 17.17, 17.29, 18.06 and 18.33 (-O-[CH(CH₃)-CH₂-O]-), 27.50 and 34.97 (CH₃, gem, alicyclic), 23.16 (CH₃, alicyclic), 44.28, 46.72 (-CH₂-, alicyclic), 31.70 (=C-(CH₃)₂, alicyclic), 36.24 (=C-(CH₃)-CH₂-NH-CO-, alicyclic), 59.21 (-CH₂-NH-CO-O-), 64.04 and 69.57 (-NH-CO-O-CH₂-CH₂-O-) and 70.45 (-O-CH₂-CH₂-O-), 72.76 and 73.20 (-O-[CH(CH₃)-CH₂-O]-), 74.98, 75.22 and 75.37 (-O-[CH(CH₃)-CH₂-O]-), 127.92 (-O-CO-CH=CH₂), 131.36 (-O-CO-CH=CH₂), 155.34 (-NH-CO-O-), 156.86 (-CH₂-NH-CO-O-), 166.06 (-O-CO-CH=CH₂)

5.2.4.2 Formulation

The formulations were made in 1 mL sample vials. 500 mg (0.0722 mmol) of macromonomer was weighed accurately in all the vials. 2.5 mg (0.5 wt%) and 10 mg (2 wt%) of ten photoinitiators were added to obtain twenty compositions. Each composition was homogenized in a vibrating mill for 5 min. The photoinitiators used were IRGACURE 651, DAROCUR TPO, IRGACURE 184, IRGACURE 2959, DAROCUR 1173, DAROCUR MBF, IRGACURE 907, IRGACURE 819, GENOCURE CQ and GENOCURE BP.

5.2.4.3 Photocuring studies

5 mg of the composition was accurately weighed on a DSC pan and subjected to photo DSC studies under a nitrogen purge of 50 mL/min. The heat flow profile obtained during the *in situ* photocuring process was recorded as a function of time under an isothermal condition of 30 and 50 °C. The intensity of irradiation was kept at 4.6 mW/cm² using a polychromatic radiation of 320-500 nm using a 100 W high pressure mercury short arc lamp. The normalized output signals in W/g against time were recorded. The rates of photopolymerizations as well as corresponding conversions were calculated for all the compositions.

5.2.4.4 Results and discussion

The prepolymer and macromonomer were characterized using IR and ^{13}C NMR spectroscopy. The total acrylate functionality in the macromonomer was calculated to be 3.8 by titration for residual unsaturation⁷ and the molecular mass was found to be 6928 by VPO. The total theoretical heat flow¹ (ΔH_{theor}) for the system was calculated to be 47.28 J/g.

The rate and conversion profiles obtained from photocuring studies of macromonomeric formulations containing ten photoinitiators at 0.5 and 2 wt% compositions at 30 and 50 °C and 4.6 mW/cm² are given below in Figures 5.7 to 5.10 (A-C).

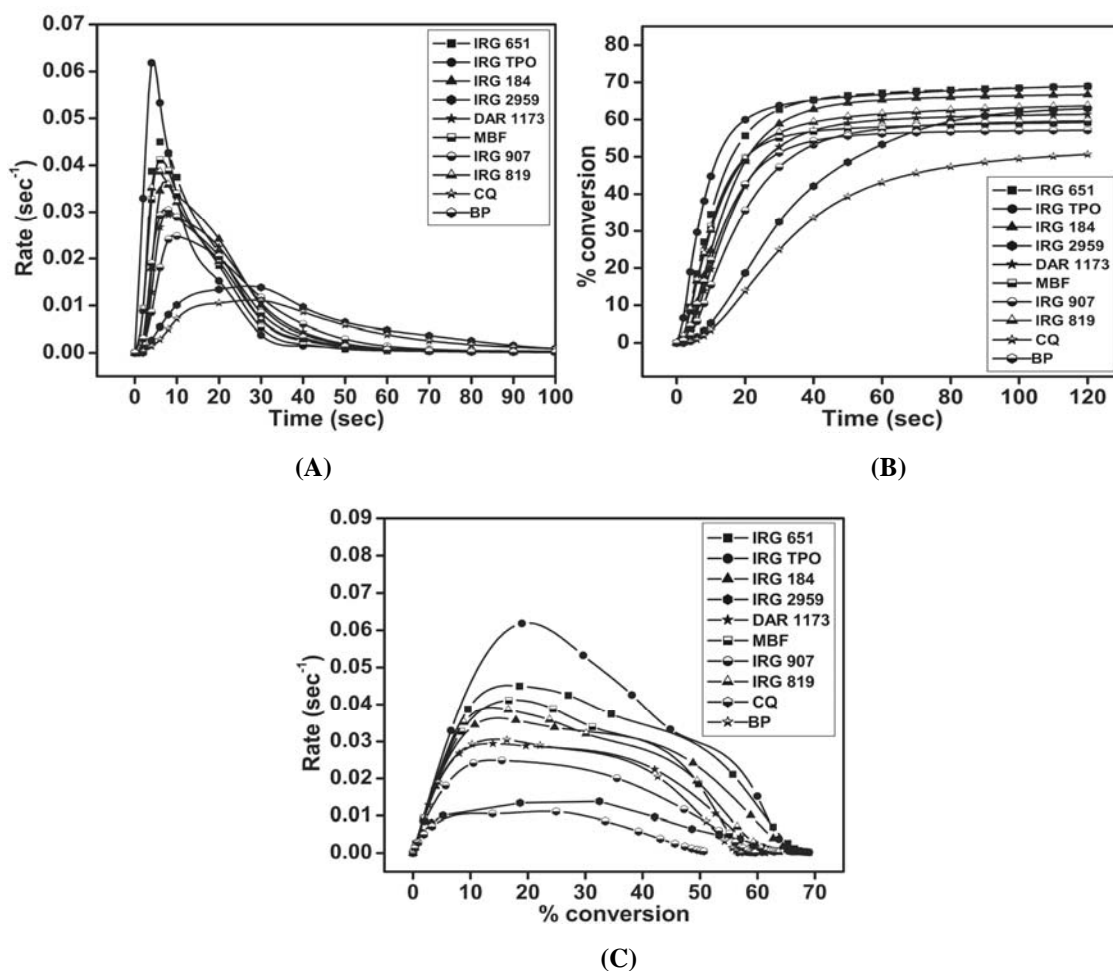
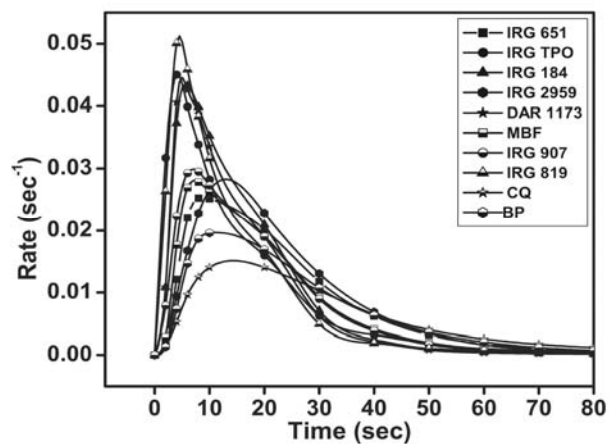
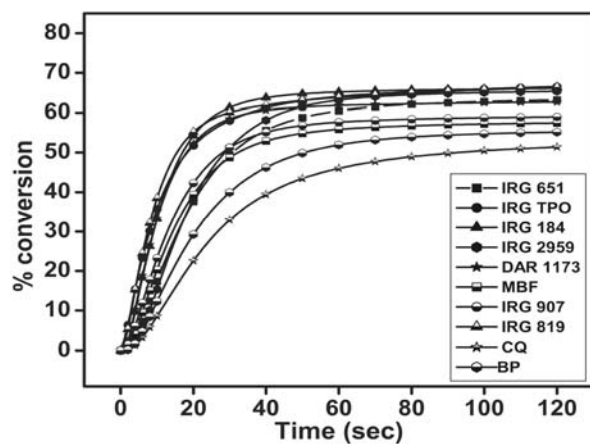


Figure 5.7(A-C) Time dependent rate and conversion profiles of macromonomeric formulations containing 0.5 wt% of ten photoinitiators at 30 °C

(A)



(B)



(C)

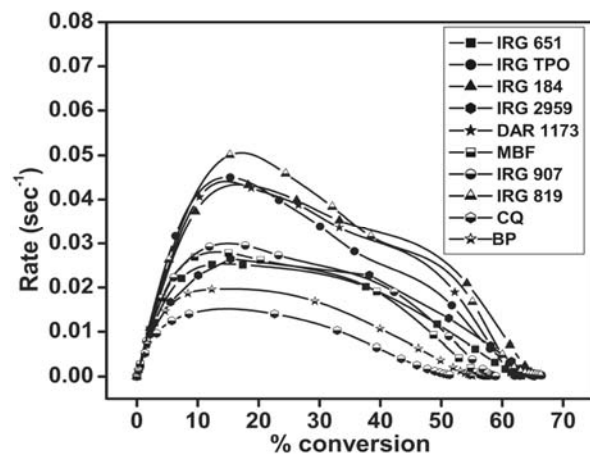
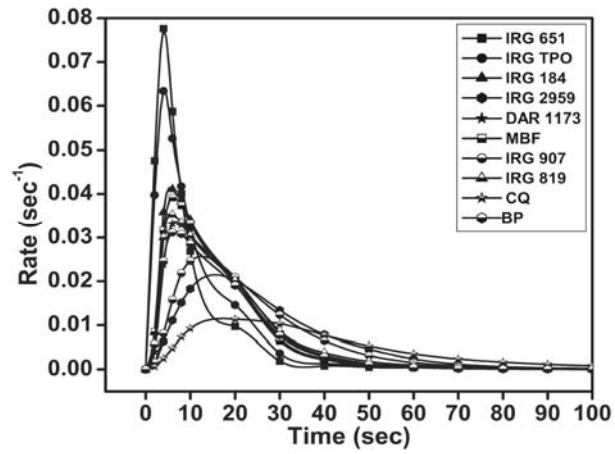
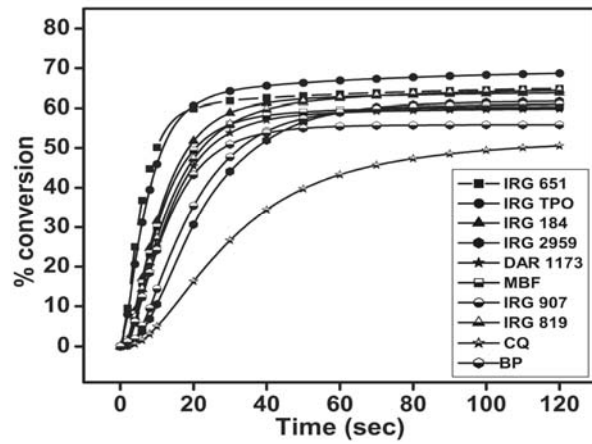


Figure 5.8(A-C) Time dependent rate and conversion profiles of macromonomeric formulations containing 2 wt% of ten photoinitiators at 30 °C

(A)



(B)



(C)

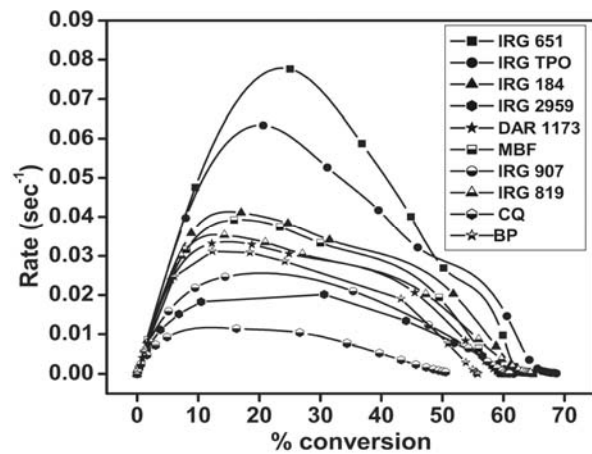


Figure 5.9(A-C) Time dependent rate and conversion profiles of macromonomeric formulations containing 0.5 wt% of ten photoinitiators at 50 °C

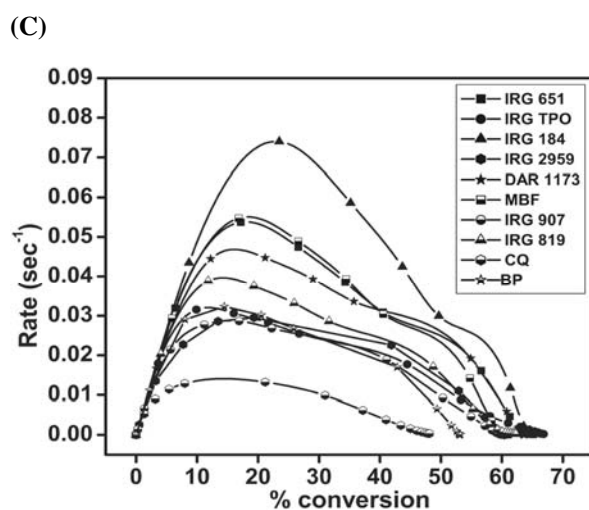
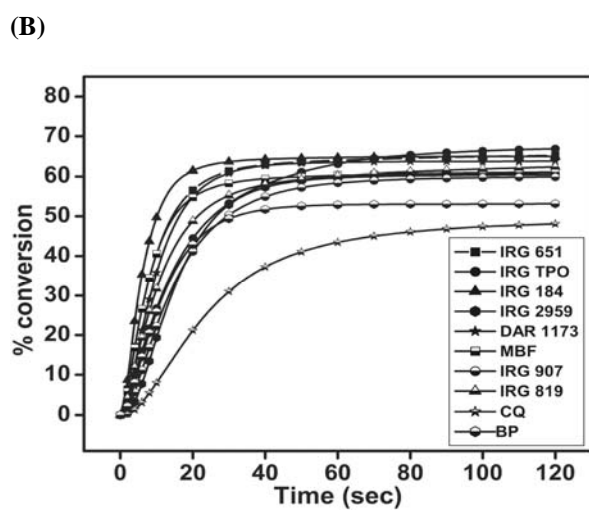
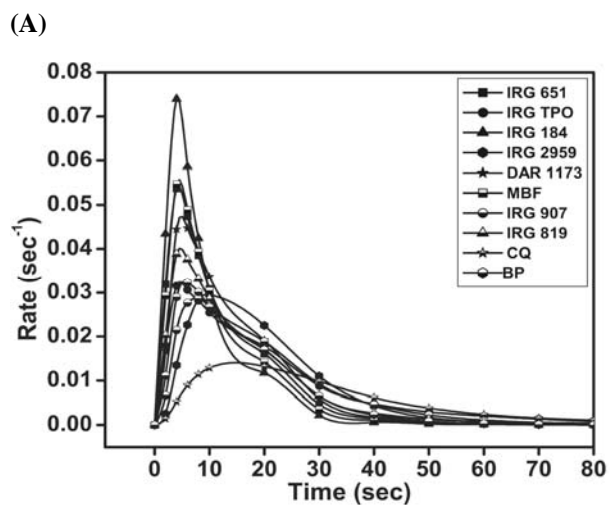


Figure 5.10(A-C) Time dependent rate and conversion profiles of macromonomeric formulations containing 2 wt% of ten photoinitiators at 50 °C

The kinetic parameters calculated are given in Tables 5.3 and 5.4.

Table 5.3 Kinetic parameters of macromonomeric formulations calculated from the heat flow profiles at 4.6 mW/cm²

Photoinitiator	% conc. of photoinitiator (w/w)	Temp (°C)	Induction Time (sec)	Peak Maximum Time (sec)	R _{p max} (x 10 ⁻²) (sec ⁻¹)	C _{max} (%)	Heat of reaction (J/g)
IRGACURE 651	0.5	30	1.57	5.40	4.52	70.03	33.11
	2	30	2.65	8.65	2.54	64.11	30.31
	0.5	50	0.22	4.09	7.77	65.67	31.05
	2	50	0.38	4.34	5.44	65.95	31.18
DAROCUR TPO	0.5	30	0.38	4.38	6.27	70.24	33.21
	2	30	0.36	4.14	4.52	67.87	32.09
	0.5	50	0.29	4.16	6.36	69.61	32.91
	2	50	0.69	4.68	3.24	68.10	32.20
IRGACURE 184	0.5	30	2.62	7	3.66	67.22	31.78
	2	30	1.36	5.59	4.35	66.33	31.36
	0.5	50	1.63	5.31	4.15	64.36	30.43
	2	50	0.27	4.18	7.42	64.85	30.66
IRGACURE 2959	0.5	30	4.97	26.93	1.41	64.17	30.34
	2	30	2.96	13.05	2.84	65.93	31.17
	0.5	50	3.29	15.57	2.15	61.95	29.29
	2	50	2.54	9.33	2.96	60.36	28.54
DAROCUR 1173	0.5	30	2.94	7.48	2.95	62.06	29.34
	2	30	1.43	4.95	4.46	62.92	29.75
	0.5	50	2.14	6.76	3.37	60.05	28.39
	2	50	0.90	4.80	4.75	63.16	29.86
DAROCUR MBF	0.5	30	1.47	6.14	4.12	59.81	28.28
	2	30	2.38	7.26	2.82	58.02	27.43
	0.5	50	1.56	6.25	3.93	60.53	28.62
	2	50	0.43	4.45	5.57	61.29	28.98
IRGACURE 907	0.5	30	3	9.11	2.52	60.36	28.54
	2	30	1.54	7.08	2.99	59.29	28.03
	0.5	50	3.08	12.64	2.57	61.38	29.02
	2	50	1.75	7.59	2.88	60	28.37
IRGACURE 819	0.5	30	1.61	5.10	3.96	64.85	30.66
	2	30	0.50	4.53	5.12	67.98	32.14
	0.5	50	1.88	5.57	3.56	65.38	30.91
	2	50	0.64	4.68	4.03	63.62	30.08
GENOCURE CQ	0.5	30	6.26	28.49	1.11	52.45	24.80
	2	30	3.51	14.42	1.52	53	25.06
	0.5	50	4.92	16.33	1.16	52.20	24.68
	2	50	3.49	14.81	1.41	49.26	23.29
GENOCURE BP	0.5	30	2.31	7.30	3.07	57.28	27.08
	2	30	3.23	10.39	1.97	55.92	26.44
	0.5	50	1.88	6.78	3.15	55.54	26.26
	2	50	1.22	5.40	3.26	52.33	24.74

From Table 5.3, we can infer that the induction time as well the peak maximum time showed a decreasing trend with increase in concentration of photoinitiator at a

particular temperature as well as with increase in temperature at a particular concentration showing the initiation has not attained a optimum value of radical concentration during the initial stages of polymerization. Certain anomalies were observed in some cases. An increase in induction and peak maximum time was observed with increase in temperature at a particular concentration in the case of IRGACURE 907 and IRGACURE 819. In these cases, the radical concentration has crossed the optimum value at 2 wt% concentration reducing the number of effective radicals involved in photopolymerization process. Hence, terminations are higher which was further enhanced by the low system viscosity at higher isothermal conditions.⁸ This reduced the quantum yield of photo initiation and hence higher values were observed at higher temperature. In the case of formulations containing IRGACURE 651, DAROCUR MBF and GENOCURE BP at 30 °C and IRGACURE 651 and DAROCUR TPO at 50 °C, an increase in concentration of photoinitiator has resulted in an increase in induction time and peak maximum time due to reduction in effective number of reacting radicals at higher concentration of photoinitiator.

The value of $R_{p \text{ max}}$ in this case was found to follow an increasing trend with increase in concentration of photoinitiator at a particular temperature as well as with increase in temperature at a particular concentration. $R_{p \text{ max}}$ was found to increase with increase in concentration of photoinitiator at many cases. Variations with decrease in value of $R_{p \text{ max}}$ with increase in concentration of photoinitiator at 30 °C were observed for IRGACURE 651, DAROCUR TPO, DAROCUR MBF and GENOCURE BP and at 50 °C for IRGACURE 651 and DAROCUR TPO. A decrease in the value of $R_{p \text{ max}}$ was also observed with an increase in temperature with formulation containing 0.5 wt% of IRGACURE 819 and DAROCUR MBF and with formulation containing 2 wt% of DAROCUR TPO, IRGACURE 907, IRGACURE 819 and GENOCURE CQ. Since similar variations were observed in induction and peak maximum time as explained earlier, we can infer that the reduction in effective radical concentration involved in reaction from the initial stages has influence up to $R_{p \text{ max}}$. In other words, increase in viscosity from autoacceleration to $R_{p \text{ max}}$ is not high enough so that the onset of reaction diffusion is only gradual. The values of final conversions varied from 52 to 70%. A trend as observed for $R_{p \text{ max}}$ was not observed in C_{max} due to enhanced influence of viscosity

dependent reaction diffusion in the deceleration step.⁹ It has to be noted that final conversions with camphoroquinone (GENOCURE CQ) and benzophenone (GENOCURE BP) were at the lower side mainly due to the lower efficiency of these initiators within the irradiation range. Benzophenone cures efficiently within the irradiation range, in presence of sensitizers such as amines.^{10,11} Camphoroquinone has π - π^* transitions around 200-300 nm, and n- π^* transition at 470 nm.¹² The emission spectra of mercury source from 320-500 nm shows nearest emission at 436 nm. Since the value of forbidden transition of camphoroquinone is very low, the formulations containing these initiators showed longer induction times and lower ultimate conversions.

Table 5.4 Evaluation of kinetic parameters of macromonomeric formulations as per autocatalytic model at 4.6 mW/cm²

Photoinitiator	% conc. of photoinitiator (w/w)	Temp (°C)	Autocatalytic		
			n	m	k (min ⁻¹)
IRGACURE 651	0.5	30	2.81	0.46	10.7
	0.5	50	3.50	0.53	23.8
	2	30	2.98	0.43	5.66
	2	50	3.04	0.40	11.3
DAROCUR TPO	0.5	30	3.01	0.45	14.4
	0.5	50	2.91	0.40	13.4
	2	30	3.43	0.40	10.1
	2	50	3.12	0.34	5.94
IRGACURE 184	0.5	30	2.50	0.38	6.85
	0.5	50	2.89	0.42	8.90
	2	30	2.75	0.44	9.55
	2	50	3.12	0.47	18.8
IRGACURE 2959	0.5	30	3.53	0.68	5.91
	0.5	50	3.50	0.68	8.32
	2	30	3.17	0.62	8.70
	2	50	3.18	0.58	8.92
DAROCUR 1173	0.5	30	2.80	0.41	6.22
	0.5	50	3.12	0.44	7.89
	2	30	2.92	0.39	8.88
	2	50	2.68	0.38	8.80
DAROCUR MBF	0.5	30	3.60	0.57	13.5
	0.5	50	3.35	0.51	11
	2	30	3.43	0.44	6.69
	2	50	3.47	0.48	14.8
IRGACURE 907	0.5	30	3.29	0.49	6.42
	0.5	50	3.38	0.58	7.68
	2	30	3.47	0.50	8.11
	2	50	3.57	0.51	8.12
IRGACURE 819	0.5	30	3.21	0.44	9.29
	0.5	50	2.95	0.38	7.08
	2	30	3.18	0.44	11.8
	2	50	3.39	0.42	8.98
GENOCURE CQ	0.5	30	4.38	0.64	4.90
	0.5	50	4.34	0.60	4.49
	2	30	4.61	0.58	5.61
	2	50	4.94	0.60	5.73
GENOCURE BP	0.5	30	3.20	0.45	7.37
	0.5	50	3.36	0.45	7.73
	2	30	3.82	0.49	5.49
	2	50	3.60	0.44	7.88

Table 5.4 provides the evaluation of variable autocatalytic kinetic model for the photocured formulations cured at 30 and 50 °C at 4.6 mW/cm². The values show that the system obeys the model to greater levels at achieved conversions, as the value of m and n are constant. The value of specific rate constant (k) was also within a range. The system

during photocuring can be assumed to undergo both bimolecular and monomolecular terminations.

5.2.5 Photopolymerization of multiacrylate macromonomer based on polytetrahydrofuran 650, isophorone diisocyanate and propylene glycol glycerolate diacrylate (System 5-4)

A multiacrylate based on PTHF 650, IPDI and PGGDA was synthesized and its photocuring studies were carried out. Estimation of kinetic parameters were done based on the heat flow profile obtained during the photopolymerization process.

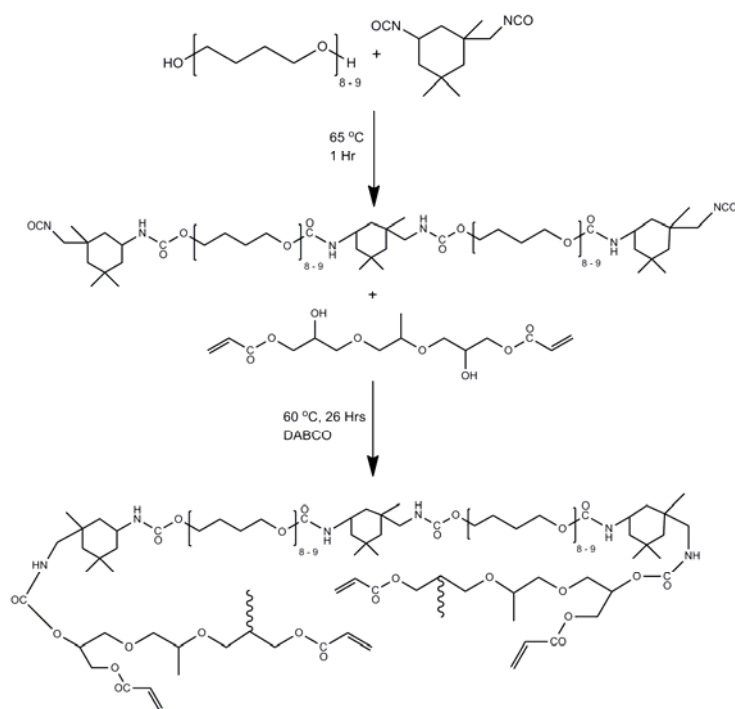


Figure 5.11 Synthesis pathway of urethane multiacrylate based on PTHF 650, IPDI and PGGDA

5.2.5.1 Procedure for synthesis

Preparation of prepolymer

To a 100 mL three neck round bottomed flask provided with a half moon stirrer and stuffing box was flushed with dry nitrogen gas for 3 min. It was then charged with 15.52 g (23.87 mmoles) of PTHF 650 and 5.33 g (24 mmoles) of IPDI at room temperature. The system was stirred at 100 rpm. The reaction temperature was increased

to 65 °C and the reaction was carried out for a period of 1 h, until the prepolymer is formed. The reaction was monitored by residual isocyanate (ASTM D 2772). IR and NMR spectra were noted.

IR: 2262 (NCO), 1712 (C=O, urethane), 3340 and 1535 (-CO-NH-, urethane), 1105 (C-O), 2928 and 2855 (-CH₂-) cm⁻¹.

¹H NMR: (CDCl₃): 0.86, 0.91 and 1.04 (CH₃, alicyclic), 1.16 to 1.31 (-CH₂-, alicyclic), 1.60, 1.64 (-O-CH₂-CH₂-CH₂-CH₂-O-), 2.90, (-CH₂-NH-CO-), 3.02 (-CH₂-NCO), 3.39 and 3.43 (-O-CH₂-CH₂-CH₂-CH₂-O-), 3.77 (-CH-NH-, alicyclic), 4.52 (-NH-CO-O-CH₂-), 4.78 (-CH₂-NH-CO-O-CH₂-).

¹³C NMR: (CDCl₃): 26.46, 26.17 and 25.86 (-O-CH₂-CH₂-CH₂-CH₂-O-), 27.59 and 35.02 (CH₃, gem, alicyclic), 23.21 (CH₃, alicyclic), 41.88, 46.36 and 47.01 (-CH₂-, alicyclic), 31.83 (=C=(CH₃)₂, alicyclic), 36.35 (=C-(CH₃)-CH₂-NH-CO-, alicyclic), 56.94 (-CH₂-NCO), 64.70 (-NH-CO-O-CH₂-CH₂-), 62.66 (-CH₂-NH-CO-O-CH₂-CH₂-), 70.21 and 70.81 (-O-CH₂-CH₂-CH₂-CH₂-O-), 155.95 (-NH-CO-O-), 157.12 (-CH₂-NH-CO-O-)

Preparation of macromonomer

To a 100 mL three neck R B flask provided with a half moon stirrer and stuffing box was flushed with dry nitrogen gas for 3 min. It was then charged with 15 g of NCO terminated prepolymer and stirred under nitrogen atmosphere at 60 °C for 5 min at 100 rpm. 15 mg of HQME was added to it. 1 g (3.01 mmol) of PGGDA was solvated in 20 mL of chloroform in a dropping funnel. The stirring speed was raised to 120 rpm and the contents of the funnel were added at a rate of 1 mL/min followed by addition of 160 mg (1.43 mmol) of DABCO. After addition, the stirring speed was reduced to 80 rpm and the temperature was maintained at 60 °C for 26 h until the residual isocyanate content was completely consumed from the IR spectrum. 20 mL of chloroform was added to the R B flask and the contents were poured in to 100 mL deionised water taken in a 500 mL separating funnel. It was then washed further four times with deionised water until the washings are devoid of excess acrylate. The chloroform layer was separated and kept over night over activated molecular sieves. The chloroform layer was decanted and dried in vacuum oven at 60 °C for 12 h to obtain the viscous macromonomer. IR and NMR spectra were noted. The molecular mass was found by VPO.

IR: 1704 (C=O, urethane), 3332 and 1538 (-CO-NH-, urethane), 1110 (C-O), 809 (CH=CH-CO-, acrylate), 2945 and 2857 (-CH₂-) cm⁻¹.

$^1\text{H NMR}$ (CDCl_3): 0.86, 0.91 and 1.04 (CH_3 , alicyclic), 1.11 to 1.—($-\text{CH}_2-$, alicyclic), 1.60, 1.64 ($-\text{O}-\text{CH}_2-\text{CH}_2-\text{CH}_2-\text{CH}_2-\text{O}-$), 2.90 ($-\text{CH}_2-\text{NH}-$), 3.39 and 3.43 ($-\text{O}-\text{CH}_2-\text{CH}_2-\text{CH}_2-\text{CH}_2-\text{O}-$), 3.77 ($-\text{CH}-\text{NH}-$, alicyclic), 4.22 ($-\text{NH}-\text{CO}-\text{O}-\text{CH}=\text{CH}_2$), 4.51 ($-\text{NH}-\text{CO}-\text{O}-\text{CH}_2-$), 4.78 ($-\text{CH}_2-\text{NH}-\text{CO}-\text{O}-\text{CH}_2-$), 5.85 and 6.40 ($-\text{CO}-\text{O}-\text{CH}=\text{CH}_2$), 6.15 ($-\text{CO}-\text{O}-\text{CH}=\text{CH}_2$).

$^{13}\text{C NMR}$ (CDCl_3): 26.46, 26.17 and 25.86 ($-\text{O}-\text{CH}_2-\text{CH}_2-\text{CH}_2-\text{CH}_2-\text{O}-$), 27.59 and 35.02 (CH_3 , gem, alicyclic), 23.20 (CH_3 , alicyclic), 41.91, 46.35 and 47 ($-\text{CH}_2-$, alicyclic), 31.83 ($=\text{C}=(\text{CH}_3)_2$, alicyclic), 36.35 ($=\text{C}-(\text{CH}_3)-\text{CH}_2-\text{NH}-\text{CO}-$, alicyclic), 55.03 ($-\text{CH}_2-\text{NH}-\text{CO}-$), 64.69 ($-\text{NH}-\text{CO}-\text{O}-\text{CH}_2-\text{CH}_2-$), 62.67 ($-\text{CH}_2-\text{NH}-\text{CO}-\text{O}-\text{CH}_2-\text{CH}_2-$), 70.21 and 70.81 ($-\text{O}-\text{CH}_2-\text{CH}_2-\text{CH}_2-\text{CH}_2-\text{O}-$), 127.97 ($-\text{O}-\text{CO}-\text{CH}=\text{CH}_2$), 132.04 ($-\text{O}-\text{CO}-\text{CH}=\text{CH}_2$), 155.96 ($-\text{NH}-\text{CO}-\text{O}-$), 157.12 ($-\text{CH}_2-\text{NH}-\text{CO}-\text{O}-$), 166.07 ($-\text{O}-\text{CO}-\text{CH}=\text{CH}_2$).

5.2.5.2 Formulation

The formulations were made in 2 mL sample vials. 1 g (0.349 mmol) of macromonomer was weighed accurately in all the vials. 5 mg (0.5 wt%) and 20 mg (2 wt%) of four photoinitiators were added to obtain eight compositions. Each composition was homogenized in a vibrating mill for 2 min. The photoinitiators used were IRGACURE 651, DAROCUR TPO, IRGACURE 184 and IRGACURE 819.

5.2.5.3 Photocuring studies

5 mg of the composition was accurately weighed on a DSC pan and subjected to photo DSC studies under a nitrogen purge of 50 mL/min. The heat flow profile obtained during the *in situ* photocuring process was recorded as a function of time under an isothermal condition of 30 and 50 °C. The intensity of irradiation was kept at 4.6 mW/cm² using a polychromatic radiation of 250-450 nm using a 100 W high pressure mercury short arc lamp. The normalized output signals in W/g against time were recorded. The rates of photopolymerizations as well as corresponding conversions were calculated for all the compositions.

5.2.5.4 Results and discussion

The prepolymer and macromonomer were characterized using IR ^1H and ^{13}C NMR spectroscopic techniques. The total acrylate functionality was calculated as 4.3 by titration for residual unsaturation⁷ and the molecular mass was found to be 2863 by VPO. The total theoretical heat flow¹ (ΔH_{theor}) for the system was calculated to be 129.45 J/g.

The rate and conversion profiles obtained from photocuring studies of macromonomeric formulations containing four photoinitiators at 0.5 and 2 wt% compositions at 30 and 50 °C and 4.6 mW/cm² are given below in Figures 5.12 (A-C) to 5.15 (A-C).

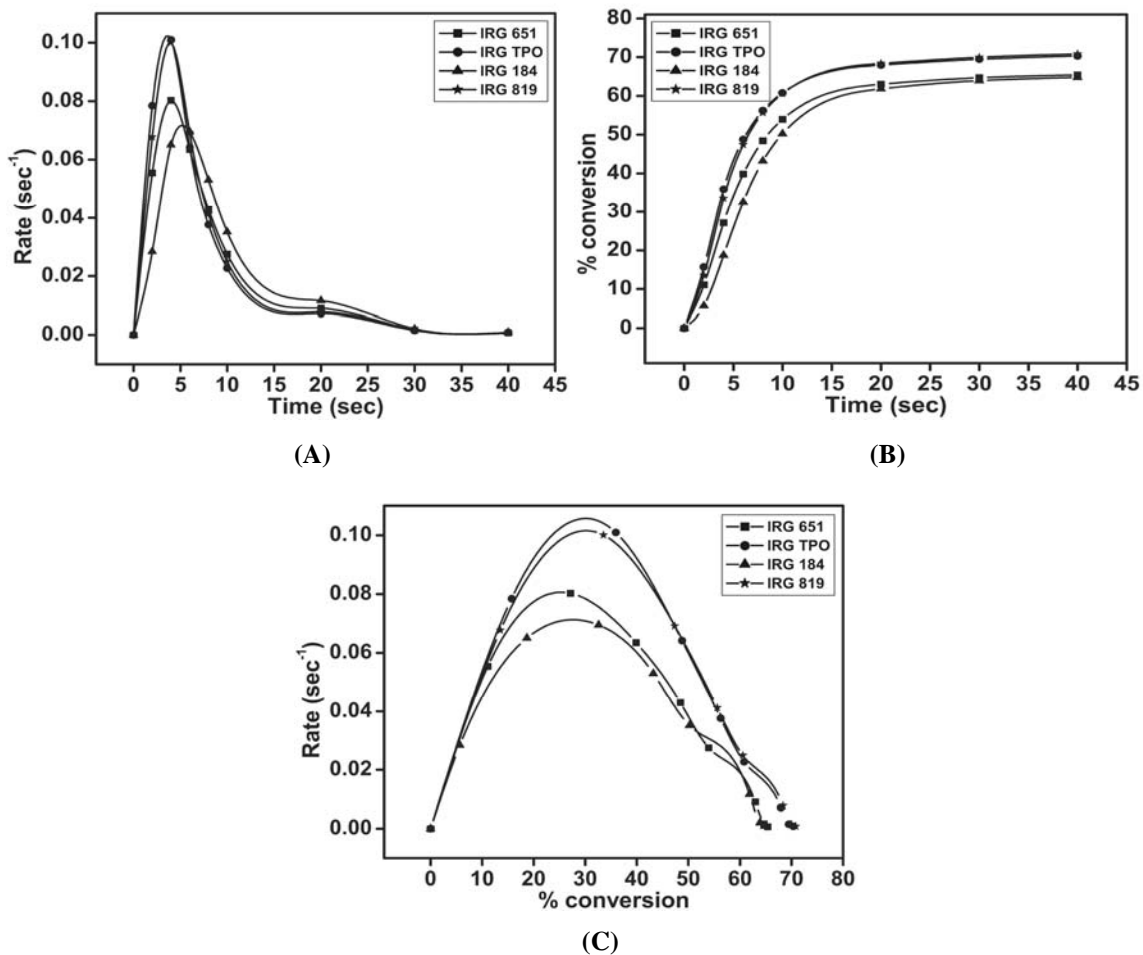
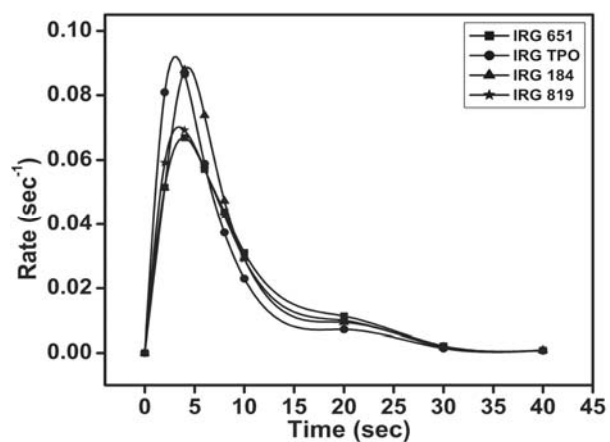
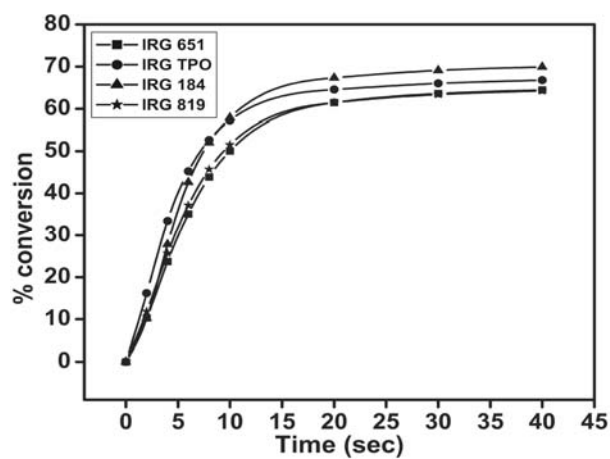


Figure 5.12(A-C) Time dependent rate and conversion profiles of macromonomeric formulations containing 0.5 wt% of four photoinitiators at 30 °C

(A)



(B)



(C)

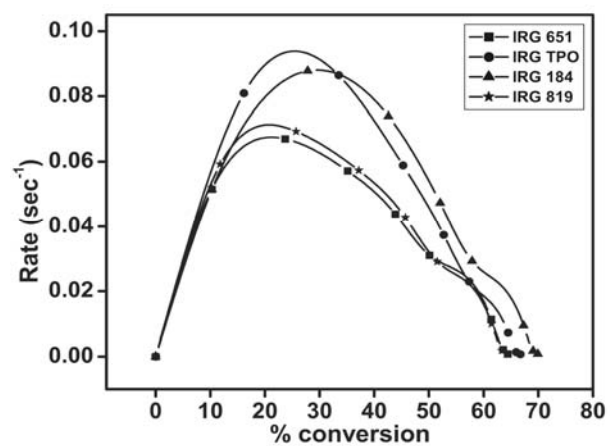
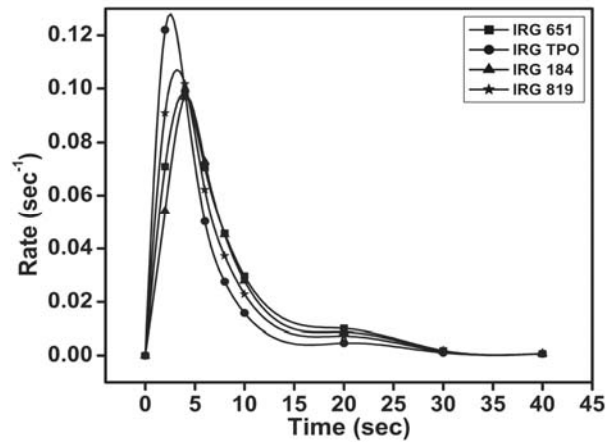
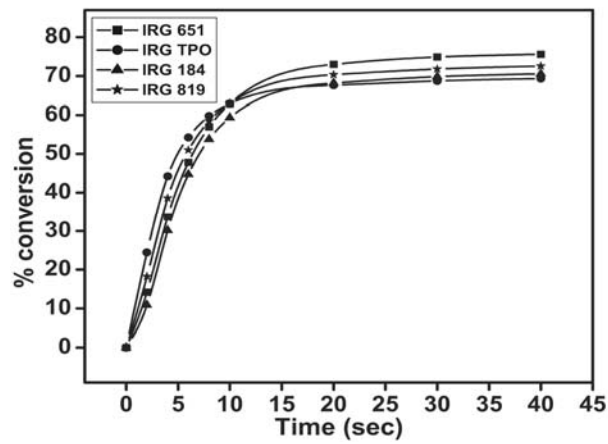


Figure 5.13(A-C) Time dependent rate and conversion profiles of macromonomeric formulations containing 2 wt% of four photoinitiators at 30 °C

(A)



(B)



(C)

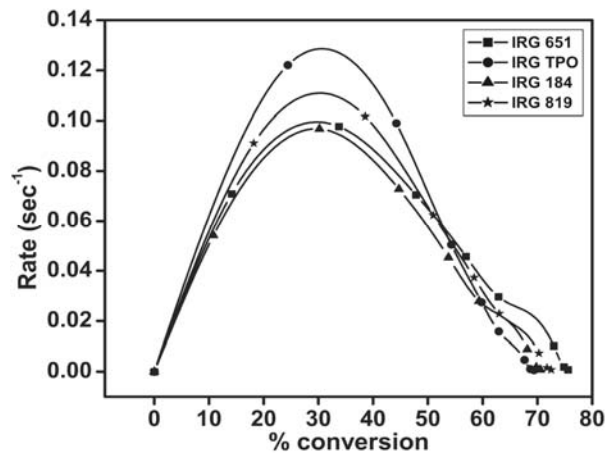


Figure 5.14(A-C) Time dependent rate and conversion profiles of macromonomeric formulations containing 0.5 wt% of four photoinitiators at 50 °C

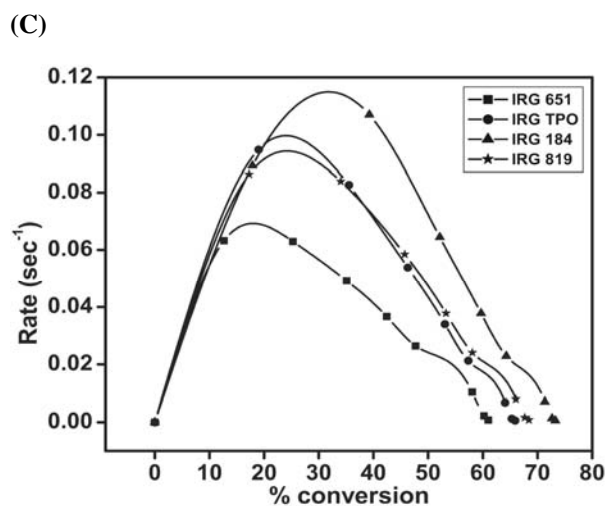
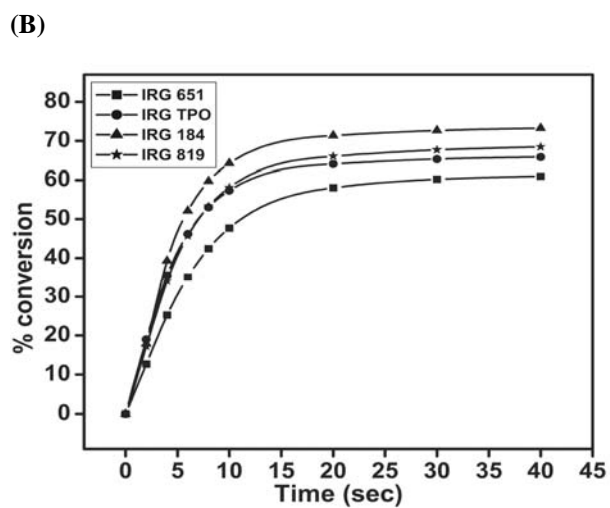
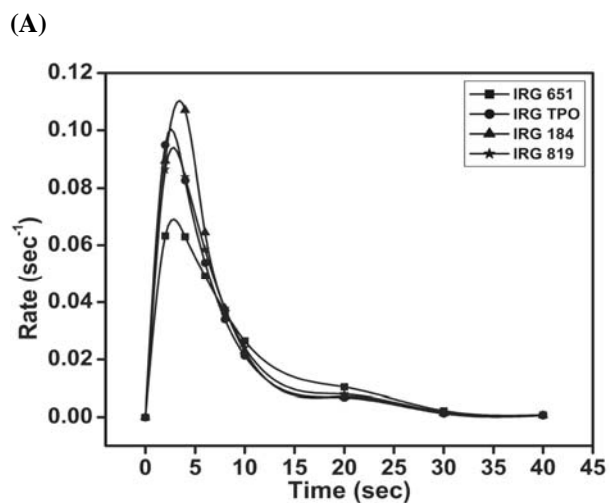


Figure 5.15(A-C) Time dependent rate and conversion profiles of macromonomeric formulations containing 2 wt% of four photoinitiators at 50 °C

The kinetic parameters calculated are given in Tables 5.5 and 5.6.

Table 5.5 Kinetic parameters of macromonomeric formulations calculated from the heat flow profiles at 4.6 mW/cm²

Photoinitiator	% conc. of photo-initiator (w/w)	Temp (°C)	Induction Time (sec)	Peak Maximum Time (sec)	R _{p max} (x 10 ⁻²) (sec ⁻¹)	C _{max} (%)	Heat of reaction (J/g)
IRGACURE 651	0.5	30	0.20	4.04	8.05	68.09	88.14
	2	30	0.20	3.83	6.70	66.84	86.53
	0.5	50	0.16	3.86	9.81	77.48	100.3
	2	50	0.16	2.82	6.91	62.23	80.56
DAROCUR TPO	0.5	30	0.13	3.62	10.2	75.13	97.26
	2	30	0.12	3.06	9.22	70.54	91.31
	0.5	50	0.08	2.52	12.81	72.74	94.16
	2	50	0.10	2.58	10.02	68.17	88.24
IRGACURE 184	0.5	30	0.51	5.27	7.18	68.47	88.64
	2	30	0.24	4.33	8.87	73.23	94.80
	0.5	50	0.24	4.19	9.71	72.95	94.43
	2	50	0.13	3.43	11.05	75.36	97.55
IRGACURE 819	0.5	30	0.17	3.99	10	76.31	98.78
	2	30	0.17	3.40	7.05	68.78	89.03
	0.5	50	0.11	3.23	10.71	76.57	99.12
	2	50	0.11	2.77	9.39	72.14	93.39

Table 5.6 Evaluation of kinetic parameters of macromonomeric formulations as per autocatalytic model at 4.6 mW/cm²

Photoinitiator	% conc. of photo-initiator (w/w)	Temp (°C)	Autocatalytic		
			n	m	k (min ⁻¹)
IRGACURE 651	0.5	30	2.94	0.49	21.1
	0.5	50	2.55	0.52	25.7
	2	30	2.66	0.39	13.8
	2	50	2.85	0.29	11.5
DAROCUR TPO	0.5	30	3.19	0.61	37.1
	0.5	50	3.45	0.57	48.8
	2	30	3.10	0.46	24.9
	2	50	3.01	0.37	21.1
IRGACURE 184	0.5	30	3.31	0.72	29.7
	0.5	50	3.03	0.64	33.8
	2	30	3.02	0.68	32.8
	2	50	2.95	0.58	37.1
IRGACURE 819	0.5	30	3.13	0.64	36.8
	0.5	50	2.95	0.53	32.7
	2	30	2.76	0.39	15
	2	50	2.97	0.44	23

Table 5.5 represents the kinetic parameters calculated from the heat flow profiles. As expected the induction times as well as the peak maximum times were found to decrease with an increase in concentration of photoinitiator at a particular temperature as well as with increase in temperature at a particular concentration. The formulations can thus be considered to have a better radical diffusion with reduced terminations at the initial stages of polymerization. The value of $R_{p \text{ max}}$ at a particular concentration was found to increase with an increase in temperature. This shows that the retardation effect of reaction diffusion is not much pronounced at $R_{p \text{ max}}$ with increase in temperature at similar initiator concentration due to better radical and/or segmental diffusion.² The glycerol moieties as well as the polyol segments can impart much better segmental diffusion due to their flexible nature which is pronounced at higher temperature.¹³ In addition, with similar radical concentration at higher temperature the initial viscosity is reduced and hence the radical diffusion shows the same trend of initiation up to $R_{p \text{ max}}$, provided the *in situ* viscosity is not very high at $R_{p \text{ max}}$. It has to be noted that in many cases, an increase in concentration of photoinitiator from 0.5 to 2 wt% at the same temperature has reduced the value of $R_{p \text{ max}}$. This is due to either higher rate of radical radical combinations occurring with increase in concentration of photoinitiator which was pronounced during the volume relaxation in autoacceleration or due to a comparatively higher influence of reaction diffusion soon after autoacceleration. In both the cases, the effective number of radicals involved in the propagation reaction gets reduced thereby reducing the value of $R_{p \text{ max}}$. The final conversion also showed the same trend as $R_{p \text{ max}}$. This system can be considered to have a gradual increase in reaction diffusion along with radical diffusion, so that the effect at $R_{p \text{ max}}$ is shown in the deceleration step. This effect is normally observed when the *in situ* viscosity build up is gradual.¹⁴

Table 5.6 shows that the formulations obey autocatalytic kinetic model to high levels of achieved conversions, as the values of m and n are constant. The value of specific rate constant (k) was also within a range.⁶ The system during photocuring can be assumed to undergo both monomolecular as well as bimolecular termination reactions.²

5.3 Conclusions

Photopolymerization of multi functional oligomers in presence of photoinitiators of various classes were carried out without the addition of reactive diluents. The first two systems involved photopolymerization of hexaacrylates while the last two systems involved photopolymerization of branched multiacrylates. The synthesized oligomers were based on urethane (meth)acrylates possessing aliphatic and cycloaliphatic backbone and functionalities varying from 3.8 to 6. Photopolymerizations were carried out with polychromatic radiation at 30 °C for hexaacrylate systems and at 30 and 50 °C for branched multiacrylate systems under a constant nitrogen purge of 50 mL/minute. In the case of hexaacrylates, photopolymerization took place in an efficient manner with moderate conversions when irradiated with 250-450 nm polychromatic radiation while low conversions were observed with oligomers when irradiated with low irradiation intensity and excitation energy of 320-500 nm.

It was also observed in system 5-1 that an increase in concentration of photoinitiator decreased the induction as well as peak maximum time with an increase in the value of $R_{p \text{ max}}$ and C_{max} . The value of $R_{p \text{ max}}$ was increased with an increase in concentration of photoinitiator. C_{max} also showed similar trend as $R_{p \text{ max}}$ showing a gradual influence of reaction diffusion during deceleration step. In the case of system 5-2, we can infer that the studied formulations had high induction and peak maximum times. It shows that the rate of initiation as well as the course of polymerization is low. This system showed a low final conversion due to low irradiation intensity and energy. The low energy irradiation range from 320-500 nm prevented the occurrence of $\pi\text{-}\pi^*$ transitions.

In the case of system 5-3, it was found in most cases that an increase in concentration of photoinitiator at a particular temperature as well as an increase in temperature at a particular concentration resulted in a decrease in induction as well as peak maximum time with an increase in the value of $R_{p \text{ max}}$. This shows that the trend from rate of initiation is observable up to $R_{p \text{ max}}$. However, the trend was not noted in similar way for C_{max} . From these observations, we can infer that an enhanced effect of reaction diffusion is observed after $R_{p \text{ max}}$ probably due to low *in situ* viscosity build up or increased radical diffusion up to $R_{p \text{ max}}$. Hence, the effect of viscosity dependent reaction

diffusion which restricts other diffusion processes can be assumed to occur in the deceleration step.

In the case of system 5-4, it was found in most cases that an increase in concentration of photoinitiator at a particular temperature as well as an increase in temperature at a particular concentration resulted in a decrease in induction as well as peak maximum time. An increase in concentration of photoinitiator at a particular temperature decreased the value of $R_{p \text{ max}}$ and C_{max} showing the influence of viscosity dependent reaction diffusion. It has to be noted that an increase in temperature at a particular concentration increased the value of $R_{p \text{ max}}$ in all cases with variations in C_{max} values in certain cases. This shows that the reduction in *in situ* viscosity at higher temperature resulted in better radical diffusion, which delayed the onset of reaction diffusion in the case of all formulations. Variations in the trend occurred for C_{max} values, due to enhancement in reaction diffusion in the deceleration step due to opposing factors.

The applicability of variable autocatalytic kinetic model on photopolymerization processes were studied using TA advantage specialty library software. The model takes into account of the heat flow profiles signal from onset of initiation to the onset of vitrification. It was observed that in certain cases the value of autocatalytic exponent (m) for the studied acrylate photopolymerization reactions were closer to 0.5. However, it cannot be said that the model is a fit to the reaction kinetics as in many cases all the experimental points did not lie within the calculated value on plotting $\log(dC/dt)$ against $\log(1-C)C^{m/n}$. The value of specific rate constant (k) did not show an increase with increase in temperature in many cases. All these systems during photocuring can be assumed to undergo both bimolecular as well as monomolecular terminations.

5.4 References

- [1] I.V. Khudyakov, J.C. Legg, M.B. Purvis, B.J. Overton., *Ind. Eng. Chem. Res.* **38**, 3353 (1999).
- [2] E. Andrzejewska., *Prog. Polym. Sci.* **26**, 605 (2001).
- [3] C. Decker., *Polym. Inter.* **45**, 133 (1988).
- [4] Photoinitiators for UV curing – Key products selection guide, Ciba Speciality Chemicals Inc., Switzerland.
- [5] R. Chandra, R.K. Soni, S.S. Murthy., *Polym. Inter.* **31**, 305 (1993).
- [6] E. Andrzejewska, L.A. Linden, J.F. Rabek., *Polym. Inter.* **42**, 179 (1997).
- [7] L.S. Luskin – *Acrylic and methacrylic acids and esters. In Encyclopedia of Industrial chemical analysis-Ablative materials to alkaloids (F.D. Snell and C.L. Hilton Ed.)* Vol.4, page 191 (1967).
- [8] S. Harrisson, S.R. Mackenzie, D.M. Haddleton., *Macromolecules* **36**, 5072 (2003).
- [9] K.S. Anseth, C.M. Wang, C.N. Bowman., *Macromolecules* **27**, 650 (1994).
- [10] N.S. Allen, E. Lam, E.M. Howells, P.N. Green, A. Green, F. Caralina, C. Peinado., *Eur. Polym. J.* **26**, 1345 (1990).
- [11] G. Ullrich, D. Herzog, R. Liska, P. Burtscher, N. Moszner., *J. Polym. Sci. Polym. Chem.* **42**, 4948 (2004).
- [12] E. Andrzejewska, L.A. Linden, J.F. Rabek., *Macromol. Chem. Phys.* **199**, 441 (1998).
- [13] J.H. Ward, A. Shahar, N.A. Peppas., *Polymer* **43**, 1745 (2002).
- [14] D.L. Kurdikar, N.A. Peppas., *Polymer* **35**, 1004 (1994).
- [15] N.S. Allen, J. Segurola, M. Edge, E. Santamari, A. Mc Mahon., *Surf. Coat. Inter.* **2**, 67 (1999).
- [16] U. Khanna, M. Chanda., *J. Appl. Polym. Sci.* **49**, 319 (1993).

Synthesis of cation exchange resins and
their catalytic evaluation for acid phase
condensation reactions

6.1 Introduction

6.1.1 Functionalization of porous polymers for use as cation exchange resins

Porous polymers are used in ion exchange applications.¹ These resins can be functionalized with active species.² Relative abundance of functionalization at the surface makes them useful for catalytic applications. Cation exchange resin can be used for catalyzing many reactions such as lactone formation, alkylation of aromatics including phenols, polymerization and acylation of olefins, acylation of aromatics, decomposition of cumene hydroperoxide and Von Pechmann reaction.³ Conventionally, acidic cation exchange resins can be made by functionalization of porous polymers prepared by suspension polymerization techniques.^{4,5} Beads with higher surface area are preferred as the pores are not found to be interconnected throughout the matrix. As a result macroporous matrix is always preferred over a microporous matrix for functionalization.

It has been observed that highly porous polymeric matrixes prepared by High Internal Phase Emulsion (HIPE) technique have interconnected pores with high surface area and pore volumes. They also have very low bulk densities and low physical strengths. The addition of inert hydrophobic porogens is mostly used in water in oil in water (W/O/W) polyHIPE synthesis. It was observed that use of these matrices for acid functionalization resulted in the rupture of the cellular morphology of the beads due to low physical strength. Hence we proposed to use W/O/W polyHIPE without added porogens. This would result in reduction of pore size in the HIPE matrix as the pores are created by the water present in the internal phase during polyHIPE synthesis. As sphere has the minimum surface area, dispersing water in the monomer surfactant system during the preparation of HIPE at high rpm (preferably over 1000) will result in the creation of small spherical droplets of water stabilized by the surfactant-monomer system. A W/O/W polyHIPE prepared by this method results in the formation of porous polymers with better physical strength than that of corresponding W/O/W polyHIPE prepared by using a hydrophobic porogen.

We functionalized the synthesized polyHIPEs with sulphonic acid groups as well as mercapto sulphonic acid groups. The functionalization was based the ring opening of oxirane / thiirane groups as well as sulphonation of aromatic ring present in the polyHIPE matrix.

The oxirane ring in a co/terpolymers involving glycidyl methacrylate as one of the monomers can result in the introduction of surface functionalized oxirane groups. Reaction of oxirane ring with sodium bisulphite results in the formation of sodium sulphonates which on acidification forms sulphonic acids.⁶ Opening of oxirane ring in the polymer with sodium sulphite in the presence of a mixture of solvent system at 80 °C followed by acidification will also yield sulphonic acids.⁷⁻⁹ The remaining oxirane groups can be converted into diols by treating with 0.5M sulphuric acid at 80 °C for two hours. The sulphonic acid group concentration can be determined by titration.¹⁰ Bisulphite addition on unsaturated compounds in the presence of peroxides or other oxidizing agents can also provide sulphonates by cleavage of π bonds.^{11,12} Homopolymerization of allyl allyl sulphonate followed by ring opening can also produce sulphonic acids.^{13,14}

Sulphonation using mineral acids are widely used for improving the surface properties of the unsaturated polymers from hydrophobic to hydrophilic nature. In this case the π bonds present in the surface is subjected to sulphonation by treatment with gaseous sulphur trioxide^{15,16}, hot concentrated sulphuric acid¹⁷⁻¹⁹ and fuming sulphuric acid.²⁰⁻²² Haloalkylated aromatic polymers can also be converted into polymeric sulphonic acids by reacting with dimethyl sulphide followed by treatment with sodium sulphite and acidification.^{23,24} Haloalkylated polymers could be first converted into mercaptoalkylated polymers which was then oxidized by hydrogen peroxide to sulphoalkylated copolymers.²⁵ Aromatic rings can also be sulphonated by mineral acids. Direct reaction of chlorosulphonic acid on styrenated polymers in the presence of an inert solvent at ambient conditions followed by treatment with base and subsequent acidification can produce pendant substituted aromatic sulphonic acids.²⁶⁻²⁸ Sulphonation of aromatic based polyHIPE has been reported.^{2,29} If DVB is used as cross linker in the polymer, then sulphonation can also occur in the aromatic ring involved in crosslinking.³⁰ Sulphonic acid groups can also be substituted in aromatic ring by treatment with acetyl sulphate.³¹⁻³³ Sulphonation using acetyl sulphate on polyHIPE monolith is reported.³⁴ Another method of sulphonation involves metallation followed by sulphination and acidification.^{35,36} Aromatic sulphonic acids are hydrolyzed in the presence of a large excess of water above 150 °C.³⁷ Styrene-DVB copolymers can be used as base matrix for subsequent functionalization by chloromethylation followed by treatment with aliphatic

diamines to obtain macroreticular chelating resins.³⁸ These resins can adsorb Zn^{2+} , Cu^{2+} , Ni^{2+} and Hg^{2+} ions efficiently from solvated mixtures.

Conversion of oxirane group to thiirane group are reported.³⁹⁻⁵¹ Oxiranes and thiiranes of optical purity can be obtained.⁵² Other methods of thiirane synthesis includes silica gel assisted synthesis of thiiranes⁵³ and conversion of olefins to thiiranes.⁵⁴ Aqueous ammonia and acetic acid⁵⁵ polymerize thiirane and the polymerization reaction is enhanced with dilute hydrochloric acid.⁵⁶ However, with concentrated hydrochloric acid thiirane forms 2-chloro thiols.⁵⁷ With hydrogen sulphide, thiirane forms dithiols⁵⁸ and with primary or secondary amines, thiiranes form amino substituted thiols.⁵⁹ Bisphenol A diglycidyl ether (BPADGE) can be converted into diepisulphides followed by thermal polymerization. This process reduces the gelation time on polymerization as compared to BPADGE.⁶⁰ Synthesis, radical polymerization and photocrosslinking of 2,3-epithiopropyl methacrylate (ETMA) are reported.⁶¹⁻⁶⁵ ETMA can also form copolymers with DVB which in turn can be modified to form a chelating resin for Hg^{2+} and Ag^{+} ions.⁶⁶ Thiiranyl ring in porous polymers can be converted into dithiols by treating with potassium hydrosulphide followed by acidification.⁶⁷ Reduction of disulphides in the presence of catalyst can also yield dithiols.^{68,69} Thiiranyl ring on treatment with hydrogen peroxide can yield β -hydroxy sulphonic acids⁷⁰ while on treatment with aqueous sodium bisulphite gives sodium salt of β -mercapto sulphonic acids.⁷¹ Oxidation of thiols can also produce sulphonic acids.⁷² Thiolated HIPE beads has been synthesized from polyHIPE containing pendant vinyl groups. The process involves addition of thioacetic acid followed by aminolysis.⁷³

6.1.2 Preparation of bisphenol and trisphenol by acid phase catalysis

Bisphenol A is synthesized by the condensation of excess phenol with acetone in acidic environment. The catalyst can be either homogenous or heterogeneous. The homogeneous catalysts include hydrogen halides, sulphuric acid, phosphoric acid, nitric acid, acetyl chloride, dimethyl sulphate, sulphur dioxide, p-toluene sulphonic acid, boron trifluoride and dodecyl benzene sulphonic acid.⁷⁴ An acid having a dissociation constant greater than 10^{-3} can catalyze the reaction.⁷⁵ Commonly used catalysts include Amberlite IR-120H, Amberlyst-15H, 31 and 131, Dowex-50-x-4, Dowex MSC-1H, Duolite C-26, Permutit QH, Chempro C-2, Purolite CT-124, Bayer K-1221 and Imac-C8P/H.⁷⁶

Fluorinated sulphonation catalyst can also be used for the synthesis of bisphenol A.⁷⁷ The preferred exchange capacity of the resin is from 3 to 5.5 meq. H⁺/g of dry resin.⁷⁸

Synthesis of mercapto sulphonic acid has been reported.⁷⁹ Synthesis of 4,4'-bisphenol A using mesoporous silica functionalized with sulphonic acid⁸⁰ as well as mercapto sulphonic acid⁸¹ groups are reported. It has been observed that the addition of low molecular weight aliphatic mercapto acid to the reaction mixture or *in situ* generation of it in the system by the addition of a corresponding salt or an ester to a level of 0.1 to 0.5 mol for each mole of ketone can reduce the time of reaction to one tenth of the time required for a particular extent of conversion.⁸² Typical synthesis procedures of the bicatalyst system involving catalyst as well as added mercaptan containing additive as cocatalyst are reported.⁸³

Alternatively, bicatalyst that contain both acidic as well as mercaptan group in the same matrix has also been used.^{81,84,85} Ring opening of side chain anchored sultone with sodium hydrosulphide followed by acidification can produce aliphatic sulphonic acid with thiol in the side chain.⁸¹ The monophenol as well as the carbonyl compound used has to be purified so as to remove accompanying substances which may act as alkylating agents directly or via intermediate compounds. Reduction of polyvinyl sulphonic acid can provide aliphatic mercapto sulphonic acid catalyst. Here half of the sulphonic acid group can be converted into chlorosulphonyl units and subsequently reduced to mercapto groups to obtain the bicatalyst.⁸⁵ Alkylation of polystyrene with 4-bromo ethyl benzyl chloride in presence of lewis acid results in the formation of an adduct, which on treatment with chlorosulphonic acid followed by treatment with sodium hydrogen carbonate will introduce sodium sulphonates on the aromatic rings. This on treatment with sodium thioacetate followed by acid hydrolysis will provide a bicatalyst having aromatic sulphonic acid with thiol groups in the side chain.⁸⁵ The phenol to acetone ratio in bisphenol A synthesis can vary from 3:1 to 40:1 with excess phenol acting as a solvent for the reaction.⁷⁸ Purification methods of bisphenol A are based on recrystallization, extraction using different solvents or high vacuum distillation, which are complex and difficult processes. Hence the selective catalysis route is preferred to obtain the 4,4'-isomer. Various by-products are formed during the synthesis process such as 2,4'-isomer, Indan and spiroindan compounds, chroman, trisphenol etc. which make the system to

appear dark. Formation of the product as well as the impurities has been studied.⁸⁶ It has been reported⁸⁷ that traces of water helps to suppress the isomerization reactions favoring an increase in the 4,4' isomer.

Similar to bisphenol synthesis, 1,1,1-tris(4'-hydroxyphenyl)ethane (THPE) can be prepared by acid catalysis. Initially, it was used as a laxative for treating constipation in mammals⁸⁸ and is widely used as a cross linker in polycarbonate manufacture.⁸⁹ It is generally prepared by the acid phase condensation of phenol and 4-hydroxy acetophenone. It can also be prepared from 2,4-pentanedione and phenol.⁸⁹ Inert solvents, catalysts and cocatalysts used for the synthesis of bisphenol A, are employed for the synthesis of THPE. Sulphonated styrene-DVB catalyst can be used for the synthesis of THPE.^{90,91} Synthesis of THPE using ion exchange resin with the addition of 3-mercaptopropionic acid has been reported.⁹²

The exchange capacity of the catalyst can vary from 2-5 meq. of H⁺/g of catalyst in dry form. The mole ratio of phenol to 4-hydroxyl acetophenone can vary from 4:1 to 20:1 and the reaction is typically carried out from 50-110 °C. Azeotropic removal of water can be done with toluene or 1,2-dichloroethane.⁹³ The absorbance of THPE detected at 422, 500 and 600 nm using HPLC is less than 0.06, 0.03 and 0.01, respectively.⁹⁴

6.2 Experimental

6.2.1 Materials

Ethylene dimethacrylate-EGDM, styrene, divinyl benzene-DVB, polyethyleneglycol octadecyl ether-Brij 72, 1,1,1-tris(4'-hydroxyphenyl)ethane-99% (from Aldrich), glycidyl methacrylate-GMA and poly-N-vinyl pyrrolidone-PVP (from Fluka), sorbitane monooleate-Span 80 (from Loba Chemie), 2,2'-Azobisisobutyronitrile or AIBN (from SRL), potassium peroxy disulphate, phenol, acetone (from Merck), 4-hydroxyl acetophenone (from Spectrochem) and 4,4'-bisphenol A-99% (GE) were used as received. 2,3-epithiopropyl methacrylate-ETMA was synthesized by a reported procedure.⁶² The HLB values of Span 80 and Brij 72 are 4.3 and 4.9, respectively.

6.2.2 Measurements

The purified beads obtained by HIPE method were subjected to various characterization studies using surface analyses techniques. Nature of beads before and after modification were noted.

6.2.2.1 Elemental analysis

6.2.2.1.1 EDX

Elemental analyses of certain synthesized HIPE beads were noted by energy dispersive X-ray spectroscopy (EDX). The energy of analyses was 20 keV.

6.2.2.2 Infrared Spectroscopy

The surface modifications of the HIPE beads were studied using (Perkin Elmer – Spectrum GX) Fourier Transform Infra Red spectrophotometer. Spectra were recorded after mulling with KBr followed by pelletization. All spectra were recorded from 4000-450 cm^{-1} with 10 scans at a resolution of 4.

6.2.2.3 BET surface area analysis

The BET surface areas of the prepared co/terpolymers as well as cation exchange resins prepared from the same were studied using a QUANTACHROME autosorb gas sorption analyzer. The analyses for surface areas were carried out using ultra pure nitrogen at a flow rate of 10 psi and the data were processed with autosorb 1 software.

6.2.2.4 Surface morphology analysis

6.2.2.4.1 Optical microscopy

The surface morphologies of the beads prepared were studied by an OLYMPUS polarized optical microscope at a magnification of 40 and 500 x. The microphotographs were recorded using a OLYMPUS digital camera.

6.2.2.4.2 Scanning electron microscopy

The surface morphologies of the beads prepared were studied using a Lieca Stereoscan 440 scanning electron microscope at three different magnifications. The energy of analyses was 20 keV.

6.2.2.5 High resolution XPS

X-ray photoelectron spectra were recorded using an ESCA-3000 (VG Scientific Ltd, England) with a 9 channeltron CLAM4 analyzer under a vacuum better than 1×10^{-8} Torr, using MgK α radiation (1253.6 eV) and a constant pass energy of 50 eV. The binding energy values were charge-corrected to the C_{1s} signal (285 eV). An XPS peak 4 software was used for deconvolution of experimental data.

6.2.2.6 High performance liquid chromatography

The high performance liquid chromatography of the acid phase reactions were carried out using a LDC Analytical HPLC unit comprising of a LDC Analytical SM4000 programmable wavelength detector, LDC Analytical CM 4000 multiple solvent delivery system, ANAMED CI 10 integrator and Zorbax C₈ 250 L X 4 mm ID column.

6.2.3 Polymerization methods and surface modification reactions

6.2.3.1 Method of HIPE copolymerization

A double walled cylindrical reactor with a three necked lid was used for the purpose. The diameter of the reactor was 11 cm with a height of 15 cm, suitable for small scale batch processes. The continuous phase consists of monomer, crosslinker, initiator and non ionic surfactant. AIBN was used as initiator in all the reactions while Span 80 was used as non ionic surfactant. Initially, 0.25 wt% of PVP in 200 mL of distilled water was kept overnight for homogenization. It was then added to a three necked double walled glass reactor provided with a metallic stirrer. Nitrogen gas was purged through one side neck of the glass reactor. The temperature of the water in the double walled compartment was kept constant at 70 °C. The HIPE of 9 g batch size was prepared by the addition of 1.6 g of Span 80 in a 100 mL plastic bottle (in the case of ETMA-DVB copolymer, 1.6 g of Brij 72 was taken) followed by heating in a water bath at 70 °C for one minute. Subsequently, calculated amount of monomer and crosslinker (as given in Table 6.1) which can impart 100% crosslink density were added. This was followed by addition of 0.2 g (1.218 mmol) of AIBN. The additives were mixed well. 0.49 g (1.813 mmol) of potassium peroxydisulphate (inorganic initiator) was solvated in 9 mL of distilled water in a beaker and added to a double walled dropping funnel with water circulating in it at 70 °C. It was then added slowly at the rate of 3 to 4 mL/min to the

homogenized monomer mixture and stirred at 1400 rpm for a period of 2 min to obtain HIPE. The formed HIPE was stirred further for two more minutes. The reactor containing 0.25 wt% of PVP in distilled water maintained at 70 °C was stirred at 300 rpm. After 10 min, the HIPE was added to it at the rate of 4 to 5 mL/min under stirring. After addition, stirring was carried for 6 h at 250 rpm (8 h for systems containing DVB) to obtain polyHIPE beads.

The formed beads were filtered under suction, washed with distilled water and further soaked in methanol for 6 h, filtered again and dried. The lodged surfactants in the formed beads were then removed in refluxing methanol in a soxhlet extractor for a period of 24 h. Refluxing was done for a period of 36 h for copolymers containing divinyl benzene. The beads obtained were then washed under suction with methanol, acetone and finally dried in vacuum oven at 60 °C. The beads were sieved through a 44 mesh sieve. Various HIPE copolymers prepared as per the above procedure and their corresponding infra red absorptions are given in Table 6.1 As the fingerprint region other than the group frequency region had most of the distinct adsorptions, a higher emphasis was given in analyzing this region.

Table 6.1 Synthesis of copolymers of HIPE with 100% crosslink density

No.	Monomer	Monomer (g & mmol)	Cross linker	Cross linker (g & mmol)	IR spectra (cm ⁻¹)
1	GMA	3.759 & 26.44	EGDM	5.241 & 26.44	908 (epoxy), 1151 (C-O-C), 1732 (C=O)
2	ETMA	3.99 & 25.25	EGDM	5 & 25.25	617 (thiirane), 1159 (C-O-C), 1731 (C=O)
3	GMA	4.697 & 33.04	DVB	4.302 & 33.04	799 (m-disubstituted phenyl ring), 841 (p-disubstituted phenyl ring), 909 (epoxy), 1171(C-O-C), 1729 (C=O)
4	ETMA	4.937 & 31.21	DVB	4.063 & 31.21	616 (thiirane), 799 (m-disubstituted phenyl ring), 1508, 834 (p-disubstituted phenyl ring), 1164(C-O-C), 1727 (C=O)

6.2.3.2 Surface modifications for copolymerized HIPE beads

The synthesized and sieved HIPE beads were subjected to surface modification reactions by sulphonation, mercapto sulphonation and aromatic sulphonation reactions.

6.2.3.2.1 Method for sulphonation of oxirane ring in copolymerized HIPE beads

Sodium sulphite, water and isopropanol in the weight ratio (10:15:75) respectively to a total weight of 25 g was prepared. It was then added to 1 g of copolymer

beads taken in a 50 mL R B flask and refluxed for a period of 5 h at 80 °C, cooled and filtered under suction. Washing was carried out in three steps. The beads were initially washed with distilled water followed by washing with 25 mL of 0.5M sulphuric acid solution and subsequently washed with deionised water until neutral, followed by wash with acetone and drying in vacuum at 50 °C for 6 h. This reaction is a modification of a reported procedure.⁹

6.2.3.2.2 *Method for mercapto sulphonation of oxirane ring in copolymerized HIPE beads*

1.5 g of copolymer having oxirane ring was taken in a 100 mL RB flask. To it were added 2 g of thiourea and 30 g of PEG 400. It was then stirred with a magnetic stirrer at room temperature for 36 h. The stirring was done slowly so that the beads do not break during stirring. The reaction mixture was filtered under suction. Washing of the beads were carried out in two steps. The beads were initially washed with distilled water until the washings were devoid of excess thiourea and PEG 400. It was finally washed with deionised water, acetone and dried in vacuum to obtain thiirated copolymer. In this reaction, other low molecular weight polymeric cosolvents such as PEG 200, PEG 600 and PTHF 250 can also be used instead of PEG 400. This reaction is a modification of a reported procedure.⁵⁰

25 mL of saturated aqueous solution of sodium hydrosulphide and sodium sulphite were prepared. To it, 10 mL of isopropanol and 1 g of thiirated copolymer were added and kept under reflux for 6 h, cooled and filtered under suction. Subsequently washed with distilled water until isopropanol, excess NaSH and Na₂SO₃ were removed. Acidified with 50 mL of 3% hydrochloric acid for 15 min and further washed with deionised water until neutral, followed by wash with acetone and drying in vacuum at 50 °C for 10 h.

6.2.3.2.3 *Method for mercapto sulphonation of thiirane ring in copolymerized HIPE beads*

1 g of copolymer having thiirane ring was treated with 25 mL of 1:1 saturated solution of sodium hydroxide and sodium sulphite in water under reflux for 24 h, cooled and filtered under suction. Initially washed with distilled water until neutral. The obtained polymer was acidified with 100 mL of 5% hydrochloric acid and subsequently washed

with deionised water until neutral, followed by wash with acetone and drying in vacuum at 50 °C for 10 h.

6.2.3.2.4 Method for aromatic sulphonation in copolymerized HIPE beads

1 g of copolymer having aromatic ring was treated with 25 mL of 2% chlorosulphonic acid in 1,2-dichloro ethane and kept at room temperature for 8 h. Filtered and washed with 50 mL of chloroform followed by washing with 100 mL of dichloro methane. The beads were soaked in 1,4-dioxan for one hour and further washed with distilled water. The washed beads were kept in 50 mL of 5% aqueous sodium hydroxide solution in a 250 mL beaker. After 30 min, it was filtered under suction, washed with distilled water until neutral and subsequently washed with 100 mL of 3% hydrochloric acid solution. Again washed with deionised water until neutral and finally washed with acetone and dried in vacuum at 50 °C for 10 h. This reaction is a modification of a reported procedure.²⁶

The surface modification results of copolymeric HIPE beads prepared with 100% crosslink density as described above are given in Table 6.2.

Table 6.2 Surface modifications of copolymers of HIPE with 100% crosslink density

Copolymer	Reactions	IR spectra
GMA-EGDM	1.a. Sulphonation	1154 (C-O-C), 1731 (C=O)
	1.b. Mercapto sulphonation	Step – 1: 617 (thiirane), 1153 (C-O-C), 1731 (C=O) Step – 2: 2586 (SH), 1156 (C-O-C), 1733 (C=O)
ETMA-EGDM	2. Mercapto sulphonation	2589 (SH). 1155 (C-O-C), 1731 (C=O)
GMA-DVB	3.a. Sulphonation	844 (p-disubstituted phenyl ring), 799 (m-disubstituted phenyl ring), 1170 (C-O-C), 1729 (C=O)
	3.b. Mercapto sulphonation	Step – 1: 617 (thiirane), 846 (p-disubstituted phenyl ring), 798 (m-disubstituted phenyl ring), 1171(C-O-C), 1729 (C=O) Step – 2: 2591 (SH), 845 (p-disubstituted phenyl ring), 799 (m-disubstituted phenyl ring), 1170 (C-O-C), 1729 (C=O)
	3.c. Aromatic sulphonation of mercapto sulphonated beads	2606 (SH), 849 (p-disubstituted phenyl ring), 798 (m-disubstituted phenyl ring), 1170 (C-O-C), 1729 (C=O)
ETMA-DVB	4.a. Mercapto sulphonation	2604 (SH), 797 (m-disubstituted phenyl ring), 835 (p-disubstituted phenyl ring), 1165(C-O-C), 1728 (C=O)
	4.b. Aromatic sulphonation of mercapto sulphonated beads	2609 (SH), 798 (m-disubstituted phenyl ring), 1510, 834 (p-disubstituted phenyl ring), 1163(C-O-C), 1728 (C=O)

6.2.3.3 Method of HIPE terpolymerization

0.25 wt% of PVP was taken in 200 mL of distilled water and kept overnight for homogenization. It was then added to a three necked double walled glass reactor provided

with a metallic stirrer. Nitrogen gas was purged through one side neck. The temperature of the water in the double walled compartment was kept constant at 70 °C. 1.6 g of Brij 72 was taken in a 100 mL plastic bottle and heated to 70 °C. Subsequently, calculated amount of two monomers and one crosslinker to a sum of 9 g (as given in Table 6.3) which can impart 100% crosslink density were added. This was followed by addition of 0.2 g (1.218 mmol) of AIBN. The additives were mixed well. 9 mL of distilled water and 0.49 g (1.813 mmol) of potassium peroxydisulphate were homogenized in a beaker and heated to 70 °C. It was then added slowly at the rate of 3 to 4 mL/min to the homogenized monomer mixture with stirring at 1400 rpm for a period of 2 min to obtain the HIPE. The obtained HIPE was further stirred for 2 more min. The reactor containing 0.25 wt% of PVP in distilled water maintained at 70 °C was stirred at 300 rpm. After 10 min, the HIPE was added to it at a rate of 4 to 5 mL/min under stirring. Stirring was carried for 12 h (16 h for systems containing styrene and DVB) to obtain polyHIPE beads.

The formed beads were filtered under suction and washed with distilled water. It was then soaked overnight in methanol and filtered again under suction and dried. The lodged surfactants in the formed beads were then removed under reflux in methanol in a soxhlet extractor for a period of 36 h (48 h for terpolymers containing styrene or DVB and 72 h for terpolymers containing styrene and DVB). The beads obtained were then washed under suction with methanol, acetone and subsequently dried in vacuum at 60 °C for 10 h. The terpolymeric beads were sieved through a 44 mesh sieve.

Table 6.3 Synthesis of terpolymers of HIPE with 100% crosslink density

No.	Monomers		Monomers (g & mmol)		Cross linker	Cross linker (g & mmol)	IR spectra
	1	2	1	2			
1	ETMA	GMA	2.043 & 12.92	1.836 & 12.92	EGDM	5.12 & 25.83	617 (thiirane), 908 (epoxy), 1155 (C-O-C), 1728 (C=O)
2	ETMA	GMA	2.539 & 16.05	2.281 & 16.05	DVB	4.179 & 32.10	617 (thiirane), 836 (p-disubstituted phenyl ring), 798 (m-disubstituted phenyl ring), 906 (epoxy), 1166 (C-O-C), 1729 (C=O)
3	styrene	GMA	1.458 & 14	1.99 & 14	EGDM	5.551 & 28	908 (epoxy), 703 and 760 (monosubstituted phenyl ring), 1144 (C-O-C), 1733 (C=O)
4	styrene	GMA	1.85 & 17.76	2.525 & 17.76	DVB	4.625 & 35.52	704 and 761 (monosubstituted phenyl ring), 851 (p-disubstituted phenyl ring), 794 (m-disubstituted phenyl ring), 909 (epoxy), 1152 (C-O-C), 1732 (C=O)
5	styrene	ETMA	1.422 & 13.66	2.161 & 13.66	EGDM	5.416 & 27.32	616 (thiirane), 702, 758 (monosubstituted phenyl ring), 1166 (C-O-C), 1728 (C=O)
6	styrene	ETMA	1.793 & 17.22	2.724 & 17.22	DVB	4.483 & 34.43	617 (thiirane), 701 and 762 (monosubstituted phenyl ring), 836 (p-disubstituted phenyl ring), 797 (m-disubstituted phenyl ring), 1166 (C-O-C), 1728 (C=O)

6.2.3.4 Surface modifications for terpolymerized HIPE beads

The synthesized and sieved HIPE beads were subjected to surface modification reactions by sulphonation, mercapto sulphonation and aromatic sulphonation reactions.

6.2.3.4.1 Method for sulphonation of oxirane ring in terpolymerized HIPE beads

The reaction was carried out as per 6.2.3.2.1 for a period of 8 h.

6.2.3.4.2 Method for mercapto sulphonation of oxirane ring in terpolymerized HIPE beads

1.5 g of copolymer having oxirane ring was taken in a 100 mL RB flask. To it was added 2.5 g of thiourea and 30 g of PEG 400. It was then stirred slowly with magnetic stirrer at room temperature for 48 h and filtered under suction. Washing was carried out with distilled water until the washings were devoid of excess thiourea and PEG 400 and subsequently washed with deionised water, acetone and dried in vacuum to obtain thiirated copolymer. 25 mL of saturated aqueous solution of sodium hydrosulphide and sodium sulphite were prepared. To it, 10 mL of isopropanol and 1 g of thiirated copolymer were added and kept under reflux for 10 h, filtered under suction.

Washing was carried out with distilled water until isopropanol, excess NaSH and Na₂SO₃ were removed. Acidified with 50 mL of 3% hydrochloric acid for 30 min and subsequently washed with deionised water until neutral followed by wash with acetone and drying in vacuum at 60 °C for 10 h.

6.2.3.4.3 *Method for mercapto sulphonation of thiirane ring in terpolymerized HIPE beads*

1 g of copolymer having thiirane ring was treated with 25 mL of 1:1 saturated solution of sodium hydroxide and sodium sulphite in water under reflux for 36 h, filtered under suction. Refluxing for 48 h was required for terpolymers containing DVB as cross linker. Washing was carried out with distilled water until neutral. The obtained polymer was acidified with 100 mL of 5% hydrochloric acid and subsequently washed with deionised water until neutral followed by wash with acetone and drying in vacuum at 60 °C for 10 h.

6.2.3.4.4 *Method for aromatic sulphonation in terpolymerized HIPE beads*

1 g of terpolymer having aromatic ring was treated with 50 mL of 2% chlorosulphonic acid in 1,2-dichloro ethane and kept at room temperature for 12 h. Filtered and washed with 50 mL of chloroform followed by washing with 100 mL of dichloro methane. The beads were soaked in 1,4 dioxan for one hour and further washed with distilled water. The washed beads were kept in 100 mL of 5% aqueous sodium hydroxide solution in a 250 mL beaker. After 30 min, it was filtered under suction. Washed further with distilled water until neutral and subsequently washed with 100 mL of 3% hydrochloric acid solution. Again washed with deionised water until neutral and finally washed with acetone and dried in vacuum at 60 °C for 10 h.

The surface modification of terpolymeric HIPE beads prepared with 100% crosslink density are given in Table 6.4.

Table 6.4 Surface modifications of copolymers of HIPE with 100% crosslink density

Terpolymer	Reaction	IR spectra
ETMA-GMA-EGDM	1. Mercapto sulphonation	2598 (SH), 1172 (C-O-C), 1716 (C=O)
ETMA-GMA-DVB	2.a. Mercapto sulphonation	2588 (SH), 841 (p-disubstituted phenyl ring), 797(m-disubstituted phenyl ring), 1166 (C-O-C), 1729 (C=O)
	2.b. Aromatic sulphonation of mercapto sulphonated beads	2597 (SH), 843 (p-disubstituted phenyl ring), 799 (m-disubstituted phenyl ring), 1167 (C-O-C), 1730 (C=O)
Styrene-GMA-EGDM	3.a. Sulphonation	703 and 760 (monosubstituted phenyl ring), 1144 (C-O-C), 1733 (C=O)
	3.b. Aromatic sulphonation of sulphonated beads	703 and 762 (monosubstituted phenyl ring), 1151 (C-O-C), 1734 (C=O)
	3.c. Mercapto sulphonation	Step – 1: 617 (thiirane), 703 and 760 (monosubstituted phenyl ring), 1146 (C-O-C), 1731 (C=O) Step – 2: 2576 (SH), 703 and 760 (monosubstituted phenyl ring), 1145 (C-O-C), 1730 (C=O)
Styrene-GMA-DVB	4.a. Sulphonation	703 and 761 (monosubstituted phenyl ring), 847 (p-disubstituted phenyl ring), 798 (m-disubstituted phenyl ring), 1152 (C-O-C), 1732 (C=O)
	4.b. Mercapto sulphonation	Step – 1: 614 (thiirane), 703 and 761 (monosubstituted phenyl ring), 847 (p-disubstituted phenyl ring), 798 (m-disubstituted phenyl ring), 1152 (C-O-C), 1732 (C=O) Step – 2: 2576 (SH), 703 and 762 (monosubstituted phenyl ring), 846 (p-disubstituted phenyl ring), 797 (m-disubstituted phenyl ring), 1153 (C-O-C), 1732 (C=O)
	4.c. Aromatic sulphonation of sulphonated beads	2592 (SH), 703 and 761 (monosubstituted phenyl ring), 847 (p-disubstituted phenyl ring), 798 (m-disubstituted phenyl ring), 1152 (C-O-C), 1732 (C=O)
Styrene-ETMA-EGDM	Mercapto sulphonation	2587 (SH), 702 and 759 (monosubstituted phenyl ring), 1158 (C-O-C), 1729 (C=O)
	Aromatic sulphonation of mercapto sulphonated beads	2601 (SH), 703 and 758 (monosubstituted phenyl ring), 1156 (C-O-C), 1733 (C=O)
Styrene-ETMA - DVB	Mercapto sulphonation	2592 (SH), 701 and 762 (monosubstituted phenyl ring), 846 (p-disubstituted phenyl ring), 797 (m-disubstituted phenyl ring), 1166 (C-O-C), 1728 (C=O)
	Aromatic sulphonation of mercapto sulphonated beads	2606 (SH), 703 and 763 (monosubstituted phenyl ring), 846 (p-disubstituted phenyl ring), 798 (m-disubstituted phenyl ring), 1168 (C-O-C), 1728 (C=O)

6.2.4 Calculation of acid exchange values

0.1 N NaOH solution was standardized using 0.1 N 99.9% aqueous solution of potassium hydrogen phthalate. The acid exchange values of the synthesized catalysts were done by treating 100 mg of dry resin with 10 mL of alcoholic standard 0.1 N NaOH solution. 10 mL of 1,4-dioxan was also added to it and the mixture was stoppered and stirred for 24 h at ambient conditions. 5 mL aliquots were then withdrawn and titrated against 0.05 N standard HCl using 4 drops of 1% phenolphthalein in methanol as indicator. A blank was also conducted without the catalyst. From the amount of NaOH consumed, the concentrations of sulphonic acid groups in meq/g were calculated for all the aromatic sulphonated HIPE based catalysts as well as for the two commercial

catalysts. For aliphatic sulphonated/mercapto sulphonated HIPE based catalysts, the titration was similarly carried out using 0.05 N standard NaOH solution with 0.01 N HCl with 4 drops of 2% phenolphthalein in methanol as indicator.

6.2.5 Acid phase catalysis

Acid phase condensation reactions with the synthesized as well as commercial catalysts were carried out for studying the condensation of phenol and acetone to form 4,4'-BPA and condensation of phenol as well as condensation of 4-hydroxy acetophenone to form 1,1,1-THPE. The percentage content and selectivity of 4,4'-BPA and 1,1,1-THPE were calculated from HPLC analyses.

6.2.5.1 Condensation of phenol with acetone

The reactions were carried out with 0.1 g of synthesized catalysts and two commercial catalysts with 4.235 g (45 mmol) of phenol, 0.66 mL (9 mmol) of acetone and 40 mg of activated neutral alumina. Condensation reactions were studied at 60 and 100 °C in presence of 4Å molecular sieves for a period of 16 h.

6.2.5.2 Condensation of phenol with 4-hydroxy acetophenone

The reactions were carried out with 0.1 g of synthesized catalysts and two commercial catalysts with 4.235 g (45 mmol) of phenol, 1.225 g (9 mmol) of 4-hydroxyacetophenone and 40 mg of activated neutral alumina. Condensation reactions were studied at 100 °C in presence of 4Å molecular sieves for a period of 16 h.

6.2.6 HPLC studies

The HPLC was used for analyzing two acid phase condensation reactions using the prepared catalysts and two commercial catalysts. The reactions studied involves the condensation of phenol and acetone to form 4,4'-BPA and the condensation of phenol and 4-hydroxy acetophenone to form 1,1,1-THPE.

6.2.6.1 HPLC study of condensation of phenol and acetone

The separation of phenol, acetone and 4,4'-BPA were achieved using a mobile phase of 40% acetonitrile in water. To set the wavelength for HPLC analysis, the λ_{\max} of 4,4'-BPA was determined by UV spectroscopy (Shimadzu UV-160) by adding 99% pure 4,4'-BPA to a 2 mL cuvette at a concentration of 2mg/mL. The value was found to be 254 nm.

The HPLC analyses were carried out using a Zorbax C₈ column with 40% acetonitrile in water as eluent at a flow rate of 1.5 mL/min. The detection wavelength was kept constant at 254 nm at a sensitivity of 0.5. The chart speed was kept constant at 2 cm/min. The conditions used for chromatographic analyses as given above were kept constant.

The samples were initially heated at 65 °C for 2-3 min and homogenized well prior to injection. Accurately weighted (about 0.2 to 0.4 g) and homogenized reaction mixture was transferred to 25 mL volumetric flasks and diluted with the mobile phase (40% acetonitrile in water). It was then filtered using 0.45 µ filter prior to injection. The filtered solution was then injected into the column and their respective areas were noted from the chromatogram. From the areas obtained and the slope of the calibration curve, the percentage contents of 4,4'-BPA in all the samples were calculated. The standard was injected in the starting and finishing on all analysis days to check steady system performance.

6.2.6.2 HPLC study of condensation of phenol and 4-hydroxy acetophenone

The separation of phenol, 4-hydroxy acetophenone and 1,1,1-THPE were achieved using a mobile phase of 35% acetonitrile in water. To set the wavelength for HPLC analysis, the λ_{max} of 1,1,1-THPE was determined by UV spectroscopy by adding pure 1,1,1-THPE to a 2 mL cuvette at a concentration of 2mg/mL. The value was found to be 275 nm.

The HPLC analyses were carried out using a Zorbax C₈ column with 35% acetonitrile in deionised water as eluent at a flow rate 1 mL/min. The detection wavelength was kept constant at 275 nm at a sensitivity of 0.5. The chart speed was kept constant at 2 cm/min. The conditions used for chromatographic analyses as given above were kept constant.

One representative sample (reaction mixture) was carried out qualitatively to understand signature of individual components. Two peaks appeared as products. For the confirmation of the peak corresponding to 1,1,1-THPE, spiking was carried out with a physical mixing of reaction mixture and standard 1,1,1-THPE.

The samples were heated at 65 °C for 2-3 min and homogenized well prior to injection. Accurately weighted (about 0.2 to 0.4 g) sample was transferred to 10 mL

volumetric flasks and diluted with the mobile phase (35% acetonitrile in water). It was then filtered using 0.45 μ filter prior to injection. The filtered solution was then injected into the column and their respective areas were noted from the chromatogram. From the areas obtained and the slope of the calibration curve, the percentage content of 1,1,1-THPE for all the samples were calculated. The standard was injected in the starting and finishing on all analysis days to check steady system performance.

6.3 Results and discussion

6.3.1 IR analysis

The IR spectra of the copolymers and terpolymers as well as the spectra of functionalized beads are given in Table 6.1 to 6.4. The spectra given are with emphasis on fingerprint region. Major absorptions at group frequency region were also noted. For aromatic systems, the fingerprint region was analyzed. It has to be noted that the aromatic peaks around 3026, 3083, 1600 and 1495 cm^{-1} were observed in many cases involving styrene or DVB. In case of GMA-DVB copolymer and terpolymers involving either styrene or DVB with GMA, the absorption for epoxy ring mentioned from 906 to 909 cm^{-1} has interference due to 900 to 910 cm^{-1} peak arising from the C-H bending absorption of the aromatic ring.^{95,96} In this case the conversion can be assigned due to the reduction in absorption intensity. The mercapto functionalization of aliphatic ring was easily attained. In the case of GMA-EGDM copolymer, the conversion of oxirane to thiirane ring and subsequent modification to mercapto sulphonic acid group noted using IR spectroscopy is given in Figure 6.1.

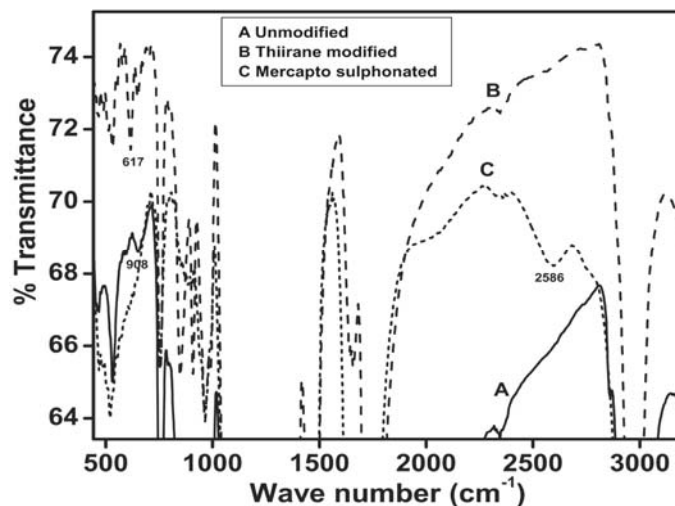


Figure 6.1(A-C) Formation of mercapto sulphonic acid catalyst from GMA-EGDM HIPE beads with 100% crosslink density in three steps using IR. (A) Unmodified copolymer, (B) thiirane modified copolymer and (C) mercapto sulphonated copolymer

Aromatic ring showed a reduction in thiol content, when subjected to mercapto sulphonation followed by treatment with low concentration of chlorosulphonic acid, probably due to the presence of unprotected thiol groups. The aromatic sulphonation of mercapto sulphonated beads in certain cases showed a weak peak corresponding to S-S stretching around 600 cm^{-1} with a reduction in the intensity of aliphatic thiol stretching frequency around $2580\text{--}2600\text{ cm}^{-1}$. This may be due to the possible formation of S-SO₃H group on treatment with chlorosulphonic acid. Sulphonic acid group provides three distinct IR absorption bands.^{97,98} These bands correspond to aromatic C-S stretch around 1124 cm^{-1} , symmetric as well as antisymmetric stretching of S(=O)₂ group around 1040 and $1080\text{--}1280\text{ cm}^{-1}$. Since all the porous polymers studied have broad C-O-C absorption from 1000 to 1250 cm^{-1} , the determination of these peaks from IR was difficult. In most cases, on sulphonation the peak for C-O-C at $1150\text{--}1170\text{ cm}^{-1}$ got further broadened, which made the assignment difficult. Hence an XPS study was carried out, which is explained in Section 6.3.2.

6.3.2 XPS analysis

Due to difficulty in interpreting sulphonic acid groups in IR spectroscopy, qualitative XPS analyses were carried out for ETMA-EGDM copolymer before and after mercaptosulphonation. Correction with carbon 1s (285 eV) was done before analyses.

The binding energies for sulphur 2p (S_{2p}) region (160-170 eV) were studied in both cases. In the case of mercapto sulphonic acid catalyst, it was observed that in addition to the thiirane binding energy for sulphide at 164 eV, three other peaks were also obtained. The peak at 162.8 eV corresponds to $2p_{3/2}$ value for polymer bound thiol.⁹⁹ Two peaks at 168.9 and 169.9 eV were also obtained. These peaks respectively correspond to sulphur $2p_{3/2}$ and $2p_{1/2}$ binding energies of sulphite species in sulphonic acid group.^{100,101} The results are given in Figure 6.2 (A-D). Due to porous nature of the copolymer, the binding energy of internally substituted thiirane also emerged out by X-ray penetration as observed in the deconvoluted spectrum. (Figure 6.2 D)

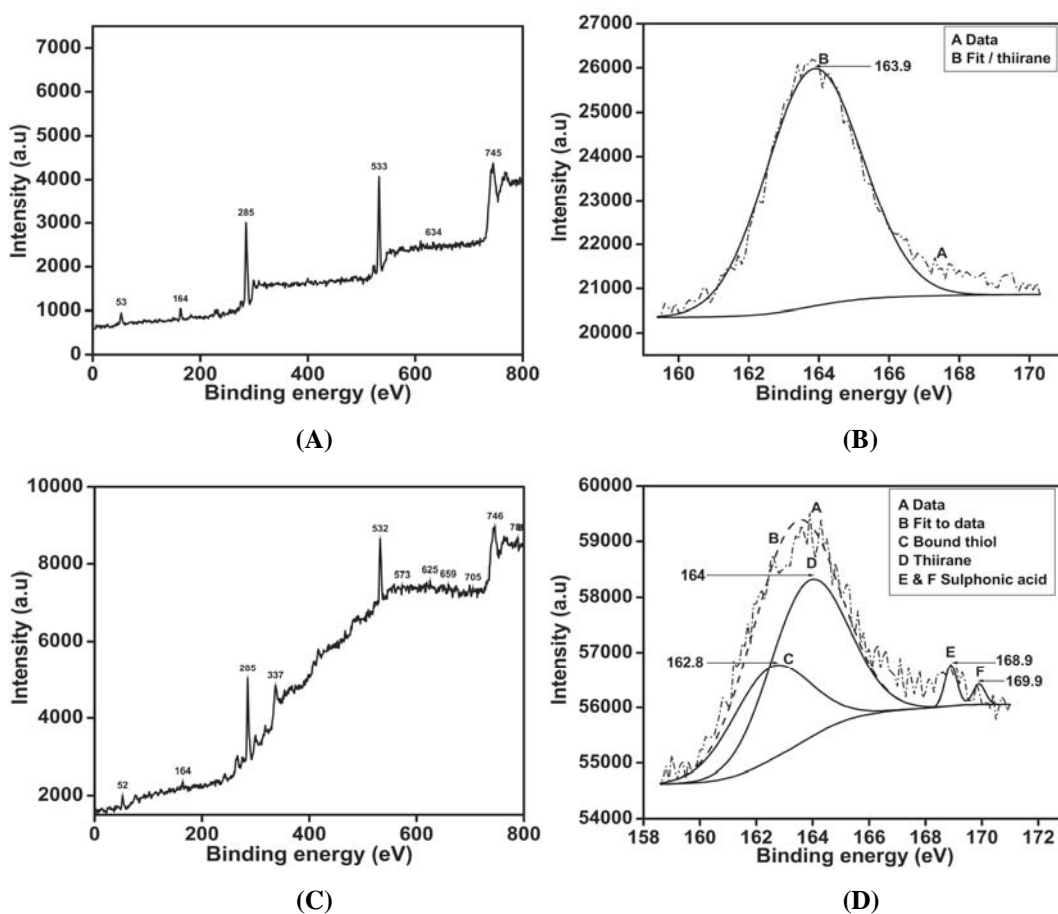
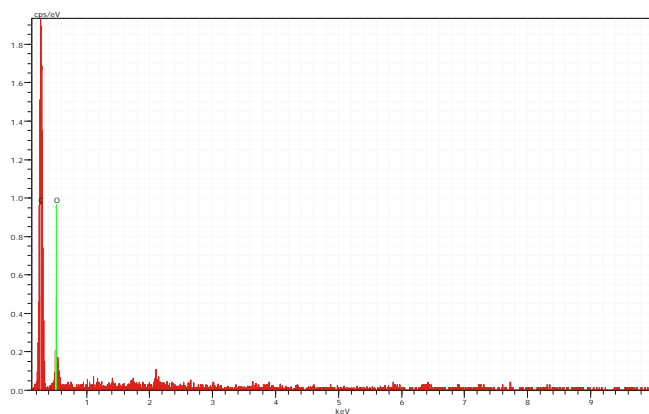


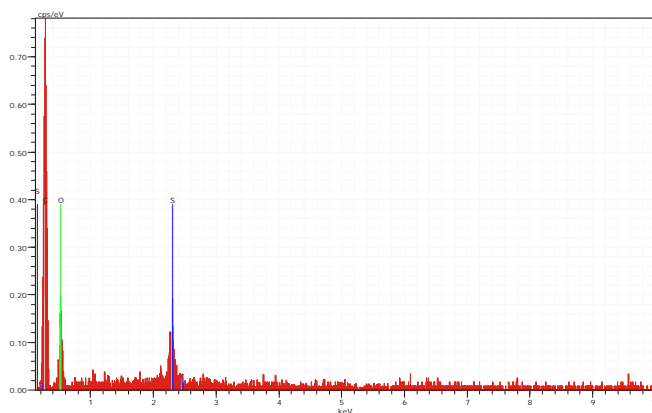
Figure 6.2(A-D) Formation of mercapto sulphonic acid catalyst from ETMA-EGDM HIPE beads with 100% crosslink density in two steps using high resolution XPS. (A-B) unmodified copolymer and (C-D) mercapto sulphonated copolymer

6.3.3 EDX analysis

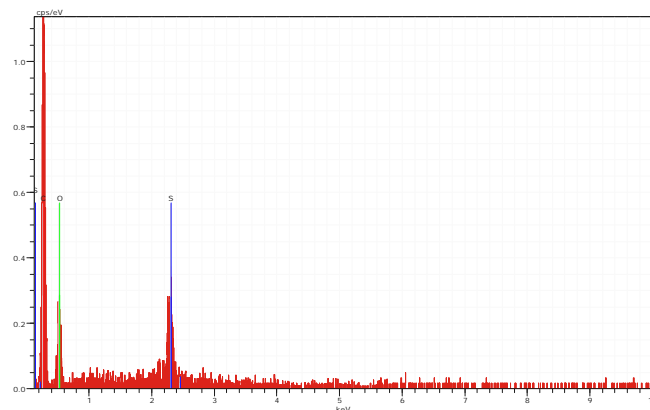
The EDX analyses were carried out to check the functional group modification occurring in the formation of sulphonic acid catalyst. Figure 6.3(A-C) represents the formation of mercapto sulphonic acid catalyst from GMA-EGDM HIPE beads with 100% crosslink density in three steps using EDX. Figure A represents unmodified copolymer while B represents surface modification with thiirane rings. Figure C represents formation of mercapto sulphonic acid catalyst by showing a higher abundance of sulphur. The percentages of sulphur from Figure A to C were 0, 0.59 and 3.08%, respectively.



A



B



C

Figure 6.3(A-C) Formation of mercapto sulphonic acid catalyst from GMA-EGDM HIPE beads with 100% crosslink density in three steps using EDX. (A) unmodified copolymer, (B) thiirated copolymer and (C) mercapto sulphonated copolymer

6.3.4 Calculation of acid exchange values

The results show that the aromatic sulphonated catalysts have a much higher acidity than that of aliphatic mercapto sulphonated or sulphonated catalysts. This is due to the higher acidity imparted by conjugation of sulphonate ion with the aromatic ring, which makes the proton more labile. It has been reported in literature that the acidity value of Amberlyst 15 dry resin varied from 3.7 to 4.8 depending on batch to batch variations in surface area as well as total acid content analyses methods.¹⁰²⁻¹⁰⁴ We preferred to use the back titration method so as to get an abrupt end point. The acid exchange values obtained for the catalysts are given below. (Table 6.5)

Table 6.5 Acid exchange values for the catalysts

Number	Co/terpolymer	Modification	meq of H ⁺ /g of catalyst
1	GMA-EGDM	Sulphonated	0.34
2	GMA-EGDM	Mercapto sulphonated	0.32
3	ETMA-EGDM	Mercapto sulphonated	0.30
4	GMA-DVB	Sulphonated	0.41
5	GMA-DVB	Mercapto sulphonated	0.39
6	GMA-DVB	Aromatic sulphonation of mercapto sulphonated	3.48
7	ETMA-DVB	Mercapto sulphonated	0.53
8	ETMA-DVB	Aromatic sulphonation of mercapto sulphonated	3.57
9	ETMA-GMA-EGDM	Mercapto sulphonated	0.23
10	ETMA-GMA-DVB	Mercapto sulphonated	0.27
11	ETMA-GMA-DVB	Aromatic sulphonation of mercapto sulphonated	4.09
12	Styrene-GMA-EGDM	Sulphonated	0.22
13	Styrene-GMA-EGDM	Mercapto sulphonated	0.19
14	Styrene-GMA-EGDM	Aromatic sulphonation of mercapto sulphonated	3.44
15	Styrene-GMA-DVB	Sulphonated	0.22
16	Styrene-GMA-DVB	Mercapto sulphonated	0.19
17	Styrene-GMA-DVB	Aromatic sulphonation of mercapto sulphonated	4.42
18	Styrene-ETMA-EGDM	Mercapto sulphonated	0.32
19	Styrene-ETMA-EGDM	Aromatic sulphonation of mercapto sulphonated	3.98
20	Styrene-ETMA-DVB	Mercapto sulphonated	0.24
21	Styrene-ETMA-DVB	Aromatic sulphonation of mercapto sulphonated	4.35
22	Amberlyst-15	Aromatic sulphonated	3.68
23	Lewatit K-2629	Aromatic sulphonated	3.82

6.3.5 Surface area analysis

The surface areas of the synthesized beads with 100% crosslink density as well as commercial beads were calculated using a BET surface area analyzer. GMA-DVB was prepared with Span 80 as surfactant while all other co/terpolymers with divinyl benzene as crosslinker were prepared with Brij 72 as surfactant. It was observed that the surface areas of the beads increased when the surfactant was changed from Span 80 to Brij 72. Comparatively lower surface area was observed when EGDM was used as crosslinker. It was also observed that the surface area of the beads decreased after functionalization. The surface area of the beads before and after modifications are given in Table 6.6.

Table 6.6 BET surface areas of unfunctionalized and functionalized beads

Number	Co/terpolymer	Bead modifications	Surface area (m ² /g)
1	GMA-EGDM	Unmodified	29.27
2	GMA-EGDM	Sulphonated	25.71
3	GMA-EGDM	Mercaptosulphonated	23.38
4	ETMA-EGDM	Unmodified	37.42
5	ETMA-EGDM	Mercaptosulphonated	34.43
6	GMA-DVB	Unmodified	50.35
7	GMA-DVB	Sulphonated	37.53
8	GMA-DVB	Mercaptosulphonated	33.44
9	GMA-DVB	Aromatic sulphonation of mercapto sulphonated	17.96
10	ETMA-DVB	Unmodified	104.74
11	ETMA-DVB	Mercaptosulphonated	89.14
12	ETMA-DVB	Aromatic sulphonation of mercapto sulphonated	74.57
13	GMA-ETMA-EGDM	Unmodified	62.83
14	GMA-ETMA-EGDM	Mercaptosulphonated	61.56
15	GMA-ETMA-DVB	Unmodified	180
16	GMA-ETMA-DVB	Mercaptosulphonated	171.41
17	GMA-ETMA-DVB	Aromatic sulphonation of mercapto sulphonated	157.28
18	Styrene-GMA-EGDM	Unmodified	61.70
19	Styrene-GMA-EGDM	Sulphonated	38.40
20	Styrene-GMA-EGDM	Mercaptosulphonated	37.89
21	Styrene-GMA-EGDM	Aromatic sulphonation of mercapto sulphonated	29.48
22	Styrene-GMA-DVB	Unmodified	240.87
23	Styrene-GMA-DVB	Sulphonated	205.46
24	Styrene-GMA-DVB	Mercaptosulphonated	207.11
25	Styrene-GMA-DVB	Aromatic sulphonation of mercapto sulphonated	172.29
26	Styrene-ETMA-EGDM	Unmodified	107.4
27	Styrene-ETMA-EGDM	Mercaptosulphonated	93.56
28	Styrene-ETMA-EGDM	Aromatic sulphonation of mercapto sulphonated	84.35
29	Styrene-ETMA-DVB	Unmodified	160
30	Styrene-ETMA-DVB	Mercaptosulphonated	128.49
31	Styrene-ETMA-DVB	Aromatic sulphonation of mercapto sulphonated	102.41
32	Amberlyst [®] 15	Aromatic sulphonated	53
33	Lewatit [®] 2629	Aromatic sulphonated	40

6.3.6 Surface morphology studies

The surface morphology of the synthesized beads were noted by optical microscopy as well as by scanning electron microscopy.

6.3.6.1 Optical microscopy

Optical microscopic data of the beads were noted after sieving through a 44 mesh sieve. The beads showed spherical nature. The data obtained for GMA-EGDM copolymer with 100% cross link density and GMA-ETMA-EGDM terpolymer; magnified to 40 and 500 times are given below in Figures 6.4(A-B) and 6.5(A-B), respectively. From the Figures we can infer that with other parameters remaining

constant, both the copolymeric as well as terpolymeric beads had almost similar dimensions.

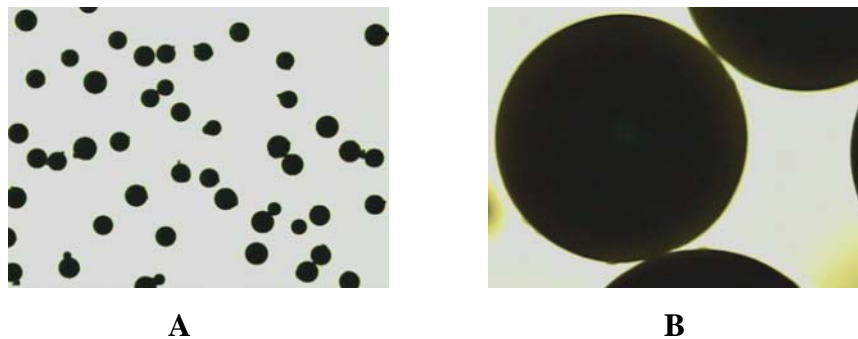


Figure 6.4(A-B) Surface morphology of the synthesized GMA – EGDM beads with 100% crosslink density measured at (A) 40 x and (B) 500 x

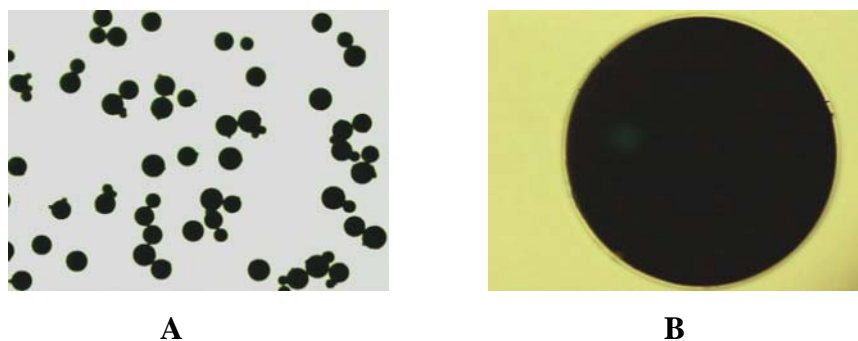


Figure 6.5(A-B) Surface morphology of the synthesized GMA-ETMA-EGDM beads with 100% crosslink density measured at (A) 40 x and (B) 500 x

6.3.6.2 Scanning electron microscopy

Scanning electron microscopic data of the synthesized HIPE beads were noted after sieving through a 44 mesh sieve while Amberlyst 15 was used as received. Pores with 300 nm were visible at 30k times magnification for the aliphatic terpolymeric mercapto sulphonated GMA-ETMA-EGDM HIPE beads while much smaller pores were observed in Amberlyst 15 even at 50k times magnification. Hence the synthesized terpolymeric HIPE beads showed a better macroporosity (>50 nm) than Amberlyst 15. The Figures obtained for Amberlyst 15 magnified to 200 and 50000 times and GMA-ETMA-EGDM terpolymer HIPE beads magnified to 100 and 30000 times are given below in Figures 6.6 (A-B) and 6.7(A-B), respectively.

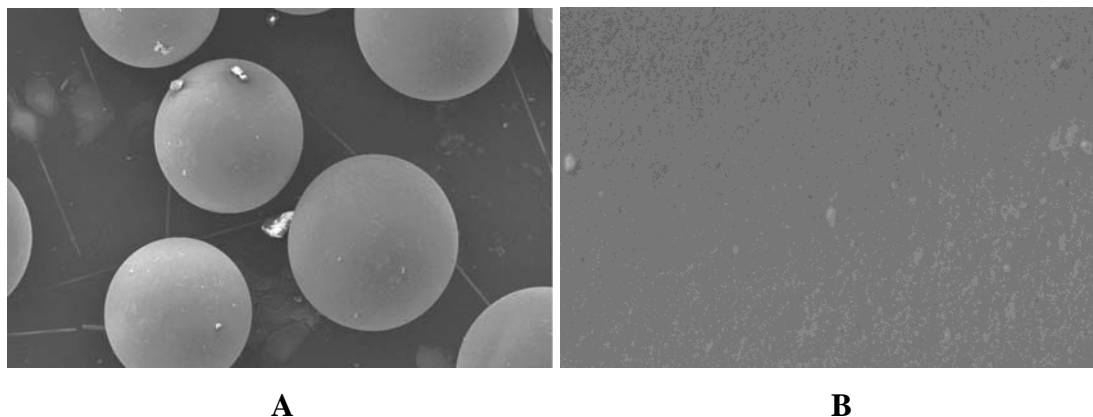


Figure 6.6(A-B) Surface morphology of Amberlyst 15 copolymer beads with 100% crosslink density magnified to (A) 200 x and (B) 50k x

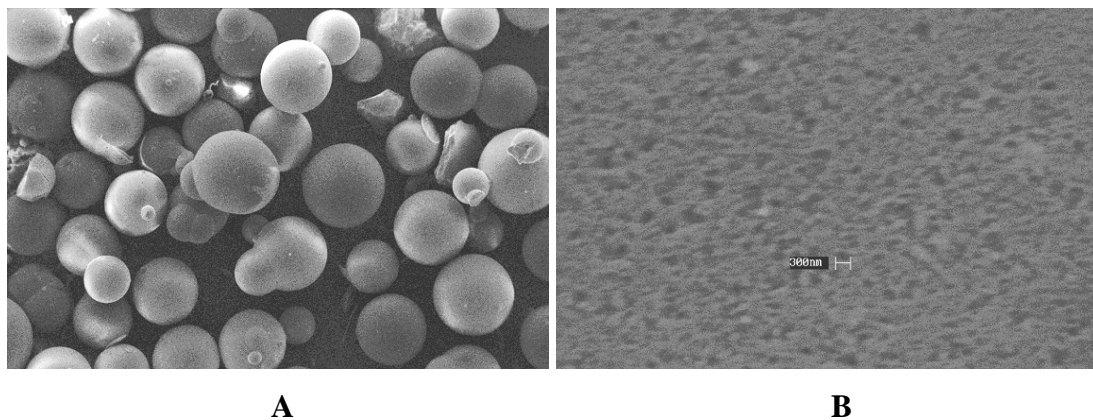


Figure 6.7(A-B) Surface morphology of the synthesized GMA-ETMA-EGDM terpolymer beads with 100% crosslink density magnified to (A) 100 x and (B) 30k x

6.3.7 HPLC analysis for acid phase condensation reactions

The percentage selectivity and conversion of HPLC analyses carried out for the two acid phase condensation reactions are given below. The percentage conversions were calculated based on area obtained from chromatogram.

6.3.7.1 Estimation of 4,4'-bisphenol A using HPLC

Separation of all the three pure standard samples obtained with 40% acetonitrile in water (A) as well as the calibration plot for 4,4'-BPA (D) are given in Figure 6.8(A-D)

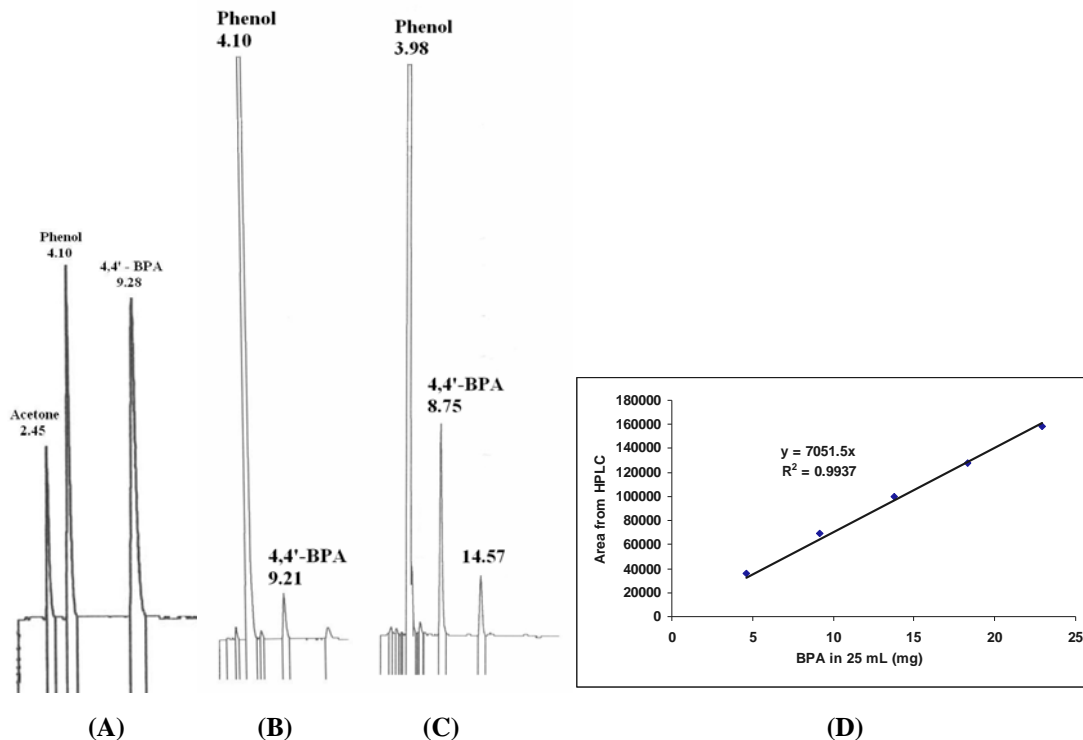


Figure 6.8(A-D) Separation of (A) standard reactants and product obtained with 40% acetonitrile in water (B) product mixture after reaction with aliphatic mercapto sulphonated styrene-GMA-EGDM catalyst at 60 °C and (C) product mixture after reaction with two step sulphonated styrene-GMA-EGDM catalyst at 60 °C and (D) HPLC calibration plot for standard 4,4'- bisphenol A

It was observed that using aliphatic sulphonated catalyst and aliphatic mercapto sulphonated catalyst, the percentage of 4,4'-BPA was below 2% in the product mixture at 60 and 100 °C while the percentage of 4,4'-BPA in the product mixture varied from 2.3 to 8.9 in the case of two step sulphonated catalysts (aromatic sulphonated and aliphatic mercapto sulphonated catalysts) and aromatic sulphonated commercial catalysts. In all cases the reaction mixture was brown in color, with two to five product peaks coming within an analysis time of 30 minutes. The amount in mg of 4,4'-BPA in each sample were calculated from the ratio of area of 4,4'-BPA in sample to the slope of calibration curve. The percentage content of 4,4'-BPA was thus calculated from the amount in mg of product mixture taken for analyses. The selectivity was calculated based on percentage area. The results obtained are given in Tables 6.7 to 6.9.

Table 6.7 Percentage content and selectivity of 4,4'-bisphenol A calculated using aliphatic mercapto sulphonated catalysts

No.	Co/terpolymer	Temp. (°C)	Wt. of sample in 25 mL (mg)	Area of 4,4'-BPA	Total area of phenolic products	Amount of 4,4'-BPA* (mg)	% of 4,4'-BPA in product mixture	Selectivity (Area %)
1	Styrene-GMA-EGDM	60	538.4	29994	33926	4.25	0.79	88.41
2	Styrene-GMA-EGDM	100	432.7	27148	35079	3.85	0.89	77.39
3	Styrene-GMA-DVB	60	266	21467	24481	3.04	1.15	87.68
4	Styrene-GMA-DVB	100	314.3	35680	43295	5.06	1.61	82.41
5	Styrene-ETMA-DVB	60	415.9	22160	24821	3.14	0.75	89.28
6	Styrene-ETMA-DVB	100	338.1	26936	36787	3.82	1.13	73.22
7	Styrene-ETMA-EGDM	60	381.5	32050	35050	4.54	1.19	91.52
8	Styrene-ETMA-EGDM	100	297.8	29828	35433	4.23	1.42	84.18
9	ETMA-GMA-EGDM	60	390.3	32021	35413	4.54	1.16	90.42
10	ETMA-GMA-EGDM	100	321.9	34270	41509	4.86	1.51	82.56
11	ETMA-GMA-DVB	60	461.2	29373	33154	4.17	0.91	88.60
12	ETMA-GMA-DVB	100	342.6	25879	32544	3.67	1.07	79.52
13	ETMA-DVB	60	346.3	40716	50745	5.77	1.66	80.24
14	ETMA-DVB	100	305.1	37373	48739	5.30	1.74	76.68
15	GMA-DVB	60	522.9	48470	58815	6.87	1.31	82.71
16	GMA-DVB	100	371.7	35610	45577	5.05	1.36	78.13
17	ETMA-EGDM	60	4.4.2	41193	44526	5.84	1.44	92.51
18	ETMA-EGDM	100	361.7	39770	47132	5.64	1.56	84.38
19	GMA-EGDM	60	469.8	42278	45852	5.99	1.27	92.21
20	GMA-EGDM	100	416.3	41674	55840	5.91	1.42	74.63

* Determined from calibration plot using 99% 4,4'-bisphenol A

Table 6.8 Percentage content and selectivity of 4,4'-bisphenol A calculated using aliphatic sulphonated catalysts

No.	Co/terpolymer	Temp. (°C)	Wt. of sample in 25 mL (mg)	Area of 4,4'-BPA	Total area of phenolic products	Amount of 4,4'-BPA* (mg)	% of 4,4'-BPA in product mixture	Selectivity (Area %)
1	Styrene-GMA-EGDM	60	426.7	36385	53991	5.16	1.21	67.39
2	Styrene-GMA-EGDM	100	374.1	44513	58454	6.31	1.69	76.15
3	Styrene-GMA-DVB	60	678.2	59898	80584	8.49	1.25	74.33
4	Styrene-GMA-DVB	100	678.9	96226	131627	13.65	2.01	73.12
5	GMA-DVB	60	471.2	31238	45496	4.43	0.94	68.66
6	GMA-DVB	100	596.8	65296	98255	9.26	1.55	76.41
7	GMA-EGDM	60	362.1	18669	26702	2.64	0.73	69.91
8	GMA-EGDM	100	326.4	34019	45863	4.82	1.47	74.18

* Determined from calibration plot using 99% 4,4'-bisphenol A

Table 6.9 Percentage content and selectivity of 4,4'-bisphenol A calculated using two step sulphonated catalysts (aromatic sulphonated and aliphatic mercapto sulphonated catalysts) and commercial aromatic sulphonated catalysts

No.	Co/terpolymer	Temp. (°C)	Wt. of sample in 25 mL (mg)	Area of 4,4'-BPA	Total area of phenolic products	Amount of 4,4'-BPA* (mg)	% of 4,4'-BPA in product mixture	Selectivity (Area %)
1	Styrene-ETMA-DVB	60	263.8	63621	82311	9	3.4	77.29
2	Styrene-ETMA-DVB	100	349.9	199182	272050	28.24	8.03	73.22
3	Styrene-ETMA-EGDM	60	597.3	133556	189178	18.94	3.17	70.60
4	Styrene-ETMA-EGDM	100	394.2	201718	272658	28.60	7.26	73.98
5	Styrene-GMA-DVB	60	390.5	101982	155299	14.46	3.70	65.67
6	Styrene-GMA-DVB	100	388	243618	400568	34.54	8.90	60.82
7	Styrene-GMA-EGDM	60	687.4	111497	146221	15.81	2.30	76.25
8	Styrene-GMA-EGDM	100	407	191309	275745	27.13	6.66	69.38
9	ETMA-GMA-DVB	60	468.5	119602	177900	16.96	3.62	67.23
10	ETMA-GMA-DVB	100	402.3	251701	326063	35.69	8.87	77.19
11	ETMA-DVB	60	647.2	110534	150539	15.68	2.42	73.43
12	ETMA-DVB	100	268.9	124438	174133	17.64	6.56	71.46
13	GMA-DVB	60	422.6	77822	118143	10.18	2.41	65.87
14	GMA-DVB	100	236	110507	158714	15.67	6.64	69.63
15	Amberlyst-15	60	391.5	81115	105197	11.50	2.94	77.02
16	Amberlyst-15	100	228.6	124641	187973	17.67	7.73	66.31
17	Lewatit K-2629	60	444.9	72421	93391	10.27	2.31	77.55
18	Lewatit K-2629	100	613.8	222596	272541	31.57	5.14	81.67

* Determined from calibration plot using 99% 4,4'-bisphenol A

It has to be noted that 4,4'-BPA synthesis under acidic condition can produce by-products. Even though 4,4'-BPA is colorless, the reaction mixture was found to be brown in color due to the formation of by-products which absorb visible light. The impurities include 2,4'-BPA, alkylated phenols, 4'-hydroxyphenyl-2,2,4-trimethyl chroman, 4'-hydroxyphenyl-2,4,4-trimethyl chroman and 2,2,4-trimethyl chromen.¹⁰⁵ With low acid exchange value catalysts, mostly two products were observed from HPLC, while other products were also observed in the case of aromatic sulphonated catalyst whose positions in chromatogram were not identified due to unavailability of standards. Hence the selectivity of 4,4'-BPA calculated based on percentage area is not accurate in the case of catalysts with higher acid content since the concentration of benzenoid chromophores can vary in each injection which in turn can vary the peak intensity.

6.3.7.2 Estimation of 1,1,1-tris(4'-hydroxyphenyl) ethane using HPLC

A representative product mixture on analysis showed two product peaks at very close proximity. Separation of standard solutions of phenol, 4-hydroxy acetophenone

and 1,1,1-THPE obtained with 35% acetonitrile in water, an example of separation for reactants and products obtained from condensation reaction under the same analysis conditions as well as confirmation of second product peak as peak for 1,1,1-THPE after spiking with pure sample are given in Figure 6.9 (A-E)

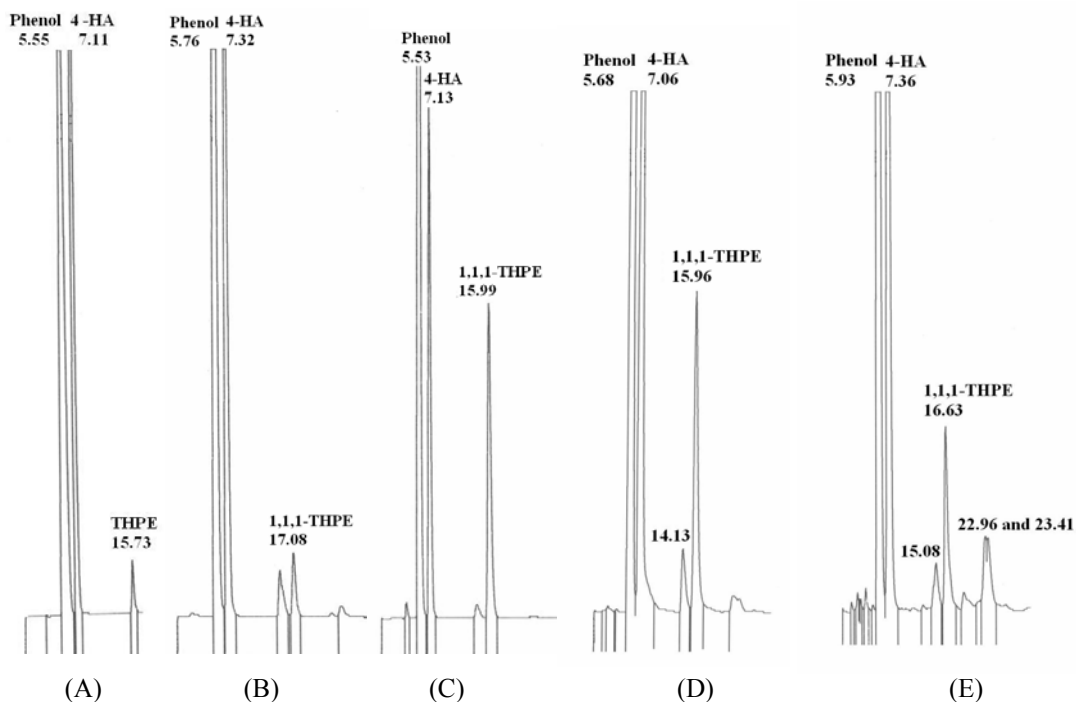


Figure 6.9(A-E) Separation of (A) standard solutions of reactants and product (B) example product mixture and (C) product mixture B after spiking with pure 1,1,1-THPE (D) product mixture after reaction with two step sulphonated styrene-GMA-DVB catalyst at 100 °C and (E) product mixture after reaction with Amberlyst 15 at 100 °C

The calibration plot obtained on plotting standard solution of 1,1,1- THPE against area obtained is given in Figure 6.10

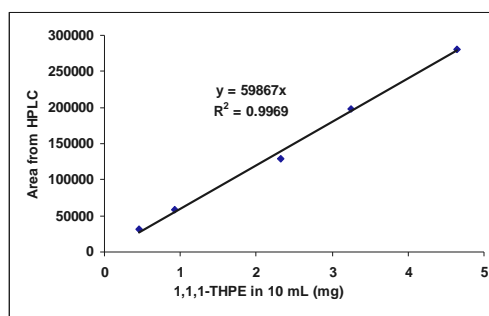


Figure 6.10 HPLC calibration plot for standard 1,1,1-tris(4'-hydroxyphenyl) ethane

It was observed that using aliphatic mercapto sulphonated catalyst, the percentage of 1,1,1-THPE was below 1% in the product mixture at 60 and 100 °C while using two step sulphonated catalysts (aromatic sulphonated and aliphatic mercapto sulphonated catalysts) carried out at 100 °C showed better results. Two commercial catalysts were also used for comparative studies. In all cases the reaction mixture was reddish brown in color with two product peaks coming within an analysis time of 30 min. The percentage content of 1,1,1-THPE was noted based on calibration curve and the selectivity was calculated based on percentage area. The amount in mg of 1,1,1-THPE in each sample was calculated from the ratio of area of 1,1,1-THPE in sample to the slope of calibration curve. The percentage content of 1,1,1-THPE was thus calculated from the amount in mg of product mixture taken for analyses. The selectivity was calculated based on percentage area. The results obtained are given in Table 6.10.

Table 6.10 Percentage content and selectivity of 1,1,1-tris(4'-hydroxyphenyl) ethane calculated using two step sulphonated catalysts (aromatic sulphonated and aliphatic mercapto sulphonated catalysts) and commercial aromatic sulphonated catalysts

No.	Co/terpolymer	Wt. of sample in 10 mL (mg)	Area of 1,1,1,-THPE	Total area of phenolic products	Amount of 1,1,1,-THPE* (mg)	% of 1,1,1,-THPE in product mixture	Selectivity (Area %)
1	Styrene-ETMA-DVB	147.2	490229	569470	8.18	5.55	86.09
2	Styrene-ETMA-EGDM	210.4	556592	661849	9.29	4.31	84.10
3	Styrene-GMA-DVB	110	407471	487602	6.8	6.17	83.57
4	Styrene-GMA-EGDM	164.2	416915	478016	6.96	4.23	87.22
5	ETMA-GMA-DVB	178.7	560024	644098	9.35	5.25	86.95
6	ETMA-DVB	210.4	509420	588383	8.5	4	86.58
7	GMA-DVB	203.9	473900	557647	7.91	3.88	84.98
8	Amberlyst-15	86.90	222180	472332	3.71	4.26	57.04
9	Lewatit K-2629	106.4	277057	511787	4.62	4.34	54.14

* Determined from calibration plot using 99% 1,1,1,-THPE

It has to be noted that 1,1,1-THPE synthesis under acidic condition can produce by-products. Even though 1,1,1-THPE is colorless, the reaction mixture is found to be reddish brown in color due to the formation of by-products, which absorb visible light. The impurities include iso THPE, mixture of ortho and para tris(hydroxyphenyl)ethane isomers, 1,1-bis(hydroxyphenyl)ethane isomers as well as other unidentified color bodies.⁹¹ Since only two products were observed from HPLC, the selectivity of 1,1,1-THPE was calculated based on percentage area as the pure standard for impurity was not available. The selectivity calculated based on percentage area is not an accurate method

as the concentration of benzenoid chromophores can vary in each injection, which in turn can vary the peak intensity. Since the conversion in reaction is much less, the error in selectivity calculated based on area can also be expected to be low.

6.4 Conclusions

Porous polymeric beads with low to moderate surface area were synthesized with 100% crosslink density using two different surfactants. The obtained beads were functionalized with sulphonic acid group or mercapto sulphonic acid groups and characterized by FTIR, EDX and XPS. The acid exchange values of the catalysts as well as the surface areas of the formed beads were noted. The surface morphologies of the beads were noted by optical microscopy and scanning electron microscopy.

The beads were used as cation exchange resins to study the acid phase condensation reactions involving phenol and acetone at 60 and 100 °C as well as between phenol and 4-hydroxy acetophenone at 100 °C. Mixture of products were obtained, from which the percentage content of 4,4'-BPA as well as 1,1,1-THPE were noted from calibration plots obtained using pure standards. Since the standards for the impurities in the reactions were not available, the percentage selectivity based on area was considered. This consideration can have errors as the benzenoid chromophore absorption varies with the concentration of injected product mixture using a UV detector. Since the final conversions were low, the selectivity values would have errors.

It was observed that in the case of reactions involving phenol and acetone with aliphatic mercapto sulphonated / sulphonated catalyst, the percentage content of 4,4'-BPA was much less than that obtained with aromatic sulphonated catalysts. Aromatic sulphonated catalysts containing mercaptan and commercial aromatic sulphonated catalysts showed much higher percentage content of 4,4'-BPA and did not show much variation in selectivity. In the case of reactions involving phenol and 4-hydroxy acetophenone, the aliphatic sulphonated/mercapto sulphonated catalyst showed very low conversion and hence the study was carried with two step sulphonated mercapto sulphonic acid catalysts and commercial catalysts at 100 °C. It was observed that this system showed better selectivity. The condensations carried out with commercial catalysts showed less selectivity.

6.5 References

- [1] Y.Chauvin, D. Commereuc, F. Dawans., *Prog. Polym. Sci.* **5**, 95 (1977).
- [2] N.R. Cameron., *Polymer* **46**, 1439 (2005).
- [3] N.M. Bortnik., *US patent* 3037052 (1962).
- [4] H.G. Yuan, G. Kalfas, W.H.Ray., *Rev. Macromol. Chem. Phys.* **C31**, 215 (1991).
- [5] E.V. Lima, P.E.Wood, A.E. Hamielec., *Ind. Eng. Chem. Res.* **36**, 939 (1997).
- [6] R.T.E. Schenck, S. Kaizerman., *J. Am. Chem. Soc.* **75**, 1636 (1951).
- [7] R.A.Stein, V.Slawson., *Anal. Chem.* **40**, 2017 (1968).
- [8] H.Shinano, S.Tsuneda, K.Saito, S.Forusaki, T.Sugo., *Biotechnol. Prog.* **9**, 193 (1993).
- [9] M.Kim, K.Saito., *Rad. Phys. Chem.* **57**, 167 (2000).
- [10] M.Kim, K.Saito., *React. Funct. Polym.* **40**, 275 (1999).
- [11] M.S.Kharasch, E.M.May, F.R.Mayo., *J. Org. Chem.* **3**, 175 (1938).
- [12] M.S.Kharasch, R.T.E. Schenck, F.R.Mayo., *J. Am. Chem. Soc.* **61**, 3092 (1939).
- [13] E.J. Goethals., *Polym. Lett.* **4**, 691 (1966).
- [14] E.J. Goethals, E.D. Witte., *J. Macromol. Sci. Chem. A5*, **1**, 63 (1971).
- [15] J. Ihata., *J. Polym. Sci. Part A: Polym. Chem.* **26**, 167 (1988).
- [16] S. B. Idage, S. Badrinarayanan, S. P. Vernekar, S. Sivaram., *Langmuir* **12**, 1018 (1996).
- [17] G. G. Cameron, B. R. Main., *Polym. Degrad. Stab.* **5**, 215 (1983).
- [18] G. G. Cameron, B. R. Main., *Polym. Degrad. Stab.* **11**, 9 (1985).
- [19] H. Tada, S. Ito., *Langmuir* **13**, 3982 (1997).
- [20] D. A. Olsen, A. J. Oстераas., *J. Polym. Sci. Part A: Polym. Chem.* **7**, 1913 (1969).
- [21] D. A. Olsen, A. J. Oстераas., *J. Polym. Sci. Part A: Polym. Chem.* **7**, 1921 (1969).
- [22] D. Fischer, H. H. Eysel., *J. Appl. Polym. Sci.* **52**, 545 (1994).
- [23] J.M. Wheaton, M.J. Hatch., *Ion exchange Ed. J.A.Marinsky, M. Dekker, New York.* 219 (1966).
- [24] F. Doscher, J. Klein, F. Pohl, H. Widdecke., *Makromol. Chem. Rapid Commun.* **1**, 297 (1980).
- [25] D.H. Clemens, W. Grove, R.J. Lange., *US Patent* 3944507 (1976).
- [26] B.N. Kolarz, A. Trochimczuk, M. Wajaczynska., *Die Angew. Makromol. Chem.* **162**, 193 (1988).
- [27] K. Miyatake, K. Oyaizu, E. Tsuchida, A.S. Hay., *Macromol.* **34**, 2065 (2001).

- [28] S. Matsumura, A.R. Hlil, C. Lepiller, J. Gaudet, D. Guay, Z. Shi, S. Holdcraft, A.S. Hay., *Macromol.* **41**, 281 (2008).
- [29] H.F.M. Schoo, G. Challa., *React. Polym.* **16**, 125 (1991).
- [30] R.J. Wakeman, Z.G. Bhungara, G. Akay., *Chem. Eng. J.* **70**, 133 (1998).
- [31] H.S. Makowski, R.D. Lundberg, G.H. Singhal., *US Patent 3870841* (1975).
- [32] Y. Tran, P. Auroy., *J. Am. Chem. Soc.* **123**, 3644 (2001).
- [33] C.C. Chu, Y.W. Wang, C.F. Yeh, L. Wang., *Macromol.* **41**, 5632 (2008).
- [34] M. Ottens, G. Leene, A.A.C.M. Beeneckers, N. Cameron, D.C. Sherrington., *Ind. Eng. Chem. Res.* **39**, 259 (2000).
- [35] J. Kerres, W. Cui, S. Reichle., *J. Polym. Sci. Polym. Chem.* **34**, 2421 (1996).
- [36] F. Wang, M. Hickner, Y.S.Kim, T.A.Zawodzinski, J.E.McGrath., *J. Memb. Sci.* **197**, 231 (2002).
- [37] N. Bothe, F. Doscher, J. Klein, H. Widdecke., *Polymer* **20**, 849 (1979).
- [38] H. Maeda, H. Egawa., *J. Appl. Polym. Sci.* **29**, 2281 (1984).
- [39] F.G. Bordwell, H.M. Andersen., *J. Am. Chem. Soc.* **75**, 4959 (1953).
- [40] B. Tamami, A.R. Kiasat., *Synth. Commun.* **26**, 3953 (1996).
- [41] N. Iranpoor, F. Kazemi., *Synthesis* **7**, 821 (1996).
- [42] M. Baltork, H. Aliyan., *Synth. Commun.* **28**, 3943 (1998).
- [43] M. Baltork, A.R. Khosropoor., *Ind. J. Chem.* **38B**, 605 (1999).
- [44] N.S. Krishnaveni, K. Surendra, M.S. Reddy, Y.V.D. Nageswar, K.R. Rao., *Adv. Synth. Catal.* **346**, 395 (2004).
- [45] K. Surendra, N.S. Krishnaveni, K.R. Rao., *Tett. Lett.* **45**, 6523 (2004).
- [46] B. Tamami, M. Kolahdoozan., *Tett. Lett.* **45**, 1535 (2004).
- [47] B. Kaboudin, H. Norouzi., *Tett. Lett.* **45**, 1283 (2004).
- [48] B. Kaboudin, H. Norouzi., *Synthesis* **12**, 2035 (2004).
- [49] B. Tamami, K.P. Borujeny., *Synth. Commun.* **34**, 65 (2004).
- [50] B. Das, V.S. Reddy, M. Krishnaiah., *Tet. Lett.* **47**, 8471 (2006).
- [51] B.P.Bandgar, N.S.Joshi, V.T.Kamble., *Tet. Lett.* **47**, 4775 (2006).
- [52] N. Spassky, P. Dumas, M. Sepulchre, P. Sigwalt., *J. Polym. Sci. Symp.* **52**, 327 (1975).
- [53] M.O. Brimeyer, A. Mehrota, S. Quici, A. Nigam, S.L. Regen., *J. Org. Chem.* **45**, 4254 (1980).

- [54] J. Kowara, A. Skowronska, J. Michalski., *Heteroatom Chem.* **8**, 429 (1997).
- [55] M. Dele'pine, P. Jaffeux., *Bull. Soc. Chim. Fr.* **29**, 136 (1921).
- [56] J.M. Stewart., *J. Org. Chem.* **28**, 596 (1963).
- [57] M. Dele'pine, S. Eschenbrenner., *Bull. Soc. Chim. Fr.* **33**, 703 (1923).
- [58] E.M. Meade, F.N. Woodward., *J. Chem. Soc.* 1894 (1948).
- [59] W. Reppe, F. Nicolai., *US Patent 2105843* (1938).
- [60] Y. Li, J. Cheng, J. Zhang., *J. Appl. Polym. Sci.* **101**, 4023 (2006).
- [61] F.A. Ogliari, M.L.T. Sordi, M.A. Ceschi, C.L. Petzhold, F.F. Demarco, E. Piva., *J. Dent.* **34**, 472 (2006).
- [62] T. Nonaka, K.Fujita., *J. Memb. Sci.* **144**, 187 (1998).
- [63] M.L.T. Sordi, M.A. Ceschi, C.L. Petzhold, A.H.E. Muller., *Macromol. Rapid Commun.* **28**, 63 (2007).
- [64] H. Egawa, T. Nonaka, T. Hurusawa., *J. Polym. Sci. Polym. Chem.* **21**, 2597 (1983).
- [65] M. Tsunooka, S. Tanaka, M. Tanaka, H. Egawa, T. Nonaka., *J. Polym. Sci. Polym. Chem.* **23**, 2495 (1985).
- [66] H. Egawa, T. Nonaka., *J. Appl. Polym. Sci.* **31**, 1677 (1986).
- [67] H. Maeda, H. Egawa., *Analyt. Chim. Acta.* **162**, 339 (1984).
- [68] L.E. Overman, D. Matzinger, E.M. O'Connor, J.D. Overman., *J. Am. Chem. Soc.* **96**, 6081 (1974).
- [69] H.C. Brown, B. Nazer, J.S. Cha., *Synthesis* **6**, 498 (1984).
- [70] J.M. Stewart, H.P. Cordts., *J. Am. Chem. Soc.* **74**, 5880 (1952).
- [71] H. Ufer, A. Freitag., *German Patent 696773* (1940).
- [72] J.A. Malero, R.V.Grieken, G.Morales., *Chem. Rev.* **106**, 3790 (2006).
- [73] A. Chemin, A. Mercier, H. Deleuze, B. Maillard, O.M. Monval., *J. Chem. Soc. Perkin Trans. I.*, 366 (2001).
- [74] K.H. Meyer, L. Bottenbruch, W. Jakob., *US patent 4387251* (1983).
- [75] D. Palmer., *US Patent 6465697* (2002).
- [76] M.J. Cipullo, E.J. Pressman., *US Patent 5723691* (1998).
- [77] R. Lloyd, B. Fayetteville, Q. Sun., *European Patent 1399403 B1* (2006).
- [78] M.J. Cipullo., *US Patent 5146007* (1992).
- [79] C.H. Schramm, H. Lemaire, R.H. Karlson., *J. Am. Chem. Soc.* **77**, 6231 (1955).

- [80] D. Das, J.F. Lee, S. Cheng., *J. Catal.* **223**, 152 (2004).
- [81] E.L. Margelefsky, R.K. Zeidan, V. Dufaud, M.E. Davis., *J. Am. Chem. Soc.* **129**, 13691 (2007).
- [82] J.E. Jansen., *US patent* 2468982 (1949).
- [83] W.C. Stoesser, E.H. Sommerfield., *US patent* 2623908 (1952).
- [84] K. Berg, G. Fennhoff, R. Pakull, H.J. Buysch, B. Wehrle, A. Eitel, C. Wulff, J. Kirsch., *US patent* 5780690 (1998).
- [85] R.M. Wehmeyer, E.L. Tasset, M.E. Walters., *US patent* 6133190 (2000).
- [86] G.D. Yadav, N. Kirthivasan., *Appl. Catal. A Gen.* **154**, 29 (1997).
- [87] B. Carvill, K. Glasgow, M. Roland., *US Patent* 7132575 (2006).
- [88] R.J. Meyer, O.E. Horsley, H.J. Eichel., *US patent* 3579542 (1971).
- [89] A.M. Dhalla, R. Gupta, G. Kishan, Y. Li, G.V. Ramanarayanan., *US Patent* 7304189 (2007).
- [90] A.K. Mendiratta., *US patent* 4400555 (1983).
- [91] H. Strutz, W. Mueller., *US patent* 4992598 (1991).
- [92] S. Sivaram, V.R. Ranade, S. Chakrapani, P.P. Wadgaonkar, P.D. Sybert, G.M. Kissinger, A.K. Mendiratta., *US Patent* 5969167 (1999).
- [93] G.R. Faler., *US patent* 4375567 (1983).
- [94] P.D. Stbert, G.M. Kissinger, A.K. Mendiratta., *US patent* 5756781 (1998).
- [95] M. Bartholin, G. Boissier, J. Dubois., *Makromol. Chem.* **182**, 2075 (1981).
- [96] C.Y. Liang, S. Krimm., *J. Polym. Sci.* **27**, 241 (1958).
- [97] M. Kaneko, H. Sato., *Macromol. Chem. Phys.* **206**, 456 (2005).
- [98] J.A. Asensio, S. Borros, P.G. Romero., *J. Polym. Sci. Polym. Chem.* **40**, 3703 (2002).
- [99] D.G. Castner, K. Hinds, D.W. Grainger., *Langmuir* **12**, 5083 (1996).
- [100] J.G.C. Shen, T.H. Kalantar, R.G. Herman, J.E. Roberts, K. Klier., *Chem. Mater.* **13**, 4479 (2001).
- [101] J.G.C. Shen, R.G. Herman, K. Klier., *J Phys Chem B* **106**, 9975 (2002).
- [102] R.A. Soldi, A.R.S. Oliveira, L.P. Ramos, M.A.F.C. Oliveira., *Appl. Catal. A* **316**, 42 (2009).
- [103] S. Talwalkar, P. Kumbhar, S. Mahajani., *Ind. Eng. Chem. Res.* **45**, 8024 (2006).
- [104] P.M. Slomkiewicz., *Appl. Catal. A* **301**, 232 (2006).

Summary and conclusions

7 Summary and conclusions

The thesis has been divided into seven chapters. Introduction to photopolymerization, Introduction to high internal phase emulsion, Aims and objectives, photopolymerization of mono and diacrylate based monomers, photopolymerization of multiacrylate based monomers, synthesis of cation exchange resins and their catalytic evaluation for acid phase condensation reactions and summary and conclusions form the seven chapters.

Chapter 1 describes the current state of knowledge in photopolymerization studies while Chapter 2 describes a general outlook on high internal phase emulsion (HIPE) polymerization. The various applications areas are also provided in the respective introductory chapters. Chapter 3 describes the aims and objectives of the research work. Chapter 4 is divided into three parts. The first part describes the synthesis and photopolymerization kinetics of polyether urethane di(meth)acrylate macromonomer in presence of reactive diluents while the second part describes the synthesis and photopolymerization kinetics of bis aromatic based di(meth)acrylates in presence of reactive diluents using photo DSC. The third part describes the feasibility of photopolymerization kinetic studies carried out on HIPEs using an external irradiation source. Chapter 5 describes the synthesis and photopolymerization kinetics of linear and branched multiacrylates using photo DSC. Chapter 6 describes the synthesis and functionalization of polyHIPEs to obtain cation exchange resins and their evaluation in acid phase condensation reactions. Chapter 7 deals with the summary and conclusions.

Photopolymerization of synthesized oligomers in the presence of reactive diluents and photoinitiators of various classes were carried out. The synthesized oligomers studied in chapter 4 (part –A) were based on urethane di(meth)acrylates possessing aliphatic and cycloaliphatic backbone. Photopolymerizations of prepared formulations were carried out with polychromatic radiation at various concentrations of different class of photoinitiators. The addition of reactive diluents decreases the viscosity with an increase in density of reactive sites in the formulations. In presence of reactive diluents, high conversions were observed with flexible oligomers having long chain ethyleneoxy and propyleneoxy linkages.

Photopolymerization of urethane acrylate oligomer based on propyleneoxy linkages in presence of 15 wt% of HEMA as reactive diluent showed high conversion at higher irradiation wavelength and intensity as compared to that of similar systems possessing 15 wt% of HEA as reactive diluent due to enhanced vitrification of the later. Photopolymerizable urethane diacrylates based on ethyleneoxy linkages in presence of 10wt% of HEA as reactive diluent was also found to show lower conversions.

Photopolymerization of polybutadiene based dimethacrylate macromonomers containing 30 wt% of HEMA with soft and partially rigid backbone were studied at high intensities. The soft segmented urethane dimethacrylate showed higher final conversions as compared partially hard segmented ones. These systems can be assumed to show better radical and reaction diffusions. The volume relaxation occurring soon after autoacceleration helped these systems to undergo enhancement in diffusion processes such as segmental and reaction diffusions, leading to final conversions. In the absence of reactive diluent, high energy radiation and high irradiation intensity, oligomers containing polybutadiene moiety in the backbone and acrylate end functionalities showed huge variations in conversions due to the overall influence in the rate of initiation and diffusion parameters.

It was found that photopolymerization can occur efficiently in presence of reactive diluents and high energy radiation (250-450 nm), even at a low intensity of 4.6 mW/cm². The influence of reactive diluent, crosslinkers as well as radical scavenger were estimated. It was found that the addition of crosslinker increased the final conversion while the addition of radical scavenger increased the induction time or in other words slows down the photo initiation process by undergoing rapid terminations. An increase in temperature from 30 to 50 °C was found to increase the rate of initiation, while the final conversion did not show any trend due to the influence of viscosity assisted reaction diffusion.

The efficacies of variable autocatalytic kinetic model on photopolymerization processes were studied using TA advantage specialty library software. The model takes into account of the heat flow profiles signal from onset of initiation to the onset of vitrification. It was observed that in many cases the value of autocatalytic exponent (m) is closer to the ideal value of 0.5 observed in the case of amine assisted epoxy/anhydride

cure reactions. All the studied systems can be assumed to undergo both bimolecular and monomolecular termination reactions.

Photopolymerization of oligomers studied in chapter 4 (part –B) were based on bis aromatic based urethane di(meth)acrylates possessing aliphatic/cycloaliphatic and aromatic backbone. The addition of reactive diluents decreased the viscosity with an increase in density of reactive sites in the formulations. As a result, the photopolymerization took place in an efficient manner with moderate to high conversions in certain cases. High conversions were observed with formulations having low initial viscosity.

The bis aromatic based urethane diacrylate with ethyleneoxy linkages containing 50 wt% of monoacrylate as reactive diluent showed a initial viscosity of 1781 cP and a maximum conversion around 71%, when irradiated at a very low intensity of 1.93 mW/cm² at 40 °C. High conversion was not occurring in this case, which can be attributed to the effect of radical/reaction diffusions occurring during the deceleration step and enhanced vitrification. Bis aromatic based urethane diacrylate with propyleneoxy linkages containing 50wt% of monoacrylate as reactive diluent showed a initial viscosity of 993 cP and a maximum conversion of around 89%, when irradiated at a low intensity of 1.93 mW/cm² at 40 °C. An increase in irradiation intensity to 4.47 mW/cm² did not cause much effect on final conversion due to influence of limitations imparted by overall diffusion processes under polychromatic conditions. An increase in isothermal condition to 70 °C at 4.47 mW/cm² resulted in an overall decrease in final conversion due to reduction in initial system viscosity and enhanced terminations occurring during the initial stages of photopolymerization. The compositions cured at higher temperature vitrified faster due to comparatively faster volume shrinkage with respect to the chemical reaction in the deceleration step.

Bis aromatic based urethane dimethacrylate with propyleneoxy linkages and sulphone moieties in the backbone and containing 75 wt% of monomethacrylate as reactive diluent, showed a initial viscosity of 1856 cP. For this system, the maximum conversion of above 68% was found to occur at an irradiation intensity of 1.78 mW/cm² at 40 and 70 °C. On increasing the irradiation intensity to 3.26 mW/cm² at 40 °C, a maximum conversion of around 75% was obtained. This showed that the final

conversion during the photopolymerization process for this system was influenced by intensity rather than increase in temperature from 40 to 70 °C. It is known that photopolymerization of dimethacrylates in most cases occur to a lower rates and higher conversion than corresponding diacrylates at similar irradiation conditions due to longer time scale for reaction diffusion for the former and earlier vitrification for the later. In this system, with methacrylate end functionalities, an increase in timescale of reaction diffusion with a decrease in rate as compared to previous two acrylate systems were obtained and is evident from the heat flow profiles. A very high conversion as expected for methacrylates was not obtained, probably due to a positive glass transition temperature of 55.5 °C for the photocured matrix which forced the system to vitrify early.

Bis aromatic based urethane diacrylate with ethyleneoxy linkages and biphenyl moieties in the backbone and containing 300 wt% of monoacrylate as reactive diluent, showed a initial viscosity of 1406 cP. The solid macromonomer was solvated with high excess of monoacrylate as reactive diluent to obtain an optimum viscosity and the maximum conversion of above 76% was obtained when irradiated at a very low intensity of 2.27 mW/cm².

From the studies at 5% conversion, formulations containing 300 wt% of excess acrylate and 0.5 wt% of IRGACURE 651 analyzed at 40 °C showed a six time value for the ratio (k_t^b/k_p) as compared to the former system under similar conditions with 50 wt% of excess acrylate as reactive diluent. This shows that at low conversions, the value of the ratio (k_t^b/k_p) for bimolecular termination increases with an increase in density of reactive sites.

From thermogravimetric analyses, we can infer that samples photocured at higher temperature showed a decrease in degradation profiles due to better crosslinking. It was also observed that photoinitiated samples on storage had undergone dark polymerization to a considerable extent as compared to completely photocured samples. Extent of dark polymerization varied depending on the nature of photoinitiated matrix. This supports the theory that photoinitiated matrix can undergo polymerization in dark over a much longer time scale of days or even months.

In chapter 4 (part-C), the photopolymerization of HIPE was successfully carried out. The final conversions in photopolymerized HIPES vary with the extent of initiation.

For emulsions containing IRGACURE 819, high conversion was obtained possibly due to the through cure (thick layer curing) property of the monomer arising from the proximity of the major absorption maximum of the photoinitiator to the major emission line of the mercury spectrum. The other factors such as diffusion of radical species can also affect the final conversion. This has been observed in the case of emulsions containing DAROCUR 1173 as compared to IRGACURE 184. The feasibility of photopolymerization of HIPE systems involving acrylates was established. The foams prepared by this method can be used in various applications such as fluid absorption, insulation, sound dampening and filtration. It can also be used for the preparation of multilayer foam articles. By varying the starting material and processing conditions, the foam structure can be tailored to obtain desired physical properties.

Photopolymerization of multiacrylates were studied in chapter-5. Photopolymerization of synthesized hexaacrylate macromonomer in presence of photoinitiators of various classes were carried out without the addition of reactive diluents. The photopolymerization took place in an efficient manner with moderate conversions when irradiated with 250-450 nm polychromatic radiation. An increase in concentration of photoinitiator decreased the induction as well as peak maximum time along with an increase in the value of R_p max and C_{max} showing a gradual influence of reaction diffusion during deceleration step. Linear hexaacrylate macromonomer irradiated with 320-500 nm radiation was found to show slow rate of polymerizations and very low conversions due to low irradiation energy. The π - π^* transition did not occur in this case as the studied photoinitiators had a λ_{max} below 320 nm.

In the case of branched multiacrylates prepared with glycerol 1,3-diglycerolate diacrylate as well as with propylene glycol glycerolate diacrylate, it was found that an increase in concentration of photoinitiator at a particular temperature as well as an increase in temperature at a particular concentration resulted in a decrease in induction as well as peak maximum time with an increase in the value of R_p max. An enhancement in polymerization rates which were shown in the initial stages of polymerization with an increase in temperature was not shown up to C_{max} due to the effect of viscosity dependent reaction diffusion which restricts overall diffusion processes.

The applicability of variable autocatalytic kinetic model on photopolymerization processes were studied using TA advantage specialty library software. All these systems can be assumed to undergo both bimolecular as well as monomolecular termination reactions.

In chapter-6, porous polymeric beads with low to moderate surface area were synthesized with 100% crosslink density using two different surfactants. The obtained beads were functionalized with sulphonic acid group or mercapto sulphonic acid groups and characterized by FTIR, EDX and XPS. The acid exchange values of the catalysts as well as the surface areas of the formed beads were calculated. The surface morphologies of the beads were evaluated by optical microscopy and scanning electron microscopy. The beads were used as cation exchange resins to study the acid phase condensation reactions involving phenol and acetone at 60 and 100 °C as well as between phenol and 4-hydroxy acetophenone at 100 °C.

It was observed that in the case of reactions involving phenol and acetone with aliphatic mercapto sulphonated / sulphonated catalyst, the percentage content of 4,4'-BPA was much less than that obtained with aromatic sulphonated catalysts. Aliphatic mercapto sulphonated catalysts showed a higher selectivity towards 4,4'-BPA as compared to that of aliphatic sulphonated catalysts at 60 °C, while the difference in selectivity was negligible at 100 °C. Aromatic sulphonated catalysts containing mercaptan and commercial aromatic sulphonated catalysts showed much higher percentage content of 4,4'-BPA and did not show much variation in selectivity. In the case of reactions involving phenol and 4-hydroxy acetophenone to form 1,1,1-THPE, the aliphatic sulphonated/mercapto sulphonated catalyst showed very low conversion and hence the study was carried with two step sulphonated mercapto sulphonic acid catalysts and commercial catalysts at 100 °C. It was observed that the synthesized catalysts showed better selectivity as compared to commercial catalysts.